LEGISLATIVE LIBRARY OF BRITISH COLUMBIA
3 3298 00268 8993

BRITISH COLUMBIA
Ministry of Energy and Mines
Energy and Minerals Division

METALLOGENY AND MINERAL DEPOSITS OF THE NELSON-ROSSLAND MAP-AREA;

PART II: THE EARLY JURASSIC ROSSLAND GROUP SOUTHEASTERN BRITISH COLUMBIA

Trygve Höy, P.Eng. and Kathryn P.E. Dunne, P.Geo.

With Contributions From:
J. Gabites, The University of British Columbia
C.I. Godwin, Consultant, Vancouver, B.C.
C.H.P. Leitch, Consultant, Saltspring Island, B.C.
J. Mortenson, The University of British Columbia
H.J. Stein, Colorado State University

BULLETIN 109

LEGISLATIVE LIBRARY
VICTORIA BC MAR 12 2002

National Library of Canada Cataloguing in Publication Data
Hoy, Trygve, 1945-
Metallogeny and mineral deposits of the Nelson-Rossland map-area. Part II, The early Jurassic Rossland group, southeastern British Columbia

(Bulletin ; 109)

Issued by Energy and Minerals Division.
Includes bibliographical references: p.
ISBN 0-7726-4625-2

1. Metallogeny - British Columbia - Salmo Region. 2. Geology, Stratigraphic - Jurassic. 3. Geology, Structural - British Columbia - Salmo Region. 4. Geology, Economic - British Columbia - Salmo Region. 5. Mines and mineral resources - British Columbia - Salmo Region. I. Dunne, Kathryn P. E., 1963- . II. British Columbia. Ministry of Energy and Mines. III. British Columbia. Energy and Minerals Division. IV. Title. V. Series: Bulletin (British Columbia. Ministry of Energy and Mines) ; 109.

QE187.H69 2001 553.4'1'0971162 C2001-960247-2

VICTORIA
BRITISH COLUMBIA
CANADA

DECEMBER 2001

102-04178/

SUMMARY

The Nelson-Rossland map area (NTS 082F/SW) contains a variety of mineral deposits and numerous past producers. Many historical mining camps in southern British Columbia are located in the region, and their development led directly to the settlement and growth of the interior of the province.

The area straddles the tectonic boundary between rocks of North America and the eastern edge of arc terranes. It has a complex tectonic and magmatic history which is reflected in the diversity of mineral deposits and occurrences. The eastern part of the area is within the Kootenay arc, a north-trending arcuate structural zone in the eastern part of the Omineca belt that is characterized by intense polyphase deformation and locally high-grade regional metamorphism. The arc developed mainly in Late Proterozoic and Paleozoic rocks of the Kootenay terrane and in miogeoclinal North American rocks. It contains lead-zinc carbonate-hosted deposits, most of which are concentrated in the southern part of the arc south and southwest of Salmo. The Sheep Creek gold camp, within mainly EoCambrian quartzites of the Hamill Group, has produced more than 23 035 kilograms of gold from gold-quartz veins.

Mesozoic volcanic arc rocks of Quesnellia, west of the Kootenay arc, contain important silver-lead-zinc mineral camps, such as the Ymir camp within mainly metasedimentary rocks, and gold-copper±molybdenum deposits in intrusive, mafic volcanic and metasedimentary rocks of the Rossland Group.

Porphyry copper-gold deposits in the Nelson-Rossland area include Katie, Shaft and occurrences adjacent to the Eagle Creek plutonic complex, all associated with mafic stocks within Early Jurassic Elise volcanic rocks. They are typical of the alkalic porphyry gold-copper class of deposits, with magnetite mineralization associated with potassic feldspar alteration and widespread regional propylitic alteration. Porphyry molybdenite deposits and related breccias are concentrated on Red Mountain west of the Rossland gold-copper vein camp and on Stewart Mountain west of Ymir. The Gold Mountain zone of Kena Gold is a new porphyry gold prospect within the Middle Jurassic, syntectonic Silver King porphyry.

A variety of skarn deposit-types are recognized within the Nelson-Rossland map-area. Copper, lead-zinc, iron and gold skarns are associated with Middle Jurassic intrusions, whereas tungsten skarns occur mainly in Early Cambrian marbles along the margins of Cretaceous intrusions. Many of these skarns are past producers, most notably the gold skarns at Second Relief and Bunker Hill, the tungsten skarns such as the Emerald Tungsten and Dodger northeast of Salmo, and the molybdenite skarns, including Coxey and Giant on Red Mountain in the Rossland camp.

Polymetallic Ag-Pb-Zn±Au veins are the most common deposit type in the Nelson-Rossland map-area. Many of the veins of the Ymir camp, those within Elise Formation rocks southwest of Nelson, and a number in the South belt of the Rossland camp are past producers. These veins are commonly along the margins of Middle Jurassic granitic stocks or batholiths.

The Rossland mining camp, the main focus of this paper, is the second largest lode gold producing camp in British Columbia, with recovery or more than 84 000 kilograms of gold and 105 000 kilograms of silver between 1894 and 1941. Vein deposits are in three main belts within or along the margins of the Middle Jurassic Rossland pluton. The North belt and Main veins are dominantly massive, intrusion-related gold-copper pyrrhotite veins, whereas those in the South Belt are dominantly polymetallic silver-lead-zinc veins. Pronounced mineral, textural and chemical zoning of these veins reflect their proximity to the Rossland pluton and to structural levels of emplacement. Due to western tilting of the area in Eocene time, eastern exposures of the Rossland veins were formed at deeper structural levels than those in the west.

Molybdenite mineralization within the camp occurs within an intrusive breccia-skarn complex on the western slopes of Red Mountain, west of and at higher structural levels than the Rossland gold-copper veins.

The relationships between various deposit-types in the Rossland camp are now well constrained. The copper-gold veins are spatially and genetically related to the *ca.* 167 Ma Rossland monzonite and associated diorite porphyry dikes. These dikes are overprinted by skarn alteration and molybdenite mineralization, dated by Re-Os at *ca.* 163 Ma. Brecciated quartz diorite dikes, spatially associated with the molybdenite mineralization, are dated at *ca.* 163 Ma, supporting a younger age for molybdenite mineralization. These dikes may be late phases of the similar *ca.* 166 Ma Rainy Day pluton located just south of the molybdenite breccia complex.

Although Rossland veins have many characteristics of intrusion-related hydrothermal veins, their strong preferred alignment and associated shearing indicate structural control as well. Their orientation, age, and timing, relative to compressive deformation and documented synkinematic plutons elsewhere in the Rossland-Nelson area, support a model for development in an east-west compressive stress regime. This is manifest in the Rossland area by east-verging thrust faults that emplace oceanic ultramafic assemblages and the Permo-Carboniferous Mount Roberts Formation onto the Rossland Group.

TABLE OF CONTENTS

CHAPTER 1
INTRODUCTION 1
Introduction 1
Previous Work 1
Acknowledgments 1

CHAPTER 2
REGIONAL GEOLOGY 3
Introduction 3
Regional Geology 3
Rossland Group 3
Archibald Formation 3
Elise Formation 3
Hall Formation 7
Plutonic Rocks 8
Early Jurassic Plutons 8
Early-Middle Jurassic Plutons 8
Middle Jurassic Plutons 9
Cretaceous Plutons 9
Cenozoic Plutons 9
Structure and Tectonics 9
Early Jurassic 9
Middle Jurassic 10
Tertiary 10

CHAPTER 3
MINERAL DEPOSITS 11
Introduction 11
Carbonate-Hosted Deposits 11
Volcanogenic Massive Sulphide Deposits 12
Porphyry Copper-Gold: Alkalic 13
Introduction 13
Katie 13
Shaft 19
Kena Gold 23
Great Western 23
Toughnut 25
Alman and Star 27
Porphyry Mo 28
Stewart 2, Bobbi and Fresno 28
Skarn Deposits 29
Gold Skarns 29
Second Relief, Inez and Rand 31
Gold-Quartz Veins 33
Introduction 33
Sheep Creek Camp 34
Other Au-Quartz Vein Deposits 36
Polymetallic Veins: Ag-Pb-Zn±Au 36
Introduction 36
Ymir Camp 37
Silver King 38
Clubine 40
Other Deposits 43
Velvet 43
Red Point 48

CHAPTER 4
ROSSLAND AREA 49
Introduction 49
Geological Setting 49
Unit Cs 49
Mount Roberts Formation 51
Rossland Group 51
Sophie Mountain Formation 54
Marron Formation 54
Intrusive Rocks 54
Early? Jurassic Monzogabbro Intrusions . . . 54
Rossland Monzonite 55
Diorite Porphyry Dikes 56
Rainy Day Pluton 56
Red Mountain Quartz Diorite Dikes 56
Ultramafic Rocks 56
Mineralization 57
Structure and Tectonics 58
Early Jurassic 58
Middle Jurassic 58
Eocene 59
Mineral Deposits 59
Red Mountain Mo Deposits 60
Introduction 60
Host Rocks 61
Molybdenite Breccia Complex 62
Mineralization 62
Re-Os Dating 64
Summary 64
Discussion 65
Regional Implications 65
Rossland Copper-Gold Veins 65
Introduction 65
North Belt 66
Evening Star 66
Monte Cristo 70

Cliff 70
Consolidated St. Elmo 71
St. Elmo 71
Mountain View 71
Jumbo 72
Discussion: North Belt 73
Main Veins 73
Centre Star - Le Roi 74
War Eagle-No. 1 74
Columbia-Kootenay 76
Other Main Vein Deposits 76
Discussion: Main Vein Deposits 76
South Belt 76
Homestake and Gopher 79
Bluebird and Mayflower 79
Robert E. Lee and North 80
Other South Belt Vein Occurrences 81
Discussion: South Belt Veins 81
Gold-Quartz Veins 81
Discussion 82
Discussion: Rossland Au-Cu Camp 82
Age Relations 82
Magmatic Controls 83
Mineralization, Geochemistry and Camp Zonation 83
Fluid Chemistry, Evolution and History 83
Structural Controls and Tectonic Setting 86
Model Summary 86
Summary: Rossland Camp 87

SELECTED BIBLIOGRAPHY 89

APPENDICES 97
1. Mineral occurrences of the Rossland-Trail map area 99
2. Sample Locations and Descriptions 109
3. Production Data: Metallic Deposits of the Rossland-Nelson Map Area 111
4. U -Pb Data 115
5. Petrographic Report on Thin and Polished Thin Sections from Rossland Camp, B.C. 121
6(a) Analyses of Samples from Deposits in the Rossland Camp (by ICP) 135
6(b) Analyses of Samples from Deposits in the Rossland Camp (by INA) 139
7. Re-Os Dating of Molybdenite, Coxey deposit, Red Mountain, B.C. 141
8. Isotopic Characterization of Lead in Galena from Mineral Deposits in the Trail Map Sheet, South-central British Columbia 143
9. Fluid Inclusion Data 159

FIGURES

2-1. Geology map of the Nelson-Rossland map-area, southeastern British Columbia 4
2-2. Stratigraphic succession. 5
2-3. Composite stratigraphic sections of the Elise Formation, Nelson-Rossland map area 5
3-1. Location and regional geology of the Katie property. 14
3-2. Drill hole plan for the Katie property, showing location of main mineralized zones. 16
3-3. Cross-sections through the Katie Main zone, Katie property 17
3-4. Regional geology map showing location of mineral deposits and occurrences in the region of the Silver King shear zone, southwest of Nelson . . 18
3-5. Geological map of the Gold Creek - Cottonwood Creek area south of Nelson 20
3-6. Geology of the Cat zone.. 21
3-7. Geology of the Shaft area. 22
3-8. Geology in the vicinity of mineralized zones, Great Western Group. 24
3-9. Geology in the vicinity of the Toughnut showing 26
3-10. Geology of the Stewart claim group, west of Ymir 30
3-11. Geology in the vicinity of the Second Relief vein-skarn deposit (from Ostensoe, 1989). 32
3-12. Geology of the Erie Lake area, showing the location of mineral deposits 41
3-13. Geology of the Clubine prospect 42
3-14. A stratigraphic section of the Hall Formation in the Keystone Mountain area 43
3-15. Geology of the Velvet mine area, southwest of Rossland.. 46
4-1. Geological map of the Rossland area 50
4-2. Geological map of the Rossland area . . . *in pocket*
4-3. Trace element diagrams of analyses of intrusive clasts in the Archibald Formation, Fruitvale and Montrose areas 52
4-4. A composite section of the Elise Formation, Rossland area 53
4.5. Plot of U-Pb zircon data, sample R313-4, Rossland monzonite 56

4-6. Plot of U-Pb zircon data from the Rainy Day pluton 57

4-7. Plot of U-Pb zircon data, sample R96-5, quartz diorite breccia dike, Red Mountain.. 57

4-8. Simplified geological map of the Rossland copper-gold camp 60

4-9. Diamond drill location plan, and simplified geology map of the Evening Star and Georgia claim area 67

4-10. Vertical section through the Evening Star deposit 68

4-11. Diagram illustrating alteration assemblages along the margins of Evening Star veins 69

4-12. A vertical model showing the distribution, tenor and alteration assemblages of veins in the Rossland Au-Cu camp. 72

4-13. Geology of the Rossland South belt vein system 78

4-14. Simplified maps of the Rossland camp, showing metal zonation patterns 84

4-15. Log fO_2 - pH diagram for the system Fe-S-O showing phase relationships at 350°C and 3 kb. 86

4-16. Model showing the evolution of gold-copper vein, polymetallic vein and molybdenite skarn deposits of the Rossland camp 88

A8-1. Location of mineral occurrences analyzed in the Trail map sheet 144

A8-2. General $^{206}Pb/^{204}Pb$ versus $^{207}Pb/^{204}Pb$ and $^{206}Pb/^{204}Pb$ versus $^{208}Pb/^{204}Pb$ plots of galena lead isotopes from mineral occurrences in the Trail map sheet.. 144

A8-3. General $^{208}Pb/^{206}Pb$ versus $^{207}Pb/^{206}Pb$ plot of galena lead isotopes from mineral occurrences in the Trail map sheet 150

A8-4. Cluster 1 data for mineral occurrences in the Trail map sheet are plotted with Jurassic to Cretaceous points for lead for an idealized Mantle, Lower Crust and Orogene 150

A8-5. Cluster 2 and Cluster 3 data for mineral occurrences in the Trail map sheet plotted with Jurassic to Cretaceous points for the plumbotectonic model for Mantle and Lower Crust 150

A9-1. Main geologic and physiographic features in the Nelson southwest portion showing location of intrusions and fluid inclusion 160

A9-2. Sketches of six compositional types of fluid inclusions identified in quartz from mineral occurrences in the Rossland Group 171

A9-3a. Histograms of temperature data, Type I fluid inclusions 173

A9-4. Histograms of temperature data, Type III fluid inclusions 174

A9-5. Histograms of temperature data, Type IV fluid inclusions 175

A9-6. Freezing point depression of water for NaCl, KCl, CaCl2, and MgCl2 solutions. 176

A9-7. Comparison of range of salinity and homogenization temperature of Rossland Group deposits to fluids in different ore deposit environments . . 184

PHOTOS

3-1a. Brecciated sulphides in Lower Cambrian Reeves limestone, Reeves MacDonald deposit. 12

3-1b. Folded sulphides in Reeves limestone, Reeves MacDonald deposit. 12

3-2. Remains of the Motherlode mill in the Sheep Creek valley 35

3-3. View of hillside above Ymir 37

3-4. View of the Main Silver King vein 38

3-5. View of the waste dumps at the Velvet deposit . 43

3-6. Ultramafic blocks mineralized with specularite and chalcopyrite, velvet mine dump. 47

4-1. Porphyritic Rossland sill 54

4-2. Coarse-grained Rossland monzonite 55

4-3. Altered quartz diorite dike from the A pit on Red Mountain 57

4-4a. View of the northwestern slope of Red Mountain showing open pits developed by Red Mountain Mines Ltd. 61

4-4b. View of Red Mountain mill site on the north side of Red Mountain; note ski runs on slopes of the mountain. 61

4-5. Red Mountain breccia, E pit, Mountain View claim diopside-rich metasediment clasts in a diopside, hornblende and minor molybdenite matrix . . . 62

4-6. Altered and veined breccia, Red Mountain . . . 62

4-7a. Dark, biotite hornfelsed metasediments cut by numerous stringers of diopside and molybdenite . 63

4-7b. Molybdenite with chlorite, calcite and epidote cut diopside-garnet skarn, B pit, Coxey deposit, Red Mountain 63

4-8. View of the headwall of E pit, Mountain View molybdenite deposit, Red Mountain. 65

4-9. Waste dump on Le Roi claim, Red Mountain, viewed to northwest. 66

4-10. Underground photo of vein and alteration, Evening Star deposit 69

4-11. Vein and alteration, Evening Star deposit. 69

4-12. View, along strike to east, of the Centre Star and Nickel Plate Au-Cu vein system 74

4-13. War Eagle Au-Cu vein here removed and infilled 75

4-14. Semi-massive sulphide vein, Homestake Ag-Zn-Pb deposit, South belt 79

4-15a. Bluebird Ag-Pb-Zn vein, South belt. Brecciated sulphide vein with angular quartz fragments in a matrix of pyrite-sphalerite-galena 80

4-15b. Bluebird Ag-Pb-Zn vein, South belt, South belt. Brecciated vein with angular, silicified and hornfelsed siltstone fragments cut by veins of mainly quartz and pyrite 80

A5-1. Sample R96-12c, Mountain View deposit, E pit 122

A5-2. Sample R96-19b, Mountain View deposit, F pit 123

A5-3. Sample R96-25b, Le Roi deposit 124

A5-4. Sample R96-35c, Centre Star deposit 126

A5-5. Sample R96-68, California deposit: Fringing alteration of secondary amphibolea round large crystals of clinopyroxene in massive skarn. 133

A5-6. Sample R96-68, California deposit: Typical "bird's-eye" alteration of pyrrhotite to intermediate FeS phases and marcasite in clinopyroxene skarn 135

A9-1. Primary inclusions trapped in quartz growth zones in quartz matrix of massive pyrite, galena sphalerite vein, Bluebird deposit. 166

A9-2. Semi-massive pyrrhotite chalcopyrite vein incorporating subhedral quartz comprising primary fluid inclusions in growth zones and overgrowths, Le Roi deposit 166

A9-3. Possible primary fluid inclusions in bands or clusters in poikilitic-textured quartz gangue from a massive sulphide vein, Jumbo deposit. 166

A9-4. Possible primary fluid inclusions trapped in growth zones in quartz from a quartz-pyrite-calcite vein, Evening Star deposit 166

A9-5. Secondary fluid inclusions occuring along healed fracture planes in quartz vein with disseminated galena, Clubine deposit. 168

A9-6. Wispy quartz texture: abundance of microfractures filled with tiny, secondary fluid inclusions in quartz vein with disseminated galena, chalcopyrite, pyrite, and sphalerite, Ace in the Hole deposit 168

A9-7. Composite plate with examples of type I, type IIIA, type IV, type V, type VI and type VII fluid inclusions at 20°C 172

A9-8. "Milled" quartz grains in a semi-massive to poorly banded pyrrhotite chalcopyrite vein at the Columbia-Kootenay deposit and a quartz vein with minor pyrite and pyrrhotite at the Consolidated St. Elmo deposit 189

A9-9. Secondary multiphaseType VI fluid inclusions in anhedral quartz vein, War Eagle deposit. . . . 190

A9-10. Clear, euhedral quartz crystal encapsulated within pyrrhotite grain, War Eagle deposit 191

TABLES

3-1. Analyses of Selected Hand Samples and 1-Metre Surface Chip Samples from the Cat and Shaft Showings 22

3-2. Analyses of Selected Samples, Great Western Group 25

3-3. Analyses of Selected Hand Samples, Toughnut Prospect 26

3-4. Mineralized Drill Intersections, Alma N and Star 28

3-5. Mineralized 'zones' In The Inez Vein, With Average Gold Content 33

3-6a. Analyses of Hand Samples from the Inez and Rand Veins, Second Relief 34

3-6b. Analyses of Hand Samples from the Rand Vein, Second Relief 34

3-7. Analyses of Selected Samples grom Trenches snd Drill Core, Silver King Deposit 39

3-8. Analyses of Selected Samples of the Clubine Property 44

3-9. Analyses of Samples of Coryell Intrusive Rocks, Velvet Deposit Area and Elsewhere. 47

3-10. Analyses of Samples of the Velvet Vein 48

4-1. Analyses of Intrusive Clasts within the Archibald Formation in the Fruitvale and Montrose Areas 52

4-2. Fe_2O_3 (Total), Feo and Fe_2O_3 Values of Selected Hand Samples of the Rossland Monzonite Showing Oxidation State Ratios 55

4-3. Drill Intersections, Novelty Property 64

A1-1. Galena Lead Isotope Analyses of Mineral Occurrences in the Trail Map Sheet 145

A2-2. Location of Mineral Occurrences Analyzed in the Trail Map Sheet 151

A3-3. Geology of Mineral Occurrences Analyzed in the Trail Map Sheet 152

A9-1. List of Quartz Vein Samples, Occurrence Names, and Estimated Age of Related Intrusions Used in this Study Sorted by Deposit Type 161

A9-2. Fluid Inclusion Nomenclature used in this Study 163

A9-3a. Melting, Homogenization and Decrepitation Temperature Data for Type I Fluid Inclusions . . . 164

A9-3b. Melting, Homogenization, Dissolution and Decrepitation Temperature Data for Type III Fluid Inclusions 166

A9-3c. Melting, Homogenization and Decrepitation Temperature Data for Type IV Fluid Inclusions . . 167

A9-3d. Melting and Homogenization Temperature Data for Type V Fluid Inclusions 168

A9-3e. Melting, Homogenization and Decrepitation Temperature DataffFor Type VI Fluid Inclusions. . 169

A9-3f. Melting, Homogenization and Decrepitation Temperature Data for Type VII Fluid Inclusions. . 170

A9-4. Salinity in Relation to Deposit Type. 170

A9-5. Paired Salinity and Homogenization Temperature Data 177

A9-6. Fluid Inclusion Composition Data: Type IV Fluid Inclusions 179

A9-7. Estimates of Minimum Pressure of Trapping Using: Method 1: Salt Dissolution After Liquid-Vapour Homogenization and Method 2: Three-Phase, Mixed Aqueous and Co2-Bearing Inclusions 181

A9-8. Fluid Characteristics of Deposits Associated with the Early Jurassic Eagle Creek Complex and Katie Stock, the Early-Middle Jurassic Silver King Pluton, the Middle Jurassic Rossland Group, Bonnington Pluton and Nelson Batholith and the Middle Cretaceous Hidden and Wallack Creek Stocks 185

CHAPTER 1 INTRODUCTION

INTRODUCTION

The Rossland Group in southeastern British Columbia is a mafic volcanic arc succession deposited along the eastern edge of Quesnellia in Early Jurassic time (Figure 1-1, in back pocket). Chemical and isotopic evidence indicate that the volcanic rocks of this arc were contaminated by continental crustal rocks and, hence, may have been deposited, at least in part, along the western edge of the North American craton (Höy and Dunne, 1997). The Rossland Group is in fault contact with rocks of the Kootenay terrane to the east and locally overlain by remnants of a post-accretionary late Cretaceous clastic succession, the Sophie Mountain Formation, or by mafic flows of the extension-related Eocene Marron Formation. The characteristics, chemistry, tectonic setting and evolution of the Rossland Group have been described in detail by Höy and Dunne (1997).

The Rossland Group contains a variety of deposits typical of volcanic arcs. These include alkalic porphyry copper-gold deposits, numerous copper, gold and polymetallic veins, and copper and gold skarns. The gold-copper veins of the Rossland camp and silver-lead-zinc veins of the Nelson and Ymir camps have been major past producers of precious and base metals. Red Mountain Mines Ltd. at Rossland had limited production of molybdenite in the early 1960s. Although mineral exploration continues to be active in Rossland Group rocks, there are currently no operating mines.

This report focuses on deposits in the Rossland Group, particularly those that have had recent exploration, and on the metallogeny of the Nelson-Rossland map area. Mineral occurrences in the Nelson-Rossland map sheet are listed in Appendix 1 and plotted on Figure 1-1. Chapter 2 is an overview of the regional geology of the area, in part summarized from Bulletin 102 (Höy and Dunne, 1997). Chapter 3 classifies many of the deposits and occurrences in the Nelson-Rossland map area, provides a brief overview of the characteristics of deposit classes, and presents and describes examples of these classes. Profiles (type descriptions) of deposits are given in Lefebure and Ray (1995) and Lefebure and Höy (1996). The metallogeny of the Rossland gold-copper, silver-lead-zinc and molybdenite camps is the subject of Chapter 4.

PREVIOUS WORK

Previous geological mapping in the Nelson-Rossland map-area has included reconnaissance mapping by the Geological Survey of Canada and the B.C. Ministry of Energy and Mines, as well as a number of university theses studies. These geological studies are described in Höy and Dunne (1997) and summarized in Chapter 2. A regional compilation map of the Nelson-Rossland area has been published by Höy and Dunne (1998) and is reproduced as Figure 1-1. Detailed mapping of many deposits and camps has also been done by exploration and mining companies. Much of this data is available in provincial assessment reports and is used and acknowledged in descriptions of individual deposits and camps in this paper.

The most detailed study of the Rossland copper-gold camp is Memoir 77 by Drysdale (1915). Mapping by Fyles (1970) focused largely on the molybdenite mineralization in the Rossland camp. Thorpe (1967), in a Ph.D. thesis, focused on the mineralogy and depositional temperatures of ores of the camp, and defined a regional zonation within the camp.

This present study includes considerable new mapping of many deposits throughout the Nelson-Rossland map area. Within the Rossland camp, the study has concentrated on morphology, petrology, alteration and geochemistry of intrusive-related gold-copper veins, polymetallic veins, skarn and molybdenite deposits.

A number of the appendices present data or separate papers by other authors. For example, Appendix 5 is a detailed petrographic report by C. Leitch of many vein and skarn samples from the Rossland camp. Appendix 8, by C. Godwin and J. Gabites, presents and interprets new Pb-Pb isotopic data from many deposits throughout the Nelson-Rossland area, and Appendix 9, by K. Dunne, is a fluid inclusion analysis of many mineralized samples from a variety of deposits, including those of the Rossland camp.

ACKNOWLEDGMENTS

We thank our field assistants during the course of regional mapping; they included M. Fournier, M. Holmes, D. Lindsay, C. Lund, H. Blyth, J. Drobe, E. Höy and H. Karem. Discussions with numerous geologists have helped in our understanding of the deposits of the Rossland-Nelson area. Some of these include C. Ash, B. Bourden, L. Dandy, E. Denny, J. Denny, J. Fyles, W. Howard, O. Janout, J. Jenks, D. Lefebure, K. Murray, G. Ray, D. Wehrle and P. Wilton.

U-Pb age dating and related discussions (Appendix 4) are through the efforts of Janet Gabites and Jim Mortensen of The University of British Columbia. We thank M. Fournier and C. McDonell for much of the drafting and R. Lett for expediting samples for chemical analyses. Janet Holland is thanked for final manuscript layout and Geological Survey Branch staff for their work in maintaining BC MINFILE and ARIS. We also thank D. Lefebure, B. Grant and J. Newell for editing fieldwork articles that formed the basis for parts of this bulletin, and C. Ash, D. Brown, B. Grant, W. Howard and A. Panteleyev for discussions and edits of this final manuscript. Finally, I (T. Höy) thank my wife, Lorraine, for years of support, encouragement and patience as I lost myself in grappling with the problems of Kootenay metallogeny.

CHAPTER 2 REGIONAL GEOLOGY

INTRODUCTION

Mineral occurrences in the Nelson-Rossland map area are listed in Appendix 1 and plotted on Figure 1-1. These occurrences include those related to or within the Rossland Group as well as others within North American rocks, post accretionary granitic rocks and onlap assemblages. Profiles (type descriptions) of these are given in Lefebure and Höy (1996) and Lefebure and Ray (1995). This bulletin, a compendium to the regional geology of the Rossland Group in southeastern British Columbia briefly overviews regional geology summarized from Bulletin 102 (Hoy and Dunne 1997, Chapter 2) and describes a number of type examples of mineral deposits in Rossland Group rocks and others in the Nelson-Rossland map area, or deposits that have had recent exploration activity (Chapter 3). Chapter 4 describes and presents models for copper-gold and molybdenum mineralization in the Rossland camp.

REGIONAL GEOLOGY

The Rossland-Nelson map area is within the Omineca belt, a zone of variably deformed and metamorphosed Proterozoic to Tertiary rocks along the boundary between accreted terranes and ancestral North America. The Omineca belt developed in Jurassic through Early Cretaceous time as Quesnellia was thrust over marginal North American and Kootenay terrane rocks and subsequently displaced eastward by folding and thrust faulting (Price, 1981; 1986). This Mesozoic compressional deformation was followed by extensional tectonics in Eocene time (Parrish, 1995). Plutonic rocks within the Omineca belt are common, and represent magmatism associated with both compressional and extensional tectonics.

The tectonic boundary between Quesnellia and North American rocks is commonly marked by mafic volcanic rocks and associated ultramafics of the oceanic Slide Mountain terrane. South of Nelson, this boundary is defined by the Waneta and Tillicum fault systems (Figure 1-1, in pocket; Figure 2-1); the contact is locally obscured or cut by either Middle Jurassic Nelson batholithic rocks or Late Cretaceous intrusions.

ROSSLAND GROUP

The Rossland Group (Figure 2-2) has been described in considerable detail by Höy and Dunne (1997). It includes clastic rocks of the Archibald Formation and correlative Ymir Group, dominantly volcanic rocks of the Elise Formation and dominantly fine-grained clastic rocks of the overlying Hall Formation (Frebold and Little, 1962; Little, 1982b). Its age is Early Jurassic, bracketed by macrofossils in the Archibald and Hall formations and U-Pb dates from tuffaceous units in the Elise Formation (Höy and Dunne, *op. cit.*).

ARCHIBALD FORMATION

The Archibald Formation is named for thick exposures of sedimentary rock along Archibald Creek, southwest of Salmo (Figure 1-1). It correlates with the Ymir Group on the east limb of the Hall Creek syncline and may be correlative with the upper part of the Slocan Group exposed north of Nelson (Little, 1962). Its age is well constrained by numerous fauna of early to late Sinemurian age (Frebold and Little, 1962; Frebold and Tipper, 1970; Höy and Dunne, 1997). The base of the Archibald is only exposed at Patterson where it unconformably overlies fine-grained siliceous rocks, argillite, carbonate and minor greenstone of the Pennsylvanian to Permian Mount Roberts Formation (*see* Figure 4-2, in pocket).

The Archibald Formation comprises a succession of interbedded siltstones, sandstones and argillites with prominent sections of interbedded conglomerate. Its total exposed thickness varies from a few tens of metres of conglomerate near Patterson to more than 2550 metres of finer grained clastic rocks near Gilliam Creek. Its contact with the overlying Elise Formation varies from abrupt to locally gradational.

Facies and thickness changes in the Archibald Formation indicate deposition in a large submarine fan with a source area to the west. Coarse clastic debris flows, and locally fluvial deposition in the Fruitvale area, pass eastward into thick sequences of A-E turbidites near Mount Kelly and finally to deep-water pelagic sediments and more distal turbidites of the Ymir Group in the Nelson area.

Debris flows, associated rapid facies changes and locally subaerial deposition in the Fruitvale area suggest deposition near a faulted basin margin. Farther west near Rossland, the Archibald Formation is missing and the Elise Formation sits unconformably on Mount Roberts Formation. These relationships indicate that the Archibald records deposition on a tectonic high in the Rossland-Patterson area and in a fault-bounded structural basin located to the east. Periodic uplift of the western block triggered debris flows along the eastern faulted margin and provided a source for clasts of Mount Roberts Formation in Archibald fanglomerates and for the distal apron of turbidite deposits to the east.

ELISE FORMATION

INTRODUCTION

The Elise Formation (Little; 1950) comprises up to 5000 metres of dominantly mafic volcanic rocks, including mafic flows, thick sequences of pyroclastic rocks, some epiclastic rocks and locally interlayered fine to medium-grained sedimentary rocks (Figure 2-3). It is exposed in the limbs of the Hall Creek syncline from Nelson to

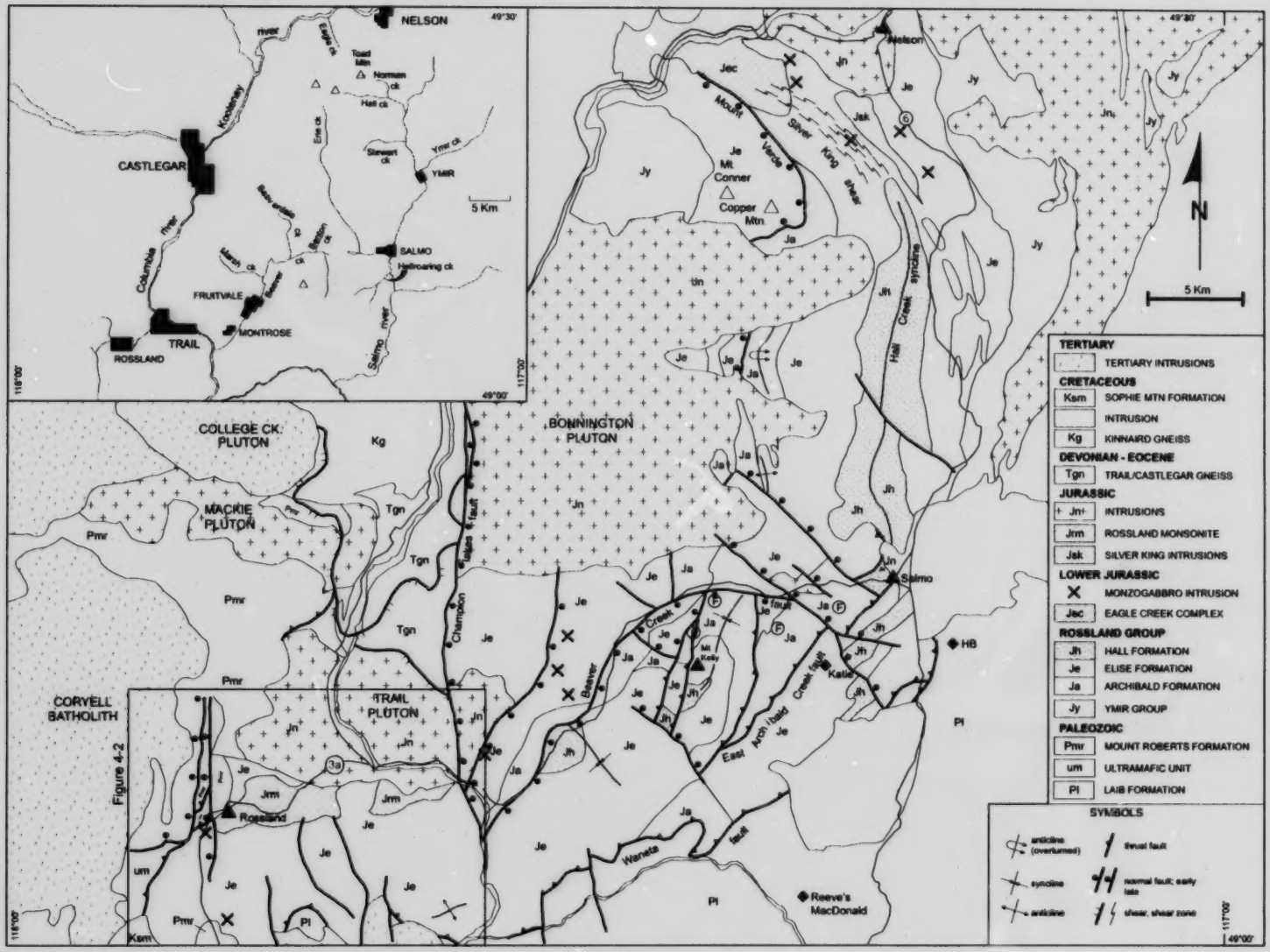

Figure 2-1. Geology map of the Nelson-Rossland map-area, southeastern British Columbia (082F/SW), showing location of deposits described in text; after Höy and Dunne, 1998; Little, 1985 and included references.

AGE			ROSSLAND - TRAIL AREA	NELSON - SALMO AREA	SLOCAN AREA
CRETACEOUS			MT SOPHIE		
JURASSIC		Upper			
		Middle			
	LOWER	Toarcian	HALL	HALL	
		Pliensbachian			
			ELISE	ELISE	
		Sinemurian	ARCHIBALD		
		Hettangian		YMIR	
TRIASSIC					SLOCAN
PERMIAN			MOUNT ROBERTS		KASLO
CARBONIFEROUS					MILFORD
DEVONIAN			TRAIL GNEISS		
SILURIAN			CS		
ORDOVICIAN				Active Nelway Reeves	LARDEAU
CAMBRIAN				LAIB	BADSHOT
PROTEROZOIC				HAMILL	HAMILL
				WINDERMERE	

Figure 2-2. Stratigraphic succession.

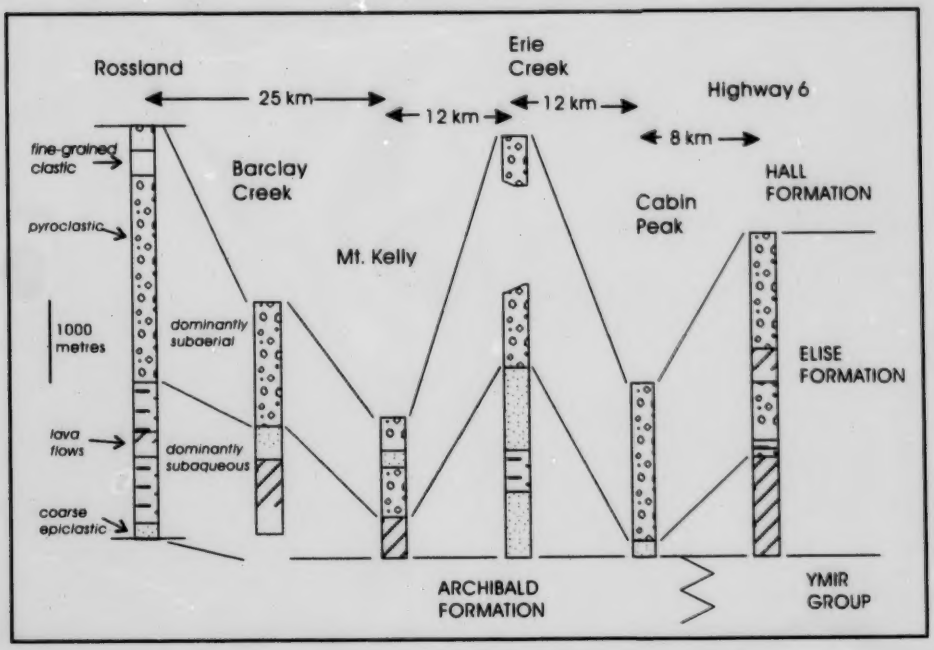

Figure 2-3.Composite stratigraphic sections of the Elise Formation, Nelson-Rossland map area (from Höy and Dunne, 1997).

Salmo, extends west to underlie a large part of the block-faulted area between Salmo and Montrose, and forms an essentially north-dipping homoclinal succession from the Washington border north to Rossland (Figure 4-2, pocket). The formation is also exposed in isolated roof pendants in Nelson-age intrusions northwest of the Nelson-Rossland map-area; for example, the dominant hostrocks of both the Willa Cu-Mo deposit near Silverton (Wong and Spence, 1995) and the Tillicum gold skarn near Burton (Ray and Spence, 1986) are Elise volcanic rocks. Detailed descriptions of the Elise Formation and its geochemistry are given by Höy and Dunne (1997).

The Elise Formation is mainly in sharp to gradational, conformable contact with underlying sedimentary rocks of the Archibald Formation (Höy and Dunne, 1997). However, on the slopes of OK Mountain west of the town of Rossland it rests unconformably on Mount Roberts Formation. In eastern exposures it is overlain conformably by sedimentary rocks of the Hall Formation, whereas in the Rossland area the Hall Formation is missing and conglomerates of the Early Cretaceous Mount Sophie Formation unconformably overlie Elise volcanic rocks (Little, 1982a; Höy and Andrew, 1991b; Figure 4-2).

The age of the Elise Formation is constrained by late Sinemurian fauna in the underlying Archibald Formation and early Toarcian fossils in the Hall Formation. As well, a number of ammonites of Sinemurian age have been discovered in interbedded siltstones and argillites in the lower few hundred metres of the Elise Formation in the Maude Creek area south of Rossland and the Waneta and Fruitvale areas to the east (Little, 1982b). These faunal ages are corroborated by a 197.1±0.5 U-Pb zircon date from an Elise crystal tuff in the Copper Mountain area southwest of Nelson (Höy and Dunne, 1997).

DESCRIPTION

The Elise Formation changes in both character and thickness from the Nelson area in the north to the Rossland area in the southwest (Figure 2-3). In the Nelson area, it includes a prominent basal succession of mafic flows, overlain by dominantly mafic to intermediate pyroclastic rocks. The mafic flows include coarse-grained augite porphyry flow breccias, less commonly, non-brecciated flow units up to a metre thick and, rarely, pillow basalts. Lahars, mafic tuffs and argillite interbeds also occur locally in the basal Elise. The upper Elise in the Nelson area comprises a sequence of mafic to intermediate flows, tuffs and minor epiclastic deposits up to 2500 metres thick. A number of cyclical sequences of pyroclastic rocks that typically grade upward from lapilli tuff to crystal tuff or fine ash tuff are common. Augite porphyry flows and flow breccias are a minor component of the upper Elise.

Tuffaceous siltstones within the upper Elise contain well-defined graded beds, basal scours, crossbeds and channels. A tuffaceous conglomerate near the base of the upper Elise consists of an interbedded sequence of conglomerate, grit, sandstone and siltstone. It forms the basal part of a thick, fining-upward succession that contains a series of fining-upward clastic cycles, generally a few to several tens of metres thick, that are coarser near the base of the succession and finer near the top.

The Elise in the Mount Kelly area is similar, with a lower section of massive augite-phyric flows and an upper section dominated by lapilli tuff, pyroclastic breccia and epiclastic slump deposits.

In the Copper Mountain - Mount Conner area southwest of Nelson, the entire Elise Formation is similar to the upper Elise of the Nelson area, dominated by pyroclastic breccias, homogeneous crystal tuff and, farther east, a heterolithic tuffaceous conglomerate. On the ridge between Copper Mountain and Mount Conner, interpreted to be lower in the Elise section, volcanic breccias and interlayered volcanic sandstones are commonly altered, with pervasive epidotization or preferential epidotization of fragments, and locally development of garnet-diopside-epidote skarn.

The total estimated thickness of the Elise Formation in the Barrett Creek area to the south is 2000 metres. The basal part consists of a succession of interlayered massive to well-bedded water-lain sandy tuffs and coarse mafic volcanic breccias. On the ridge northwest of Cabin peak and on the slopes to the southwest, the Elise includes sections with beds of dominantly planar-bedded to locally massive, fine to coarse-grained, green augite-rich fine tuff, up to a few tens of metre thick, interbedded with lapilli tuff or massive flows. The restricted distribution of fine tuff beds, their bed forms, associated structures and the volcanic facies indicate that they are surge deposits. Interlayered lapilli tuff or pyroclastic breccia contain augite porphyry and less abundant augite-plagioclase clasts in a dark green augite-rich crystal matrix. Massive flows are similar in mineralogy and composition. They are commonly a few metres thick with sharp basal contacts; others appear to have gradational contacts with surge deposits.

The upper part of the Elise Formation, exposed on the ridge east of Cabin Peak and northeast of Midday Peak, comprises thick accumulations of well-bedded, dominantly crystal-rich surge deposits that are interlayered with some augite and augite-plagioclase phyric flows and overlain by mafic lapilli tuff, blocky tephra and massive to flow-brecciated augite-plagioclase flows.

In the Fruitvale area east of Rossland, the Elise Formation is characterized by variable lithologies and rapid facies changes. A lower succession of mafic flows and an upper succession of intermediate to mafic pyroclastic and epiclastic rocks occurs only locally (Andrew *et al.*, 1990a). Lower Elise exposed on Highway 3a just west of Montrose consists of a thick succession of debris flows with a variety of large clasts including debris eroded from the underlying Mount Roberts Formation and possibly the Archibald Formation.

South of Rossland, the Elise Formation comprises dominantly mafic to intermediate lapilli tuffs interlayered with prominent sections of thinner bedded mafic crystal and fine lapilli tuffs. Tuffaceous siltstone and argillaceous siltstone occur locally throughout the succession. Mafic flows are subordinate and tuffaceous conglomerates are es-

sentially restricted to the basal part of the succession. The succession thins to the southwest, towards exposures of underlying Mount Roberts Formation near Patterson, and is underlain to the east by a thick sequence of lapilli tuffs and augite phyric flows that correlate with lower Elise rocks near Mount Kelly.

DEPOSITIONAL MODEL

Schematic sections of the Elise Formation from Nelson to Rossland are illustrated on Figure 2-3. Thicknesses of the Elise vary considerably, from greater than 5000 metres in an incomplete section south of Rossland to approximately 1800 metres in the Mount Kelly area. It is difficult to correlate individual units, suggesting that there are a number of discrete volcanic centers. However, in all areas subaqueous lava flows, debris flows or turbidites are overlain by dominantly subaerial pyroclastic and associated coarse epiclastic deposits.

A model for deposition of the Elise Formation involves initial effusive submarine mafic lava flows that dominate in the Nelson area along the eastern margin of exposed Elise volcanism, and in the Mount Kelly area east of Rossland. The extent of this volcanism south of Rossland is not known. Coarse debris flows with large blocks of augite porphyry, as well as debris from underlying Mount Roberts Formation exposed just west of Montrose, suggest that at least some lower Elise flows were deposited farther west and subsequently slumped eastward into a structural basin.

North of Erie Lake, a thicker section, abrupt facies changes and abundant coarse mafic pyroclastic and epiclastic deposits (Andrew and Höy, 1991) indicate contemporaneous explosive volcanism and slumping, characteristics of deposits on the flanks of a stratovolcano. The abundance of subaqueous epiclastic deposits, including tuffaceous siltstone turbidites and debris flows, as well as the documented submarine volcanism to the north and west, suggest that the early Erie Lake area stratovolcano was dominantly marine. However, it is possible that much of this subaqueous debris originated in the subaerial or possibly shallow marine parts of the volcano (Höy and Dunne, 1997).

Uppermost Elise volcanic rocks throughout the entire area are dominated by mafic to intermediate pyroclastic rocks, coarse debris flows, minor lava flows and, only locally, marine fine turbidites and waterlain sandstone and siltstone. Marked facies changes, both vertical and lateral, major thickness changes, the abundance of subaerial pyroclastic flow deposits associated with surge deposits, coarse debris facies indicative of high relief, air-fall deposits and minor lava flows are typical of deposits associated with stratovolcanoes. These volcanoes are centered in two areas: near Rossland and in the Erie/Stewart creek area. Surge, pyroclastic flow deposits and intrusion of a small mafic plug, the Mammoth intrusion in the Cabin Peak area, indicate a third, smaller volcanic center. Facies and thickness changes near Mount Kelly also suggest deposition on the flanks of a stratovolcano with possible proximal volcaniclastic facies in the north, medial flank facies farther south and distal volcaniclastic facies in an epiclastic apron in the Tillicum Creek area. Considering the proximity, large volume and relief of the volcanic complex in the Erie Lake area to the northeast, it is likely that a considerable portion of Elise deposits northeast of Mount Kelly are derived from this northern source.

The Rossland area has the thickest preserved accumulation of Elise volcanic rocks. Coarse pyroclastic volcanism was typically followed by relative subsidence and quiescence with deposition of subaqueous, but possibly very shallow-water tuffaceous siltstones and sandstones. This implies that relative subsidence in western deposits of the Elise Formation was greater than that farther east, possibly due to the large volume of extruded volcanic material, and was accommodated by reactivation of older growth faults.

Geochemistry

The geochemistry of Elise volcanic rocks is described in detail by Höy and Dunne (1997). Early work by Beddoe-Stephens and Lambert (1981) suggested that the Elise Formation has similarities with shoshonitic or alkalic rocks of young island arcs and that the Rossland Group accumulated in a back-arc sedimentary basin, with a volcanic arc to the west.

Based on major element data, volcanic rocks of the Elise Formation have an alkaline to subalkaline affinity. The basaltic to andesitic nature of these rocks is suggestive of mature island or continental margin arcs. Trace element data support a transitional to shoshonitic affinity and an oceanic island arc setting. However, high concentrations of K, Ba, Rb and Sr, and immobile trace element and REE data, are more comparable with values typical of continental margin arc basalts and andesites. We suggested (Höy and Dunne, 1997) that this may be due, in part, to contamination during ascent through crustal rocks of the North American plate. This implies that Elise Formation volcanics were formed close to the North American continental margin above an extended and thinned continental prism, or possibly above thinned continental crust in an oceanic environment. Supportive isotopic evidence for formation close to the continental margin includes xenocrystic cores in zircons in Elise volcanic tuffs with dates similar to those of North American crustal rocks (Höy and Dunne, 1997).

HALL FORMATION

The Hall Formation, dated by macrofossils as early Toarcian (Tipper, 1984; Little, 1950), includes up to 2100 metres of sedimentary rocks that overlie volcanics of the Elise Formation. Contacts with the Elise range from conformable to locally unconformable with an erosional coarse basal conglomerate. The Hall Formation can be subdivided into three broadly defined members: (1) a lower, rusty-weathering black siltstone and argillite succession, passing upward into (2) a coarse sandstone and conglomerate succession of the middle Hall, overlain locally by (3) dominantly carbonaceous siltstone of the upper Hall (Andrew and Höy, 1991; Höy and Dunne, 1997).

Based on sedimentary rock types and the abundance of marine fossils, the Hall Formation has been interpreted to have been deposited in a littoral to offshore environment

(Little, 1950; Mulligan, 1951). It was deposited on an irregular paleosurface, after a hiatus of several million years following volcanism of the Elise Formation. The few reliable fossils in the Hall indicate an early Toarcian age (Freebold and Little, 1962; Tipper, 1984), whereas underlying Elise rocks are Sinemurian in age (Little, 1982b; Höy and Dunne, 1997). There is no evidence of Pliensbachian deposition of either Elise Formation or Hall Formation. Supportive evidence for a hiatus between Elise and Hall deposition is the local occurrence of a prominent basal conglomerate in the Hall that contains large and abundant clasts of Elise Formation rocks.

The Hall Formation is interpreted to have been deposited in a marine structural basin on an irregular paleosurface developed after arc volcanism of the Elise Formation. Early Hall sediments may be shallow water lagoonal, followed by coarse clastic deposits derived from fault-bounded marginal highlands to the west and northeast.

PLUTONIC ROCKS

Plutonic rocks are extensive throughout the Nelson-Rossland area. They include mafic sills and stocks interpreted to be Early Jurassic in age and related to Elise arc magmatism, numerous Middle Jurassic batholiths and stocks, including the Silver King plutonic suite and the Nelson batholith, and a number of Late Cretaceous stocks that cut Mesozoic fabrics in the eastern part of the area. Cenozoic plutonic rocks are more abundant in western exposures and many are related to Eocene extension.

A variety of mineral deposits are spatially associated with these intrusive rocks. Deposit types include copper-gold porphyry mineralization within small Early Jurassic stocks and dikes, copper-gold vein mineralization along the margins of the Rossland monzonite, many occurrences of gold and copper skarns, porphyries associated with Nelson age intrusions, lead-zinc-silver veins of the Ymir camp along the margin of the Nelson batholith, and tungsten and gold skarns related to the Late Cretaceous intrusions. Mineralization that can be clearly related to Cenozoic plutonism is more difficult to document, although the unusual Velvet deposit may have formed during intrusion of the Eocene Coryell batholith.

The following descriptions of plutonic rocks in the Rossland-Nelson area are summarized largely from Dunne and Höy (1992).

EARLY JURASSIC PLUTONS

A number of mafic, high-K alkalic plutonic complexes within the Rossland Group are interpreted to be subvolcanic intrusions, comagmatic with the Elise Formation. These include the Katie and Shaft plutons as well as a number of other small mafic plugs and sills scattered throughout the Rossland-Nelson area. The Rossland monzonite, initially interpreted as an Early Jurassic pluton (Dunne and Höy, 1992; Höy and Dunne, 1997), has a Middle Jurassic (*ca.* 167 Ma) age (*see* Chapter 4).

EAGLE CREEK PLUTONIC COMPLEX

The Eagle Creek plutonic complex west of Nelson, referred to as 'pseudodiorite' (Mulligan, 1952), is generally a medium to coarse-grained mafic intrusion, in part gneissic (Mulligan, 1951; 1952; Little, 1982a,b; Lindsay, 1991). On the basis of extensive petrography and rock geochemistry at the Moochie occurrence, Lindsay (1991) described it as a metadiorite. It ranges in composition from a quartz monzonite to a hornblende syenite, with diorite and gabbro the most common phases. It locally includes coarse ultramafic phases, and clinopyroxenite occurs along the margins of the complex.

A number of gold-copper showings have been explored within or along the margins of the Eagle Creek plutonic complex. These include vein, skarn and possibly porphyry mineralization (*e.g.*, Star and Alma N, Chapter 3).

MONZOGABBRO INTRUSIONS

A number of monzogabbro/gabbro sills or small stocks occur throughout the exposures of the Elise Formation (Höy and Dunne, 1997). They are typically tabular, lensoid or sill-like, several tens of metres thick and can often be traced for several kilometres. Others are subrounded, discordant plutons. They are fine to medium grained and commonly porphyritic with 30 to 40 percent plagioclase phenocrysts in dark green-grey matrix. They are petrographically distinct from the Eagle Creek plutonic complex, Rossland monzonite or Silver King intrusions. Monzogabbro stocks can occur anywhere within the Elise Formation but tend to be mainly in the upper part. Examples in the Rossland- Nelson map-area include the Shaft, Mammoth and Katie intrusions. Mineralization associated with these intrusions is described in Chapter 3.

These small widely scattered monzogabbros are interpreted to be high-level synvolcanic intrusions. They are restricted to the Elise Formation, have diffuse, commonly brecciated margins, have a volcanic arc geochemical signature (Höy and Dunne, 1997) and are locally associated with copper-gold-magnetite mineralization (*e.g.*, Katie and Shaft prospects).

EARLY-MIDDLE JURASSIC PLUTONS

A number of generally highly deformed feldspar porphyries, referred to as the Silver King intrusions (Dunne and Höy, 1992), occur within the Elise Formation south of Nelson. They have been dated as Aalenian (*ca.* 174-178 Ma) and are interpreted to be syntectonic granitoids. Locally, as in the Silver King deposit area, copper, lead, zinc, gold and silver mineralization is spatially associated with these intrusions. However, the relationship between mineralization and these intrusions is unclear (*see* Chapter 3).

Silver King plutonic rocks are typically porphyritic, characterized by euhedral to subhedral plagioclase (An28-60) phenocrysts in a fine-grained greenish grey groundmass. As the porphyry has few preserved mafic minerals and plagioclase is generally An <50, it is classified as a leucodiorite porphyry. Based on major element chemistry, analyzed Silver King intrusive samples are dominantly

quartz monzodiorites and granodiorites. This nomenclature contrasts with the leuco-diorite classification based on petrography, probably due to the lack of complete identification of fine-grained matrix minerals as well as locally intense alteration.

MIDDLE JURASSIC PLUTONS

Many Middle Jurassic plutons occur throughout the Nelson-Rossland area. Typically, they are complex, with early alkaline magmatism followed by calcalkaline and finally, formation of two mica granite. They include the Kuskanax, Nelson, Bonnington and Trail batholiths (Figures 1-1; 2-1), as well as numerous smaller stocks. Based on U-Pb analyses of zircons, the ages of these granitic plutons range from *ca.* 173 Ma to 160 Ma (Ghosh, 1995a,b; Parrish and Wheeler, 1983). Most phases of the Nelson batholith are dated *ca.* 167 Ma (*see* summary in Ghosh, *op. cit.*) with a young, coarse megacrystic phase dated at 161±1 Ma (Ghosh, *op.cit.*) and an equigranular biotite granite dated at 158.9±1 Ma (Sevigny and Parrish, 1993). The Bonnington pluton has a number of 167 Ma dates (Parrish and Wheeler, *op. cit.*; Ghosh, *op. cit.*) and the Trail pluton is dated at 169 ± 3 Ma (Carr *et al.*, 1987). The Rossland monzonite, host for many of the veins of the Rossland camp, is also dated at *ca.* 167 Ma (*see* Chapter 4).

These Middle Jurassic intrusions are continental arc granitoids that have undergone considerable crustal contamination (Ghosh, 1995a). They record continued subduction of an ancestral Cache Creek ocean with obduction and onlap of the eastern edge of Quesnellia with the North American craton.

Many Middle Jurassic plutons have a variety of mineralized veins or skarns along their margins; the Rossland gold-copper and molybdenite deposits (Chapter 4) occur within and adjacent to the Rossland monzonite. The Slocan, Ainsworth, Ymir (Chapter 3) and Nelson mining camps all occur along the borders of the Nelson batholith, inferring a genetic link. Alternatively, Beaudoin *et al.* (1992a,b) have argued that the Slocan camp is related to Eocene extensional tectonics.

CRETACEOUS PLUTONS

Early and Late Cretaceous granitic rocks postdate Jurassic regional metamorphism and deformation. However, some are intensely foliated and sheared by Eocene extensional faults. In the Rossland area, these plutonic rocks include Castlegar orthogneisses (*ca.* 100-110 Ma) and pegmatites dated at *ca.* 70-80 Ma (Parrish, 1992). Cretaceous plutons, such as the Wallack Creek and Hidden Creek stocks near Salmo, are typically highly evolved S-type leucogranites and granodiorites. Many are associated with tungsten and minor copper and zinc mineralization; the Invincible, Dodger, Emerald and Feeney mines near Salmo are in skarn deposits along the contact of a small Cretaceous stock with Lower Cambrian Badshot Formation limestone.

CENOZOIC PLUTONS

Cenozoic plutonic rocks are common north and west of Rossland. Their relationships to the complex Tertiary history of south central British Columbia has been investigated by Parrish *et al.*, 1988; Carr, 1991, and references therein). They are mainly late Paleocene to early Eocene in age, and range in composition from I-type quartz monzonites of the Ladybird suite to alkaline Coryell intrusions. Paleocene intrusions may be related to a final phase of compressional tectonism in the eastern Cordillera whereas Eocene magmatism, including both plutonic rocks and alkalic volcanics (Marron Formation), record regional extension associated with normal faulting.

STRUCTURE AND TECTONICS

A tectonic model for deposition of the Rossland Group in southeastern British Columbia and subsequent tectonic history has been presented in Höy and Dunne (1997) and is reviewed only briefly here. The Rossland Group, built on deformed and possibly imbricated Permian arc-derived clastic rocks, ophiolitic assemblages and associated sediments, and thin? continental crustal rocks, is the youngest and most eastern of the volcanic arc units of Quesnellia. It is interpreted to have been deposited along the western margin of North America, thrust eastward in late Early Jurassic through Middle Jurassic time, and carried eastward with telescoping of the miogeoclinal prism through Paleocene time.

EARLY JURASSIC

Early Jurassic tectonism associated with volcanic arc development in the Rossland Group involved local extension with uplift and erosion in the west and deposition of coarse clastics of the Archibald Formation in a deepening structural basin to the east. There are no recognized ultramafic clasts that would confirm imbrication and uplift of Slide Mountain lithologies prior to deposition of arc volcanics, as is demonstrated in the Greenwood area (Fyles, 1995). Farther east within the Archibald basin, lithologies become finer grained, dominated by turbidite deposition, and in western exposures of the correlative upper part of the Ymir Group, by argillaceous sediments and carbonate muds.

Arc volcanism began in Sinemurian time with deposition of submarine shoshonitic flows above exposures of the Ymir Group and eastern exposures of the Archibald Formation. There are also mafic tuffs above shallower water to locally subaerial exposures of the Archibald in the Fruitvale area east of Rossland. Late Elise time is marked by dominantly mafic pyroclastic volcanism in stratovolcanoes. A number of small comagmatic mafic intrusions, including those at the Katie and Shaft deposits, occur throughout the Elise Formation and are commonly associated with elevated copper and gold values.

The unconformably overlying Hall Formation records essentially post-arc deposition in a marine structural basin.

A suite of plagioclase porphyry intrusions, the Silver King suite, of early Middle Jurassic age, are interpreted to be syntectonic plutons (Dunne and Höy, 1992) that may record the first onlap of the eastern margin of Quesnellia with the edge of cratonic North America.

MIDDLE JURASSIC

Middle Jurassic deformation records continued compression as the eastern edge of Quesnellia was thrust over North American miogeoclinal rocks. The age of this deformation and associated regional metamorphism is constrained by plutonic rocks. The *ca.* 174-178 Ma Silver King intrusion is deformed, but to the west folds in the Elise Formation are truncated by the *ca.* 167 Ma Nelson batholith. These folds are also cut by the Mount Verde fault, a listric normal fault that is also older than the Nelson batholith.

Middle Jurassic deformation in the Rossland-Nelson map area is dominated by east-verging folds and thrust faults. Folds are broad to locally tight, generally south-plunging, with a prominent axial planar foliation and locally pronounced fold axes mineral lineations. In general, the intensity of deformation and grade of regional metamorphism within Rossland Group rocks increases to the south and east, towards the tectonic boundary with North American rocks.

South of Nelson, the Rossland Group has been folded into broad north-trending and east-verging folds. The Hall Creek syncline, cored by the Hall Formation, is the most prominent fold in the map-area. It is a tight, south-plunging, west-dipping overturned fold that extends from west of Nelson to southwest of Ymir, and continues southwest of Salmo as the Hellroaring Creek syncline. A pronounced cleavage in clastic rocks of the Hall Formation and a penetrative foliation in the Elise Formation parallel the axial plane of the syncline. Northwest of the closure of the Hall Formation, at deeper structural levels, the core of the syncline forms a zone of intense shearing more than a kilometre in width. This shear zone, referred to as the Silver King shear, continues northwestward into the Elise Formation and intrusive rocks of the Eagle Creek plutonic complex, and appears to die out at higher structural levels along the limbs of the Hall Creek syncline. This zone of shearing is the loci of sulphide deposits, such as Silver King, southwest of Nelson.

A large upright to overturned, south-plunging fold, the Mount Kelly syncline, is exposed in the Mount Kelly area west of the Hellroaring Creek syncline (Fitzpatrick, 1985; Höy and Andrew, 1990b). Archibald Formation rocks in its hinge zone are gently to tightly folded and locally thickened. More competent Elise Formation rocks are concentrically folded and Hall Formation in the core is strongly cleaved. Overturned thrust faults east of the Mount Kelly syncline displace the syncline eastward, over the west limb of the Hellroaring Creek syncline. These thrusts dip steeply to the east, probably due to regional tilting related to Eocene extension (Wingate, 1993), resulting in apparent normal movements.

A number of north to northeast-trending, west-dipping normal faults occur northwest of Mount Kelly (Figure 1-1). They cut the early folds and faults but are cut and sealed by Middle Jurassic intrusions. They may be southern extensions of the Mount Verde fault west of Nelson, a large normal fault that records post Early Jurassic, probable Bajocian, extension, as these faults are cut by *ca.* 165 Ma plutons.

Farther west in the Rossland area, an essentially homoclinal succession of Rossland Group rocks extends northward from the United States border to the town of Rossland (Figures 4-1, 4-2). This succession is in the footwall of an east-verging thrust, exposed just west of Rossland, that contains remnants of ultramafic rocks with ophiolitic affinities. Other parallel faults in the immediate area have both reverse and normal movements, the latter probably reflecting Eocene reactivation of Jurassic thrust faults. Gold-quartz veins, such as the I.X.L. and Midnight, appear to be associated with the ultramafic rocks and thrust faults (*see* Chapter 4).

TERTIARY

Extensional faulting, uplift and tilting of structural blocks (Wingate, 1993) was synchronous with volcanism of the Marron Formation west of Rossland and intrusion of syenitic and granitic plutonic rocks such as in the western part of the Nelson-Rossland map area during Eocene time (Parrish *et al.*, 1988). Displacement on these faults changed markedly along strike, from tens of kilometres on the Slocan fault north of Castlegar to zero displacement at its southern extension, the south end of the Champion Lake fault east of Rossland (Figures 1-1, 2-1).

CHAPTER 3 MINERAL DEPOSITS

INTRODUCTION

The Nelson-Rossland map area (082F/SW) contains a wide variety of mineral deposits and numerous past producers. Many of the historical mining camps in southern British Columbia are located in this area, and their discovery led directly to the settlement and development of the interior of the province. The names, Rossland, Trail, Salmo, Ymir and Nelson are forever tied to the early mining history of British Columbia, and these towns are still the centre of active and continued mineral exploration.

This chapter concentrates on deposits in the Rossland Group, but also reviews briefly other deposit types within the map area. The deposits are classified using the nomenclature of the British Columbia mineral deposit profiles (Lefebure and Ray, 1995; Lefebure and Höy, 1996). Deposits in the historical Rossland gold-copper camp are described in Chapter 4.

The Nelson-Rossland map area straddles the tectonic boundary between rocks of North America and the eastern edge of arc terranes. This area has a complex tectonic and magmatic history that is reflected in both the diversity and numbers of mineral deposits and occurrences. The eastern part of the map area is within the Kootenay arc, a north-trending arcuate structural zone in the eastern part of the Omineca belt that is characterized by intense polyphase deformation and locally high-grade regional metamorphism. The arc developed mainly in Late Proterozoic and Paleozoic rocks of the Kootenay terrane and in miogeoclinal North American rocks. It contains a number of lead-zinc carbonate-hosted deposits, most of which are concentrated in the southern part of the arc southeast and south of Salmo (Figure 1-1). The Sheep Creek gold camp, within mainly EoCambrian quartzites of the Hamill Group, has produced more than 23 035 kg of gold from gold-quartz veins.

Mesozoic volcanic arc rocks of Quesnellia, west of the Kootenay arc, contain important silver-lead-zinc mineral camps, such as the Ymir camp within mainly metasedimentary rocks, and gold-copper ± molybdenum deposits in mafic volcanic rocks and metasediments of the Rossland Group. These deposits are the focus of this study and are described in detail below.

Plutonic rocks of mainly Middle Jurassic or Early to Middle Cretaceous age are abundant within this part of the Omineca belt. They record post-accretionary magmatism and hence have geochemical and petrological signatures that reflect continental crustal contributions. Deposits within and along the margins of these plutonic rocks include a variety of porphyry types, copper-gold, tungsten and molybdenum skarns, and numerous precious metal and polymetallic veins.

The concentration of metallic mineral deposits in the southern part of the Omineca belt coincides with a marked change in the structural grain from easterly, south of Salmo, to more northerly farther north. This prominent deflection follows the loci of earlier structures that developed along or parallel to changes in the inferred western cratonic margin of North America, or to underlying basement anisotropies. In Middle Cambrian time, the southwesterly deflection parallels a change from platformal rocks of the Nelway Formation in the south to deeper water facies of the Lardeau Group to the north (Höy, 1982a,b). In Late Proterozoic time, fluvial quartzites of the Hamill Group and Quartzite Range and Reno formations were shed northward in alluvial fans (Devlin and Bond, 1987), inferring a tectonic high south of the Nelson-Rossland map area. Farther east in the Purcell anticlinorium, Windermere-age block faulting (Lis and Price, 1976) and fundamental changes in the character and thickness of Middle Proterozoic Purcell Supergroup rocks (Höy, 1993; 2000) are evidence of northeast-trending structures that parallel the southwest deflection of the southern Kootenay arc (Höy, 1982a,b). The coincidence of basement and early tectonic features with post-accretionary structures implies that tectonic transport during Laramide contractual deformation may have been parallel to these early structures.

It is suggested that the distribution of many deposits in southeastern British Columbia is controlled, at least in part, by these deep crustal structures. These structures influenced the orientation of extensional faults in Middle and Late Proterozoic time, and the eventual rifted continental margin in Eocambrian time. They appear to have controlled the distribution of granitic magmas, outflow of hydrothermal fluids, and a variety of mineral deposits.

CARBONATE-HOSTED DEPOSITS

Carbonate-hosted deposits in the Nelson-Rossland map area (Appendix 1), commonly referred to as 'Kootenay arc lead-zinc deposits', are essentially restricted to the Early Cambrian Badshot Formation, referred to as the Reeves member of the Laib Group in the Salmo area. The larger deposits ranged in size from 6 to 10 million tonnes and contained 1-2% lead, 3-4% zinc and trace silver. The Reeves MacDonald mine produced, until its closure in 1977, 5.8 million tonnes of ore containing 0.98% lead, 3.5% zinc and 3.4 g/t silver. None of these deposits are presently in production, but considerable recent work has focused on the Red Bird deposit, a southern oxidized extension of the Reeves MacDonald, and on gold-bismuth zones at the Jersey deposit.

'Kootenay arc' deposits generally consist of lenses, irregular bands, disseminated grains or massive zones of pyrite, sphalerite and galena in dolomite or chert zones within highly deformed limestone (Fyles and Hewlett, 1959; Fyles,

1970). They are irregular in outline and commonly elongate parallel to the structural grain. Contacts with country rocks may be sharp or gradational.

Deposits of the Salmo camp are within fine-grained dolomite of the Reeves limestone. The dolomite is texturally different from more typical barren, well-banded limestone. The dolomite is poorly banded, flecked with black, irregularly streaked or crackled. Breccia zones with dolomite fragments surrounded by sulphides are present in many of the deposits (Photo 3-1a). Sulphides are typically folded along with their country rocks (Photo 3-1b). Massive dolomite typically contains only sparse mineralization.

The origin of these deposits is enigmatic. Fyles and Hewlett (1959) described the deposits as replacements controlled by the dominant phase 2 folds, and locally by faults. They described the close spatial association of mineralization to structures and the brecciated nature of some of the ore. Sangster (1970) and Addie (1970), emphasizing their stratabound nature and laminated sulphides, described the deposits as syngenetic with sulphides accumulating in small basins in a deep-water platformal succession. Höy (1982a) suggested that 'Kootenay arc' lead-zinc deposits have a diagenetic-syngenetic origin, with some sulphides accumulating in shallow water carbonate facies but others in collapsed breccia zones in lithified Badshot carbonate, a model which is similar to that ascribed to massive sulphide deposits in the MacMillan Pass area in Yukon Territories (Turner and Rhodes, 1990) and to some Irish-type Zn-Pb deposits (Hitzman, 1995).

However, Pb-Pb isotopic analyses of galenas from a number of the Kootenay arc lead-zinc deposits in the Salmo area suggest that these deposits have a replacement origin. The data plot as a well-defined, linear trend that closely follows an Upper Crustal model growth curve from middle Paleozoic through to Jurassic (Appendix 8). Pb-Pb data are "markedly radiogenic", as is common to many carbonate-replacement deposits (Godwin *et al.*, 1982), making interpretation difficult. Godwin and Gabites (in Appendix 8) suggest that the data may indicate a mixing trend from a Cretaceous point on the North American shale model curve to the Jurassic-Cretaceous on the Upper Crustal curve, with the data compatible with a Jurassic age. As these deposits are intensely folded during Middle Jurassic deformation, their age, based on this tenuous Pb isotopic data and their deformational history would be restricted to Early Jurassic, supportive of the model presented by Fyles and Hewlett (1959).

In summary, the intense deformation characteristic of Kootenay arc deposits has modified most of the original features of these deposits making any models of their origin tenuous. In this paper they are classified as carbonate-hosted deposits, a general term that can be applied to a variety of lead-zinc deposits, including Irish types, mantos or Mississippi-Valley types.

VOLCANOGENIC MASSIVE SULPHIDE DEPOSITS

A few mineral occurrences in the Nelson-Rossland map area are tentatively classified as volcanogenic massive sulphide deposits (Appendix 1). They are in mixed sediment-volcanic successions in the basal part of the Elise Formation or the upper part of the underlying Ymir Group or Archibald Formation. The Silver 1 deposit, within the Elise, is located on the east side of Cottonwood Creek, 5 kilometres southeast of Nelson (Figure 1-1, 2-1); the Hungary Man, 16 kilometres southwest of Nelson, is in rocks that have been tentatively assigned to the Ymir Group. A new discovery, Silver Lynx, in Ymir Group rocks approximately 10 kilometres west of Nelson may also be a polymetallic massive sulphide deposit.

The Silver 1 and Silver Hawk occurrences, and other showings in the immediate area, consist of galena, sphalerite, pyrite and minor chalcopyrite zones that parallel the prominent north-trending schistosity, and probable primary layering, in Elise Formation chloritic and biotitic schists. The mineralized zone has been exposed for a strike length of about 65 metres with a width of 1 to 3 metres. Assays are variable; values of 0.5 to 5.65% lead, 4 to 13.45% zinc and 13 to 497 g/t silver have been reported. A grab sample across 3 metres, from a trench 9 metres south of the main

Photo 3-1a. Brecciated sulphides (mainly pyrite) in Lower Cambrian Reeves limestone, Reeves MacDonald deposit.

Photo 3-1b. Folded sulphides (mainly pyrite) in Reeves limestone, Reeves MacDonald deposit.

shaft, assayed 58 g/t silver, 1.85% lead and 7.36% zinc (Taylor, 1978).

Mineralization at the Hungary Man was discovered in 1900, and two shafts and a crosscut were subsequently developed. The showing consists of massive to semi-massive sulphides in a schistose volcanic-sedimentary sequence, mapped as part of the Ymir Group (Figure 2-2), but possibly within the basal part of the Elise Formation. Sulphide lenses up to 7 metres in thickness and 30 metres in length are within a mineralized north-south trending zone, up to 300 metres in length, that parallels the structural grain and inferred layering. Sulphides include pyrrhotite, pyrite and minor chalcopyrite in quartz gangue. Mineralization appears to be concentrated along a volcanic-diorite contact in mineralized shear and breccia zones. Hence, although classified as volcanogenic massive sulphide Besshi-type in BC MINFILE (and Appendix 1), it is possible that it is an 'intrusion-related gold-sulphide vein'.

Similar style mineralization occurs on the adjacent Connor and Anne-Marie claims. A channel sample from an exposure along Connor Creek assayed 4.42 g/t gold and 2.4 g/t silver over 1 metre (Akhurst, 1989).

The Silver Lynx property was discovered in September, 2000, by Bruce Doyle and subsequently optioned to Cassidy Gold Corp. Work to date, and proposed in the summer of 2001, includes a geochemical survey, geological mapping, prospecting, sampling and a geophysical survey. The geochemical survey has outlined a lead-zinc-silver anomaly greater than 800 metres in length and up to 300 metres in width. Mineralization is reported to be "near the contact between felsic volcanic rocks and black argillaceous sediments"; a selected grab sample from a roadcut of semi-massive sphalerite, galena, chalcopyrite and pyrrhotite assayed 24.59 % Zn, 22.35 % Pb, 0.21 % Cu and 556.4 g/t silver (Cassidy Cold Corp., report).

The possible recognition of volcanogenic massive sulphide deposits in the Rossland Group has some important exploration implications. These occurrences are in eastern, more basal exposures of the Elise Formation, in subaqueous mixed volcanic-sedimentary successions. The potential for classical volcanogenic massive sulphides may be considerably less in more western exposures of the Elise Formation, as large parts of these exposures are subaereal or shallow water, on the flanks of stratovolcanoes (Höy and Dunne, 1997). However, the potential for precious-metal rich Eskay-type deposits (Alldrick, 1995) in the Rossland Group must be considered, particularly if felsic components of the Elise Formation are recognized. These deposits are within shallow-water, volcanic arc successions commonly associated with felsic volcanics in bimodal suites.

Felsic volcanic centres within the Elise have not been well documented, although foliated rocks of rhyolitic and dacitic composition are known. Some of these rhyolites are flow-banded Tertiary-age dikes such as occur throughout the Rossland camp area, in the Champion Lakes area, and on the Gus-Swift claims southeast of Salmo. Other occurrences are highly sheared sericite schists that are similar in appearance to sheared felsic volcanic rocks. A sericite schist at the Great Western property, p. 84) between 185.3±3 and 165.5±4 Ma in age, (Höy and Dunne, 1997) is a sheared intrusive rock at least 10 million years younger than the Elise Formation. However, there are some reported felsic volcanic rocks in the Elise, such as at the Silver King deposit, which may be evidence of local bimodal volcanism, and hence may enhance considerably the potential for additional discoveries of volcanogenic massive sulphide deposits.

PORPHYRY COPPER-GOLD: ALKALIC

INTRODUCTION

Porphyry copper-gold deposits related to alkalic rocks in the Canadian Cordillera occur within the pre-accretionary Triassic-Jurassic arc terranes (McMillan and Panteleyev, 1995; Lang *et al.*, 1995a, b; McMillan *et al.*, 1995). Some of these deposits in British Columbia include Galore Creek, Mount Polley, Afton and Copper Mountain.

General characteristics and settings of these porphyries are well described by McMillan *et al.* (*op. cit.*) and Lang *et al.* (*op. cit.*) and summarized by Panteleyev (1995). Alkalic porphyry copper-gold deposits have been further subdivided into those in silica-undersaturated or silica-saturated systems (Lang *et al.*, 1992a, b). Silica-undersaturated systems are more strongly alkalic, dominated by syenite porphyries and containing high concentrations of magnetite. Diorites, monzodiorites and monzonites are the most common igneous phases in silica-saturated systems. Molybdenum content is generally low in both, and copper/gold ratios are similar.

Alteration assemblages in alkalic systems are typically zoned vertically and laterally (Lang *et al.*, 1995). Albitic alteration is commonly associated with mineralization in silica-saturated systems; potassium-calc-silicate in silica undersaturated. Sulphide-rich propylitic assemblages may surround these assemblages. In contrast with calc-alkalic deposits, sericitic, argillic and aluminosilicate alteration assemblages are generally absent or of minor importance in alkalic systems.

Within the Nelson-Rossland map area, porphyry copper-gold deposits include Katie, Shaft and possibly occurrences adjacent to the Eagle Creek plutonic complex, all associated with mafic stocks within Early Jurassic Elise volcanic rocks. The Gold Mountain zone of Kena may be a gold porphyry, related to the more felsic Silver King pluton. Associated plutonic rocks are dominantly alkalic, ranging from dominantly silica-undersaturated (Eagle Creek complex) to silica-saturated. They are typical of alkalic porphyry gold-copper class of deposits, with magnetite mineralization associated with potassic feldspar alteration and widespread regional propylitic alteration.

KATIE (082F/SW290)

Names: Katie, Jim
Location: Lat. 49°08'53" N; Long. 117°20'09" W
Elev. 1420 metres

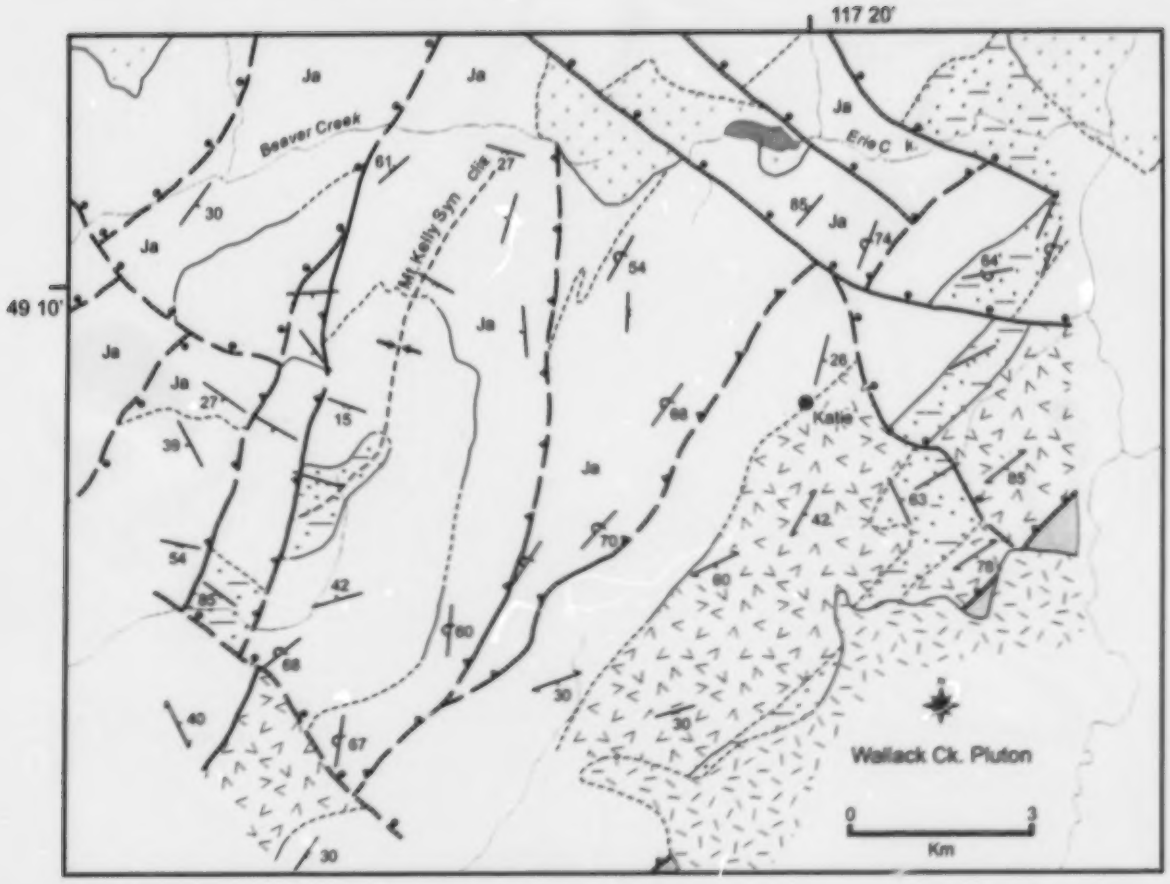

LEGEND

Cretaceous

Wallack Creek pluton

Jurassic

Nelson intrusion

Early Jurassic

Rossland Group

Jh - Hall formation: argillite, siltstone

Je - Elise formation

Je8 - Intermediate to mafic tuff

Je1,4 - Mafic flows, tuff

Archibald Formation

Ja Siltstone, conglomerate, argillite

Paleozoic

Laib formation (?)

Geological contact (defined : assumed)

Fault (defined : assumed)

River, creek

Fault - thrust

Fault - normal

Syncline

Mineral Showing

Layering (tops unknown)

Layering

Foliation

Overturned layering

Figure 3-1. Location and regional geology of the Katie property (after Höy and Andrew, 1990a).

INTRODUCTION

The Katie deposit is located 7 kilometres southwest of the town of Salmo (Figure 2-1). Access to the property is via the Hellroaring Creek logging road which leaves Highway 3, 2 kilometres south of Salmo. Topography on the property ranges from gentle to moderately steep slopes at elevations from 1250 to 1700 metres; outcrop is generally sparse. The following report is summarized from Cathro *et al.* (1993).

Katie is a porphyry gold-copper deposit in dominantly mafic and shoshonitic volcanic rocks of the Elise Formation that are intruded by subvolcanic mafic dikes and sills. Mineralization comprises disseminated and stockwork pyrite, chalcopyrite and magnetite, and late, sheared gold and silver-bearing veins.

Anomalous copper values were first indicated in Hellroaring Creek stream sediments by the 1977 National Geochemical Reconnaissance Survey (GSC Open file 514). A geochemical survey by Amoco Canada Petroleum Company Limited in 1980 identified anomalous copper values in soils (MacIsaac, 1980). Most work in the 1980s focused on adjacent shear-hosted gold-silver targets on the Gus, Swift, Elise and Lisa claims (Andrew and Höy, 1990).

The Katie claims were staked by Ken Murray in 1985 and subsequent soil geochemistry outlined a coincident gold-copper anomaly (Murray, 1987). Balloil Lassiter Petroleum Limited optioned the property in 1988 and completed geological and geophysical surveys and drilled four holes totaling 305 metres. The best intersection assayed 0.24% copper and 0.20 g/t gold (McIntyre and Bradish, 1990).

Yellowjack Resources Limited acquired the property in 1990 and formed a joint venture with Hemlo Gold Mines and Brenda Mines Ltd. to explore the property. Noranda Exploration Company, the operator, conducted geological mapping, geochemical and geophysical surveys, and drilled 34 holes totaling 8260 metres (McIntyre and Bradish, 1990; McIntyre, 1991; Kemp, 1992). In 1992, Yellowjack took over as operator and drilled an additional 18 holes totaling 4477 metres.

REGIONAL GEOLOGY

The Katie property is underlain by mainly mafic to intermediate volcanic rocks of the Elise Formation in the northwestern limb of the Hellroaring Creek syncline (Figure 3-1). Drill information indicates that numerous subvolcanic sills, the 'Katie intrusions', cut these volcanic rocks. They are spatially associated with both alteration and mineralization.

Tight folds and, locally, shearing and a penetrative foliation deform Elise rocks in the area. Shear zones are more intense south of the Katie prospect, closer to the core of the Hellroaring Creek syncline, and are associated with intense carbonate-sericite-silica alteration (Andrew and Höy, 1990). This shearing appears to predate both Cretaceous (Wallack Creek) and Middle Jurassic (Nelson-age) intrusions. Late northwest-trending normal faults, possibly related to Eocene extension, offset earlier structures and the Cretaceous intrusions.

The Wallack Creek stock is a leucocratic, equigranular intrusion ranging in composition from granodiorite to granite. Although it truncates shearing in the limbs of the Hall Creek syncline, its margin is locally sheared and foliated. Limited trace and major element analyses of the stock indicate that it is metaluminous to slightly peraluminous with a CIPW normative composition of quartz, orthoclase and albite (Einersen, 1994).

PROPERTY GEOLOGY

The Elise Formation, the dominant host for Katie mineralization, is made up of mainly augite and plagioclase phyric mafic volcanic rocks that have been assigned to the Lower Elise. These include monolithic pyroclastic breccias and lapilli, crystal and fine tuff. They are medium to dark green in colour, and massive to vaguely laminated. Pyroxene phenocrysts are completely altered to actinolite, chlorite, epidote and biotite, and plagioclase is variably sausseritized or sericitized.

The Hall Formation is exposed on the east side of the property and has been intersected in a fault block in one drill hole (DDH 25) northeast of the Main zone.

Intrusive rocks range in composition from gabbro to monzonite and are composed of nearly equal proportions of feldspar and dark green mafic minerals, mainly hornblende and lesser pyroxene. In drill core, intrusive lithologies alternate with volcanic rocks suggesting that they probably occur as thick sills or dikes (Cathro *et al.*, 1993). In thin sections, intrusive rocks are generally equigranular, although porphyritic phases are recognized. Mafic phases comprise up to 40% plagioclase (An_{50-65}), 15% orthoclase, altered pyroxene and hornblende, and trace apatite and magnetite. More intermediate phases are dominated by plagioclase (An_{10-45}) with up to 30% orthoclase and perthite; these K-feldspars are interpreted to be largely due to potassic alteration. Sphene is commonly present but apatite is notably absent.

The original composition of the Katie intrusions is difficult to determine due to the pervasive potassium alteration. The lack of sharp contacts and chilled margins, and the similar overall petrographic composition, suggest that the intrusions are synvolcanic (Cathro *et al., op. cit.*)

A number of late, post-mineralization dikes are intersected in drill holes. They include a plagioclase porphyry similar to the Silver King intrusions, other feldspar porphyries and microdiorites, and numerous lamprophyres.

The structure of the Katie deposit area is not well known, due largely to the lack of outcrop. Correlation of units in drill core suggests that bedding strikes northwest, in contrast to the more regional northeast trends, and dips steeply northeast. Shear zones, recognized in the Main zone, appear to crosscut porphyry-stage alteration and mineralization. Their attitude is not known.

MINERALIZATION AND ALTERATION

Drilling on the Katie prospect has defined three areas of low-grade porphyry copper-gold mineralization, the "Main", "West" and "17" zones (Figure 3-2). Reserves in

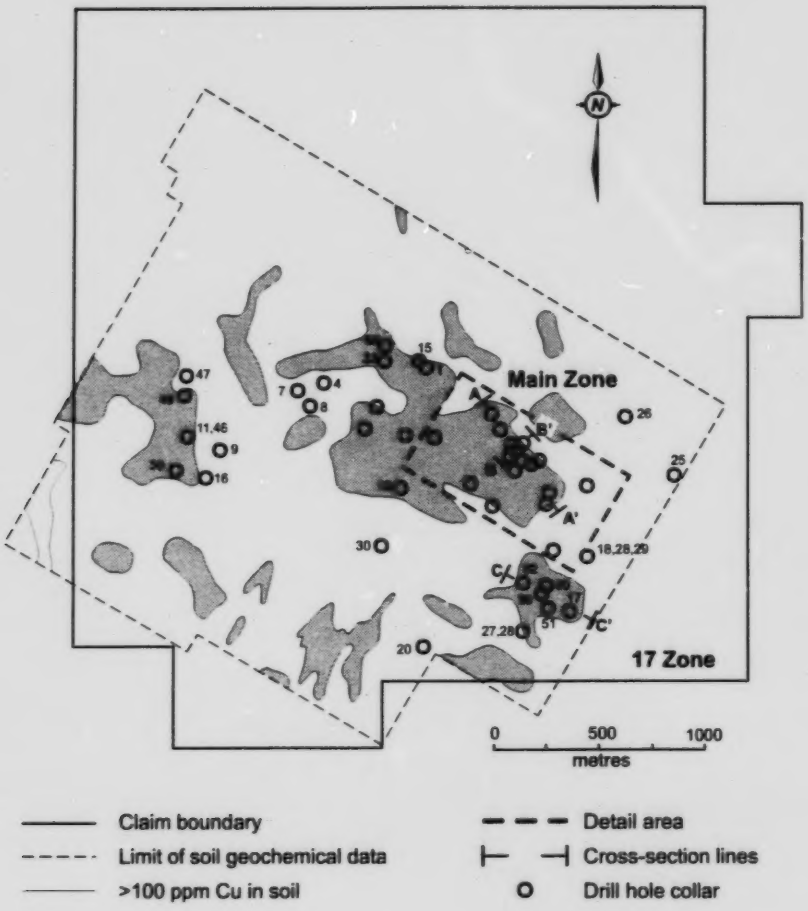

Figure 3-2. Drill hole plan for the Katie property, showing location of main mineralized zones. Also shown is the location of cross-section of Figure 3-3 (from Cathro *et al.*, 1993).

the Main zone are calculated at 55 million tonnes containing 0.17% copper (K. Murray, personal communication, 1998).

Cathro *et al.* (1993) recognized at least two stages of mineralization: an alkalic porphyry copper-gold stage and a later, shear-hosted gold-silver-copper-antimony-arsenic stage.

Alkaline Porphyry Stage

Porphyry-stage mineralization consists mainly of pyrite, lesser chalcopyrite and bornite, and traces of pyrrhotite, sphalerite, tetrahedrite and ?chalcocite. Total sulphide content ranges from 1 to 10% and averages about 2%. Sulphides occur disseminated in both volcanics and intrusive rocks and in narrow veinlets with quartz, calcite, K-feldspar, chlorite and epidote. Limonite, malachite and azurite are common on fractures, with partial oxidization extending to depths of over 100 metres.

Copper content generally ranges from 400 ppm to about 1%, and gold, up to 0.5 grams/tonne. Correlation between copper and gold analyses suggests that gold occurs mainly in chalcopyrite. Other elements, such as silver, lead, zinc, arsenic and antimony, have relatively low concentrations.

Up to several percent magnetite is present in most rock types, with the exception of the strongly potassic altered zones. Magnetite occurs as veins, irregular aggregates, breccia fillings, and in narrow zones of coarse secondary magnetite above mineralized intervals (Figure 3-3). A slightly oxidized surface sample of this secondary magnetite contained 14 200 ppm copper and 2 800 ppm gold (Cathro *et al.*, 1993). Accessory minerals, commonly associated with magnetite, include rutile, sphene, ilmenite and leucoxene.

Propylitic alteration in the Katie deposit area is characterized by saussurization of feldspars to a greenish grey mixture of chlorite, epidote, sericite and calcite. Pyroxene grains have been altered to chlorite, sericite and actinolite. Albite is locally developed adjacent to sulphides. As well, calcite, epidote and chlorite-pyrite stringers cut mineralization.

Potassic alteration is characterized by a grey, green, pink or brownish mottled, vaguely granular rock composed

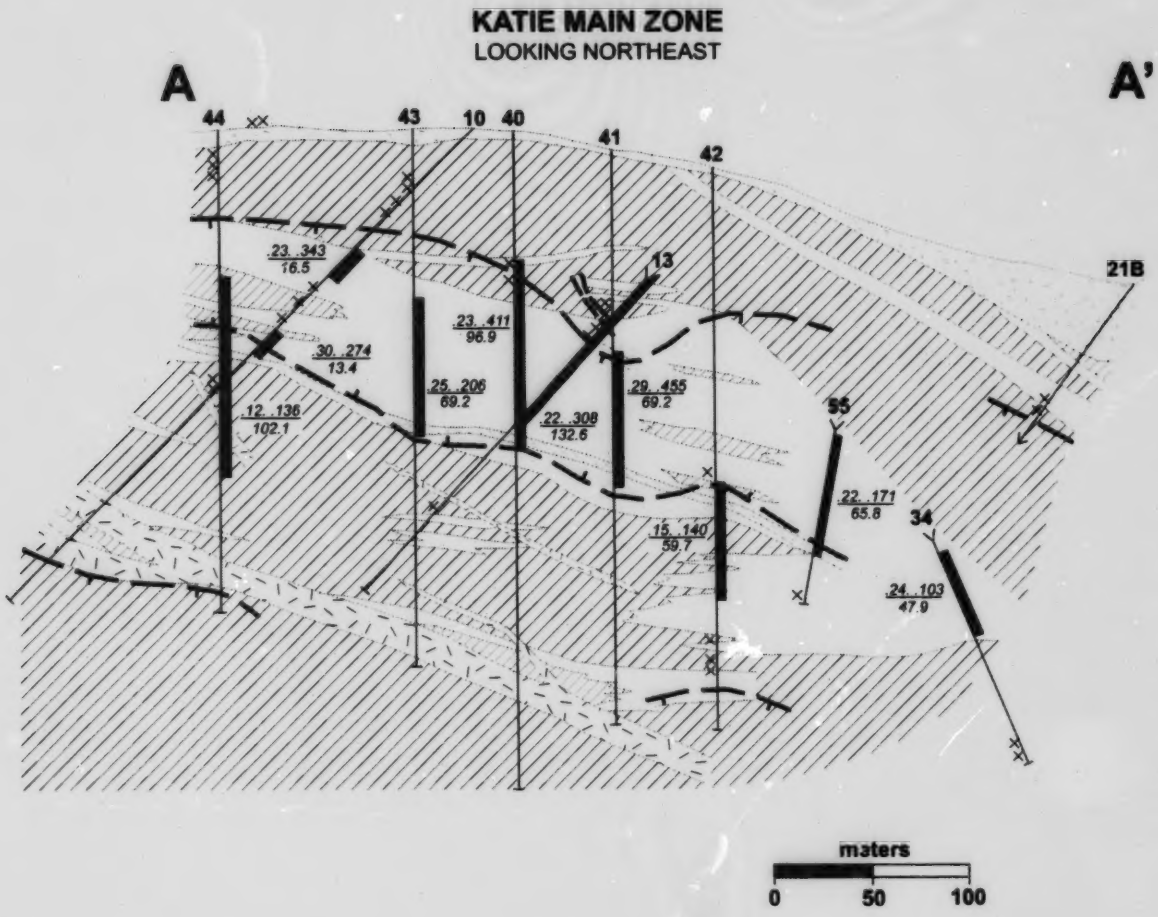

LEGEND

Overburden

Quartz-carbonate healed shear zone

LATE DIKES

Lamprophyre

LOWER JURASSIC ROSSLAND GROUP
ELISE FORMATION

Gabbro, monzogabbro, monzonite

Andesitic to basaltic flows and tuffs

Boundary of stockwork and pervasive Potassium feldspar and biotite alteration

×××× Coarse secondary magnetite

Diamond drill-hole

Offsection drill-hole

30 .274
13.4
Mineralized interval in %Cu. G/t Au / meters

Figure 3-3. Cross-sections through the Katie Main zone, Katie property. The location of the section is shown on Figure 3-2 (from Cathro *et al.*, 1993).

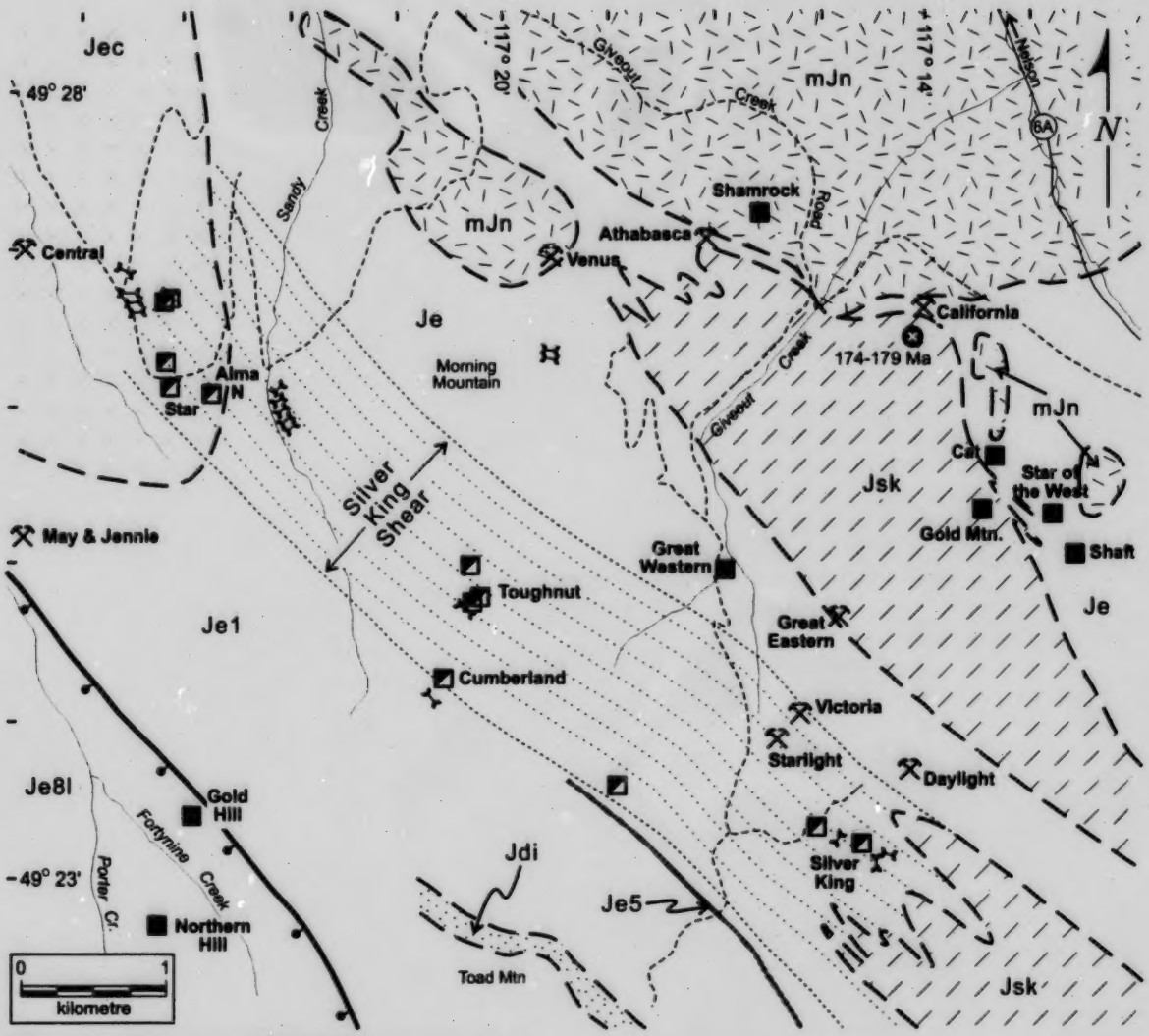

Figure 3-4. Regional geology map showing location of mineral deposits and occurrences in the region of the Silver King shear zone, southwest of Nelson (after Höy and Andrew, 1989; Figure 1-1, in pocket).

of K-feldpar, plagioclase and lesser quartz, biotite and chlorite. K-feldpar replaces the groundmass, rims plagioclase grains, and occurs in narrow veins, quartz vein selvages, or irregular flooded zones associated with quartz, pyrite and chalcopyrite. Coarse secondary biotite is also present.

A late, retrograde hydrous alteration overprints prograde alteration types. Sericite replaces plagioclase and secondary K-feldpar and chlorite replace secondary biotite and amphibole (Getsinger, 1992). Abundant late calcite, epidote and chlorite-pyrite stringers cut the potassic alteration and may also be part of this late retrograde stage.

Shear-related Au-Ag-Cu-Sb-As Stage

Although not common, mylonitic shear zones carry significant gold values (1 to 3 ppm), silver (10 to 60 ppm), up to 1% copper, and anomalous levels or arsenic and antimony. The sheared rocks are pervasively altered to an assemblage of quartz, sericite and carbonate and contain weakly to strongly contorted quartz-dolomite-sulphide veins. The veins contain minor but locally abundant concentrations of pyrite, chalcopyrite, tetrahedrite and arsenopyrite and traces of molybdenite and specular hematite.

The attitude of the mylonite shears is not known, but one set appears to strike northwest. The shears appear to be younger than the porphyry stage mineralization. They may be related to the early shearing recognized on the limbs of the Hellroaring Creek syncline, and parallel to the inferred northwest trend of layering in the deposit area.

SUMMARY AND DISCUSSION

Katie is an alkaline copper-gold porphyry deposit in mafic to shoshonitic volcanic rocks of the Elise Formation and a series of mafic, comagmatic(?) dikes and sills. A potassic alteration zone is surrounded by a wide area of pervasive propylytic alteration. Mineralization is closely associated with zones of biotite and K-feldspar alteration, in an area that measures at least 1800 metres by 500 metres. Coarse-grained secondary magnetite-cemented breccias are commonly associated with mineralization, locally concentrated above sulphide zones.

Shear zones, with local enrichment of gold and silver, and containing as well copper, arsenic and antimony, cut porphyry-style mineralization. The age of this shearing and related mineralization is not known. It is probably related to northeast-trending shearing that is recognized immediately to the south and appears to be pre-Middle Jurassic in age; however, there are more brittle northwest-trending faults farther to the northwest that are interpreted to be related to Eocene extension.

SHAFT (082F/SW331)

Names: Shaft, Cat, Magpie, Eldorado, Dolly

Location: Lat. 49°26'11" N; Long. 117°16'28" W
Elev. 1400 metres

INTRODUCTION

The Shaft occurrence is a gold-copper deposit associated with highly sheared mafic intrusive rocks approximately 7 kilometres south of Nelson (Figure 2-1; 3-4). It was located in 1987 near old trenches and adits that are believed to have been developed between 1900 and 1904. In the fall of 1987, South Pacific Gold Corporation optioned the property and undertook geological mapping, trenching, magnetic and induced polarization surveys (Seywerd, 1988), soil and rock geochemistry and 760 metres of diamond drilling. More recently, Sultan Minerals Inc. optioned the property, and the adjoining Kena, and resampled and assayed trenches and drill core.

REGIONAL GEOLOGY

The Shaft property is on the eastern limb of the Hall Creek syncline, a tight south plunging fold with Hall Formation in its core and Elise and Archibald formations on its limbs. Intrusive rocks in the vicinity of the Shaft deposit include the Silver King intrusion a few hundred metres to the west, a number of small Nelson-age (*ca.* 165 Ma) intrusions just to the north and a highly sheared and elongated diorite intrusion that, in part, hosts mineralization (Figure 3-5). Both the Silver King and the diorite are deformed by northwest trending shearing concentrated on the limbs of the Hall Creek syncline.

Much of the Shaft property is underlain by augite porphyry flows and lapilli, crystal and fine-grained tuffs of the upper part of the Elise Formation. These mafic to intermediate-composition volcanic rocks are intruded by an elongate, fine to medium-grained mafic intrusive complex that is commonly locally brecciated. Due to the local intense shearing and foliation, it is often difficult to distinguish it from mafic tuffs. The complex is tabular, up to 50 metres in width and 5 kilometres in strike length. Although it appears to be a sill, it is probable that it crosscuts the Elise hostrocks and has been transposed into parallelism.

The intrusive complex is a porphyritic intrusion that ranges in composition from quartz diorite to monzodiorite with minor diorite (Andrew and Höy, 1989). It is similar to other small mafic intrusions in the Elise Formation, such as the Katie, that are interpreted to be subvolcanic intrusions (Dunne and Höy, 1992). It comprises an intergrowth of 30 to 45% anhedral to subhedral calcic plagioclase (An 55-60), 5 to 10% orthoclase, rare microcline and 2 to 3% quartz. The feldspars are strained and have been variably altered to sericite. Biotite (10 to 25%) and ?K-feldspar are widely distributed. Biotite occurs as sheaves of tabular crystals, commonly intergrown with chlorite, that have grown parallel to schistosity; some masses retain a prismatic shape, perhaps pseudomorphic after hornblende or augite. Epidote and magnetite are common accessory minerals, and apatite, sphene, hematite and malachite are present in trace amount. Fine-grained chalcopyrite, pyrite and magnetite are disseminated throughout. Carbonate, mainly calcite, occurs as irregular veinlets, generally intergrown with quartz and, locally, biotite and feldspar.

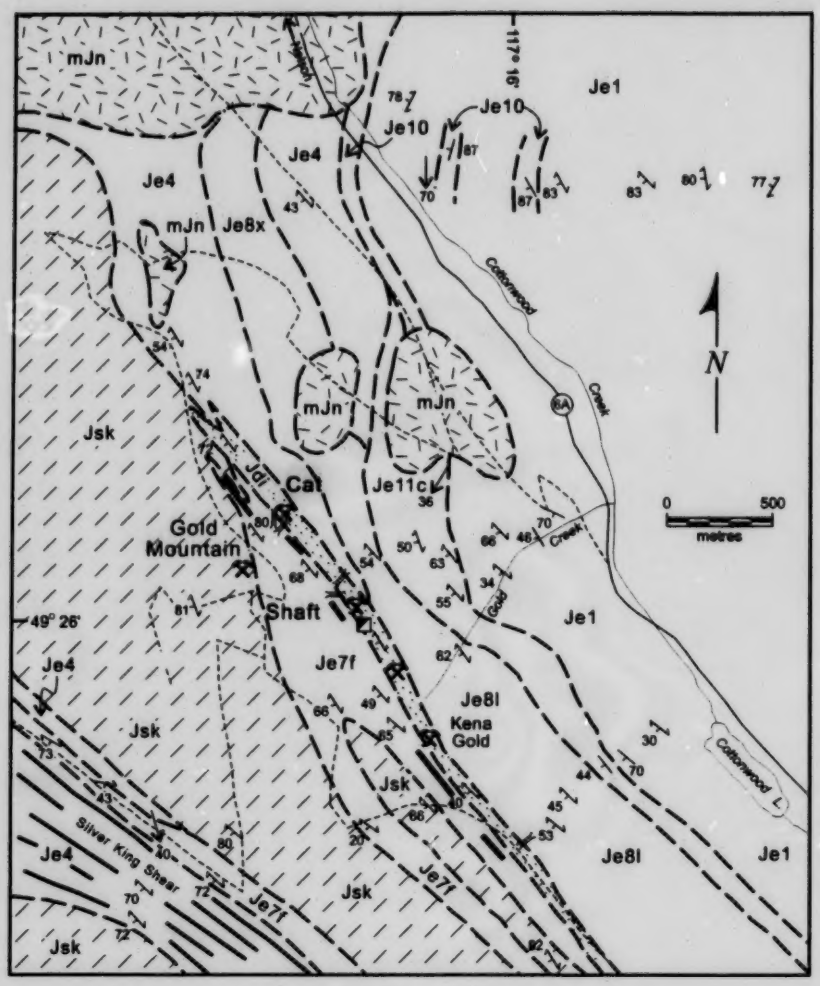

Legend

MIDDLE JURASSIC

mJn — NELSON intrusions: Jn1, granodiorite, quartz monzonite; Jn2, diorite porphyry; Jn3, breccia.

LOWER OR MIDDLE JURASSIC (?)
intrusive units

Jsk — SILVER KING intrusions: plagioclase porphyry; locally intensely sheared.

Jdi — fine to coarse, granular diorite.

LOWER JURASSIC
ROSSLAND GROUP

Je — ELISE FORMATION: mafic to intermediate flows, tuffs, epiclastic deposits and subvolcanic intrusions.

upper ELISE FORMATION

epiclastic units

Je11 — tuffaceous conglomerate: Je11c, predominantly intermediate to felsic volcanic and intrusive clasts; Je11b, mixed mafic felsic clasts; Je11a, predominantly mafic volcanic clasts.

Je10 — tuffaceous siltstone, sandstone: Je10a, argillaceous siltstone.

pyroclastic units

Je8 — andesite tuff, minor basaltic tuff: Je8l, lapilli tuff with plagioclase ± augite-bearing volcanic clasts; Je*x, plagioclase ± augite crystal tuff.

Je7 — basaltic tuff: Je7f, mafic, fine tuff.

Je4 — augite ± plagioclase basalt flows, flow breccias.

lower ELISE FORMATION

Je1 — augite ± plagioclase basalt flows, flow breccias, subvolcanic intrusions.

Figure 3-5. Geological map of the Gold Creek - Cottonwood Creek area south of Nelson, showing the location of the properties *(see* also regional map, Figure 1-1).

MINERALIZATION AND ALTERATION

Two principal copper-gold showings, the Shaft and the Cat approximately 500 metres apart, were identified on the Shaft claims in 1987 (Figures 3-6 and 3-7).

Mineralization on the Shaft occurs mainly in the monzodiorite intrusion, but also in the Elise tuffs and in the margins of the Silver King porphyry. It comprises up to one percent magnetite, and a high proportion of sulphides, including up to 15% pyrite, 3% chalcopyrite and rare pyrrhotite. Chalcopyrite occurs mainly as disseminations, small discrete patches, thin discontinuous laminae and fracture fillings, whereas pyrite and magnetite are mainly disseminated throughout the intrusive complex. Sulphides occur both within the breccia fragments and in the matrix. Malachite forms on fracture surfaces adjacent to chalcopyrite in surface exposures.

At the Cat zone (Figure 3-6), sulphides are concentrated within the matrix of a crackle breccia. The mineralization forms a lens, approximately 9 by 5.5 metres in dimension. Assays from this showing averaged 1.37 g/t gold and 0.7% copper (South Pacific Gold Corp., report, 1988).

The monzodiorite and Elise tuffs are both variably altered to a chlorite-epidote-carbonate-sericite assemblage. Although this assemblage resembles that typically found in greenschist facies regional metamorphism elsewhere in the Nelson area, the extent of alteration at the Shaft showing is far more intense. This suggests that probable early potassic

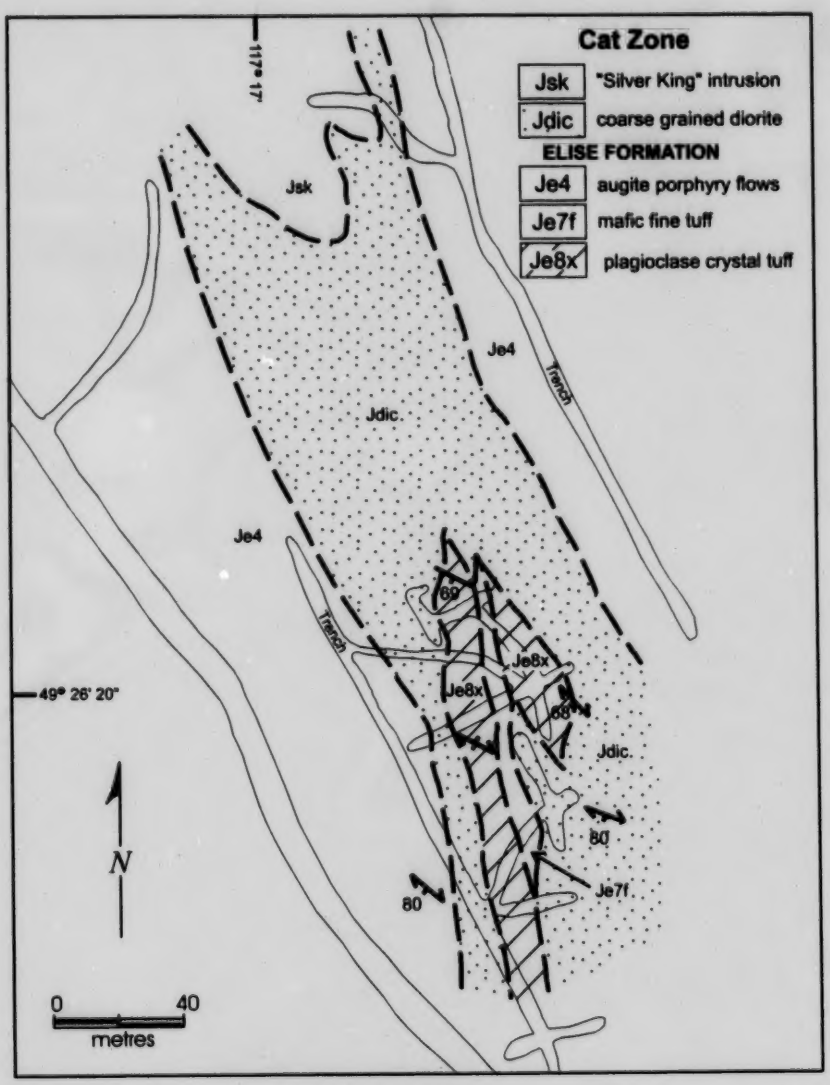

Figure 3-6. Geology of the Cat zone.

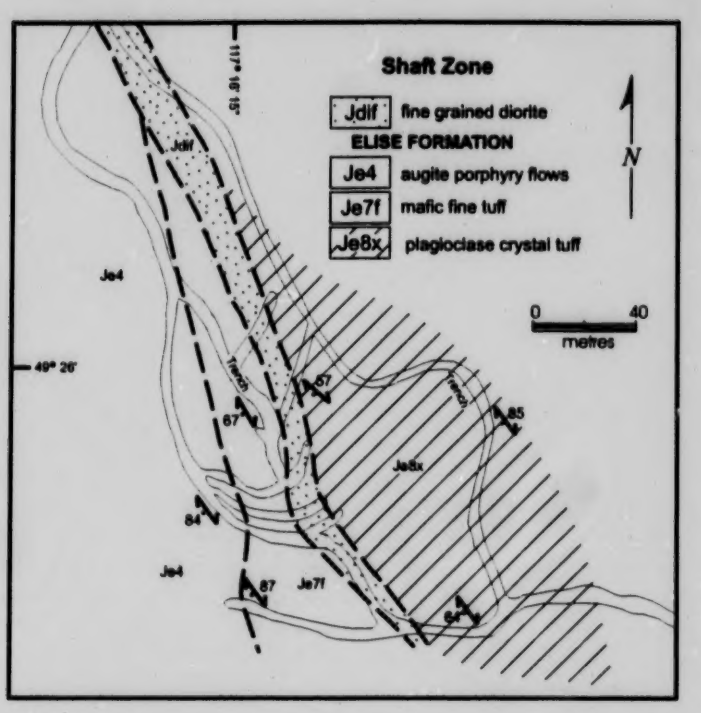

Figure 3-7. Geology of the Shaft area.

TABLE 3-1
ANALYSES OF SELECTED HAND SAMPLES AND 1-METRE SURFACE CHIP SAMPLES FROM THE CAT AND SHAFT SHOWINGS

Lab No.	Sample	Type	Au ppb	Ag ppm	Cu ppm	Pb ppm	Zn ppm	Co ppm	Ni ppm	As ppm
Cat showing										
36475	R79-1	chip	160	<0.3	820	6	95	22	4	8
36476	R79-2	chip	32	<0.3	760	8	107	42	66	12
36477	R79-3	chip	<20	<0.3	320	9	95	24	4	10
36478	R79-4	chip	203	<0.3	146	11	108	22	4	8
36479	R79-10	chip	564	<0.3	480	5	125	32	11	8
36480	R79-15	chip	191	1.0	720	10	340	26	4	23
36481	R79-17	chip	552	1.0	405	10	119	26	4	53
36482	R79-18	chip	<20	<0.3	111	9	123	22	4	6
36483	R79-21	chip	<20	<0.3	104	11	105	24	4	9
36511	R79-4A	grab	54	0.3	173	6	112	25	4	10
36512	R79-9	grab	50	0.3	186	7	114	24	4	9
36513	R79-12A	grab	2030	23.0	0.84%	3	22	82	4	2
36514	R79-12	grab	82	0.5	610	6	139	37	10	6
36515	R79-13	grab	1860	2.0	0.63%	7	137	36	4	13
36516	R79-14	grab	185	1.0	640	7	246	26	4	22
36517	R79-16	grab	526	7.0	0.40%	9	219	24	4	35
36518	R79-17	grab	340	1.0	630	10	115	23	4	44
Shaft showing										
36484	R80-1a	chip	864	2.0	0.70%	13	101	34	6	12
36485	R80-1b	chip	1980	1.0	0.47%	10	81	33	4	9
36486	R80-4	chip	32	0.3	165	6	152	26	7	7
36487	R80-5	chip	300	0.7	0.27%	11	128	27	8	8
36488	R80-6	chip	2420	1.0	0.64%	13	92	23	4	7
36489	R80-9	chip	1200	1.0	0.51%	15	102	36	80	11
36490	R80-17	chip	200	<0.3	0.18%	12	68	30	12	20
36491	R80-21	chip	446	6.0	0.32%	49	710	34	8	61
36492	R80-24	chip	187	0.3	610	15	80	25	19	11
36493	R80-26	chip	133	1.0	0.10%	14	65	21	5	27

alteration was overprinted by propylitic alteration, with a later assemblage of sericite-carbonate-quartz.

Surface grab samples at the Shaft zone assayed an average of 6.2 g/t gold and 1% copper (Jenks, 1988). The best intersection in drill core is 5.4 metres containing 6.9 grams gold and 1% copper. Resampling and assaying of trenches in 1999 yielded 5.64 g/t Au and 0.95% Cu over a "true" mineralized width of 12 metres, including 2 metres containing 14.14 g/t Au and 1.73% Cu (Sultan Minerals Inc., report, 2000).

Analyses of selected hand samples and 1-metre surface chip samples are shown in Table 3-1; gold correlates positively with copper and with cobalt. High gold and copper concentrations also correspond with zones of intense chlorite-sericite-carbonate alteration. Lead, zinc and arsenic show a positive correlation, although concentrations are noticeably lower (Table 3-1).

DISCUSSION

Mineralization at the Shaft and Cat prospects is in Lower Jurassic Elise Formation tuffs and a mafic, possibly synvolcanic, monzodiorite intrusion. Potassic and intense propylitic alteration are spatially associated with the intrusion and the Au-Cu mineralization. Regional metamorphism to greenschist grade and intense shearing have overprinted host rocks and mineralization.

The nature of the mineralization and alteration and its association with an intrusive body suggest that Shaft may be part of a highly sheared alkali porphyry Cu-Au prospect, similar to the Katie deposit.

KENA GOLD (082F/SW237)

Names: Kena Gold, Kena 7, Cottonwood
Location: Lat. 49°25'33" N; Long. 117°15'57" W
Elev. 1500 metres

Kena Gold is located approximately 7 kilometres south of Nelson (Figure 3-5). Kena Gold and a number of other occurrences or zones in the area, including Shaft, Cat, South Gold, Gold Mountain and Kena Copper, have now been combined as the Kena property, owned by Sultan Minerals Inc.

The regional geology of the Kena property area is described above (*see* Shaft). The area is underlain by mainly mafic flows and tuffs of the upper Elise Formation which are intruded by the Middle Jurassic Silver King pluton. The Elise Formation is commonly brecciated and sheared, and in the vicinity of mineralization, silicified and potassic altered.

Mineralization at Kena Gold consists mainly of broad zones of disseminated pyrite and chalcopyrite within a silicified and brecciated diorite intrusion, and the host Elise metavolcanics. One drill hole, LK86-20, averaged 1.1g/t Au over its entire 136.85 m length, with a 31.43 metre zone containing 2.3 g/t Au (Sultan Minerals Inc. Report).

GOLD MOUNTAIN ZONE

Name: Gold Mountain
UTM: 5475907N; 479363W
Elev. 1483 metres

The Gold Mountain zone, located several hundred metres southwest of the Cat showing, was discovered by Sultan Minerals Inc. in 2000. This brief desciption, summarized mainly from a report by Sultan Minerals (July, 2001), describes the results of their recent exploration of the zone. It is outlined by a gold soil geochemical anomaly that measures 2000 metres by 600 metres. In contrast with other zones on the Kena property, this zone is within and along the margins of the Silver King porphyry. It consists of disseminated and fracture-filled pyrite with elevated gold contents. One drill hole at the south end of the zone averaged 0.4 g/t Au over its entire 235.5 metre length, including 24 metres containing 1.1g/t Au and 9 metres of 2.3 g/t Au. Analyses of hand samples have returned values up to 5.48 g/t Au, and chip samples of trenches averaged 1.43 g/t Au, with a 3-metre chip sample containing 11.38 g/t Au.

Preliminary work on the Gold Mountain zone by Sultan Minerals suggests that the deposit may by a porphyry gold deposit, related to the Silver King pluton.

GREAT WESTERN (082F/SW333)

Names: Great Western, White Witch, Thistle, Aberdeen
Location: Lat. 49°26'17" N; Long. 117°18'47" W
Elev. 1432 metres

INTRODUCTION

The Great Western Group is located 6 kilometres south of Nelson near the confluence of the west and main forks of Giveout Creek. Mineralization comprises a number of gold-copper zones in highly sheared mafic volcanic rocks of the Elise Formation and felsic intrusive (?) rocks.

Access to the property is via the Giveout Creek road for 3.5 kilometres, which leaves Highway 6, 6.2 kilometres south of Nelson, and then the Silver King mine road for 2 kilometres (Figure 3-4).

The property was initially discovered in the early 1900s and a number of small pits and trenches were dug. Systematic exploration began in 1979 when Asarco Exploration Company of Canada Ltd. registered the Aberdeen claims. Asarco conducted soil sampling, geophysics and diamond drilling in nine holes in the period 1972-1982. In 1985, Lindex Explorations Ltd. entered into an option agreement with Asarco Ltd. (Aberdeen claims) and R.J. Borden (Great Western claims).

Lectus Developments Ltd. began surveying, sampling and trenching on the claims in 1986, and in 1987 drilled 21 holes. Pacific Sentinel Gold Corp. did extensive work over a large area in 1989-1990, termed the Great Western Star Project that included considerable trenching, sampling, geophysics, geochemistry and 5,880 metes of diamond drilling. Most of this work, however, was concentrated on other occurrences or areas, most notably on the Toughnut claims (*see* below).

REGIONAL GEOLOGY

The Great Western Group lies on the eastern margin of the Silver King shear zone, a zone more than a kilometre wide that extends northwest from the closure of the Hall

Formation in the core of the Hall Creek syncline (Figure 3-4). Rocks are locally intensely sheared and therefore it is often difficult to distinguish original rock types. Much of the upper Elise is missing in this area, perhaps removed by this shearing.

The Elise succession is intruded by the Silver King porphyry, dated at *ca.* 174-178 Ma (Höy and Dunne, 1997). The porphyry is deformed and metamorphosed, with intense shearing concentrated along its margins.

Augite porphyry flows, mafic tuff and intermediate lithic tuffs underlie the southwestern part of the Great Western claims. The succession is interpreted to be inverted as it occurs on the western limb of the overturned Hall Creek syncline. Supportive evidence for a generally overturned succession includes possible inverted graded beds in drill core (P.B. Read, personal communication, 1989) and rare bedding-cleavage intersections recognized in thin limestone layers.

The mafic volcanic rocks comprise predominantly green phyllites and schists. Lapilli tuff units, containing stretched mafic clasts in a schistose matrix, are observed locally. Foliated and sheared mafic flows and flow breccias occur in the footwall of the most northerly mineralized zone (Figure 3-8). Elsewhere, foliated green phyllite without recognizable clasts is interpreted to be derived from mafic fine tuff. Within these mafic volcanic rocks are a number of zones of intense carbonate-sericite-quartz alteration that are conformable to foliation and contain the gold-copper mineralization. A number of these zones are cored by felsic intrusive lenses.

One of these lenses, now largely altered to a carbonate-sericite-quartz assemblage, is exposed in the most northerly mineralized zone (Figure 3-8). U-Pb dating of zircon fractions restricts its age to between 185.3±3 and 165.5±4 Ma. The lens is generally less than a metre thick and at least 200 metres in length. It contains broken quartz grains, altered plagioclase phenocrysts and minor secondary biotite in a fine-grained schist matrix. Accessory minerals include biotite, apatite and tourmaline; fine-grained euhedral pyrite is concentrated mainly as stringers parallel to the foliation.

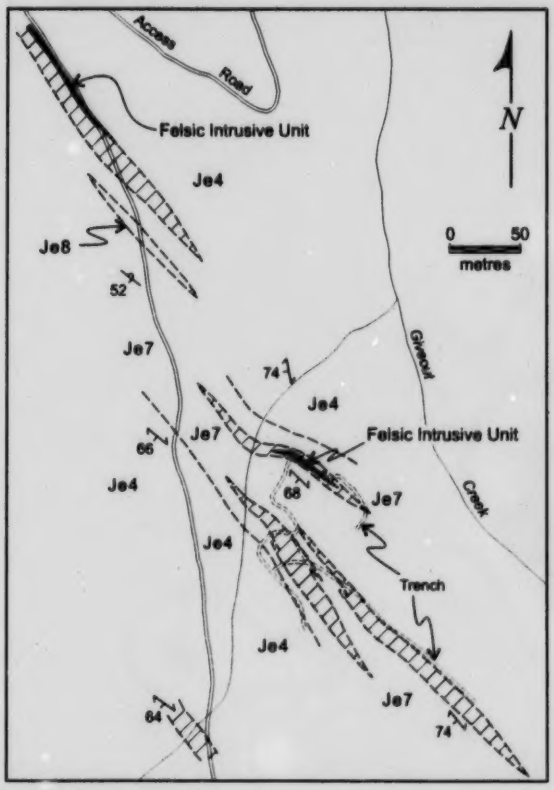

LOWER JURASSIC
ROSSLAND GROUP
Upper Elise Formation

▨	mineralized carbonate-sericite-quartz alteration zone
Je8	andesite lapilli tuff
Je7	mafic tuff, fine ash
Je4	augite ± plagioclase basalt flows, flow breccias

Figure 3-8. Geology in the vicinity of mineralized zones, Great Western Group.

MINERALIZATION AND ALTERATION

Three principal zones of gold-copper mineralization occur in the immediate area. These are the Giveout Creek North and South zones, discovered in 1987, and the Black Witch zone located to the north.

Mineralization occurs in zones of intense carbonate-quartz-sericite alteration in both mafic units and in the associated "felsic" lenses. The alteration zones are 5 to 10 metres in width and several hundred metres in length. They contain 2 to 3% sulphides, dominantly pyrite with minor chalcopyrite, as foliation parallel discontinuous stringers but also pervasive disseminations throughout. Although most mineralization is deformed along with the host rocks, some occurs as late, post-kinematic, crosscutting quartz veins.

Analyses of randomly selected grab and chip samples of the Great Western Group are shown in Table 3-2. Gold content does not appear to correlate positively with other metals but copper, silver and lead have strong positive correlations as do cobalt, zinc and nickel (Höy and Andrew, 1989c). The best intercept in drill core at the Great Western Group was 7 metres containing 9.7 g/t gold; the highest reported assay was 58 g/t gold over 0.9 metres (George Cross Newsletter, Nov.17, 1987).

SUMMARY AND DISCUSSION

The age and origin of gold-copper mineralization at the Great Western occurrence is not known. Zones have been referred to as 'conformable gold deposits' (Höy and Andrew, 1989c). They appear to be spatially associated with

TABLE 3-2
ANALYSES OF SELECTED SAMPLES, GREAT WESTERN GROUP

Lab No.	Sample No.	Sample type	Au ppb	Ag ppm	Cu ppm	Pb ppm	Zn ppm	Co ppm	Ni ppm	As ppm
36467	R78-2	chip	63	<0.3	22	3	13	16	4	<1
36468	R78-1	chip	23	<0.3	29	3	63	29	15	5
36469	R78-19	chip	197	<0.3	24	3	21	20	15	10
36470	R78-21	chip	223	2	480	10	40	19	17	3
36471	R78-23	chip	464	2	214	8	36	40	22	6
36472	R78-23e	chip	931	1	83	6	30	28	18	5
36473	R78-24	chip	208	<0.3	14	3	38	28	23	4
36500	R78-11	chip	25	<0.3	108	8	112	36	29	27
36507	R78-3	grab	20	0.7	66	3	93	33	55	5
36508	R78-5	grab	168	0.3	18	3	67	67	41	14
36509	R78-13	grab	78	0.3	25	6	94	94	60	8
36510	R78-16	grab	82	0.8	211	6	68	68	22	5

felsic to intermediate intrusions, are aligned parallel to the prominent foliation, have conspicuous alteration envelopes, and are sheared and foliated along with their country rocks. They may be porphyry gold prospects, with mineralization associated with small, high level? intrusions, that owe their conformable nature to overprinting by the intense deformation. The chemistry, mineralogy, age and pre to syntectonic form suggest that the intrusion may be related to the Silver King porphyry. Recognition of probable gold porphyry mineralization here and at the Gold Mountain zone on the Kena property enhances considerably the potential for this style of mineralization in the Silver King intrusions.

TOUGHNUT (082F/SW294)

Names: Toughnut, Great Western Star
Location: Lat. 49°26'11" N; Long. 117°20'31"W
Elev. 1770 metres

INTRODUCTION

The Toughnut occurrence is located on Toad Mountain, 7 kilometres southeast of Nelson and 2 kilometres southeast of the Star showings (Figure 3-4). Access is via the Giveout Creek and Silver King roads, south of Nelson. Despite moderately steep relief in the area, exposures are largely limited to those in Giveout Creek, road cuts and the summit of Morning Mountain.

The Toughnut vein, discovered in the late 1880s, had some underground work done in 1890-1891. In 1974, Granby Mining Company drilled three holes totaling 186 metres. In 1985-1986, L. Addie established a grid over the area and did some soil and rock geochemistry and a magnetometer survey (Addie, 1986); this program identified coincident gold geochemical and magnetic anomalies. Geophysical work in the Toughnut area for Lectus Developments Ltd. identified two strong IP anomalies (Lloyd, 1988). The anomalous areas were trenched by Pacific Sentinel Gold Corp. in 1989, and considerable soil and rock geochemistry followed (Dawson *et al.*, 1989). The property was drilled in 1989-1990 for a large, low-grade copper-gold target.

REGIONAL GEOLOGY

The Toughnut area is underlain by Elise volcanic rocks, comprising dominantly augite phyric mafic tuffs, flows?, and a quartz feldspar porphyry (Addie, 1986; Figure 3-9). It is within the Silver King shear, a wide zone of shearing in the limbs and the core of the Hall Creek syncline.

Mafic volcanic rocks of the Elise have a pervasive carbonate alteration, with 1 to 2% disseminated pyrite and minor disseminated magnetite. Fine-grained, pale grey to dark green schists are interpreted to be quartz and feldspar crystal tuffs of intermediate composition (Dawson *et al.*, 1989). They are typically intensely altered with abundant silicification, sericite and iron carbonate. Pyrite, and locally chalcopyrite and malachite, are disseminated throughout the alteration.

The quartz-feldspar porphyry is medium to coarse grained with sericitized plagioclase crystals, 'eyes' of quartz, and chloritized hornblende in a bleached, sericitized matrix. It is interpreted to be a high level, possibly subvolcanic, sill (*see*, for example, Dawson *et al.*, *op. cit.*). Alternatively, it may be a sheared marginal phase of one of the Silver King intrusions.

A number of fine-grained biotite lamprophyre dikes and sills, with only minor disseminated pyrite and magnetite, cut other units in the Toughnut area.

MINERALIZATION AND ALTERATION

The Toughnut showing was first described as a vein "four to eight feet" wide that "contains ore of a high grade character" (GSC Annual Report 1890-1891). Addie (1986) described mineralized shears that contain gold, silver, tetrahedrite, galena, chalcopyrite, pyrite, sphalerite and pyrolusite in a quartz-carbonate gangue. Analyses of three hand picked samples from old working are presented in Table 3-3.

More detailed work by Dawson *et al.* (1989) and Ronning (1990) have defined more clearly the various styles of mineralization in the Toughnut area. Two to 5% disseminated pyrite is common throughout the intermediate

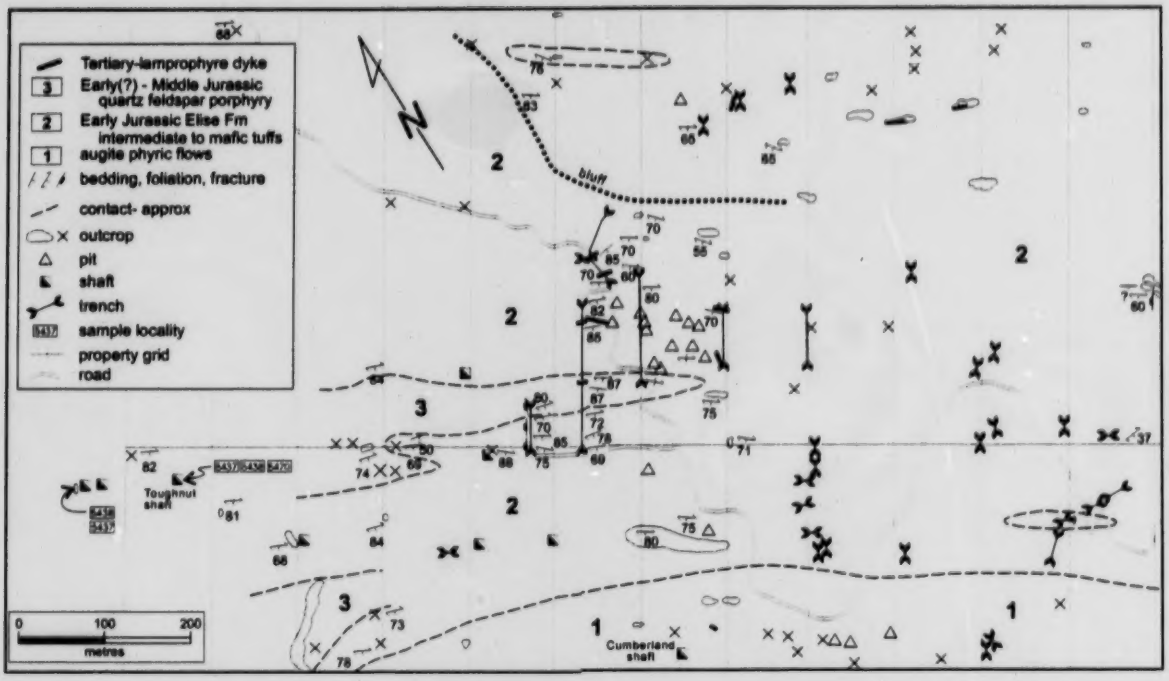

Figure 3-9. Geology in the vicinity of the Toughnut showing (after Dawson *et al.*, 1989).

TABLE 3-3
ANALYSES OF SELECTED HAND SAMPLES, TOUGHNUT PROSPECT

Sample number	Type	Au ppb	Ag ppm	Cu ppm	Pb ppm	Zn ppm	Mn ppm	Mo ppm	Sb ppm	As ppm
Addie-1	grab		1	12	188	950	>9999	5	30	17
Addie-2	grab	150	52	4633	2724	>9999	7241	77	810	46
Addie-3	grab	1400	32	584	>9999	>9999	4313	90	570	12
5437	grab	415	180	212	1.26%	5.21%				
5438	grab	165	200	580	10.06	3.02				
5459	grab	110	126	2876	2.45	6.3				
5461	grab	260	159	1016	7.36	1.48				
5470	grab	560	36	185	0.19	1.51				

Note (Addie samples): Ag, Cu, Pb, Zn, Mn, Mo, Sb analyses, ICP, Chemex Labs Ltd., Vancouver
Au, As, FA and AA, Chemex Labs, Vancouver (Addie, 1986)
(other samples: Acme Analytical Laboratories, Vancouver (Dawson et al., 1989)

quartz crystal tuffs, and in numerous veinlets in these and other more mafic tuffs. A number of quartz veins, including those that were worked near the turn of the century, contain galena, chalcopyrite, sphalerite and rare tetrahedrite, and are enriched in gold and silver (*see* Table 3-3). These veins typically parallel the regional foliation, striking approximately 120 degrees and dipping steeply southwest; one vein, on which early workings were developed, can be traced discontinuously for at least 120 metres. Other sulphide-bearing quartz veins clearly cut across the regional north-trending foliation.

Chalcopyrite also occurs rarely with only pyrite in small veinlets or veins; one 5 cm wide vein contained 10 g/t gold and 0.1% copper (Dawson *et al., op. cit.*). Chalcopyrite, galena and sphalerite are also locally disseminated in zones of chloritic, sericitic or iron carbonate altered Elise volcanic rocks. Sericite zones are locally associated with altered and sheared quartz-feldspar porphyry intrusive lenses. Silicification is locally common, as is enrichment of gold and silver. Chlorite and iron carbonate alteration is more common in the more mafic assemblages.

Drilling intersected some gold enriched zones up to several tens of metres thick in Elise volcanic rocks. These are commonly in brittle K-feldspar altered zones, with disseminated pyrite and elevated arsenic values. Diamond drill hole GWS-90-18, at a depth of 106 metres, intersected 26

metres assaying 1.49 g/t gold and 25-50 ppm arsenic (Ronning, 1990).

DISCUSSION

The origin of these and numerous other occurrences in the Silver King shear zone are debatable (*see* also, Silver King, below). A number of veins farther northwest, close to the margin or within the Eagle Creek plutonic complex (*e.g.*, Star, 082F/SW083) are interpreted to be related to, and perhaps remobilized from, sheared gold-copper porphyry deposits. Others within the shear zone may be related to intense alteration within or along the margins of Silver King intrusions.

Quartz-carbonate-sulphide veins in the Toughnut area, both parallel to and crosscutting the Silver King shear, may also be remobilized from larger low grade deposits of disseminated mineralization. The tenor of these veins, carrying base metal sulphides and chalcopyrite, and with elevated gold content, is similar to some porphyry mineralization. Furthermore, the widespread alteration in hostrocks, disseminated sulphide content, potassic alteration, and spatial relationship with intrusive rocks, support porphyry style mineralization. The elongation of mineralized zones parallel to the Silver King shear, as indicated in both soil geochemistry and geophysical surveys, may be due to structural extension.

ALMA N AND STAR (082F/SW083)

Names: Star, Alma N, Great Western Star, Gold Eagle, Ron, Ja, Pb, Bee
Location: Lat. 49°26'55" N; Long. 117°21'45" W
Elev. 1493 metres

INTRODUCTION

Alma N and Star are gold-copper prospects near the margin of the Eagle Creek plutonic complex seven kilometres southwest of Nelson (Figure 3-4). They are accessible by the Giveout Creek road that leaves Highway 3a, 6 kilometres south of Nelson. The original Alma N showing is located about 400 metres southeast of the Star occurrence. These are dominantly veins, although associated dispersed mineralization, commonly within the intrusion, and pervasive K-feldspar alteration, suggest similarities with copper-gold porphyry deposits. They are in the Silver King shear zone, within either the Eagle Creek complex or Elise volcanic rocks.

Alma N and Star were discovered in 1897. Cockfield (1936) reported minor underground work and a small ore shipment to the Trail smelter that returned 21.6 g/t gold, 75 g/t silver and 1.2% copper. In 1912, some ore was shipped to the Granite-Poorman mill. In 1984, U.S. Borax explored these prospects under the terms of an option agreement with Reymont Gold Mines Limited. Work included soil geochemical surveys, I.P., reverse circulation drilling and diamond drilling.

Pacific Sentinel Gold Corp. optioned a large area, including the Alma N and Star prospects, from Reymont Gold Mines and Lectus Development, and in 1989 began an exploration program that included geological mapping, line cutting, soil geochemistry, magnetometer and I.P. surveys, trenching and rock geochemistry (Dawson *et al.*, 1989). Work by Pacific Sentinel in 1990 concentrated on diamond drilling, with 5,880 metres drilled in 26 holes, mainly in the Alma N and Star showing areas, but also at the Toughnut occurrence located farther south. The target of this exploration program was a "bulk mineable copper-gold deposit with similarities to a porphyry system. Volcanogenic massive sulphide are a secondary target" (Ronning, 1990).

REGIONAL GEOLOGY

The Alma N and Star showings are near the contact of the Eagle Creek plutonic complex with Elise volcanic rocks. Intense shearing and alteration related to the Silver King shear zone is pervasive throughout the area. The Eagle Creek plutonic complex, or "pseudodiorite" (Mulligan, 1952) is generally a medium to coarse-grained mafic intrusion, in part gneissic, with syenitic to ultramafic phases (Mulligan, 1951, 1952; Little, 1982a,b). In the vicinity of the Moochie occurrence, it is a metadiorite (Lindsay, 1991). Its age is not known; however, it has been interpreted to be cogenetic with the Elise Formation (Dunne and Höy, 1992; Höy and Dunne, 1997). It is cut by the Middle Jurassic Nelson intrusion and by the Silver King shear zone.

Contacts of the Eagle Creek plutonic complex with the Rossland Group rocks are generally sharp, locally marked by coarse-grained clinopyroxenite that comprises mainly augite with lesser green amphibolite and secondary chlorite. Within the Silver King shear, the complex is altered so that plagioclase is commonly saussuritized, sericitized and/or partially replaced by chlorite; muscovite, chlorite and calcite overprint and surround plagioclase and microcline and segregated albite and epidote show fine-grained cataclastic textures.

Elise volcanic rocks in the vicinity of the showings are now mainly chlorite schists, also due to intense shearing and alteration in the Silver King shear zone. These rocks are interpreted to be within the upper Elise; however, the lower-upper Elise contact is not well established here so it is possible that they are mafic tuffs of the lower Elise.

MINERALIZATION AND ALTERATION

Alma N

The Alma N is at the contact of schistose Elise rocks and the Eagle Creek complex. The contact is "an indistinct zone several tens of metres across typified by large xenoliths of partially digested volcanic rock within potassically altered leucocratic monzonite" (Dawson *et al.*, 1989). Pyrite is disseminated throughout the contact zone, increasing from 1-2% in the country rock to 3-5% in the intrusion. Gold content correlates positively with increasing pyrite content and potassic alteration. In the Silver King shear zone, higher gold content is associated with strong quartz-sericite alteration and pyrite content up to 10 percent.

Cockfield (1936, p. 70) described decomposed dioritic rock at the contacts, specks of pyrite, manganese on joint planes, and a number of faults. The Elise Formation is described as a schist "impregnated with pyrite and stained with malachite". Cockfield (*op. cit.*) also reported "gold values"

in quartz and silicified country rock along this contact. A "dioritic" rock, with little pyrite or quartz, carried a rich "streak of ore". Numerous grab samples of unaltered to oxidized Elise and intrusive rock, reported by Cockfield, contained gold values that ranged up to 31 grams/tonne.

Considerable drilling by Pacific Sentinel Gold Corp. concentrated on the contact mineralization of the Alma N zone. Mineralized drill intersections are listed in Table 3-4. These mineralized zones are within an altered "monzodiorite", with disseminated and fine fracture-controlled pyrite, magnetite and minor chalcopyrite (Ronning, 1990). Alteration includes bleaching, locally pervasive K-feldspar, and late calcite veinlets.

Star

The Star deposit is in sheared rocks within the Eagle Creek monzodiorite complex. Cockfield (1936) described it as a north-trending, nearly vertical shear that contains an irregular quartz vein locally up to 35 centimetres in width. The vein "includes a considerable amount of country rock and the whole is mineralized with pyrite, chalcopyrite and malachite. The sulphides are not confined to the vein but are found in the sheared rock on either side" (p. 70).

Drilling by U.S. Borax, summarized in Dawson *et al.* (1989) and tabulated below, intersected wide zones of low grade mineralization in generally medium to coarse-grained monzonite that are cut by considerably higher grade veins. Drill hole S-48 intersected several centimetre-wide quartz-carbonate veins. Drill hole S-51, collared 200 metres to the north, intersected a wide zone of intense potassic alteration with abundant secondary biotite and orthoclase and locally up to 50% sericite. Mineralization here comprises widespread, finely disseminated pyrite, chalcopyrite and minor bornite (Dawson, *op. cit.*). This mineralization apparently trends northwest, parallel to the Silver King shear zone. Trenching along the extension of the zone uncovered monzonite with disseminated chalcopyrite and malachite and northwest trending fractures with higher (one percent) chalcopyrite concentrations.

TABLE 3-4
MINERALIZED DRILL INTERSECTIONS, ALMA N AND STAR
(summarized from Dawson *et al.*, 1989)

Drill hole	Interval (metres)	Length	Au (ppm)	Ag (ppm)	Cu (%)
Alma-N					
89-01	29.05-47.95	18.9	4.06	3.8	0.027
89-01	51.13 - 62.0	10.87	0.02	1.7	0.008
89-02	89.0 - 102	13	1.65	2.3	0.028
Star					
S-48	60.96 - 61.57	0.61	8.21	31	1.02
S-48	61.57 - 62.48	0.91	18.51	2.9	0.22
S-51		73	0.788		0.16

DISCUSSION

Early exploration work in the Star and Alma N area focused on the small high grade gold veins. However, more recent work has recognized the potential for larger, high tonnage, low grade gold-copper mineralization.

Widely dispersed chalcopyrite and pyrite occur near the margins of the Eagle Creek plutonic complex, associated with widespread K-feldspar and biotite alteration. Locally, this style of mineralization extends out into altered and sheared Elise Formation mafic volcanics, although there the grades are lower. Mineralization appears to be largely prekinematic, locally sheared out or concentrated parallel to the northwest trend of the Silver King shear.

The style of mineralization, its concentration in the margins of the Eagle Creek plutonic complex, and association with pervasive potassic alteration, suggest that it is a porphyry gold-copper prospect. Concentration within and parallel to the Silver King shear may be due to later remobilization. Higher grade veins, such as Star and Alma N, may also record late remobilization.

PORPHYRY Mo

Porphyry molybdenite deposits within the Nelson-Rossland map area are concentrated on Red Mountain west of the Rossland gold-copper vein camp and on the Stewart claims west of Ymir. The Red Mountain deposits are described in Chapter 4; the Stewart deposits, below. A number of other porphyry Mo occurrences are listed in Appendix 1 and plotted on Figure 1-1. For summaries, refer to BC MINFILE.

STEWART 2 (082F/SW229), BOBBI (250) and FRESNO (251)

INTRODUCTION

The Stewart molybdenite occurrences are associated with a multistage intrusive complex in the Elise and Hall formations due west of Salmo (Figure 3-10). Base and precious metal occurrences on the Stewart property include the Free Silver (082F/SW277) and May Blossom (082F/SW070), discovered in 1896. Arrow Tungsten (082F/SW311) is a tungsten± copper-zinc-molybdenum skarn occurrence in the Hall Formation just north of the Breccia 2 molybdenite complex (Figure 1-1).

Work on the Fresno group by Copper Horn Mining from 1969 to 1970 included geological mapping, and magnetometer and geochemical surveys (Manning, 1967). Quintana Minerals Corp. held a large part of the property in 1969-1970, then called the Salmo Group, and carried out extensive surface exploration for base and precious metals. In the late 1970s, Eric and Jack Denny acquired the Stewart property, which included Fresno, Main Molly, West Anomaly, Arrow Tungsten, Free Silver and May Blossum. In 1979 it was optioned to Shell Canada which did geochemical and geophysical surveys, geological mapping and diamond drilling (Turner, 1980). After cessation of mineral exploration by Shell Canada, Selco optioned the Stewart claims, and carried out extensive exploration in the early 1980s, including mapping, considerable rock geochemistry, soil

sampling, airborne geophysical surveys and diamond drilling (Grant, 1983; Hickling, 1983; Carpenter, 1984). More recent work, including additional mapping concentrated in the Stewart Mo - Arrow Tungsten area, Gold Hill on the southwestern Stewart claims, and the Craigtown Creek gold anomaly area, is summarized by Kaufman (1995). The Stewart claims are presently held by Eric and Jack Denny.

This brief summary concentrates on the geology of the molybdenite occurrences at and adjacent to the Stewart Group. Descriptions of other occurrences on the claim group, listed in Appendix 1, are found in BC MINFILE. This review is taken largely from the referenced assessment reports, some unpublished data supplied by Eric Denny (BC Property File) and from BC MINFILE.

REGIONAL GEOLOGY

The Stewart property area is underlain by Hall Formation metasediments in the core of the Hall Creek syncline, and Elise Formation metavolcanics on the east limb of this syncline (Figure 3-10). The Elise-Hall contact generally trends northward, but is offset to the east in the vicinity in the claim area, probably due to a late southeast-trending right-lateral fault. This fault is cut by a composite porphyritic quartz monzonite stock that is probably a phase of the Nelson batholith. Molybdenite-bearing breccia zones occur within the stock, the Arrow Tungsten occurrence is along its northern margin, and the May Blossum and Free Silver vein occurrences are close to its southern margin.

Coryell intrusive rocks, of Eocene age, cut the Hall Formation in the vicinity of the West Anomaly and just south of the Nelson stock. A prominent suite of late north-trending rhyolite dikes cut the eastern lobe of the Nelson stock, the Coryell stock, and both Elise and Hall Formation rocks (Figure 3-10).

MOLYBDENITE MINERALIZATION

Three main areas of molybdenite mineralization are known: showings on the Stewart 2 claim, Fresno farther east, and Bobbi just northeast of the Stewart 2 claim. As well, molybdenite occurs in a zone of quartz stockwork in a small Middle Jurassic(?) quartz monzonite intrusion, of probable Nelson age, on the West Grid (Hickling 1983).

Molybdenite mineralization on the Stewart 2 claim is concentrated mainly in two breccia complexes along the western edge of the quartz monzonite porphyry. One of these breccias is a pipelike body that contains disseminated molybdenite; molybdenite also occurs on fractures and in narrow quartz veins. The breccia is associated with intense pyrite-sericite alteration. Molybdenite also occurs in quartz stockwork zones with pyrite and pyrrhotite, K-feldpar alteration and more distal propylitic alteration. Reported reserves are 204,000 tonnes grading 0.37% MoS_2.

The Fresno showing is located on Quartz Creek, about 1.5 kilometres west of Main Showing (Figure 3-10). Molybdenite mineralization, with pyrite, occurs as selvages on fracture surfaces within sheared felsic intrusions.

The Bobbi occurrence is located 2 kilometres northwest of Ymir. Molybdenite, scheelite and minor chalcopyrite are found with sericite in quartz veins and in fractures in a quartz monzonite plug. Fluorite is a common accessory mineral in the intrusion, and very minor disseminated chalcopyrite, sphalerite and galena occur in adjacent sedimentary rocks.

SKARN DEPOSITS

A variety of skarn deposits are recognized within the Nelson-Rossland map-area. Copper, lead-zinc, iron and gold skarns are associated with Middle Jurassic intrusions, whereas tungsten skarns occur mainly in Early Cambrian marbles along the margins of Cretaceous intrusions. A wollastonite skarn north of Rossland is in the Permian Mount Roberts Formation, adjacent to the Tertiary Coryell batholith. Many of these skarns are past producers, most notably the gold skarns at Second Relief and Bunker Hill, the tungsten skarns such as the Emerald Tungsten and Dodger northeast of Salmo, and the molybdenite skarns, including Coxey and Giant on Red Mountain in the Rossland camp (Appendix 1). Exploration continues to be active on a number of these deposits, with considerable recent work in the vicinity of Bunker Hill and on the Rossland Wollastonite, as well as the Mammoth molybdenite skarn drilled in late October, 1998.

The geology of the various skarn types in British Columbia has been dealt with extensively by G.E. Ray and the following overview descriptions are taken largely from his work (Ray and Webster, 1997). Deposit descriptions are summarized from BC MINFILE, assessment reports and field visits during the course of our regional mapping. A number of vein deposits have extensive skarn envelopes that contain dispersed mineralization and have been described as skarns.

GOLD SKARNS

Gold skarns, skarns in which gold is the primary or dominant economic mineral, occur within either Rossland Group rocks or Late Paleozoic rocks adjacent to Middle Jurassic intrusions. Gold skarns are typically within calcareous rocks and can be broadly separated into pyroxene-rich, garnet-rich or epidote-rich varieties (Ray and Dawson, 1998). Mineral and metal zonings are typical of gold skarns. At the Nickel Plate deposit near Hedley, proximal garnet-dominated assemblages containing higher copper-gold ratios give way distally to diopsidic skarns that contain the gold deposits (Ray and Dawson, 1994) and at the QR deposit near Likely, the richest gold mineralization occurs within 50 metres of the distal epidote skarn (Ray and Dawson, 1998; Fox and Cameron, 1995).

All gold skarns within the Nelson-Rossland map-area have been found along the margins of Middle Jurassic intrusions, including the Nelson and Bonnington batholiths and the Rossland monzonite (Appendix 1). Most are within the Elise Formation and many occur adjacent to vein deposits. Copper mineralization is common in many, and lead-zinc-silver mineralization is characteristic of the associated veins. Second Relief, a polymetallic vein with locally, well-developed skarn envelopes, is here described as a gold skarn. However, it has many similarities with the intru-

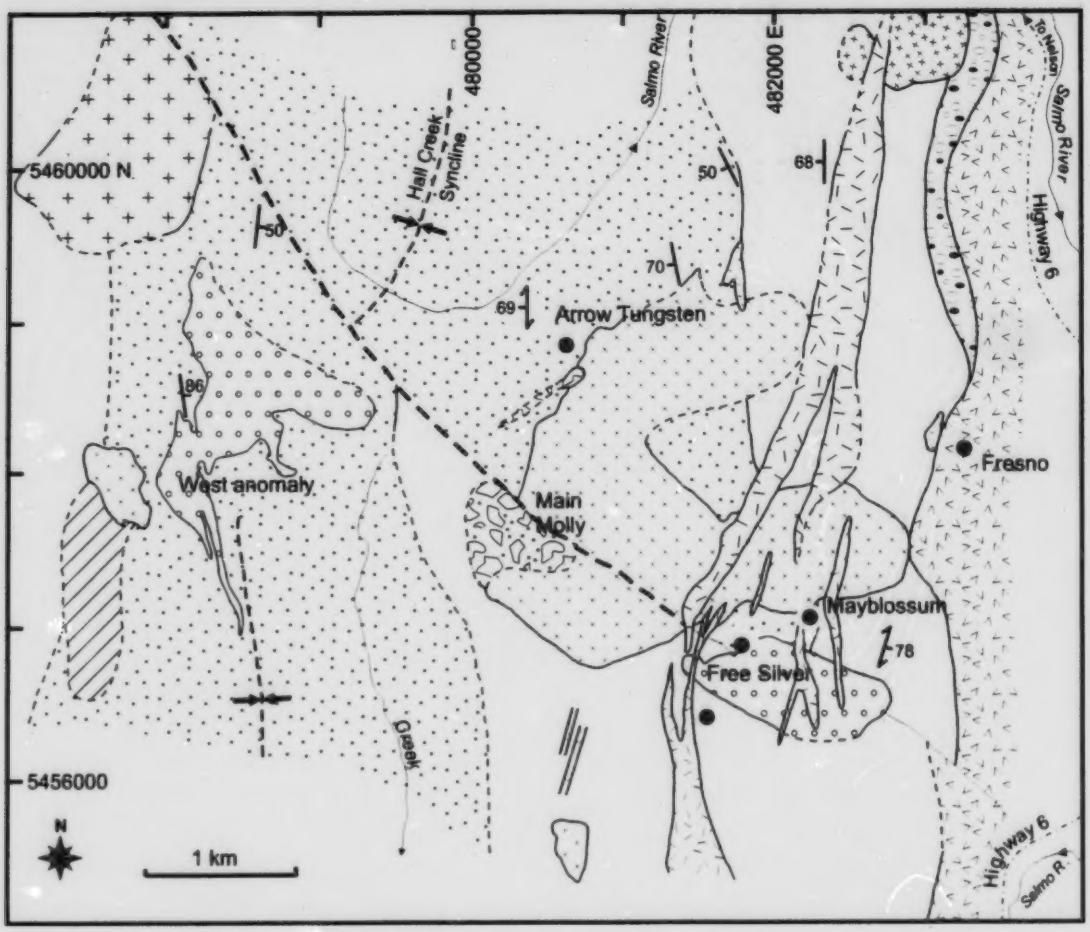

Legend

Cenozoic

Tertiary

Ktr - Rhyolite dike

Middle Eocene

Ec - Coryell intrusion

Mesozoic

Middle Jurassic

Nelson intrusion

- breccia
- quartz monzonite
- granodiorite
- diorite porphyry

Early Jurassic

Jdi - Fine to medium-grained hornblende diorite

Hall Formation

Jh - Siltstone, sandstone, & argillite

Elise Formation

Je - Undivided volcaniclastics

Je 11b - Tuffaceous conglomerate, mafic to felsic clasts

Je4 - Augite-phyric flows, flow breccia

Geological contact (defined : assumed)

Fault

River, creek

Highway

Mineral Showing

Foliation

Layering

Syncline

Figure 3-10. Geology of the Stewart claim group, west of Ymir (modified from Carpenter, 1984 and cited Selco reports).

sion-related gold-sulphide veins described below and in Chapter 4.

SECOND RELIEF (082F/SW187), INEZ AND RAND (082F/SW216)

INTRODUCTION

Second Relief, Inez and Rand are past-producing vein/skarn deposits located along Erie Creek, approximately 20 kilometres south-southwest of Nelson. They are accessible by a road that follows Erie Creek north from Highway 3a west of Salmo.

Vein mineralization at the Second Relief was discovered in the late 1890s and intermittent production continued from 1900 to 1948, with 3 118 kg of Au, 858 kg of Ag, 20 210 kg of Pb and 1 057 kg of Zn recovered from 205 316 tonnes of ore (Appendix 3).

Interest in the Second Relief area continued after production ceased, with Calmark Explorations Ltd. conducting both surface and underground mapping in 1969 (Read, 1969), and Homestead Resources Inc., mapping, soil geochemistry, minor geophysics and some diamond drilling in 1984 (Sookochoff, 1984). In 1988, Hawkeye Developments Ltd. amalgamated most of the claims in the area and began an extensive survey with road rehabilitation, sampling and some surface excavating. The program continued in 1989 with the establishment of a large grid, soil sampling, geological mapping, trenching, and magnetometer, VLF-EM and seismic surveys (Ostensoe, 1989). Reverse circulation and diamond drilling tested a number of the veins. Additional work, including underground rehabilitation and sampling, were recommended on two of the veins, the No. 2 and Ida D.

REGIONAL GEOLOGY

The Second Relief area is underlain by a panel of folded and faulted Archibald and Elise Formation rocks surrounded on the north, east and south by the Bonnington batholith. The Elise Formation is in the core of a north-trending syncline, with upper Archibald Formation exposed immediately to the east (Höy and Andrew, 1989b). However, underground work in the late 1930s suggested that the structure is considerably more complex with local reversals of bedding common.

The Archibald Formation comprises dark, thin-bedded argillites and argillaceous siltstones with, locally, concentrations of disseminated pyrite. Adjacent to intrusive rocks, the Archibald is altered to a dark, fine-grained biotite hornfels. The overlying Elise Formation is the main host for the mineralized veins. It consists of dominantly lapilli tuffs with plagioclase and/or augite-phyric clasts. Feldspar crystal tuffs and mafic, fine tuffs are less common.

A variety of dikes occur throughout the area; some diorite and diorite porphyry dikes are clearly early and cut by the veins whereas other "granitic" dikes are post mineralization (Cockfield, 1936). A prominent diorite porphyry dike, with phenocrysts of oligoclase and quartz in a fine-grained dark grey to green matrix, trends northeast closely following the footwall of the Second Relief vein. Small north projections of the dike are cut by the vein, indicating that the vein is post dike. U-Pb data of zircons collected from a probable southwest extension of this dike yielded a 168.9±8 Ma age (Höy and Dunne, 1997). This dike and the mineralization are both cut by "granite porphyry dikes" that trend more northerly (Cockfield, 1936).

The Mount Verde fault (previously referred to as the Red Mountain fault; Höy and Dunne, *op. cit.*) is a vertical to steeply west dipping fault that is inferred to separate the Archibald from the Elise. Small, generally north-trending faults, offset the Second Relief vein.

MINERALIZATION

The Second Relief mine area includes at least eight subparallel veins that strike northeast and dip steeply northwest in altered volcanics and argillaceous quartzites of the Elise and Archibald Formations. These include the Second Relief or No.1 vein, No.'s 2 to 5, the Ida D and the Inez and Rand veins (Figure 3-11). The veins are sheared, generally quartz-poor, and irregularly mineralized with pyrite and/or pyrrhotite with variable magnetite, chalcopyrite and sphalerite, and trace molybdenite. Gold and silver contents are variable, but concentrated in the quartz, pyrite, epidote, garnet and magnetite bearing veins; visible gold has been reported locally. In general, more massive pyrrhotite and chalcopyrite veins contain less gold. Local skarn envelopes and gangue assemblages include abundant epidote with some diopside, garnet, feldspars, quartz and carbonate.

Second Relief

The Second Relief is the main vein in the camp area, accounting for most of the production. It follows the hanging wall contact of a diorite porphyry dike. The vein strikes 050° and dips steeply northwest. It has a strike length of 300 metres and has been mined to a depth of 400 metres. To the northeast where the vein and dike pass from volcanics to slates, their trend changes from discordant to parallel the trend of the slates and metal values in the vein decrease substantially.

The No. 2 vein parallels the Second Relief vein in the footwall of the porphyry dike. Its width is up to 2.4 metres and its length, greater than 300 metres. Gold assays between 0.137 to 34.2 g/t across one metre or more are reported (Ostensoe, 1989). The No. 2 vein is similar to the Second Relief vein, hosted by fragmental volcanic rocks and mineralized with pyrite, pyrrhotite, magnetite, sphalerite, chalcopyrite and, locally, visible fine-grained gold. Quartz content is variable, and a silicified envelope surrounds the vein.

The No. 3 vein is a narrow stringer, approximately 45 metres southeast of the Second Relief vein. It has no obvious mineralization.

The No. 4 vein, approximately 90 metres southeast of Second Relief, has been exposed by open cuts over a length of 15 metres. 'Greenstone' (Elise volcanic rocks) occurs in its hanging wall and diorite in its footwall. It is a quartz vein up to a metre wide that contains pyrrhotite and chalcopyrite. A 0.5 metre wide sample assayed 12.3 g/t gold (Ostensoe; 1989).

The No. 5 vein, 10 metres farther southeast, comprises massive pyrrhotite and chalcopyrite with only minor pyrite

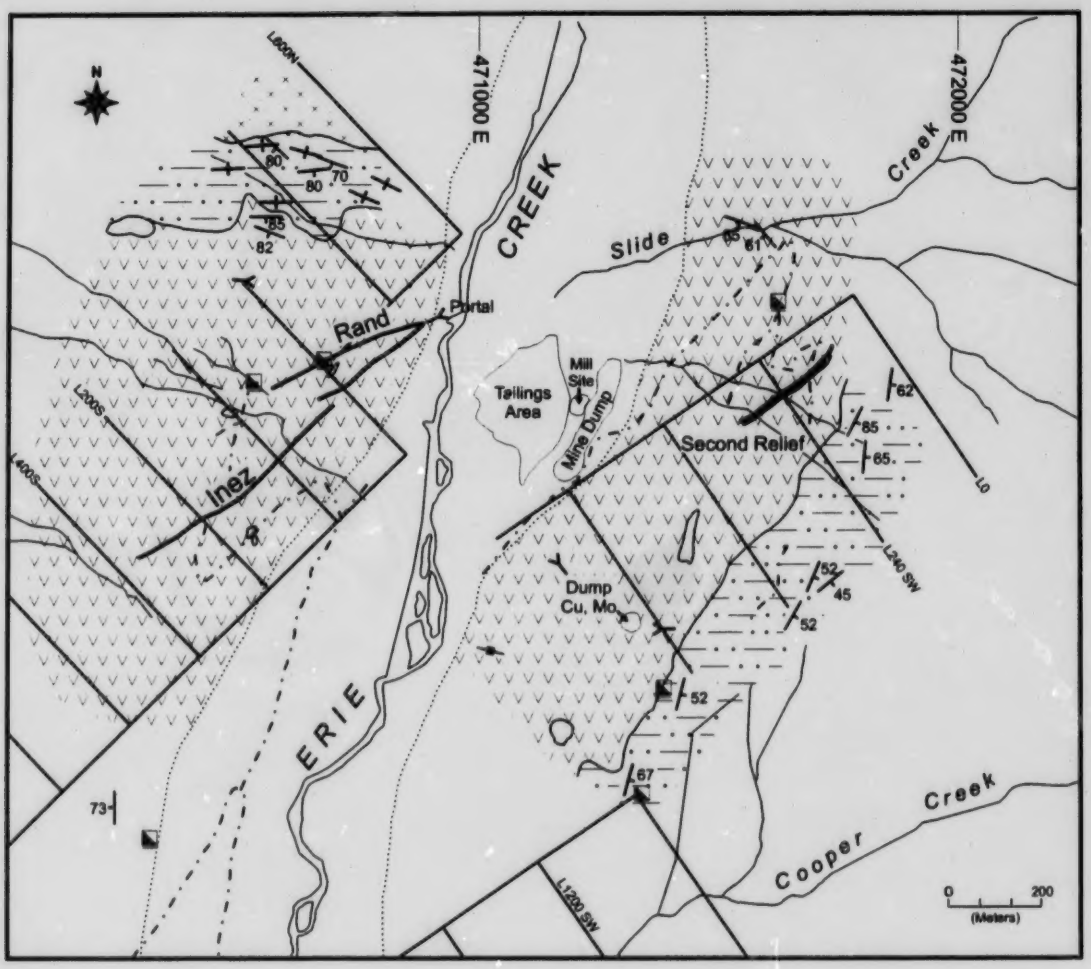

Legend

Mesozoic
Middle Jurassic

- Nelson intrusion
- Feldspar porphyry

Early Jurassic
Archibald formation

- Argillite, argillaceous siltstone, quartzite

Elise Formation

- Lapilli tuff, minor ash tuff

- Veins
- Geological contact (approximate)
- Abandoned Mineshaft
- Adit
- River, creek
- Road
- Layering - inclined
- Layering - vertical
- Jointing

Figure 3-11. Geology in the vicinity of the Second Relief vein-skarn deposit (from Ostensoe, 1989).

and quartz. It is generally less than a metre in width, although underground it is locally up to 1.5 metres wide. O'Grady (1933, p. 236) reported assays of approximately 7.7, 12.5 and 11.5 g/t gold across widths of 30, 100 and 107 centimetres. More recent assays returned values of 0.07 and 26.53 g/t gold (Ostensoe, 1989).

The Ida D vein occurs in the central portion of the property, about 150 metres west of the Second Relief vein. It has produced approximately 34 280 grams of gold (Appendix 3). Samples of the vein taken at the portal in 1988 assayed 0.10 to 35.65 g/t gold (Ostensoe; 1989). As well, samples of pyritic alteration zones in the central portion of the property were reported to assay 6.2 g/t gold over widths of more than 7 metres (Vancouver Stockwatch, Sept. 12, 1989).

Rand and Inez

The Rand and Inez veins occur west of the Second Relief vein system, on the west side of Erie Creek (Figure 3-11). Production from these veins is not known as it is included in production figures for Second Relief. The veins were first described by Cockfield (1936, p. 12): "A vein has been traced continuously for about 800 feet by a series of open-cuts. It strikes north 70 degrees east, dips 75 degrees northwest, and ranges from 1 to 3 feet wide.....The quartz is well mineralized with pyrite".

A considerable amount of the work in the late 1980s was directed towards exposing and exploring these veins. The veins trend northeast and dip steeply north; they appear to converge towards the northeast, and near the portal are approximately 15 metres apart. The Rand vein has been traced on surface and underground for a total distance of 420 metres; the Inez, approximately 750 metres. Mineralization is generally erratic, comprising lenses of massive sulphides that typically range in strike length from 0.4 to 9 metres. Mineralization consists of pyrite, pyrrhotite and chalcopyrite with flakes and minute particles of gold.

The Inez vein is in Elise fragmental volcanic rocks that contain bands of silicified, hornfelsed sedimentary rocks. A banded, pale buff-coloured, one metre thick rhyolite dike occurs in the footwall at the portal. At least seven zones with possible significant mineralization have been reported with values up to 21.6g/t gold in one zone 0.37 metres in width and 17 metres in length (Table 3-5).

Results from sampling the Inez and Rand veins during this study are shown in Table 3-6. These are selected grab samples across the width of the veins at three locations on the Inez (344-3, 344-4 and 344-6) and two on the Rand (349-1 and 349-3). Other individual samples include 344-5b and 349-2. Gold content in virtually all samples is significant, with values to 29 ppm in the Inez and 33 ppm in the Rand. Copper content is variable, but generally low, and both lead and zinc contents are generally low. Although molybdenite is locally visible, Mo is not abundant with maximum values of a few tens parts per million.

DISCUSSION

These veins were first described as fissure veins by Cockfield (1936). They are clearly structurally controlled, as they are locally sheared and have a common and pronounced northeast structural trend. This trend parallels a number of early plagioclase porphyry dikes, dated at *ca.* 169 Ma. The close spatial association with these dikes, their common structural control, and the high temperature skarn assemblages in some veins, suggest a genetic link. One of these dikes forms the footwall of the Second Relief vein but, in detail, mineralization locally cuts and, therefore, postdates the dike. A number of drill holes at the Inez vein encountered massive, locally coarse-grained feldspar porphyry at variable depths, but generally greater than 60 to 70 metres, within sections of epidotized Elise fragmental rocks, suggesting the presence of an underlying intrusion.

The veins have many similarities with the massive sulphide veins of the Rossland camp, including a similar mineralogy, alteration, metal content, and structural control. Both vein camps are also related to similar age intrusions that may be earlier, more mafic phases of the Middle Jurassic Nelson granitic suite.

GOLD-QUARTZ VEINS

INTRODUCTION

Gold-quartz veins, commonly referred to as Mother Lode veins or mesothermal lode gold deposits, typically occur along major structures, including continental collisional sutures or crustal breaks in stable cratons. Within British Columbia, the largest Au-quartz vein camp is Bralorne; other important camps are the Atlin and Cassiar districts. In the Nelson-Rossland map-area, most Au-quartz veins are within quartzites of the Reno and Quartzite Range formations in the Sheep Creek camp southeast of Salmo. Others occur along major fault structures to the west of the Rossland gold camp (Chapter 4), and in sheared Elise Formation rocks and the Eagle Creek plutonic complex south of Nelson (Appendix 1).

Due to their economic importance, mesothermal gold veins have been the focus of many studies; summaries of their characteristics and settings have been presented by Hodgson (1993), Kerrich and Wyman (1990), Roberts (1987) and Ash and Alldrick (1996). They typically contain native gold in a quartz and carbonate gangue, with variable but generally minor amounts of sulphide minerals such as pyrite, arsenopyrite, galena, sphalerite and chalcopyrite. Alteration is usually restricted, with silicification, pyritization

TABLE 3-5
MINERALIZED 'ZONES' IN THE INEZ VEIN, WITH AVERAGE GOLD CONTENT
(from Ostensoe, 1989)

Zone	length (m)	average width (m)	gold (g/T)
A	15	0.63	8.8
B	17	0.73	21.6
C-II	15.5	2	2.9
C-II	15.5	0.7	8.6
D	26	2.37	5.8
E	35.5	0.9	8.4
F	17	1.93	4.4

TABLE 3-6A
ANALYSES OF HAND SAMPLES FROM THE INEZ AND RAND VEINS, SECOND RELIEF

Sample No	Au (ppb)	Ag (ppm)	Cu (ppm)	Pb (ppm)	Zn (ppm)	Co (ppm)	Ni (ppm)	Mo (ppm)	Cr (ppm)	As (ppm)	Note
344-3d	7613	2	400	12	340	30	2	<10	15	39	silicified vein
344-3e	2821	1	324	26	24	38	2	<10	19	37	disseminated sulphides
344-3f	535	0.5	410	46	240	34	3	<10	20	40	disseminated sulphides
344-3g	2949	2	685	14	190	38	5	<10	22	0.28%	quartz vein with sulphides
344-4c	2071	2	740	192	210	24	2	<10	<10	15	sulphide veining
344-4d	3187	3	0.27	32	2.37%	31	2	22	<10	8	sulphide veining
344-4e	9399	2	512	62	84	47	<2	11	<10	34	silicified, disseminatd sulphides
344-4f	394	1	196	32	350	40	2	<10	<10	19	silicified, disseminated sulphides
344-4h	4003	2	740	16	104	18	33	10	15	0.32%	quartz-pyrrhotite veining
344-4j	17328	2	490	14	250	24	<2	<10	<10	47	sericite, sulphides
344-3j	19375	4	0.10%	14	74	28	3	<10	<10	64	epidote-garnet skarn
344-5b	5034	2	580	12	68	48	<2	<10	12	99	quartz vein with sulphides
344-6e1	237	2	0.11%	12	97	27	20	<10	62	24	skarn
344-6e2	1156	2	0.11%	6	132	29	14	<10	65	18	skarn
344-6f	29395	5	0.17%	6	93	64	9	10	49	36	disseminated sulphides
344-6h	284	<.5	191	16	60	39	13	<10	66	14	skarn
344-6j	49	<.5	1	<4	<2	<2	<2	<10	35	2	skarn
344-6l	75	<.5	79	18	85	37	2	<10	<10	21	minor skarn, epidote

TABLE 3-6B
ANALYSES OF HAND SAMPLES FROM THE RAND VEIN, SECOND RELIEF

Sample No	Au (ppb)	Ag (ppm)	Cu (ppm)	Pb (ppm)	Zn (ppm)	Co (ppm)	Ni (ppm)	Mo (ppm)	Cr (ppm)	As (ppm)	Note
349-1b	1565	1	0.10%	8	885	42	2	<10	<10	25	thin pyrite veinlet
349-1e	24	0.5	124	12	70	24	2	<10	<10	6	disseminated sulphides in diorite
349-1g	7872	1	875	14	54	33	25	11	<10	30	silicified, veinlets
349-1h	6292	2	0.14%	12	60	22	2	<10	<10	245	quartz-pyrite veins
349-1j	6481	1	0.11%	12	83	33	2	<10	<10	16	skarn
349-2	33356	19	0.19%	26	59	56	32	20	24	205	skarn
349-3b	452	1	239	40	47	35	5	<10	26	14	quartz-pyrite veins
349-3c	4276	<.5	345	8	10	72	3	<10	21	182	silicified, veinlets
349-3d	27		143	12	25	67	2	10	20	6	silicified, veinlets
349-3f	153	1	356	14	44	56	13	10	49	25	silicified, veinlets

Notes: Au by fire assay, ICP; Ag, Cu, Pb, Zn, Co, Ni, Mo, As, by Atomic absorption; Cr by XRF

and sericitization occurring a few metres adjacent to the veins, and carbonate alteration, to several tens of metres. Most veins have sharp contacts with wallrocks. They commonly occur in high-angle faults, typically as en-echelon veins; some are associated with broad areas of fracturing with gold and sulphides occurring in quartz veinlets or stockworks. Although intrusive rocks are not associated with all Au-quartz veins, many occur along the margins or within syn to post-collisional, felsic to intermediate plutons.

SHEEP CREEK CAMP

Introduction

The Sheep Creek camp, located 12 kilometers southeast of Salmo (Figure 1-1), includes more than a dozen past-producing gold-quartz vein deposits in dominantly EoCambrian quartzites of the Reno and Quartzite Range formations. Production from this camp, between 1899 and 1988, totaled 23 101 859 grams of gold (761,456 ounces) and 9 102 786 grams of silver (280,495 ounces) from 1.53 million tonnes of ore; remaining reserves in these deposits are estimated to be approximately 3 940 kilograms of gold (Schroeter and Lane, 1991). The largest individual produc-

ers in the camp were the Queen, Reno and Kootenay Belle deposits (Appendix 1).

The first mine in the camp, the Yellowstone, was discovered in 1896 and began production in 1899. Shortly after, the Queen (1900), Motherlode (1906), and Kootenay Belle (1905) mines began production (Photo 3-2). This early production was concentrated mainly in upper levels of veins that had been enriched by oxidation and leaching. The second period of mining began in 1928 when a new vein on the property, the Reno, was brought into production and other older mines reopened (Mathews, 1953). Production in the camp reached its peak in 1937 and continued at high levels until 1942. A 100-ton cyanide mill was built on the Kootenay Belle mine in 1934 and operated until the mine closed in 1942. Gold Belt Mining Company Limited was formed in 1932, and after acquisition by North American Mines, Inc., a 150-ton mill was installed in 1943.

In 1934 a number of properties, including Queen, Yellowstone, Alexandra, Vancouver and Midnight were amalgamated under the newly formed Sheep Creek Mines Ltd. This company produced from the Queen vein until 1938, and intermittently from other properties until 1970.

Exploration and development work has continued on a number of properties of the Sheep Creek camp. In 1982 some rehabilitation work and drilling were done by Carl Creek Resources, and in 1984 approximately 2 000 tonnes of low grade ore were shipped to the Trail smelter. Work in 1986 by Gunsteel Resources Inc. and Nugget Mines Ltd. was concentrated on the Nugget Mine and included underground rehabilitation, installation of surface facilities and minor drilling (Allen, 1987). Two tunnels explored the Nugget and Calhoun veins. Another company in the Sheep Creek camp, Goldrich Resources Inc., concentrated exploration on their Goldbelt property (Ellerington, 1987). This work included underground rehabilitation and mapping, geophysical and geochemical surveys and diamond drilling on a number of the veins. Some exploration has continued into the 1990s, including a self potential survey at the Reno mine (Endersby, 1992).

REGIONAL GEOLOGY

Veins of the Sheep Creek camp are mainly within quartzitic rocks of the Reno and Quartzite Range Formations. These comprise massive, thick-bedded quartzites, argillaceous quartzites and minor argillite deposited as a north to northwest prograding fluvial-deltaic complex along the ancestral western margin of North America in latest Pre-Cambrian to Early Cambrian time. They are overlain by the Laib Group, consisting of impure marbles, calcareous schists, phyllites of the Truman or Mohican Formation, and the immediately overlying Lower Cambrian Reeves or Badshot marble. Overlying rocks of the Upper Laib or Lardeau Group are within the Kootenay terrane.

The structure of the area is well described by Mathews (1953). It is dominated by the Sheep Creek anticline, a major overturned isoclinal fold that has been traced from south of the United States border to north of the Sheep Creek camp. In the vicinity of the camp, it consists of a larger eastern anticline and a western subsidiary anticline (Mathews, 1953). These are cored by rocks of the Reno and Quartzite Range formations, with the Laib Group exposed in an intervening syncline. The folds trend north, have steep east-dipping axial surfaces, and plunge at low angles to the south and, locally, to the north. Most of the veins are on the west limb of the main eastern anticline and in the core and limbs of the western anticline.

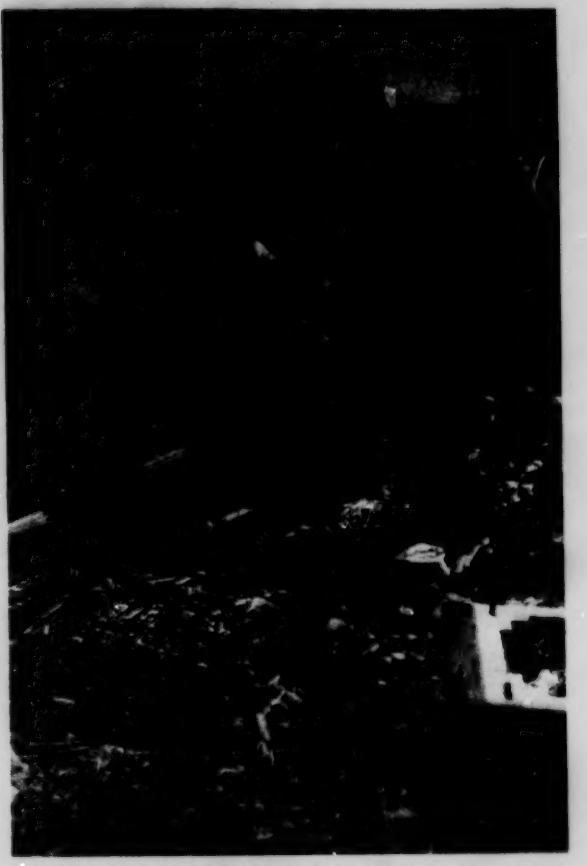

Photo 3-2. Remains of the Motherlode mill in the Sheep Creek valley, viewed towards the west, in the historical Sheep Creek gold camp.

Four well-defined sets of faults are recognized by Mathews (1953) in the camp. All the productive gold veins occur within a group of northeast-trending, generally southeast-dipping faults. These have up to 60 to 70 metres right-hand strike-slip motions and several tens of metres of normal displacement. Many are listric. These faults, referred to as the vein fractures, are refracted as they cross from argillaceous units into more competent quartzites, resulting in tensional regimes in quartzitic units. A north-trending quartz porphyry sill swarm cuts these northeast-trending faults.

A few northwest-trending faults, with left-lateral strike-slip motion may be the same age as the vein faults; these, however, contain no mineralization.

Two fault sets clearly post-date mineralization. North-trending, east-dipping faults, with normal displace-

ments up to 300 metres, and "flat-lying" faults with displacements of a few metres have been recognized in underground workings and on surface (Mathews, 1953).

A number of early Cretaceous stocks are exposed in the vicinity of the Sheep Creek camp, but none appear to be spatially related to the veins. As well, north-trending quartz porphyry sills and dikes, referred to as a sill swarm, occur throughout the mine area. The total width of the swarm ranges up to 50 metres, with individual sills varying from a few to 10 metres in thickness. The age of these sills, relative to faulting and mineralization, is not well known. According to Mathews (*op. cit.*), they cut the northeast-trending vein faults and vein quartz, but appear to be earlier than the sulphide and gold mineralization. Evidence for post-dike mineralization includes rare pyrite veinlets cutting the quartz porphyry, grains of sphalerite along the vein-porphyry contact and low gold values in the porphyry.

MINERALIZATION

Gold mineralization in the Sheep Creek camp occurs as Au-quartz veins within northeast-trending fault zones. These veins may be branching or occur as en-echelon arrays and can have been explored to depths up to 600 metres. A general description of veins is taken from Mathews (1953, p. 50):

"The gold deposits of the Sheep Creek camp consist essentially of quartz veins containing as a rule minor amounts of sulphides. Pyrite is the most abundant sulphide; sphalerite and galena are present, but as a rule it is only where the veins cut limestone that these two minerals occur in commercial quantities." Other reported vein minerals include calcite, sericite, scheelite, wolframite, chalcopyrite, chalcocite, arsenopyrite, marcasite, tetrahedrite, ruby silver and gold.

"Nearly all the production of gold has been from those parts of the veins where one or both walls consist of quartzite of either the Nugget or the Nevada members of the Quartzite Range Formation. Vein fractures cutting argillite are generally devoid of quartz or are occupied by only a thin band of barren vein matter. The extent of the productive part of any vein along the vein is, therefore, limited by the distribution of the favorable quartzite in its walls."

"The upper limit of orebodies is most commonly the ground surface, or in the Western anticline the crest of the quartzite beds, but in places in the southern part of the camp, even within a single type of rock, veins become narrower upward to the point that they cannot be mined economically. In general.... vein widths are average or greater than average on the lowest levels of most mines. However, high grade ore occurs less abundantly in the lower levels, and the proportion of the vein that could be mined profitably diminishes."

Recognition of vein quartz is often difficult within the host quartzites, particularly as vein contacts may be gradational into the host rock. In general, vein quartz is coarser grained, milky white in colour and may be banded parallel to the walls.

Gold occurs as isolated grains, generally from a few microns to 30 microns in size. Most gold occurs associated with sulphides, commonly along quartz-pyrite contacts or, less commonly, along contacts of other sulphides. Approximately 30% occurs in quartz, and very minor amounts in sulphide grains.

OTHER AU-QUARTZ VEIN DEPOSITS

A number of deposits within and along the margins of the Eagle Creek complex west of Nelson have been classified as Au-quartz veins (Appendix 1, Figure 1-1). Although most were small producers, the Kenville (Granite-Poorman) deposit has produced 2 024 216 grams of gold and 861 085 grams of silver. Other gold-quartz veins occur west of the main Rossland gold camp within fault zones in ultramafics and Elise Formation rocks.

KENVILLE (Granite-Poorman) (082F/SW086)

The Kenville deposit, staked in 1888, was one of the first vein deposits discovered in the Nelson area. It produced intermittently for more than 50 years until its closure in 1954. In 1995, Anglo Swiss Industries Ltd. and Teck Corporation, with Teck as operator, conducted prospecting, an induced polarization survey and 1140 metres of diamond drilling (Thomson, 1995). The veins form a northwest-trending system of quartz veins within mafic to ultramafic intrusive rocks of the Eagle Creek plutonic complex parallel to the northwest trend of the Silver King shear to the southeast. The veins comprise milky to glassy quartz with pyrite, chalcopyrite and minor amounts of galena, scheelite, sphalerite and some visible gold (BC MINFILE data). Disseminated sulphides occur in adjacent hostrocks; plagioclases in these rocks are commonly replaced by albitic and potassic feldspars, and ferromagnesium minerals by biotite and epidote.

ROSSLAND AREA

Au-quartz veins in the Rossland area are within mainly mafic metavolcanic rocks of the Elise Formation near the northern, faulted contact with an east-trending serpentinite (Fyles, 1984). In contrast with the veins of the Rossland camp, inferred to be genetically related to intrusion of the Rossland monzonite, these Au-quartz veins are assumed to be related to east-directed thrust faults that carried Mount Roberts Formation, unconformably overlying Rossland Group and ultramafic rocks over Rossland Group rocks.

Production from this camp totaled 1 094 000 grams of gold and 496 000 grams of silver; the largest individual producers were the I.X.L (811 746 grams Au) and Midnight (245 311 grams). They are described in more detail in Chapter 4.

POLYMETALLIC VEINS: Ag-Pb-Zn±Au

INTRODUCTION

Polymetallic Ag-Pb-Zn±Au veins are the most common deposit type in the Canadian Cordillera and constitute one of the largest silver resources in the world. They are

common throughout the Nelson-Rossland map-area, and many are past producers. These past producers include many of the veins of the Ymir camp, those within Elise Formation rocks southwest of Nelson, and a number in the South belt of the Rossland camp. These latter veins are described in Chapter 4.

Polymetallic veins have traditionally been considered to be related to intrusion of granitic stocks or batholiths. Supporting evidence includes the close spatial association of these veins and intrusions; many of the veins in the Nelson-Rossland map area are within or along the margins of the Nelson batholith or other small, related stocks. Beaudoin *et al.* (1992a; 1992b) have stressed the close genetic ties of these veins with major structures that appear to have formed late in the evolution of an orogen. As evidence, they cite the apparent age difference between intrusions and mineralization.

Polymetallic Ag-Pb-Zn±Au veins typically contain galena and sphalerite, with minor pyrite, chalcopyrite and sulphosalt minerals in a carbonate and quartz gangue (Lefebure and Church, 1996). They are generally narrow and steeply dipping, within fractures or fault zones. Wall rock alteration is commonly of limited extent, comprising sericitization, silicification and pyritization.

Appendix 1 lists the known polymetallic veins within the Nelson-Rossland map area. Examples described below typify the main camps; the Ymir camp, dating back to 1899, is the largest of these vein camps.

YMIR CAMP

The Ymir camp includes numerous silver-gold-lead-zinc veins in the Ymir Group and Nelson batholith east and north of the town of Ymir (Photo 3-3). Most descriptions of these veins date back to the time of their discovery and development (Drysdale, 1915; Cockfield, 1936); recent work is detailed in a number of company assessment reports. The veins are in an irregular north to northeast-trending belt within the Ymir Group and the southern 'tail' of the Nelson batholith. This belt parallels the regional foliation trend in the Ymir Group as well as the Ymir-Nelson contact. It also coincides with the tectonic boundary between Quesnellia and North American rocks, a boundary that is exposed as the Waneta fault to the southwest but is obscured in the Ymir camp by the Nelson batholith 'tail'.

The camp was discovered in the late 1800s with production beginning at the Ymir, Dundee and Protection deposits in 1899 (Appendix 3). Production reached a peak in the 1930s and was, during these years, the largest silver-producing camp in the British Commonwealth. Production from these deposits ceased in the early 1950s, with total production of 43 006 kilograms of silver and 8 294 kilograms of gold.

The Ymir Group consists of several hundred metres of argillaceous quartzites overlain by a thick succession of grit, siltstone and argillite with discontinuous bands of thin-bedded impure limestone. It has a prominent north-trending foliation, and appears to be internally folded. The 'tail' of the Nelson batholith comprises three subvertical, subparallel, compositionally distinct sheets separated by thin screens of country rock (Vogl and Simony, 1992). High temperature mylonitic fabrics, with dextral sense of displacement, appear to coincide with the northern extension of the Waneta fault, implying at least some motion on the fault either synchronously or immediately after emplacement of the batholith (Vogl and Simony, *op. cit.*). Farther north, however, pendants within the Nelson batholith expose the Waneta fault and there it is clearly truncated by the batholith (Figure 1-1).

Many of the veins in the Ymir camp have a strong structural control, with associated shearing and local development of gouge. They can extend over more than a kilometre in length and many individual mines or showings, such as Yankee Girl, Dundee and Two Star deposits, are along the same structure. This structure trends northeast, cross-cutting Ymir stratigraphy into the Nelson batholith. The most prominent vein attitudes are north-northeast and steeply west-dipping, parallel to shears in Elise Formation rocks farther west (Figure 2-1). Commonly veins follow the main shears as well as small cross faults between shears. For example, at the Centre Star deposit (082F/SW066), two vein sets, one trending northeast and the other north to northwest, are within or parallel to faults between two more northerly-trending shear faults (Cockfield, 1936). The northeast-trending veins are mineralized extension or dilation faults whereas the less mineralized north-trending veins parallel the flattening or compressional faults within a northeast trending shear zone with right-lateral motion.

Most veins contain galena, sphalerite, pyrite and pyrrhotite in a quartz-rich gangue. Native gold is common in some of the veins, and native silver is reported from the Elise deposit. Chalcopyrite and, less commonly, arsenopyrite occur in many of the veins, generally associated with pyrrhotite. In some veins (e.g., Centre Star), a vertical zoning is apparent, with pyrite more abundant at higher levels and pyrrhotite in lower levels. Vein gangue is mainly quartz with locally minor carbonate, either dolomite or siderite, sericite or tourmaline. Oxidation of some veins has produced limonite and occasionally cerussite or manganite.

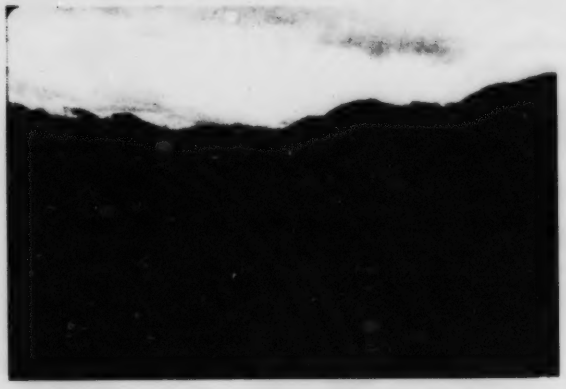

Photo 3-3. View of hillside above Ymir, showing location of some of the historical Ymir silver mines.

A regional precious metal zonation, based on published production data (Appendix 3) is apparent. In general, more northern veins have higher gold/silver ratios than those in the very southern part of the camp. These variations appear to be independent of host lithologies, alteration assemblages or type or degree of shearing. The only noted mineralogical change that accompanies these changes is a higher concentration of arsenopyrite in the more northern deposits. Due to limited recovery of zinc or copper, it is difficult to determine if there is consistent variation in base metal ratios.

Wall rock alteration is generally limited to silicification and sericitization. Disseminated pyrite, extending several metres into the country rock is also common. Some veins are highly fractured and brecciated, and others contain graphitic fault gouge.

The age of these veins is not known. Their close spatial association with the tail of the Nelson batholith suggests a genetic link. Their formation in dextral shear zones that may be related to the northern extension of the Waneta fault implies an age synchronous with latest motion on the fault. However, many veins appear to crosscut the prominent north-trending foliation in the Ymir Group and some, such as the Wilcox deposit, cut the mylonitic fabric within Nelson batholith rocks. These mylonites are typical of high temperature shear zones, suggesting formation during or shortly after intrusion (Vogl and Simony, 1992). Brittle fractures and veins within the shears imply formation after cooling through the ductile-brittle transition, possibly as late as Cretaceous time as K-Ar biotite dates in the 'tail' have Cretaceous ages (Archibald *et al.*, 1983). However, Pb isotope analyses, discussed in detail in Appendix 8, group these veins with polymetallic and gold-quartz veins of the Nelson and Rossland camps. This data suggests that the deposits may be related to I-type granitic rocks of Jurassic age.

SILVER KING (082F/SW176)

Names: Silver King, Dandy, Ollie, King, F.S., D50, D45, Iroquois, Kohinoor, Kootenay, Bonanza
Location: Lat. 49°25'18" N; Long. 117°18'00" W;
Elev. 1800 metres

INTRODUCTION

The Silver King mine is located 4.5 kilometres south of Nelson on the northeast side of Toad Mountain (Figures 1-1, 3-4). It comprises a number of sheared polymetallic veins in the Elise Formation. It is accessible via the Giveout Creek and Silver King roads, south of Nelson. Exposures are generally scarce in the area, and growth of brush and timber are heavy (Photo 3-4).

The Silver King deposit, discovered in 1886, spurred exploration and initiation of mining in the Nelson area. Production began on a large scale in 1896 and continued through to 1910 by Hall Mining and Smelting Co. Ltd. and Kootenay Development Syndicate; further intermittent production continued, mainly by Consolidated Mining and Smelting Ltd, until about 1949. Total production from the Silver King veins is greater than 200 000 tonnes with recovery of 138 214 kg of silver, 6 789 million kg of copper and 8 896 grams of gold (Appendix 3).

In 1965, New Cronin Babine Mines Ltd. undertook an extensive re-evaluation of the property, reopened underground workings, and from 1965 to 1967 drilled 3710 metres in 54 holes. This work identified a new vein, the King vein, and increased the total proven reserves to 75 026 tonnes containing 295 g/t Ag, 2.1% Cu and 0.9% Pb.

Sproatt Silver Mines conducted a geochemical and geophysical survey in 1973, and outlined two coincident anomalies, one over the Iroquois vein and a second on a new target located 200 metres farther south (White and Cruz, 1973).

In 1981, Hecate Gold Corporation did some sampling and mapping, and in 1983, Mine Quest Exploration Associates Ltd., for Host Ventures Ltd., conducted an exploration program that included 566 metres of diamond drilling, considerable trenching, sampling and mapping (Aylward, 1983).

Proposed work (1998) by Amulet Resources Ltd., current operators, includes an I.P. survey and drilling of three or four holes.

The property geology in this report is based largely on the published results of these exploration programs.

REGIONAL GEOLOGY

Silver King is within the Elise Formation in the Silver King shear zone (Figure 3-4). The Silver King intrusion, a leuco-diorite porphyry characterized by 30 to 60% plagioclase phenocrysts, is located approximately one kilometre to the northeast; similar, highly sheared intrusive rocks are exposed just to the southeast in the Silver King shear zone and the core of the Hall Creek syncline. Two samples of the Silver King intrusion have yielded U-Pb zircon ages of 177±3.0 Ma and 172±6.0 Ma (Höy and Dunne, 1997).

The Elise Formation in the Silver King deposit area comprises highly sheared, mafic volcanic rocks. These have been assigned to the Lower Elise (Höy and Andrew, 1989a;b); however, due to the structural complexity in the

Photo 3-4. View of the Main Silver King vein, looking towards the northwest.

area, it is possible that they are a mafic component of the Upper Elise.

The Silver King shear is a zone of intense shearing, nearly a kilometre in width, that trends northwest from the core of the Hall Creek syncline, through the Elise volcanics and into the Eagle Creek plutonic complex. To the southeast it deforms the Silver King intrusion, then appears to die out farther south at higher structural levels in the limbs of the Hall Creek syncline (Figure 1-1). The age of the shearing and associated folding is bracketed between the *ca.* 175 Ma Silver King intrusion and essentially post-kinematic *ca.* 165 Ma Nelson batholith.

PROPERTY GEOLOGY

The Elise Formation in the deposit area comprises dominantly augite phyric volcanic rocks and chlorite schist. Previous workers (*e.g.*, H.L. Hill, 1965, unpublished report) have interpreted the more massive units as mafic intrusions within schistose tuffs, whereas Wiswall (1981; in Aylard, 1983), based largely on the gradational nature of the contacts, suggested that these are more competent mafic flows and clastic rocks preserved as cores within sheared tuffaceous volcanics.

The clastic volcanic rocks are either coarse mafic pyroclastic breccias or flow breccias. They typically contain the veins and anomalous metal values, possibly due to their more competent nature. "Pods of felsic material", generally concordant with foliation, include "quartzite" and "rhyolitic" material, interpreted to be both metasediments and felsic volcaniclastics (Wiswall, 1981). It is possible that the 'rhyolite' is similar to the felsic intrusive lenses on the Great Western property that are at least 10 million years younger than the Elise Formation (Appendix 4). Alternatively, the "rhyolite" may be older, Elise-age felsic volcanics.

The Silver King porphyry intrudes the chlorite schists, with "apothyses of Silver King porphyry in chlorite schist, xenoliths of the schist, and sharp, cross-cutting contacts" (Wiswall, 1981). It is not an important host for Silver King mineralization.

MINERALIZATION AND ALTERATION

The veins of the Silver King camp include the Main Silver King vein, the Iroquois vein, the King vein and the Kohinoor vein. All trend northwest, within and approximately parallel with the Silver King shear. The veins comprise mainly quartz with calcite, iron carbonate and minor hematite; sulphide minerals include pyrite, chalcopyrite, galena, minor sphalerite and locally, trace stromeyerite, tetrahedrite and bornite. Large prominent lamellae of a black, submetallic mineral may be manganite (Mulligan, 1952). Regional alteration within the shear includes pervasive development of calcite and replacement of mafic minerals by chlorite; iron carbonate, sericite and locally K-feldspar alteration occur more proximal to the veins.

The Iroquois structure has been traced or is inferred to have a strike length of nearly three hundred metres. It comprises irregular stringers and massive quartz with abundant disseminated pyrite, concentrations of chalcopyrite and galena, and minor bornite. Sulphides are commonly concentrated in east-west cross fractures within the shear zone. The immediate hangingwall and footwall are bleached, probably due to sericite and silica alteration. Assays of a number of grab samples, listed in Table 3-7, show silver content up to 456 grams/tonne. Drilling intersected bleached zones with disseminated pyrite, two to five metres in width, with intensely silicified intervals containing abundant stringer pyrite and variable sphalerite; however, silver content is low in these zones, up to 48 grams/tonne (Aylward, 1983).

The Main Silver King vein structure is located 300 metres north of the Iroquois vein. It has a strike length of at least 700 metres and appears to be on strike with the King vein, 300 metres farther east. The vein has a gangue of quartz and iron carbonate, with variable concentrations of pyrite, chalcopyrite, galena and sphalerite; in general, lead and zinc content increase to the west. Although mineralization is erratic within the Main vein, widths up to 15 metres are noted by Lorimer (1967). Locally higher sulphide concentrations occur in cross-fractures, similar to those in the Iroquois vein. In the open pit area, an east-west structure, the footwall vein, appears to intersect the Main vein and is the location of most past production as well as present reserves.

Drilling of the King vein in 1965-1967 outlined a reserve of 37 000 tonnes containing 346 g/t Ag and 2.8% Cu (Lorimer, 1967). Further drilling in 1983 also intersected the vein (Table 3-7) and trenching located the vein, for the first time, at surface. It occurs as a highly weathered and fractured structure within augite phyric, manganese-altered Elise volcanic rocks; recognized sulphides include pyrite,

TABLE 3-7
ANALYSES OF SELECTED SAMPLES FROM TRENCHES AND DRILL CORE, SILVER KING DEPOSIT

Sample number	Type	Au ppm	Ag ppm	Cu %	Pb %	Zn %
Iroquois vein						
21391	1 m chip	<0.1	209	1.74	0.36	1.2
21342	3 m chip	1.1	487	0.17	0.59	1.32
21345	3 m chip	0.3	206	0.27	0.71	1.86
Main vein						
21206	1.2 m chip	0.1	103	0.33	0.29	0.00
ddh SKD9	0.5 m	0.9	219	0.56	0.04	0.01
ddh SKD8	0.9 m	0.35	113	0.46	0.02	0.02
ddh SKD10	0.5 m	0.7	110	0.11	0.01	0.00
98SK-1	grab	312 ppb	559	5.02	1.53	2.10
King vein						
21210	1 m chip	<0.1	29	0.2	0.47	0.06
21211	1 m chip	<0.1	16	0.08	0.43	0.05
ddh SKD2	0.5 m	0.1	298	1.54	0.11	0.17
Kohinoor vein						
21227	0.5 m chip	0.006	52	0.42	0.84	0.69

Note: analyses by Chemex Labs Ltd., Vancouver, B.C.
data from Aylward, 1983; sample 98SK-1;
selected hand sample, this study

chalcopyrite and galena (Aylward, 1983). Minor disseminated sulphides, including chalcopyrite, also occur in the footwall of the vein.

The Kohinoor vein, located about 150 metres south of the King vein, was discovered by the 1965-1967 drill program, and subsequently drilled and trenched in 1983. Mineralization is discontinuous and erratic. Trench SKTR 4 exposed a 0.5 metre-wide silicified zone with minor pyrite, chalcopyrite, galena and sphalerite in sheared mafic volcanics. An assay of a 0.5 metre chip sample is listed in Table 3-7.

SUMMARY AND DISCUSSION

The Silver King deposit consists of a number of Ag-Pb-Zn-Cu veins in Elise volcanics in the Silver King shear. The distribution and concentration of sulphides in the Silver King veins are controlled by the shear, cross-fractures, and the occurrence of more competent units of the Elise. There appears to be no correlation between vein sulphides and the Silver King or Nelson intrusions.

The origin and age of these veins is not known. It is possible that they are synkinematic veins, related to development of the Silver King shear. Alternately, they are earlier than the shear zone, possibly distal polymetallic veins related to the Eagle Creek plutonic complex. Copper-gold porphyry and vein mineralization occur within and along the margins of this complex.

CLUBINE (082F/SW200)

Names: Clubine, Comstock, Boulder City
Location: Lat. 49°14'15" N; Long. 117°16'10" W
Elev. 1037 metres

INTRODUCTION

Mineralization on the Clubine property includes a number of zones of silver-lead-zinc ± gold mineralization in argillite and mafic volcanic rocks near the contact of Early Jurassic Hall and Elise formations. These zones are exposed in a number of trenches at the Maggie Zone on the northeast ridge of Keystone Mountain, and at the past producing Clubine-Comstock mine about one kilometre west of the confluence of Key and Boulder Mill creeks, 5 kilometres north of Salmo (Figure 3-12).

Access to the property is via the Boulder Creek road (4-wheel drive) that leaves the Salmo-Ymir highway 4 km north of Salmo.

EXPLORATION HISTORY

Work on the Clubine property between 1926 and 1942 by Clubine Comstock Gold Mines Ltd. concentrated on the Clubine-Comstock occurrence, a northwest-trending gold-silver-lead-zinc bearing quartz vein system on Key Creek, 4 kilometres north of Salmo. The Clubine-Comstock workings are on five levels; quartz veins in the uppermost level have elevated lead-zinc values whereas the lower levels have higher gold values (B.C. Report of the Minister of Mines, 1934). Total production from the mine, mainly from 1936 to 1939, was 3 616 tonnes with recovery of 123 293 grams of gold, 239 463 grams of silver and 818 kilograms of zinc (Appendix 3). About 83 percent (2 990 tonnes) of the total was mined in 4 years from 1936 to 1939.

During this time other precious and base metal quartz vein deposits in the vicinity of Keystone Mountain were also in production. These included the Second Chance (BC MINFILE 082F/SW201), Keystone (082F/SW202), Gold Hill (082F/SW204) and Arlington (082F/SW205). The Arlington deposit produced 69 823 tonnes with recovery of 1 700 339 grams of gold, 4 334 578 grams of silver, 520 420 kilograms of lead and 456 920 kilograms of zinc.

In 1989, diamond drilling by YellowJack Resources Ltd. intersected gold-bearing quartz veins and silicified zones beneath the No. 5 level of the Clubine-Comstock occurrence (Cooke, 1990; Figure 3-13). The Maggie Zone to the northwest, an area of anomalous silver, lead, zinc and copper, was discovered in 1990 by YellowJack Resources Ltd. during the course of geophysical and soil geochemical work over the whole of the Clubine property. Trenching on this zone uncovered significant lead-zinc and silver-bearing quartz-carbonate veins.

REGIONAL SETTING

The Clubine property lies on the east limb of the Hall Creek syncline just north of Salmo (Figure 3-12). The Hall Creek syncline is a tight, south-plunging fold that can be traced from north of Hall Creek in the Nelson area, to Salmo. Near Salmo, it is cut by the Erie Creek fault, a Tertiary east-side-down normal fault, but is exposed south of Salmo as an overturned, east-dipping syncline called the Hellroaring Creek syncline. Both Hall and Hellroaring Creek synclines are the earliest structures recognized in the Salmo area.

A slaty cleavage in clastic rocks and a penetrative foliation in volcanic rocks parallel the axial planes of the Hall Creek and Hellroaring Creek synclines. A number of faults or shear zones in the volcanic rocks parallel the margins of the synclines (Andrew and Höy, 1991).

East and northeast-dipping normal faults, such as the Erie Creek fault, are the youngest structures in the Clubine area. They may be related to Middle Eocene extension recognized throughout southeastern British Columbia.

The Early Cretaceous Hidden Creek granite stock intrudes the eastern part of the Clubine area and a granite stock, of unknown age, intrudes south of Keystone Mountain. The Hidden Creek stock comprises 10 to 15% plagioclase (An_{60-86}), 15 to 20% microperthite, 50 to 60% orthoclase, 25 to 30% quartz, up to 2% biotite and 1 to 2% opaques. Numerous small dikes, one-half to two metres wide, trend north to northwest across the property (Figure 3-13). They are of various compositions including lamprophyre, hornblende diorite, quartz porphyry and massive rhyolite and are probably mainly Middle Eocene in age.

PROPERTY GEOLOGY

The eastern part of the Clubine property is underlain by mafic volcanic rocks of the Elise Formation; the western part, by the Hall Formation. The Elise Formation consists of augite porphyry flows and lapilli, crystal and fine tuffs. Unaltered primary mafic minerals are rare in the augite por-

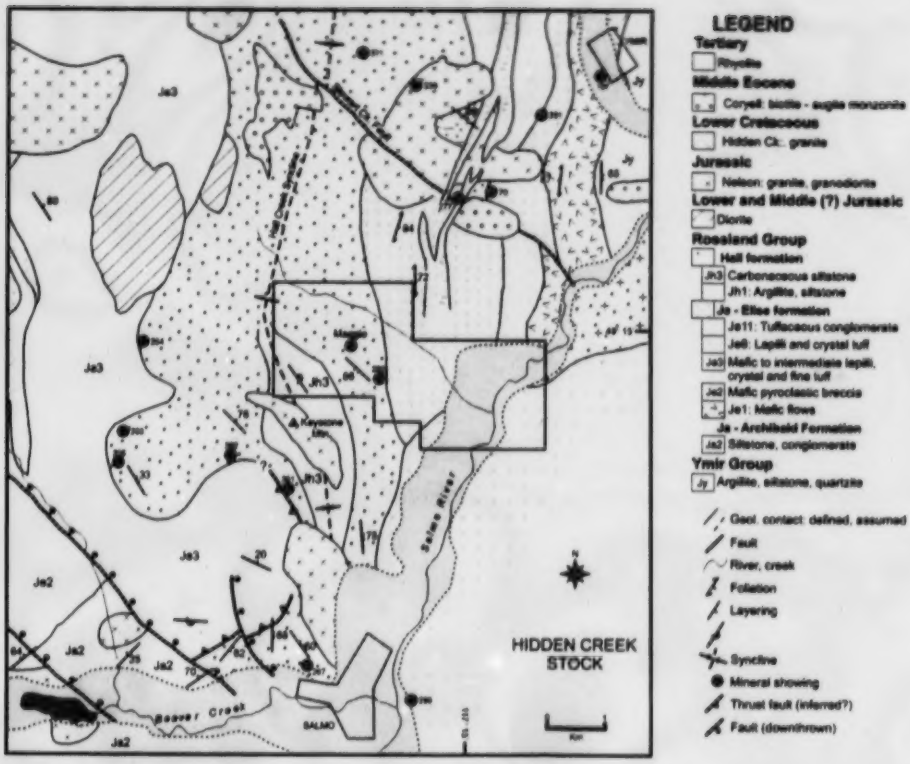

Figure 3-12. Geology of the Erie Lake area, showing the location of mineral deposits (after Höy and Andrew, 1989; 1990; Little, 1960; 1965; Mulligan, 1952 and Fitzpatrick, 1985).

phyry flows but relict blue-green amphibole (15-20%) and green biotite (10-15%) can sometimes be distinguished. The mafic minerals are variably altered to chlorite and epidote. Apatite is a common accessory mineral in the flows. Lapilli tuffs contain subrounded to subangular volcanic fragments (up to 5 cm in diameter) that vary from coarse augite porphyry to crystal and fine tuff. The crystal tuffs contain 20 to 25% plagioclase (An_{55-59}) and minor (5 to 10%) albite. Most mafic minerals are variably altered to chlorite and epidote. The volcanic succession is intruded by a lensoid monzogabbro sill near the contact with the Hall Formation north of Key Creek. A number of these monzogabbro/gabbro sills or small stocks occur throughout the exposures of the Elise Formation and are interpreted to be high-level syn-Elise intrusions (Dunne and Höy, 1992).

The contact between the Hall and Elise formations is not exposed on the property. However, discordant bedding attitudes in the Elise and Hall suggest either a disconformable or faulted contact. The exposed thickness of the Hall in the Clubine area is approximately 1700 metres (Figure 3-14). It is divisible into a lower, rusty-weathering black siltstone and argillite succession and an upper carbonaceous siltstone unit. A central coarse conglomeratic phase, seen elsewhere in exposures of the Hall Formation, is missing. The upper Hall appears to be laterally discontinuous; it is only recognized in the vicinity of Keystone Mountain. Occasional rip-up clasts and flame structures in the Hall Formation that indicate facing directions and bedding/cleavage intersections imply that the property is on the east limb of the Hall Creek Syncline.

MINERALIZATION AND ALTERATION

A number of quartz and quartz-carbonate precious and base-metal vein occurrences are in the upper 500 metres of the Hall Formation and lower part of the Elise, in the Keystone Mountain area. They generally trend north to northwest and dip steeply northeast and include variable amounts of galena, pyrite, chalcopyrite with minor sphalerite, tetrahedrite and pyrrhotite.

The Clubine property has two principle showings; the Clubine-Comstock workings (082FSW200) and the Maggie Zone.

The Clubine-Comstock, hosted mainly by the Elise Formation, has lenses of quartz and quartz-carbonate up to 0.5 metres wide with variable amounts of pyrite, chalcopyrite, galena and minor sphalerite and pyrrhotite. The lenses or veins of the main workings are commonly brecciated and parallel to the footwall of a biotite lamprophyre dike. Gold (34.6 g/t over 21.6 m in level No. 2 and 14.7 g/t over 8.6 m in level No. 5) occurs in the vein quartz and also within broad silicified and pyritic zones (Cooke, 1990). The No. 1 level workings, in the Hall Formation 60 metres west of the main workings, have veins with lesser gold content but higher lead and zinc values.

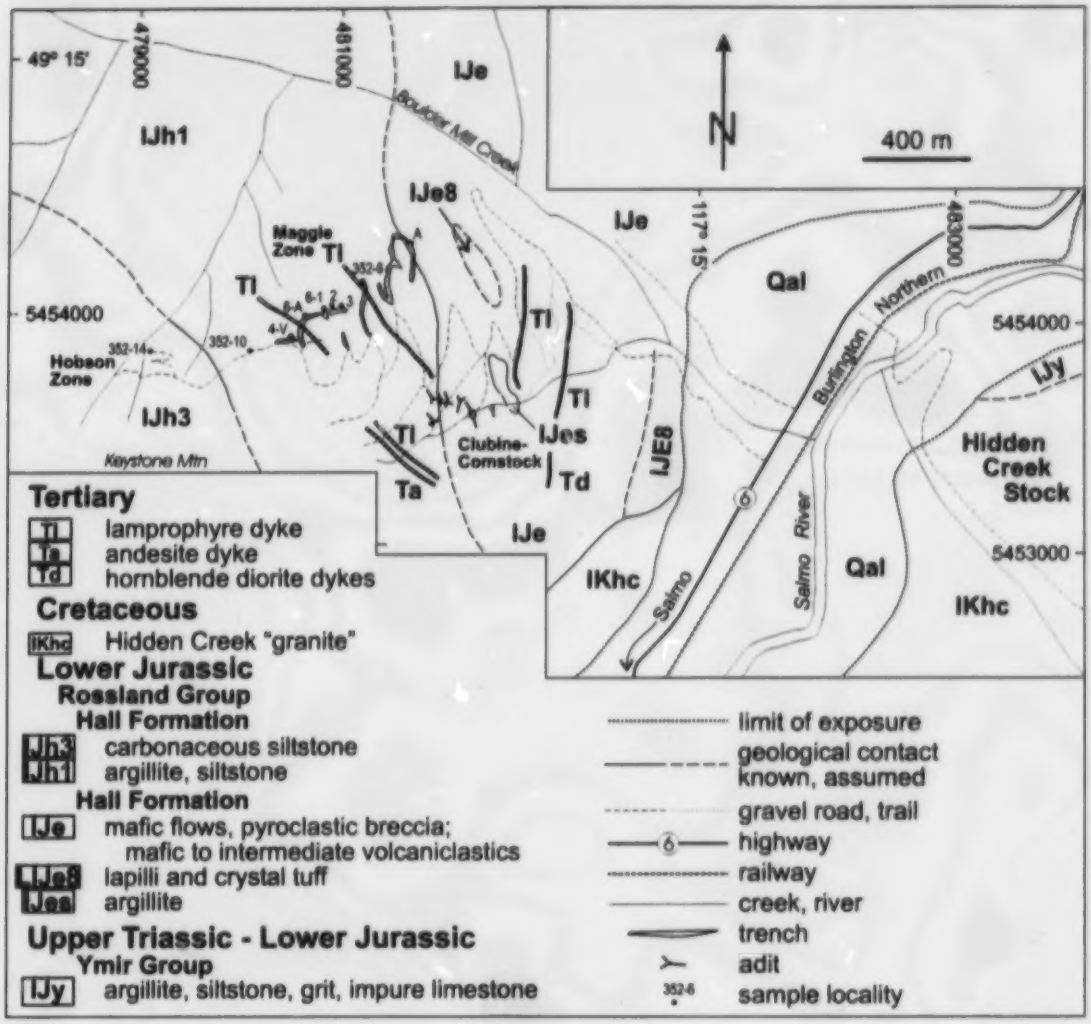

Figure 3-13. Geology of the Clubine prospect (from Dunne *et al.*, 1992).

The Maggie Zone consists of 12 to 15 cm widths of brecciated quartz and quartz-carbonate veins. In thin section, vein material appears as translucent quartz and rarely carbonate crystals crosscut by a dense network of wispy microfractures defined by tiny (<2 microns) fluid inclusions. The wispy quartz texture is commonly observed in veins formed at deep crustal levels (>4 km) (Reynolds, 1991). The selvages of the veins are commonly marked by 2 to 3 cm of massive 'steely' galena and/or 8 to 10 cm of coarse-grained, euhedral, slightly oxidized galena (90%), pale sphalerite (<3%) and trace pyrite. This zone has high silver and lead but low gold and zinc values (Table 3-8). A distinctive yellow-green alteration envelope of mica(?) and iron carbonate(?), 5 to 10 centimetres wide, surrounds some of the veins in the Maggie zone.

Analyses of selected vein samples from the Clubine property, not including the Clubine-Comstock workings, are given in Table 3-8. This data indicate a strong positive correlation between gold, silver and lead (Dunne *et al.*, 1992). Zinc and molybdenum also have a positive correlation, although the actual concentrations of these elements are relatively low.

SUMMARY AND DISCUSSION

The concentration of veins near the contact of the Elise and Hall formations may result from shearing near the sedimentary/volcanic contact.

The age of these veins is not known. They may be associated with either the Middle Jurassic Nelson intrusions or the Early Cretaceous Hidden Creek stock, an interpretation supported by Pb isotope data (Appendix 8). However, it is possible that the veins are Tertiary as they trend north, parallel to Tertiary structures, and some are spatially associated with Tertiary dikes.

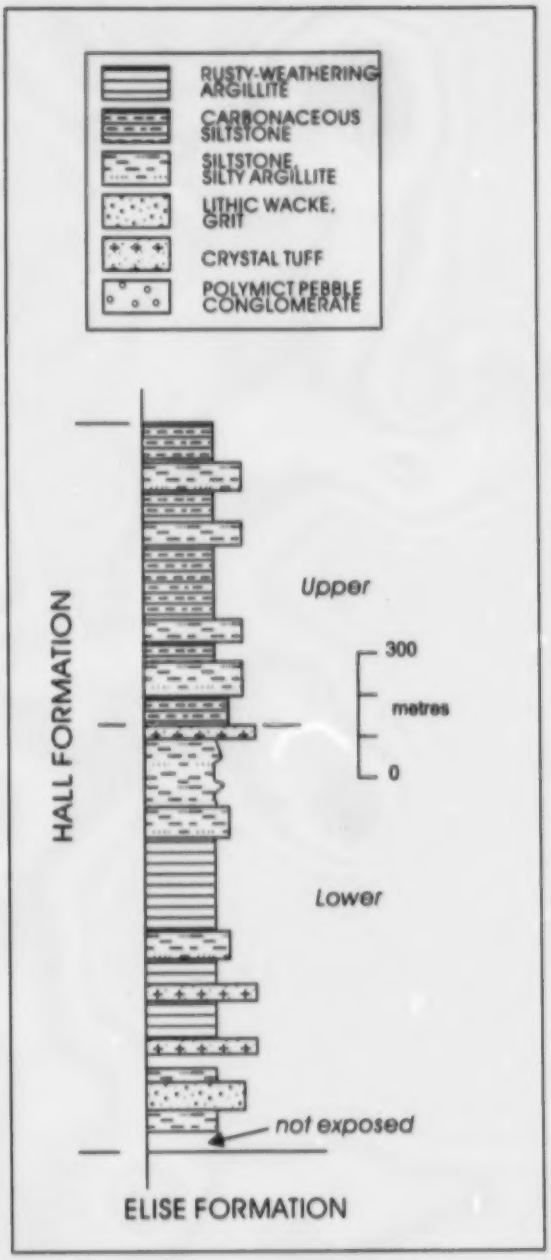

Figure 3-14. A stratigraphic section of the Hall Formation in the Keystone Mountain area (from Höy and Dunne, 1997).

The variation in composition from gold-bearing at the Clubine-Comstock to silver-lead bearing at the Maggie zone may reflect the different host rocks for these two systems: Elise volcanic rocks versus Hall argillite, respectively. However, dominantly gold-bearing quartz veins have been reported elsewhere in the Hall Formation at the Keystone, Canadian King and Arlington deposits. It is possible that the Maggie veins were deposited in the same vein system as the Clubine-Comstock but at a deeper structural level.

OTHER DEPOSITS

VELVET (082F/SW162)

Names: Velvet (L.2521), Portland (L.2523), Velvet-Portland
Location: Lat. 49°00'45" N, Long. 117°54'50" W
Elev. 1200 metres

INTRODUCTION

The Velvet Mine is a gold-silver-copper vein system within ultramafic pendants in Middle Eocene Coryell intrusive rocks southwest of Rossland (Figures 1-1, 4-2, in pocket). The host ultramafic rocks contain large xenoliths(?) of mafic volcanic rocks and are intruded by Coryell and later dikes. The age and origin of these veins is not known; they may be related to deformation in Early to Middle Jurassic time or to Middle Eocene tectonic-magmatic events.

Access to the area is by a well-maintained gravel road that extends approximately 13 km southwest from Rossland. Property access is via two 4-wheel-drive roads that branch north from the main road (Figure 3-15).

Between 1901 and 1964, the Velvet Mine produced 88 833 tonnes of ore yielding 620 785 grams gold, 664 359 grams silver, 1 154 104 kg copper and minor amounts of lead and zinc (Appendix 3). Potential reserves on the property are 450 000 tonnes containing 12 g/t gold, 31 g/t silver and 6.5% copper (International Prospectors and Developers, Nov/Dec 1983).

EXPLORATION HISTORY

The Velvet and Portland Crown-granted claims were located in 1896 at approximately 1200 metres elevation on the northwest slope of Sophie Mountain in the valley of Big Sheep Creek south of Rossland (Photo 3-5). These adjacent claims were developed separately until 1904 when Velvet-Portland Mines Ltd. formed and acquired both properties. The Velvet mine was operated intermittently by this and several other companies until 1967, with closures between the years 1916-20, 1928-32, and 1942-52. In 1978,

Photo 3-5. View of the waste dumps at the Velvet deposit, with mainly dark ultramafic blocks in the foreground and rusty-weathering pyritic rocks in the backround.

TABLE 3-8
ANALYSES OF SELECTED SAMPLES OF THE CLUBINE PROPERTY
(from Dunne *et al.*, 1992)

Lab[1]	Sample	Width	ppb Au[2]	Ag[3]	Cu[3]	% Pb[3]	% Zn[3]	Co[3]	Ni[3]	Mo[3]	As[3]	Cr[4]	Ba[4]	Sr[4]
42076	Club6-1	grab	9	6	21	0.23	0.26	16	30	<10	85	102	1375	99
42077	Club6-A	0.20 m	3	7	32	0.24	0.19	49	590	<10	925	1372	177	582
42079	Club4-V	0.20 m	14	8	137	1.47	1.93	44	7	<10	21	36	745	18
42083	352-1	grab	21	372	8600	1	1.05	15	44	13	205			
42084	352-6	grab	34	1789	154	49	0.38	12	3	11	1400			
42085	352-14	grab	46	57	103	11.3	2.1	39	5	<10	107			
42086	Club4-1	0.20 m	279	2230	3300	73	1.43	2	5	<10	95			
42087	Club4-3	0.15 m	20	6	37	0.49	0.39	48	49	16	75	95	1125	17
42088	Club6-2	grab	4	26	31	0.65	3.03	42	14	<10	95	47	695	254
42089	Club6-3	grab	9	618	312	11.3	3.91	42	18	<10	23			

Lab[1] No.	Sample Width	Au[5] ppm	Ag[5] ppm	Cu[5] ppm	Pb[5] %	Zn[5] %	Co[5] ppm	Ni[5] ppm	Mo[5] ppm	As[5] ppm	Cr[5] ppm	Ba[5] ppm	Sr[5] ppm
38777	grab	0.03	0.5	13	0.0002	0	6	4	3	13	40	145	137
38778	grab	0.03	1.2	31	0.01	0.45	215	380	42	31	10	599	155
38779	grab	0.03	0.3	57	0.008	0	80	549	2	20	234	120	79
38780	grab		83.7	783	4.27	0.19	21	27	12	14516	9	85	25
38781	grab	0.03	13.9	86	0.49	0.09	19	23	10	77	11	91	26
38782	grab	0.03	17.8	399	0.39	0.13	18	41	8	12167	7	168	97
38783	grab	0.03	468.6	237	64.25	0.34	8	7	5	3083	2	14	31
38784	grab	0.03	2	19	0.41	0	3	5	2	38	5	30	6
38785	grab	0.03	8.3	96	0.58	0.3	13	26	2	80	6	48	128
38786	grab	0.03	21.9	99	0.72	0.46	16	41	8	39	7	48	74
38787	grab	0.03	211.7	2149	4.51	0.43	15	64	7	868	55	207	151
38788	grab	0.1	376.2	5853	55.34	0.98	1	10	1	106	2	22	29
38789	grab	0.13	26.1	124	1.35	0.27	8	31	9	85	19	92	19
38790	grab	0.03	41.1	94	0.96	0.09	2	12	11	17	5	96	6
38791	grab	0.13	0.7	88	0.01	0.01	13	6	2	25	6	71	58
38792	grab	0.03	0.9	11	0.02	0.01	2	5	3	8	4	20	14
38793	grab	0.03	0.4	7	0.02	0	2	12	3	5	9	15	5

Sample No.	Sample Width	Ag[2] ppm	Pb[2] %	Zn[2] %
Tr3-#2	grab	81.4	4.27	0.19
Tr4-#3	grab	1637	54.25	0.34
Tr6-#1	grab	818.7	39.26	5.45
Tr6-#4	0.25 m	1992	55.34	0.98
Tr6-#4	2 m	447.4	16.77	0.4

1. Lab No. 42076 to 42089: analyses by Ministry of Energy, Mines and Petroleum Resources Laboratory
   Lab No. 38777 to 38793: analyses by Acme Analytical Laboratories Ltd.
2. Analyses by fire assay/Induction Coupled Plasma
3. Analyses by atomic absorption spectrophotometry
4. Analyses by X-ray fluorescence
5. Analyses by Induction Coupled Plasma

Velvet Exploration Co. Ltd. acquired the property and in 1980, 1000 metres of drilling was carried out. In 1982, approximately 930 tonnes of rock from the ore pile on the 8th level and the dump on the 1st level, containing 5.5 g/t gold, was shipped to the H.B. mill in Salmo (George Cross Newsletter, May 25, 1982).

The Velvet workings are on 8 levels, each approximately 30 metres apart; a vertical shaft serviced all levels. In 1903 the mine was flooded to the 400 level and in 1937, to the 600 level (Peters, 1937). Long adits were opened from surface at the 400 and 600 levels to drain the mine. A 180-metre adit on the 800 level is connected to the 600 level by a raise (BC Property File). The size and shape of ore shoots and extent of mine workings are shown in Drysdale (1915) and Peters (1937).

The only other deposit in the vicinity of the Velvet Mine is the Douglas (082F/SW161), which was in production from 1948 to 1950. This is a silver-lead-zinc vein in coarse clastic rocks of the Upper Cretaceous Sophie Mountain Formation, which are intruded by several Middle Eocene Coryell dikes. Most recent work in the area is on the Santa Rosa property one kilometre east of the Velvet Mine (Keyser and Smith, 1988).

REGIONAL GEOLOGY

The Velvet Mine area is underlain by ultramafic cumulate rocks intruded on the west by the Middle Eocene Coryell batholith. Large blocks of mafic volcanic rocks, up to 70 metres wide, occur within the ultramafic rocks. Generally north-trending Middle Eocene, and possibly Middle Jurassic, granite, pulaskite, augite-biotite porphyry and biotite-potassium feldspar porphyry dikes, up to 6 metres wide, are common. Bedrock exposures are limited; outcrops are found mainly at road cuts, trenches and ridge crests.

West of Rossland, these ultramafic bodies are interpreted to be in thrust contact with both the Pennsylvanian - Permian Mt. Roberts Formation and Early Jurassic Rossland Group (Figure 4-1). They are dunitic to wehrlitic ultramafic cumulates of probable oceanic affinity, perhaps part of the Slide Mountain Terrane (Ash, 2001).

The Coryell intrusions are exposed mainly as a batholith, which extends from the USA border north to the Castlegar area and from Christina Lake east to Granite Mountain just west of Rossland. Numerous U-Pb zircon ages from the Coryell intrusions (*e.g.*, 51.7±0.5 Ma; Bevier, 1987) and field relationships on Old Glory Mountain that indicate that the Coryell is genetically related to the Marron Formation (Little, 1982a; Monger, 1968) support a Middle Eocene age. The Coryell batholith varies from coarse-grained, inequigranular and locally porphyritic syenite to medium-grained porphyritic syenite, granite, quartz monzonite and monzonite. Small stocks and dikes of the Coryell occur throughout the Rossland-Salmo-Nelson area. These are generally more mafic than the batholith, consisting of augite-biotite monzonite and hornblende monzonite (Little, 1982a,b).

The Coryell intrusions generally have a pinkish-red colour but adjacent to areas of hydrothermal alteration or metasomatism, appear green due to chloritization of mafic minerals.

PROPERTY GEOLOGY

The Velvet Mine is within dunite and wehrlite ultramafic cumulates intruded by Coryell rocks. The ultramafic rocks are exposed as four pendants, the largest approximately 600 by 150 metres in area (Figure 3-15). Ultramafic outcrops are a medium-brown colour on weathered surfaces; a penetrative foliation or shearing is generally present. In thin section, ultramafics comprise antigorite + serpentine after olivine, magnetite, spinel, chrysotile and other opaques in a serpentine mat (Little, 1982a).

Xenoliths of mafic volcanic rocks occur within the ultramafics in the Velvet mine area. The shaft on the Portland claim is reported to be in a large xenolith of pyritized, silicified greenstone (Drysdale, 1915). Mafic flows, pyroclastic breccia, tuff and minor siltstone crop out south of Santa Rosa Creek (Figure 3-16). These exposures have undergone widespread propylitic alteration (Keyser and Smith, 1988).

Samples of Coryell batholith exposures comprise, in general, microperthite and/or orthoclase, minor plagioclase, pyroxene, biotite and/or hornblende, less than 10% quartz and accessory apatite, sphene, zircon, magnetite and allanite (Little, 1982a). Samples from the Velvet Mine area are similar, with megacrysts of biotite (~10%), pyroxene (~5%), plagioclase (~10-15%), orthoclase (1-2%) and microperthite (1%) in a finer-grained matrix of quartz (3%), plagioclase (10%) and orthoclase (~60%). Apatite and sphene commonly occur as accessory minerals.

Whole-rock analyses from two 'fresh' (pink-coloured) samples of Coryell intrusive rocks from the Velvet Mine area were compared with four samples of 'average' Coryell rocks (Table 3-9). Samples from the Coryell batholith generally plot as metaluminous ($Al_2O_3 < Na_2O+K_2O$) in the high clinopyroxene and sphene field of Debon and Le Fort (1983). Velvet Mine area samples fall into the quartz monzonite and monzodiorite fields, which is within the syenite to monzodiorite compositional range of the Coryell batholith.

MINERALIZATION AND ALTERATION

Shear zones cutting the ultramafic rocks in the Velvet mine area contain veins of quartz and calcite with specularite, chalcopyrite and pyrite; galena and sphalerite occur in lesser amounts (Photo 3-6). Locally, chalcopyrite is massive, particularly along the margins of the ore shoots. Minor scheelite may be sparsely disseminated in the ore (Stevenson, 1943, p. 154). Drysdale (1915, p. 78) reported a lens of molybdenite half a metre thick at the Velvet mine. The veins generally strike north parallel to the main dike system and dip steeply west. Drysdale (1915, p. 157) described the vein wallrock as "impregnated for some feet", indicating a significant alteration envelope. Little (1960, p. 182) suggested that the wallrock had been replaced in part by quartz, calcite and sulphide minerals. He described the Velvet mine as shear zone-related, containing veins or stockwork of veinlets with disseminated sulphides.

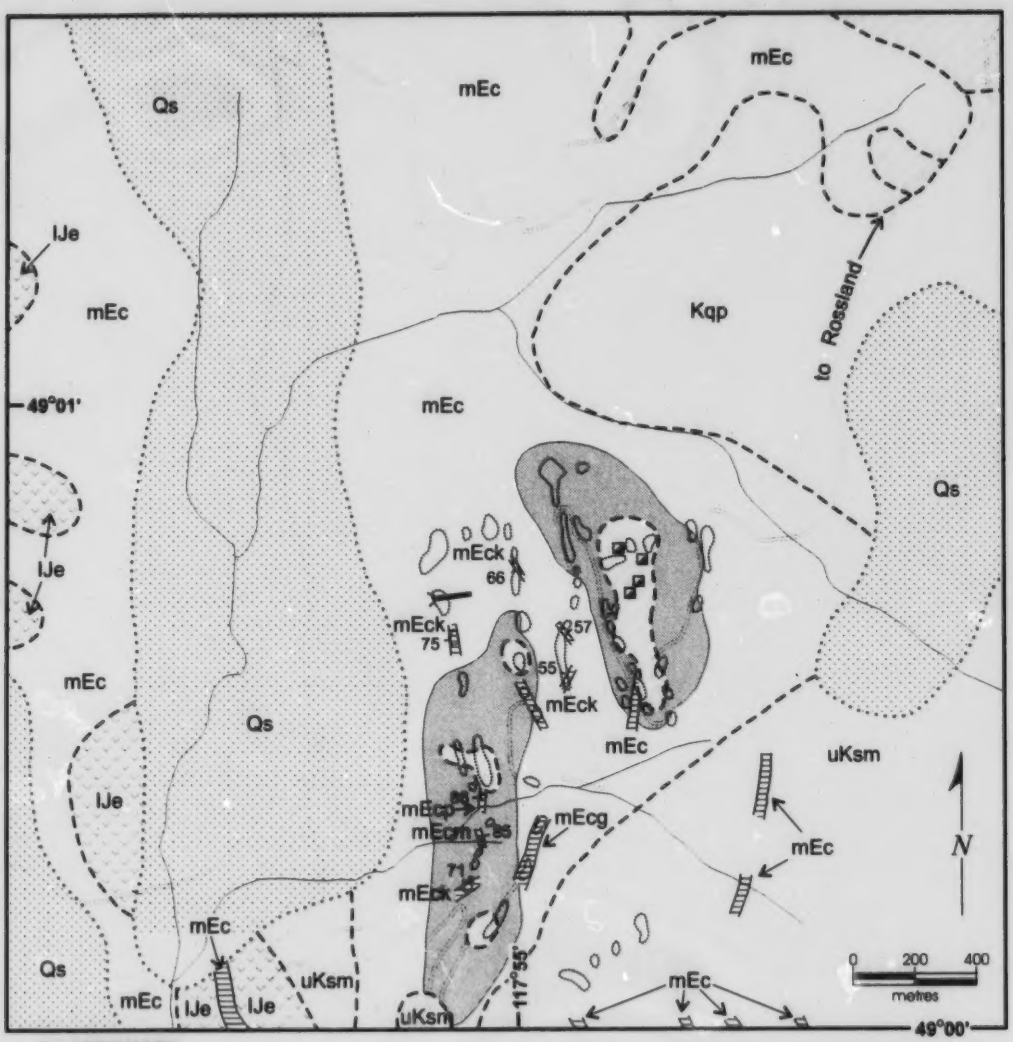

QUATERNARY

Qs — unconsolidated sediments

TERTIARY - Middle Eocene

mEc — syenite, quartz monzonite; minor dykes of granite (mEcg), pulaskite (mEcp), monzonite (mEcm), Kspar porphyry (mEck)

MESOZOIC - Cretaceous

Kqp — quartz-feldspar porphyry

- Upper Cretaceous

uKsm — Sophie Mountain Formation: coarse conglomerate; minor siltstone, argillite

- Lower Jurassic

lJe — Elise Formation: mafic flows, pyroclastic breccia; mafic to intermediate tuff, tuffite

PALEOZOIC

ultramafic cumulates, dunite and wehrlite

alteration zones

57 — dykes; strike and dip

rock outcrops

geological contact

adit

shaft

roads

rivers

Figure 3-15. Geology of the Velvet mine area, southwest of Rossland.

TABLE 3-9
ANALYSES OF SAMPLES OF CORYELL INTRUSIVE ROCKS, VELVET DEPOSIT AREA AND ELSEWHERE

Lab No.	Field	SiO_2	TiO_2	$Al2O_3$	Fe_2O_3	MnO	MgO	CaO	Na_2O	K_2O	P_2O_5	Total
36243	45-11	45.25	1.97	12.51	10.86	0.20	7.14	9.10	2.20	4.54	2.08	97.87
42004	286-6	54.33	1.18	15.37	7.94	0.15	4.30	5.81	3.84	4.40	0.77	99.07
41690	325-10	59.94	0.47	17.33	5.60	0.11	1.58	8.10	3.29	0.67	0.16	99.67
41692	325-16	57.48	0.79	14.97	6.23	0.12	4.26	3.90	4.35	4.83	0.49	99.22
41693	325-22	70.87	0.20	14.73	1.84	0.01	0.25	0.13	4.29	5.50	0.04	98.82
41694	329-13	61.77	0.75	15.91	5.68	0.07	2.32	3.39	3.89	2.60	0.19	99.34
42387	347-3	53.39	0.85	14.40	7.84	0.15	6.17	7.31	3.00	4.49	0.59	99.06

Lab No.	Field	Ni	Cr	Ba	Sr	Zr	Y	Nb	Ta	V	La
36243	45-11	103	157	5523	2779	364	44	166	9	248	267
42004	286-6										
41690	325-10					63	13	5	15	116	
41692	325-16					325	26	68	15	110	
41693	325-22					387	21	53	15	11	
41694	329-13					87	16	5	15	213	
42387	347-3	65	244	2135	1301	139	21	37	15	164	66

Samples 325-10,16 and -22 are from the Velvet mine area.
Locations and descriptions are given in Appendix 8.

Assays from a number of hand samples of the Velvet veins are shown in Table 3-10. One sample contains 34 ppm gold and 0.2% copper. There appears to be little correlation between copper and gold content. Cu/Au ratios vary from 1 to 710000 and Cu/Ag, from 0.064 to 0.00061. High nickel content in some samples reflects the ultramafic host.

The main Velvet vein occurs in the Kelley stope, the richest area of the mine (Peters, 1937). The Main vein trends north-south and dips 70° west. Four productive veins, including the South and Stable veins, occur 20, 40, 60 and 105 metres east of, and parallel to, the Main vein. Ore zones occur at the intersection of north-trending veins with crosscutting dikes or faults. Sulphides in the veins have been largely altered to limonite and malachite in the upper three levels of the mine (Drysdale, 1915, p. 157; Little, 1960, p. 182). Later crosscutting east-trending veins are barren.

Photo 3-6. Ultramafic blocks mineralized with specularite and chalcopyrite, Velvet mine dump (photo width, approximately 20 cm).

Within approximately 100 metres of the serpentinized ultramafics, Coryell intrusive rocks are propylitized to a green colour, with chloritization of biotite (20%), breakdown of feldspars to epidote (20%), sericite and clay minerals (25%) and addition of quartz (up to 20%). Drysdale (1915) described the Coryell wallrock adjacent to veins in the Velvet mine as "a mottled grey irruptive rock, with coarse siliceous and chloritic phases, which is much epidotized in places". The wide distribution of altered Coryell rocks in the Velvet mine area is outlined in Figure 3-15; it may be a useful exploration parameter for mineral exploration in Coryell batholith rocks.

SUMMARY AND DISCUSSION

The origin of copper-gold-silver veins at the Velvet Mine is not well understood. They may have formed as mesothermal veins along structures related to Middle? Jurassic thrust faults marginal to ophiolitic crustal and/or mantle lithologies. Alternatively, there has been some suggestion that the mine may be a skarn, although there is little published evidence of calc-silicate mineral assemblages or limy protoliths. Skarn occurrences possibly associated with Coryell intrusions include the May Blossom, Jumbo, Stewart 2, Kimbarb and Rossland Wollastonite (BC MINFILE 082F/SW070, 111, 229, 326 and 341).

It is possible that the veins are related to extension during emplacement of the Middle Eocene Coryell intrusions. Their dominant north-south orientation is parallel to Coryell dikes. Furthermore, the pervasive alteration of the Coryell

TABLE 3-10
ANALYSES OF SAMPLES OF THE VELVET VEIN
(From this study, Drysdale (1915) and George Cross Newsletter #297)

Sample No		Au (ppb)	Ag (ppm)	Cu (ppm)	Pb (ppm)	Zn (ppm)	Co (ppm)	Ni (ppm)	Mo (ppm)	Cr (ppm)	Note
V. 2800	41536	10	5	0.71%	39	205	15	0.10%	<10		massive mag. + cp
V. 3500	41537	34510	27	2182	36	65	223	228	<10	<10	vein spec. + sulph.
322-13	41538	1116	56	880	618	55	31	10	<10	<10	c.g. bi-feldspar syenite(?)
98V-1	53832	3318	7.5	1.78%	18	42	35	46	2	11	vein spec., mag + cp
98V-3	53834	6338	25.5	3.07%	9	173	78	18	<2	6	cc vein, spec +cp

Notes: Au by fire assay, ICP; Ag, Cu, Pb, Zn, Co, Ni, Mo, As, by Atomic absorption; Cr by XRF

rocks adjacent to ultramafic rocks that host the veins suggests a syn to post-Coryell age. However, it is possible that this alteration is simply a contact altered phase of the Coryell, unrelated to mineralization.

RED POINT (082F/W366)

Names: Red Point, Gold Dust
Location: Lat. 49°05'00" N, Long. 117°43'34" W
Elev. 1100 metres

INTRODUCTION

Red Point is located approximately 5 kilometres southwest of Trail on the northern ridge of Lookout Mountain. It was initially staked in 1893 and by 1897 a large amount of underground development had been done on the property. The property was drilled by Tomex Resources in 1988 and by Gamah International Ltd. in 1997. Gamah Resources, the operator for Loumic Resources Ltd. who had optioned the property from the owner, M. Gerg, drilled a total of six holes for a total of 1 014 metres. This work resulted in a "the discovery and delineation of a bulk tonnage gold deposit" (Ermanovics and Downing, 1997).

REGIONAL GEOLOGY

Red Point is within a sequence of mainly basaltic to andesitic lapilli tuff of the Elise Formation. These include augite-phyric lapilli tuff, lapilli tuff with plagioclase ± augite-bearing clasts and crystal tuff. Ermanovics and Downing (1998, p. 3) report that drill intersections of Lower Elise in this area are dominantly "felsic/siliceous and agglomeratic".

The Elise succession on the northern ridge of Lookout Mountain defines a north-northwest trending and plunging syncline. Bedding on the ridge north of Lookout Mountain swing from north-trending, west-dipping to east-west trending in the core of the syncline near the summit of Lookout Mountain.

Elise Formation in the Red Point area is surrounded by intrusive rocks (Figure 4-2, in pocket). The area is within an embayment of the Rossland monzonite; the monzonite is exposed less than a kilometre to the west and less than 2 kilometres to the east. The Trail pluton truncates the Rossland monzonite immediately to the north of Red Point and Sheppard and Coryell intrusions, both of Eocene age, are exposed just south of the summit of Lookout Mountain. A number of generally north-trending, late dikes cut Elise metavolcanics. These commonly have flow textures suggestive of a volcanic origin; however, they are Eocene in age, as they are post-tectonic, cutting Elise stratigraphy and regional foliation at high angles.

MINERALIZATION

Mineralization on the property is variable, including disseminated sulphides, sulphide clasts in Elise volcaniclastics, some spectacular sulphide-matrix breccias, and veins and fracture filling (Ermanovics and Downing, 1997). Disseminated sulphides consist mainly of pyrite, pyrrhotite and minor chalcopyrite, most commonly in fragmental Elise volcanic rocks. Sulphide clasts, up to 6 cm in diameter, consist mainly of massive pyrrhotite and pyrite. Vein and fracture-controlled pyrrhotite, pyrite and chalcopyrite may contain minor carbonate, quartz and chlorite gangue.

Drill holes intersected anomalous gold and copper values, with gold in the range of 2-12 ppm over two metre lengths, in sections with "agglomerate/breccia and breccia" that contained up to 6% pyrrhotite, pyrite and minor chalcopyrite (Ermanovics and Downing, *op. cit.*). Average copper values were less than 750 ppm, with the highest value of 1991 ppm obtained in one 2-metre interval.

The origin of this low-grade, but potentially large-tonnage gold-copper deposit, is not known. Ermanovics and Downing (*op. cit.*) note that mineralization is best developed in volcaniclastic rocks, regardless of their composition, implying a porosity/permeability control. Furthermore, they note that the sulphide clasts indicate "pyroclastic or epiclastic" sulphide deposition with local hydrothermal enrichment.

Red Point has some similarities with the Harper Creek deposit in the Eagle Bay assemblage north of Kamloops. There, disseminated sulphides, minor layered sulphides and fracture-controlled sulphides in mafic volcaniclastics were interpreted as a "volcanogenic disseminated sulphide deposit" (Höy, 1997). Red Point also has similarities with a copper-gold porphyry deposit. Considerable more work on this deposit is required to understand and classify it.

CHAPTER 4 ROSSLAND AREA

INTRODUCTION

The Rossland mining camp is the second largest lode gold producing camp in British Columbia, with recovery or more than 85 900 kilograms of gold and 109 500 kilograms of silver between 1894 and 1941. Vein deposits are in three main belts, referred to as the North belt, Main veins and South belt (Figure 4-1). Mineralization in the Rossland camp also includes molybdenite deposits on the western slopes of Red Mountain and a number of high-grade gold-quartz veins in the Sheep Creek valley and on the eastern slopes of O.K. Mountain just west of Rossland. These latter veins have been described in Chapter 3.

Gold-copper vein deposits of the Rossland camp have been described by a number of authors; the most comprehensive reports are by Drysdale (1915), Gilbert (1948) and Thorpe (1967). Stevenson (1936) described in some detail the workings of the gold-quartz veins west of Rossland, and Fyles (1984), the setting of the camp and the molybdenite deposits on Red Mountain. The regional geology in the vicinity of the camp is presented in Höy and Andrew (1991a) and summarized by Höy and Dunne (1997).

The origin and age of gold-copper veins in the Rossland camp and the relationship, if any, between these veins and other styles of mineralization in the immediate camp vicinity, have been the focus of considerable discussion and debate. The purpose of this chapter is to summarize the regional geology around Rossland, to describe the main deposit types, and to present a model for intrusive-related gold-sulphide veins. The importance of this deposit type, referred to as "intrusion-related Au-pyrrhotite veins" by Alldrick (1993) and initially believed to be restricted to a number of Jurassic occurrences in British Columbia (Alldrick, *op. cit.*), is enhanced considerably by recognition of a number of other examples, including massive sulphide-gold veins in the Chibougamou camp in Quebec (Kirkham *et al.*, 1997) and at the 17 Mile porphyry Cu-Au deposit in Western Australia (Rowins, 2000). Furthermore, the Rossland model has been applied to exploration on a number of similar style veins in the Greenwood camp west of Rossland (L. Caron, personal communication, 1998).

GEOLOGICAL SETTING

The geology of the Rossland area is illustrated on Figure 4-1. The southern part of the area is underlain mainly by volcanic rocks of the Early Jurassic Elise Formation. These rest unconformably on meta-sedimentary rocks of the late Paleozoic Mount Roberts Formation and are in apparent fault contact with underlying rocks of Unit Cs, interpreted to be mainly a siliciclastic assemblage of the Slide Mountain terrane. Locally, the Elise Formation is unconformably overlain by coarse conglomerates of the Late Cretaceous Mount Sophie Formation.

A number of igneous suites intrude these rocks. The Rossland sill, a subvolcanic monzogabbro intrusion and the Rossland monzonite both host a considerable number of the productive veins of the Rossland camp. The intrusions are cut by the Middle Jurassic Trail pluton and by alkaline Coryell intrusions of Middle Eocene age. The Eocene Sheppard intrusions occur as stocks in the southeastern part of the area or form north-trending felsic dikes; they are also cut by the Coryell intrusions.

UNIT CS (CHARBONNEAU CREEK ASSEMBLAGE)

Rocks assigned to Unit Cs are restricted to the southeastern part of the Rossland area. The more western of the two exposed areas was mapped in detail (Höy and Andrew, 1991a). It includes tan to black-coloured argillite, silty argillite and minor siltstone, a massive pale grey limestone, some massive dolomite and dolomitic siltstone. These rocks are locally silicified, sheared, brecciated and veined. To the east, north of the Pend O'Reille River, these rocks include mafic volcanic rocks with MORB signatures (Einersen, 1994). Tight, minor folds occur locally, and crenulated phyllites indicate at least two periods of deformation.

The intense shearing and brecciation, particularly along the margins of Unit Cs, and the truncation of adjacent units in the Elise Formation, suggest a faulted contact between Cs and the Elise. It is probable that this fault contact is the western extension of the Waneta fault, a thrust fault that is interpreted to mark the boundary of Quesnellia with Slide Mountain and North American rocks.

Unit Cs is late Paleozoic in age; in correlative exposures farther east, Little (1982b) described brachiopods of possible Late Mississippian age and Einersen (1994) identified abundant *holothurian sclerites* of probable Mississippian to Pennsylvanian age (C.M. Henderson, written communication to J. Einersen). Einersen (*op. cit.*) divided Unit Cs into two assemblages, the Charbonneau Creek and Harcourt Creek assemblages. The western exposures of Cs south of Rossland are included in the Charbonneau Creek assemblage that Einersen (*op. cit.*) correlates with the Upper Mississippian McHardy assemblage of the Milford Group; the more easterly Harcourt Creek assemblage is correlated with the Davis assemblage of the Kootenay terrane.

The McHardy assemblage is considered by Klepacki and Wheeler (1985) to be part of a siliciclastic succession beneath mafic volcanic rocks in the Slide Mountain terrane. Hence, the Charbonneau Creek assemblage may represent the most southern exposures of Slide Mountain in British Columbia. Alternatively, W. Howard (personal communication, 2000) favours correlation of the Charbonneau Creek assemblage with Kootenay terrane rocks, specifically the Davis assemblage of the Milford Group. The assemblage is

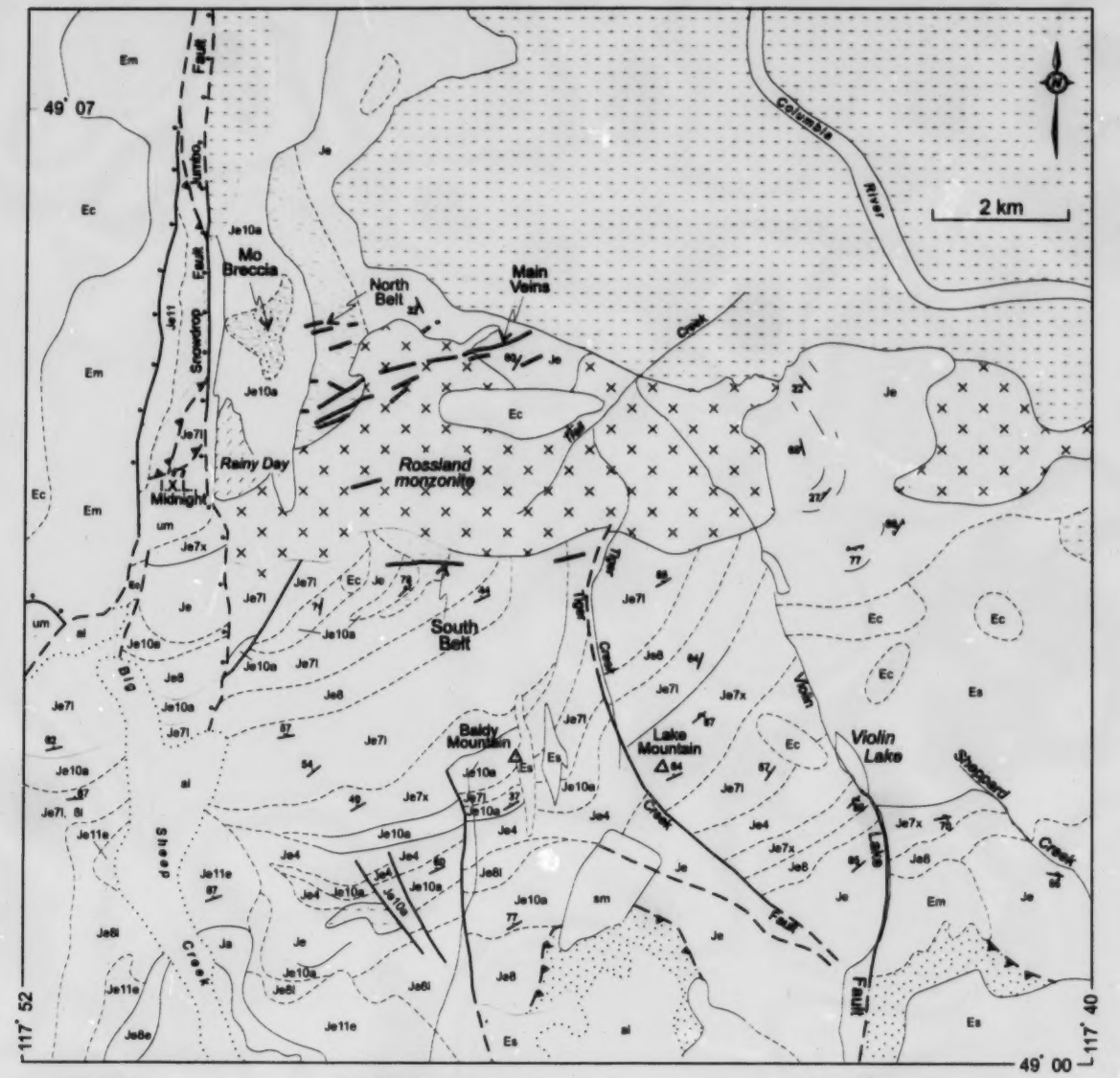

Figure 4-1. Geological map of the Rossland area, Rossland-Trail map sheet (082F/04); after Höy and Andrew (1991b), Fyles (1984), Little (1982b) and Drysdale (1915). *See* Figure 4-2, in pocket for detail.

within a thrust panel, separated from overlying Quesnel rocks by the Waneta fault and from underlying Kootenay terrane rocks by the Tillicum Creek fault.

The Charbonneau Creek assemblage appears to record mainly shallow-water deposition in a lagoonal and shoal environment (Einersen, 1994). Possible correlation with the McHardy assemblage, and inferred stratigraphic ties with the Davis assemblage, which unconformably overlies the Lardeau Group of the Kootenay terrane (Roback, 1993; Roback *et al.*, 1994; Klepacki and Wheeler, 1985; Klepacki, 1985), suggested deposition as a "marginal basin assemblage" along the western ancestral North American margin (Einersen, *op. cit).*

MOUNT ROBERTS FORMATION

The Mount Roberts Formation consists of a succession of dominantly fine-grained siliceous rocks, argillite, carbonate and minor greenstone and conglomerate of Pennsylvanian and possibly Permian age (Little, 1982b; Höy and Dunne, 1997). In the Rossland area, the formation is exposed near Patterson at the United States border, and on the eastern slopes of Mount Roberts and Granite and OK mountains northwest of Rossland (Figure 4-1). These localities are described by Little (1982b) and Höy and Andrew (1991a) and the exposures on Mount Roberts, by Fyles (1984).

The Patterson exposures comprise dominantly fine-grained siliceous siltstone, dark grey to black argillite or pale grey-green silty chert. Numerous fine, irregular hairline fractures typically cut the more siliceous units; quartz veining is less common. These units are either massive or thinly laminated. Locally, graded and scoured sandstone lenses occur within the siltstone and provide rare stratigraphic-top indicators. Carbonate units, including grey brecciated limestone and rusty weathering, well-bedded fossiliferous dolomite, are conspicuous near the uppermost exposures of the Mount Roberts Formation.

Outcroppings on the eastern slopes of Mount Roberts and Granite Mountain are similar, comprising mainly black to grey siliceous argillite and siltstone. Rare silt scours, graded beds and a number of bedding-cleavage intersections indicate that the Mount Roberts Formation at this location faces west. Thicker bedded, graded siltstone and sandstone beds are locally interbedded with thin, impure dolomite and limestone lenses. These units also face west and are unconformably overlain by volcanic breccias of the Elise Formation.

The Mount Roberts Formation is locally 'basement' to arc rocks of Quesnellia, with the Rossland Group unconformably overlying it at Patterson and elsewhere. It unconformably? overlies the Trail gneiss, a succession of amphibolites, gneisses and schists, that may contain rocks as old as Devonian (Simony, 1979). The Mount Roberts Formation may correlate with the Davis or Keen assemblages of the Milford Group of the Kootenay terrane (Wheeler and McFeely, 1991) or with the Harper Ranch subterrane of Quesnellia (Roback, 1993, Roback and Walker, 1995). Supportive evidence for correlation with the Milford Group includes similar lithologies, including conglomerates that contain plutonic and quartzitic cobbles, and lithic fragments of quartzite and grit, suggestive of a cratonic source (Roback and Walker, 1995). As well, detrital zircon grains with U-Pb ages that range from Devonian to PreCambrian are similar to those in cratonic rocks of North America.

Roback and Walker (*op. cit.*), however, prefer a model that includes the Mount Roberts Formation as part of the Harper Ranch rocks, separated from the western margin of North America, and developed in part on rift-generated continental fragments. Sandstones appear to have both a magmatic arc and a "recycled orogen" provenance, suggestive of deposition in a shelf-slope environment near an active arc (Roback and Walker, *op. cit.*). Alternatively, it is possible that the sources of these sandstones were, in part, the eroded Late Devonian arcs of the western Kootenay terrane, such as occur in the Eagle Bay assemblage. Therefore this provides additional support for a tie to North America. These interpretations lend further support to a model that places formation of arc volcanics of the Rossland Group along the attenuated ancestral margin (Höy and Dunne, 1997). As well, a leucocratic sill that intruded the Slide Mountain McHardy assemblage has been dated at 196 Ma Roback (1993, p. 82). As the McHardy assemblage can be 'tied' to marginal North America, it implies Rossland-age intrusive activity and, by inference, deposition of the Rossland Group close to North America.

ROSSLAND GROUP

The Rossland Group in the Rossland area includes a coarse basal conglomerate, correlated with the Archibald Formation, and an overlying thick accumulation of mafic flows, pyroclastic rocks and interlayered metasedimentary rocks of the Elise Formation (Höy and Andrew, 1991a; Höy and Dunne, 1997). The Hall Formation is missing, due to nondeposition or to erosion prior to deposition of the unconformably overlying Mount Sophie Formation. The age of the Elise Formation is constrained by late Sinemurian fossils in the upper part of the Archibald Formation, a 197 Ma U-Pb zircon age from tuffs within the formation, and Toarcian fossils in the Hall Formation (*see* summary and references, Chapter 2).

The Archibald Formation at Patterson consists of a veneer of conglomerates, up to several hundred metres thick, that lies unconformably on the Mount Roberts Formation. The Mount Roberts paleosurface is irregular, resulting in isolated patches of Archibald in depressions in the surface and small outcrops of Mount Roberts on paleohighs (Figure 3-4, in Höy and Dunne, 1997). Most commonly, a limestone unit in Mount Roberts lies along the paleosurface.

The Archibald Formation is typically a heterolithic pebble conglomerate with subrounded to subangular clasts of grey-green siliceous siltstone, argillaceous siltstone, limestone, and minor chert, quartzite and a variety of plagioclase porphyries in an argillaceous or granular sandy matrix. Locally, a coarse limestone breccia derived from the underlying Mount Roberts Formation is at the base of the

TABLE 4-1
ANALYSES OF INTRUSIVE CLASTS WITHIN THE ARCHIBALD FORMATION IN THE FRUITVALE AND MONTROSE AREAS

Lab No.	Field No.	SiO_2 %	TiO_2 %	Al_2O_3 %	Fe_2O_3 %	MnO %	MgO %	CaO %	Na_2O %	K_2O %	P_2O_5 %	SUM %	Zr ppm	Nb ppm	Sr ppm	Y ppm	V ppm	Nd ppm	Rb ppm
54483	Montrose -1	65.7	0.43	15.21	1.25	0.05	1.95	5.8	4.38	1.95	0.1	99.2	102	11	576	22	100	<5	38
54484	Montrose -3	60.2	0.37	17.26	4.86	0.11	1.8	7.07	5.05	0.58	0.14	99.4	71	11	646	18	75	<5	<5
54485	Archibald -1	53.7	0.6	14.6	4.65	0.18	1.58	10.21	3.75	2.11	0.17	99.2	106	10	543	22	144	<5	40

NOTES
Oxide analyses: Fused disc - X-ray fluorescence; trace elements: pressed pellet XRF
SUM = Sum of oxides
Laboratory = Cominco Research Labs.

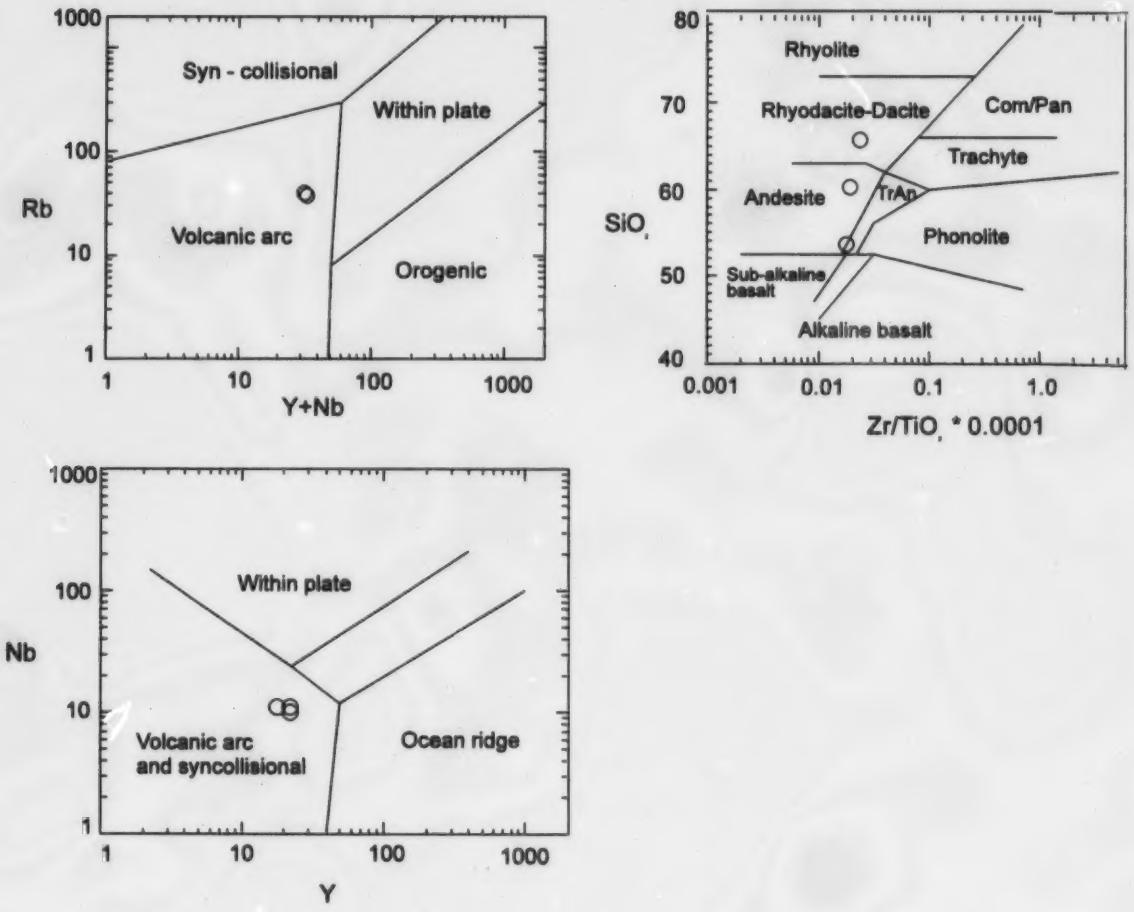

Figure 4-3. Trace element diagrams of analyses of intrusive clasts in the Archibald Formation, Fruitvale and Montrose areas, showing their subvolcanic arc provenance.

Archibald. The argillaceous matrix is commonly tinged purple, suggestive of subaerial exposure. Bedding, clast-sorting or winnowing, grading or other features indicative of fluvial environments are lacking. These sedimentary conglomerates are distinct from tuffaceous conglomerates in the Elise as they contain virtually no volcanic clasts or a tuffaceous matrix.

The origin of the porphyritic clasts within the basal part of the Archibald Formation is not known. A number of these clasts in the Fruitvale and Montrose areas have been analyzed (Table 4-1). Low Nb, Y and Rb values (Figure 4-3) indicate a volcanic arc provenance, suggesting derivation from subvolcanic arc plutons that were exposed in Early Jurassic time. It is most likely that these clasts record plutonism in the underlying Mount Roberts Formation, but also possible that they record Triassic plutonism, related to Nicola arc volcanism, or older Devonian plutonism associated with arc volcanics of the Kootenay terrane.

The Elise Formation in the Rossland area is described in considerable detail by Höy and Dunne (1997). It comprises a north to northwest-dipping homoclinal succession that extends north from Patterson to Rossland. A composite section is illustrated on Figure 4-4.

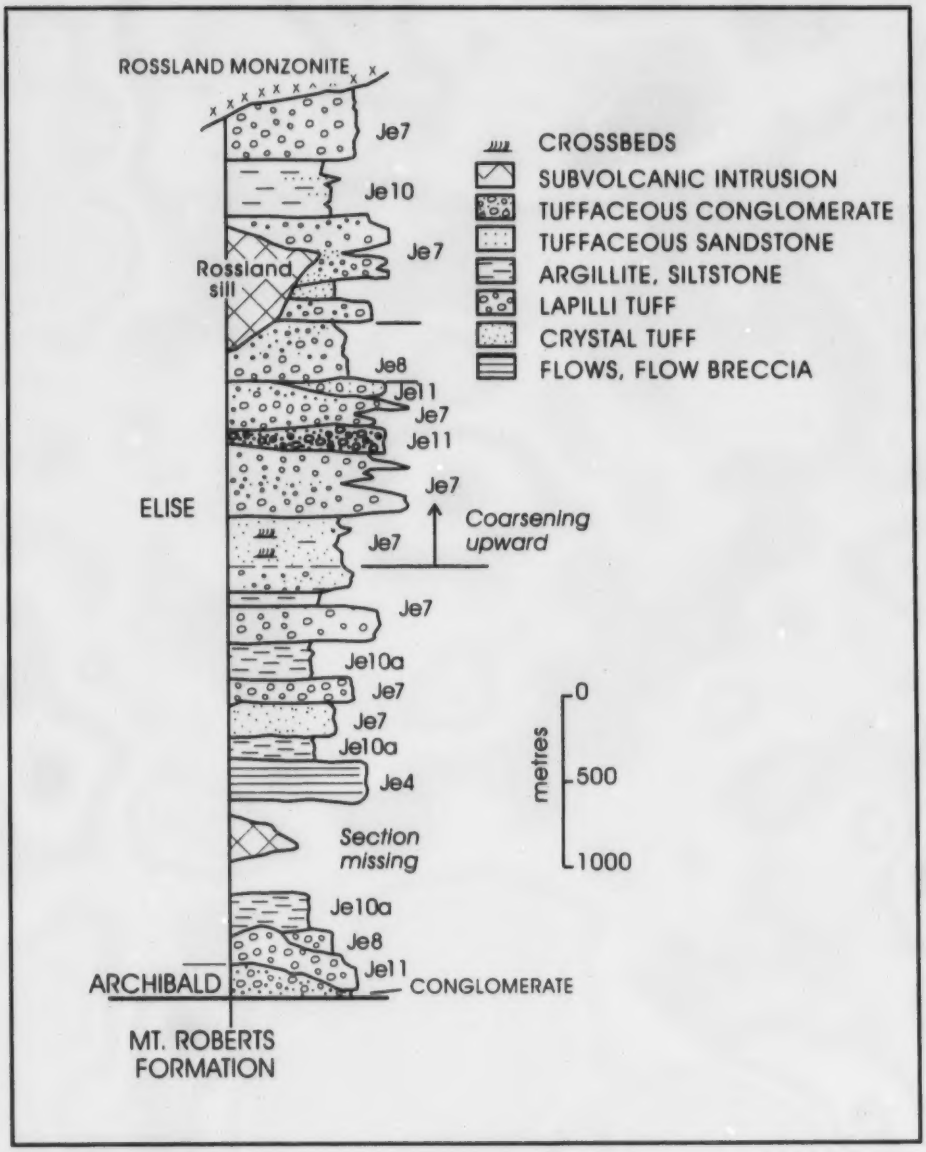

Figure 4-4. A composite section of the Elise Formation, Rossland area (from Höy and Dunne, 1997).

The base of the Elise is a gradational contact with the Archibald, placed where either volcanic clasts are first noticed or the matrix becomes tuffaceous. Plagioclase-porphyry lapilli tuff of Unit Je8l locally overlies the tuffaceous conglomerate. Argillaceous turbidite siltstones (Unit Je10a) and mafic flows and flow breccias (Unit Je4) overlie the tuffaceous conglomerates and lapilli tuffs. The mafic flows comprise massive augite porphyry, flow breccias and possible minor lapilli tuff; it is the only significant mafic flow succession in the Rossland area.

Unit Je7x is a succession of dominantly fine mafic tuff beds that generally coarsen upward into crystal tuffs that contain small, widely scattered augite porphyry lapilli and numerous plagioclase and augite crystals. Layers of lapilli tuff and, less commonly, pyroclastic breccias become more prominent near the top of the succession. These are interpreted to be mainly surge and pyroclastic flow deposits recording subaerial to possibly very shallow water conditions.

South of the Rossland monzonite, interbedded argillaceous siltstone and tuffaceous sandstones of units Je10 and 10a host a number of vein deposits of the South belt (Höy and Andrew, 1991a,b). They may correlate with rust-weathering argillites and siltstones on the west slope of Red Mountain, host to the Red Mountain molybdenite deposits. Mafic lapilli tuffs of Je8l overlie these metasediments.

In summary, the Elise Formation in the Rossland area comprises dominantly mafic to intermediate lapilli tuffs interlayered with prominent sections of tuffaceous siltstone and argillaceous siltstone. Mafic flows are subordinate and tuffaceous conglomerates are essentially restricted to the basal part of the succession. The Elise Formation in the Rossland area was deposited on a structural high that is exposed in the Patterson area and on the eastern slopes of Mount Roberts. Virtually the entire basal succession of the Rossland Group, the Archibald Formation, and a considerable part of the lower Elise is missing. Despite this, the Elise in the Rossland area represents one of the thickest successions recognized, in excess of 5000 metres.

SOPHIE MOUNTAIN FORMATION

The Sophie Mountain Formation (Bruce, 1917; Little, 1960) is exposed on Mount Sophie, on the ridge a few kilometres southeast of Baldy Mountain, and on the ridge north of Lake Mountain (Höy and Andrew, 1991b). The formation comprises poorly sorted, heterolithic conglomerate with thin interbeds of argillite and argillaceous siltstone. The conglomerate consists dominantly of rounded clasts of quartzite and other sedimentary rocks. Clasts derived from the underlying Elise Formation are rare or absent. The Sophie Mountain Formation represents deposition in small, structurally controlled basins in Late Cretaceous time.

MARRON FORMATION

The Middle Eocene Marron Formation (Bostock, 1940; Church, 1973; Little, 1982b; Fyles, 1984) is exposed on the eastern slopes of OK Mountain and Mount Roberts just west of Rossland and to the east of Goodeve Creek. The formation comprises dark grey, green and, locally, mauve andesitic flows and minor lapilli tuff, tuffaceous sandstone and tuffaceous conglomerate. It is in fault contact with the Elise Formation near Rossland (Fyles, 1984) but unconformably overlies the Elise in the southwest part of the map area; it is intruded by Middle Eocene Coryell intrusions.

INTRUSIVE ROCKS

Numerous intrusive rocks, ranging from batholithic bodies to small stocks and dikes, occur throughout the Rossland area. They are described in considerable detail by Fyles (1984), Little (1982b) and Höy and Dunne (1997) and hence will be only briefly described here.

EARLY? JURASSIC MONZOGABBRO INTRUSIONS

The Rossland sill (Fyles, 1984), exposed on the east slopes of Red Mountain and just south of the Rossland monzonite, hosts many of the western extensions of the Main Rossland veins and virtually all of the North belt veins. It is an inequigranular to porphyritic augite porphyry intrusion (Photo 4-1). It is interpreted to be an Early Jurassic subvolcanic intrusion, similar to many other, small Elise Formation-age, monzogabbro intrusions throughout the Rossland Group.

Elsewhere in the Rossland area, monzogabbro or gabbro stocks are also found in the Elise Formation on the ridge southwest of Deer Park Hill and on the southern slopes of Malde Mountain. As well, a similar small intrusion occurs in the Mount Roberts Formation west of Patterson. These intrusions are fine to medium grained and generally porphyritic with 30-40% plagioclase phenocrysts in dark green-grey matrix. Farther east in the Nelson area, they host copper-gold porphyry mineralization (*see* Chapter 3). They are petrographically distinct from the Eagle Creek plutonic complex, Rossland monzonite and Silver King intrusions.

Based on their chemistry and mineralogy, these monzogabbro intrusions are interpreted to be Elise-age subvolcanic intrusions. Although they have not been dated,

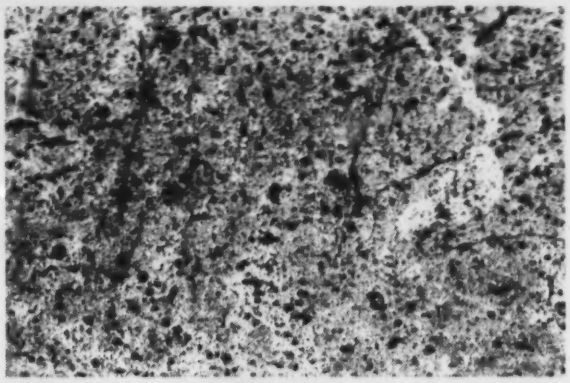

Photo 4-1. Porphyritic Rossland sill; note large (to 0.5 cm) augite phenocrysts in a plagioclase, orthoclase, hornblende, biotite and augite matrix; also note thin chlorite veins.

they may be similar in age to a number of known Early Jurassic mafic plutons recognized elsewhere in the southern Cordillera, and interpreted to record more extensive arc magmatism. The Lexington porphyry in the Greenwood camp is dated at *ca.* 200 Ma (Church, 1992) and a diorite near Christina Lake has a 197 ± 5 Ma age (Acton *et al.*, 1999); a similar massive to foliated diorite on the southwest side of the Valhalla complex is dated at 193 ± 1 Ma (Parrish, 1992). As well, a leucocratic sill that intrudes the McHardy assemblage in the Slide Mountain terrane is dated at 196 Ma (Roback, 1993). The recognition of inheritance in zircons from some of these plutons, in particular the Lexington porphyry, and the occurrence of at least one within Slide Mountain terrane that can be tied to Kootenay terrane stratigraphy (Klepacki, 1985; Roback, *op. cit.*) support a model for deposition of the Rossland Group close to marginal North America.

These plutons record arc magmatism and are part of a suite of subvolcanic intrusions related to the Early Jurassic arc volcanics of the Elise Formation.

ROSSLAND MONZONITE

The Rossland monzonite, centered on the town of Rossland, hosts many of the Main veins of the Rossland camp. It has been described by numerous workers, including Drysdale (1915), Bruce (1917), Gilbert (1948), Little (1960, 1963, 1982b), Fyles (1984), Höy and Andrew (1991a,b) and Höy and Dunne (1997). The following description is summarized largely from Höy and Dunne (*op. cit.*).

The Rossland monzonite is a composite stock with coarse to fine-grained phases, and mafic-rich to intermediate (feldspar-dominated) phases (Photo 4-2). Fe_2O_3/FeO ratios of a number of hand samples (Table 4-2) indicate that the more mafic phases tend to be more oxidized, in contrast to reduced, intermediate phases. Contacts between these phases range from gradational to intrusive with, more commonly, coarse grained or more feldspathic phases being younger (Drysdale, 1915). More mafic monzodiorite rocks comprise 40-60% andesine, up to 25% orthoclase, and augite variably replaced by hornblende and biotite. Magnetite and apatite are ubiquitous accessory minerals, sphene is rare, and a small amount of quartz occurs as late, resorbed crystals. It can grade to a dark greenish black rock comprised dominantly of pyroxene and hornblende with abun-

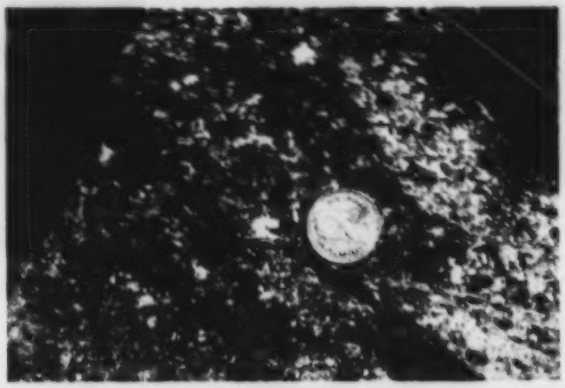

Photo 4-2. Coarse-grained Rossland monzonite, consisting of mainly large augite, partially replaced by hornblende, orthoclase and plagioclase, from the Iron Colt deposit (2.5 cm coin scale).

TABLE 4-2
FE_2O_3 (TOTAL), FEO AND FE_2O_3 VALUES OF SELECTED HAND SAMPLES OF THE ROSSLAND MONZONITE SHOWING OXIDATION STATE RATIOS

[Samples with Fe_2O_3/Fe_2O_3+FeO ratios greater than ~0.4 are considered oxidized, those below, more reduced]

Lab No.	Field No.	Fe_2O_3(t) %	FeO %	Fe_2O_3	Fe_2O_3/Fe_2O_3+FeO	Fe_2O_3/FeO
36429	R91-14	10.99	5.84	4.50	**0.435203532**	**0.770549315**
36432	R93-5	10.72	6.64	3.34	0.334733865	0.503157831
36966	R99-8	4.16	2.72	1.14	0.294836962	0.418111765
42005	286-9	10.16	6.17	3.30	0.348694364	0.535377472
42007	287-7	8.41	4.35	3.58	**0.451162621**	**0.822033333**
42008	287-14	6.97	3.34	3.26	**0.493805789**	**0.975526347**
41680	313-4	9.53	5.69	3.21	0.360437232	0.56356819
41684	318-3	7.03	4.12	2.45	0.37304495	0.59501068
41685	320-14	12.69	6.07	5.94	**0.494773318**	**0.979309555**
41686	323-3	8.56	5.23	2.75	0.344439095	0.525411281
41688	324-22	8.42	3.48	4.55	**0.56676953**	**1.30824023**
36427	R91-6	6.23	3.99	1.80	0.310394055	0.450103509

Analytical methods:

FeO: Acid decomposition / acid soluble / volumetric

Fe_2O_3(t): X-ray fluorescence (*see* Bulletin 102)

Fe_2O_3 = % Fe_2O_3(t) - (% FeO)(1.1113)

dant biotite. Other phases include monzonite and, at the Centre Star deposit, an exposure of biotite clinopyroxenite several metres across.

There has been considerable debate regarding the age of the Rossland monzonite and its relationship to the Elise volcanics. Höy and Dunne (1997), based on petrographic evidence, the locally intense alteration of the pluton, contact relationships with the Elise rocks, and chemistry suggested that it was a subvolcanic intrusion, comagmatic with the Elise Formation. Furthermore, U-Pb zircon data seemed to support an Early Jurassic age (Höy and Dunne, *op. cit.*), although J. Gabites and J. Mortenson (personal communication, 1996) suggested that these data indicated a Middle Jurassic age for the Rossland monzonite.

Uranium-lead zircon data from another Rossland monzonite sample are presented in Appendix 4 and plotted in Figure 4-5. Concordant data from two fractions indicate a 167.5 ± 0.5 Ma age for the Rossland monzonite. These data support a Middle Jurassic age for the Rossland monzonite, a similar age as the Nelson, Trail and Bonnington plutonic rocks.

DIORITE PORPHYRY DIKES

Diorite porphyry dikes, referred to as diorite porphyrite by Drysdale (1915) and Gilbert (1948), are common in underground workings in the area of the Main veins. The similar orientation and their close proximity to the veins suggest a genetic link (Drysdale, *op. cit.*). Drysdale suggested that these were phases of the Middle Jurassic Trail pluton, whereas Gilbert (*op. cit.*) concluded that they grade into the Rossland monzonite, and may be a dike or marginal contact phase. This interpretation is supported by Fyles (1984) who noted similar hornblende porphyries in the margins of the Rossland monzonite and intense alteration of these dikes, in contrast to less altered dikes that appear to be related to the Trail pluton.

RAINY DAY PLUTON

The Rainy Day pluton is a small quartz diorite stock exposed along Highway 22 just west of the town of Rossland.

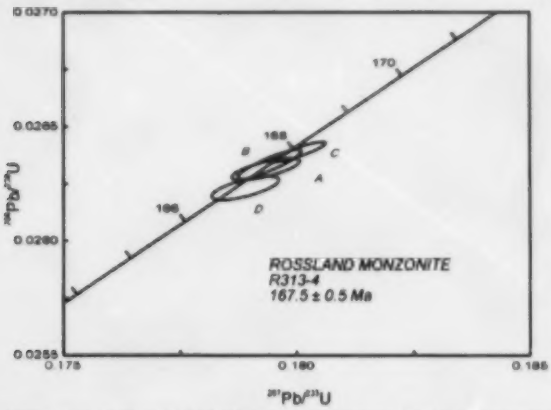

Figure 4-5. Plot of U-Pb zircon data, sample R313-4, Rossland monzonite (*see* Appendix 4 for data).

It is considered important in the metallogeny of the Rossland camp as it, and possibly associated dikes on Red Mountain (Eastwood, 1966; Fyles, 1984), are interpreted to have been the source of molybdenite mineralization in the camp. The following description of the stock is taken mainly from Fyles (1984).

The pluton varies from a central, more massive quartz diorite to a marginal porphyritic zone. It comprises approximately 50% plagioclase, 15-20% quartz, 5-15% orthoclase microperthite, 10-15% biotite, 5% hornblende and 5% augite.

Contacts with Elise Formation country rocks are generally sharp and irregular. The pluton is truncated to the west by the Coryell intrusion and is in sharp contact with the Rossland monzonite in the south. Fyles (*op. cit.*, p. 21) suggested that "the relationships between the two stocks are not entirely conclusive" but that "dike-like masses of quartz diorite appear to extend from the Rainy Day pluton into the Rossland monzonite indicating that the monzonite is older".

"The Rainy Day pluton is highly fractured with a network of intersecting veinlets containing very fine-grained pyroxene, quartz, hornblende, biotite, chlorite, carbonates and sulphides (pyrite and molybdenite)" (Fyles *op. cit.*, p. 22).

U-Pb analyses of a composite sample of the Rainy Day pluton, collected along the roadcut west of Rossland, are tabulated in Appendix 4, and shown on Figure 4-6. A York regression through these fractions gives an upper intercept age of 174.6 ± 3.6 Ma, which is probably the upper limit on its age. A weighted mean of the $^{206}Pb/^{238}U$ of the most concordant fractions, A and B, gives the best estimate of the lower limit on the age of the pluton, at 166.3 ± 1.4 Ma. The large uncertainty in this date does not resolve the question of the relative ages of the Rainy Day and Rossland plutons.

RED MOUNTAIN QUARTZ DIORITE DIKES

Three dikes, described by both Eastwood (1966) and Fyles (1984), occur in the vicinity of the molybdenite mine on the western slopes of Red mountain. The similarity in alteration and composition to the Rainy Day pluton suggests that they are part of a common magmatic suite. One of these dikes, the A zone dike, is intensely altered, brecciated and veined or replaced by molybdenite. It is described in more detail below (*see* Red Mountain Mo deposits).

A smaller dike within the A pit, also brecciated and cut by veins of molybdenite (Photo 4-3), has yielded a lower intercept U-Pb zircon age of 162.3 +1.2/–2.5 Ma (Figure 4-7; Appendix 4).

The dikes generally strike east with steep dips. The largest (Figure 4-2, in pocket) is up to 100 metres in thickness and 600 metres in length. Others are smaller and discontinuous, but several extend several hundred metres in length.

ULTRAMAFIC ROCKS

Ultramafic rocks in the vicinity of the Rossland camp are described by Fyles (1984) and Ash (2001). Fyles (*op.*

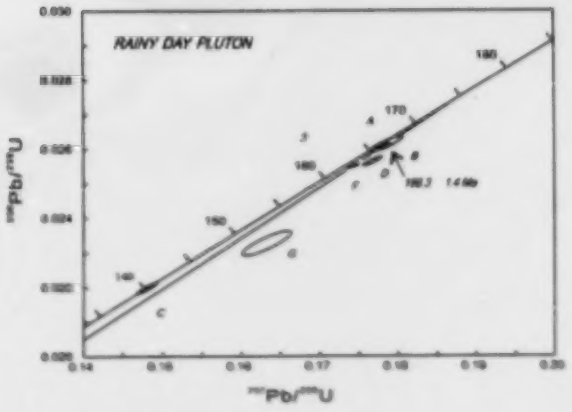

Figure 4-6. Plot of U-Pb zircon data from the Rainy Day pluton (*see* Appendix 4 for data).

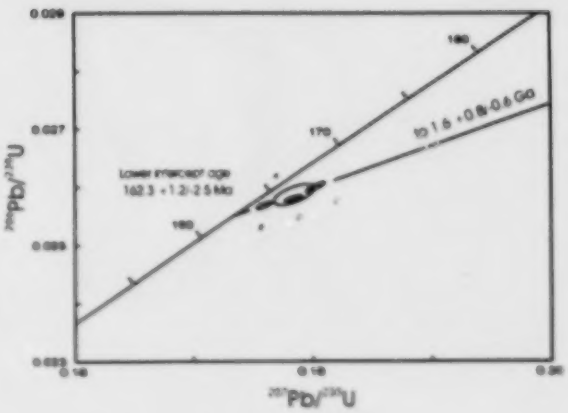

Figure 4-7. Plot of U-Pb zircon data, sample R96-5, quartz diorite breccia dike, Red Mountain (*see* Appendix 4 for data).

cit.) suggested that these bodies of "serpentinite" are probably within faults and Höy *et al.* (1992) interpreted that they were tectonically emplaced during a period of regional compression in Middle Jurassic time

Detailed studies of one of these, the O.K ultramafic body located in the Little Sheep Creek valley just west of Rossland (Fyles, *op. cit.*; Figure 4-1) have been undertaken by Ash *et al.* (1992) and Ash (2001). They described it as mainly an olivine wehrlite with erratically distributed areas of dunite and pyroxene-bearing dunite.

The O.K ultramafic body is in fault contact with surrounding host rocks. Fine-grained mafic volcanic rocks exposed along its northern contact may be of oceanic crustal affinity, related to the ultramafics (Ash *et al., op. cit.*) rather than part of the oceanic arc Elise Formation (Höy and Andrew, 1991b). These volcanic rocks host a number of very high-grade quartz veins, including the IXL, O.K and Midnight deposits.

Early interpretations of the origin and age of the O.K. ultramafic body, and others in the Rossland area such as the larger Record Ridge body farther south, have varied considerably. Drysdale (1915) suggested that they are altered augite porphyry stocks, and Fyles (1984) inferred that they are plutonic, possibly Late Cretaceous rocks. Little (1982b) suggested that they were part of an ophiolitic assemblage, related to the Late Paleozoic Mount Roberts Formation.

Ash (2001) confirmed that these are plutonic cumulate bodies. Furthermore, based on detailed petrographic studies and analyses of platinum group elements in massive chromite from the Record Ridge ultramafic, Ash further concluded that these bodies have an ophiolitic rather than an Alaskan-type affinity. Ash (2001) suggested that, based on the close spatial and structural association with the Mount Roberts Formation, this formation, the ultramafic bodies, and possibly related mafic volcanic rocks, be referred to as the Mount Roberts Assemblage. However, it is not resolved if this assemblage is therefore part of the oceanic Slide Mountain terrane; the Mount Roberts Formation has also been interpreted to be part of the Kootenay (Wheeler and McFeely, 1991) or Quesnel (Roback, 1993; Roback and Walker, 1995) terranes.

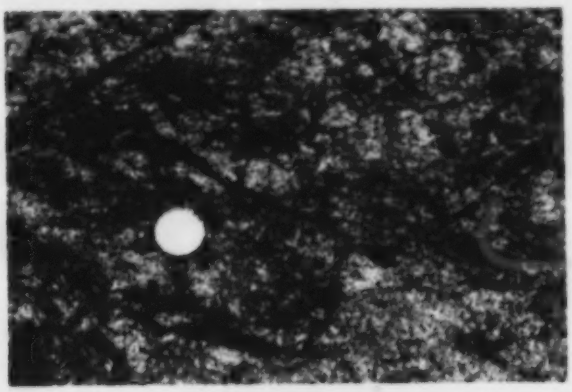

Photo 4-3. Altered quartz diorite dike from the A pit on Red Mountain; this dike is locally intensely brecciated and veined with molybdenite. It has yielded a 162.3 Ma U-Pb zircon date.

MINERALIZATION

Two occurrences of chromite mineralization in ultramafic rocks in the Rossland area are documented in B.C. MINFILE.

The **Vandot** occurrence (082F/SW130) is in the Record Ridge ultramafic body between the two main forks of Sophie Creek, seven kilometres southwest of Rossland. Massive pods, lenses and veins of chromite and magnetite are exposed in a number of pits within serpentinite. As well, millerite, linnaeite and pyrite are reported (BC MINFILE). One of these lenses is up to 30 cm in width and strikes 330 degrees. Analyses of a number of samples of this mineralization are reported in Assessment Report 4927. These samples contain trace silver and gold, 1.0 to 1.4 g/t platinum, and up to 160 ppm cobalt, 0.23% nickel and 16.5% chromium.

A second chromite occurrence, referred to as **Little Sheep Creek ultramafics** (082F/SW214) is located in the Little Sheep Creek valley approximately 3 km southwest of Rossland. This occurrence is associated with minor asbestos.

Fyles (1984, p. 23) describes exploration for nickel near the northern contact of a mass of serpentinite on the Midnight property along the west side of Little Sheep Creek: "exploration companies sampled underground workings and reported several thousand tonnes of serpentinite averaging 0.25% nickel. Selected samples assayed as high as 0.45% nickel. In samples submitted to R.V. Kirkham of the Geological Survey of Canada, pyrite, millerite (NiS) and a mineral of the linnaeite group were identified. Ten samples taken by (Fyles) at various places throughout the two masses of serpentinite exposed in the area gave nickel assays of less than 0.24 per cent."

STRUCTURE AND TECTONICS

The structure of the Rossland area has been well described by Fyles (1984) and Little (1982b). Fyles divided the area into two domains separated by the "Rossland break", an east-trending zone marked by a number of faults and intrusions, including the Rossland monzonite, Rainy Day pluton and serpentinites. Fyles suggested that the Rossland break is a zone of "structural weakness that may have originated when the Rossland Group was laid down..." (Fyles, 1984, p.29). South of the break, structures trend northeasterly whereas to the north, they trend northerly.

Detailed mapping, concentrated largely south of Rossland (Höy and Andrew, 1991a; 1991b) has, in large part, confirmed the structures outlined by Fyles. However, correlation of both map units and structural patterns to those farther east has allowed a better understanding of the stratigraphic position of the Rossland mining camp and of the tectonic evolution of the area. Three phases of deformation affecting Rossland-age rocks are recognized:

- extensional tectonism during deposition of lower Rossland Group rocks in Early Jurassic time;
- east-directed thrust faulting and associated minor folding before intrusion of Middle and Late Jurassic plutons;
- normal faulting in Eocene time.

EARLY JURASSIC

The Rossland area is underlain by a tectonic high, bounded by growth faults, that is first evident in early Rossland time (Höy and Dunne, 1997). The basal sedimentary succession of the Rossland Group, the Archibald Formation, records deposition in a fault-bounded structural basin located east of the Rossland map area, in the Beaver Creek valley (Andrew *et al.*, 1990a,b). The source area, based on facies analyses, was inferred to lie immediately to the west. In the Rossland area, the Archibald Formation is missing or represented by a thin basal conglomerate and the entire lower part of the Elise Formation is generally missing (Figures 4-1, 4-4) confirming the presence of a tectonic high and source area here. The orientation and exact position of the bounding growth faults are not known; however, the rapid facies changes in Elise rocks just east of Waneta suggest that the late north-trending faults located there might be the loci of some of the syndepositional Rossland growth faults. The location of other north-trending faults, including the Eocene Champion Lake fault, may also be controlled or modified by either fault-controlled facies changes in Rossland Group rocks or Rossland-age growth faults. Finally, the east-trending Rossland break also appears to record a zone of structural weakness in Rossland time (Fyles, 1984) suggesting that the uplifted tectonic high in the Rossland area may have been controlled by an orthogonal pattern of block faults. Block-faulted regions, with fault-bounded basins and tectonic highs, generally record extensional tectonics. These areas tend to localize later structures and intrusions and hence are favourable sites for structurally controlled mineral deposits.

MIDDLE JURASSIC

A period of compressive tectonism, evident throughout the Rossland Group in Middle Jurassic time, produced tight folds, a penetrative cleavage and intense shearing in eastern exposures, and more open, upright folds and thrust faults farther west. Southeast of the Rossland area, the Waneta and Tillicum Creek faults record further reworking of the Quesnellia - Slide Mountain - Kootenay terrane boundary. The Waneta fault, initially recognized by Fyles and Hewlett (1959) in the Salmo area, separates rocks of the ?Slide Mountain Charbonneau Creek assemblage from those of Quesnellia (Einersen, 1994). The Tillicum Creek fault separates the Charbonneau Creek assemblage from the Harcourt Creek assemblage, correlated by Einersen (*op. cit.*) with the Milford Group Davis Creek assemblage of the Kootenay terrane. Both faults contain slivers of ultramafic rocks along them and, hence, both are interpreted to be thrusts that place Quesnel rocks and oceanic rocks onto Kootenay terrane and North American rocks.

The Waneta fault has been traced westward into the Rossland area (Little, 1982b; Höy and Andrew, 1991a; 1991b) where it is covered by the Late Cretaceous Sophie Mountain Formation or the Eocene volcanic rocks of the Marron Formation (Figure 4-1).

The Snowdrop fault west of Rossland is a west-dipping structure, marked by intense shearing and brecciation, that places a west-facing panel of Mount Roberts Formation and basal Elise on younger Elise Formation (Sections A-A', B-B', Figure 4-2, in pocket). Related folds are concentrated in only a few areas; the Rossland area is essentially a west to northwest-dipping homoclinal succession of Rossland Group rocks (Fyles, 1984; Höy and Andrew, 1991a;b).

The age of this compressive deformation is constrained in the Nelson area to be post- Toarcian (*ca.* 187 Ma), the youngest age of Rossland Group rocks, and pre-intrusion of middle Jurassic Nelson plutons (*ca.* 167 Ma). Furthermore, Höy and Andrew (1997, p. 84) have argued that the *ca.* 174-178 Ma 'Silver King intrusions' (south of Nelson) are a syncollisional intrusive suite that records the earliest onlap

of the eastern margin of Quesnellia with North American crustal rocks. Farther north in the Kootenay arc, Colpron *et al.* (1996) constrain "juxtaposition of the Intermontane superterrane over the North American margin" between 187-173 Ma and post-emplacement, southwest-verging deformation between 173-168 Ma. High temperature shear zones within the 'tail' of the Nelson pluton south of Nelson, suggest strain may have continued along the Waneta fault during emplacement of the batholith (Vogl and Simony, 1992).

EOCENE

Steeply dipping, generally north-trending normal(?) faults occur throughout the Rossland area. A number of these on the slopes of Mount Roberts just west of Rossland have been described in considerable detail by Fyles (1984). As described above, they appear to be along a major structural break that was the locus for earlier thrust emplacement of ultramafic rocks.

The OK fault appears to be a listric normal fault that is overturned to the east at higher structural levels (Fyles, 1984; Stinson, 1995). Marron Formation rocks in the western block have been down-dropped in excess of 600 metres (Fyles, *op. cit.*). Similarly, the Jumbo fault is inferred to be overturned at higher structural levels, with a steep east-dip near surface exposures. It is interpreted to be downthrown to the west (Fyles, *op. cit.*). Shattered syenites along the east side of the fault indicate movement after Eocene emplacement of the Coryell intrusion. The Snowdrop fault lies in the panel of Mount Roberts Formation rocks between the OK and Jumbo faults. It is a west-dipping fault that is inferred to be older than, and unrelated to the normal faults. A spectacular breccia with large angular fragments and a quartz-calcite-hornblende-sulphide matrix is exposed along the Cascade highway just northwest of the gold-quartz veins in the Jumbo Creek valley. Höy and Andrew (1991a) suggested that this may be from an earlier thrust fault, related to emplacement of ophiolitic rocks.

North-trending faults southeast of Rossland, of inferred Eocene age, include the Violin Lake, Tiger Creek and Malde Creek faults (Figure 4-1). The Violin Lake fault is a vertical structure with an unknown amount of displacements (Little, 1985). It appears to truncate the Waneta fault and possibly the Eocene Marron Formation in the south, but produces little, if any offset of the Rossland monzonite; hence, it may die out to the north. The Tiger Creek fault is inferred from truncation and displacements of units in the Elise Formation (Figure 4-1). However, it also dies out northward as it displaces the Rossland monzonite only minimally. A number of north-trending faults with minor right-lateral displacement in the Malde Creek area, southwest of the Tiger Creek fault, may follow the loci of Rossland-age growth faults. They are associated with pronounced facies changes in the Rossland Group, and appear to die out up-section.

These late faults are younger than the Eocene intrusive and extrusive events. The Jumbo fault brecciates Middle Eocene Coryell intrusive rocks; the OK and Violin Lake faults truncate Middle Eocene lavas of the Marron Formation, and a western splay of the Tiger Creek fault truncates Sheppard intrusions in the Mount Sophie Formation (Figure 4-1). These faults are probably related to Eocene extensional events in southern British Columbia (Parrish *et al.*, 1988; Corbett and Simony, 1984).

Wingate (1993) and Wingate and Irving (1994), based on paleomagnetic evidence, have shown that the Rossland area has been tilted westward in excess of 30° due to rotational movement on Eocene listric extensional faults, such as the Kettle fault and newly named Arrow Lake fault proposed to cut through the Coryell intrusion. This tilting has rotated earlier faults, including thrusts such as the Waneta and Tillicum Creek, and possibly earlier (?) Tertiary faults described above. It also affected pre-Tertiary rocks, including the Rossland monzonite, and hence has allowed an oblique view through a major mineral deposit camp, with deeper structural levels exposed in the east and shallower levels farther west.

MINERAL DEPOSITS

The following sections describe the molybdenite breccias on the western slopes of Red Mountain, the copper-gold veins of the North belt and Main veins, the South belt lead-zinc-silver veins and high-grade gold-quartz veins located approximately 4 kilometres southwest of Rossland in the Little Sheep Creek valley (Figure 4-8). These latter veins are in highly altered "greenstones" adjacent to a small unit of serpentinite. The various deposits are classified, constraints are placed on their ages, and a metallogenic model is presented that integrates these somewhat diverse deposit types.

Most of the mines and veins of these camps are not described individually in this report, as access and sampling was largely restricted to dump material; the descriptions of many of the veins by Drysdale (1915) and of the molybdenite mineralization by Fyles (1984) still remain the most comprehensive.

Molybdenum deposits on Red Mountain produced about 1.75 million kilograms of molybdenum from approximately 1 million tonnes of ore between 1966 and 1972 (Appendix 3; B.C. MINFILE data). Molybdenite occurs dominantly in quartz veins and veinlets cutting a coarse breccia complex in a west-dipping and facing, hornfelsed and skarned siltstone succession (Fyles, 1984). The molybdenite and host quartz diorite intrusive breccias have been dated at 162-163 Ma by Re-Os and U-Pb methods respectively (*see* below and Appendices 4 and 7), which is younger than the Rossland monzonite and associated gold-copper veins.

Drysdale (1915) divided the veins of the Rossland camp into three main belts, termed the North belt, Main veins and South belt. All veins trend east-west, with variable but generally steep northerly dips. The veins cross the western exposures of the Rossland monzonite, the Rossland sill, and metavolcanic and metasedimentary rocks of the structurally higher Elise Formation to the west.

We conclude in this paper that Cu-Au vein mineralization of the Rossland camp is spatially and genetically related

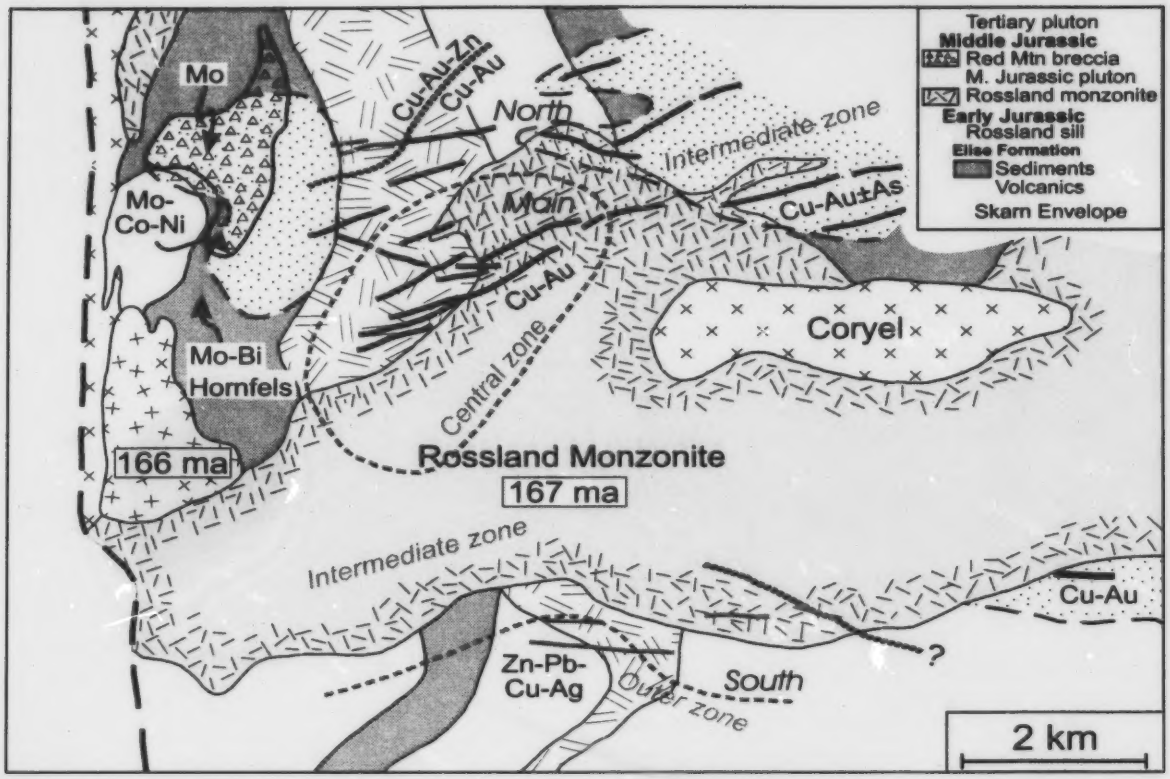

Figure 4-8. Simplified geological map of the Rossland copper-gold camp (for details, *see* Figure 4-2, in pocket); modified from Drysdale (1915), Thorpe (1967), Fyles (1984), Cominco Ltd. unpublished data and Höy and Dunne (1997).

to diorite porphyry dikes, which are late phases of the Rossland monzonite. Furthermore, we suggest that the diverse character, mineralogy, alteration and tenor of these veins are related largely to depth of emplacement and proximity to the Rossland pluton. Skarn alteration and associated higher temperature Au-Cu veins occur in eastern, structurally deeper exposures whereas more brittle Pb-Zn-Ag veins occur at higher structural levels in western exposures in the South belt. This model is compatible with paleomagnetic data that suggests that the Rossland monzonite and host Rossland Group were tilted down to the west in Eocene time, thereby exposing progressively shallower structural levels in the west.

RED MOUNTAIN Mo DEPOSITS

INTRODUCTION

The molybdenite deposits on the western slopes of Red Mountain have been described in considerable detail by Fyles (1984), and this summary is based in part on his work. Recent work by Webster *et al.* (1992) and Ray and Webster (1997) describes the general characteristics of molybdenite skarns and the mineralogy and chemistry of the Red Mountain deposits.

Exploration for molybdenum on the western and upper slopes of Red Mountain began in 1962 by Torwest Resources Ltd. and subsequently continued on the southern slopes by Cascade Molybdenite Mines Ltd. (Fyles, 1984). Production by Red Mountain Mines Ltd. began in 1966 from a number of shallow pits and, until 1972, produced 1,748,871 kilograms of molybdenum from 939,397 tonnes of ore (Coxey deposit, Appendix 3) (Photos 4-4a and 4b). Geological mapping, geochemical and geophysical surveys, and drilling were carried out by Minefinders Inc. from 1972 to 1974. In 1981, David Minerals drilled nine short holes on the Novelty to test for gold, molybdenum and cobalt mineralization (Richardson, 1982).

Molybdenite occurs within a breccia-skarn complex that contains irregular, generally north-striking intrusive breccia dikes. The breccia complex trends roughly north-south, with a maximum exposed length of 2 700 metres and a width up to 1 200 metres (Figure 4-8). It extends across the Mountain View, Nevada, Coxey, Novelty and Giant claims. It is developed in fine-grained metasediments near the top of the exposed Elise Formation. A sill complex, referred to as the Rossland sill, intrudes the Elise Formation just east of the molybdenite deposits and is, in turn, intruded by the Rossland monzonite. Numerous north-trending dikes cut the monzonite, the Rossland sill and the Elise Formation rocks in the vicinity of the molybdenite breccia complex.

Photo 4-4a. View of the northwestern slope of Red Mountain showing open pits developed by Red Mountain Mines Ltd. in the late 1960s and early 1970s. Note mill site in the saddle at left of photo (Photo 4b).

Photo 4-4b. View of Red Mountain mill site on the north side of Red Mountain; note ski runs on slopes of the mountain.

HOST ROCKS

The molybdenite breccia complex is exposed on the western slopes of Red Mountain within an assemblage of generally west to southwest-dipping, dark grey to black siltstones and argillites. These metasediments are typically rusty weathering containing disseminated pyrrhotite and minor pyrite. Occasional white quartzite layers and calcsilicates, suggestive of a calcareous protolith, are also noted.

Hornfelsed and skarned argillite and siltstone, within and adjacent to the breccia complex, are pale to medium green, grey, buff or purplish brown, laminated to massive hard "cherty" rocks (Fyles, 1984). They comprise fine-grained quartz and feldspar with variable biotite, pyroxene (diopside?) and hornblende, and locally minor garnet and epidote. Typical alteration paragenesis includes early biotite hornfelsing with a purple-brown colouration, followed by prograde skarn diopside ± quartz and minor molybdenite mineralization, then chlorite- amphibole-molybdenite veining with bleached envelopes, and finally late thin carbonate-epidote veins.

These metasediments have been correlated with either the Elise Formation (Fyles, 1984) or the Mount Roberts Formation that implied a thrust contact with underlying Rossland sill (Höy and Andrew, 1991b). Fyles (*op. cit.*) recognized sills and dikes of the Rossland sill complex cutting overlying metasediments, evidence of an intrusive contact. We support the correlation with the Elise Formation and hence, the interpretation of an intrusive contact between the metasediments and the Rossland sill; detailed mapping (Figure 4-2) illustrates the irregular, intrusive character of the contact. The contact, which is intersected by drilling on the Gertrude property, shows no sign of shearing or brecciation, and thin pyrrhotite veins, similar to veins of the Rossland gold camp, cut the contact and overlying metasediments.

The Rossland sill has been interpreted to be an Elise-age subvolcanic intrusion, similar to other monzogabbro intrusions within the Rossland Group. However, Fyles (1984, p. 19) describes fragmental textures with "subrounded blocks a few centimetres to as much as a metre across that are somewhat lighter in colour than the main mass of porphyry but essentially the same composition." These fragmental textures are also noted in Gertrude drill core, as are thin layers of green, fine-grained, bedded and occasionally graded tuffs. Hence, it is probable that the Rossland sill is a composite volcanic-intrusive complex that includes sill and dike material as well as Elise augite-phyric flows with flow breccia textures and ash and crystal tuffs.

A number of dikes, described by Fyles (1984), cut the metasediments and the molybdenite breccia complex. Diorite porphyry dikes or 'diorite porphyrites' of Drysdale (1915) are closely related to gold-copper vein mineralization in the Rossland camp. In contrast to Tertiary dikes, these dikes trend westerly, parallel to the veins, and are clearly altered and mineralized. On the western slopes of Red Mountain, similar porphyry dikes and sills form "irregular masses several metres across or lenticular sill-like sheets up to a few metres thick lying parallel to bedding in the hornfelsed siltstone" (Fyles, 1984, p.26). This diorite porphyry is "thermally metamorphosed, fractured, bleached, and mineralized with pyrrhotite and molybdenite, (and) is older than the dikes related to the Trail granodiorite". If these dikes are the same age as those that are related to copper-gold vein mineralization, then the copper-gold mineralization must be older than the molybdenite mineralization.

Large irregular masses of aphanitic to porphyritic intrusions, referred to as andesite or meta-andesite by Fyles (1984), occur as dikes or lenses in the vicinity of the molybdenite pits. They are early, cut by the north trending Eocene dikes and, as shown by Fyles (*op. cit.*), are also cut by the quartz diorite breccias which host the molybdenite mineralization. Their relationship to other intrusive rocks is not known; it is possible that they are Elise-age intrusions, phases of the Rossland sill, or perhaps related to the Rossland monzonite. Gilbert (1948) correlated them with the diorite porphyrites, but Fyles (*op. cit.*) concluded that "although this correlation is plausible, it is by no means certain".

Lamprophyre dikes of Tertiary age generally trend northerly with steep to vertical dips. They are typically dark and fine grained with biotite crystals and abundant potassic feldspar. "Diorite" dikes form a north 20° west swarm that cuts the breccia complex in the D and E pits. They are also dark and fine grained, with small hornblende needles. Their northerly trend and post-molybdenite mineralization emplacement suggest that they are also of Tertiary age.

MOLYBDENITE BRECCIA COMPLEX

Fyles (1984, p. 47) described the breccia complex, shown on Figure 4-8, in considerable detail. "Much of the hornfels and hornfelsic siltstone on Red Mountain comprises a breccia with angular blocks ranging up to 30 metres. The attitude of bedding and colour laminations which reflects bedding show that smaller blocks, from a few centimetres to a few metres across, have random orientation (Photo 4-5). Larger blocks, however, are only slightly disoriented from the normal low westerly dip of the siltstone....the margins of the Breccia complex dip steeply and are very irregular. The base appears to be controlled by bedding.... Most of the molybdenite mineralization is within the Breccia complex."

The matrix of the breccia consists of mainly fine-grained silicate minerals and rock fragments, with rare coarse-grained silicates, quartz, calcite, garnet, scheelite or molybdenite.

Within the breccia complex are irregular, generally east-trending intrusive breccia dikes, referred to above and by Fyles (1984) as 'Red Mountain diorite dikes'. They comprise subrounded fragments of generally medium-grained, equigranular quartz diorite with clasts up to 0.5 metres in diameter. Locally, concentrations of molybdenite occur within the endoskarn in the quartz diorite breccia. Along the margins of the intrusive breccia, hornfels also occurs as breccia fragments, and in their central portions, non-brecciated quartz diorite may occur. Chloritic alteration is locally intense, producing a pale green colour, and many fragments have pronounced bleached reaction rims along their margins (Photo 4-6).

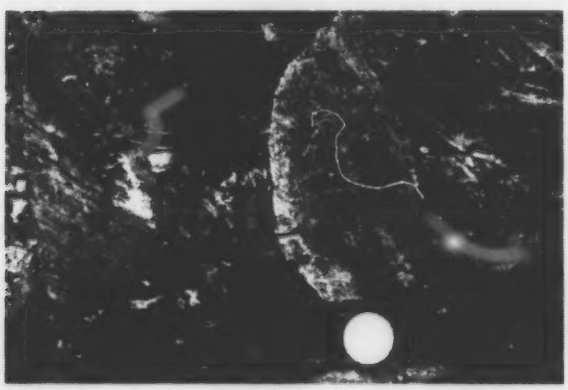

Photo 4-5. Red Mountain breccia, E pit, Mountain View claim (sample R96-20); diopside-rich metasediment clasts in a diopside, hornblende and minor molybdenite matrix (2 cm coin scale).

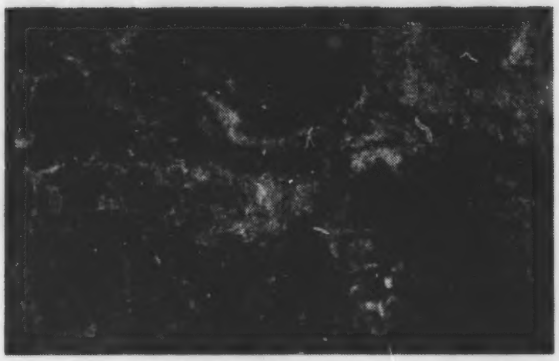

Photo 4-6. Altered and veined breccia, Red Mountain. Note (1) early biotite hornfels cut by bleached stringers (2) pale green diopside with minor dispersed molybdenite and (3) cross-cutting molybdenite-chlorite veins (2 cm coin scale).

As noted above, U-Pb analyses of zircons from one of these brecciated dikes yielded a 162.3 +1.2/-2.5 Ma age.

MINERALIZATION

Extensive molybdenite mineralization is largely confined to the breccia complex. It is restricted to a depth of less than 200 metres; deeper drill holes discovered only minor disseminated molybdenite and scheelite.

Molybdenite is generally associated with the intense skarn alteration. Mineralization is present as coarse molybdenite, with variable but generally minor pyrrhotite, arsenopyrite, pyrite, and locally minor chalcopyrite, bismuth, bismuthinite and variable amounts of scheelite. The molybdenite occurs in the skarn matrix or in sulphide veins cutting skarn.

Coxey (082FSWE110)

Most production from Red Mountain came from the Upper A, A, Upper B and B pits on the Coxey claim near the center of the breccia complex. Skarn alteration increases towards the upper, more eastern exposures (Webster *et al.*, 1992). Brecciation, biotite hornfelsing and prograde, mainly diopside ± garnet skarn alteration are intense (Photos 4-7a and 7b). The garnets are grossularite-andradite solid solutions and 'diopside', hedenbergite-diopside solid solutions (Ray and Webster, 1997). Late veins with coarse-grained dark chlorite, calcite and epidote cut the breccia-skarn. Molybdenite, pyrrhotite, arsenopyrite and pyrite, with minor scheelite and magnetite, occur in the skarn as well as in the later veins, commonly with chalcopyrite.

Mountain View (082FSW140)

The Mountain View claim is located upslope and northeast of the Coxey. Production was limited to two pits on the property, the E and the F pits (Photo 4-8). Recovered grades of 0.10% tungsten from these pits was the highest mined on Red Mountain.

Detailed petrographic studies show that the skarn in the Mountain View E pit (sample R96-12c, Appendix 5) com-

prises mainly granular quartz, K-feldspar, clinopyroxene (diopside) and garnet, cut by diopside-molybdenite veins. Molybdenite also occurs in veins with calcite, wollastonite(?) and minor ilmenite, locally altered to a sphene, rutile and pyrite assemblage. A second sample (R96-12a) is dominantly massive garnet intergrown with diopside that is partially replaced by tremolite. Late veinlets contain quartz, calcite, pyrrhotite and chalcopyrite. In the F pit, a thin pyrrhotite-pyrite-chalcopyrite vein cuts the "diopside" skarn. Wallrock to the vein (R96-19b) contains biotite, replaced by amphibole and epidote, and pyrite ± chalcopyrite locally rimmed by pyrrhotite and magnetite. Other gangue minerals include quartz and carbonate (ankerite or siderite).

Analyses of a number of samples from the pits on the Mountain View claim indicate unusually high concentrations of a number of elements (Appendix 6). One sample (R96-12a) contains 3800 ppm uranium, and a second sample (R96-12c) high lanthanum (1800 ppm), cerium (1100 ppm) and neodymium (150 ppm). Tungsten and copper values are also high, but gold is generally less than a few hundred ppb.

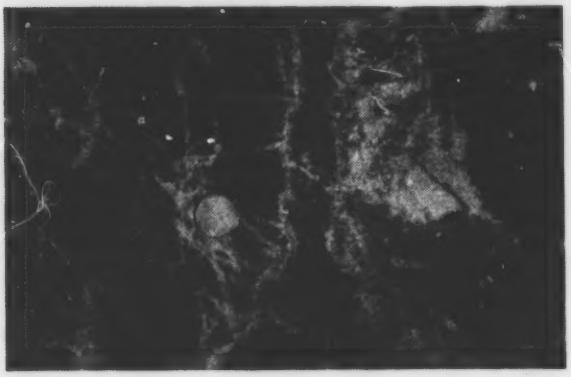

Photo 4-7a. Dark, biotite hornfelsed metasediments cut by numerous stringers of diopside and molybdenite, B pit, Coxey deposit, Red Mountain (sample R96-18) (2.5 cm coin scale).

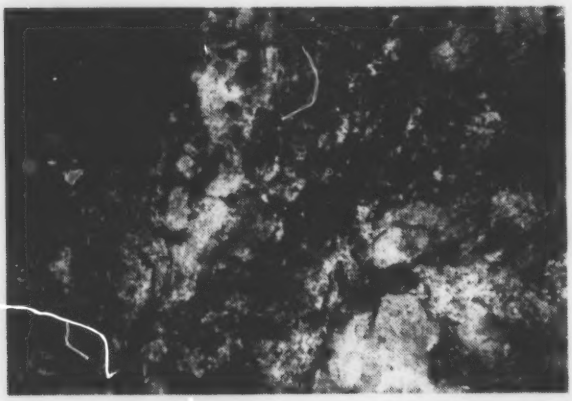

Photo 4-7b. Molybdenite with chlorite, calcite and epidote cut diopside-garnet skarn, B pit, Coxey deposit, Red Mountain (sample R96-17) (2.5 cm coin scale).

Nevada

The Nevada claim is the most western of the molybdenite-producing claims on Red Mountain. In the D pit, a number of late, north-trending dark, fine-grained Tertiary dikes cut pale green diopside skarn. Skarn alteration is less intense than in the Coxey pits to the east, and includes abundant biotite hornfels and diopside, but only minor garnet. Molybdenite, with only minor pyrrhotite, occurs in the skarn and in thin fractures cutting the skarn. One sample of mineralized skarn (R96-15, Appendix 6) contained 2.5% Mo and 3300 ppm barium, but low copper and gold values. A second sample from the B pit contained 4600 ppm Ba (Appendix 6, sample R96-7a.

Novelty (082FSW107)

The Novelty claim is located due south of the Coxey. It has a small exploration pit, and most recently was explored by nine diamond drill holes (Richardson, 1982). The best mineralized intersections are listed in Table 4-3.

Mineralization and chemistry of the Novelty are unusual. It is mainly a molybdenite-arsenopyrite-pyrrhotite skarn with low copper content. The skarn comprises mainly plagioclase (andesine?) and diopside with sulphides, and minor sphene, calcite, sericite, biotite and apatite. Nickel content is high (Appendix 6), as is cobalt which produces cobalt bloom (erythrite) on fracture surfaces. Bismuth and bismuthinite are also abundant; Thorpe (1967, p. 26) reported that "an isolated area of bismuth was observed to include a number of small crystals of molybdenite".

Gold content, generally low throughout the molybdenite breccia complex, is high in the Novelty pit. One analysis of a skarn sample contained 114 ppm gold and a second, 43.3 ppm (samples R96-7a, R96-7b; Appendix 6). Thorpe (1967) described blebs of gold disseminated in siliceous skarn adjacent to veins and patches of arsenopyrite and molybdenite.

Giant (082FSW109)

The Giant is the most southern of the claims within the breccia complex. Production from the Giant property is included in that of the California claim (Appendix 3); 3 900 tonnes are reported to have been shipped from the Giant prior to operations being suspended in 1903 (Drysdale, 1915). In 1966, 17 drill holes indicated an open pit reserve of 50 000 tonnes containing 0.282% MoS_2 and 1.16 g/t gold. In 1971, indicated reserves for the Novelty and Giant were 706 177 tonnes containing 0.2% MoS_2 and 1.9 g/t gold (David Minerals Ltd., Statement of Material Facts, Dec 23, 1980).

Considerable trenching and stripping on the Giant claim have exposed a number of highly altered intrusive and metasedimentary rocks, alteration and sulphides. In general, exposures in the stripped area are silicified, skarned and brecciated, and contain disseminated pyrite or pyrrhotite which results in brown to tan coloured outcrops. Exposed rocks include an irregular mass of a granular,

TABLE 4-3
DRILL INTERSECTIONS, NOVELTY PROPERTY
(Exploration by David Minerals, 1981; *see* Richardson, 1982)

Hole	From	To	Length Metres	Au g/T	Mo %	Co %
RN 81-1	5.0	6.5	1.5	27.6	0.655	0.063
	26.0	38.5	12.5	6.7	0.151	0.178
RN 81-2	29.0	34.0	5.0	17.7	0.785	0.110
RN 81-3	1.5	16.8	15.3	1.9	0.200	0.057
RN 81-5	7.45	13.3	5.85	3.8	0.196	0.110
	15.25	23.0	7.75	1.3	0.226	0.014
RN 81-6	20.65	26.5	5.85	0.4	0.515	0.008
	38.0	42.5	4.5	3.6	0.171	0.039
RN 81-8	38.7	41.5	2.8	5.6	0.048	0.064
	45.0	47.25	2.25	1.5	0.043	0.100
RN 81-9	26.3	30.0	3.7	2.4	0.067	
	32.5	35.5	3.0	8.8	0.099	0.300
	38.5	47.0	8.5	1.3	0.138	0.028

leucocratic, rusty-weathering pyritic intrusion, as well as north-trending lamprophyre and other mafic dikes. Diopsidic skarn alteration in the metasediments appears to be overprinted by sericitic alteration with associated dispersed pyrite. Hence, the original distribution of the skarn alteration may have been considerably larger.

Several styles of mineralization occur on the property: (1) a narrow north-striking, east-dipping vein with cobalt, nickel, arsenic, bismuth, and molybdenum values, (2) an east-west striking pyrrhotite-chalcopyrite vein that is similar to the gold-copper veins of the Rossland camp, and (3) molybdenite, pyrrhotite, bismuth, bismuthinite and minor chalcopyrite in the breccia-skarn complex. All appear to have elevated gold content.

The north-striking vein has gradational boundaries and parallels a fine-grained syenitic dike. Mineralization comprises mainly pyrrhotite with locally abundant native bismuth, bismuthinite, arsenopyrite, pyrite and some molybdenite and chalcopyrite. Native gold occurs dispersed in the sulphides. Analyses of selected hand samples of the vein and immediate skarn hostrocks returned high gold content (5 to 17 ppm), arsenic, nickel, cobalt (4100 to 6000 ppm) and selenium (R96-62a,b,c; Appendix 6).

An east-west trending pyrrhotite vein with minor chalcopyrite cuts silicified sediments. An analysis (R96-61b) returned 0.1% copper and 10.5 ppm gold.

Hornfelsed metasediments, and locally diopside skarn alteration of a metasedimentary breccia, contain irregular masses and veins of molybdenite and pyrrhotite with concentrations of bismuth and bismuthinite locally. Pyrrhotite, pyrite, arsenopyrite and minor chalcopyrite(?) also occur dispersed throughout the metasediments. Analysis of the skarn (R96-62d, Appendix 6) also shows that it contains, at least locally, high gold and copper values as well as anomalous nickel, cobalt, uranium, selenium, cerium, neodymium and samarium.

Re-OS DATING

A sample of molybdenite from the B pit on the Coxey claim was analyzed at AIRIE, Colorado State University, to obtain a Re-Os date. An age of 162.9±0.5 Ma was determined (*see* Appendix 7 for data). A similar age for the host intrusive breccia in the A pit is independent supportive evidence for the age of molybdenite mineralization on Red Mountain.

SUMMARY

Molybdenite and scheelite occur within a skarn-intrusive breccia complex on the western slopes of Red Mountain west of and structurally above the gold-copper veins of the Rossland camp. The breccia complex is largely developed in fine-grained metasedimentary rocks of the Elise Formation, but is also intimately associated with quartz diorite breccia dikes.

Molybdenite and minor scheelite mineralization in the complex appears to be associated with prograde K-Mg-Ca metasomatism that produced diopside, garnet, K-feldspar, calcic plagioclase, variable but generally minor quartz as well as other skarn minerals. It overprints an earlier biotite hornfels and is cut by late, epidote-amphibole veins that also contain pyrrhotite, pyrite, chalcopyrite and rare molybdenite.

Molybdenite mineralization is associated with a variety of other elements that may have a crude camp zonation. In eastern exposures, garnet is abundant and disseminated sulphides are prominent producing rusted outcrops. The molybdenite occurs with locally high concentrations of scheelite (tungsten) and anomalous uranium, lanthanum, cerium and neodymium. Gold and copper contents are low, except in rare crosscutting pyrrhotite-chalcopyrite veins. In southern exposures on the Novelty and Giant claims, gold content is high, and mineralization comprises molybdenite and arsenopyrite with high nickel, cobalt, bismuth, barium and selenium values. Within the central part of the complex, in the eastern pits of the Coxey claim, molybdenite and ar-

senopyrite with only minor scheelite and low copper-gold values, predominate. The most western and structurally highest exposures consist of brecciated endoskarns with molybdenite and locally high barium values.

DISCUSSION

The age of the molybdenite mineralization is 162.9±0.9 Ma, based on Re-Os dating. However, its relationship to intrusive events or to the gold-copper veins of the Rossland camp is less certain. The close spatial association of molybdenite mineralization with the Red Mountain quartz diorite dikes, incorporation of dike fragments in the breccia complex, and a *ca.* 162 Ma U-Pb zircon age (Figure 4-7), indicate that the molybdenite is related to the dikes. It has generally been assumed that this mineralization is associated with the *ca.* 166 Ma Rainy Day quartz diorite (Figure 4-6), an intrusion exposed less than a kilometre to the south that contains minor molybdenite mineralization (Fyles, 1984).

Based on similar chemistry and mineralogy with the Rainy Day pluton, and a slightly younger age than this pluton and the Rossland pluton, we suggest that the Red Mountain dikes are a late phase of these plutons, a phase that was associated with explosive volatiles that brecciated, altered and mineralized host Elise metasediments.

"Andesite" intrusions in the skarn complex are early, as they are overprinted by both skarn alteration and molybdenite mineralization. However, they are not brecciated and it is not known if they are cogenetic with the Red Mountain dikes in the breccia complex. Fyles (1984, Figure 5) shows them cut by these dikes, supporting an older age.

As discussed below, copper-gold veins of the Rossland camp are spatially and genetically related to the *ca.* 167 Ma Rossland monzonite and associated diorite porphyry dikes. Similar porphyry dikes within the breccia complex (distinct from the Red Mountain dikes) are overprinted by skarn alteration and molybdenite mineralization. This supports a model of early Cu-Au vein mineralization followed by brecciation, skarn alteration and molybdenite mineralization associated with 162-163 Ma quartz diorite dike emplacement.

However, thin pyrrhotite-chalcopyrite veins, the western extension of the veins of the North belt in the Rossland camp, appear to cut skarn alteration (but not breccia) related to molybdenite mineralization in the F pit on the Mountain View claim. This implies that molybdenite mineralization is older than the veins. It is probable, however, that these thin veins formed earlier and were unaffected by later skarn alteration.

In summary, we conclude that there are several periods of intrusive activity, and two main periods of sulphide mineralization and alteration in the Red Mountain camp area:

- *ca.* 195-197 Ma: deposition of Elise Formation, followed by intrusion of Rossland sill.
- early "andesite" dike emplacement.

Photo 4-8. View of the headwall of E pit, Mountain View molybdenite deposit, Red Mountain.

- *ca.* 167 Ma: intrusion of the Rossland monzonite, diorite porphyry dikes and gold-copper vein mineralization.
- *ca.* 166 Ma: coeval, or slightly younger, intrusion of Rainy Day pluton, skarn alteration, some molybdenite mineralization.
- 162-163 Ma: Red Mountain dike emplacement, brecciation, intense skarn alteration and molybdenite mineralization.

REGIONAL IMPLICATIONS

Molybdenum occurrences, such as the Stewart and Mammoth within the Nelson-Trail map-area are generally associated with Middle Jurassic Nelson-age intrusions, occurring as molybdenite skarns or porphyries, and associated with tungsten mineralization and breccia complexes (*see* Chapter 3). We conclude that molybdenite mineralization, brecciation and skarn alteration on Red Mountain is similar, related to late dike phases of the Middle Jurassic Rainy Day quartz diorite.

ROSSLAND COPPER-GOLD VEINS

INTRODUCTION

Copper-gold veins in the Rossland camp were divided by Drysdale (1915) into three main belts, referred to as the North belt, Main veins and South belt (*see* Figure 4-8). Production from the Rossland veins, mainly between 1897 and the early 1940s, are summarized in Appendix 3. In total, 85 904 623 grams of gold (~2.76 million ounces), 109 509 814 grams of silver (~3.52 million ounces) and 71 502 kilograms of copper were recovered from the mines of the Rossland camp. Of that, 98 percent came from the Main veins, and 80 percent of this production came from deposits in a central core zone between two large north-trending Tertiary lamprophyre dikes. Deposits in this central zone include the Le Roi, Centre Star, Nickel Plate, Josie and War Eagle mines (Photo 4-9).

Thorpe (1967) first described a clearly defined mineralogical and chemical zonation, also shown on Figure 4-8. A

Photo 4-9. Waste dump on Le Roi claim, Red Mountain, viewed to northwest.

'central' zone located along the western edge of the Rossland monzonite and into the Rossland sill is dominated by massive pyrrhotite with persistent but minor chalcopyrite; an 'intermediate' zone, peripheral to the central zone has veins that contain arsenopyrite, pyrite, cobalt, bismuth minerals and molybdenite in addition to pyrrhotite and chalcopyrite. The 'outer' zone south of the Rossland monzonite is marked by veins that contain galena and tetrahedrite.

Veins of the North belt are entirely within the 'intermediate' zone whereas Main veins extend westward from the 'intermediate' zone into the 'central' zone. Most veins of the South belt are within the 'outer' zone.

The purpose of the following sections is to describe the intrusive-related gold-sulphide veins, attempt to relate these to the structurally higher molybdenite skarn-breccia complex described above, and to develop a model that integrates these with the lead-zinc-silver veins of the South belt and the structural and magmatic history of the area.

NORTH BELT

The North belt comprises a zone of discontinuous veins that extend west from Monte Cristo Mountain to the northern ridge of Red Mountain. The veins trend east and dip north at 60° to 70°. Veins in the North belt are mainly pyrrhotite with chalcopyrite in a gangue of altered rock with minor lenses of quartz and calcite. The largest, on the Cliff and Consolidated St. Elmo claims, are exposed for almost 100 metres along strike. However, more eastern exposures of the vein system (Monte Cristo, Evening Star, Cliff) contain considerable arsenopyrite and, locally, trace ?molybdenite, scheelite and cobalt minerals whereas farther west (St. Elmo, Consolidated St. Elmo) sphalerite and galena are common.

EVENING STAR (82FSW102)

Introduction

The Evening Star vein is mainly within metasediments of the Elise Formation along the north edge of the Rossland monzonite. It was in production intermittently from 1896-1908 and 1932-1939, with recovery of 56.7 kilograms of gold, 21.5 kilograms of silver and 1 276 kilograms of copper from 2 859 tonnes of ore, representing a recovered gold grade of approximately 20 g/tonne. This production was mainly from a wide and irregular northeast-striking vein of arsenopyrite, pyrrhotite, pyrite and chalcopyrite (Drysdale, 1915). The veins have a high cobalt content with danaite, a cobaltiferous arsenopyrite, and samples of pyrrhotite containing 1.58% cobalt and 0.67% nickel oxide (Drysdale, *op. cit.*).

Cominco Ltd. optioned the Evening Star claim in 1980 and explored its potential as a low-grade gold stockwork deposit. However, the option was dropped after discouraging results in seven percussion drill holes. In the early 1980s, Gallant Gold Mines optioned the Georgia property, which included a number of the eastern extensions of veins of both the North belt and Main veins and did considerable prospecting, mapping, rock-chip sampling and some geophysical surveying (Troup *et al.*, 1984), and in 1986, conducted some diamond drilling (Hardy, 1986). Exploration in the late 1980s by Antelope Resources included geological mapping, rock geochemical sampling, electromagnetic geophysical surveys, as well as underground rehabilitation and considerable underground drilling (Fowler and Wehrle, 1990). The drilling intersected both thin, irregular veins and zones of mineralized and altered country rocks. The best intersection, in diamond-drill hole 88-37, contained 35.7 g/t gold over 4.4 metres.

In 1990-1991, Vangold Resources continued exploration, with geophysical surveys and some limited drilling, resulting in reported reserves in the "main zone" of 20 000 tonnes grading 17 g/t gold (Wehrle, 1995). Hole NB-91-11, located approximately 125 metres southwest of the main zone (Figure 4-9), intersected 3.1 metres grading 27 g/t gold. Additional drilling in 1994 concentrated on this extension of the main zone. Hole NB-94-5 intersected 1.5 metres grading 12 g/t gold "in a strongly altered volcanogenic sediment containing a 25% mixture of pyrrhotite, pyrite, arsenopyrite and chalcopyrite" (Wehrle, 1995, p.7), and NB-94-6, approximately 3 metres grading 14 g/t gold. A vertical hole, NB-94-7, drilled to test the down dip extension intersected 4.6 metres grading 5 g/t Au at 72.3 metres depth.

Description

The vein system consists of irregular, discontinuous veins within altered Elise metasediments and underlying Rossland monzonite. Veins in the Rossland monzonite are generally not as rich nor have the pronounced alteration envelopes as those in the metasediments (Figure 4-10). The veins are parallel to and within numerous diorite porphyry dikes that extend, at depth, into the main mass of the Rossland monzonite. As with other veins in the Rossland camp, their strong structural control is indicated by the prominent regional as well as local preferred orientations, and the prominent shearing both within and along the margins of some of the vein (Photo 4-10). This structural control is also apparent in the parallel orientation of some Rossland monzonite dikes. Late, north-trending, steeply dipping feldspar porphyry dikes, of probable Eocene age, cut the veins,

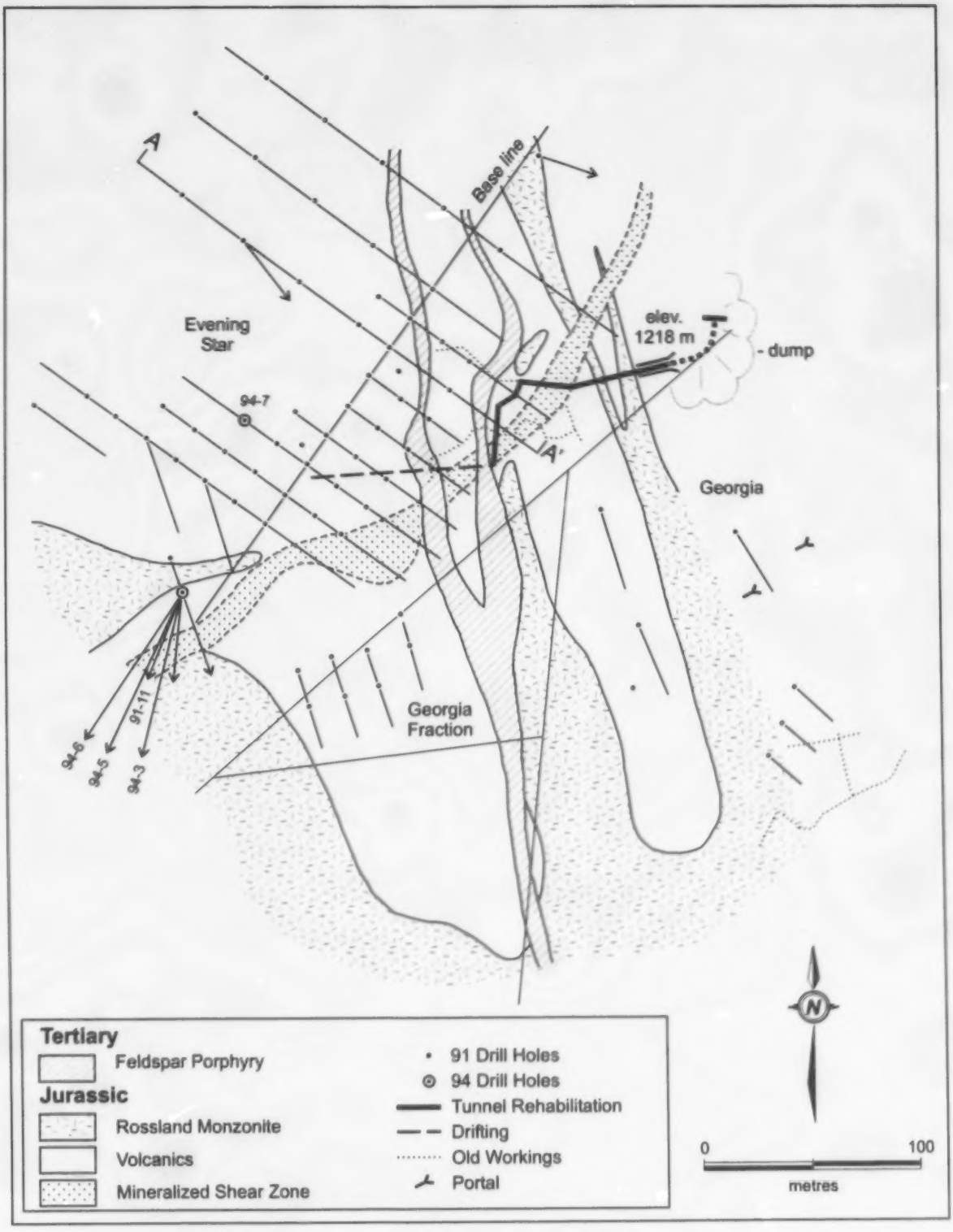

Figure 4-9. Diamond drill location plan, and simplified geology map of the Evening Star and Georgia claim area, North Belt, Rossland camp (from Wehrle, 1995).

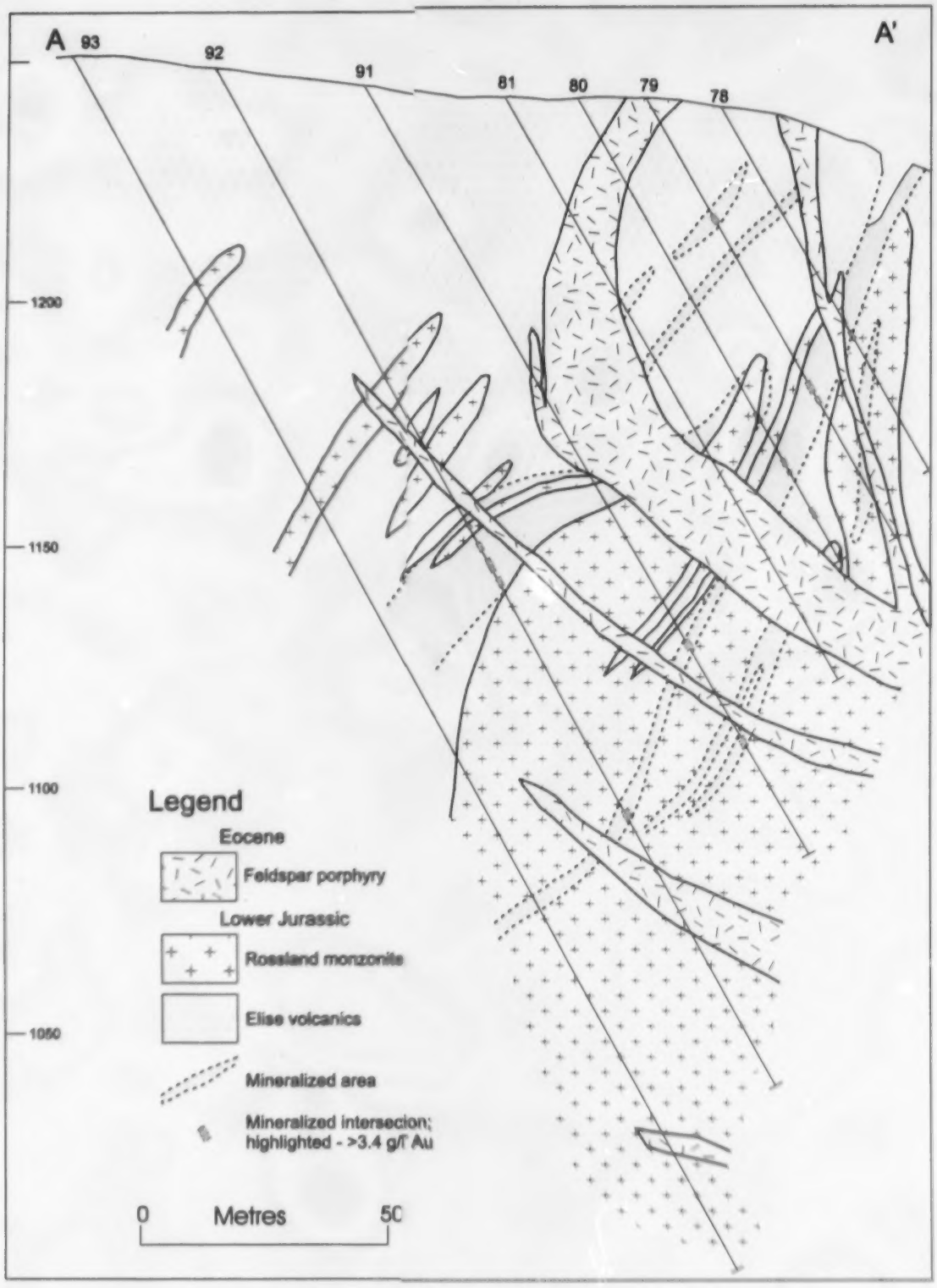

Figure 4-10. Vertical section through the Evening Star deposit, viewed to the northeast (*see* figures 4-2 and 4-9 for location); section and data from unpublished data, D. Wehrle, Vangold Resources, Inc.

associated alteration and the Rossland monzonite (Figures 4-9, 4-10).

The mineralogy of the Evening Star veins consists of mainly pyrrhotite and arsenopyrite. Chalcopyrite is intimately intergrown with pyrrhotite or occurs as finely dispersed grains. Pyrite, typically after pyrrhotite, and minor sphalerite, molybdenite and magnetite, and trace danaite, bismuthinite and erythrite (cobalt bloom), have been identified (Thorpe, 1967). Gangue minerals in the veins include calcite, a dark green amphibole (termed hornblende, below), chlorite, quartz, fine-grained biotite and minor epidote.

Alteration assemblages are zoned, with more proximal skarn alteration and distal biotite hornfelsing. The distribution of these assemblages, based mainly on examination of specimens from an ore stockpile, is illustrated schematically in Figure 4-11. Sulphides form massive to semi-massive elongate pods and lenses within a medium to dark green skarn assemblage of mainly hornblende, chlorite, epidote, diopside, garnet and plagioclase. An envelope of siliceous, biotitic hornfels, commonly cut by thin hornblende-sulphide veins, surrounds the skarn assemblage (Photo 4-11). The siliceous zone extends out into biotite ± epidote hornfels; thin sulphide veins as well as some disseminated sulphides and locally, low gold grades persist in this zone (Figure 4-10). The distal, biotite hornfels grades laterally into regional, propylitically altered metasediments. Thin quartz-calcite-pyrite veins cut all other assemblages. This mineralogical zonation is reflected in a local chemical zonation as well, with proximal sulphide-Fe-Mg rich assemblages and distal potassic alteration.

A general gradation of skarn mineral assemblages away from the Rossland monzonite has been noted by Stinson and Patterson (1993, p. 250):

"Pockets of garnetiferous skarn, the highest metamorphic grade observed, occur locally in the ore zone within 10 metres of the igneous contact. These exhibit a coarse-grained skarn assemblage of andraditic garnet, diopside and plagioclase, which in turn is overprinted by hornblende along growth zones in garnet, and by quartz, calcite and zeolites. Minor arsenopyrite and pyrite are disseminated in this rock, and chalcopyrite and pyrrhotite are mainly confined to late quartz-carbonate veins."

"Farther out from the monzonite contact (20 to 40m) pockets of lower grade skarn are found within the hydrothermally altered country rock. The skarn consists of diopside and plagioclase, overprinted by actinolite and later epidote and clinozoisite. Minor minerals present include sphene, apatite, sericite and tourmaline. These assemblages are cut by carbonate and quartz-carbonate veins. In the ore zone, arsenopyrite, pyrrhotite, chalcopyrite and other opaque minerals are disseminated in highly variable amounts."

"Still farther out from the monzonite (40+ m) the volcanics are dominantly fine grained and strongly silicified. These are cut by veins of diopside, wollastonite and/or actinolitic amphibole, 0.5 to 5 millimeter wide, which are partly replaced by calcite. Some actinolite veins contain ar-

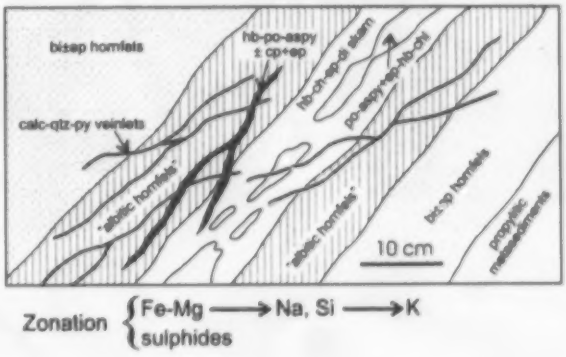

Figure 4-11. Diagram illustrating alteration assemblages along the margins of Evening Star veins (bi-biotite; ep-epidote; calc-calcite; qtz-quartz; hb-hornblende; po-pyrrhotite; chl-chlorite; di-diopside; aspy-arsenopyrite; cp-chalcopyrite).

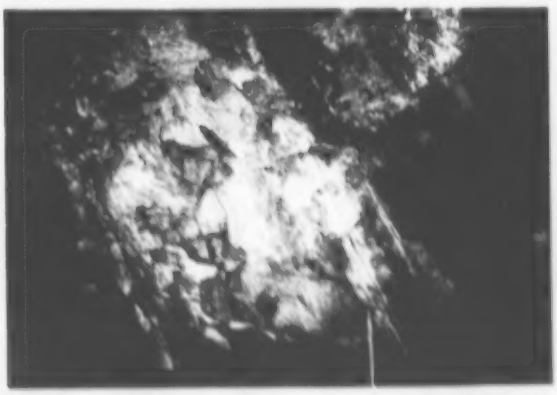

Photo 4-10. Underground photo (1995) of vein and alteration, Evening Star deposit. Note thin chlorite-pyrrhotite-arsenopyrite veins with bleached envelopes near pencil and thin massive sulphide vein at left of photo. Also note late cross-cutting pyrrhotite-calcite veins.

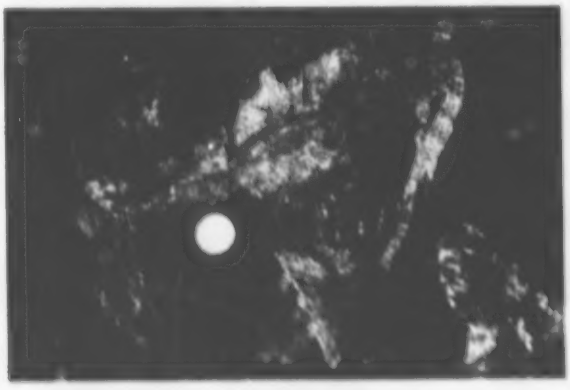

Photo 4-11. Vein and alteration, Evening Star deposit. Dark biotite hornfels is cut by diopside-hornblende-epidote-chlorite-sulphide vein with bleached envelopes; late calcite-pyrite veins cut skarn (see text and Figure 4-11 for details).

senopyrite along their margins, suggesting it might have been formed at these same time as the actinolite alteration. Pyrrhotite is present in the veins as a replacement of arsenopyrite and actinolite."

"These assemblages are crudely arranged outward from the Rossland monzonite, in a similar fashion to skarn zones in the Hedley district as described by Ray *et al.* (1987). This marked spatial association with the monzonite provides evidence in favour of it being the source of heat and possibly mineralizing fluids for the Evening Star deposit."

Stinson and Patterson (1993) noted two main stages of sulphide mineralization. Early pyrite, arsenopyrite and gold (± bismuth) are followed by chalcopyrite and pyrrhotite. This correlation of gold with arsenopyrite contrasts with the conclusion by Thorpe (1967) that most of the gold occurs in solid solution with chalcopyrite. Stinson and Patterson (*op. cit.*) also noted late replacement of sulphides by magnetite, and minor hematite and marcasite alteration.

In summary, a simplistic sulphide-alteration paragenesis includes early siliceous biotite hornfelsing, overprinted by intense prograde skarn alteration, followed by retrograde skarn and massive sulphide veining, and finally late pyrite-calcite veining.

Fluid Inclusion Data

Detailed fluid inclusion data and discussion are presented in Appendices 9a and 9b. Primary fluid inclusions in growth zones in quartz from a quartz-pyrite-calcite vein include aqueous (H_2O-NaCl) Type I, carbonic (CO_2-trace CH_4/N_2) Type V and mixed aqueous and carbonic (H_2O-CO_2-NaCl) Type IV. Homogenization temperatures from Types I and IV fluid inclusions are moderately high from 307°C to 370°C and salinities low to moderate, from 5.5 to 18.5 eq. wt. % NaCl. Estimated trapping pressures for two Type IV inclusion assemblages are 1529 and 2273 bars, corresponding to trapping depths of between about 5.7 and 8.6 km lithostatic load.

MONTE CRISTO (082FSW101)

The Monte Cristo claim group is located just west of the Evening Star claims (Figure 4-2, in pocket). Production from Monte Cristo is not tabulated in Appendix 3 as ore from this vein, and from a number of others in the Rossland camp, were included in the production of the Centre Star-War Eagle mines.

In contrast to the Evening Star veins, the Monte Cristo veins strike west-northwesterly and are mainly within the Rossland monzonite. Locally, the host monzonite is altered to an endoskarn with an amphibole-quartz-biotite ± pyroxene(?) assemblage. The margins of the vein are generally sheared, and late calcite veinlets extend into the country rock.

The Monte Cristo vein is mainly massive pyrrhotite with less chalcopyrite and magnetite in a dark green gangue. A "10-inch streak of arsenopyrite" was noted by Drysdale (1915). Chalcopyrite occurs intergrown with pyrrhotite, in calcite (± quartz-chlorite) stringers and disseminated in the gangue. Pyrite occurs in late veinlets with chlorite and carbonate. Analyses of a hand sample of massive sulphide (R96-46A; Appendix 6) returned 844 ppb Au, <5 ppm Ag and approximately 10% Cu. Mo (419 ppm) and Zn (134 ppm) values were low, but Co (982 ppm) was relatively abundant. Drysdale (*op. cit.*) also reported that the gold content of the massive sulphide vein was low, although one crosscutting(?) vein assayed 27 g/t Au. (p. 109). Drysdale also noted that analyses of pyrrhotite from Monte Cristo returned 0.13% NiO and trace Co.

Vein gangue mineralogy consists of mainly sericitized albitic(?) plagioclase (An 0-5?) and pale green mica (Appendix 5). The plagioclase appears to be secondary, forming small subhedral crystals. These grains are typically pervasively altered to sericite and, closer to their margins, green phengitic (Fe-rich) sericite. This green mica also appears to pseudomorph former amphibole(?) crystals. Amphibole also occurs as needle-like laths adjacent to pyrrhotite, associated with quartz and tourmaline. Clear feldspar grains may be K-feldspar (2-3%).

In general, wall-rock alteration of the Monte Cristo veins is not as pervasive as at Evening Star, probably reflecting the intrusive host.

CLIFF (082FSW136)

The Cliff vein is mainly within the Rossland sill west of Monte Cristo. Total reported production from the Cliff includes that of the Consolidated St. Elmo to the west: 14 868 grams of gold, 99 530 grams of silver and 24 195 kg of copper from 1 915 tonnes of milled ore (Appendix 3), resulting in a recoverable grade of 7.8 g/t Au. This grade is comparable to the average analysis of 1 236 tonnes shipped in 1904 (Drysdale, 1915), and analysis of a selected hand sample of the vein reported in Appendix 6 (R96-48A: 6.2 ppm Au).

The Cliff-Consolidated St. Elmo vein strikes east-west and dips 60°-70° north. It is well exposed at a portal on the east side of the Cliff claim where it occurs as a massive chalcopyrite-pyrrhotite vein approximately 2 metres thick within biotite hornfelsed Rossland(?) sill. The exposed footwall contact is sheared and sharp; only minor disseminated pyrrhotite occurs in the footwall, with minor late fractures, some bleaching but no obvious skarn alteration. The hangingwall contact is also sheared, and the hangingwall host is rusty weathering and bleached with chlorite, hornblende and pyrrhotite alteration.

A polished section of the massive sulphide from this exposure (R96-48a, Appendix 5) indicates that the host is mainly coarsely crystalline clinopyroxene, partly retrograded to actinolite, and is cut by fine fractures filled with limonite. Fine sulphide fractures cutting the pyroxene also contain amphibole, suggesting sulphide mineralization is related to late retrograde alteration rather than the prograde clinopyroxene (?diopsidic) skarn alteration.

Chalcopyrite in this sample occurs with quartz and minor chlorite in veinlets. It also occurs as massive concentrations intimately intergrown with pyrrhotite. Thorpe (1967) also reported the occurrence of native bismuth veins in ar-

senopyrite and pyrrhotite, as well as minor magnetite and trace scheelite.

In summary, a paragenetic sequence involves early prograde skarn alteration, followed by retrograde alteration to amphibole, accompanied by sulphide-quartz ± chlorite veining. Pyrrhotite and possibly chalcopyrite and arsenopyrite appear to be earlier formed sulphides, followed by native bismuth, then pyrite. This sequence is generally similar to that described at the Evening Star vein.

CONSOLIDATED ST. ELMO (082FSW135)

The Consolidated St. Elmo is the western extension of the Cliff vein. It also strikes westerly, dips at steep angles to the north and is mainly within the Rossland sill. Production from the Consolidated St. Elmo is included in the data for the Cliff deposit (Appendix 3).

The Consolidated St. Elmo vein contrasts in many features from the structurally lower Cliff vein. Vein samples on a dump at the Consolidated St. Elmo suggest that this portion of the North vein contains more quartz than the Cliff, and skarn alteration is less prominent and more closely confined to gangue within the vein. Arsenopyrite was not observed, but has been reported by Thorpe (1967). Pyrite and sphalerite are common, and minor scheelite is reflected in high tungsten values (*see* Appendix 6).

The silver content and silver/gold ratio of the Consolidated St. Elmo is also higher than the more eastern, structurally lower veins, with pyrargyrite, a ruby silver, identified by Thorpe (*op. cit.*).

A polished section of a semi-massive sulphide sample (R96-51c; Appendix 5) indicates that the skarn gangue is mainly fine-grained ?calcic plagioclase with coarser clinopyroxene (probably diopside), minor sphene, minor K-feldspar, possible garnet, and sulphides. Quartz veins, with epidote, zoisite and clinozoisite, and along the vein margins, sulphides associated with biotite, Fe-rich chlorite, diopside and garnet, cut the skarn. Pyrrhotite is the dominant sulphide, with intergrown chalcopyrite, and magnetite along the margins.

Late alteration includes rare actinolite after pyroxene, pyrargyrite (after tetrahedrite; Thorpe, 1967) and local replacement of pyrrhotite to pyrite. Other samples, however, show intimate intergrowth of pyrite and sphalerite.

The mineralogy and less developed skarn alteration support a model of the North veins developing at higher structural levels in the west. Paragenesis indicates early prograde diopsidic skarn development, followed by pyrrhotite, chalcopyrite and magnetite-epidote-chlorite-quartz veining. Although minor pyrite appears to form after pyrrhotite, massive pyrite intergrown with sphalerite, may be early.

Fluid Inclusion Data

Fluid inclusions were evaluated in two quartz-sulphide veins with 'milled' or finely brecciated textures, that cut the skarn (Appendix 9b). The abundance of fluid inclusion-filled fractures and small size of the inclusions resemble a quartz texture termed 'wispy'. The fluid inclusions are characterized by aqueous (H_2O-NaCl) Type I, mixed aqueous and carbonic (H_2O-CO_2-NaCl) Type IV, carbonic (CO_2-t r CH_4/N_2)Type V, multiphase (H_2O-NaCl-unknown phases) Type VI and mixed carbonic and multiphase (H_2O-CO_2-NaCl-unknown phases) Type VII. There is no evidence of sylvite, halite or other readily soluble phases since dissolution of daughter minerals was not observed on heating to decrepitation temperatures (300°C to 327°C).

Homogenization temperatures from Types I and VI fluid inclusions are unusually low, from 102°C to 194°C (Tables A9-3a and A93e; Appendix 9a), and salinities of Type I and IV inclusions are low to moderate, from 6.4 to 20 eq. wt. % NaCl (Table 5). Sample R96-51a probably formed at depths > 10 km lithostatic load given a 150°C 'pressure correction'.

ST. ELMO (082FSW134)

The St. Elmo vein, within Elise Formation metasediments adjoins the Consolidated St. Elmo to the west. It comprises mainly pyrite, pyrrhotite, sphalerite and minor chalcopyrite. In 1908, 70 tonnes of ore were shipped to the Trail smelter, with recoverable grades of 98 g/t silver, 1.3 g/t gold and 2.06% copper. Drysdale (1915) reported that an adit driven along the vein had some molybdenite, sphalerite and galena in the walls. It is not clear if this mineralization was within the veins or, more likely, within the vein host-rocks. Reported molybdenite reserves on the St. Elmo claim are 59 052 tonnes containing 0.28% MoS_2 (*see* BC MINFILE).

MOUNTAIN VIEW (082FSW140)

Although the Mountain View claim is considered to be mainly a molybdenite prospect related to other molybdenite occurrences on Red Mountain, it was originally staked to cover the most western extension of the North belt Consolidated St. Elmo-Cliff vein system. As such, it is important as it provides details regarding possible relationships between the molybdenite mineralization and the copper-gold veins.

Drysdale (1915, p. 135) described an east-west striking, 10 metre thick and 60 metre long vein "which averaged $25 to the ton in gold" (approx. 28g/t). A thin pyrrhotite-pyrite ± chalcopyrite(?) vein, trending 080° and dipping 85°N, is visible on the east wall of the Mountain View E pit. This vein cuts hornfelsing and skarn related to the molybdenite breccia complex, suggesting that they formed later than the molybdenite (Fyles, 1970). However, as noted above, we argue that molybdenite mineralization is younger than the vein and that alteration associated with molybdenite mineralization may selectively replace only reactive host rocks and not the earlier sulphide vein; brecciation does not extend to this area.

JUMBO (082FSW111)

The Jumbo mine is located on the west side of Jumbo Creek, 3.2 kilometres northwest of Rossland. It is unusual as

it occurs west of the molybdenite breccia complex, considerably separated from other veins of the North belt.

Drysdale (1915) described the vein as ranging up to 10 metres in width and consisting mainly of pyrrhotite, with minor chalcopyrite and trace pyrite, bismuthinite, sylvanite, molybdenite, arsenopyrite and free gold. Dark green gangue, described by C. Leitch (sample R96-28a; Appendix 5), is mainly granular clinopyroxene (diopside?) and quartz with minor sulphides and trace zoisite. The vein is within tan to pale grey, fine-grained rusted metasediments of the upper part of the Elise Formation. Pervasive skarn alteration, typical of exposures to the east, is not evident in surface exposures.

Drysdale (1915) also noted the "close association" of mineralization, particularly the high gold content, with syenite dikes that cut across the veins. The dikes "of aplite or syenite are intrusive into the vein at low angles and are themselves mineralized .... fine-grained syenite or aplitic dykes are closely connected with the rich pay streaks and such dykes are in places impregnated with or have seams of sulphides".

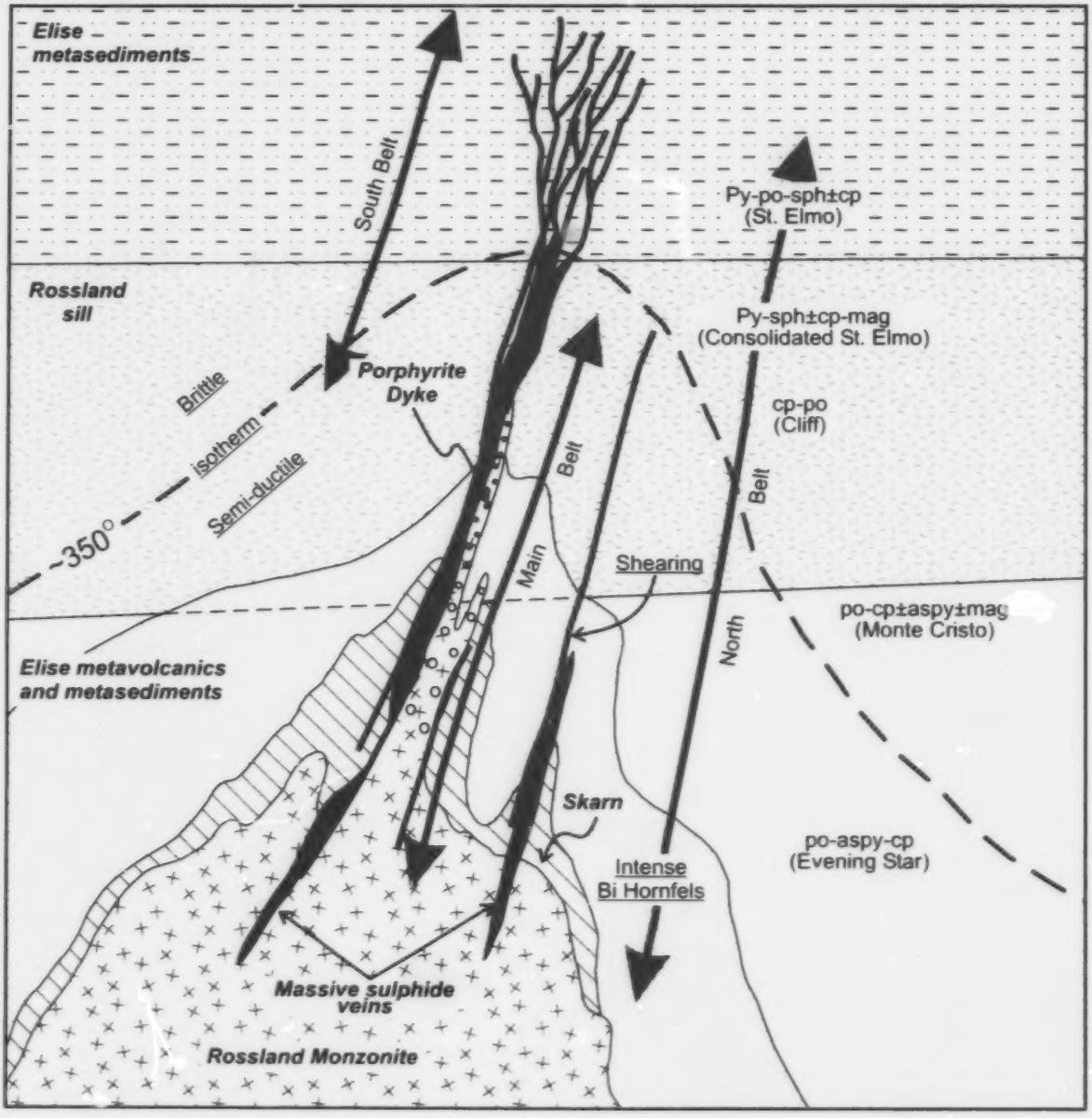

Figure 4-12. A vertical model showing the distribution, tenor and alteration assemblages of veins in the Rossland Au-Cu camp.

Fluid Inclusion Data

The fluid inclusions in quartz gangue from a massive sulphide vein comprise aqueous (H_2O-NaCl) Type I, carbonic (CO_2-trace CH_4/N_2) Type V, mixed aqueous and carbonic (H_2O-CO_2-NaCl) Type IV, multiphase (H_2O-NaCl-unknown phases) Type VI and mixed carbonic and multiphase (H_2O-CO_2-NaCl - unknown phases) Type VII phases (Appendix 9).

Primary fluid inclusion homogenization temperatures for multiphase Type VI inclusions range from 145°C to 267°C. Fluid inclusion assemblage 5-1 exhibited homogenization to the vapour phase at 210°C; all other observed homogenization temperatures were to the liquid phase. Secondary fluid inclusion homogenization temperatures for Type I and VI inclusions are moderate and range from 183°C to 231.5°C (Tables A9-3a, 3e; Appendix 9a). Salinities of aqueous fluid inclusions from the same assemblagee low at 5.2 eq. wt. % NaCl.

DISCUSSION: NORTH BELT

A simplistic model for the North belt veins is shown in Figure 4-12. The veins trend westward. The Evening Star veins cut Elise metasediments and the northeastern fringes of the Rossland monzonite. The Monte Cristo veins cut the Rossland monzonite, the Cliff and Consolidated St. Elmo are in the Rossland sill, the St. Elmo is in overlying Elise metasediments, and the most western, Mountain View, cuts the fringes of the alteration halo around the molybdenite breccia complex near the summit of Red Mountain.

A number of features indicate that eastern portions of the North belt veins developed at deeper structural levels. Evening Star veins have more diffuse margins and locally well developed and extensive skarn in the hostrocks. Skarn involves early biotite hornfelsing, followed by prograde diopsidic skarn, then sulphide-quartz-calcite veining associated with retrograde hornblende (?actinolite), chlorite and epidote. To the west, intensity and amount of skarn alteration decrease, due only in part to less reactive host rocks. Diopside skarn assemblages are essentially restricted to the immediate vein at the Monte Cristo, Cliff and Consolidated St. Elmo, and in these deposits the vein boundaries are typically sharp and locally sheared, with alteration of the host rocks limited to bleaching, minor biotite hornfelsing and minor disseminated pyrrhotite. Farther west, St. Elmo and Mountain View veins also have discrete, sharp boundaries. However, the Mountain View vein and, to a lesser extent, the St. Elmo vein, is in skarn alteration related to the molybdenite breccia complex.

The mineralogy and tenor of the North belt vein system also changes progressively to the west. Massive pyrrhotite, arsenopyrite and chalcopyrite, dominant in the east (Evening Star and Monte Cristo), give way to the west to mainly pyrrhotite, pyrite, chalcopyrite and sphalerite (Consolidated St. Elmo), pyrite, pyrrhotite and sphalerite with only minor chalcopyrite (St. Elmo) and finally mainly pyrite and pyrrhotite at the Mountain View. As well, the eastern veins contain high cobalt and nickel; these and the intermediate veins contain bismuth, and western veins have increasing silver content and silver/gold ratios. Molybdenite in host rocks of the western veins and possibly scheelite, reported at Cliff, may not be related to Rossland vein mineralization, but rather is probably associated with the molybdenite breccia complex to the west. Gold content is highest in the eastern part of the vein system, and appears to generally decrease to the west. Copper content is highest in the central part where the veins cross the Rossland sill, somewhat less in the structurally deeper Evening Star vein, and least in most western exposures. These values are also reflected in the zonation of Au/Cu ratios, illustrated in Figure 4-14, which show a general decrease towards the northern lobe of the Rossland monzonite.

However, the Jumbo deposit farther west has mineralogy more typical of the more eastern North belt veins and the Main veins. It is possible that this is due to its deeper structural level, in the valley of Jumbo Creek, or that it may be related to a separate body of Rossland monzonite, exposed just over a hundred metres to the north (Figure 4-2).

As discussed below, the Rossland veins were developed prior to westward tilting of the area in Eocene time. Hence, the Rossland veins, including those of the North belt, allow a view through a vein system that illustrates deeper structural levels in eastern exposures and more shallow exposures farther west.

MAIN VEINS

The Main veins extend west-southwest from the eastern slopes of Columbia-Kootenay Mountain to the southern slopes of Red Mountain (Figure 4-8). These veins are described by Drysdale (1915), Gilbert (1948), Thorpe (1967) and Fyles (1984) and this summary is based in part on these previous reports.

The veins are dominantly massive pyrrhotite and chalcopyrite with minor molybdenite in the War Eagle (Thorpe, 1967) and Centre Star (Drysdale, 1915). Gangue content is minor, mainly calcite and quartz.

The veins parallel well-defined fractures that trend 060° to 070° (Centre Star - Le Roi) and 120° (War Eagle) and generally dip steeply (60° to 80°) to the north. Other less pronounced mineralized fractures trend approximately east-west and also dip to the north. The veins are in Rossland monzonite in the east and continue west into augite porphyry of the Rossland sill. Farther west in Elise metasediments, the veins are more diffuse and less well developed.

Many of the veins follow the margins or are within diorite porphyry dikes that extend westward from the Rossland monzonite into the Rossland sill. The dikes are altered and mineralized, as well as locally sheared. Elsewhere, and commonly along strike or down dip, veins are along the margins of the Rossland monzonite and in shear zones in the monzonite or the Rossland sill.

The veins are commonly truncated by north-trending structures, including two large lamprophyre dikes of Tertiary age, referred to as the Josie and the Nickel Plate dikes. Gilbert (1948, p.193) concluded that the ore was post-emplacement of these dikes because shoots of the

Main veins normally stopped abruptly against the dikes, "ores commonly thicken against the dike contacts and send off minor branches along them, and that there is some mineralization in many places, or a stringer representing the vein, within the dikes themselves". Alternatively, the dikes may parallel older north-trending structures that controlled vein distribution, and sulphides may have been locally remobilized during Tertiary deformation and magmatism.

CENTRE STAR (082FSW094) - LE ROI (082FSW093)

The Centre Star - Le Roi vein is the largest and most productive vein system in the Rossland camp. It extends westward within the Rossland monzonite, then follows the southern edge of a tongue of Rossland monzonite into Rossland sill. The vein was mined almost continuously over this length, a strike distance of nearly a kilometre (Photo 4-12). Although the veins are typically depicted as continuous, they actually "are made up of a series of shoots more or less *en echelon* in strike and dip.....the veins are a series of ore shoots of no great width or strike length, with their greatest dimension along dip. On dip, they usually die out gradually, either through loss of width or loss of metalliferous content. On the strike the same may occur, but more commonly they end abruptly against a dike or other cross structure." (Gilbert, 1948, p. 193). Drysdale (1915, Map 146A) showed the veins extending west of the Josie dike, but offset to the south and with reduced width. Shearing of the vein is common, with mineralized zones forming discontinuous lenses within a through-going shear.

The Centre Star - Le Roi vein system has simple mineralogy in contrast to the more complex ores of the South and North belts. The vein comprises massive pyrrhotite, less chalcopyrite and traces of native silver and molybdenite. There is a close correlation between copper content and total silver + gold content, with the total metal values increasing to the west in the Le Roi deposit (Thorpe, 1967). This zonation may, however, simply reflect the tendency for metal content to be higher in the Rossland sill than in the Rossland monzonite.

Drysdale (*op. cit.*) noted that the ore appears to become more siliceous at depth, and although copper tends to decrease, gold content appears to remain constant. A sample from the Le Roi dump (R96-25b, Appendix 5) is a piece of silicified and hornfelsed Rossland sill cut by narrow stringers of magnetite, chalcopyrite and pyrrhotite. Quartz in this sample occurs in both the veinlets and as an alteration in the host rock with secondary biotite and fine-grained ?albite.

Samples from the Centre Star area have similar mineralogy to the Le Roi portion of the vein. Massive sulphides are mainly pyrrhotite with irregular patches of pyrite, minor chalcopyrite and scattered grains of magnetite. Gangue is generally minor, comprising calcite, less quartz, and minor actinolite, chlorite, biotite and plagioclase. Immediate host rocks are biotite-hornfelsed and silicified Rossland monzonite or hornblende porphyrite (R96-35b; Appendix 5).

Photo 4-12. View, along strike to east, of the Centre Star (foreground) and Nickel Plate (across highway) Au-Cu vein system. Exposures on left are the altered hangingwall of the Centre Star vein.

The Le Roi - Centre Star vein continues to increasing depths as a shear zone and mineralization dies out into a "broad band of silicified granodiorite containing calcite, chlorite, biotite, epidote, and pyrite but without important ore shoots" (Drysdale, 1915, p. 52). It extends to the east-northeast into the **Idaho** and **Enterprise** claims.

Fluid Inclusion Data

Fluid inclusions in quartz were evaluated from a Le Roi dump sample of a quartz-sulphide vein in hornblende porphyrite that contained fine-grained to disseminated sulphides (Appendix 9b). The quartz-sulphide vein is brecciated and cut by coarse pyrrhotite-chalcopyrite sulphide stringers.

Quartz from the vein typically occurs as anhedral, irregular-shaped grains with abundant tiny fluid inclusions which give the grains a cloudy appearance. These inclusions were too small for evaluation. The cloudy quartz grains are occasionally overgrown by euhedral clear quartz that contained no fluid inclusions. The cloudy quartz texture resembles 'wispy' quartz (Reynolds, 1991) which typically forms in deep environments.

The coarse sulphide stringers from sample R96-24a have trapped a broken fragment of an earlier? generation of quartz vein. Secondary? fluid inclusions within this fragment include aqueous (H_2O-NaCl) Type I, multiphase (H_2O-NaCl-unknown phases) Type VI and mixed carbonic and multiphase (H_2O-CO_2-NaCl-unknown phases) Type VII phases. The only homogenization temperature attained was 206.2°C for a fluid inclusion assemblage containing Type VII inclusions.

WAR EAGLE (082FSW097) - No. 1

The War Eagle vein system trends west-northwest. To the east it approaches the Centre Star vein but farther west it diverges to the north from the Le Roi vein. Here, numerous other east-trending veins formed within the wedge between the War Eagle and the Le Roi, including the very productive Josie vein. Farther west, the War Eagle vein appears to be

offset to the south along the Josie dike with its western extension west of the dike referred to as the No. 1 vein.

In contrast with the sheared and irregular Le Roi vein system, the War Eagle - No. 1 vein generally has a well-defined hangingwall and footwall, and is typically fairly uniform in width and gold grades (Photo 4-13). The War Eagle has a surface strike length of at least 600 metres; the main stope is approximately 150 metres in length with a pitch length of 250 metres and an average width of 2.5 metres. It commonly follows the contacts of hornblende porphyrite dikes and the Rossland sill. At intersections with north-trending structures, and in particular the northwest-trending "K" fault, the vein can thicken substantially. Small north-trending veins or "ore shoots" locally occur along the lower contact of cross-cutting biotite lamprophyre dikes (Drysdale, 1915).

The War Eagle vein contains mainly massive pyrrhotite and chalcopyrite with minor quartz-calcite gangue. Locally, the vein has a crude sulphide banding. Sphalerite is uncommon, but has been reported in a vein cutting massive pyrrhotite and chalcopyrite (Drysdale, 1915) or locally within the main vein and partially replaced? by pyrrhotite (Thorpe, 1967). Trace amounts of molybdenite, native silver and native gold have also been reported. Large pyrite cubes can occur in the massive pyrrhotite-chalcopyrite ore.

Adjacent to the vein, the host augite porphyry of the Rossland sill is commonly altered to a texture-destructive assemblage of mainly plagioclase, actinolite, biotite, minor sphene and trace apatite.

Fluid Inclusion Data

Details of fluid inclusion studies of three samples from the War Eagle deposit are given in Appendices 9a and 9b. R96-31b is from the footwall of the War Eagle vein system, R96-58, from the northwest extension of the War Eagle vein and R96-71a, from the entrance to the War Eagle portal.

Sample R96-58 is a clinopyroxene-amphibole skarn with (1) minor cloudy quartz and associated fracture-controlled? pyrrhotite and chalcopyrite. Inclusions in the quartz produce a 'wispy' texture, characteristic of deep environments. Rare fluid inclusions large enough to observe in the quartz are characterized by multiphase (H_2O-NaCl-unknown phases) Type VI fluid inclusions. One Type VI assemblage homogenization temperature of 141°C was recorded.

Photo 4-13. War Eagle Au-Cu vein here removed and infilled; exposures on right (south) are in the immediate footwall of the vein.

Sample R96-71a consists of highly fractured, cloudy, anhedral quartz (1) cut by fractures filled with chalcopyrite, pyrrhotite, clear quartz (2) and magnetite(?). Fluid inclusions in the early, cloudy quartz are typically less than one micron in size which makes them unusable for fluid inclusion petrography. The 'wispy' texture of the quartz is characteristic of deep (> 4 km) environments.

The clear quartz (2) that is associated with sulphides in fractures contains salt-saturated (H_2O-NaCl) Type III and carbonic (H_2O-CO_2-NaCl) Type IV inclusions (Appendix 9). Salt-saturated fluid inclusions have one contained solid phase, commonly cubic, which is approximately the same size as the vapour bubble. The homogenization temperatures from fluid inclusions in assemblages FIA 1-1 and 2-3 are low (156°C and 170°C) whereas the two salt phases, presumably halite, melted at 285°C and 331°C respectively. Calculated salinities for these samples are 37 and 41 eq. wt. % NaCl. Homogenization temperatures from Type IV fluid inclusions range from 243°C to 342°C and salinities, from 4 to 10 eq. wt. % NaCl.

Estimates of minimum fluid pressures from Type III inclusions in sample R96-71a are 2443 and 2872 bars, using dissolution of halite, and in Type IV inclusions, 1692 bars, using volume ratios of liquid-to-vapour and homogenization temperatures for CO_2 and H_2O (*see* Appendix 9). These trapping pressures correspond to trapping depths of about 9.2 km, 10.8 km and 6.4 km lithostatic load respectively.

Sample R96-31b consists of mainly semi-massive pyrrhotite and pyrite, minor chalcopyrite, traces of magnetite(?), and (2) 5% clear quartz gangue. These sulphides are cut by (3) a one centimetre wide quartz vein. Note that secondary quartz is associated with sulphides in sample R96-31c, collected at the same location (Appendix 5).

Fluid inclusions in the vein quartz (3) are secondary occurring typically along healed fractures. They are characterized by aqueous (H_2O-NaCl) Type I, mixed aqueous and carbonic (H_2O-CO_2-NaCl) Type IV, multiphase (H_2O-NaCl- unknown phases) Type VI and mixed carbonic and multiphase (H_2O-CO_2-NaCl-unknown phases) Type VII. Multiphase fluid inclusion assemblage 2-4 (Appendix 9) exhibits evidence of sylvite, halite or another readily soluble phase since dissolution of one of five daughter minerals occurs at 329°C, after homogenization at 298°C.

The homogenization temperature from a secondary Type I was 208°C and corresponding salinity moderate at 15 eq. wt. % NaCl. Homogenization temperatures from secondary Type VI fluid inclusions to a liquid phase are low to moderate, from 160°C to 300°C.

Types IV and VII inclusions contain trace concentrations of CH_4 or N_2. Homogenization temperatures range from 295°C to 316°C.

In summary, the paragenetic sequence of quartz deposition in the War Eagle vein is as follows: (1) anhedral quartz with wispy texture that appears to be associated with early skarn alteration, (2) euhedral to subhedral clear quartz, sometimes embayed, associated with massive pyrrhotite and chalcopyrite deposition, and (3) late anhedral quartz veinlets (with minor sulphides?) cutting earlier massive sulphides.

'Wispy' textures in the (1) early anhedral quartz suggest a deep environment (> 4 km, probably > 8 km) (Reynolds, 1991). The clear quartz in the massive sulphide veins (2) contains Type IV CO_2 fluid inclusions and NaCl-saturated inclusions with liquid-vapour homogenization temperatures <220°C and salinity of <41 eq. wt. % NaCl. Estimates of depth of emplacement of these sulphide-quartz veins range from 6.4 to 10.8 km. Fluid inclusions in the late anhedral quartz veinlets (3) are characterized by CO_2 (Type IV) and multiphase (Type VI) inclusions which are also indicative of formation in deep environments.

COLUMBIA-KOOTENAY (082FSW151)

The Columbia-Kootenay is the eastern extension of the Main vein system. It is located 1.6 km northeast of Rossland on the east slope of Columbia Kootenay Mountain. The mineralized vein system trends northeast and dips from 45°-75° northwest. Surface exposures at the portals are mixed metasediments and volcaniclastics of the Elise Formation. Drysdale (1915) described the vein at a contact between "biotite-bearing monzonite" in the hangingwall, presumably the Rossland monzonite, and augite porphyrite of the Elise Formation. No diorite porphyrite dikes, typical of vein contacts farther west, were noted.

The vein consists of mainly massive pyrrhotite with minor arsenopyrite and trace native bismuth and bismuthinite. "Much of the ore, which is made up of sulphides in a calcite and altered rock gangue, appears to be laminated. The ore is also found massive or scattered through the gangue or along small fracture planes in the walls." (Drysdale, *op. cit.*, p. 128). Vein gangue mineralogy includes calcite, diopside, quartz, plagioclase, minor K-feldspar and biotite, and secondary actinolite (sample R96-39a, Appendix 5). Host rocks to the veins are commonly altered to diopside-garnet skarn, and may contain disseminated sulphides.

Fluid Inclusion Data

Fluid inclusions from three samples from the Columbia waste dump were studied (Appendix 9). Sample R96-39a is a clinopyroxene-plagioclase? skarn retrograde altered to actinolite (Appendix 5), and cut by stringers of pyrrhotite, minor chalcopyrite, quartz (2) and trace magnetite. Fluid inclusions in the quartz are secondary and include aqueous (H_2O-NaCl) Type I, carbonic (CO_2-trace CH_4/N_2) Type V and multiphase (H_2O-NaCl-unknown phases) Type VI inclusions (Appendix 9a).

Homogenization temperatures for Type I inclusions are 237°C and 246°C with corresponding salinities of 4.4 and 4.7 eq. wt. % NaCl. Homogenization temperatures for Type VI inclusions are slightly higher at 269°C and 301°C. A second assemblage (3-1, Appendix 9a) contained Types I and V inclusions, with the Type I inclusions having a salinity of 4.4 eq. wt. % NaCl and homogenizing at 237.5°C. Type V carbonic inclusions are essentially pure CO_2 with less than 2 mol. % CH_4/N_2.

Sample R96-42b comprises massive arsenopyrite, pyrite, pyrrhotite, minor chalcopyrite and (2) quartz in a crudely banded, folded and almost gneissic-textured altered rock. Euhedral arsenopyrite overprints and is later than the other sulphides and quartz. Secondary? fluid inclusions include aqueous (H_2O-NaCl) Type I, carbonic (CO_2-trace CH_4/N_2) Type V, and multiphase (H_2O-NaCl-unknown phases) Type VI.

Type I homogenization temperatures range from 288°C to 346°C with corresponding salinities from 10.7 to 16.6 eq. wt. % NaCl. Type VI fluid inclusions homogenize between 157°C and 303°C. The presence of observable CO_2 phases at room temperature is typical of deep depositional environments. The absolute minimum depth of trapping for secondary Type I fluids is 1.0 to 1.7 km based on boiling curves for NaCl solutions under hydrostatic conditions (after Haas, 1971).

Sample 'Columbia' consists of a quartz, calcite, chlorite, biotite vein with sulphides and broken fragments. Aqueous (H_2O-NaCl) Type I and multiphase (H_2O-NaCl-unknown phases) Type VI inclusions were noted. Homogenization temperatures for Type I inclusions range from 272°C to 377°C with corresponding salinities from 6 to 12 eq. wt. % NaCl, and Type VI inclusions homogenize between 199°C and 293°C.

In summary, CO_2 (Type IV) inclusions in sample R96-42b probably indicates deep (>4 km) deposition.

OTHER MAIN VEIN DEPOSITS

The **Josie** (082FSW147) vein trends west-southwest, north of and approximately parallel to the Le Roi vein. It comprises three main veins, the Hamilton, the North Annie and Annie. The main ore shoot pitches steeply to the west; it has well-defined contacts, similar to the War Eagle.

The mineralogy of the Josie vein is comparable to the Le Roi vein, dominated by pyrrhotite and chalcopyrite. A sample of the vein (R96-74, Appendix 5) has massive pyrrhotite intergrown with minor chalcopyrite and magnetite, with late coarse subhedral pyrite crystals. Analysis of this sample returned relatively high manganese content (1248 ppm) and high La (240 ppm) and Se (290 ppm). Massive fine-grained sphalerite was observed in veinlets and blebs from samples from the 275 metre level.

Skarn alteration comprises amphibole, calcite and ?garnet. Dump samples are commonly biotite hornfelsed, silicified or rarely skarn-altered Rossland sill.

Annie (082FSW148) may be the western faulted extension of the Josie vein or the extension of a number of smaller veins between the Le Roi and the Josie. It is mainly within Rossland sill west of the north-trending Josie and Tramway dikes. The Annie vein is similar to the Le Roi veins and con-

sists of massive pyrrhotite with some chalcopyrite in west-trending discontinuous shear zones.

A number of Main veins are in Rossland monzonite east of those described above. In general, veins within the monzonite have lower gold grades than those in the Rossland sill to the west, even though they may still comprise massive sulphide.

The **Iron Colt** (082FSW100) is the most eastern extension of the Main vein system. Limited production, mainly in 1995, recovered 21 586 grams of gold. Recent work by Antelope Resources included geophysical surveys, diamond drilling and some underground exploration. Samples from a dump are dominantly Rossland monzonite, many which have undergone pervasive carbonate alteration or less intense albitic alteration. Other samples have a pronounced green cast due to pervasive propylitic alteration. Disseminated pyrite is also common. Vein samples include massive to semi-massive pyrrhotite with minor arsenopyrite and chalcopyrite in a calcite-quartz-?albite gangue. An analysis of one of these samples (R96-40B; Appendix 6) returned 15.8 ppm gold, 7.8% As and high cobalt content (.. <5 ppm).

The **Iron Horse** (082FSW099) is located due west of Iron Colt. There is little available information on this segment of the Main vein. It consisted of massive sulphide with low gold grades; in 1903, limited production recovered 746 grams of gold from 27 tonnes of ore. Sulphide-rich samples on a dump include massive to semi-massive pyrrhotite with minor chalcopyrite and late pyrite crystals, mafic intrusive samples (Rossland monzonite?) with 30 to 40% wispy pyrrhotite veinlets, and sulphide breccias with pyrrhotite and pyrite forming the matrix to angular Rossland monzonite clasts. Calcite and quartz occur as gangue minerals and host monzonite samples may have minor dispersed secondary biotite and ?chlorite, and may be veined with calcite.

Virginia (082FSW098) is also in Rossland monzonite, west of Iron Horse. It trends east-northeast parallel to the main Centre Star vein system. Farther west and on strike is the **Iron Mask** (082F/SW096) vein. It had considerable production from 1897 to 1899 and after consolidation with other properties by Consolidated Mining and Smelting Company in 1907. Although the Main vein system trends to the west, Drysdale (1915) reported that considerable production came from cross fractures that intersected the main veins. These mineralized cross fractures were, apparently, more pronounced in the upper levels of a number of deposits near the intersections of the Centre Star - Le Roi vein system and the War Eagle vein.

DISCUSSION: MAIN VEIN DEPOSITS

The distribution of veins is schematically shown on Figure 4-8. They extend westward from within the Rossland monzonite into the Rossland sill, commonly following the contact of monzonite and sill, or the margins of porphyrite dikes.

The pronounced metal and mineralogical zoning in North and South belt veins is less apparent in the Main vein system. However, in common with these other veins, more eastern Main veins formed at deeper structural levels than those in the west. More eastern exposures, such as the Iron Colt, have more intense alteration in the host rocks, with dispersed pyrite and more pronounced carbonate alteration and biotite hornfelsing. At depths, carbonate and silica alteration as well as biotite hornfelsing increase in the Le Roi vein. As well, small wispy sulphide veins extend into the country rock, in contrast to the better-defined and more continuous veins in western exposures (War Eagle). Shearing along veins is more pronounced in the more western Le Roi - Centre Star vein than in eastern veins. Farther west, these sheared veins diffuse into "shattered and minutely fractured" metasediments of the Elise Formation (Drysdale, 1915, p. 51).

Although the Main veins are dominated by massive pyrrhotite and chalcopyrite, gold content appears to vary with either structural depth or host lithology. Eastern veins, though still mainly massive sulphide, typically have lower gold content than those in the more western Main veins. Arsenopyrite, more common in eastern exposures in the North belt, is also found in the Iron Colt, the most eastern portion of the Main veins.

SOUTH BELT

The principal veins in the South belt trend approximately east-west and dip steeply north or south. They are within siltstones, lapilli tuff and augite porphyry of the Rossland Group several hundred metres south of the Rossland monzonite. More northern and eastern veins in the South belt are similar to the typical copper-gold mineralization of the Main veins and North belt, whereas western and southern veins contain appreciably more lead, zinc and silver, and are within the "outer zone" of Thorpe (1967). White (1949) distinguished a third "transitional" vein type in the South belt which is gradational in mineralogy and metal content between the Main Rossland veins and those of the South belt. Figure 4-13 illustrates the geology of the South belt vein area, and distinguishes the main vein types.

The Lily May, located in 1887, was the first vein to be discovered in the Rossland camp. The Mayflower (1889), Homestake (1890) and Bluebird (1900) were subsequently discovered. Production from most of these veins is limited, generally between tens to hundreds of tonnes (Appendix 3); Bluebird, the largest producer, mined 7 239 tonnes, mainly in the middle to early 1970s producing a total of 3 911 kg silver, 12 857 grams of gold, as well as lead, zinc and minor copper.

The separate crown granted claims of the South belt were largely assembled by Rossland Mines Ltd. in 1947 and from then through to 1956 they underwent considerable exploration, underground development and some production from the Bluebird-Mayflower zone. Exploration in the 1960s included mainly geophysical work and soil surveys. From 1972-1980, Ross Island Mining Co., formerly Rossland Mines Ltd. leased the group of claims covering the South belt veins, referred to as the Bluebird-Homestake

claim group, to Standonray Mines with resultant mining of the Bluebird vein.

From 1981-1986, Bryndon Ventures Ltd. (previously Ross Island Mining Co. Ltd.), established a grid on the Bluebird-Homestake group, carried out a VLF electromagnetic survey, 530 metres of trenching and 631 metres of diamond drilling. Work continued in 1987-1988 under an option agreement with Antelope Resources Ltd. and operator, Pacific Vangold Mines Ltd, and funding in part by the provincial government Mineral Exploration Incentive Program (FAME program) (York-Hardy *et al.*, 1988). Limited diamond drilling on a number of the veins continued through the early 1990s by Antelope Resources or Pacific Vangold Mines in an attempt to define additional reserves.

Three main vein zones are recognized in the South belt (Yorke-Hardy *et al., op. cit.*). The most northern, the 'Homestake-Gopher' trends east-west, parallel to the southern margin of the Rossland monzonite, the 'North shear zone' just to the east trends east-northeast, and the 'Bluebird-Mayflower' parallels the Homestake-Gopher vein system 200-300 metres farther south (Figure 4-13). Shearing along vein margins and brecciated ore textures indicate that the veins follow fault zones; however, displacements on these are minimal.

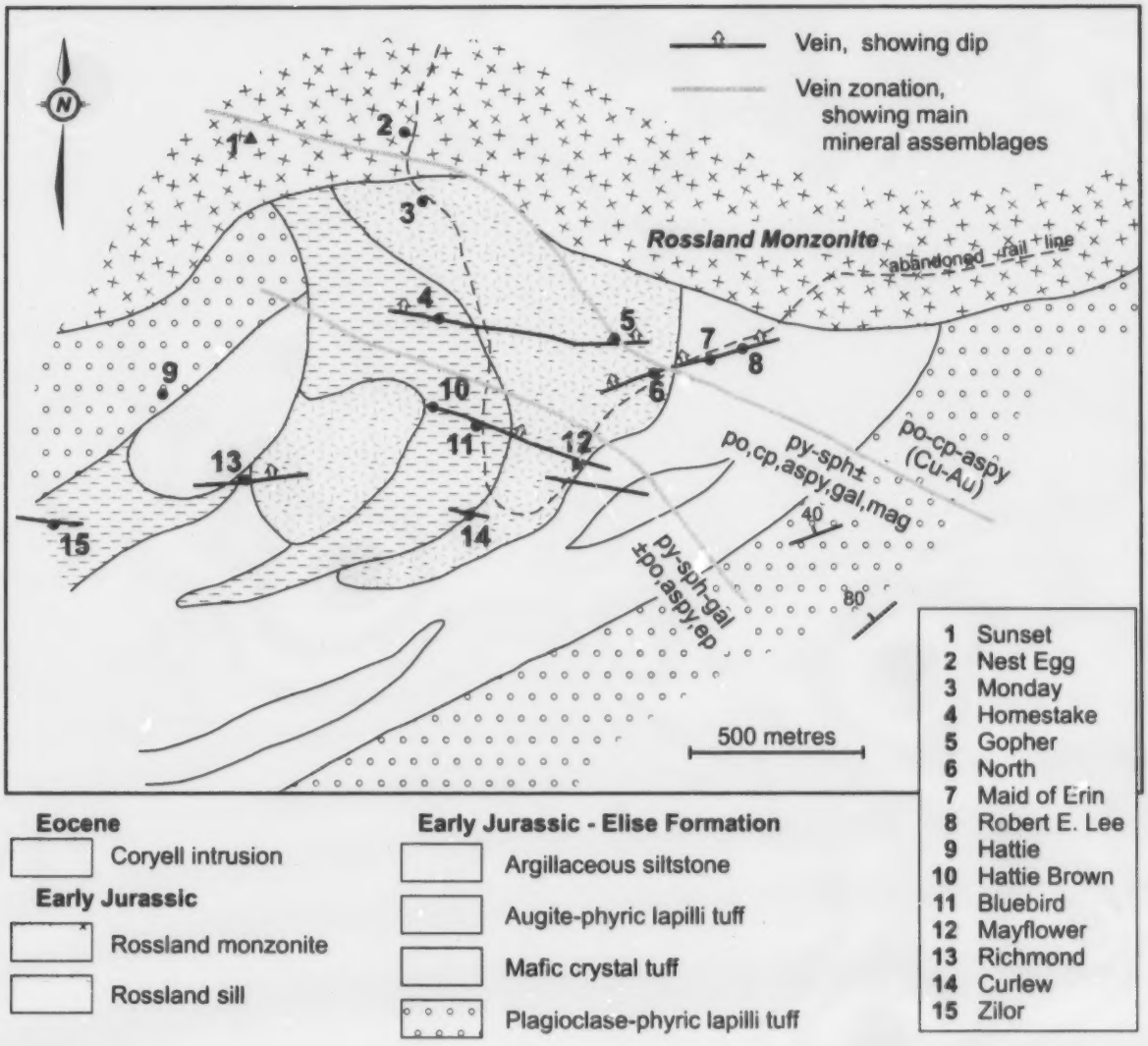

Figure 4-13. Geology of the Rossland South belt vein system (after Fyles, 1984; Höy and Andrew, 1991).

HOMESTAKE (082FSW123) AND GOPHER (082FSW125)

The Homestake-Gopher vein strikes approximately 100° and dips steeply north. It has been traced along strike for 650 metres, from the Gopher in the east to the Homestake farther west. In the early 1900s, 236 tonnes of ore were mined from the Homestake with a recoverable grade of 317 g/t silver and 3.9 g/t gold. Assays of a number of samples of vein material from the Homestake dump are given in Appendix 6.

The Homestake vein is mainly within the Rossland sill, close to its western contact with the Elise Formation. The sill adjacent to the vein is altered to chlorite, and veined with carbonate?-quartz, minor epidote-amphibole skarn, with early pyrrhotite, is noted in some dump samples. A sample (R96-67d; Appendix 5) is intensely altered with most plagioclase replaced by secondary sericitized albite, and pervasive vein-fracture alteration with sericite, amphibole and chlorite, and minor sphene and apatite. Late, cross-cutting fractures contain calcite-quartz-epidote-chlorite assemblages.

The Homestake vein in underground workings is approximately 2 metres wide, with a 0.2 metre sulphide band in the footwall and a 0.5 metre band in the hangingwall. Sulphides (Photo 4-14) comprise mainly pyrite with variable sphalerite and pyrrhotite, and lesser chalcopyrite, arsenopyrite, galena and magnetite (Appendix 5). Pyrrhotite appears to be early, and is locally pervasively altered to marcasite. Sulphides are streaked due to shearing, and locally recrystallized producing 'sieve' textures with porphyroblasts of arsenopyrite and pyrite in other sulphides (Thorpe, 1967). Gangue minerals include quartz, epidote (clinozoisite?), biotite and actinolite. Elsewhere, sericite with biotite, tourmaline, chlorite and carbonate occur in the veins.

The eastern extension, the Gopher vein, is similar to the Main Rossland veins. It contains mainly pyrrhotite, chalcopyrite, sphalerite and minor arsenopyrite, bismuth and bismuthinite in quartz-calcite gangue.

Fluid Inclusion Data

An analyzed sample of the Homestake vein (MI-123) consists of quartz intergrown with sulphides and chlorite as well as crushed and broken quartz fragments. The sample is cut by a calcite-quartz vein.

Secondary? fluid inclusions in the early quartz, intergrown with sulphide, includes aqueous (H_2O-NaCl) Type I, salt-saturated (H_2O-NaCl) Type III, carbonic (CO_2-trace CH_4,N_2) Type V, multiphase (H_2O-NaCl-~unknown phases) Type VI and mixed aqueous and carbonic (H_2O-CO_2-NaCl) Type IV (Appendix 9). In one inclusion assemblage, the Type I inclusion has a salinity of 7.5 eq. wt. % NaCl and homogenizes at 262°C and the Type IIIA inclusion homogenizes at 255°C with a salinity of 31.1 eq. wt. % NaCl; the Type V CO_2 inclusion homogenizes at 24.1°C. In a second assemblage, Type IV fluid inclusions CO_2 homogenizes at 28.5°C and H_2O at 300.8°C. An estimate of minimum fluid pressure using volume ratios of liquid - to - vapour and homogenization temperatures for CO_2 and H_2O (Type IV) inclusions is 1262 bars, corresponding to a depth of about 4.8 km.

BLUEBIRD (082FSW145) AND MAYFLOWER (082FSW146)

The Bluebird and its probable eastern extension, Mayflower, are located several hundred metres south of the Homestake-Gopher vein. The vein zone trends approximately 120-130°, and dips to the north at 50–65°; however, within this zone, some individual vein shoots strike east-northeast, towards the North-Maid of Erin system. The vein zone can be traced or extrapolated for at least 600 metres, from the Mayflower in Rossland sill in the southeast to the Bluebird in argillaceous siltstones in the northwest (Figure 4-13). The Battle Brown (082F SW359) occurs to the northwest along the structure; however, there is little reported data on this deposit, other than it is apparently a silver-bearing galena vein occurrence.

The Bluebird vein comprises mainly pyrite, sphalerite, galena and pyrrhotite with variable arsenopyrite and minor to trace chalcopyrite, boulangerite and stibnite in a quartz-calcite gangue (Photo 4-15a). Pyrrhotite is early, occurring as relict grains or inclusions in other sulphides. Vein boundaries are sharp, in contrast to wispy or disseminated vein textures noted in deeper level vein deposits. Vein textures vary from brecciated, with quartz cutting sulphides, to massive or less commonly crudely banded or streaked sulphides (Photo 4-15b). Commonly, angular hornfelsed siltstone clasts and grains occur in sulphide matrix, yielding brecciated textures. These fragments are typically altered to fine-grained sericite, carbonate and quartz. Late calcite-quartz veinlets cut the sulphide vein.

The grade recovered during mining was 540 g/t silver and 1.8 g/t gold. An assay of a semi-massive sphalerite-arsenopyrite-galena hand sample returned 260 g/t silver and 4.45 g/t gold (R96-86A; appendices 5 and 6).

Photo 4-14. Semi-massive sulphide vein, Homestake Ag-Zn-Pb deposit, South belt. Sulphides comprise mainly pyrite, sphalerite, pyrrhotite and minor galena in a gangue of quartz and minor epidote, chlorite, biotite and actinolite (sample R96-67a).

A second sample assayed 280 g/t silver and 4.96 g/t gold (Appendix 6).

The **Mayflower** vein is a rich massive sulphide vein located along the abandoned rail line southeast of Bluebird (Figure 4-13). Although the vein/shear structure trends towards Bluebird, individual sulphide veins within it trend to the northeast. It is possible therefore that these ore shoots are dilation or extensional veins within a left-lateral shear zone that trends easterly or east-southeasterly.

Mayflower is within the Rossland sill near its eastern contact with dominantly augite phyric flows of the Elise Formation. It is described by Drysdale (1915, p. 168): "the vein strikes north 60 degrees east..... The ore is very similar to the Bluebird mine but more massive. Blende (sphalerite), galena, a little arsenopyrite, and pyrrhotite occur in the ore which in places is well banded." Magnetite is also common, and tetrahedrite, with high silver content, and a ruby silver ("pyrargyrite) are also reported (Thorpe, 1967). Boulangerite also occurs in the Mayflower vein, as it does in all the South belt veins other than Homestake. Dominant gangue minerals are quartz and carbonate, with minor chlorite.

In contrast to vein textures at the Bluebird, sulphides in the Mayflower vein are typically finer grained and commonly crudely banded or sheared. Vein boundaries are not as distinct, and sulphides may occur disseminated in immediate host rocks resulting in gradational vein contacts. As well, brecciation is less intense in the Mayflower. These textures suggest emplacement at deeper structural levels, in a transitional brittle-ductile environment.

Fluid Inclusion Data

Sample M3-145 consists of angular and brecciated, hornfelsed siltstone clasts in a matrix of pyrite, galena and minor chalcopyrite in a quartz gangue. Euhedral quartz in quartz overgrowths contain both primary and secondary? inclusions (Appendix 9).

Primary inclusions include aqueous (H_2O-NaCl) Type I, carbonic (CO_2-trace CH_4/N_2) Type V and multiphase (H_2O-NaCl-unknown phases) Type VI (Appendix 9). Homogenization temperatures for Types I and VI fluid inclusions range from 286°C to 310°C; salinity for Type I inclusions is low at 7.9 eq. wt.% NaCl. Secondary fluid inclusions in the anhedral quartz are characterized by aqueous (H_2O-NaCl) Type I and multiphase (H_2O-NaCl-unknown phases) Type VI inclusions. Homogenization temperatures for Types I and VI fluid inclusions range from 245°C to 248°C , with 17.8 eq. wt. % NaCl salinities for Type I.

ROBERT E. LEE (082FSW131) AND NORTH (82FSW128)

These veins, referred to as the "North shear zone" by Yorke-Hardy *et al.* (1988), trend southwestward, from the Robert E. Lee claim within augite phyric lapilli tuffs and pyroclastic breccias of Unit Je7 just south of the Rossland monzonite, through the Maid of Erin or North deposit near the eastern extension of the Homestake-Gopher vein, into Rossland sill south of Gopher (Figure 4-13). In contrast with other veins of the South belt, this vein is more typical of the Main Rossland veins, dominated by pyrrhotite and containing appreciable chalcopyrite.

The North showing has received considerable recent exploration by Antelope Resources Ltd., including trenching, mapping, sampling and diamond drilling (Yorke-Hardy *et al., op. cit.*). This work was concentrated largely southwest of the Maid of Erin vein occurrence. Chip samples across one meter intervals in four of six trenches across the structure returned values averaging 12 g/t Au and 33 g/t Ag. As well, six drill holes tested the vein, with the best intersection consisting of 2 meters grading 22.7 g/t Au and 31.2 g/t Ag (Sampson, 1986).

The Robert E. Lee vein trends approximately 070° and dips steeply to the north. It ranges up to approximately 1 metre in thickness. The vein is mainly massive sulphide, consisting of arsenopyrite partially replaced by pyrrhotite (Thorpe, 1967), with less pyrite and chalcopyrite, minor sphalerite and trace bismuth, in a fine-grained grey quartzitic gangue. Hostrock samples on the dump are green

Photo 4-15a. Bluebird Ag-Pb-Zn vein, South belt. Brecciated sulphide vein with angular quartz fragments in a matrix of pyrite-sphalerite-galena (sample R96-66) (2 cm coin scale).

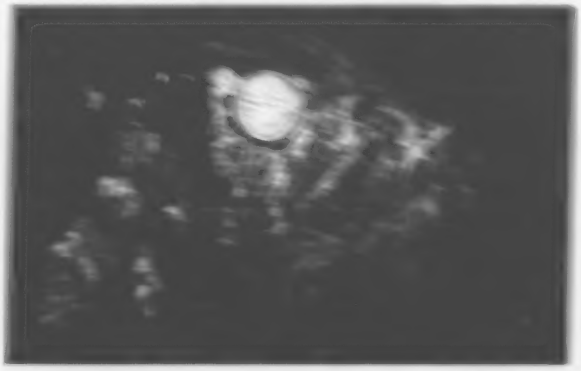

Photo 4-15b. Bluebird Ag-Pb-Zn vein, South belt. Brecciated vein with angular, silicified and hornfelsed siltstone fragments cut by veins of mainly quartz and pyrite (sample R96-66b) (2 cm coin scale).

biotite-hornfelsed metavolcanics that locally contain wispy, irregular sulphide veinlets and disseminated sulphides.

Assays of samples from the Robert E. Lee dump are given in Appendix 6. A massive pyrrhotite sample, containing sphalerite and minor chalcopyrite and arsenopyrite, contained 0.34% Cu, 2.28% Zn, 17 ppm Ag and 3.4 ppm Au.

OTHER SOUTH BELT VEIN OCCURRENCES

A number of other isolated vein occurrences are known in the South belt south of the Rossland monzonite. The **Carlew** vein (082F/SW154) is south of and parallel to the Bluebird vein. It is similar to the Bluebird vein, with pyrite, sphalerite, galena and arsenopyrite and some stibnite, chalcopyrite, pyrrhotite and boulangerite in a quartz gangue.

The **Richmond** (082F/SW143), **Lily May** (153) and **Elise** (223) are all located west of the Bluebird vein. They are typical of the South belt veins, comprising mainly galena and sphalerite, with pyrite, pyrrhotite and variable but generally minor chalcopyrite. Boulangerite and marcasite occur in the Richmond vein, and magnetite and minor stibnite in the Lily May. Limited production of the Richmond and Lily May veins yielded high silver values (Appendix 3); 37 tonnes from the Lily May contained 509 g/t Ag and 3.3 g/t Au, and 11 tonnes of a galena-rich sample from Richmond contained 1312 g/t Ag and 28 g/t Au.

The **Hattie** (082F/SW142) is north of the Lily May and Richmond and is more typical of the Main Rossland veins. It contains mainly arsenopyrite, chalcopyrite and pyrrhotite with minor native bismuth, bismuthinite and native gold (Thorpe, 1967). Limited production from 1934 to 1939 recovered approximately 15 g/t gold and 52 g/t silver.

Fluid Inclusion Data, Lily May (082FSW153)

Fluid inclusion data from quartz in a quartz-carbonate-sulphide vein are presented in Appendix 9, sample M3-153. Inclusions are characterized by aqueous (H_2O-NaCl) Type I, carbonic (CO_2-trace CH_4/N_2) Type V and mixed aqueous and carbonic (H_2O-CO_2-NaCl) Type IV fluid inclusions.

A single Type I inclusion has a salinity of 11.7 eq. wt. % NaCl and homogenizes to the liquid phase at 392.5°C.

DISCUSSION: SOUTH BELT VEINS

A systematic mineral and metal zoning is apparent in veins of the South belt (Figure 4-13). In general, veins farther from the Rossland monzonite contain mainly galena, sphalerite and pyrite in contrast to pyrrhotite-chalcopyrite-sphalerite veins closer to the intrusion. Furthermore, veins change in both ores and texture to the west. The Robert E. Lee and Gopher, the most easterly veins, are fairly typical of the Main Rossland gold-copper veins, although both contain minor sphalerite. Sphalerite and pyrite become more prominent to the west and are the dominant sulphide minerals at Homestake. Similarly, the Bluebird-Mayflower vein changes systematically to the west; pyrrhotite is the dominant iron sulphide at Mayflower whereas pyrite predominates at Bluebird. As well, sulphides at Mayflower are typically finer grained and sheared, with locally gradational contacts with country rock, in contrast to brittle brecciated textures at Bluebird.

These changes are comparable to those noted in the North belt veins, although developed at higher structural levels largely within a brittle regime. They support a model that involves westward tilting of the Rossland vein system so that deeper levels are now exposed farther east and shallower levels, associated with brittle faulting, in more western exposures. These differences also suggest that mineralization is related to the Rossland monzonite, as the transition between brittle and ductile shearing tends to parallel the southern margin of the intrusion.

Sulphides in many veins of the South belt are sheared producing banded or gneissic textures. This is most evident in more eastern exposures, such as at the Mayflower, but is common in most galena and sphalerite-bearing veins that developed or were deformed in a semi-ductile regime. Galena typically forms textures referred to as "steel galena" while other less ductile sulphides such as pyrite and pyrrhotite become finely granulated. At higher structural levels, brittle brecciated textures develop. These textures imply vein formation pre-shearing.

GOLD-QUARTZ VEINS

A number of high grade gold-quartz veins are concentrated in the Little Creek valley just west of the town of Rossland. They have been described by Drysdale (1915) and Stevenson (1935). Fyles (1984) discussed their local setting, and Ash (2001) has discussed their origin in light of their regional tectonic setting. This report overviews their geology, based mainly on these previously published papers as well as company assessment reports, and attempts to place them in relation to other deposits of the Rossland camp.

The veins are mainly within a panel of fault-bounded massive greenstone and ultramafic rocks that trend north in the Little Sheep creek valley just west of Rossland (Fyles, 1984). The age of the greenstones is not known. Fyles (1984) tentatively correlated them with the Elise Formation but Ash (2001) noted that they are distinct from the Elise. The greenstones are fine grained and dense with local to pervasive chloritic alteration, silicification and chloritization. Fibrous amphibole, magnetite and serpentine are common within them. An exposure on the Cascade Highway comprises hornfelsed mafic volcanics, highly brecciated with plagioclase phyric clasts and locally a sulphide matrix. The ultramafic rocks have been described above; they are mainly variably serpentinized dunites and websterites of inferred oceanic affinity (Ash, 2001).

The ultramafic rocks are inferred to have been tectonically emplaced along east-directed thrust faults. The age of this thrust faulting is not known but is correlated with Middle Jurassic compressive deformation recognized in more eastern exposures of the Rossland Group (Höy and Andrew, 1990b). The thrust belt is the loci for later normal faults and intrusion of Eocene dykes, intrusive plugs and mafic volcanic rocks of the Marron Formation. These faults have been

reactivated to produce steeply-dipping late faults with inferred west-side-down movement (Fyles, 1984); the OK fault to the west places Eocene Marron Formation against Pennsylvanian-Permian Mount Roberts Formation, and the Jumbo fault to the east separates the greenstones from the Elise Formation that contains "abundant intrusions and widespread thermal metamorphism.....taken as evidence that rocks east of the fault represent a deeper thermal regime" (Fyles, 1984, p. 31).

The gold-quartz veins are on the **L.X.L.** (082FSW116), **O.K.** (117), **Midnight** (119) and Dominion (**Snowdrop** - 115) crown-granted claims. They were discovered in 1891 and had relatively continuous but minor production between 1899 and 1974, totaling 1 081 816 grams of gold (Appendix 3). The L.X.L. produced 811 746 grams of gold with a recovered grade of 153 g/t and the Midnight, 245 31 grams with a recovered grade of 43 g/tonne. During the 19 10s this work was done by a number of lessees. In 1969, work by Howe International and Cinola Tull Mines consisted of 1 766 metres of surface and underground drilling, 23 metres of development drifting and bulk sampling. Work on the Midnight Mine claim group in 1993-1994, which incorporated the past-producing crown-granted claims, included some geological mapping, geophysical work and drilling (Smithson, 1995). This work continued through 196 under option to Minefinders Corporation Ltd. with considerable underground rehabilitation, drilling and sampling (Smithson, 1996).

The veins are quartz-ankerite-gold veins that typically range from a few centimetres to 0.5 metres but locally up to 2 metres in width. According to Fyles (1984), the mineralized parts of the veins "pinch and swell and change attitude". They are commonly discontinuous with total length and down-dip extensions of the "strongest mineralized zones" less than 100 metres. The principal vein on the Midnight trends 160° and dips 65° west; on the Snowdrop the veins trend northeast and dip 30° southeast (Fyles, *op. cit.*). Sulphide mineral content of the veins is variable though generally minor; sulphides include pyrite, galena, sphalerite and minor chalcopyrite. Reported gangue minerals include quartz, ankerite, calcite and, in one sample, prehnite (Thorpe, 1967).

In addition to the spectacular high-grade veins, Smithson (1995, 1996) reported that "mineralization at the Midnight Mine occurs as disseminations in broad zones of carbonate-altered ultramafics that are intruded by a north-trending lamprophyre-like swarm... High grade gold zones and gold-bearing quartz veins occur adjacent to some of the pre-mineral dikes within both ultramafic and adjacent volcanic rocks.... Silica-carbonate alteration of the serpentinized ultramafic was encountered across broad zones that contain low grade gold mineralization". Tabulation of assay results from Holes 1, 2 and 3 shows a total of 95.3 metres averaging 1.74 g/t Au; this included 40 metres in Hole 1 (1.7 g/t Au), 7.5 metres in Hole 2 (1.78 g/t Au) and 47.8 metres in Hole 3 (1.7 g/t Au).

DISCUSSION

The gold-quartz veins in Little Sheep Creek are located west-southwest of, and on direct strike with the Main veins of the Rossland camp. They are in a structural panel that is down-dropped relative to the Main veins. This led Fyles (1984, p. 52) to suggest that they may be an "upper extension of the same or a similar mineralizing system as the copper-gold deposits of the main camp". This view is implicit in the thesis of Thorpe (1967) who included these veins in his regional thermal and zonation study of the Rossland camp.

Relatively low-temperature sulphide assemblages, dominant quartz-carbonate gangue with locally prehnite, and brecciated textures support the interpretation that these are lower temperature than the Rossland Main veins, supporting a model for higher level emplacement.

The age of these veins is not known but can be reasonably deduced to be a similar age as the Main veins (*see* below). They must be contemporaneous with or postdate shearing along the margins of the serpentinites as they occur within the serpentinites and the greenstones immediately to the north. Intense regional compressive deformation in the Rossland-Trail area is post-deposition of the Toarcian Hall Formation and mainly pre-intrusion of the Middle Jurassic (*ca.* 165-170 Ma) Nelson suite; Höy and Dunne (1997) argued that the 174-178 Ma Silver King intrusive suite are early to synkinematic plutons. As the Rossland veins are in shear zones within the Rossland monzonite (*ca.* 167 Ma), shearing must have continued after intrusion of the monzonite. Hence, it is probable that the gold-quartz veins are late synkinematic, post-intrusion of the Rossland and Rainy Day plutons.

DISCUSSION: ROSSLAND AU-CU CAMP

AGE RELATIONS

Re-Os dating of massive molybdenite mineralization in the intrusive-breccia skarn complex on the western slopes of Red Mountains indicates it is 162.9±0.9 Ma. This age is in agreement with a U-Pb zircon age of *ca.* 162.3+1.2/-2.5 Ma for the host brecciated quartz diorite dikes within the complex. The similar Re-Os and U-Pb ages provide one example showing high precision and robustness of dating molybdenite mineralization by Re-Os methods (Stein *et al*, 1997; Selby and Creaser, 2001).

U-Pb dating of the Rainy Day pluton, a small quartz diorite stock just south of the molybdenite mineralization and inferred to be the source of this mineralization (Fyles, 1984) indicates an upper age limit of 174.6 Ma and a lower age of 166.3 Ma. Field relations indicate that the Rainy Day pluton is younger than the Rossland monzonite, dated at *ca.* 167 Ma; hence, it is concluded that the date of the most concordant fractions, *ca.* 166 Ma, is the age of the Rainy Day pluton. Furthermore, the similar but slightly younger quartz diorite dikes in the intrusive breccia complex may be late phases of the pluton.

Copper-gold veins in the Rossland camp and polymetallic veins of the South belt are within and along the

margins of the Rossland monzonite and associated east-trending diorite porphyrite dikes. These porphyrite dikes have only yielded titanites, dated at *ca.* 155 and 135 Ma, which probably record metamorphic overprinting. Farther west, the porphyrite dikes are overprinted by skarn alteration within the breccia complex. These relationships support a model of gold-copper vein mineralization related to the 167 Ma Rossland monzonite, followed by brecciation, skarn alteration and molybdenite mineralization related to late (163-162 Ma) phases of the Rainy Day pluton.

MAGMATIC CONTROLS

The close spatial association of Cu-Au veins with the Rossland monzonite and zonation of both vein mineralogy and alteration assemblages relative to the monzonite indicate a genetic link. This zonation is particularly evident in the South belt where pyrrhotite-chalcopyrite veins occur closer to the intrusion whereas dominantly galena-sphalerite-pyrite veins are farther south.

Pb isotopic analyses of a number of the South belt veins also support a magmatic influence. Data from these veins, as well as a number of other polymetallic veins elsewhere in the Rossland Group (Cluster 2 in Appendix 8), suggest relatively radiogenic lead and an upper crustal lead source with a minor component of mantle lead; the data define an elongated Pb isotopic mixing trend from the Jurassic on the radiogenic pericratonic model curve to Jurassic-Cretaceous mantle model lead isotopes. These veins are all within or along the margins of Jurassic plutons that are interpreted to have facilitated mixing of upper crustal lead with mantle lead.

Analyses of fluid inclusions in quartz in Rossland veins also suggest that these veins may be hydrothermal-magmatic. Three generations of vein quartz are recognized in many of the samples (see, for example, War Eagle, above and Appendix 9). Early cloudy quartz grains, characterized by abundant small inclusions that define a 'wispy' texture, are cut by the main sulphide veins that have a clear quartz gangue. These are cut by late anhedral quartz ± calcite veins that contain only minor sulphides. This paragenesis reflects the main stages of vein development throughout the camp: early prograde skarn alteration, followed by massive sulphide veins and finally late quartz-pyrite veining.

Fluid inclusions in vein quartz associated with massive sulphide mineralization include aqueous, multiphase (H_2O-NaCl), mixed aqueous and CO_2 bearing and occasional salt-saturated or CO_2-rich inclusions. The composition, salinity and homogenization temperatures of these inclusions are similar to those in other intrusion-related gold systems (Appendix 9, Figure 8). In particular, high salinity fluids associated with main stage mineralization is suggestive of a hydrothermal-magmatic source, and CO_2 inclusions are typical of fluids proximal to deeper level intrusions. Calculated pressures are relatively high, suggesting emplacement at depths up to 11 km.

MINERALIZATION, GEOCHEMISTRY AND CAMP ZONATION

A simplistic camp zonation, developed along the northwestern margin of the Rossland monzonite, consists of a 'central' zone dominated by pyrrhotite and chalcopyrite, an 'intermediate' zone with veins that contain arsenopyrite, pyrite, cobalt, bismuth minerals and molybdenite in addition to pyrrhotite and chalcopyrite, and an 'outer' zone with veins of galena, sphalerite and tetrahedrite (Thorpe, 1967). The Cu-Au veins change systematically in tenor, alteration and structural style from deeper levels in the east to more shallow levels farther west. This is evident in many individual veins, with progressive change along strike to the west from pyrrhotite-arsenopyrite-chalcopyrite assemblages, to assemblages dominated by pyrrhotite-chalcopyrite, then pyrrhotite-sphalerite-chalcopyrite and finally, brittle pyrite-sphalerite-galena.

The interpretation that molybdenite mineralization developed after and probably unrelated to copper-gold vein mineralization allows refinement of zonation patterns in the camp and a better understanding of fluid chemistry and migration. Massive molybdenite mineralization, although overlapping the western extension of several of the North belt and Main veins, is generally separated from these veins and trends more northerly. Molybdenite mineralization in the Coxey, Novelty, Mountain View and Giant deposits is associated with high concentrations of a variety of elements, including As, Ba, W, Ni, Co and Bi. In addition, U, La, Ce and Nd concentrations are also anomalously high. Gold and copper content in these deposits is variable and, at the Giant deposit, is largely concentrated in a crosscutting, west-trending vein that is similar to the Main veins.

Hence, it is probable that at least two separate mineralizing events produced the camp zonation patterns: an earlier Cu-Au dominant system and a later Mo-dominant system. Figure 4-14, based on analyses of hand samples tabulated in Appendix 6, illustrates a revised Rossland camp zonation. Within the Main and North belt veins, Cu/Cu+Zn and Au/Cu ratios increase at deeper levels and closer proximity to the Rossland monzonite. Due to more limited sampling, metal zonation in the molybdenite camp is not well defined. However, Mo appears to be dominant in more northern deposits, Mo-Co-Ni in a central zone, and Mo-Bi in the most southern deposits. Two distinct trends in the zonation pattern of absolute Mo values, a southwesterly trend parallel to the Main veins and a more northerly trend parallel to the molybdenite skarn complex (Figure 4-14d), are also suggestive evidence for two distinct but overlapping mineralizing systems.

FLUID CHEMISTRY, EVOLUTION AND HISTORY

Due to lack of fluid inclusion data and limited sampling there is little direct evidence on the nature of the fluids forming the molybdenite complex; hence, they are not discussed further. However, considerable information about temperature, chemistry and evolution of fluids forming the Rossland sulphide veins and related polymetallic veins in the South

belt can be determined, either directly through fluid inclusion studies or indirectly through mineralogy and chemistry of the veins themselves or their alteration halos.

Temperatures

Temperatures of ore deposition can be estimated by considering the stability fields of coexisting sulphides. For example, arsenopyrite and pyrite, occurring together in veins of the South belt, restrict temperatures to below approximately 490°C (Clark, 1960a; Kretschmar and Scott, 1976; Sharp *et al.*, 1985). Arsenopyrite and pyrrhotite, occurring together in eastern exposures of the Main veins and in the North belt, are stable to much higher temperatures.

Despite considerable discussion and caution regarding the applicability of sphalerite and arsenopyrite geothermometry, the compositions of these minerals do provide further constraints to formational temperatures. Temperature estimates based on arsenopyrite compositions, formed under an assumed pressure of 1000 bars, ranged from above 600°C for the Evening Star and "S.E. of Cliff", above 525°C for Cliff, 510-540°C for Novelty, 480-510°C for Giant and Gertrude, 465-500°C for Bluebird, to 430-460°C for the Robert E. Lee (Thorpe, 1967). Based on Fe and Mn content in sphalerite, Thorpe (*op. cit.*) suggested temperatures from the Evening Star might have been above 545°C and from the Bluebird deposits in the South belt, between 440-450°C.

Native bismuth, common as a late mineral in many of the deposits, is only stable at temperatures below its melting point at approximately 270°C. However, it is possible that bismuth may have been deposited in a higher temperature mineral, such as a sulphosalt, and retrograded to native bismuth during late-stage, low temperature veining (Thorpe, *op. cit.*).

Gangue and contact alteration assemblages further constrain temperature estimates of ore formation. Pre-ore prograde diopside-garnet-plagioclase skarn assemblages indicate metamorphic temperatures greater than approximately 500°C and silicate assemblages associated with vein mineralization, specifically amphibole and biotite, indicate somewhat lower temperatures, above approximately 450°C.

Homogenization temperatures of fluid inclusions in quartz associated with sulphide veining range from 150 to approximately 370°C. The higher temperatures are from aqueous Type I inclusions in the Evening Star and Columbia-Kootenay veins and are interpreted to record minimum fluid temperatures.

In summary, copper-gold in the Main veins was probably deposited from solutions above 500°C, after a thermal peak that may have reached temperatures of 600°C. Lead-zinc-silver veins in the South belt are lower temperature, generally forming below 450°C. Brittle textures in South belt veins suggest even lower temperatures. Fluid inclusions in late quartz veins (based on only one sample from the War Eagle deposit) have low homogenization temperatures, ranging up to 300°C.

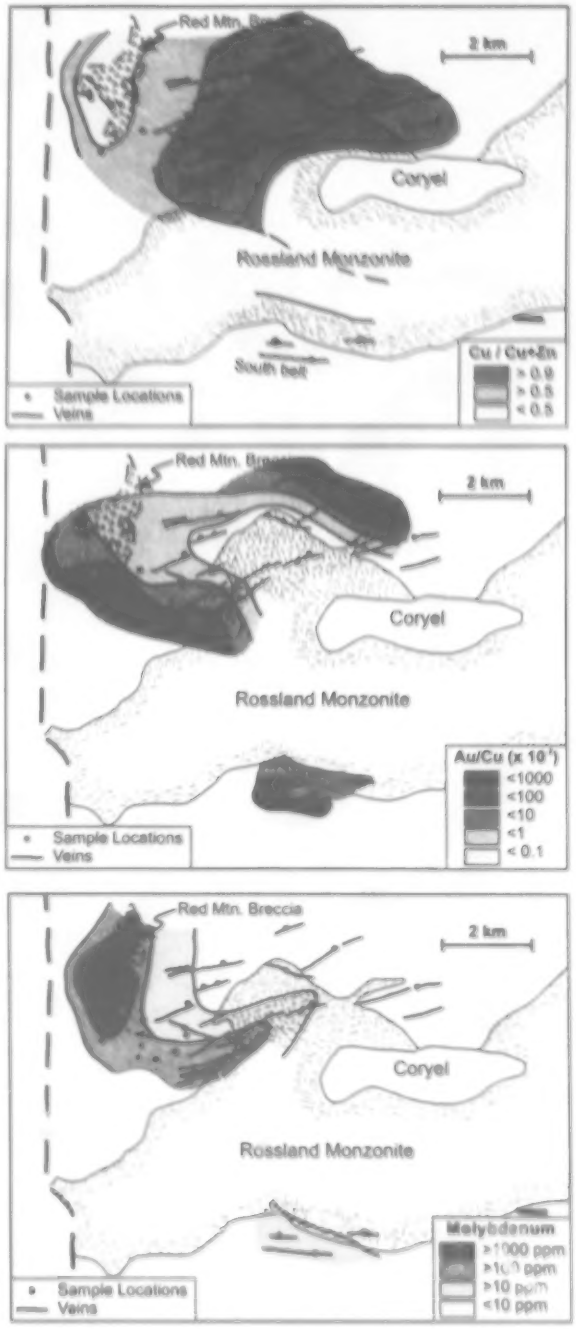

Figure 4-14. Simplified maps of the Rossland camp, showing metal zonation patterns, from assay data listed in Appendix 6; (a) Cu/Cu+Zn (b) Au/Cu*10^3 (c) Mo.

Chemistry

Eastern extensions of the Main veins, in deeper structural levels and within metasediments, illustrate a paragenetic evolution from early siliceous biotite hornfelsing, overprinted by intense prograde skarn alteration, and followed by retrograde skarn and massive sulphide mineralization, and finally late pyrite-calcite veining. Early prograde skarn alteration involves metasomatism by Si, Mg and K dominated fluids, producing mainly quartz, diopside, plagioclase, K-feldspar and garnet, whereas the main stage of vein mineralization is associated with hydrolysis and development of quartz and hydrous Fe-Mg silicates including amphibole, biotite, epidote and chlorite. Late veins are dominantly pyrite, calcite and quartz, reflecting evolution to more Ca-rich fluids.

Progressive changes in fluid chemistry (and trapping temperatures or pressures), based on fluid inclusion studies in quartz associated with these stages of vein development are not readily apparent, mainly due to limited number of analyses of both the early and late stage veins. Quartz in prograde skarn assemblages is characterized by small inclusions that produce 'wispy' textures characteristic of high pressures; due to their small size most are unsuitable for analysis. In one sample, however, this early quartz contains aqueous and rare multiphase assemblages, the latter suggesting possibly highly saline solutions.

Fluid inclusion data from veins associated with the main stage of sulphide deposition indicate fluids with moderate and high salinities of 4-20 and 37-41 eq. wt. % NaCl (and homogenization temperatures of 150 to 377°C and pressures of 1500 to 2900 bars).

The coexistence of aqueous, salt-saturated and CO_2 inclusions suggests that phase separation may have occurred from an original supercritical H_2O-NaCl-(CO_2) fluid producing salt-saturated brine and a gas phase. However this is not supported directly by fluid inclusion evidence of similar homogenization temperature ranges and homogenization to the vapour phase of Type III inclusions. Phase separation would, however, support transport of metals, including gold, as mainly chloride complexes. The zonation from copper dominant to zinc dominant veins along strike is additional evidence for chloride complexing; zinc and lead transport in hydrothermal fluids is dominantly as chloride complexes.

It is also possible that some of the carbonic (CO_2-rich) fluids may be metamorphic in origin, as proposed by Newberry *et al.* (1995) for some Alaskan intrusion-related gold deposits. However, a dominant magmatic origin for Rossland vein fluids is favoured because (1) Elise sediments are generally noncalcareous and (2) skarn mineralogy suggest Ca metasomatism and CO_2 fluid introduction on vein margins.

Fluid inclusions in late quartz-(calcite) veins (based on only one sample from the War Eagle deposit) may be similar, with aqueous, carbonic, and multiphase inclusions. However, the mineralogy of these veins suggests lower temperatures and/or more oxidized fluids.

The high sulphide content of the veins indicates that the fluids were acidic. The abundance of pyrrhotite in the Main veins, restriction of hematite as a late replacement mineral, and presence of carbonic ($CO_2 \pm CH_4$) fluid inclusions suggest that the ore-forming fluids were reduced. However, the relatively high copper content is more typical of more oxidized fluids. Although the Rossland monzonite commonly contains accessory magnetite, Fe_2O_3/FeO ratios indicate that phases of the intrusion range from oxidized to reduced.

In contrast, the slightly younger Rainy Day pluton is more reduced, and is associated with molybdenite and tungsten mineralization. This suggests magmatic evolution, with progressive reduction in oxidation state from more mafic monzodiorite phases typical of the Rossland monzonite to quartz diorites of the Rainy Day pluton. Late veins, and South belt veins more distal from the Rossland monzonite, both with pyrite, may have been deposited from lower temperature, more oxidized fluids. Again, this may reflect fluid evolution perhaps caused by mixing with meteoric fluids.

Copper-gold mineralization in intrusion-related systems is typically associated with I-type, magnetite-bearing plutons with relatively high oxidation states. This contrasts with more reduced, S-type granitic systems that host tin, tungsten and molybdenite deposits (*e.g.*, Newberry, 1998; Thompson *et al.*, 1999; Ray *et al.*, 2000). However, Rowins (2000) and Thompson *et al.* (*op. cit.*) have suggested that some copper-gold deposits are related to reduced, ilmenite-bearing I-type granitic rocks, a model supported for gold-copper veins of the Rossland camp.

In summary, metals that formed the Rossland veins were transported mainly as chloride complexes in a relatively hot, saline, probably acidic magmatic-hydrothermal fluid.

Deposition

Precipitation of metals, carried as chloride complexes, can be caused by a variety of factors, but was probably mainly due to a reduction in temperature, salinity and/or pressure. As well, an increase in the pH of the solution or a decrease in its oxidation state could also promote metal precipitation. It is probable that many of these factors played a role, accounting for the complexity in the fluid inclusions, and the diverse but pronounced mineralogy and metal zonation within the camp.

The zonation of copper-gold to lead-zinc is compatible with a decrease in temperature with distance from the Rossland monzonite. As well, unmixing of original highly saline H_2O-CO_2-salt solutions, with resultant increase in pH, may have facilitated early copper-gold precipitation. This marked decrease in the solubility of both gold and copper with increasing pH is illustrated in Figure 4-15. Also shown is a proposed fluid evolution path, restricted by precipitation of mainly pyrrhotite and chalcopyrite, and the common occurrence of carbonate gangue in some veins and CO_2-rich fluid inclusions.

The prominent structural control to Rossland veins and their brecciated nature implies rock fracturing that would allow sudden pressure drops with resultant metal precipita-

tion. Finally, mixing of saline hydrothermal-magmatic fluids with cooler pore or meteoric fluids, as expected in fractured wallrocks of the Rossland monzonite, would further enhance sulphide deposition.

STRUCTURAL CONTROLS AND TECTONIC SETTING

Rossland veins have many characteristics typical of intrusion-related hydrothermal veins. However, their strong preferred alignment and associated shearing are indicative of structural controls as well. Furthermore, a structural control to emplacement of the Rossland monzonite and porphyrite dikes is also clearly evident. The two main vein orientations, west-southwest and west-northwest, suggest a dominant east-west compressive stress. This compression is related to the east-verging thrusts documented immediately to the west; these thrusts emplace oceanic ultramafic assemblages and the Permo-Carboniferous Mount Roberts Formation on to the Rossland Group (Höy and Dunne, 1997). The relatively high pressures recorded in Rossland vein fluid inclusions may be due, in part, to increased lithostatic pressure beneath these thrust plates.

The relative timing of Middle Jurassic intrusions, such as the Rossland monzonite, and tectonic shortening and overlap during thrust tectonics have been documented farther east in the Nelson-Rossland area. There, Nelson-age (165-170 Ma) intrusions are late synkinematic to post-kinematic.

The tectonic setting of the Cu-Au veins has been discussed by many previous workers. For example, Höy *et al.* (1992, p. 268) concluded that the camp occurs in "a dominantly mafic volcanic pile spatially associated with an oceanic assemblage ... is associated with felsic intrusive rocks and ultramafic bodies, and occurs along a major structural break". Furthermore, we acknowledged that "most (mesothermal) gold mineralization is interpreted to have formed in an accretionary tectonic setting, considerably later than the host volcanic rocks, with fluid flow focused by crustal faults (Kerrick and Wyman, 1990)". We concluded that despite the apparent similar setting for Rossland Group rocks, additional chronological and isotopic data were necessary to conclude that Rossland mineralization is related to this accretionary or collisional process.

Data presented in this paper supports a model for gold-copper vein mineralization related to intrusion of the *ca.* 167 Ma Rossland monzonite, late to post intense compressional deformation. Ash (2001) also recognized the importance of crustal structures in localizing the Rossland Cu-Au camp. Ash (*op. cit.*) concluded that, in common with other lode gold camps in the province, the Rossland camp occurs along a terrane-collisional boundary between ophiolitic assemblages and Rossland arc rocks.

MODEL SUMMARY

More eastern veins and related skarn alteration formed at deeper structural levels along the margins of and within the Rossland monzonite. Shearing of hot, crystallized or partially crystallized mafic intrusive material, as is seen

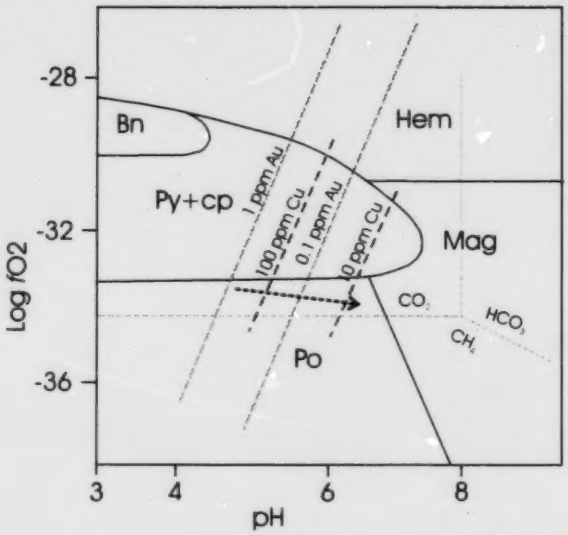

Figure 4-15. Log fO_2 - pH diagram for the system Fe-S-O showing phase relationships at 350°C and 3 kb. Arrow shows postulated fluid path during deposition of pyrrhotite and chalcopyrite; diagram after Ettner *et al.* (1993) and Pollard (1999).

along many of the vein margins, would be possible in this environment by increasing fluid pressures to lithostatic pressures (or higher?) and/or by suddenly increasing strain rates (Fournier, 1999). High fluid pressures can only develop beneath an impermeable seal, a barrier that may have developed near the ductile-brittle transition (*see* Figure 4-12). This seal would allow accumulation of higher temperature and pressure magmatic-hydrothermal fluids in the upper (western) levels of the Rossland monzonite and in immediate host rocks. Fluxing of these fluids with the magma concentrated sufficient metals to eventually precipitate massive sulphide veins.

Breaching of the impermeable seal allowed sudden escape of fluids into a brittle environment characteristic of the more western Main veins, North belt veins and most of the South belt veins. This breaching was due to a combination of factors. The buildup of hydrostatic pressure from fluids evolving from the crystallizing magma eventually resulted in hydrostatic pressures greater than the tensile strength of the rock. Tectonic activity enhanced rock fracturing; that this activity is associated with emplacement of the Rossland monzonite is inferred by the east-west alignment of the intrusion and the strong structural control of the porphyrite dykes, the common host for Rossland veins. Intrusion of these dykes may, as well, have provided a breach of the barrier and a conduit for escaping fluids. Resultant rapid drop in hydrostatic pressure, fluid unmixing and possibly mixing with cooler fluids, caused precipitation of metals from the dominantly magmatic-hydrothermal fluids. This reduction in fluid pressure caused the brittle-ductile transition to be depressed to deeper structural levels, thus allowing shearing of the more eastern and Main veins that formed in more ductile environments.

F2

The argument that the Rossland veins are magmatic-hydrothermal veins, related to intrusion of the Rossland monzonite and associated porphyrite dikes, explains some anomalous features. Massive sulphide veins, in contrast to more typical quartz and carbonate-rich mesothermal veins or to veins that show evidence of repeated hydrothermal pulses with associated reintroduction of metals, require that the fluids contained high concentrations of both metals and sulphide. These concentrations are possible in the relatively high temperature and pressure fluids that are documented here. These were supercritical fluids (*see* Figure 5 in Fournier, 1999) capable of carrying considerable dissolved base and precious metals, particularly if they contained H_2S as well as chloride complexes, as a reduced complexing agent (*e.g.*, Heinrich *et al.*, 1992).

The relatively unusual but extensive skarn alteration associated with deeper levels of the Rossland veins are also readily explained by a magmatic origin. This skarn alteration is zoned around the Rossland monzonite, as is the tenor and alteration assemblages of the veins themselves.

One of the fundamental features of intrusive-related massive sulphide veins appears to be the requirement that the magma intruded 'hot' rocks. This allowed the brittle-ductile transition, and impermeable barrier, to be considerably distant from the intrusion and hence allowed a larger volume of rock for concentrations of magmatic-hydrothermal fluids, their fluxing with the intrusion, and resultant concentrations of metals and sulphide species. These elevated geothermal gradients can occur in subvolcanic environments, where high-level magma intrudes a relatively hot volcanic pile (Alldrick and Höy, 1997) or in an area such as Rossland where multiple intrusive phases were emplaced just prior to veining.

This model for Rossland veins is compatible with some of the conclusions of other recent studies of the Rossland camp. Höy and Dunne (1997) argued that the veins appear to be spatially and probably genetically related to the Rossland monzonite, a model developed in large part by Thorpe (1967). Höy and Dunne (*op. cit.*) suggested, however, that the monzonite is a subvolcanic intrusion, a conclusion that is not supported by U-Pb zircon dating nor fluid inclusion studies that suggest relatively deep emplacement.

The chemistry, mineralogy and form of the Rossland veins is similar in many aspects to some deposits in the Cloncurry Cu-Au district in the Mount Isa area of Australia, summarized by Williams (1999). For example, the Eloise deposit, discovered in 1988 by BHP, is characterized by massive pyrrhotite-chalcopyrite veins that carry appreciable gold and silver.

Alldrick (1996) and Alldrick and Höy (1997) used the term 'intrusion-related gold-sulphide vein' to describe the Rossland veins and other similar veins such as Snip, Scottie Gold and Johnie Mountain in Jurassic Hazelton Group rocks in central British Columbia. Their basic model, that massive gold-copper sulphide-rich veins are concentrated along the ductile-brittle transition above an intrusion, is the model still adhered to in this paper. However, their conclusion that these intrusions are subvolcanic or volcanic arc-related intrusions only holds for the more northern veins. We believe that a necessary requirement for this model is relatively 'hot' hostrocks or a high geothermal gradient, which may form in a number of settings including a subvolcanic environment but also in areas such as Rossland characterized by extensive plutonic magmatism.

SUMMARY: ROSSLAND CAMP

Skarn molybdenum, intrusive-related copper-gold veins, polymetallic veins and lode gold-quartz veins have been extensively mined in the Rossland area. They are in a region that has been tectonically active since Early Jurassic time and which has been intruded repeatedly. Based on field observations and considerable new age dating, the relationships between tectonism, magmatism and mineralization can be constrained more closely and is summarized below (Figure 4-16).

- Sinemurian (*ca* 200 Ma): tectonic high in the Rossland area, with deposition of Archibald Formation sediments farther east in a structural basin.
- Late Sinemurian (*ca.* 197-195 Ma): arc volcanism of the Elise Formation, deposited on the Archibald Formation or unconformably on Mount Roberts Formation basement.
- Late Sinemurian(?) intrusion of the subvolcanic Rossland sill complex; (farther east, similar intrusions are associated with alkali copper-gold porphyry mineralization, such as Katie).
- Pliensbachian: minor tectonic activity and uplift; (early synkinematic intrusions recognized farther north, such as the *ca* 184 Ma Alwyn Creek stock).
- Toarcian: Sediments of the Hall Formation deposited unconformably on the Elise Formation.
- Early Middle Jurassic: intense compressional deformation, tectonic emplacement of ultramafic rocks just west of Rossland; (to the north and east, intrusion of synkinematic ca. 174-178 Ma Silver King plutons).
- Middle Jurassic (*ca.* 167 Ma): intrusion of the Rossland 'monzonite' and diorite porphyrite dikes; (Nelson and Trail plutons); syn to late-kinematic **Rossland Cu-Au and polymetallic veins**; [Second Relief veins and skarn mineralization (*ca.* 169 Ma) north of Salmo].
- Middle Jurassic (*ca.* 166-162 Ma): intrusion of Rainy Day pluton, quartz diorite dikes on Red Mountain; brecciation, skarn alteration and **molybdenite mineralization** on Red Mountain.
- Late Cretaceous: Sophie Mountain deposited unconformably on Rossland Group.
- Eocene: extension and westward tilting to expose oblique view of Rossland camp.

In summary, deposits in the Rossland area record two main periods of mineralization, both related to intrusion of Middle Jurassic plutons. East-trending copper-gold and polymetallic veins of the Rossland camp are spatially and genetically related to the 167 Ma Rossland monzonite and

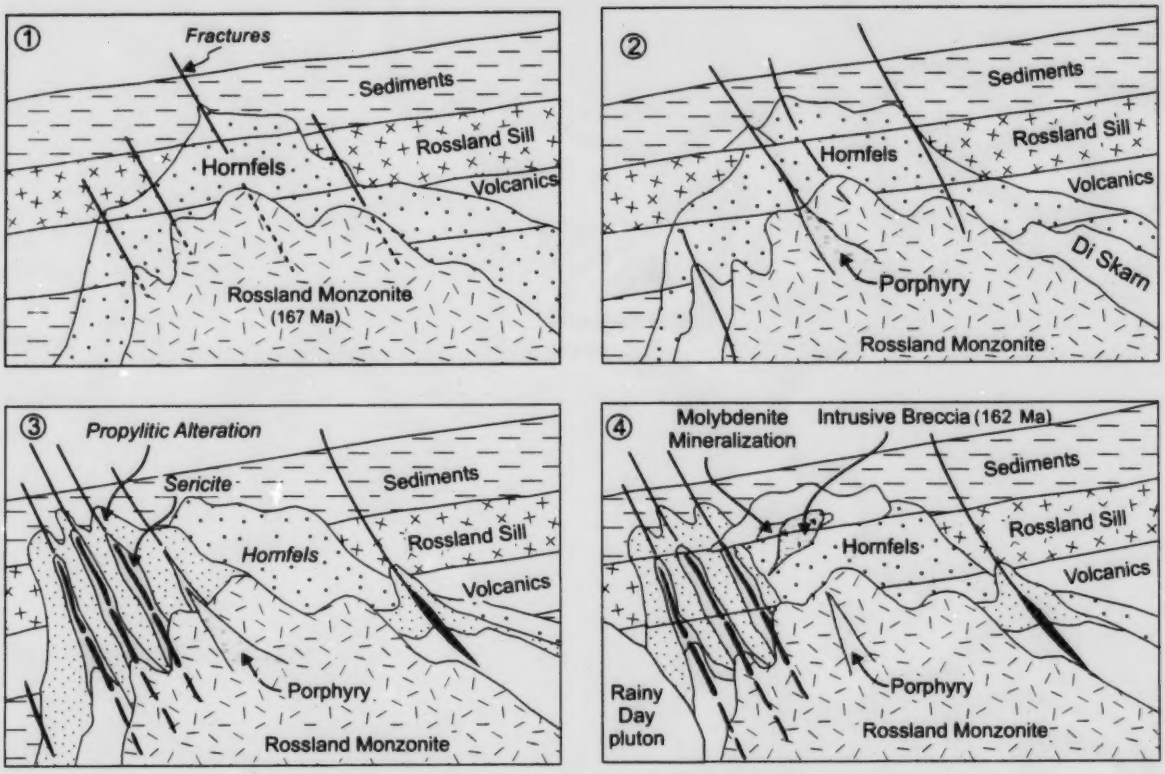

Figure 4-16. Model showing the evolution of gold-copper vein, polymetallic vein and molybdenite skarn deposits of the Rossland camp. Vein deposits are related to intrusion of the Rossland monzonite and diorite porphyry at ca. 167 Ma (2 and 3) and molybdenite, to intrusion of the ca. 166 Ma Rainy Day pluton and associated 162-163 Ma dikes (4).

associated east-trending diorite porphyrite dikes. These veins are parallel to and within the 'Rossland break', a zone of fractures, faults and intrusions that mark a pronounced change in the structural grain in the Rossland area, probably related to east-west compression associated with crustal-scale thrust faulting.

Due to Eocene tilting, the Rossland camp provides an oblique view through a major, intrusive-related gold-copper and polymetallic vein camp. More eastern deposits were formed at deeper structural levels than those in the west, resulting in systematic changes in the structural style, mineralogy and tenor of veins and related deposits from east to west.

The molybdenite breccia-skarn complex, mainly to the west of and structurally above the Rossland veins, is related to 162-163 Ma quartz diorite dikes that may be late phases of the compositionally similar *ca.* 166 Ma Rainy Day pluton.

SELECTED BIBLIOGRAPHY

Addie, G.G. (1970): The Reeves-MacDonald mine, Nelway, British Columbia; *in* Lead-zinc Deposits in the Kootenay Arc, Northeastern Washington and Adjacent British Columbia; *State of Washington, Department of Natural Resources*, Bulletin 61, pages 79-88.

Addie, G. (1986): Preliminary geochemical and geophysical report on the Morning Toad property, Nelson Mining District, British Columbia; *B.C. Ministry of Energy, Mines and Petroleum Resources*, Assessment report 13,893.

Akhurst, K. (1989): Geochemical, geophysical and geological report on the Connor Creek property, Nelson Mining Division, B.C.; *B.C. Ministry of Energy and Mines*, Assessment report 18,518.

Alldrick, D.J. (1993): Geology and metallogeny of the Stewart Mining Camp, Northwestern British Columbia; *B.C. Ministry of Energy, Mines and Petroleum Resources*, Bulletin 85, 105 pages.

Alldrick, D.J. (1995): Subaqueous hot spring Au-Ag; *in* Selected British Columbia Mineral Deposit Profiles, Volume 1, Lefebure, D.V. and Ray, G.E., Editors, *B.C. Ministry of Employment and Investment*, Open File 1995-20, pages 55-57.

Alldrick, D.J. (1996): Intrusion-related gold-pyrrhotite veins; *in* Selected British Columbia Mineral Deposits Profiles, Volume 2, Lefebure, D.V and Höy, T., Editors, *B.C. Ministry of Employment and Investment*, Open File 1996-13, pages 57-58.

Alldrick, D.J. and Höy, T. (1997): Intrusion-related gold-pyrrhotite veins; *in* The Gangue, Grant, B. Editor, *Mineral Deposit Division*, Newsletter, Issue 55, Pages 8-10.

Allen, G.M. (1987): Nugget Mines Ltd. - Sheep Creek gold camp, Nelson Mining Division, British Columbia; *B.C. Ministry of Energy, Mines and Petroleum Resources*, Assessment report 16,704.

Aylward, P.S. (1983): Silver King property, drilling, trenching and compilation of previous work; *B.C. Ministry of Energy, Mines and Petroleum Resources*, Assessment report 12611.

Andrew, K.P.E. and Höy, T. (1988): Preliminary geology and mineral deposits of the Rossland Group between Nelson and Ymir, southeastern British Columbia; *B.C. Ministry of Energy, Mines and Petroleum Resources*, Open File 1988-1.

Andrew, K.P.E. and Höy, T. (1989): The Shaft showing, Elise Formation, Rossland Group; *in* Exploration in British Columbia 1988; *B.C. Ministry of Energy, Mines and Petroleum Resources*, pages B21-28.

Andrew, K.P.E. and Höy, T. (1990): Geology and exploration of the Rossland Group in the Swift Creek area; *in* Exploration in British Columbia 1989; *B.C. Ministry of Energy, Mines and Petroleum Resources*, pages 73-80.

Andrew, K.P.E. and Höy, T. (1991): Geology of the Erie Lake area with emphasis on stratigraphy and structure of the Hall Formation, southeastern British Columbia; *in* Geological Fieldwork 1990, Newell, J.M and Grant, B., Editors, *B.C. Ministry of Energy, Mines and Petroleum Resources*, Paper 1991-1, pages 9-20.

Andrew, K.P.E., Höy, T., and Drobe, J. (1990a): Stratigraphy and tectonic setting of the Archibald and Elise formations, Rossland Group, Beaver Creek area, southeastern British Columbia; *in* Geological Fieldwork 1989, Newell, J.M. and Grant, B., Editors, *B.C. Ministry of Energy, Mines and Petroleum Resources*, Paper 1990-1, pages 19-27.

Andrew, K.P.E., Höy, T., and Drobe, J. (1990b): Geology of the Rossland Group, Beaver Creek area, southeastern British Columbia (82F/4E); *B.C. Ministry of Energy, Mines and Petroleum Resources*, Open File 1990-9.

Andrew, K.P.E., Höy, T. and Simony, P. (1991): Geology of the Trail map-area, southeastern British Columbia; *B.C. Ministry of Energy, Mines and Petroleum Resources*, Open File 1991-16.

Archibald, D.A., Glover, J.K., Price, R.A., Farrar, E. and Carmichael, D.M. (1983): Geochronology and tectonic implications of magmatism and metamorphism, southern Kootenay Arc and neighbouring regions, southeastern British Columbia. Part I: Jurassic to mid-Cretaceous; *Canadian Journal of Earth Sciences*, volume 12, pages 1891-1913.

Arculus, R.J. and Powell, R. (1986): Source component mixing in the regions of arc magma generation; *Journal of Geophysical Research*, Volume 91, pages 5913-5926.

Ash, C.H. and Alldrick, D. (1996): Au-quartz veins; *in* Selected British Columbia Mineral Deposits Profiles, Volume 2, Lefebure, D.V and Höy, T, Editors, *B.C. Ministry of Employment and Investment*, Open File 1996-13, pages 53-56.

Ash, C.H., Macdonald, R.W.J. and Arksey, R.L. (1992): Towards a deposit model for ophiolite related mesothermal gold in British Columbia (82F/4); *in* Geological Fieldwork 1991, Newell, J.M. and Grant, B., Editors, *B.C. Ministry of Energy, Mines and Petroleum Resources*, Paper 1992-1, pages 253-260.

Ash, C.H. (2001): Ophiolite-related mesothermal lode gold in British Columbia: a deposit model; *B.C. Ministry of Energy, Mines and Petroleum Resources*, Bulletin 108, 140 pages.

Aylward, P.S. (1983): Silver King property, drilling, trenching and compilation of previous work; *B.C. Ministry of Energy, Mines and Petroleum Resources*, Assessment report 12611.

Beddoe-Stephens, B. (1977): The petrology and geochemistry of the Rossland Group volcanic rocks, southern British Columbia; *University of Alberta*, Unpublished Ph.D. thesis, 390 pages.

Beddoe-Stephens, B. and Lambert, R. St. J. (1981): Geochemical, mineralogical and isotopic data relating to the origin and tectonic setting of the Rossland volcanic rocks, southeastern British Columbia; *Canadian Journal of Earth Sciences*, Volume 18, pages 858-868.

Beaudoin, G., Sangster, D.F. and Godwin, C.I. (1992a): Isotopic evidence for complex Pb sources in the Ag-Pb-Zn-Au veins of the Kokanee Range, southeastern British Columbia; *Canadian Journal of Earth Sciences*, Volume 29, pages 418-431.

Beaudoin, G., Roddick, J.C. and Sangster D.F. (1992b): Eocene age for Ag-Pb-Zn vein and replacement deposits of the Kokanee Range, southeastern British Columbia; *Canadian Journal of Earth Sciences*, Volume 29, pages 3-14.

Bevier, M.L. (1987): A Pb isotopic study of the Valhalla Complex and its surrounding rocks, southeastern British Columbia: preliminary interpretations; *in* Radiogenic Age and Isotopic Studies: Report 1, *Geological Survey of Canada*, Paper 87-2, pages 13-20, 1987.

Bodnar, R.J. (1995): Fluid-inclusion evidence for a magmatic source for metals in porphyry copper deposits; in Magmas, Fluids and Ore Deposits, J.F.H. Thompson, Editor, *Mineralogical Association of Canada*, Short Course volume 23, pages 139-152.

Bostock, H.S. (1940): Keremeos, British Columbia; *Geological Survey of Canada*, Map 341A.

Bruce, E.L. (1917): Geology and ore deposits of Rossland, British Columbia; *B.C. Ministry of Energy, Mines and Petroleum Resources*, Bulletin 4.

Carpenter, T.H. (1983): Assessment report, Stewart 2, 3, 4, 9, 11, 12, Ruby and Free Silver, Royal, Maggie, Jock 1 and Jock 2, Stewart 1,8,10 and Houlton, Stewart 5, 6, 7 and 13; *B.C. Ministry of Energy, Mines and Petroleum Resources*, Assessment report 12,241.

Carpenter, T.H. (1984): Assessment report, Stewart 1, 2, 3, 4, 5, 6, 7. 8, 9, 10, 11, 12, 13, Ruby and Free Silver, Royal, Maggie, Jock 1 and Jock 2, and Houlton claims; *B.C. Ministry of Energy, Mines and Petroleum Resources*, Assessment report 13,166.

Carr, S.D. (1984): Ductile shearing and brittle faulting in Valhalla gneiss complex, southeastern British Columbia; *in* Current Research, Part A, *Geological Survey of Canada*, Paper 85-1A, pages 89-96.

Carr, S.D. (1991): Three crustal zones in the Thor-Odin-Pinnacles area, southern Omineca Belt, British Columbia; *Canadian Journal of Earth Sciences*, Volume 28, pages 2003-2023.

Carr, S.D., Parrish, R.R. and Brown, R.L. (1987): Eocene structural development of the Valhalla complex, southeastern British Columbia; *Tectonics*, Volume 6, pages 175-196.

Cathro, M.S., Dunne, K.P.E. and Naciuk, T.M. (1993): Katie - an alkaline porphyry copper-gold deposit in the Rossland Group, southeastern British Columbia; *B.C. Ministry of Energy, Mines and Petroleum Resources*, Geological Fieldwork 1992, Paper 1993-1, pages 233-247.

Church, B.N. (1973): Geology of the White Lake basin; *B.C. Ministry of Energy, Mines and Petroleum Resources*, Bulletin 61, 120 pages.

Church, B.N. (1986): Geological setting and mineralization in the Mount Attwood-Phoenix area of the Greenwood mining camp (82E); *B.C. Ministry of Energy, Mines and Petroleum Resources*, Paper 1986-2, 65 pages.

Church, B.N. (1992): The Lexington porphyry, Greenwood mining camp, southern British Columbia; *B.C. Ministry of Energy, Mines and Petroleum Resources*, Geological Fieldwork 1991, Paper 1992-1, pages 295-297.

Clark, L.A. (1960): The Fe-As-S system: Phase relations and applications; *Economic Geology*, Volume 55, Part I, pages 1345-1381; Part II, pages1631-1652.

Cockfield, W.E., (1936): Lode gold deposits of Ymir- Nelson area, British Columbia; *Geological Survey of Canada*, Memoir 191, 78 pages.

Colpron, M., Price, R.A., Archibald, D.A. and Carmichael, D.M. (1996): Middle Jurassic exhumation along the western flank of the Selkirk fan structure: thermobarometric and thermochronometric constraints from the Illecillewaet synclinorium, southeastern British Columbia; *Geological Society of America*, Bulletin 108, pages 1372-1392.

Cooke, D.L. (1990): Geological and geochemical report, Clubine property, Nelson M.D., *YellowJack Resources Ltd.*, private report, September 1990.

Corbett, C.R. and Simony, P.S. (1984): The Champion Lake Fault in the Trail-Castlegar area of southeastern British Columbia; *in* Current Research, Part A; *Geological Survey of Canada*, Paper 84-1A, pages 103-104.

Crowe, G.G. (1981): The structural evolution of the Mackie plutonic complex, southern British Columbia; unpublished M.Sc. thesis, *University of Calgary*, Calgary, 154 pages.

Daly, R.A. (1912): North American Cordillera, forty-ninth Parallel; *Geological Survey of Canada*, Memoir 38, Parts 1, 2 and 3.

Dawson, G.M (1889): Report on a portion of the West Kootenai District, British Columbia; *Geological Survey of Canada*, Annual reports 1888-1889.

Dawson, G.J., Austen, B.E.K. and Heinrich, S. (1989): Great Western Star gold-copper project, Nelson Mining Division, British Columbia; *B.C. Ministry of Energy, Mines and Petroleum Resources*, Assessment report 19,503.

Debon, F. and Le Fort, P. (1983): A chemical-mineralogical classification of common plutonic rocks and associations; *Transactions of the Royal Society of Edinburgh*: Earth Sciences, Volume 73, pages 135-139.

Devlin, W.J. and Bond, G.C. (1987): The initiation of the Early Paleozoic Cordilleran miogeocline: evidence from the uppermost Proterozoic - Lower Cambrian Hamill Group of southeastern British Columbia; *Canadian Journal of Earth Sciences*, Volume 25, pages 1-19.

Drysdale, C.W. (1915): Geology and ore deposits of Rossland, British Columbia; *Geological Survey of Canada*, Memoir 77.

Drysdale, C.W. (1917): Ymir mining camp, British Columbia; *Geological Survey of Canada*, Memoir 94.

Dunne, K.P.E and Höy, T. (1992): Petrology of Lower and Middle Jurassic intrusions in the Rossland Group, southeastern British Columbia; *in* Geological Fieldwork 1991, *B.C. Ministry of Energy, Mines and Petroleum Resources*, Paper 1992-1, pages 9-19.

Dunne, K.P.E., Höy, T. and Fraser, A. (1992): Geology and exploration of the Clubine showing, Rossland Group, Salmo area; B.C. *Ministry of Energy, Mines and Petroleum Resources*, Exploration in British Columbia, pages 61-66.

Eastwood, G.E.P (1966): Rossland camp; *BC. Ministry of Mines*, Annual report 1967, pages 200-207.

Einersen, J.M. (1994): Structural geology of the Pend d'Oreille area and tectonic evolution of the southern Kootenay Arc; unpublished Ph.D. thesis, *The University of Calgary*, 172 pages.

Ellerington, J.D. (1987): Geological, geochemical and geophysical report, Salmo Goldbelt project; *B.C. Ministry of Energy, Mines and Petroleum Resources*, Assessment report 16,728.

Endersby, A. (1992): Report on self-potential survey on the Chrissy Group of claims at Reno mine, Nelson Mining Division British Columbia; *B.C. Ministry of Energy, Mines and Petroleum Resources*, Assessment report 22,043.

Erdmer, P. (1987): Blueschist and eclogite in mylonitic allochthons, Ross River and Watson Lake areas, southern

Yukon; *Canadian Journal of Earth Sciences*, Volume 24, pages 1439-1449.

Ermanovics, I. and Downing, B. (1997): Geology and results of a diamond drill program of the Red Point claim block area, Trail, British Columbia; *B.C. Ministry of Energy and Mines*, Assessment report 25,249.

Fitzpatrick, M. (1985): The geology of the Rossland Group in the Beaver Valley area, southeastern British Columbia; unpublished M.Sc. thesis, *University of Calgary*, 150 pages.

Fournier, R.O. (1999): Hydrothermal processes related to movement of fluid from plastic into brittle rock in the magmatic-epithermal environment; *Economic Geology*, Volume 94, pages 1193-1211.

Fowler, F.H. and Wehrle, D.M. (1990): Assessment report on the Columbia-Kootenay claim group, Rossland, British Columbia; *B.C. Ministry of Energy, Mines and Petroleum Resources*, Assessment report 20,158.

Fox, P.E. and Cameron, R.S. (1995): Geology of the QR gold deposit, Quesnel River area, British Columbia; *in* Porphyry Deposits of the Northwestern Cordillera of North America, Schroeter, T.G., Editor, *Canadian Institute of Mining, Metallurgy and Petroleum*, Special Volume 46, pages 829-837.

Frebold, H. (1959): Marine Jurassic rocks in Nelson and Salmo areas, Southeastern British Columbia; *Geological Survey of Canada*, Bulletin 49.

Frebold, H. and Little, H.W. (1962): Paleontology, stratigraphy, and structure of the Jurassic rocks in Salmo map-area, British Columbia; *Geological Survey of Canada*, Bulletin 81.

Frebold, H. and Tipper, H.W. (1970): Status of the Jurassic in the Canadian Cordillera of British Columbia, Alberta, and southern Yukon; *Canadian Journal of Earth Sciences*, Volume 7, pages 1-20.

Fyles, J.T. (1970): Geological setting of lead-zinc deposits in the Kootenay Lake and Salmo areas of British Columbia; *in* Lead-zinc Deposits in the Kootenay Arc, Northeastern Washington and Adjacent British Columbia; *State of Washington, Department of Natural Resources*, Bulletin 61, pages 41-53.

Fyles, J.T. (1984): Geological setting of the Rossland mining camp; *B.C. Ministry of Energy, Mines and Petroleum Resources*, Bulletin 74, 61 pages.

Fyles, J.T. (1990): Geology of the Greenwood - Grand Forks area, British Columbia (82E/1); *B.C. Ministry of Energy, Mines, and Petroleum Resources*, Open File 1990-25.

Fyles, J.T. (1995): Day 3 (Morning): Knob Hill Group, Attwood Group and Brooklyn Formation; *in* Field Trip Guidebook B2, *Geological Association of Canada*, Victoria, B.C., pages 40-49.

Fyles, J.T. and Hewlett, C.G. (1959): Stratigraphy and structure of the Salmo lead-zinc area; *British Columbia Department of Mines*, Bulletin 41, 162 pages.

Getsinger, J.S. (1992): Petrography of fourteen samples from the Katie project; unpublished report, *CME Consulting Limited and Yellowjack Resources Limited*.

Ghosh, D.P. (1995a): Nd and Sr isotopic constraints on the interactions of the Intermontane Superterrane with the western edge of North America in the southern Canadian Cordillera; *Canadian Journal of Earth Sciences*, Volume 32, pages 1740-1758.

Ghosh, D.P. (1995b): U-Pb geochronology of Jurassic to Early Tertiary granitic intrusives from the Nelson-Castlegar area, southeastern British Columbia; *Canadian Journal of Earth Sciences*, Volume 32, pages 1668-1680.

Godwin, C.I., Sinclair, A.J. and Ryan, B.D. (1982): Lead isotope models for the genesis of carbonate-hosted Zn-Pb, shale-hosted Ba-Zn-Pb, and silver-rich deposits in the northern Canadian Cordillera, *Economic Geology*, Volume 77, pages 82-94.

Goldfarb, R.J., Leach, D.L., Miller, M.L. and Pickthorn, W.J. (1986): Geology, metamorphic setting, and genetic constraints of epigenetic lode-gold mineralization within the Cretaceous Valdez Group, south-central Alaska; *in* Turbidite-hosted Gold Deposits, Keppie, J.D., Boyle, R.W. and Haynes, S.J., Editors, *Geological Association of Canada*, Special Paper 32, pages 87-105.

Grant, B. (1983): Assessment report, Stewart moly project; *B.C. Ministry of Energy, Mines and Petroleum Resources*, Assessment report 11,670.

Haas, J.L. Jr. (1971): The effect of salinity on the maximum thermal gradient of a hydrothermal system at hydrostatic pressure; *Economic Geology*, Volume 66, pages 940-946.

Halwas, D.B. and Simony, P.S. (1986): The Castlegar gneiss complex, southern British Columbia; *in* Current Research, Part A, *Geological Survey of Canada*, Paper 86-1A, pages 583-587.

Hardy, J.L. (1986): Geological and diamond drilling report on the Georgia property, Trail Creek Mining Division, British Columbia; B.C. *Ministry of Energy, Mines and Petroleum Resources*, Assessment report 15,432.

Heather, K.B. (1985): The Alwin Creek gold-copper-silver deposit, southeastern British Columbia; unpublished M.Sc. thesis, *Queen's University*, Kingston, Ontario, 253 pages.

Hickling, E. (1983): Geology report. Stewart west grid, project 10138; *B.C. Ministry of Energy, Mines and Petroleum Resources*, Assessment report 12251.

Hill, H.I. (1965): Report on the Silver King group, Nelson, B.C.; unpublished report, *B.C. Ministry of Energy, Mines and Petroleum Resources*, Property File.

Hitzman, M.W. (1995): Mineralization in the Irish Zn-Pb-(Ba-Ag) orefield; *in* Irish Carbonate-hosted Zn-Pb Deposits; Anderson, K., Ashton, J., Earls, G., Hitzman, M., and Sears, S., Editors, *Society of Economic Geologists*, Guidebook series, Volume 21, pages 25-61.

Hodgson, C.J. (1993): Mesothermal lode-gold deposits, *Geological Association of Canada*, Special Paper 40, pages 635-678.

Hodgson, C.J., Chapman, R.S.G. and MacGeehan, P.J. (1982): Application of exploration criteria for gold deposits in the Superior Province of the Canadian Shield to gold exploration in the Cordillera; *in* Precious Metals of the Northern Cordillera, Levinson, A.A., Editor, *Association of Exploration Geochemists*, pages 173-206.

Höy, T. (1982a): Stratigraphic and structural setting of stratabound lead-zinc deposits in southeastern British Columbia; *Canadian Institute of Mining and Metallurgy*, Bulletin, Volume 75, pages 114-134.

Höy, T. (1982b): The Purcell Supergroup in southeastern British Columbia: lead-zinc deposits in Precambrian sulphide deposits; *in* H.S. Robinson Memorial Volume, Hutchinson, R.W., Spence, C.D. and Franklin, J.M., Editors, *Geological Association of Canada*, Special Paper 25, pages 127-147.

Höy, T. (1997): Harper Creek: a volcanogenic sulphide deposit within the Eagle Bay assemblage, Kootenay Terrane, south-

ern British Columbia; *in* Geological Fieldwork 1996, *B.C. Ministry of Energy, Mines and Petroleum Resources*, Paper 1997-1, pages 199-209.

Höy, T. and Andrew, K.P.E. (1988): Preliminary geology and geochemistry of the Elise Formation, Rossland Group, between Nelson and Ymir, southeastern British Columbia; *in* Geological Fieldwork 1987, Newell, J.M and Grant, B., Editors, *B.C. Ministry of Energy, Mines and Petroleum Resources*, Paper 1988-1, pages 19-30.

Höy, T. and Andrew, K.P.E. (1989a): The Rossland Group, Nelson map area, southeastern British Columbia; *in* Geological Fieldwork 1988, Newell, J.M. and Grant, B., Editors, *B.C. Ministry of Energy, Mines and Petroleum Resources*, Paper 1989-1, pages 33-43.

Höy, T. and Andrew, K.P.E. (1989b): Geology of the Rossland Group, Nelson map-area, southeastern British Columbia; *B.C. Ministry of Energy, Mines and Petroleum Resources*, Open File Map 1989-1.

Höy, T. and Andrew, K.P.E. (1989c): The Great Western Group, Elise Formation, Rossland Group; *in* Exploration in British Columbia 1988, *B.C. Ministry of Energy, Mines and Petroleum Resources*, pages B15-19.

Höy, T. and Andrew, K.P.E. (1990a): Structure and tectonics of the Rossland Group, Mount Kelly - Hellroaring Creek area, southeastern British Columbia; *in* Geological Fieldwork 1989, Newell, J.M. and Grant, B., Editors, *B.C. Ministry of Energy, Mines and Petroleum Resources*, Paper 1990-1, pages 11-17.

Höy, T. and Andrew, K.P.E. (1990b): Geology of the Mount Kelly-Hellroaring Creek map area, southeastern British Columbia; *B.C. Ministry of Energy, Mines and Petroleum Resources*, Open File Map 1990-8.

Höy, T. and Andrew, K.P.E. (1991a): Geology of the Rossland area, southeastern British Columbia (82F/4E); *in* Geological Fieldwork 1990, Newell, J.M. and Grant, B., Editors, *B.C. Ministry of Energy, Mines and Petroleum Resources*, Paper 1991-1, pages 21-31.

Höy, T. and Andrew, K.P.E., (1991b): Geology of the Rossland -Trail area, southeastern British Columbia (82F/4); *B.C. Ministry of Energy, Mines and Petroleum Resources*, Open File 1991-2.

Höy, T. and Dunne, K.P.E. (1997): Early Jurassic Rossland Group, southern British Columbia: Part I - stratigraphy and tectonics; *B.C. Ministry of Employment and Investment*, Bulletin 102, 124 pages.

Höy, T. and Dunne, K.P.E. (1998): Geological compilation of the Trail map-area, southeastern British Columbia; B.C. Ministry of Energy and Mines, Geoscience Map 1998-1.

Höy, T., Dunne, K.P.E. and Wehrle, D. (1992): Tectonic and stratigraphic controls of gold-copper mineralization in the Rossland camp, southeastern British Columbia; *in* Geological Fieldwork 1991, Newell, J.M. and Grant, B., Editors, *B.C. Ministry of Energy, Mines and Petroleum Resources*, Paper 1992-1, pages 261-271.

Jenks, J. (1988): The Shaft mineral claims, Nelson Mining Division, British Columbia; *South Pacific Gold Corp.*, private report, January, 1988.

Joseph, N.L. (1990): Geologic map of the Colville 1:100,000 quadrangle, Washington-Idaho; *Washington Division of Geology and Earth Resources*, Open File 90-13, 78 pages.

Kaufman, M.A. (1995): Stewart claim group, Nelson M.D. assessment report; *B.C. Ministry of Energy, Mines and Petroleum* Resources, Assessment report 24,123.

Kemp. R. (1992): Report on the drilling activities carried out on the Katie Group of claims, Nelson Mining Division, NTS 82F/3; *B.C. Ministry of Energy, Mines and Petroleum Resources*, Assessment report 22,200.

Kerrich, R. (1989): Geodynamic setting and hydraulic regimes: shear zone hosted mesothermal gold deposits; *in* Mineralization and Shear Zones, Bursnall, J.T., Editor, *Geological Association of Canada*, Short course notes, Volume 6, pages 89-128.

Kerrich, R. and Fyfe, W.S. (1981): The gold-carbonate association: source of CO_2, and CO_2 fixation reactions in Archean lode deposits; *Chemical Geology*, Volume 33, pages 265-294.

Kerrich, R. and Wyman, D. (1989): Geodynamic setting of mesothermal gold deposits: an association with accretionary tectonic regimes; *Geology*, volume 18, pages 882-885.

Keyser, H.J. and Smith, G. (1988): Report on the 1987 geochemical assessment work on the Santa Rosa property; *British Columbia Ministry of Energy, Mines and Petroleum Resources*, Assessment report 17,681, 17 pages.

Kirkham, R.V., Robert, F., Sinclair, W.D., Pilote, P, and Daigneault (1997): Chibougamau mining district, Quebec, Canada: vein Cu-Au and porphyry Cu (-Mo) deposits related to a composite Archean tonalitic batholith; *in* Mineral Deposits: Research and Exploration, Papunen, H., Editor, *A.A. Balkema*, Rotterdam, pages 647-649.

Klepachi, D.W. (1985): Stratigraphy and structural geology of the Goat Range area, southeastern British Columbia; unpublished Ph.D. thesis, *Massachusetts Institute of Technology*, 268 pages.

Klepachi, D.W and Wheeler, J.O. (1985): Stratigraphic and structural relations of the Milford, Kaslo and Slocan Groups, Lardeau and Nelson map areas, British Columbia; *in* Current Research, Part A, *Geological Survey of Canada*, Paper 85-1A, pages 277-286.

Kretschmar, U. and Scott, S.D. (1976): Phase relations involving arsenopyrite in the system Fe-As-S and their application; *Canadian Mineralogist*, Volume 14, pages 364-386.

Krogh, T.E. (1973): A low contamination method for hydrothermal decomposition of zircon and extraction of U and Pb for isotopic age determinations; *Geochimica et Cosmochimica Acta*, Volume 29, pages 485-494.

Lang, J.R., Lueck, B., Mortensen, J.K., Russel, J.K., Stanley, C.R., and Thompson, J.F.H. (1995a): Triassic-Jurassic silica-undersaturated and silica-saturated alkalic intrusions of the Canadian Cordillera of British Columbia: Implications for arc magmatism; *Geology*, Volume 23, pages 451-454.

Lang, J.R., Stanley, C. and Thompson, J.F.H. (1995b): Porphyry copper-gold deposits related to alkalic igneous rocks in the Triassic-Jurassic arc terranes of British Columbia; *in* Porphyry Copper Deposits of the American Cordillera; F.W. Pierce and J.C. Bone, Editors, *Arizona Geological Society*, Digest 20, pages 219-236.

LeClair, A.D. (1986): Geology, Midge Creek area (82F/10); *Geological Survey of Canada*, Open file 1352.

Lefebure, D.V. and Church, B.N. (1996): Polymetallic veins Ag-Pb-Zn±Au; *in* Selected British Columbia Mineral Deposit Profiles, Volume 2, Lefebure, D.V. and Höy, T., Edi-

tors, *B.C. Ministry of Employment and Investment*, Open file 1996-13, pages 67-70.

Lefebure, D.V. and Höy, T. (1996): Selected British Columbia mineral deposit profiles, Volume 2; *B.C. Ministry of Employment and Investment*, Open file 1996-13, 172 pages.

Lefebure, D.V. and Ray, G.E. (1995): Selected British Columbia mineral deposit profiles, Volume 1; *B.C. Ministry of Employment and Investment*, Open file 1995-20, 135 pages.

Lindsay, D.D. (1991): Geology, geochemistry and petrography of the Moochie Cu-Au occurrence, Nelson, British Columbia; unpublished B.Sc. thesis, *Carleton University*, 51 pages.

Little, H.W. (1950): Salmo map-area, British Columbia; *Geological Survey of Canada*, Paper 50-19, 43 pages.

Little, H.W. (1960): Nelson map-area, west-half, British Columbia; *Geological Survey of Canada*, Memoir 308, 205 pages.

Little, H.W. (1962): Trail map-area, British Columbia; *Geological Survey of Canada*, Paper 62-5.

Little, H.W. (1963): Rossland map-area, British Columbia; *Geological Survey of Canada*, Paper 63-13.

Little, H.W. (1964): Geology, Ymir map-area, British Columbia; *Geological Survey of Canada*, Map 1144A.

Little, H.W. (1965): Geology, Salmo map area, British Columbia; *Geological Survey of Canada*, Map 1145A.

Little, H.W. (1982a): Geology, Bonnington map area, British Columbia; *Geological Survey of Canada*, Map 1571A.

Little, H.W. (1982b): Geology, Rossland-Trail map-area, British Columbia; *Geological Survey of Canada*, Paper 79-26, 38 pages.

Little, H.W. (1985): Geological Notes, Nelson west-half (82F,W1/2) map-area; *Geological Survey of Canada*, Open File 1199.

Lorimer, M.K. (1967): Report on the Silver King mine, Nelson Mining Division, B.C.; unpublished internal report, *New Cronin Babine Mines Ltd.*, referenced in Aylward, 1983.

Lloyd, J. (1988): A geophysical report on a time domain induced polarization survey on the Toughnut property, *B.C. Ministry of Energy, Mines and Petroleum Resources*, Assessment report 18, 889.

MacIsaac, B. (1980): Soil geochemistry report, Jim Group, Nelson Mining Division, 082F/3W; *B.C. Ministry of Energy, Mines and Petroleum Resources*, Assessment report 8258.

McAllister, A.L. (1950): Geology of the Ymir map-area, British Columbia; unpublished Ph.D. thesis, *McGill University*, 160 pages.

McAllister, A.L. (1951): The Geology of the Ymir map-area, British Columbia; *Geological Survey of Canada*, Paper 51-4.

McIntyre, T.J. (1991): Report on the drilling activities carried out on the Katie Group of claims, Nelson Mining Division, NTS 82F/3; *B.C. Ministry of Energy, Mines and Petroleum Resources*, Assessment report 21,704.

McIntyre, T.J. and Bradish, L. (1990): Geological and geochemical survey on the Katie group of claims, Nelson Mining Division, NTS 82F/3; *B.C. Ministry of Energy, Mines and Petroleum Resources*, Assessment report 20331.

McMillan, W.J. and Panteleyev, A. (1995): Porphyry copper deposits of the Canadian Cordillera; *in* Porphyry Copper Deposits of the American Cordillera; F.W. Pierce and J.C. Bone, Editors, *Arizona Geological Society*, Digest 20, pages 203-218.

McMillan, W.J., Thompson, J.F.H., Hart, C.J.R. and Johnston, S.T. (1995): Regional geological and tectonic setting of porphyry deposits in British Columbia and Yukon Territory; *in* Porphyry Deposits of the Northwestern Cordillera of North America, Schroeter, T.G., Editor, *Canadian Institute of Mining, Metallurgy and Petroleum*, Special Volume 46, pages 40-57.

Manning, M.J. (1967): Report on geochemical and geological surveys conducted on the Fresno claim group of Copper Horne Mining Ltd., *B.C. Ministry of Energy and Mines*, Assessment report 1083.

Mathews, W.H. (1953): Geology of the Sheep Creek camp; *British Columbia Department of Mines*, Bulletin 31, 94 pages.

Middlemost, E.A.K. (1989): Iron oxidation ratios, norms and the classification of volcanic rocks; *Chemical Geology*, Volume 77, pages 19-26.

Monger, J.W.H. (1968): Early Tertiary stratified rocks, Greenwood map-area, British Columbia; *Geological Survey of Canada*, Paper 67-42.

Monger, J.W.H. and Berg, H.C. (1984): Lithotectonic terrane map of Western Canada and southeastern Alaska; *in* Lithotectonic Terrane Maps of the North America Cordillera, Silberling, N.J. and Jones, D.L., Editors, *United States Geological Survey*, Open file report 84-523.

Monger, J.W.H., Wheeler, J.O., Tipper, H.W., Gabrielse, H., Harms, T., Struik, L.C. Campbell, R.B., Dodds, C.J., Gehrels, G.E. and O'Brien, J. (1991): Part B. Cordilleran terranes; *in* Upper Devonian to Middle Jurassic assemblages, Chapter 8 of Geology of the Cordilleran Orogen in Canada, Gabrielse, H. and Yorath, C.J., Editors, *Geological Survey of Canada*, No. 4, pages 281-327.

Mortimer, N. (1986): Late Triassic arc-related, potassic igneous rocks in the North America Cordillera; *Geology*, Volume 14, pages 1035-1078.

Mulligan, R. (1951): The Geology of the Nelson (Bonnington) and adjoining part of Salmo map areas, British Columbia; unpublished Ph.D. thesis, *McGill University*, 202 pages.

Mulligan, R. (1952): Bonnington map area, British Columbia; *Geological Survey of Canada*, Paper 52-13, 37 pages.

Murphy, C.M., Gerasimoff, M., Van der Heyden, P., Parrish, R.R., Klepachi, D.W., McMillan, W.J., Struik, L.C. and Gabites, J. (1994): New geochronological constraints on Jurassic deformation on the western edge of North America, southern Canadian Cordillera; *in* Jurassic Magmatism and Tectonics of the North American Cordillera, Miller, D.M. and Anderson, R.G., Editors, *Geological Society of America*, Special Paper 299, pages 159-171.

Murray, K. (1987): Soil geochemistry of the Katie group area, Salmo, B.C.; NTS 82F/3SW; *B.C. Ministry of Energy, Mines and Petroleum Resources*, Assessment report 15781.

Nesbitt, B.E. and Muehlenbachs, K. (1989): Geology, geochemistry, and genesis of mesothermal lode gold deposits of the Canadian Cordillera: evidence for ore formation from evolved meteoric water; *Economic Geology*, Monograph 6, pages 535-563.

Newberry, R.J. (1998): W- and Sn-skarn deposits - a 1998 status report; *in* Lentz, D.R., Editor, Mineralized Intrusion-related Skarn Systems; *Mineralogical Association of Canada*, Short Course Series, volume 26, pages 289-336.

Newberry, R.J., McCoy, D.T., and Brew, D.A. (1995): Plutonic-hosted gold deposits in Alaska: igneous versus metamorphic origin; *in* Ishihara, S., and Czamanske, G.K.,

Editors, Proceedings of the Sapporo International Conference on Mineral Resources in the NW Pacific Rim, *Resource Geology*, Special Issue, 18, pages 57-100.

Ostensoe, E.A. (1989): Report of work, Second Relief, Erie, B.C., 82F/SW; *B.C. Ministry of Energy and Mines*, Assessment report 19,839, 30 pages.

Panteleyev, A. (1992): Gold in the Canadian Cordillera - a focus on epithermal and deeper environments, *in* Ore Deposits, Tectonics and Metallogeny in the Canadian Cordillera, Grant, B. and Newell, J.M., Editors, *B.C. Ministry of Energy, Mines and Petroleum Resources*, Paper 1991-4, pages 163-212.

Panteleyev, A. (1995): Porphyry Cu-Au: alkalic; *in* Selected British Columbia Mineral Deposit Profiles, Volume I; Lefebure, D. and Ray, G.E., Editors, *B.C. Ministry of Energy, Mines and Petroleum Resources*, Open file 1995-20, pages 83-86.

Parrish, R.R. (1984): Slocan Lake fault: a low angle fault zone bounding the Valhalla gneiss complex, Nelson map-area, southern British Columbia; *in* Current Research, Part A, *Geological Survey of Canada*, Paper 84-1A, pages 323-330.

Parrish, R.R. (1992): U-Pb ages of Jurassic-Eocene plutonic rocks in the vicinity of the Valhalla complex, southeast British Columbia; *in* Radiogenic Age and Isotope Studies: Report 5, *Geological Survey of Canada*, Paper 91-2, pages 115-134.

Parrish, R.R. (1995): Thermal evolution of the southeastern Canadian Cordillera; *Canadian Journal of Earth Sciences*, Volume 32, pages 1618-1642.

Parrish, R.R., Carr, S.D. and Parkinson, D.L. (1988): Eocene extensional tectonics and geochronology of the southern Omineca belt, British Columbia and Washington; *Tectonics*, Volume 7, pages 181-212.

Parrish, R.R. and Wheeler, J.O. (1983): A U-Pb zircon age from the Kuskanax batholith, southeastern British Columbia; *Canadian Journal of Earth Sciences*, Volume 20, pages 1751-1756.

Peters, J.M. (1937): Engineer's report, Velvet Portland mine, Rossland Mining District, British Columbia, Canada; *British Columbia Ministry of Energy, Mines and Petroleum Resources*, Property file (82FSW162), 9 pages.

Potter, P.J. (1999) Metallogenesis of Fe oxide-Cu-Au deposits, Part F; *in* Short Course on Fe Oxide-copper-gold Deposits, *Economic Geology Research Unit, James Cook University and MDRU*, Short course, pages F1-F21.

Powell, W.G. and Ghent, E.D. (1966): Low-pressure metamorphism of the mafic volcanic rocks of the Rossland Group, southeastern British Columbia; *Canadian Journal of Earth Sciences*, Volume 33, pages 1402-1409.

Preto, V.A. (1977): The Nicola Group: Mesozoic volcanism related to rifting in southern British Columbia; *in* Volcanic Regimes in Canada, Barager, W.R.A., Coleman, L.C. and Hall, J.M., Editors, *Geological Association of Canada*, Special Paper 16, pages 39-57.

Preto, V.A. (1979): Geology of the Nicola Group between Merritt and Princeton; *B.C. Ministry of Energy, Mines and Petroleum Resources*, Bulletin 69.

Price, R.A. (1981): The Cordilleran foreland thrust and fold belt in the southern Canadian Rocky Mountains; *in* Thrust and Nappe Tectonics; McClay, K.R. and Price, N.J., *Editors*; *Geological Society of London*, Special Publication number 9.

Price, R.A. (1986): The southeastern Canadian Cordillera: thrust faulting, tectonic wedging, and delamination of the lithosphere; *Journal of Structural Geology*, Volume 8, pages 239-254.

Ray, G.E. and Dawson, G.L. (1994): The geology and mineral deposits of the Hedley gold skarn district, southern British Columbia; *B.C. Ministry of Energy, Mines and Petroleum Resources*, Bulletin 87, 156 pages.

Ray, G.E. and Dawson, K.M. (1998): Mineralized skarns in the Canadian Cordillera; *in* Mineral Intrusion-related Skarn Systems, Lentz, D.R., Editor, *Mineral Association of Canada*, Short course volume 26, pages 475-518.

Ray, G.E., Dawson, G.L., and Simpson, R. (1987): The geology and controls of skarn mineralization in the Hedley camp, southern British Columbia; *B.C. Ministry of Energy, Mines and Petroleum Resources*, Geological Fieldwork 1986, pages 65-79.

Ray, G.E. and Spence, A. (1986): The Potassium-rich volcanic rocks at Tillicum Mountain - their geochemistry, origin, and regional significance; *British Columbia Ministry of Energy, Mines and Petroleum Resources*, Geological Fieldwork 1985, Paper 1986-1, pages 45-49.

Ray, G.E. and Webster, I.C.L. (1997): Skarns in British Columbia; *B.C. Ministry of Employment and Investment*, Bulletin 101, 260 pages.

Ray, G.E., Webster, I.C.L., Ballantyne, S.B., Kilby, C.E. and Cornelius, S.B. (2000): The geochemistry of three tin-bearing skarns and their related plutonic rocks, Atlin, northern British Columbia; *Economic Geology*, Volume 95, page 1349-1365.

Read, W.S. (1969): Geological, geochemical, geophysical report, Rand Group, Erie Creek, Nelson Mining Division; *B.C. Ministry of Mines and Energy*, Assessment Report 2146, 25 pages.

Reesor, J.E. and LeClair, A.E. (1983): Nelson East-Half Map Area; *Geological Survey of Canada*, Open File 929.

Reynolds, T.J., (1991): Short course on fluid inclusions, *Mineral Deposit Research Unit, The University of British Columbia*, Short course 6 notes.

Richardson, P.W. (1982): Diamond drilling report on the Novelty claim, Rossland property; *B.C. Ministry of Energy, Mines and Petroleum Resources*, Assessment report 9942.

Roback, R.C. (1993): Late Paleozoic to Middle Mesozoic tectonic evolution of the Kootenay arc; unpublished Ph.D. thesis, *University of Austin at Texas*, 192 pages.

Roback, R.C., Sevigny, J.H. and Walker, N.W. (1994): Tectonic setting of the Slide Mountain terrane, southern British Columbia; *Tectonics*, Volume 13, pages 1242-1258.

Roback, R.C., Schiarizza, P., Nelson, J., Fyles, J., Ferri, F., Höy, T., Ash, C. and Danner, W.R. (1995): Late Paleozoic arc and oceanic terranes and their external relationships, southern Quesnellia; *in* Field Trip Guidebook B2, *Geological Association of Canada*, Victoria, B.C., 79 pages.

Roback, R.C. and Walker, N.W. (1995): Provenance, detrital zircon U-Pb geochronometry, and tectonic significance of Permian to Lower Triassic sandstone in southeastern Quesnellia, British Columbia and Washington; *Geological Society of America*, Bulletin, Volume 107, pages 665-675.

Roberts, R.G. (1987): Ore deposits model # 1; Archean lode gold deposits; *Geoscience Canada*, Volume 14, pages 37-52.

Roedder E. (1984): Fluid inclusions; *Mineralogical Society of America*, Reviews in Mineralogy, Volume 12, *Bookcrafters Inc.*, Chelsea, Michigan, 644 pages.

Ronning, P.A. (1990): Great Western Star project, diamond drilling, Nelson Mining division, British Columbia; *B.C. Ministry of Energy, Mines and Petroleum Resources*, Assessment report 20,063.

Rowins, S.M. (2000) Reduced porphyry copper-gold deposits: a new variation on an old theme; *Geology*, Volume 28, pages 491-494.

Sangster, D.F. (1970): Metallogenesis of some Canadian lead-zinc deposits in carbonate rocks, *Geological Association of Canada*, Proceedings, Volume 22, pages 27-36.

Schroeter, T.G. and Lane, R.A. (1991): A century of gold production in British Columbia (1890-1990); *B.C. Ministry of Energy, Mines and Petroleum Resources*, Open File 1991-19. 42 pages.

Selby, D. and Creaser, R.A. (2001): Re-Os geochronology and systematics in molybdenite from the Endako porphyry molybdenum deposit, British Columbia, Canada; Economic Geology, Volume 96, pages 197-204.

Sevigny, J.H. and Parrish, R.R. (1993): Age and origin of late Jurassic and Paleocene granitoids, Nelson batholith, southern British Columbia; *Canadian Journal of Earth Sciences*, Volume 30, pages 2305-2314.

Seraphin, R.H., Church, B.N. and Shearer, J.T. (1995): The Lexington-Lone Star copper-gold porphyry: an Early Jurassic cratonic linear system, southern British Columbia; *in* Porphyry Deposits of the Northwestern Cordillera of North America, Schroeter, T.G., Editor, *Canadian Institute of Mining and Metallurgy*, Special volume 46, pages 851-854.

Seywerd, M. (1988): Geophysical report on a magnetometer, VLF-EM and IP survey on the Shaft project, Nelson Mining District; *B.C. Ministry of Energy, Mines and Petroleum Resources*, Assessment report 14472.

Sharp, Z.D., Essene, E.J. and Kelly, W.C. (1985): A re-examination of the arsenopyrite geothermometer: pressure considerations and applications to natural assemblages; *The Canadian Mineralogist*, Volume 23, pages 5-7-534.

Simony, P.S. (1979): Pre-Carboniferous basement near Trail, British Columbia; *Canadian Journal of Earth Sciences*, Volume 16, pages 1-11.

Smith, A.D., Brandon, A.D. and Lambert, R.St.J. (1995): Nd-Sr isotope systematics of Nicola Group volcanic rocks, Quesnel terrane; *Canadian Journal of Earth Sciences*, Volume 32, pages 437-446.

Smith, M.J. (1974): Geology of the Harper Ranch Group (Carboniferous-Permian) and Nicola Group (Upper Triassic), northwest of Kamloops, British Columbia; unpublished M.Sc. thesis, *The University of British Columbia*, Vancouver, 211 pages.

Smith, M.T. and Gehrels, G.E. (1992): Structural geology of the Lardeau Group near Trout Lake, British Columbia: implications for the structural evolution of the Kootenay arc; *Canadian Journal of Earth Sciences*, Volume 29, pages 1305-1319.

Smith, A.D., Brandon, A.D. and Lambert, R. St. J. (1995): Nd-Sr isotopic systematics of the Nicola Group volcanic rocks, Quesnel terrane; *Canadian Journal of Earth Sciences*, Volume 32, pages 437-446.

Smithson, T. (1995): Final geological and drilling report on the Midnight claim group, Rossland, B.C.; *B.C. Ministry of Energy and Mines*, Assessment report 23 857.

Smithson, T. (1996): Geological and drilling report on the Midnight and IXL claim group; *B.C. Ministry of Energy and Mines*, Assessment report 25 007.

Sookochoff, L. (1984): 1984 Assessment report, diamond drilling, Grand Union; *B.C. Ministry of Energy, Mines and Petroleum Resources*, Assessment report 13,039.

Steiger, R.H. and Jager, E. (1977): Subcomission on geochronology: convention on the use of Decay constants in geo- and cosmo-chronology; *Earth and Planetary Science Letters*, Volume 36, pages 359-362.

Stein, H.J., Markey, R.J., Morgan, J.W., Du, A. and Sun, Y. (1997): Highly precise and accurate Re-Os ages for molybdenite from the Qinling molybdenum belt, Shaanxi Province, China; *Economic Geology*, Volume 92, pages 827-835.

Stevenson, J.S. (1936): Rossland camp; *B.C. Ministry of Mines*, Annual report of the Minister of Mines, 1935, pp. E4-E10.

Stevenson, J.S. (1943): Tungsten deposits of British Columbia; *B.C. Department of Mines*, Bulletin 10 (revised).

Stinson, P. (1995): Emplacement of the Coryell batholith; unpublished M.Sc. thesis; *The University of Calgary*, 151 pages.

Stinson, P. and Patterson, D.R.M. (1993): Petrology of the Evening Star claim, Rossland, B.C.; *B.C. Ministry of Energy, Mines and Petroleum Resources*, Geological Fieldwork 1992, Paper 1993-1, pages 249-254.

Stoffel, K.L. (1990): Geological map of the Republic 1:100,000 quadrangle, Washington; *Washington Division of Geology and Earth Resources*, Open file report 90-10, 62 pages.

Streckeisen, A. (1976): To each plutonic rock its proper name; *Earth Science Reviews*, Volume 12, pages 1-33.

Taylor, A.P. (1978): Geological report on the John claims for Warrior Resources and adjacent areas 3 miles south of Nelson, Nelson M.D., B.C.; *B.C. Ministry of Energy, Mines and Petroleum Resources*, Assessment report 7377.

Thompson, J.F.H., Sillitoe, R.H., Baker, T., Lang, J.R. and Mortensen, J.K. (1999): Intrusion-related gold deposits associated with tungsten-tin provinces, *Mineralium Deposita*, Volume 32, pages323-334.

Thomson, G.R. (1995): Diamond drilling report on the Kenville mine property; *B.C. Ministry of Energy, Mines and Petroleum Resources*, Assessment report 23,859.

Thorpe, R.I. (1967): Mineralogy and zoning of the Rossland area; unpublished Ph.D. thesis, *University of Wisconsin*.

Thorpe, R.I. and Little, H.W. (1973): Discussion, the age of sulphide mineralization at Rossland; *Economic Geology*, Volume 68, pages 1337-1346.

Tipper, H.W. (1984): The age of the Jurassic Rossland Group of southeastern British Columbia; *in* Current Research, Part A, *Geological Survey of Canada*, Paper 84-1A, pages 631-632.

Troup, A.G., Freeze, J.C. and Butterworth, B.P. (1984): Geological and geophysical report on the Georgia property, Trail Creek Mining Division, British Columbia; *B.C. Ministry of Energy, Mines and Petroleum Resources*, Assessment report 14,236.

Turner, G.W. (1980): Assessment report, Stewart claims, Nelson Mining Division; *B.C. Ministry of Energy and Mines*, Assessment Report 7722.

Turner, J. S. and Campbell, I.H. (1984): Convections and mixing in magma chambers; *Earth Science Review*, Volume 23, pages 255-352.

Turner, R.J.W. and Rhodes, D. (1990): Boundary Creek zinc deposit (NIDD property), MacMillan Pass, Yukon: sub-seafloor sediment-hosted mineralization associated with volcanism along a late Devonian syndepositional fault; *in* Current Research, Part E *Geological Survey of Canada*, Paper 90-1E, pages 321-336.

Vogl, J.J. and Simony, P.S. (1992): The southern tail of the Nelson batholith, southeast British Columbia: structure and emplacement; *in* Current Research, Part A; *Geological Survey of Canada*, Paper 92-1A, pages 71-76.

Walker, J.F. (1934): Geology and mineral deposits of the Salmo map-area, British Columbia; *Geological Survey of Canada*, Memoir 172, 102 pages.

Webster, I.C.L., Ray, G.E. and Pettipas, A.R. (1992): Selected mineralized skarns in British Columbia; *in* Geological Fieldwork 1991, Newell, J.M. and Grant, B., Editors, *B.C. Ministry of Energy, Mines and Petroleum Resources*, Paper 1992-1, pages 235-252.

Wheeler, J.O. and McFeely, P. (1991): Tectonic assemblage map of the Canadian Cordillera and adjacent parts of the United States; *Geological Survey of Canada*, Map 1712A, Scale 1:2,000,000.

Wehrle, D. (1995): Final technical report, Evening Star/Gertrude-Georgia project, Explore B.C. Program-94-95/M-186; B.C. *Ministry of Energy, Mines and Petroleum Resources*, Assessment report 25,363.

White, W.H. (1949): Rossland South belt; *B.C. Minister of Mines*, B.C. Annual report 1949, pages 150-163.

White, G.B. and Cruz, E.D. (1973): Geophysical, geochemical report, Sproat River Mines Ltd., Silver King mine property, Nelson area, B.C.; *B.C. Ministry of Energy, Mines and Petroleum Resources*, Assessment report 4701.

Williams, P. (1999) The Cloncurry Cu-Au System, Part G; *in* Short Course on Fe Oxide-copper-gold Deposits, *Economic Geology Research Unit, James Cook University and MDRU*, Short course, pages G1-G82.

Wingate, M.T.D. (1993): Extension in high-grade terranes of the southern Omineca Belt: evidence from paleomagnetism; unpublished M.Sc. thesis, *University of Victoria*, 128 Pages.

Wingate, M.T.D. and Irving, E. (1994): Extension in high-grade terranes of the southern Omineca Belt, British Columbia: evidence from paleomagnetism, *Tectonics*, Volume 13, pages 687-711.

Wiswall, G. (1981): Report on the Silver King mines, 1981; unpublished report, *Hecate Gold Corporation*.

Wong, R.H. and Spence, C.D. (1995): Copper-gold mineralization in the Willa breccia pipe, southeastern British Columbia; *in* Porphyry Deposits of the Northwestern Cordillera of North America, Schroeter, T.G., Editor, *Canadian Institute of Mining, Metallurgy and Petroleum*, Special volume 46, pages 401-409.

Yorke-Hardy, R.W., Fowler, F.G. and Boniwell, J.B. (1988): Technical report on preliminary exploration on the Bluebird-Homestake claim group, Trail Mining Division, B.C.; *B.C. Ministry of Energy, Mines and Petroleum Resources*, Assessment report 16751.

APPENDICES

APPENDIX 1
MINERAL OCCURRENCES OF THE ROSSLAND-TRAIL MAP AREA
(FROM B.C. MINFILE)

MINFILE NO.	NAME	STATUS	CODE	COMMENT (host)	COMMODITIES						TERRANE
	Carbonate Hosted										
082FSW018	Lomond	Past Producer	E12	Nelway	Fe	Pb	Zn	Ag			North America
082FSW060	Caviar	Showing	E12	Nelway	Zn						North America
082FSW004	HB (L.12672)	Past Producer	E13	Reeves	Pb	Zn	Ag	Cd	Cu	Au	North America
082FSW005	Lucky Boy	Showing	E13	Reeves	Zn	Pb					North America
082FSW006	Black Rock North	Showing	E13	Reeves	Zn	Pb	Cu	Ge	Ga		North America
082FSW007	Black Rock South	Showing	E13	Reeves	Zn	Pb					North America
082FSW009	Jersey	Past Producer	E13	Reeves	Pb	Zn	Ag	Cd	W	Mo	North America
082FSW012	Jackpot Main	Developed Prospect	E13	Reeves	Pb	Zn	Cd	W			North America
082FSW013	Jackpot East	Developed Prospect	E13	Reeves	Zn	Pb	W				North America
082FSW014	Hunter	Past Producer	E13	Reeves	Ag	Au	LS	Zn	Pb		North America
082FSW015	Double Standard	Past Producer	E13	Reeves	Ag	Au	LS	Zn	Pb		North America
082FSW017	Last Chance	Showing	E13	Active	Pb	Zn					Kootenay
082FSW022	Oxide	Showing	E13	Reeves	Zn	Pb	Ag	Au	Mn		North America
082FSW024	Red Bird (L.13465)	Developed Prospect	E13	Reeves	Zn	Pb	Ag	Cd			North America
082FSW026	Reeves MacDonald	Past Producer	E13	Reeves	Zn	Pb	Ag	Cd	Cu	Ga	North America
082FSW027	Point	Prospect	E13	Reeves	Zn	Pb					North America
082FSW028	O'Donnell	Past Producer	E13	Reeves	Zn	Pb	Ag	Cd	Cu	Ga	North America
082FSW029	Prospect	Developed Prospect	E13	Reeves	Zn	Pb					North America
082FSW031	Shanango	Showing	E13	Reeves	Pb	Zn	Ag				North America
082FSW034	Tungsten King 2	Showing	E13	Reeves	Zn	Pb	Ag				North America
082FSW219	Annex (L.14070)	Past Producer	E13	Reeves	Ag	Pb	Zn	Cd	Cu		North America
082FSW244	Mayflower (L.9189)	Showing	E13	Reeves	Zn						North America
082FSW255	Jackpost West	Developed Prospect	E13	Reeves	Zn	Pb					North America
082FSW256	Jackpot Lenwick	Developed Prospect	E13	Reeves	Zn	Pb					North America
082FSW310	Emerald	Past Producer	E13	Reeves	Pb	Ag	Zn	Mo			North America
082FSW322	Tungsten King 2	Showing	E13	Reeves	Ag	Pb	Zn				North America
082FSW249	Garnet (L.10809)	Past Producer	E13	Elise	Zn	Pb					Kootenay
082FSW001	Aspen (L.12471)	Past Producer	J01	Reeves	Ag	Au	Pb	Zn			North America
082FSW025	Red Rock	Past Producer	J01	Reeves	Pb	Zn	Ag				North America
082FSW033	Truman	Prospect	J01	Reeves	Pb	Zn	Ag				North America
082FSW305	Aspen Showing	Showing	J01	Reeves	Pb	Zn	Ag	Au			North America
082FSW231	Silver 5	Showing	J01	Elise	Ag	Pb	Zn	Cu			Quesnel
082FSW003	Ed	Past Producer	J01	Nelway	Pb	Zn	Ag				North America
082FSW008	Iron Cap	Prospect	J01	Active	Pb	Zn	Ag	Au			Kootenay
	Volcanogenic Massive Sulphide (Besshi?)										
082FSW230	Silver 1	Showing	G03	Elise	Ag	Pb	Zn	Cu			Quesnel
082FSW235	Hungary Man	Showing	G03	Elise	Au	Cu					Quesnel
	Au-quartz Veins										
082FSW035	Donnybrook	Past Producer	I01	Reno	Au	Pb	Zn	Cu			North America
082FSW036	Reno (L.12684)	Past Producer	I01	Reno	Au	Pb	Zn	Ag	Cu	Hg	North America
082FSW037	Bluestone (L.9054)	Past Producer	I01	Reno	Au	Ag					North America
082FSW038	Cayote (L.8343)	Past Producer	I01	Reno	Au	Ag					North America
082FSW039	Fawn	Past Producer	I01	Quartzite Range	Au						North America
082FSW040	Nugget (L.8341)	Past Producer	I01	Quartzite Range	Au	Ag	Pb	Zn	Si	Cu	North America
082FSW041	Motherlode (L.8818)	Past Producer	I01	Reno	Au	Ag	Pb	Zn	Cu		North America
082FSW042	Golden West	Developed Prospect	I01	Reno	Au						North America
082FSW043	Golden Belle (L.9917)	Past Producer	I01	Reno	Au						North America
082FSW044	Gold Belt	Past Producer	I01	Reno	Au	Ag	Pb	Zn	Cu		North America
082FSW045	Navada (L.8869)	Past Producer	I01	Reno	Au	Ag	Pb	Zn			North America
082FSW046	Kootenay Belle	Past Producer	I01	Reno	Au	Ag	Pb	Zn	W		North America

APPENDIX 1 CONTINUED

MINFILE NO.	NAME	STATUS	CODE	COMMENT (host)	COMMODITIES						TERRANE
082FSW047	Eureka	Showing	I01	Quartzite Range	Au						North America
082FSW048	Queen (L.1076)	Past Producer	I01	Quartzite Range	Au	Ag	Pb	Zn			North America
082FSW049	Vancouver	Past Producer	I01	Quartzite Range	Au	Ag					North America
082FSW050	Midnight (L.13476)	Past Producer	I01	Quartzite Range	Au	Ag					North America
082FSW052	Yellowstone	Past Producer	I01	Reno	Au	Ag	Pb	Zn			North America
082FSW055	Bonanza (L.10161)	Past Producer	I01	Reno	Au	Ag	Pb				North America
082FSW056	Clyde (L.8873)	Prospect	I01	Reno	Au						North America
082FSW064	Nevada (L.3504)	Developed Prospect	I01	Ymir Group	Au	Ag	Pb	Zn			Quesnel
082FSW072	Tamarac (L.3802)	Past Producer	I01	Nelson/Elise	Au	Ag					plutonic
082FSW078	Fog Horn (L.5204)	Showing	I01	Nelson	Au	Pb					plutonic
082FSW079	Gold Cup	Past Producer	I01	Nelson/Elise	Au	Ag	Cu				plutonic
082FSW086	Kenville	Past Producer	I01	Eagle Creek "pseudodiorite"	Ag	Au	Pb	Zn	Cu	Cd	Quesnel
082FSW087	Venango (L.4757)	Past Producer	I01	Eagle Creek "pseudodiorite"	Au	Ag	Pb	Zn	W		Quesnel
082FSW088	Royal Canadian (L.633)	Past Producer	I01	Eagle Creek "pseudodiorite"	Au	Ag	Zn	Pb	W		Quesnel
082FSW090	Miracle	Developed Prospect	I01	Elise	Au	Ag					Quesnel
082FSW091	May & Jennie (L.3943)	Past Producer	I01	Eagle Creek "pseudodiorite"	Au	Ag					Quesnel
082FSW092	Gold Hill	Past Producer	I01	Elise	Au	Ag	Cu				Quesnel
082FSW115	Snowdrop	Developed Prospect	I01	Elise/ultramafics	Au	Ag	Cu	Pb			Quesnel
082FSW116	I.X.L.	Past Producer	I01	Elise/ultramafics	Au	Ag	Cu	Pb	Zn	Ni	Quesnel
082FSW117	O.K.	Past Producer	I01	Elise/ultramafics	Au	Ag	Cu	Pb	AB		Quesnel
082FSW118	Golden Drip (L.539)	Past Producer	I01	Elise/ultramafics	Au	Ag	Pb	Zn	Cu	AB	Quesnel
082FSW119	Midnight (L.1186)	Past Producer	I01	Elise/ultramafics	Au	Ag	Pb	Zn	Cu	Ni	Quesnel
082FSW120	Norway (L.1628)	Developed Prospect	I01	Nelson	Ag	Au					plutonic
082FSW168	Athabasca	Past Producer	I01	Elise/Nelson	Au	Ag	Pb	Zn	Cu	W	Quesnel
082FSW188	Harriet	Past Producer	I01	Elise	Au	Ag					Quesnel
082FSW196	Pilot-Good Hope	Developed Prospect	I01	Nelson	Au	Ag	Pb	Zn			plutonic
082FSW201	Second Chance	Past Producer	I01	Hall	Au	Ag					Quesnel
082FSW248	Paradise (L.728)	Showing	I01	Eagle Creek "pseudodiorite"	Au	Ag	Cu				Quesnel
082FSW258	Gold 1-2	Prospect	I01	Sheppard/Coryel	Au	Ag	Pb				Kootenay
082FSW260	Heather	Showing	I01	Quartzite Range	Au						North America
082FSW276	North Star	Showing	I01	Elise	Au						Quesnel
082FSW324	Tec Gold	Showing	I01	Elise	Au	Cu					Quesnel
082FSW354	Oro Fino (L.2011)	Showing	I01	Elise	Au	Ag	Cu				Quesnel
	Intrusion-related Au-sulphide Veins										
082FSW093	Le Roi	Past Producer	I02	Rossland monzonite	Au	Ag	Cu				Quesnel
082FSW094	Centre Star (L.588)	Past Producer	I02	Rossland monzonite	Au	Ag	Cu	Mo			Quesnel
082FSW095	Nickel Plate (L.537)	Past Producer	I02	Rossland monzonite	Au	Ag	Cu				Quesnel
082FSW096	Iron Mask (L.688)	Past Producer	I02	Rossland monzonite	Au	Cu	Ag				Quesnel
082FSW097	War Eagle (L.680)	Past Producer	I02	Rossland monzonite	Au	Ag	Cu				Quesnel
082FSW098	Virginia (L.681)	Past Producer	I02	Rossland monzonite	Au	Ag	Cu				Quesnel

APPENDIX 1 CONTINUED

MINFILE NO.	NAME	STATUS	CODE	COMMENT (host)	COMMODITIES						TERRANE
082FSW099	Iron Horse (L.795)	Past Producer	I02	Rossland monzonite	Au	Cu					Quesnel
082FSW100	Iron Colt (L.796)	Producer	I02	Elise	Au	Ag	Cu	Co			Quesnel
082FSW101	Monte Cristo (L.802)	Developed Prospect	I02	Rossland monzonite	Au	Cu	Ag	Ni	Co		Quesnel
082FSW102	Evening Star	Producer	I02	Elise	Au	Ag	Cu	Ni	Co	Mo	Quesnel
082FSW103	City of Spokane (L.804)	Showing	I02	Rossland monzonite	Au	Cu					Quesnel
082FSW104	Red Mountain (L.1000)	Showing	I02	Rossland sill	Au	Cu					Quesnel
082FSW105	Black Bear (L.538)	Past Producer	I02	Rossland sill	Au	Cu	Ag				Quesnel
082FSW108	Gertrude (L.690)	Showing	I02	Elise	Mo	Au	Cu	Zn	Bi		Quesnel
082FSW111	Jumbo (L.965)	Past Producer	I02	Elise	Au	Ag	Mo	Cu	Bi		Quesnel
082FSW113	California (L.956)	Past Producer	I02	Elise	Au	Cu	Ag	Zn			Quesnel
082FSW114	White Bear (L.1149)	Past Producer	I02	Rossland sill	Au	Cu	Ag				Quesnel
082FSW121	Spitzee (L.2520)	Past Producer	I02	Rossland monzonite	Au	Ag	Cu	W			Quesnel
082FSW122	Deer Park (L.932)	Past Producer	I02	Elise	Au	Cu	Ag	Mo	Fe	W	Quesnel
082FSW126	Tuesday (L.1278)	Showing	I02	Rossland monzonite	Cu	Au	Ag				Quesnel
082FSW128	North	Prospect	I02	Elise	Au	Ag	Cu	Zn			Quesnel
082FSW129	Mabel (L.1202)	Past Producer	I02	Rossland monzonite	Au	Ag	Cu				Quesnel
082FSW131	Robert E. Lee	Past Producer	I02	Elise	Au	Ag	Cu	Zn	Bi	Pb	Quesnel
082FSW132	Phoenix (L.953)	Past Producer	I02	Rossland monzonite	Au	Ag	Cu				Quesnel
082FSW133	Abe Lincoln (L.1296)	Showing	I02	Rossland monzonite	Au	Cu					Quesnel
082FSW135	Consolidated St. Elmo	Past Producer	I02	Rossland sill	Au	Cu	Ag	Pb	W		Quesnel
082FSW136	Cliff (L.921)	Past Producer	I02	Rossland sill	Au	Cu	Ag	W	Bi		Quesnel
082FSW137	Southern Belle	Showing	I02	Rossland monzonite	Au						Quesnel
082FSW138	Golden Chariot	Showing	I02	Rossland monzonite	Au	Cu					Quesnel
082FSW142	Hattie (L.1054)	Past Producer	I02	Elise	Au	Ag	Cu	Bi			Quesnel
082FSW147	Josie (L.536)	Past Producer	I02	Rossland monzonite	Au	Ag	Cu				Quesnel
082FSW148	Annie (L.730)	Past Producer	I02	Rossland monzonite	Au	Ag	Cu				Quesnel
082FSW149	Georgia (L.928)	Past Producer	I02	Elise	Au	Ag	Cu				Quesnel
082FSW151	Columbia-Kootenay	Past Producer	I02	Elise	Au	Cu	Ni	Bi			Quesnel
082FSW152	Crown Point	Past Producer	I02	Elise	Au	Cu	Ag				Quesnel
082FSW162	Velvet (L.2521)	Past Producer	I02	serpentinite, Coryell, Elise	Cu	Au	Ag	Pb	Zn	Mo	Quesnel
082FSW165	Nest Egg (L.1048)	Prospect	I02	Rossland monzonite	Au	Cu	Ag				Quesnel
082FSW195	Mascot (L.1344)	Showing	I02	Elise	Cu						Quesnel
082FSW208	Commander (L.960)	Showing	I02	Rossland monzonite	Au	Cu	W				Quesnel
082FSW246	View (L.645)	Showing	I02	Elise	Cu						Quesnel
082FSW286	Silverine (L.732)	Past Producer	I02	Elise	Au	Ag	Cu	Bi			Quesnel

APPENDIX 1 CONTINUED

MINFILE NO.	NAME	STATUS	CODE	COMMENT (host)	COMMODITIES						TERRANE
082FSW356	Debbie	Showing	I02	Elise/Nelson?	Au	Cu	Ag				Quesnel
082FSW361	Cam 2	Showing	I02	Rossland monzonite	Au	Ag	Cu				Quesnel
082FSW363	Sternwinder	Showing	I02	Elise/Nelson	Au	Cu					Quesnel
	Polymetallic Veins Ag-Pb-Zn±Au										
082FSW019	Lone Silver	Past Producer	I05	Nelway	Ag	Au	Pb	Zn	Cu		North America
082FSW020	Meadow View	Showing	I05	Laib	Ag	Au	Cu	Mo			Kootenay
082FSW030	Salmo-Consoldiated	Prospect	I05	Nelson / Active	Au	Pb	Zn	Ag			Kootenay
082FSW051	Alexander	Past Producer	I05	Quartzite Range	Pb						North America
082FSW053	Ore Hill (L.2073)	Past Producer	I05	Laib	Au	Ag	Pb	Zn			Kootenay
082FSW054	Summit (L.10010)	Past Producer	I05	Laib	Au	Ag	Pb	Zn			Kootenay
082FSW061	United Verde	Developed Prospect	I05	Active	Ag	Pb	Zn	Au			Kootenay
082FSW062	Lucky Strike	Past Producer	I05	Nelway / Laib	Au	Ag	Pb	Zn	Cu		North America
082FSW063	Porcupine (L.4634)	Past Producer	I05	Index?	Au	Ag	Pb	Zn	Sn	Cu	Kootenay
082FSW065	Blue Nellie (L.2936)	Showing	I05	Ymir / Nelson	Pb	Zn					Quesnel
082FSW066	Center Star	Past Producer	I05	Ymir / Nelson	Au	Ag	Pb	Zn			Quesnel
082FSW067	Dundee	Past Producer	I05	Ymir / Nelson	Au	Ag	Pb	Zn			Quesnel
082FSW068	Yankee Girl	Past Producer	I05	Ymir / Nelson	Au	Ag	Pb	Zn	Cd		Quesnel
082FSW069	Two Star	Prospect	I05	Ymir / Nelson	Au	Ag	Pb	Zn			Quesnel
082FSW070	May Blossom (L.5666)	Showing	I05	Elise / Tertiary intrusion	Ag	Pb	Zn	Au	Mo	W	Quesnel
082FSW071	Ronoke (L.3402)	Showing	I05	Nelson	Au	Pb	Cu				plutonic
082FSW073	Protection	Past Producer	I05	Ymir / Nelson	Au	Ag	Pb	Zn	Cd	Cu	Quesnel
082FSW074	Ymir (L.1708)	Past Producer	I05	Ymir / Nelson	Au	Ag	Pb	Zn			Quesnel
082FSW075	Ymir-Good Hope	Past Producer	I05	Ymir / Nelson	Au	Ag	Zn	Pb	Cu	Cd	Quesnel
082FSW076	Blackcock (L.2922)	Past Producer	I05	Nelson / Ymir	Au	Ag	Pb	Zn			plutonic
082FSW077	Wilcox	Past Producer	I05	Nelson	Au	Ag	Pb	Zn			plutonic
082FSW080	Dumas (L.5727)	Prospect	I05	Ymir / Nelson	Au	Ag	Pb	Zn			Quesnel
082FSW081	Oild Timer (L.4662)	Prospect	I05	Ymir / Nelson	Au	Ag	Pb	Zn	Cu		Quesnel
082FSW084	Eureka (L.5552)	Past Producer	I05	Eagle Creek "pseudodiorite"	Cu	Au	Ag	Pb	Zn		Quesnel
082FSW085	Central (L.4801)	Past Producer	I05	Nelson / Elise	Cu	Ag	Au				plutonic
082FSW089	Good Hope	Past Producer	I05	Elise	Au	Ag	Cu				Quesnel
082FSW112	Gold Hill (L.640)	Past Producer	I05	Mount Roberts	Ag						Quesnel
082FSW123	Homestake (L.936)	Past Producer	I05	Elise	Ag	Au	Cu	Pb	Zn		Quesnel
082FSW124	Monday (L.995)	Past Producer	I05	Elise	Ag	Zn	Pb	Cu			Quesnel
082FSW125	Gopher (L.1050)	Prospect	I05	Elise	Au	Ag	Cu	Zn	Bi		Quesnel
082FSW139	John	Prospect	I05	Elise	Ag	Zn	Pb				Quesnel
082FSW141	Good Friday	Showing	I05	Elise	Pb	Zn					Quesnel
082FSW143	Rirchmond (L.1508)	Past Producer	I05	Elise	Ag	Pb	Au	Cu	Zn		Quesnel
082FSW145	Blue Bird (L.1053)	Past Producer	I05	Elise	Ag	Pb	Zn	Au	Cu	Sb	Quesnel
082FSW146	Mayflower (L.799)	Past Producer	I05	Elise	Ag	Au	Pb	Zn	Cd		Quesnel
082FSW150	Shawn	Showing	I05	Reno	Au	Ag	Cu	Pb			North America
082FSW153	Lily May (L.1052)	Past Producer	I05	Elise	Ag	Cu	Pb	Zn	Au		Quesnel
082FSW154	Curlew (L.1220)	Past Producer	I05	Elise	Ag	Au	Pb	Zn	Cu	Sb	Quesnel
082FSW155	Red Eagle (L.1615)	Past Producer	I05	Elise	Ag	Pb	Cu	Zn			Quesnel
082FSW156	Nature Boy	Prospect	I05	Rossland monzonite	Ag	Pb	Zn				Quesnel
082FSW157	Ural (L.2944)	Prospect	I05	Elise	Au	Ag					Quesnel

APPENDIX 1 CONTINUED

MINFILE NO.	NAME	STATUS	CODE	COMMENT (host)	COMMODITIES						TERRANE
082FSW158	Casino Red Cap	Past Producer	105	Elise	Au	Ag	Pb	Zn			Quesnel
082FSW159	Columbia	Prospect	105	Elise	Au	Ag					Quesnel
082FSW160	Sunset (L.6563)	Past Producer	105	Elise	Ag	Au	Pb	Zn	Cu		Quesnel
082FSW161	Douglas (L.2865)	Past Producer	105	Sophie Mountain	Ag	Pb	Zn	Cu			Quesnel
082FSW164	Union (L.944)	Past Producer	105	Mount Roberts	Pb	Zn	Ag	Au	Cu	Bi	Quesnel
082FSW166	Venus (L.4293)	Past Producer	105	Elise/Nelson	Au	Ag	Pb	Cu	Zn		Quesnel
082FSW169	California (L.1677)	Past Producer	105	Elise/Nelson	Au	Ag	Pb	Zn	Cu		Quesnel
082FSW170	Shamrock (L.2234)	Developed Prospect	105	Elise/Silver King	Ag	Pb	Zn	Au			Quesnel
082FSW171	Irene (L.4151)	Past Producer	105	Elise/Silver King	Au	Ag					Quesnel
082FSW172	Great Eastern	Past Producer	105	Elise/Silver King	Au	Ag					Quesnel
082FSW173	Victoria-Jessie	Past Producer	105	Elise/Silver King	Au	Ag	Cu				Quesnel
082FSW174	Starlight (L.684)	Past Producer	105	Elise/Silver King	Au	Ag	Cu				Quesnel
082FSW175	Daylight-Berlin	Past Producer	105	Elise/Silver King	Au	Ag	Pb	Zn	Cu		Quesnel
082FSW176	Silver King (L.141)	Past Producer	105	Elise/Silver King	Ag	Cu	Au	Pb	Zn		Quesnel
082FSW177	Referendum	Past Producer	105	Elise	Au	Ag	Pb	Zn			Quesnel
082FSW178	Northern Light	Past Producer	105	Elise	Au	Ag	Cu				Quesnel
082FSW179	Golden Eagle	Past Producer	105	Elise/Nelson	Au	Pb	Zn	Ag	Cu		Quesnel
082FSW180	Celtic Queen	Showing	105	Elise	Au	Ag	Zn	Pb			Quesnel
082FSW181	Gold King (L.12411)	Past Producer	105	Elise	Au	Cu	Ag				Quesnel
082FSW182	Bear (L.14714)	Past Producer	105	Elise/dike	Au	Ag	Cu				Quesnel
082FSW183	Fern (L.374)	Past Producer	105	Elise	Au	Ag	Cu				Quesnel
082FSW184	Canadian Belle	Past Producer	105	Hall	Au	Ag	Cu				Quesnel
082FSW185	Golden Age	Past Producer	105	Elise	Au	Ag	Cu	Pb	Zn	W	Quesnel
082FSW186	Euphrate	Past Producer	105	Elise	Au	Ag	Pb	Zn	Cu		Quesnel
082FSW189	Porto Rico (L.2385)	Past Producer	105	Elise	Au	Ag	Cu	Pb	Zn		Quesnel
082FSW190	Spotted Horse	Past Producer	105	Elise	Au	Ag	W				Quesnel
082FSW191	Commodore	Past Producer	105	Nelson	Ag	Au					plutonic
082FSW192	Elise (L.1310)	Developed Prospect	105	Ymir/Nelson	Ag	Au	Pb	Zn	Cu		Quesnel
082FSW193	Arizona (L.13026)	Past Producer	105	Ymir/Nelson	Au	Ag	Pb	Zn			Quesnel
082FSW194	Ymir Belle	Prospect	105	Ymir/Nelson	Au	Pb	Zn	Ag			Quesnel
082FSW197	Myrtle	Past Producer	105	Elise	Au	Ag	Pb	Zn			Quesnel
082FSW198	Dewey (L.14431)	Past Producer	105	Ymir/Nelson	Ag	Au	Pb	Zn	Cu		Quesnel
082FSW199	Howard (L.12538)	Past Producer	105	Active/Nelson	Ag	Pb	Zn	Au	Cd	Cu	Kootenay
082FSW200	Clubine	Past Producer	105	Hall	Au	Ag	Pb	Zn	Cu		Quesnel
082FSW202	Keystone (L.5137)	Past Producer	105	Hall	Au	Ag	Pb	Zn	Cu		Quesnel
082FSW203	Canadian King	Past Producer	105	Hall	Au	Ag	Pb				Quesnel
082FSW204	Gold Hill	Past Producer	105	Hall	Au	Ag	Cu				Quesnel
082FSW205	Arlington (L.3648)	Past Producer	105	Hall	Au	Ag	Pb	Zn			Quesnel
082FSW207	Silver Dollar	Past Producer	105	Hall	Au	Ag	Pb	Zn	Cu		Quesnel
082FSW208	Perrier	Past Producer	105	Elise	Au	Ag	Pb	Zn	Cu		Quesnel
082FSW209	Catherine (L.4437)	Past Producer	105	Elise/Nelson	Au	Ag	Pb	Zn	Cu		Quesnel
082FSW210	Hummingbird	Past Producer	105	Elise/Nelson	Au	Ag	Pb	Zn	Cu		Quesnel
082FSW217	Eureka (L.946)	Showing	105	Rainy Day pluton	Mo	Cu					plutonic
082FSW222	Whitewater (L.529)	Past Producer	105	Elise/Nelson	Au	Ag	Pb	Zn	Mo		Quesnel
082FSW223	Zilor (L.1051)	Showing	105	Elise	Ag	Au	Pb	Zn	Cu		Quesnel
082FSW226	Hattie	Showing	105	Archibald	Mo	W	Cu	Ag			Quesnel
082FSW227	Rex	Showing	105	Eagle Creek plutonic complex	Cu						Quesnel
082FSW232	Hilltop	Showing	105	Windermere/ Nelson	Pb	Zn	Cu				North America
082FSW233	Ness	Showing	105	Laib/ Nelson	Cu						Kootenay
082FSW236	Bluestar	Showing	105	Cs	Au	Cu	Ag	Pb	Zn		Kootenay

APPENDIX 1 CONTINUED

MINFILE NO.	NAME	STATUS	CODE	COMMENT (host)	COMMODITIES						TERRANE
082FSW238	Last Chance	Showing	I05	Elise	Ag	Cu	Pb	Zn	Au		Quesnel
082FSW239	Atlin-Nome	Showing	I05	Ynir / Nelson	Au						Quesnel
082FSW240	M	Showing	I05	Active	Zn	Pb					Kootenay
082FSW241	Rosa (L.2460)	Showing	I05	Archibald	Ag	Pb	Zn	Au			Quesnel
082FSW242	Grand Prize (L.933)	Showing	I05	Elise	Pb	Bi					Quesnel
082FSW243	Waneta 6	Showing	I05	Cs/Sheppard	Ag	Pb	Cu	Au	As	Sb	Kootenay
082FSW245	Wolf Lake	Prospect	I05	Windermere/ Nelson	Au	Ag	Cu				North America
082FSW254	Jack Pot (L.4789)	Showing	I05	Eagle Creek plutonic complex	Cu	Ag	Au				Quesnel
082FSW257	Davne	Prospect	I05	Nelway/ Laib	Au	Ag	Pb	Zn	Cu		Kootenay
082FSW259	Joint (L.8344)	Showing	I05	Active	Pb	Zn	Au	Ag			Kootenay
082FSW261	Caribou	Past Producer	I05	Active	Au	Ag	Pb	Zn			Kootenay
082FSW264	Cal	Showing	I05	Elise/ ultramafics	Au	Ag	Cu	Pb	Zn		Quesnel
082FSW265	Big Horn	Showing	I05	Reno/ Nelson	Au	Ag	Cu	Zn	W		North America
082FSW267	Armstrong	Past Producer	I05	Nelson	Ag	Pb	Zn	Au			plutonic
082FSW274	Josie (L.3925)	Showing	I05	Eagle Creek plutonic complex	Au	Cu	Ag				Quesnel
082FSW277	Free Silver (L.2902)	Showing	I05	Elise	Ag	Pb	Zn	Cu	Mo		Quesnel
082FSW281	Shiloh (L.3847)	Showing	I05	Ymir/Nelson	Au	Zn	Pb				Quesnel
082FSW283	Allouez	Showing	I05	Elise	Au	Ag	Cu				Quesnel
082FSW285	Cristine (L.1219)	Showing	I05	Mount Roberts	Au	Cu					Quesnel
082FSW295	Mitzie 1	Showing	I05	Elise	Ag	Pb	Zn	Cu	Au		Quesnel
082FSW298	Helen (LOT 1151)	Showing	I05	Sheppard	Au	Ag	Cu	Pb	Zn	Mo	plutonic
082FSW299	Rachel	Past Producer	I05	Nelson	Au	Ag	Pb				plutonic
082FSW300	Ben Hassen (L.3663)	Showing	I05	Archibald/	Ag	Pb	Zn	Au	Cu		Quesnel
082FSW301	Arnold (L.4079)	Showing	I05	Archibald/ Nelson	Ag	Au	Cu	Pb	Zn		Quesnel
082FSW302	Rhea	Showing	I05	Elise/Nelson	Au	Ag	Cu	Pb	Zn		Quesnel
082FSW303	Root	Showing	I05	Ymir/ elson	Au	Ag	Pb	Zn	Cu		Quesnel
082FSW304	Lasca 1	Showing	I05	Nelson	Pb	Zn					plutonic
082FSW306	Santa Rosa	Showing	I05	Elise/Coryel	W	Au	Ag	Cu	Pb	Zn	Quesnel
082FSW308	Flying Dutchman	Showing	I05	Elise	Au	Ag	Cu	Pb			Quesnel
082FSW309	Star of the West	Showing	I05	Elise	Ag	Pb	Zn	Au			Quesnel
082FSW312	Caribou Showing	Showing	I05	Mount Roberts	Au	Ag					Quesnel
082FSW313	Summit (L.4229)	Showing	I05	Ymir/Nelson	Pb	Zn	Mn				Quesnel
082FSW314	Pingree (L.3685)	Showing	I05	Elise	Au	Cu					Quesnel
082FSW316	Bluebird	Showing	I05	Nelson/Ymir	Au	Ag	Pb				plutonic
082FSW317	Sterling (L.2926)	Showing	I05	Ymir/Nelson	Pb	Zn					Quesnel
082FSW318	Lasca 2	Showing	I05	Nelson	Au	Ag	Pb	Zn			plutonic
082FSW319	Lasca 3	Showing	I05	Nelson	Pb	Ag	Zn				plutonic
082FSW323	Silverado	Showing	I05	Elise	Au	Ag	Pb	Zn			Kootenay
082FSW325	Maud S.(L.1442)	Showing	I05	Nelson/Elise ?	Au	Cu	Pb				plutonic
082FSW329	Gold Queen	Showing	I05	Nelson/Ymir	Ag	Au	Pb	Zn			plutonic
082FSW330	Marilyn 1-12	Showing	I05	Active	Ag	Pb	Zn				Kootenay
082FSW334	Jennie Bell	Showing	I05	Elise ?	Au	Ag	Pb				Quesnel
082FSW335	Canadian Pacific	Showing	I05	Ymir	Au	Pb	Zn				Quesnel
082FSW336	Three Friends	Showing	I05	Elise/Silver King	Au	Ag	Cu				Quesnel
082FSW349	Wewa	Showing	I05	Nelson	Cu	F					plutonic
082FSW350	Ace in the Hole	Showing	I05	Elise	Ag	Au	Pb	Cu	Zn		Quesnel
082FSW352	Vermont	Showing	I05	Elise/Sophie Mountain	Ag	Pb	Zn	Cu			Quesnel
082FSW355	Keno 9	Showing	I05	Elise	Au	Cu	Ag				Quesnel

APPENDIX 1 CONTINUED

MINFILE NO.	NAME	STATUS	CODE	COMMENT (host)	COMMODITIES						TERRANE
082FSW357	Trillicum (L.11013)	Showing	I05	Marron/Coryel	Pb	Zn	Cu				Overlap assemblage
082FSW358	Aurous	Showing	I05	Elise	Au	Cu	Ag				Quesnel
082FSW359	Hattie Brown	Past Producer	I05	Rossland sill	Au	Ag	Pb				Quesnel
082FSW362	Gold Dust	Showing	I05	Elise	Au	Cu	Ag				Quesnel
082FSW364	Little Giant (L.1992)	Showing	I05	Elise/Rossland monzonite	Au						Quesnel
082FSW368	Victory-Triumph	Prospect	I05	Coryel/Sophie Mountain	Cu	Au					plutonic
082FSW369	Olga (L.4201)	Showing	I05	Coryel/Sophie Mountain	Au	Ag	Pb				plutonic
082FSW373	Erie	Showing	I05	Archibald	Ag	Au	Pb	Zn	Cu		Quesnel
	Cu+/-Ag Quartz Veins										
082FSW284	New York Central	Showing	I06	Nelson	Au						plutonic
082FSW344	Silver Hill	Showing	I06	Windermere	Ag						North America
082FSW360	CQ	Showing	I06	Elise/pulaskite dike	Au						Quesnel
	Tungstern Veins										
082FSW221	Independent	Showing	I12	Elise	W						Quesnel
082FSW234	Blue Eyes	Showing	I12	Trail pluton	W	Mo					plutonic
	Copper Skarns										
082FSW082	Queen Victoria	Past Producer	K01	Ymir/Nelson	Cu	Ag	Au				Quesnel
082FSW211	Mammoth (L.14694)	Showing	K01	Elise/Nelson	Cu	Mo	Ag	Pb	Zn	Au	Quesnel
082FSW225	St. Louis (L.935)	Showing	K01	Elise/Trail pluton	Cu						Quesnel
	Pb-Zn Skarns										
082FSW023	Pete Creek	Showing	K02	Reeves/Nelson	Zn	Pb	Ag				North America
082FSW032	Silver Bell	Showing	K02	Active/Nelson	Zn	BA					Kootenay
082FSW057	Elm	Showing	K02	Active/Nelson	Zn	W	F				Kootenay
082FSW058	Udiville (L.15851)	Showing	K02	Reeves/Nelson	Pb	Zn	Ag	W	Mo		North America
	Fe Skarns										
082FSW163	Lord Roberts	Prospect	K03	Mount Roberts/ Nelson	MA	Fe	Cu	Ag	Bi		Quesnel
	Au Skarns										
082FSW002	Bunker Hill	Past Producer	K04	Laib/Nelson	Au	Ag	W	Mo			Kootenay
082FSW127	Sunset (L.954)	Past Producer	K04	Elise/Rossland monzonite	Au	Ag	Cu	Fe			Quesnel
082FSW167	SDR	Showing	K04	Elise/Rossland monzonite	Au	Cu	MA	Zn	Ag		Quesnel
082FSW187	Second Relief	Past Producer	K04	Elise/ Bonnington	Au	Ag	Pb	Zn	Cu	Mo	Quesnel
082FSW216	Rand (L.14666)	Prospect	K04	Elise/ Bonnington	Au	Ag	Cu				Quesnel
082FSW266	Beaver Creek	Past Producer	K04	Archibald/ Nelson	Au	Ag	Pb	Zn	Cu		Quesnel
082FSW282	Monarch (L.2082)	Prospect	K04	Elise/Nelson	Cu	Ag	Au	Mo	Pb	Zn	Quesnel
082FSW340	Strawberry Flats	Showing	K04	Mount Roberts / Nelson	Au	Ag	Cu	Pb	Zn		Quesnel
	W Skarns										
082FSW010	Emerald Tungsten	Past Producer	K05	Reeves/K Emerald stock	W	Mo	Bi	Au			North America
082FSW011	Dodger (L.12083)	Past Producer	K05	Reeves/K Dodger stock	W	Mo	Au				North America

APPENDIX 1 CONTINUED

MINFILE NO.	NAME	STATUS	CODE	COMMENT (host)	COMMODITIES						TERRANE
082FSW016	Jumbo (L.12688)	Showing	K05	Active/K Lost Creek stock	W	Mo					Kootenay
082FSW059	Victory Tungsten	Developed Prospect	K05	Reeves/K granite	W	Mo					North Ame
082FSW218	Invincible (L.12084)	Past Producer	K05	Reeves/K Dodger stock	W	Mo					North Ame
082FSW228	Loto 3	Showing	K05	Rossland/Nelson	W	Cu					Quesnel
082FSW247	Feeney (L.9074)	Past Producer	K05	Reeves/K Emerald stock	W	Mo					North Ame
082FSW280	M.U.T.	Showing	K05	Active/Lost Creek stock	Mo	W	U				Kootenay
082FSW311	Arrow Tungsten	Prospect	K05	Hall/J Nelson	W	Mo	Zn	Cu	Pb		Quesnel
082FSW320	Comet (L.14761)	Showing	K05	Reeves/K stock	W						North Ame
082FSW321	Alfie (L.15091)	Showing	K05	Reeves/K Emerald stock	W						North Ame
	Mo Skarns										
082FSW106	Golden Queen	Developed Prospect	K07	Elise	Mo	W	Cu				Quesnel
082FSW107	Novelty (L.958)	Developed Prospect	K07	Elise	Au	Mo	Co	U	Bi		Quesnel
082FSW109	Giant (L.997)	Past Producer	K07	Elise	Au	Mo	Cu	Co	Ni	Bi	Quesnel
082FSW110	Coxey	Past Producer	K07	Elise/Rossland monzonite	Mo	Cu	W	Au			Quesnel
	Wollastonite Skarns										
082FSW341	Rossland Wollastonite	Showing	K09	Mount Roberts/Coryel	W						Quesnel
	Subvolcanic Cu-Au-Ag										
082FSW372	Independence	Showing	L01	Elise	Au	Cu	Ag				Quesnel
	Porphyry Cu-Au: Alkalic										
082FSW083	Star (L.3687)	Past Producer	L03	Elise/Eagle Creek plutonic complex	Au	Cu	Ag	Pb			Quesnel
082FSW237	Kena 7	Showing	L03	Elise/Nelson?, Silver King?	Cu	Au	Pb	Zn			Quesnel
082FSW290	Katie	Prospect	L03	Elise/Early ? J stock	Cu	Au					Quesnel
082FSW291	Gus	Showing	L03	Elise	Au	Ag	Pb	Zn	Cu		Quesnel
082FSW294	Toughnut (L.199)	Showing	L03	Elise/Silver King?	Au	Ag	Cu	Pb	Zn		Quesnel
082FSW331	Shaft	Showing	L03	Elise/Early J stock	Au	Cu					Quesnel
082FSW332	Kena Copper	Showing	L03	Elise	Cu						Quesnel
082FSW333	Great Western	Prospect	L03	Elise	Au	Cu					Quesnel
082FSW353	MOR 1	Showing	L03	Elise/Early ? J stock	Au	Cu					Quesnel
082FSW365	Vinon	Showing	L03?	Elise	Au	Cu					Quesnel
082FSW366	Red Point (L.1200)	Showing	L03?	Elise	Au	Ag	Cu				Quesnel
082FSW021	Molly (L.14232)	Past Producer	L05	Lost Creek stock	Mo	W	U				plutonic
082FSW134	St. Elmo (L.923)	Past Producer	L05	Red Mountain breccia	Mo	Cu	W	Ag	Au		Quesnel
082FSW140	Mountain View (L.682)	Past Producer	L05	Red Mountain breccia	Mo	W	Cu	Au	Ag	Pb	Quesnel
082FSW213	Copper King	Showing	L05	Erie stock	Mo	Cu	W	Zn	Pb	Ag	plutonic
082FSW220	Curlett	Showing	L05	Elise/Nelson	Mo						Quesnel

APPENDIX 1 CONTINUED

MINFILE NO.	NAME	STATUS	CODE	COMMENT (host)	COMMODITIES						TERRANE
082FSW224	Rainy Day (L.1339)	Showing	L05	Rainy Day stock	Mo						plutonic
082FSW229	Stewart 2	Developed Prospect	L05	Nelson	Mo	W	Au	Ag	Pb	Zn	plutonic
082FSW250	Bobbi	Showing	L05	quartz diorite stock	Mo	W	Cu	F	Au	Pb	plutonic
082FSW251	Fresno	Showing	L05	Nelson	Mo						plutonic
082FSW268	Meadows	Showing	L05	Nelson	Mo	Ag	Au				plutonic
082FSW287	Kirkup	Showing	L05	Trail pluton	Cu	Mo	W				plutonic
082FSW326	Kimbarb	Showing	L05	Ladybird granite	Mo	GS					plutonic
082FSW328	Marble Edge (L.2354)	Showing	L05	Nelson pegmatite	Mo						plutonic
	Porphyry W										
082FSW144	Alva	Showing	L07	Nelson	W						plutonic
	Podiform Chromite										
082FSW130	Vandot	Showing	M03	serpentinite	Cr	Ni	Pt	Co	Ti	Fe	Slide Mountain
082FSW214	Little Sheep CK Ultramafics	Showing	M03	serpentinite	Cr	Ni	AB				Slide Mountain
	Five-element Veins Ni-Co-As-Ag±(Bi, U)										
082FSW272	Crescent	Showing	I14	Castlegar gneiss	Nb	Ta	U	Th	Ti	Y	plutonic
	Rare Element Pegmatite - NYF Family										
082FSW212	Mota	Showing	O02	Castlegar gneiss	U						Quesnel
082FSW252	Roma	Showing	O02	Castlegar gneiss	U	Th					Quesnel
082F3W270	Lucky-Bill-Tag	Showing	O02	Nelson	U						plutonic
082FSW271	Gibson Creek	Showing	O02	Nelson	U	Th					plutonic
082FSW273	U3O8	Showing	O02	Castlegar gneiss	U						Quesnel
082FSW275	Jackass	Showing	O02	Nelson	U						plutonic
	Placer										
082FSW269	Acorn	Showing	C01	Surficial placers	W	Au					overlap
	Industrial Minerals										
082FSW296	Nelson Clay	Past Producer	B06	Fireclay	clay						Quesnel
082FSW315	Castlegar Junction	Showing	B06	Fireclay	clay						Quesnel
082FSW351	Three Sisters	Showing	P02	Kyanite-sillimanite schists	KY						North America
082FSW327	Ymir Graphite	Showing	P04	Crystalline flake graphite	GT						Kootenay
082FSW293	Rossland Granite	Past Producer	R03	Dimension stone -GR granite		DS	BS				plutonic
082FSW297	Ymir Pulaskite Quarry	Developed Prospect	R03	Dimension stone -DS granite		BS					plutonic
082FSW342	Granite	Past Producer	R03	Dimension stone -BS granite		DS					plutonic
082FSW343	Nelson Granite	Past Producer	R03	Dimension stone -DS granite							plutonic
082FSW278	Keith	Past Producer	R06	Dimension stone -FS sandstone		DS	BS	AT			plutonic
082FSW279	Kootenay Stone	Producer	R06	Dimension stone -BS sandstone		DS	FS	Si			plutonic

APPENDIX 1 CONTINUED

MINFILE NO.	NAME	STATUS	CODE	COMMENT (host)		COMMODITIES			TERRANE
082FSW288	Sheep Creek Quartzite	Past Producer	R06	Dimension stone - sandstone	DS	FS			plutonic
082FSW345	Lot 4636	Past Producer	R06	Dimension stone - sandstone	DS	BS			plutonic
082FSW346	Sharon	Past Producer	R06	Dimension stone - sandstone	BS	DS	FS		plutonic
082FSW347	Riverside	Past Producer	R06	Dimension stone - sandstone	DS	BS			plutonic
082FSW348	B & B	Past Producer	R06	Dimension stone - sandstone	DS	BS			plutonic
082FSW374	South Fork Silica	Past Producer	R07	Silica sandstone	Si				North America
082FSW215	Swift Creek	Past Producer	R09	Limestone	LS	MB	BS		North America
082FSW253	Purex Lime	Prospect	R09	Limestone	LS	DO			North America
082FSW262	Wallace Creek	Showing	R09	Limestone	LS				North America
082FSW289	Sheep Creek Marble	Past Producer	R09	Limestone	MB	LS	DS	BS	North America
082FSW292	Pend D'Oreille	Showing	R09	Limestone	LS				North America
082FSW307	Lost Creek	Producer	R09	Limestone	LS				North America
082FSW337	Reno Limestone	Past Producer	R09	Limestone	LS				North America
082FSW338	Waneta Limestone	Showing	R09	Limestone	LS				Quesnel
082FSW339	South Salmo River	Showing	R09	Limestone	LS				North America
	Unknown								
082FSW263	Jero 5	Showing		Elise	Ag	Au			Quesnel
082FSW367	Knight Teplar	Showing		Unit Cs	Au				Kootenay
082FSW370	Falu (1350)	Showing		Mount Roberts	Au				Quesnel
082FSW371	Highland (L.1049)	Showing		Mount Roberts	Cu				Quesnel

Notes:
AB - asbestos; MA - magnetite; LS - limestone; MB - marble; DS - dimension stone; BS - building stone; DO - dolomite; FS - flagstone; AT - aggregate; GS - gemstones; GT - graphite; GR - granite; KY - kyanite

APPENDIX 2
SAMPLE LOCATIONS AND DESCRIPTIONS

Field No.	Zone	UTM North	UTM East	Deposit	Description
R96-4	11	439652	5437636	Coxey, A pit	diopside-Mo skarn
R96-4B	11	439652	5437636	Coxey, A pit	garnet-diopside-Po-Cp skarn
R96-6	11	439531	5437770	Coxey, Upper A pit	Mo-diopside skarn
R96-7A	11	439724	5437299	Novelty	Mo-Po diopside skarn
R96-7B	11	439724	5437299	Novelty	cobalt bloom in pale green diopside skarn
R96-8	11	439737	5437653	Coxey, Upper A pit	Po-Cp diopside skarn
R96-12A	11	439840	5437842	Mountain View, E pit	garnet-diopside skarn with Po-Cp vein
R96-12C	11	439840	5437842	Mountain View, E pit	Mo-garnet skarn
R96-12D	11	439840	5437842	Mountain View, E pit	Po-Cp vein
R96-15	11	439442	5437865	Nevada, D pit (Coxey)	Mo-diopside skarn, veins
R96-17	11	439450	5437716	Coxey, B pit	Mo-Po vein in diopside skarn
R96-18C	11	439457	5437661	Coxey, B pit	Mo-Py in diopside skarn
R96-19A	11	439874	5437792	Mountain View, F pit	coarse Mo-Po breccia
R96-19B	11	439874	5437792	Mountain View, F pit	semi-massive Po-Py-Cp vein
R96-19C	11	439874	5437792	Mountain View, F pit	Mo veins in Elise metasediment
R96-20B	11	439862	5437826	Mountain View, F pit	Po breccia
R96-20C	11	439862	5437826	Mountain View, F pit	garnet-diopside-Mo skarn
R96-24A	11	440669	5436612	Le Roi dump	massive Po-Cp vein in hornblende porphyrite
R96-24B	11	440669	5436612	Le Roi dump	massive Po-Cp vein in Rossland sill
R96-24C	11	440669	5436612	Le Roi dump	Po-Cp vein in Rossland sill
R96-25B	11	440598	5436759	Le Roi dump	mafic sill cut by Po-Cp veins
R95-28A	11	439138	5437759	Jumbo	Po diopside skarn
R96-28D	11	439138	5437759	Jumbo	rusted, siliceous metasediment
R96-31A	11	440645	5437021	War Eagle	semi-massive Po-Cp vein
R96-31B	11	440645	5437021	War Eagle	semi-massive Po-(Cp) vein
R96-31C	11	440645	5437021	War Eagle	disseminated Po in highly altered host
R96-35B	11	441213	5436920	Centre Star	vein altered Rossland monzonite
R96-35C	11	441213	5436920	Centre Star	massive Po-Py-(Cp) vein
R96-39A	11	443193	5437695	Kootenay-(Columbia)	mineralized (Po-Cp) skarn
R96-40B	11	443176	5437691	Iron Colt	Po-Aspy-Cp vein
R96-42A	11	442994	5437633	Columbia	disseminated and vein Cp-Po in garnet "skarn"
R96-42B	11	442994	5437633	Columbia	semi-massive Aspy-(Po)-Cp vein
R96-44A	11	442089	5437749	Evening Star	semi-massive Po-Aspy-(Cp) in altered Rossland monzonite
R96-45B	11	441449	5437247	Evening Star	altered Elise metasediments, Py-calcite veinlets
R96-45E	11	441449	5437247	Evening Star	diopside-Aspy-Po skarn
R96-46A	11	441443	5437761	Monte Christo	massive Po-Cp vein/skarn
R96-47A	11	441604	5438111	vein occurrence	diopside skarn with minor vein/disseminated Po-Cp
R96-48A	11	440937	5437775	Cliff	massive Po-Cp vein/skarn
R96-51B	11	440457	5437718	Consolidated St. Elmo	massive Po-Cp-(Sph) vein
R96-51C	11	440457	5437718	Consolidated St. Elmo	semi-massive Po-Cp-Py vein
R96-52	11	440709	5437607	Red Mountain	massive Po-Py-(Cp) vein
R96-53A	11	440483	5437077	No 1 (W. of War Eagle)	semi-massive Po-Cp-Aspy vein
R96-53D	11	440483	5437077	No 1 (W. of War Eagle)	semi-massive Po-Cp vein
R96-54	11	440527	5437211	Monita	semi-massive Po-Cp vein

APPENDIX 2 CONTINUED

Field No.	Zone	UTM North	UTM East	Deposit	Description
R96-55	11	440556	5437341	vein occurrence	semi-massive Po-Cp vein
R96-60A	11	440175	5437218	Gertrude	altered porphyrite with disseminated Po
R96-60B	11	440175	5437218	Gertrude	semi-massive Po-(Cp) vein
R96-60C	11	440175	5437218	Gertrude	massive Po-(Cp-Sph) vein
R96-61A	11	449639	5437079	Giant	altered intrusion with disseminated Py
R96-61B	11	449639	5437079	Giant	semi-massive Po-(Cp) vein
R96-62A	11	449638	5437137	Giant	Bi-bismuthite-Mo-(Cp) in siliceous metasediment
R96-62B	11	449638	5437137	Giant	altered Elise metasediments with Aspy-Po-Bi veins
R96-62C	11	449638	5437137	Giant	disseminated and fracture-controlled Py-Po
R96-62D	11	449638	5437137	Giant	disseminated Py-Mo in altered metasediment
R96-63	11	449526	5437065	Giant	disseminated Po in diopside skarn
R96-64A	11	441888	5434637	Mayflower	massive Sph-Po-Py vein
R96-64B	11	441888	5434637	Mayflower	massive Sph-Gal-Py-Aspy vein
R96-64C	11	441888	5434637	Mayflower	Py-Sph-Po-(Gal) in biotite hornfels
R96-65A	11	443139	543674	Robert E. Lee	semi-massive Aspy-Po-Cp vein
R96-65B	11	443139	543674	Robert E. Lee	massive Po-(Cp-Sph-Aspy) vein
R96-66A	11	441570	5434632	Bluebird	semi-massive Py-Sph-Aspy-Gal vein
R96-66B	11	441570	5434632	Bluebird	Py-Sph-Gal-(Aspy) vein
R96-67A	11	441552	5434770	Homestake	semi-massive Py-Sph-?o-Gal vein
R96-67B	11	441552	5434770	Homestake	semi-massive Po-Cp vein
R96-67C	11	441552	5434770	Homestake	massive Py-Cp-Sph-Gal vein
R96-69	11	441977	5437313	Iron Horse	semi-massive to disseminated Po-Cp in amphibolite
R96-70	11	441814	5437313	Iron Horse	Po-Py-(Cp) in brecciated Rossland monzonite
R96-70A	11	441814	5437313	Iron Horse	semi-massive Po-Py in amphibolite
R96-71A	11	441412	5437067	War Eagle	massive Po-Cp in altered Rossland monzonite
R96-72	11	440709	5437607	Red Mountain	semi-massive Po-(Cp) vein
R96-73	11	440280	5436812	Annie	massive Po-Cp in quartz gangue
R96-74	11	440462	5436812	Josie	massive Po-Py-(Cp) in skarn
R96-74A	11	440462	5436812	Josie	disseminated Po-Py in altered "host"
R95-74B	11	440462	5436812	Josie	Po-Cp vein in Rossland sill?

Notes

Po - pyrrhotite; Cp - chalcopyrite; Sph - sphalerite; Gal - galena; Aspy - arsenopyrite; Bi - bismuth; Py - pyrite; Mo - molybdenite

UTM coordinates: Nad 87

See Appendix 5 for detailed petrographic descriptions of selected samples and Appendix 6 for analyses.

APPENDIX 3
PRODUCTION DATA; METALLIC DEPOSITS OF THE ROSSLAND-NELSON MAP AREA

MINFILE No.	NAME	MINED (tonnes)	MILLED (tonnes)	silver (grams)	gold (grams)	lead (kg)	zinc (kg)	copper (kg)	cadmium (kg)	molybdenum (kg)	production (from - to)	
082FSW001	ASPEN (L.12471)	28	0	36359	31	431	365	0	0	0	1918	1934
082FSW002	BUNKER HILL	340	0	9642	3298	0	0	0	0	0	1933	1942
082FSW003	ED	257	0	1462	124	1646	784		0	0	1953	1970
082FSW004	HB (L.12672)	6656101	6628195	31543666	2862	51178298	272911903	889	2019586		1912	1978
082FSW008	IRON CAP	5	0	5785			0	0	2268	0	1914	1914
082FSW009	JERSEY (L.9070)	8134702	8128809	21483869		114935331	263715580		2011236		1944	1970
082FSW011	DODGER	332986	336235		0	0	0	0	0	0	1971	1972
082FSW014	HUNTER V	56820	0	8464402	31413	0	0	0	0	0	1902	1929
082FSW018	LOMOND	18	0	1182		4401	436	0	0	0	1948	1949
082FSW019	LONE SILVER	174	0	693941	2674	10746	3693	0	0	0	1909	1941
082FSW021	MOLLY (L.14232)	171	0		0	0	0	0	0	11366	1914	1917
082FSW025	RED ROCK	525	0	154738	155	85059	94987	16		0	1935	1979
082FSW026	REEVES MACDONALD	5846021	5817828	19842003		57692784	203616006	27584	1215665	0	1949	1971
082FSW030	SALMO-CONSOLIDATED	6	0	2343		46	83	0	0	0	1917	1937
082FSW036	RENO (L.12684)	293924	288915	2424075	5269714	68457	44811		0	0	1929	1979
082FSW039	FAWN	68	64	404	4074		0	0	0	0	1915	1935
082FSW040	NUGGET (L.8341)	36968	28519	283053	777791	3294	1273		0		1907	1988
082FSW041	MOTHERLODE	67444	63108	588106	1256988	10968	4264	3010		0	1906	1985
082FSW044	GOLD BELT	236502	232861	1061298	2512906	10457	6605	681	0	0	1934	1979
082FSW046	KOOTENAY BELLE	305610	252310	1306232	3507079	52517	59335		0	0	1904	1967
082FSW048	QUEEN (L.1076)	653165	649686	3121278	9453072	7769	3063	0	0	0	1902	1970
082FSW049	VANCOUVER	347	0	12815	29983	0	0	0	0	0	1909	1933
082FSW052	YELLOWSTONE	15473	15306	96357	174457	181	120	0	0	0	1899	1970
082FSW053	ORE HILL (L.2073)	2241	885	168424	88612	80257	75651	0	0	0	1906	1940
082FSW054	SUMMIT	1094	907	37883	27059	13728	12988	0	0	0	1906	1938
082FSW055	BONANZA	14	0	2861	124	118	0	0	0	0	1963	1963
082FSW062	LUCKY STRIKE	55	0	65191	2456	2318	1115	0	0	0	1938	1963
082FSW063	PORCUPINE	109	0	18507	134	1130	2633	1052		0	1926	1971
082FSW064	NEVADA (L.3504)	9	0	1773	62	546	381	0	0	0	1937	1937
082FSW066	CENTER STAR	51458	50595	2955219	386145	966401	475628	0	0	0	1936	1950
082FSW067	DUNDEE	2717	168	472144	30886	204302	211781	0	0	0	1899	1951
082FSW068	YANKEE GIRL	370616	285203	22036290	3850118	6198334	6474173	0	0	0	1907	1951
082FSW072	TAMARAC (L.3802)	346	0	404	8040	0	0	0	0	0	1899	1959
082FSW073	PROTECTION	14788	0	2576104	333391	688611	703233	10	514	0	1899	1973
082FSW074	YMIR (L.1708)	327646	325101	14283898	3410319	4778178	813341	0	0	0	1899	1973
082FSW075	YMIR-GOOD HOPE	41	8	3950	902	0	0	0	0	0	1903	1905
082FSW076	BLACKCOCK	2614	1095	97260	31850	43163	36821	0	0	0	1899	1942
082FSW077	WILCOX	14555	13453	526635	241982	98224	30649	0	0	0	1901	1943
082FSW079	GOLD CUP	24	0		1244	0	0	0	0	0	1925	1925
082FSW081	OLD TIMER (L.4662)	46	0	2578	184	326	116	0	0	0	1980	1980
082FSW082	QUEEN VICTORIA	45352	4397	950010	7651		0	672630	0	0	1907	1961
082FSW083	STAR (L.3687)	1163	0	85	5599		0	42	0	0	1904	1934
082FSW084	EUREKA (L.5552)	8995	3603	1124747	19190	713		159170	0	0	1905	1954

APPENDIX 3, CONTINUED

MINFILE No.	NAME	MINED (tonnes)	MILLED (tonnes)	silver (grams)	gold (grams)	lead (kg)	zinc (kg)	copper (kg)	cadmium (kg)	molybdenum (kg)	production (from - to)	
082FSW085	CENTRAL (L.4801)	21	0	1710	62		0	1331	0	0	1907	1924
082FSW086	KENVILLE	181395	158212	861116	2029068	23488	15149	1582		0	1890	1954
082FSW087	VENANGO (L.4757)	809	160	13655	11758	57	57	0	0	0	1939	1963
082FSW088	ROYAL CANADIAN	113	0	3454	3359	15	27		0	0	1896	1941
082FSW089	GOOD HOPE	48	0	2489	2799	0	0	0	0	0	1911	1944
082FSW090	MIRACLE	24	0	778	311	0	0	0	0	0	1944	1944
082FSW091	MAY & JENNIE	272	0	933	1213	0	0	0	0	0	1906	1906
082FSW092	GOLD HILL	115	0	7837	9424		0	1558	0	0	1903	1925
082FSW127	SUNSET (L.954)	30	0	809	373		0	99	0	0	1898	1908
082FSW139	JOHN	7	0	404		79	145	0	0	0	1954	1954
082FSW157	URAL (L.2944)	8	0	311	218	0	0	0	0	0	1935	1936
082FSW158	CASINO RED CAP	5514	0	23949	81334	6009	5982	0	0	0	1951	1965
082FSW159	COLUMBIA	1	0	93	31	0	0	0	0	0	1937	1937
082FSW160	SUNSET (L.6563)	13	0	3639		1420	1940	0	0	0	1952	1964
082FSW161	DOUGLAS (L.2865)	9	0	591		592	479	0	0	0	1948	1950
082FSW162	VELVET (L.2521)	88842	21613	664359	620785	37	25	1154104		0	1901	1964
082FSW163	LORD ROBERTS	7	0	187		0	0	22	0	0	1924	1924
082FSW164	UNION (L.944)	31	0	37945	187	5019	2558	0	0	0	1937	1952
082FSW166	VENUS (L.4293)	5411	4197	95486	107120	432		6	0	0	1900	1941
082FSW168	ATHABASCA	41779	20219	201798	631826	9333	13947	13	0	0	1898	1943
082FSW169	CALIFORNIA (L.1677)	1454	0	122607	70231	8085	19478	0	0	0	1910	1947
082FSW170	SHAMROCK	8	0	1213	31	280	354	0	0	0	1937	1948
082FSW171	IRENE (L.4151)	15	0	342	249	0	0	0	0	0	1939	1939
082FSW172	GREAT EASTERN	34	0	1774	1276	0	0	0	0	0	1934	1939
082FSW173	VICTORIA-JESSIE	3255	0	94119	3793		0	83577	0	0	1907	1949
082FSW174	STARLIGHT (L.684)	21	0	2936	583		0	200	0	0	1937	1981
082FSW175	DAYLIGHT-BERLIN	327	0	4977	8832	70	68	0	0	0	1937	1949
082FSW176	SILVER KING (L.141)	202049	0	138214612	8896	15234	4071	6789739		0	1889	1958
082FSW177	REFERENDUM	386	0	3683	1839	288	328	9		0	1907	1985
082FSW178	NORTHERN LIGHT	31	0	1835	62		0	124	0	0	1907	1907
082FSW179	GOLDEN EAGLE	104	0	4385	3951	2028	1082	0	0	0	1925	1958
082FSW181	GOLD KING	7	0	621	341		0	51	0	0	1931	1940
082FSW182	BEAR	114	0	1897	4167		0	0	0	0	1937	1942
082FSW183	FERN (L.374)	11277	8619	16515	196448		0	0	0	0	1896	1942
082FSW184	CANADIAN BELLE	24	0	280	840		0	23	0	0	1939	1940
082FSW185	GOLDEN AGE	155	0	9673	1243	225	227	107	0	0	1928	1973
082FSW186	EUPHRATES	307	10	76543	14401	8246	5287	0	0	0	1928	1960
082FSW187	SECOND RELIEF	207022	205316	858347	3117637	1057	147	20210		0	1900	1959
082FSW188	HARRIET	144	0	1772	10265	0	0	0	0	0	1936	1941
082FSW189	PORTO RICO	5740	5528	46405	178470	138	51	322		0	1897	1969
082FSW190	SPOTTED HORSE (L.5375)	47	0	2083	1649	0	0	0	0	0	1901	1937
082FSW191	COMMODORE	45	0	7371	62	0	0	0	0	0	1940	1940

APPENDIX 3, CONTINUED

MINFILE No.	NAME	MINED (tonnes)	MILLED (tonnes)	silver (grams)	gold (grams)	lead (kg)	zinc (kg)	copper (kg)	cadmium (kg)	molybdenum (kg)	production (from - to)	
082FSW192	ELISE (L.1310)	5	0	9331	0	0	0	0	0	0	1896	1896
082FSW193	ARIZONA (L.13026)	296	230	7216	4604	0	0	0	0	0	1905	1946
082FSW194	YMIR BELLE	9	0	311	218	0	0	0	0	0	1899	1938
082FSW196	PILOT-GOOD HOPE	7	0	671	249	0	0	0	0	0	1905	1905
082FSW197	MYRTLE	25	0	2053	528	122	183	0	0	0	1934	1938
082FSW198	DEWEY (L.14431)	40	0	4915	156	1700	1786	0	0	0	1949	1952
082FSW199	HOWARD (L.12538)	20091	19806	1613871	212121	1059009	343307		68	0	1937	1970
082FSW200	CLUBINE	3616	0	239463	123293		818	0	0	0	1926	1942
082FSW201	SECOND CHANCE	10	0	155	280	0	0	0	0	0	1932	1934
082FSW202	KEYSTONE (L.5137)	1989	0	188044	84476	22744	21493	177	0	0	1901	1981
082FSW203	CANADIAN KING	440	0	80526	37976	1224	0		0	0	1900	1912
082FSW204	GOLD HILL	19	0	1027	560	0	0	0	0	0	1932	1942
082FSW205	ARLINGTON (L.3648)	69823	15182	4334578	1700339	520420	456920	0	0	0	1900	1970
082FSW207	SILVER DOLLAR	5607	0	1818469	50916	52597	60230	170		0	1947	1977
082FSW208	PERRIER	2027	256	94803	34681	14384	21144	0	0	0	1913	1946
082FSW209	CATHERINE (L.4437)	135	0	15240	5599	3717	1969	0	0	0	1928	1941
082FSW210	HUMMINGBIRD	97	0	6407	1959	1692	6126	0	0	0	1933	1960
082FSW219	ANNEX (L.14070)	763314	763314	34052093		7136975	42679634	16492	482244		1970	1975
082FSW222	WHITEWATER	40	0	1804	1151	0	0	0	0	0	1890	1933
082FSW257	DAVNE	4	0	5361	342	193	68	0	0	0	1938	1938
082FSW266	BEAVER CREEK	55	0	4976	560	0	0	0	0	0	1940	1941
082FSW267	ARMSTRONG	13	0	671	31	0	0	0	0	0	1939	1939
082FSW282	MONARCH (L.2082)	153	0	31103	529		0	4627	0	0	1918	1918
082FSW283	ALLOUEZ	12	0	4665		5443	0	0	0	0	1918	1918
082FSW286	SILVERINE (L.732)	82	0	2178	1493	0	0	0	0	0	1934	1944
082FSW295	MITZIE 1	59	0	1026	218		0	3538	0	0	1910	1910
082FSW299	RACHEL	0	14	3851	946	1335	0	0	0	0	1980	1980
082FSW310	EMERALD	28751	0	705292		6788936	19771	0	0	0	1906	1925
082FSW312	CARIBOU SHOWING	59	0	3670	584	0	0	0	0	0	1938	1940
082FSW359	HATTIE BROWN	29	0	21772		86	0	0	0	0	1909	1909
Note: Jersey produced 6232248 kg tungsten and Dodger, 1183818 kg tungsten.												
Rossland Camp												
082FSW093	LE ROI	2445376	0	52971737	34019495		0	44692881	0	0	1898	1942
082FSW094	CENTRE STAR	2065331	0	23147008	34164625		0	13366167	0	0	1897	1917
082FSW095	NICKEL PLATE	18685	0	335787	291778		0	209376	0	0	1901	1913
082FSW097	WAR EAGLE	300169	0	12036613	5659751		0	5021436	0	0	1898	1905
082FSW098	VIRGINIA (L.681)	95	0	1866	2395		0	943	0	0	1899	1899
082FSW099	IRON HORSE (L.795)	27	0		746		0	272	0	0	1903	1903
082FSW100	IRON COLT (L.796)	1434	1434	466	21586		0	0	0	0	1936	1995
082FSW102	EVENING STAR	2859	0	21521	56701		0	1276	0	0	1896	1939
082FSW105	BLACK BEAR (L.538)	1314	0	9891	5474		0	4214	0	0	1919	1919
082FSW110	COXEY	920136	939397		0	0	0	0	0	1748871	1966	1972
082FSW111	JUMBO (L.965)	30794	0	12347	435597		0	0	0	0	1903	1942

APPENDIX 3, CONTINUED

MINFILE No.	NAME	MINED (tonnes)	MILLED (tonnes)	silver (grams)	gold (grams)	lead (kg)	zinc (kg)	copper (kg)	cadmium (kg)	molybdenum (kg)	production (from - to)	
082FSW112	GOLD HILL (L.640)	9	0	31103	0	0	0	0	0	0	1894	1894
082FSW113	CALIFORNIA (L.956)	4131	0	23265	113246		0	1330	0	0	1898	1913
082FSW114	WHITE BEAR	17028	0	229104	72905		0	142064	0	0	1903	1920
082FSW115	SNOWDROP	6	0	16640	6843	0	0	0	0	0	1931	1957
082FSW116	I.X.L.	5292	54	270531	811746	256	154	8306		0	1899	1984
082FSW117	O.K.	293	0	14991	17916		0	154	0	0	1909	1939
082FSW118	GOLDEN DRIP	233	0	10910	12039	462	60	39		0	1923	1982
082FSW119	MIDNIGHT (L.1186)	5682	0	182978	245311	3925	2142	670	0	0	1927	1984
082FSW120	NORWAY (L.1626)	1	0	156	0	0	0	0	0	0	1936	1936
082FSW121	SPITZEE (L.2520)	5910	0	97290	55207		0	52264	0	0	1900	1905
082FSW123	HOMESTAKE (L.936)	236	0	74927	933		0	91	0	0	1901	1908
082FSW124	MONDAY (L.995)	64	0	13468		2226	3467	0	0	0	1937	1937
082FSW129	MABEL (L.1202)	23	0	1244	1058		0	694	0	0	1906	1906
082FSW131	ROBERT E. LEE	11	0		684		0	0	0	0	1896	1896
082FSW132	PHOENIX (L.953)	279	0	16016	4697		0	3212	0	0	1912	1942
082FSW134	ST. ELMO (L.923)	70	0	6874	93		0	1446	0	0	1908	1908
082FSW136	CLIFF (L.921)	1915	0	99530	14868		0	24195	0	0	1898	1936
082FSW142	HATTIE (L.1054)	21	0	1090	310	0	0	0	0	0	1934	1939
082FSW143	RICHMOND (L.1508)	11	0	14432	311	912	0	0	0	0	1912	1912
082FSW145	BLUE BIRD (L.1053)	7239	1211	3910823	12857	181088	207496	864	0	0	1908	1978
082FSW146	MAYFLOWER (L.799)	884	617	376780	4136	25785	49390		139	0	1907	1949
082FSW147	JOSIE (L.536)	568700	0	15544721	9792252		0	7965035	0	0	1898	1922
082FSW149	GEORGIA (L.928)	49	0	653	466	0	0	0	0	0	1933	1939
082FSW151	COLUMBIA-KOOTENAY	144	0		68520	0	0	0	0	0	1896	1904
082FSW152	CROWN POINT	714	0	6065	9456		0	3600	0	0	1905	1906
082FSW153	LILY MAY (L.1052)	37	0	18506	124	407	578	549		0	1910	1935
082FSW154	CURLEW (L.1220)	6	0	3608	62	0	0	0	0	0	1908	1908
082FSW155	RED EAGLE (L.1615)	6	0	4354		381	0	0	0	0	1908	1908
082FSW156	NATURE BOY	4	0	964		54	41	0	0	0	1949	1949
082FSW165	NEST EGG (L.1048)	72	0	1555	435		0	718	0	0	1907	1934
Totals (Rossland Camp):		**8405290**	**942713**	**109509814**	**85904623**	**215496**	**263328**	**71501796**	**139**	**1748871**		

APPENDIX 4
U-PB ZIRCON DATA, ROSSLAND-NELSON AREA

By Janet Gabites and Jim Mortenson,
The University of British Columbia

R313-4: ROSSLAND MONZONITE

Sample: R313-4, Rossland Monzonite

Collected by: T. Höy, 1990

Location: 082F/4; Zone 11, 444678E, 5435207N (Nad 87)
Located approximately 2.5 km southeast of Rossland, just east of Tiger Creek (*see* Figure 4-2, in pocket).

Sample description: Fine to medium-grained, fresh, granular, mafic phase of the Rossland monzonite.

Age problem: Confirmation of Middle Jurassic age for the Rossland monzonite, host and source for Rossland gold-copper veins.

Zircon description: About five kg of this relatively mafic variant of the Rossland Monzonite intrusion yielded abundant pale pink broken grains of zircon. The coarsest, best quality material was strongly abraded and then split into four fractions.

Interpretation: Concordant and overlapping fractions A and B provide the basis for the best age estimate of 167.5±0.5 Ma. Fraction C appears to contain minor inherited zircon and D has lost traces of Pb (Figure A4-1).

Data

Fraction[1]	Wt mg	U2 ppm	Pb*[3] ppm	$^{206}Pb/^{204}Pb$[4]	Pb[5] pg	^{208}Pb[6] %	Isotopic ratios (1σ,%) 7 $^{206}Pb/^{238}U$	$^{207}Pb/^{235}U$	$^{207}Pb/^{206}Pb$	Apparent ages (2σ,Ma) $^{206}Pb/^{238}U$	$^{207}Pb/^{206}Pb$
A c,N2,p,b	0.055	756	21	7133	10	15.7	0.02631 (0.09)	0.1793 (0.16)	0.04943 (0.09)	167.4 (0.3)	168.2 (4.4)
B c,N2,p,b	0.079	918	26	4860	25	17	0.02634 (0.12)	0.1794 (0.19)	0.04941 (0.09)	167.6 (0.4)	167.4 (4.3)
C c,N2,p,b	0.056	999	28	9711	10	16	0.02639 (0.09)	0.1801 (0.15)	0.04948 (0.09)	167.9 (0.3)	170.8 (4.0)
D c,N2,p,b	0.036	752	21	4544	10	16.3	0.02618 (0.10)	0.1785 (0.17)	0.04946 (0.12)	166.6 (0.3)	169.8 (5.4)

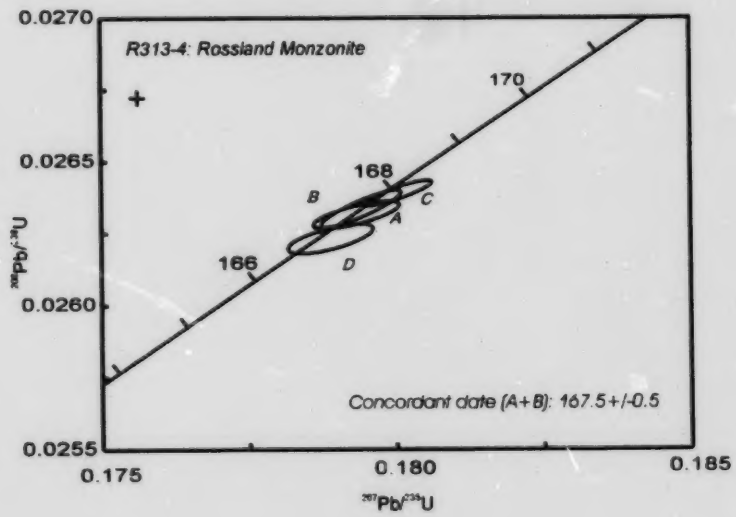

H88R-RDP: RAINY DAY PLUTON

Sample: H88R-RDP, Rainy Day pluton

Collected by: T. Höy, 1988

Location: 082F/4; Zone 11, 439398E, 5437671N (Nad 87)
Located along Highway 22 just west of Rossland (see Figure 4-2, in pocket)

Sample description: Medium-grained quartz diorite, porphyritic, cut by thin quartz veins that may contain minor molybdenite.

Age problem: The Rainy Day pluton is assumed to be related to quartz diorite dikes that host molybdenite mineralization on Red Mountain (see sample R96-5, Appendix 4).

Zircon description: Zircons are clear, colourless to pale tan prisms with some clear inclusions. The population contains two morphologies; long thin needles with aspect ratio of 1:4-6, and stubby, multifaceted tabular prisms. The short crystals were picked for analyses. The titanite is clear and pale yellow, occurring as platy shards which contain some inclusions.

Interpretation: Of the four zircon and three titanite fractions analyzed, all but two plot close to concordia between 160 and 170 Ma (Figure A4-2). A York regression through these fractions gives an upper intercept age of 174.6±3.6 Ma, which is likely the upper limit on the age. A weighted mean of the $^{206}Pb/^{238}U$ ages of fractions A and B, the most concordant fractions, gives the best estimate of the lower limit on the age of the rock, at 166.3±1.4 Ma. There appears to be only a very minor component of inherited old zircon in this rock. The titanites have probably lost lead, causing them to give younger $^{206}Pb/^{238}U$ ages.

Data

Fraction[1]	Wt	U2	Pb*[3]	$^{206}Pb/^{204}Pb$[4]	Pb[5]	^{208}Pb[6]	Isotopic ratios (1σ,%) 7			Apparent ages (2σ,Ma)[7]	
	mg	ppm	ppm		pg	%	$^{206}Pb/^{238}U$	$^{207}Pb/^{235}U$	$^{207}Pb/^{206}Pb$	$^{206}Pb/^{238}U$	$^{207}Pb/^{206}Pb$
A N2,+a abr	0.976	309	8	2450	203	11.4	0.02613 (0.43)	0.1786 (0.58)	0.04976 (0.27)	166.3 ±1.4	174.2 ±13
B M2, -a+d abr	0.328	717	19	5556	69	10.4	0.02608 (0.15)	0.1782 (0.23)	0.04956 (0.11)	166.0 ±3.4	174.3 ±5
C N2, -d+e abr	1.158	712	16	3067	355	9.8	0.02198 (0.39)	0.1481 (0.44)	0.04886 (0.14)	140.2 ±1.1	140.9 ±6
D M2, -d+e abr	0.623	722	19	3595	201	10.3	0.02564 (0.26)	0.1768 (0.34)	0.05001 (0.14)	163.2 ±0.8	195.5 ±6
F M2, -d+e	0.21	721	18	5026	49	9.2	0.02551 (0.13)	0.1744 (0.22)	0.04957 (0.12)	162.4 ±0.8	175.0 ±5
G Ti l	0.754	253	7	306	982	20	0.02327 (0.77)	0.1633 (0.96)	0.05089 (0.48)	148.3 ±0.8	236 ±22

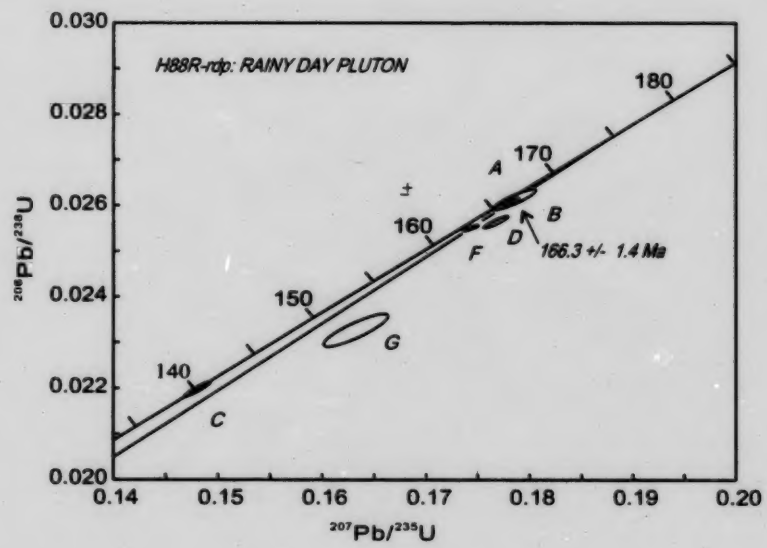

R96-5: RED MOUNTAIN DIORITE DIKE

Sample: R96-5, Red Mountain diorite dike

Collected by: T. Höy, 1996

Location: 082F/4; Zone 11, 439576E, 5437671N (Nad 87) Sample is located in the A pit on the western slopes of Red Mountain (see Figure 4-2, in pocket).

Sample description: Small, medium-grained, equigranular quartz diorite dike in the headwall of the A pit, intensely altered and cut by molybdenite veins.

Age problem: As the dike hosts the molybdenite mineralization on Red Mountain, a date restricts the age of this mineralization. It also restricts the age of the earlier Rossland copper-gold veins.

Zircon descriptions: Pale yellow, clear prismatic zircon with abundant clear inclusions was recovered from this sample.

Interpretation: Three analysed fractions give a lower intercept age of 162.3 +0.7/-1.0 Ma (Figure A4-3). An upper intercept of 1.5 Ga gives an estimate of the average age of inherited zircon in the analysed grains.

Data

Fraction[1]	Wt	U2	Pb*[3]	$^{206}Pb/^{204}Pb$[4]	Pb[5]	^{208}Pb[6]	Isotopic ratios (1σ,%) 7			Apparent ages (2σ,Ma)[7]	
	mg	ppm	ppm		pg	%	$^{206}Pb/^{238}U$	$^{207}Pb/^{235}U$	$^{207}Pb/^{206}Pb$	$^{206}Pb/^{238}U$	$^{207}Pb/^{206}Pb$
A cc,N2,p	0.135	435	11	7405	13	7.3	0.02587 (0.34)	0.1784 (0.48)	0.05002 (0.37)	164.7 (1.1)	196 (17.0)
B cc,N2,p	0.13	444	11	5636	17	7.2	0.02569 (0.12)	0.1759 (0.18)	0.04967 (0.11)	163.5 (0.4)	179.7 (5.0)
C cc,N2,p	0.11	431	11	5296	15	7.2	0.02600 (0.16)	0.1802 (0.22)	0.05027 (0.10)	165.5 (0.5)	207.7 (4.6)

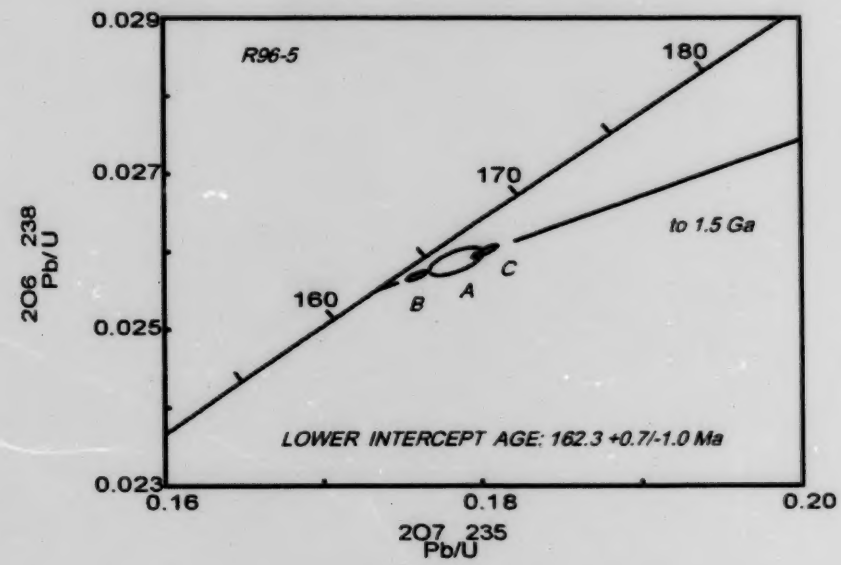

GUS-2: TERTIARY SILL

Sample: Gus-2, Tertiary sill

Collected by:T. Höy, 1997

Location: 082F/3, Zone 11, 476500E, 5441000N (Nad 87)

Sample description: Leucocratic, flow banded rhyolite dike or sill.

Age problem: This unit is one of a number of layer-parallel, rhyolitic sills within the Rossland Group; some of these have been interpreted to be rhyolite flows within the Middle Jurassic Elise Formation.

Zircon description: This sample yielded brown, translucent to opaque zircon with some visible growth zoning, and in some grains, visible cores. Five fractions were processed, of which three have been analysed .

Interpretation: Three analysed fractions indicate the presence of inherited zircon and, as is clearly demonstrated by fraction C, Pb loss. A two point regression through fractions A and D give a lower intercept age of 87.3 +1.2/-1.9 Ma (Figure A4-4).

Data

Fraction[1]	Wt mg	U2 ppm	Pb*[3] ppm	$^{206}Pb/^{204}Pb$[4]	Pb[5] pg	^{208}Pb[6] %	Isotopic ratios (1σ,%) 7			Apparent ages (2σ,Ma) 7	
							$^{206}Pb/^{238}U$	$^{207}Pb/^{235}U$	$^{207}Pb/^{206}Pb$	$^{206}Pb/^{238}U$	$^{207}Pb/^{206}Pb$
A m,M20,p,s	0.016	9759	137	281	529	10.8	0.01392 (0.24)	0.0924 (0.77)	0.04813 (0.61)	89.1 (0.4)	105 (29)
C ff,M20,p,s	0.016	7766	106	328	343	11.4	0.01341 (0.20)	0.0895 (0.65)	0.04838 (0.52)	85.9 (0.3)	118 (25)
D m,N20,p,s	0.06	9989	158	316	2015	10.2	0.01574 (1.1)	0.1098 (2.2)	0.05058 (1.1)	100.7 (2.2)	222 (51/52)
E f,N20,p,s	0.1	9786	138	199	4798	11	0.01390 (0.37)	0.0954 (1.1)	0.04977 (0.85)	89.0 (0.6)	185 (39/40)
F ff,N20,p,s	0.097	10637	152	856	1108	10.7	0.01410 (0.21)	0.0943 (0.36)	0.04848 (0.23)	90.3 (0.4)	123 (11)

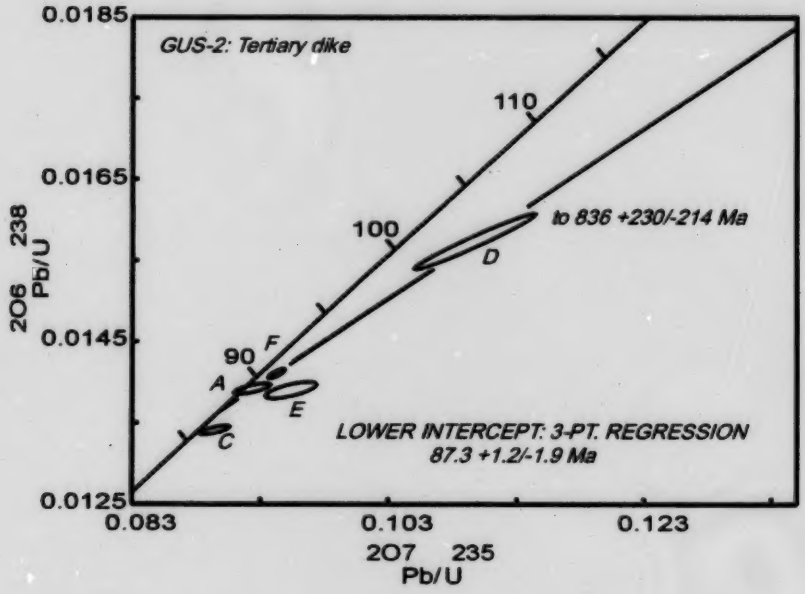

NOTES

Analytical techniques are listed in Mortensen *et al.* (1995).

[1]Upper case letter = fraction identifier; All zircon fractions air abraded: 10-30% of outer portions of grains removed; Grain size, intermediate dimension: cc= >180 μm and <134μm, c=<180 μm and >134μm; m=<134μm and >104μm; f= < 104μm and > 74μm; f f= < 74μm and >62μm; Magnetic codes:Franz magnetic separator sideslope at which grains are nonmagnetic (N) or Magnetic (M); *e.g.*, N1=nonmagnetic at 1°; Field strength for all fractions =1.8A; Front slope for all fractions=20°; Grain character codes: b= broken fragments, e=elongate, eq=equant multifaceted ,ov=ovoid; p=prismatic, s=stubby, t=tabular, ti=tips; Additional codes for detrital single grains: Colour: co=colourless; pp= pale pink; vp = vivid pink; py= pale yellow; tan = tan; Clarity; cl = clear; tr = translucent;

[2] U blank correction of 1pg ± 20%; U fractionation corrections were measured for each run with a double ^{233}U-^{235}U spike (about 0.004/amu).

[3]Radiogenic Pb

[4]Measured ratio corrected for spike and Pb fractionation of 0.0035/amu ± 20% (Daly collector) and laboratory blank Pb of 2-10 pg ± 20%. Laboratory blank Pb concentrations and isotopic compositions based on total procedural blanks analysed throughout the duration of this study.

[5]Total common Pb in analysis based on blank isotopic composition

[6]Radiogenic Pb

[7] Corrected for blank Pb, U and common Pb. Common Pb corrections based on Stacey Kramers model (Stacey and Kramers, 1975) at the age of the rock or the $^{207}Pb/^{206}Pb$ age of the fraction.

REFERENCES

Mortenson, J.K., Ghosh, D.K. and Ferri, F. (1995): U-Pb geochronology of intrusive rocks associated with copper-gold porphyry deposits in the Canadian Cordillera; in Porphyry Deposits of the Northwestern Cordillera of North America, Schroeter, T.G., Editor, *Canadian Institute of Mining, Metallurgy and Petroleum*, Special Volume 46, pages 142-158.

Stacey, J.S. and Kramers, J.D. (1975): Approximation of terrestrial lead isotopic evolution by a two-stage model; *Earth and Planetary Science Letters*, volume 26, pages 207-221.

APPENDIX 5
PETROGRAPHIC REPORT ON THIN AND POLISHED THIN SECTIONS FROM ROSSLAND CAMP, BC

By Craig H.B. Leitch, P.Eng, P.Geo
492 Isabella Point Road, Salt Spring Island, B.C. V8K 1V4

(Note: locations are given in Appendix 2, and analyses of many of these samples in Appendix 6)

SUMMARY:

This is a suite of mainly skarn-altered rocks, in many cases with a visible intrusive igneous protolith. Semi-massive to locally massive sulfides are common in the samples, grading in some cases to vein- or fracture-controlled sulfides. The samples can be roughly divided into several general types:

1) Clinopyroxene-feldspar (±garnet) skarn, commonly retrograded to an assemblage containing actinolitic amphibole±epidote, quartz, sphene chlorite, carbonate generally closely associated with sulfide minerals (samples R96-12c, 39a, 48a, 51c, 68, 7a, 28a, 12a, 4b, 45e). Feldspar in these samples ranges from calcic plagioclase (?bytownite) through andesine to albite and probable ?K-feldspar.
2) Amphibole (?actinolite/tremolite)-biotite-epidote-quartz-sphene-apatite-carbonate±chlorite-relict feldspar, with sulfides generally closely related to the skarn minerals; these could be in part more altered versions of 1) above (samples R96-19b, 46a, 53c, 60b, 24c, 35b, 67d, 31c). Feldspar ranges from sericitized alkali feldspar (?albitic or oligoclase to ?K-feldspar); dark (schorlitic) tourmaline is important in 46a, and ?allanite (REE-bearing epidote) in 24c.
3) Massive sulfides, mainly pyrrhotite-pyrite-chalcopyrite; may contain magnetite, sphalerite and arsenopyrite (samples R96-35c, 60c, 65a, 66a, 67a, 67c, 74), and rare molybdenite (R96-12c, 7a), marcasite (R96-67a), and galena and sulfosalt such as ?boulangerite (R96-66a, 67a). Gangue inclusions in these samples include actinolite/tremolite-calcite-quartz-biotite-chlorite-sericite-sphene-apatite-sericitized feldspar (plagioclase to ?K-feldspar)-garnet-tourmaline; in other words, these samples grade to the skarn types above with decrease in the amount of sulfides present, and this division is purely arbitrary.
4) Other: R96-25b is a ?plagioclase-quartz- biotite- magnetite±apatite assemblage after a ?mafic sill cut by stringers of quartz-pyrrhotite-chalcopyrite ± pyrite, tourmaline, magnetite and sphalerite. Sample R96-62b is a ?fine ash tuff or metasediment (?plagioclase- amphibole-biotite-epidote-sphene) cut by arsenopyrite-?Kspar-epidote veins with silicified envelopes. Minor oxidation to limonite is noted in many samples.

SAMPLE: R96-7a

Deposit: Novelty

Summary: Plagioclase-pyroxene ?skarn altered rock retrograded to calcite actinolite and chalcopyrite near a pyrrhotite-molybdenite vein.

Hand sample description: Biotite hornfels, but with appreciable quartz, siliceous alteration, and intergrowth of molybdenite and pyrrhotite (which is magnetic) plus minor chalcopyrite. The wallrock away from the vein shows minor reaction to cold dilute HCl.

Petrography:
Modal mineralogy in thin section:

Plagioclase (?andesine and vein albite) 65%

Clinopyroxene (?diopside) 20%

Amphibole (secondary, ?Fe-rich actinolite) 5%

Opaques (pyrrhotite, molybdenite, chalcopyrite) 5%

Sphene 2%

Carbonate (?calcite) 2%

Sericite <1%

Apatite <1%

This slide consists essentially of fine to medium-grained plagioclase containing scattered fine to medium-grained crystals of clinopyroxene (also found along narrow veinlets), minor but significant sphene and traces of opaques and apatite. Extinction on 010 in the plagioclase up to 22 degrees suggests a composition as calcic as andesine. The rock is probably the result of skarn alteration of an originally intermediate to mafic igneous rock.

A pyrrhotite-rich vein contains a narrow selvage of molybdenite; the envelope contains pyrrhotite and chalcopyrite. The vein contains alkali feldspar (?albite) and minor sericite (after? feldspar). In association with the wallrock sulfides, pyroxene is altered to dark green (Fe-rich) amphibole, probably actinolite, and traces of fine-grained carbonate (? calcite).

SAMPLE: R96-12a

Deposit: Mountain View, E pit

Summary: Massive garnet±clinopyroxene skarn with interstitial/fracture-controlled pyrrhotite-chalcopyrite; minor tremolite-quartz-carbonate.

Hand sample description: Diopside-biotite-amphibole skarn with fine, fracture-controlled pyrrhotite and chalcopyrite; it is magnetic, but shows no reaction to cold dilute HCl.

Petrography:
Modal mineralogy in thin section:

Garnet 85%
Opaques (pyrrhotite, chalcopyrite) 10%
Clinopyroxene (diopside) 3-5%
Amphibole (secondary, ?tremolite) <1%
Quartz, carbonate (veinlets) <1%

Massive garnet forms euhedral crystals up to 3 mm in diameter that in places poikilitically enclose or are intergrown with clinopyroxene crystals. Sulfides are primarily interstitial to the silicate minerals or in abundant extremely fine networks of fractures cutting the silicates. Clinopyroxene forms coarse subhedra up to 2.5 mm across; the crystals are fractured/veined by sulfides and pale amphibole (?tremolite) plus traces of sericite. In places the pyroxene is partly replaced by sheaf-like fibrous ?tremolite that is partly stained by limonite from oxidation of sulfides. Traces of quartz and carbonate occur in other veinlets cutting the rock that also contain significant sulfides (mainly pyrrhotite).

Photo A5-1. Sample R96-12c, Mountain View deposit, E pit: Photomicrograph quartz±Kfeldspar altered rock cut by veins of clinopyroxene (cpx) -garnet (gt) -Fe carbonate, in places associated with or forming a border around molybdenite (opaque) and ?wollastonite (wo); transmitted light, uncrossed polars, field of view 2.5 mm.

SAMPLE:R96-12c

Deposit: Mountain View, Pit E

Summary: Quartz - Kspar - clinopyroxene - garnet - Fe carbonate - molybdenite- ?wollastonite - ?zoisite skarn (minor retrograde amphibole).

Hand sample description: Hand specimen is a fine-grained grey, green, buff and pinkish skarn or calc-silicate hornfels cut by irregular stringers and fractures filled with molybdenite. Calcite is abundant along a network of late white fractures that also appear to contain a white bladed mineral such as ?zeolite or wollastonite. The rock is not magnetic.

Petrography:
Modal mineralogy in polished thin:

Quartz (largely secondary) 5%
K-feldspar (largely secondary) 0%
?Clinopyroxene 10%
Molybdenite 5%
Garnet 5%
Carbonate (?mainly Fe-calcite) 3%
Unidentified (?wollastonite) 1-2%
Amphibole (?actinolite) <1%
?Zoisite <1%
Ilmenite, sphene/rutile±pyrite <1%

In general, this section consists of granular quartz containing patches of feldspar that in places is loosely associated with garnet, cut by stringers of clinopyroxene that are in places associated with molybdenite (Photo A5-1). Carbonate, possibly ferroan as indicated by minor limonite stain in thin section, is associated with the skarn minerals (pyroxene, garnet) but also found along more through-going fractures.

Quartz crystals are sub- to anhedral, mostly <1 mm in diameter, and strongly fractured, with minor undulose extinction. Feldspar forms rounded to subhedral crystals up to 2 mm in diameter that are untwinned and have negative relief compared to quartz, suggesting K-feldspar. Most is probably secondary; it occurs in irregular patches and along veinlets, in places forming very fine-grained (20 micron) aggregates. The white colour in hand specimen indicates an absence of fine hematite usually found in K-feldspar that causes the salmon-pink colour.

Crystals of the mineral tentatively identified as ?clinopyroxene are generally so small (<0.1 mm in maximum dimension) that it is difficult to be sure of their identity. However, they have moderate birefringence, strong positive relief, and approximately 45° extinction. Rare retrograding to a dark green amphibole (extinction angle about 25 degrees) supports the identification of pyroxene.

Molybdenite is the main opaque phase, forming sub- to euhedral flakes up to 0.25 mm in diameter intergrown with the ?pyroxene garnet and in places carbonate. In the semi-massive molybdenite patch at one corner of the slide, molybdenite is intergrown with major amounts of another mineral that is unidentified (similar in relief to the ?pyroxene, but with uniformly low birefringence and with small extinction angle near 30°, suggesting ?wollastonite), and minor amounts of ?zoisite (anomalous blue birefringence) and carbonate. At the margins of this semi-massive molybdenite area, molybdenite is fringed by ?pyroxene and garnet. A few subhedral crystals of ?ilmenite up to 0.25 mm across are mixed with the molybdenite; elsewhere, former ?ilmenite laths up to 1 mm long are altered to a mixture of fine-grained sphene, rutile and traces of pyrite.

SAMPLE: R96-19b

Deposit: Mountain View, F Pit

Summary: Quartz - actinolite / epidote (after biotized mafics) skarn with abundant pyrrhotite-magnetite-pyrite-chalcopyrite.

Hand sample description: Semi-massive pyrrhotite-pyrite-chalcopyrite in greenish-grey, fine-grained, siliceous ?skarn matrix. The rock is strongly magnetic but shows no reaction to cold dilute HCl.

Petrography:
Modal mineralogy in polished thin:
Quartz (secondary) 35%
Amphibole (?tremolite-actinolite) 25%
Pyrrhotite 10%
Pyrite 10%
?Magnetite 5%
Epidote-group (including ?zoisite) 5%
Relict biotite 5%
Chalcopyrite 3-5%
Apatite <1%

This slide consists essentially of irregularly shaped patches of mafic minerals and sulfides hosted in and cut by a matrix of quartz (also in places with sulfides). The mafic minerals comprise cores of brown biotite surrounded by pale green amphibole plus epidote (?clinozoisite and ?zoisite); sulfides are primarily fine-grained pyrrhotite (intimately mixed with ?magnetite) surrounding cores of coarse pyrite and lesser chalcopyrite (Photo A5-2). Sulfide and oxide minerals appear to rim what may have been formerly coarse mafic crystals with rounded to subhedral outlines up to 4 mm long.

At the cores of these ?relict mafic crystals, biotite forms pale to medium brown subhedral to ragged (?corroded) flakes mainly <0.15 mm in diameter that appear to be altered to the surrounding amphibole (lath-like subhedra mostly <0.25 mm long with pale green pleochroism suggesting ?tremolite-actinolite). In places various epidote-group minerals are present as sub- to euhedral crystals up to 0.15 mm long, with either strong birefringence and pale yellow pleochroism (?clino-zoisite) or weak, anomalous blue birefringence and no pleochroism (?zoisite). Minor ? apatite occurs with the epidote-group minerals, forming 0.1 mm long stubby prisms that reinforce the idea that former mafic mineral sites are replaced. Rare garnet forms irregular masses up to 0.5 mm across associated with margins of the mafic relics.

Pyrrhotite occurs as sub- to anhedral crystals <0.25 mm in diameter, partly oxidized in places (?along retrograde fractures) to supergene FeS phases with "bird's-eye" textures. The ?magnetite occurs as fine (<0.1 mm) sub- to anhedral crystals that are opaque, arguing against sphalerite with a very high Fe content. In many cases the ?magnetite forms a ?reaction rim around pyrrhotite, separating it from silicates. Pyrite forms coarse sub- to euhedral crystals up to several mm in diameter, intergrown at margins with subhedral chalcopyrite up to almost 1 mm in diameter.

The matrix that consists of coarse, rounded to subhedral quartz crystals in places contain inclusions of radiating needles of pale green amphibole and pale brown biotite. In places these needles are aligned, giving an erroneous impression of twinned plagioclase. Minor Fe-stained carbonate (?ankerite or siderite) occurs as rosettes up to 20 microns diameter, surrounding and ?replacing the margins of sulfides along the late retrograde fractures.

SAMPLE: R96-24c

Photo A5-2. Sample R96-19b, Mountain View deposit, F pit: Euhedral pyrite (py) in intermixed pyrrhotite (po) and chalcopyrite (cp) plus some magnetite (mt); gangues are mostly quartz (qz), and actinolite (ac) and epidote (ep) close to sulfides; reflected and part transmitted light, uncrossed polars; field of view 2 mm.

Deposit: Le Roi dump

Summary: Actinolite-biotite±chlorite altered intermediate rock; quartz actinolite-pyrrhotite-chalcopyrite±?allanite veining.

Hand sample description: Pyrrhotite and chalcopyrite vein in altered Rossland sill. The rock is magnetic but shows no reaction to cold dilute HCl.

Petrography:
Modal mineralogy in thin section:
Plagioclase (phenocrysts, groundmass) 45%
Amphibole (secondary, ?actinolite) 30%
Biotite (?largely secondary) 5%
Quartz (partly secondary, in veins) 5%
Opaques (pyrrhotite, chalcopyrite) 3%
Chlorite 1-2%
?Allanite or REE-bearing epidote <1%
Apatite, rutile <1%

Relict plagioclase phenocrysts and biotite-actinolite±chlorite altered relict mafic phenocrysts, both up to 1.5 mm in size, are visible in a matrix of fine-grained feldspar and minor biotite, actinolite and opaques. Fine-grained sulfides (mainly pyrrhotite and chalcopyrite) are closely associated with the altered mafic sites. Most sulfide mineralization is present along irregular veinlets containing minor quartz and associated with the strong actinolite alteration. Traces of rutile occur in altered biotite; minor apatite is also associated with altered mafic sites. Rare clots of strongly pleochroic ?allanite are found with actinolite veining.

SAMPLE: R96-25b

Deposit: Le Roi dump

Summary: Relict ?mafic sill (?plagioclase - biotite - magnetite - apatite) cut by stringers of quartz - pyrrhotite - chalcopyrite - tourmalinite - pyrite.

Hand sample description: A mineralized sill; dark grey, fine-grained, partly siliceous rock with a vague fragmental

texture caused by faintly visible rounded ?clasts up to 1 cm in diameter, cut by narrow stringers of magnetite, pyrrhotite and chalcopyrite (rare pyrite). The rock is strongly magnetic but shows no reaction to cold dilute HCl.

Petrography:
Modal mineralogy in polished thin:

?Plagioclase feldspar 35%

Quartz (secondary) 30%

Biotite 15%

Pyrrhotite 10%

Magnetite 5%

Chalcopyrite 3%

Tourmaline (schorl) 1%

Pyrite <1%

Apatite <1%

Sphalerite tr

This slide consists essentially of coarse-grained quartz in what appear to be mostly veinlets cutting and replacing areas of fine-grained ?feldspar, biotite opaques and minor apatite (?representing relict wallrock). Fine-grained to disseminated sulfides and magnetite occur in the relict wallrock; minor coarser-grained sulfides occur in the quartz veinlets. Most coarse-grained sulfides occur in the cross-cutting sulfide stringers (with minor magnetite) (Photo A5-3).

Quartz crystals are interlocking subhedra usually less than about 0.5 mm in diameter; they show little strain (almost no undulose extinction or fracturing). In the fine-grained relict wallrock areas, slightly negative relief of most of the small (mainly <50 micron) subhedral lath-shaped crystals suggests they may be ?albitic plagioclase feldspar. They are intimately intergrown with similar-sized to slightly larger euhedral flakes of brown biotite and lesser pyrrhotite plus magnetite (subhedra to 0.3 mm). Rare chalcopyrite forms crystals up to 0.1 mm in diameter. Rare coarse dark green (schorl) tourmaline forms radiating sheaves of sub- to euhedral crystals up to 0.5 mm long, or separate crystals to 1 mm, closely associated with stringer sulfides.

Photo A5-3. Sample R96-25b, Le Roi deposit: Stringer of quartz-pyrrhotite-chalcopyrite-magnetite-pyrite-tourmaline (tm) cutting finer-grained plagioclase-quartz-biotite (bi) altered ?mafic sill; reflected and part transmitted light, uncrossed polars, field of view 2 mm.

In the sulfide stringers, pyrrhotite forms subhedra up to 1.5 mm long associated with masses of chalcopyrite; traces of sphalerite form inclusions in the chalcopyrite. Pyrrhotite contains rare euhedra of magnetite up to 0.3 mm in diameter and minor euhedral pyrite up to 1 mm in diameter; in places, magnetite contains subhedral inclusions of chalcopyrite.

As the field notes indicate, this sample is a quartz-biotite altered ?mafic sill (the abundance of biotite and magnetite, and presence of apatite support this interpretation). Sulfide mineralization appears to be associated with quartz stringers and Fe-rich (schorl) tourmaline, possibly overlapping or overprinting magnetite.

SAMPLE: R96-28a

Deposit: Jumbo

Summary: Layered clinopyroxene-quartz pyrrhotite skarn.

Hand sample description: Massive pyrrhotite in dark green granular matrix; strongly magnetic but no reaction to cold dilute HCl.

Petrography:
Modal mineralogy in thin section is simple:

Clinopyroxene (?diopside) 65%

Quartz (secondary) 25%

Opaque (pyrrhotite) 10%

Limonite <1%

?Zoisite <1%

About 2/3 of this slide consists of fine to coarse granular clinopyroxene (?diopside) with minor pyrrhotite; the other 1/3 contains significant quartz in addition to pyroxene and pyrrhotite. There is a vaguely layered appearance due to a 1 cm thick band of almost monomineralic pyroxene across the center of the slide, followed by a transition to quartz-rich rock across a gradational contact. In the quartz-rich rock, large (to 1 mm) anhedral crystals or aggregates of quartz enclose both pyroxene and sulfides poikilitically. Traces of ?zoisite surround some of the larger sulfide grains; rarely sulfide occurs along narrow veinlets. Partial oxidation of sulfides has produced minor limonite along fractures.

SAMPLE: R96-31c

Deposit: War Eagle

Summary: Amphibole-biotite-pyrrhotite/pyrite-quartz-sphene altered zones in plagioclase-rich intermediate intrusive rock.

Hand sample description: Pale green biotite-chlorite-epidote-plagioclase with dark biotite-chlorite-pyrrhotite network. Rock is magnetic but shows no reaction to cold dilute HCl.

Petrography:
Modal mineralogy in thin section:

Plagioclase (altered) 40%

Amphibole (secondary, ?actinolitic) 25%

Biotite (secondary) 25%

Opaque (pyrrhotite, pyrite) 1-2%

Quartz (secondary, veinlets) 1-2%

Sphene 1%

Clay-sericite (after plagioclase) <1%

Apatite <1%

The bulk of this rock consists of intermediate intrusive (plagioclase, mafic relics) that is cut by zones of more intense, texture-destructive alteration to secondary biotite and amphibole plus minor sulfides. Plagioclase forms small subhedral ?relict phenocrysts up to 1 mm in diameter with an altered appearance suggestive of ?albitization plus abundant fine flakes of clay-sericite, secondary biotite, amphibole and sphene. Former mafic crystals of similar size are altered to secondary biotite and amphibole plus minor sphene and rare apatite. In the most intensely altered zones, brown biotite is replaced by greenish (?Fe-rich) biotite and deeper green (?more Fe-rich) actinolitic amphibole; at the centers of these zones, sulfides (pyrrhotite surrounding cores of pyrite) are associated with a little secondary quartz. Note that chlorite and epidote are absent in thin section.

SAMPLE: R96-35b

Deposit: Centre Star

Summary: Amphibole-biotite-epidote-pyrrhotite+quartz, clay/sericite, chlorite-altered intermediate intrusive rock.

Hand sample description: Contact of vein - fractured, rusted dark (biotite)-quartz hornfels alteration and chlorite-pyrrhotite veins. The rock is magnetic but shows no reaction to cold dilute HCl.

Petrography:
Modal mineralogy in thin section:

Plagioclase (?oligoclase; altered) 65%

Amphibole (secondary, ?actinolite) 15%

Biotite (partly secondary; rare chlorite) 10%

Opaque (pyrrhotite, limonite) 3%

Epidote (?clinozoisite) 2-3%

Clay-sericite (after plagioclase) 2-3%

Sphene 1-2%

Quartz (secondary) 1%

Apatite, allanite (?) <1%

This is a typical fine-grained intermediate intrusive rock (Rossland monzonite), composed of altered plagioclase and mafic relics with a hypabyssal (high-level) texture. Plagioclase forms subhedra ranging from <0.1 mm to almost 1 mm in diameter, with extinction angle and relief suggesting sodic oligoclase near albite (probably a secondary composition), and partly altered to fine clay-sericite and minor (secondary) biotite. The secondary biotite, which also affects former mafic crystals (where it is associated with minor sphene and traces of apatite), is greenish (more Fe-rich) or brown (magnesian); it forms very fine flakes. Only rarely is biotite chloritized. Amphibole is also common as a secondary mineral, forming subhedra to 0.35 mm that replace whole sections of the rock but are particularly concentrated along fractures, closely associated with the sulfides (pyrrhotite, partly oxidized to limonite) and minor secondary quartz, colourless epidote (?Fe-poor, clinozoisite) and brown ?allanite.

SAMPLE: R96-35c

Deposit: Centre Star

Summary: Massive pyrrhotite-pyrite- chalcopyrite-magnetite with "augen" of calcite-quartz-actinolite-biotite-?sericitzed feldspar.

Hand sample description: Massive sulfide vein, essentially pyrrhotite with coarse euhedral pyrite and traces of chalcopyrite. The rock is weakly magnetic, and contains rounded patches or "augen" of carbonate that react strongly to cold dilute HCl.

Petrography:
Modal mineralogy in polished thin section:

Pyrrhotite 55%

Pyrite 20%

Carbonate (?mainly calcite) 10%

Quartz (secondary) 5%

Amphibole (?actinolite) 2-3%

Chalcopyrite 2-3%

Magnetite 2-3%

Biotite 1-2%

Feldspar (?sericitized plagioclase) 1-2%

Pyrrhotite forms a matrix to irregular-shaped masses of pyrite with minor chalcopyrite, or carbonate or carbonate-quartz. Scattered grains of magnetite are also found in the pyrrhotite.

Pyrrhotite forms subhedral to anhedral crystals up to about 0.4 mm in diameter in a granular aggregate, with fairly common triple junctions suggesting annealing after deformation. Most crystals show incipient alteration or oxidation along cleavages and margins. Intergrown magnetite forms skeletal or sieve-textured crystals with subhedral outlines up to 1 mm in diameter. Inclusions are mainly pyrrhotite and chalcopyrite (not pyrite).

Pyrite occurs as large, mainly euhedral crystals up to several mm in diameter that appear to have overgrown all other minerals (they now contain rounded inclusions of pyrrhotite, chalcopyrite, magnetite, and gangue carbonates and silicates; Photo A5-4). Small aggregates of carbonate containing minute inclusions of ?sphene are along margins of the pyrite masses.

Chalcopyrite generally occurs as irregular masses or subhedral crystals up to 0.7 mm across, and in veinlets cutting the pyrite masses. This does not necessarily indicate that chalcopyrite formed later than pyrite; it commonly indicates the greater ease of recrystallization and therefore remobilization of chalcopyrite compared to the brittle pyrite. Minor chalcopyrite also occurs intergrown with pyrrhotite, but usually only around the edges of pyrite crystals.

In the rounded "augen" of gangue minerals, carbonate (likely calcite) forms subhedral to rounded (granular, crushed-looking) crystals mostly <0.5 mm in diameter (visible in hand specimen). Variable amounts of fine-grained

Photo A5-4. Sample R96-35c, Centre Star deposit: Subhedral, sieve-like pyrite in matrix of magnetite-pyrrhotite and minor chalcopyrite; silicate inclusions are quartz-calcite-actinolite-biotite-sericitized feldspar (not distinguishable in reflected light); uncrossed polars; field of view 2 mm.

quartz and other silicates are also present; quartz forms rounded to subhedral crystals, some displaying triple junctions with adjoining quartz crystals. Lesser pale green amphibole with small extinction angle near 18 degrees (?actinolite) form ragged subhedra to 0.25 mm in size; most are partly altered at margins and along cleavages to limonite. Rare biotite forms small subhedral flakes or patches of smaller flakes that look secondary (after some other mafic mineral). In places there are also aggregates of fine-grained, partly sericitized ?feldspar, likely plagioclase.

SAMPLE: R96-39a

Deposit: Kootenay - (Columbia) waste dump.

Summary: Clinopyroxene- ?plagioclase -?skarn, retrograded to actinolite associated with stringery pyrrhotite-chalcopyrite-?Kfeldspar.

Hand sample description: Dark green, skarny, mafic-looking rock with abundant fine to medium-grained disseminated to stringer sulfides (mainly pyrrhotite and chalcopyrite). The rock is strongly magnetic but shows no reaction to cold dilute HCl.

Petrography:
Modal mineralogy in polished thin section:

Clinopyroxene (?diopside) 40%

Secondary amphibole (?actinolite) 30%

Relict ?plagioclase feldspar 15%

Pyrrhotite 10%

?K-feldspar (secondary) 3%

Chalcopyrite 1-2%

Sericite, ?clay (after plagioclase) 1%

Magnetite <1%

This slide is composed mostly of coarsely crystalline clinopyroxene, partly to largely altered to amphibole, with interstitial relict feldspar (likely plagioclase), sulfides, and magnetite. Where sulfide concentrations are greatest there is a transition from disseminated to net-textured (matrix) sulfides, or stringer sulfides.

Clinopyroxene forms elongated, feathery to lath-shaped crystals up to 4 mm long with approximately 40-45 degree maximum extinction angle. Most crystals are colourless, suggesting an Fe-poor variety such as diopside. Alteration is extensive to needle- or lath-shaped, finer grained, strongly pleochroic dark green amphibole (likely actinolite) crystals that are mainly less than 0.3 mm long. In places a second, almost colourless amphibole occurs (?tremolite).

Interstitial ?feldspar lacks euhedral shapes since it fills spaces, and does not display twinning. Most is relatively fine-grained, occurring together in patches with vague outlines up to 1.5 mm in size that likely represent former ?plagioclase crystals. Clouding and alteration to fine clay-sericite-limonite is common; inclusions of needle-like actinolite are also common. Minor ?K-feldspar is intergrown with amphibole and sulfides; the ?K-feldspar is difficult to compare relief with the ?plagioclase due to alteration of the latter. This may be a former mafic rock such as gabbro, or diopside skarn, that has been altered or retrograded to secondary amphibole.

Sulfides appear to be most closely associated with amphibole as is usual in skarn systems; however, in places poikilitic crystals of chalcopyrite up to 1 mm across are intergrown with pyroxene. Pyrrhotite forms subhedral to irregular crystals up to 0.75 mm in diameter, commonly intergrown with sub- to anhedral chalcopyrite. Pyrrhotite commonly shows partial oxidation to intermediate (transitional) FeS phases along cleavages, rims and fractures. Rare magnetite is intergrown with the sulfides, but the amount seen does not explain the observed strong magnetism of the rock, suggesting that some of the pyrrhotite is also magnetic.

SAMPLE: R96-45e

Deposit: Evening Star

Summary: Clinopyroxene-epidote- actinolite- arsenopyrite-sphene veins cutting Kfeldspar(?)-quartz altered intrusive rock, late carbonate.

Hand sample description: Skarn with pervasive epidote-?diopside cut by sulfide-pale green (pyroxene-epidote) and dark green (amphibole) veins (that also show reaction to cold dilute HCl). Hand specimen shows that sulfide is mostly arsenopyrite; minor pyrrhotite is magnetic.

Petrography:
Modal mineralogy in thin section:

?K-feldspar 35%

Arsenopyrite 20%

Clinopyroxene (?diopside) 20%

Epidote/clinozoisite 15%

Amphibole (secondary, ?actinolite) 5%

Quartz (secondary) 2-3%

Carbonate (calcite) 1-2%

Pyrrhotite 1%

Sphene <1%

The rock consists mainly of alkali feldspar (likely Kfeldspar), forming interlocking, irregular-shaped anhedra up to 1.5 mm diameter with strong secondary appearance (sub-grain development, poikilitic inclusions). Patches and vein-like areas of clinopyroxene and epidote (some pyroxene may be altered to epidote) are closely associated with the semi-massive to vein-like arsenopyrite. In places the pyroxene is altered to fibrous dark green amphibole (?actinolite) that is also associated with the sulfides and, locally, coarsely crystalline sphene.

SAMPLE: R96-46a

Deposit: Monte Christo (North belt vein)

Summary: Pyrrhotite-chalcopyrite-magnetite in alkali feldspar-green mica-?actinolite skarn, stringers of sulphide-calcite-quartz-tourmaline.

Hand sample description: Mainly "massive sulfide" (pyrrhotite, chalcopyrite, magnetite) in dark green matrix. The rock is strongly magnetic and shows moderate reaction to cold dilute HCl.

Petrography:
Modal mineralogy in polished thin section:

Pyrrhotite 35%

Feldspar (?secondary, albitic) 25%

Green mica, sericite 20%

Amphibole (?tremolite-actinolite) 5%

Quartz (secondary) 5 %

Carbonate (mainly calcite) 2-3%

Magnetite 2-3%

Chalcopyrite 2-3%

?K-feldspar (secondary) 2-3%

Tourmaline (schorl) <1%

This slide consists of areas of pyrrhotite and areas of silicate gangue (mostly sericitized ?plagioclase mixed with a pale green mica). Rarely observed twinning with extinction near 15 degrees suggests an albitic alkali feldspar near An0-5. Around sulfide clots, feldspar is commonly clear/less cloudy (?K-feldspar), but it is difficult to see any relief difference between it and the major alkali feldspar making up the rock.

The bulk of the feldspar may actually be a secondary alkali feldspar of mainly albitic composition; it forms small subhedral crystals that are commonly composed of finer-grained sub-domains, suggesting a secondary (or recrystallized) origin. Sericite flakes in the feldspar are mainly subhedral; they make up (replace) as much as 40% of the feldspar crystal, grading at the margins of the feldspar crystals to larger, sub- to euhedral flakes of pale green mica (like muscovite/sericite but probably phengitic, *i.e.* with significant iron; some could be transitional to "green biotite", an Fe-rich biotite). Vaguely defined areas of the green mica in places suggest replacement of former ?amphibole crystals. Adjacent to the major pyrrhotite masses, needle-like laths up to 0.15 mm long of amphibole (deeper green, slightly oblique extinction) are seen. Also in these areas, there are clusters of subhedral quartz crystals and sporadic crystals of bright blue tourmaline (likely Fe-rich schorl) as euhedra to 0.15 mm long.

Masses of pyrrhotite up to several cm across are composed of subhedral crystals up to about 1 mm in diameter. Magnetite occurs as common rounded to subhedral inclusions of <0.2 mm diameter in the pyrrhotite, especially at edges of the masses. Chalcopyrite is most common intergrown with pyrrhotite in carbonate-rich (± minor quartz and chlorite) stringers, or disseminations outside the major pyrrhotite masses; chalcopyrite occurs as subhedral crystals or aggregates up to 0.3 mm in size. Carbonate forms subhedral elongated (flattened, deformed) crystals up to 0.35 mm long, intergrown with similarly elongated quartz crystals up to 0.25 mm long. Chlorite forms bright green, ragged subhedra to 0.2 mm diameter with anomalous blue birefringence indicating ?fairly high Fe content. These relations suggest late emplacement (or ?remobilization) of chalcopyrite.

SAMPLE: R96-48a

Deposit: Cliff

Summary: Clinopyroxene (?diopside) skarn retrograded to amphibole (?actinolite) and chalcopyrite-pyrrhotite-quartz±chlorite veining.

Hand sample description: Massive sulfides with remnant augite (or hornblende); hand specimen is mainly stringery chalcopyrite and lesser pyrrhotite in rusty, fairly siliceous matrix. The rock is magnetic but shows no reaction to cold dilute HCl.

Petrography:
Modal mineralogy in polished thin section:

Clinopyroxene (?diopside) 70%

Chalcopyrite 20%

Pyrrhotite 5%

Quartz (secondary; veins only) 2-3%

Secondary amphibole (?actinolite) 2-3%

Chlorite (veinlets only) <1%

Limonite <1%

The bulk of this sample consists of coarsely crystalline clinopyroxene, partly retrograded to pale green amphibole (?actinolite) near the sulfide stringers. The pyroxene occurs as interlocking subhedral to rarely euhedral crystals up to 3 mm long with maximum extinction angle c^Z 45 degrees and no colour or pleochroism, suggesting ?diopside. Interstices between crystals are commonly filled with minor, fine-grained bright green amphibole (?actinolite) as sub- to anhedral crystals up to 0.25 mm in size, in places mixed with a little quartz and sulfides. Extinction angle in the amphibole is small, around 12 degrees. Fine sulfide fracture veinlets cutting pyroxene also contain amphibole, suggesting sulfide mineralization was closely associated with late (retrograde) skarn formation rather than with early (prograde diopside) skarn formation. Abundant fractures in the clinopyroxene are filled with limonite, probably derived from oxidation of sulfides.

Most of the chalcopyrite in this sample is found in quartz veins (up to about 1.5 mm thick) that form an intimate network crackling the rock. Quartz in these veins occurs as euhedral to subhedral crystals up to 0.5 mm long, in places containing abundant wispy trails of secondary fluid inclusions sub-parallel to the trend of the veinlet. Certain veinlets also contain minor chlorite. The chlorite forms subhedral flakes, oriented in sub parallel fashion oblique to the vein walls; they replace amphibole where the vein cuts amphibole.

Chalcopyrite forms irregular masses up to 4 mm long composed of aggregates of subhedral crystals. A minor proportion of chalcopyrite occurs as extremely fine-grained disseminations or fractures in clinopyroxene. In places, lesser pyrrhotite is mixed with the chalcopyrite, forming sub- to euhedral crystals up to 1 mm in diameter that are intimately intergrown with chalcopyrite around the edges. Traces of incipient oxidation to intermediate FeS phases are found in ractures in pyrrhotite.

In summary, this appears to be a pyroxene skarn that has undergone retrograde alteration to amphibole, with the retrograde alteration accompanied by sulfide mineralization and quartz-rare chlorite veining.

SAMPLE: R96-51c

Deposit: Consolidated St. Elmo

Summary: Calcic plagioclase-clinopyroxene-pyrrhotite-sphene skarn cut by quartz-epidote-pyrrhotite±chalcopyrite-pyrite magnetite-Kfeldspar veins.

Hand sample description: Skarn with approximately 30% sulfides (pyrite-pyrrhotite-chalcopyrite, and fine-grained sphalerite) in quartz matrix ± epidote-?chlorite, possibly ?diopside. The rock is strongly magnetic but shows no reaction to cold dilute HCl.

Petrography:

Modal mineralogy in polished thin section:

?Calcic plagioclase 40%

Quartz (secondary) 20%

Clinopyroxene (?diopside) 15%

Pyrrhotite 15%

Epidote (including ?zoisite) 3%

Sphene 3%

Sericite 2%

Magnetite 1%

Pyrite <1%

Amphibole (secondary, ?actinolite) <1%

K-feldspar (secondary) <1%

The bulk of this slide consists of areas of fine-grained ?calcic plagioclase and minor clinopyroxene, containing clots of coarse-grained pyroxene, sulfide and minor sphene, cut by thick (up to 1 cm) veins of quartz-sulfides and, in places, epidote-group minerals.

Plagioclase (?) forms aggregates of mainly very fine-grained, anhedral, highly interlocked crystals rarely over 0.15 mm in diameter. Significant positive relief compared to quartz, and the skarn setting, suggest a calcic composition (twinning is only rarely vaguely discernible). Most pyroxene mixed with the plagioclase is sub- to anhedral and <50 microns in size; minor sericite is also present, forming ragged subhedral flakes. Sphene occurs as rounded patches up to 0.2 mm across composed of fine-grained aggregates. In the clots, pyroxene forms subhedral to ragged crystals with extinction angle about 40 degrees; lack of colour suggests calcic diopside. There is only rare incipient alteration of pyroxene to green secondary amphibole (?actinolite) as fibrous subhedral crystals up to 0.1 mm long. Rare ?K-feldspar occurs as subhedral grains, suggested by negative relief compared to quartz; it could be more abundant, but staining tests should confirm this.

Quartz veins are up to 0.5 cm thick, mainly composed of sub- to anhedral quartz crystals, but in places with patches of epidote-group minerals (including epidote with yellow pleochroism, zoisite with anomalous blue birefringence, and ?clinozoisite). Quartz is commonly strained (undulose extinction, fractured, sub-grain development). Sulfides occur mainly at the margins of veins, or in clots within them, locally associated with pyroxene, epidote and minor amounts of hydrobiotite, Fe-rich chlorite, and semi-isotropic, altered masses that could be ?altered garnets.

Pyrrhotite forms mainly subhedral to anhedral crystals (outlines determined by their interstitial character between silicate mineral grains) up to about 0.35 mm in diameter. Minor incipient oxidation to intermediate FeS phases is present along fractures, cleavage and rims of the crystals. Rarely, very minor chalcopyrite is intergrown with pyrrhotite. In this location, rounded aggregates of magnetite up to 1.5 mm across contain abundant lath-shaped inclusions of pyrrhotite. Magnetite appears to surround the margins of pyrrhotite.

SAMPLE: R96-53a

Deposit: West of War Eagle, No. 1

Summary: Pyrrhotite-quartz-biotite-amphibole-minor relict plagioclase-chalcopyrite-arsenopyrite altered rock (?possibly mafic protolith).

Hand sample description: Semi-massive pyrrhotite-chalcopyrite with dark green matrix of quartz-amphibole-chlorite; also abundant dispersed biotite. Hand specimen is strongly magnetic but shows no reaction to cold dilute HCl.

Petrography:

Modal mineralogy in polished thin section:

Pyrrhotite 35%

Quartz (secondary) 25%

Biotite 20%

Amphibole (?actinolite) 15%

Chalcopyrite 2%

?Relict plagioclase 1-2%

Sericite (after plagioclase) 1%

Apatite <1%

Arsenopyrite <1%

Sphalerite <1%

This sample consists mainly of pyrrhotite, quartz and mafic minerals (biotite, amphibole) in patches or aggregates that have an apparent random pattern.

Pyrrhotite forms patches with irregular outlines up to 1.2 cm across, composed of subhedral crystals that rarely contain euhedral crystals of arsenopyrite. Minor intermixed chalcopyrite occurs as sub- to anhedral crystals up to 0.5 mm in diameter. Rare red-brown (moderate to high Fe-content) sphalerite is closely associated with the chalcopyrite.

Quartz, which most commonly is closely associated with sulfides, forms subhedral crystals mostly less than about 0.75 mm in size. The crystals are mainly clear and unstrained.

The mafic minerals are concentrated in patches with rounded to irregular outlines up to 1 cm across; cores of these areas are generally biotite-rich, surrounded by amphibole-rich areas. Biotite forms euhedral flakes up to 0.5 mm in diameter with pale brown pleochroism; amphibole forms lath- to needle-like crystals, with pale green pleochroism suggesting intermediate actinolite-tremolite. Minor ragged crystals of ?sericitized plagioclase with anhedral outlines occur at the margins of the mafic areas. Rare euhedral prisms of apatite up to 0.1 mm in diameter are intergrown with the mafic areas; together with the abundant biotite/amphibole, a mafic protolith such as gabbro is suggested.

SAMPLE: R96-60b

Deposit: Gertrude

Summary: Quartz-pyrrhotite-?relict feldspar-arsenopyrite-amphibole-sphene-minor chalcopyrite-limonite-apatite altered ?mafic rock.

Hand sample description: Semi-massive pyrrhotite in a pale grey very siliceous, possible feldspar host (no green colour); hand specimen is a sulfide-cemented breccia consisting of white siliceous angular fragments up to 5 cm in diameter in a matrix of pyrrhotite-arsenopyrite-minor chalcopyrite. The rock is strongly magnetic but shows no reaction to cold dilute HCl.

Petrography:

Modal mineralogy in polished thin section:

Quartz (secondary) 40%

Pyrrhotite 20%

Relict feldspar (?) 15%

Arsenopyrite 10%

Amphibole (?tremolite-actinolite) 10%

Sphene 1-2%

Chalcopyrite 1%

Limonite 1%

Apatite <1%

Sericite <1%

This slide consists essentially of a fine-grained mixture of quartz and possibly ?relict feldspar plus lesser pale green amphibole, in places with abundant sulfides. Quartz crystals are anhedral to rounded and range up to 0.35 mm in diameter; they commonly show strong undulose extinction and sub-grain development, indicating strain and recrystallization. It is difficult to be sure of the presence of feldspar; the distinction between it and quartz is based mainly on the clarity of the quartz and the presence of abundant fine inclusions of amphibole, sphene and in places ?sericite in the ?relict feldspar. Where relief difference is visible, it appears that the feldspar has a significantly lower index of refraction than quartz, suggesting ?K-feldspar, but this is difficult to be sure of in anhedral grains mostly <20 microns in diameter.

Amphibole, closely associated with sulfides and limonite, occurs as pale green, subhedral lath-shaped to fibrous crystals; the colour suggests an intermediate member of the tremolite-actinolite series. Sphene forms abundant aggregates of fine anhedral to subhedral crystals. Unusually abundant apatite forms rounded prismatic crystals up to 0.2 mm long, suggesting that although the rock looks felsic now, much of the quartz is secondary and the rock may have originally been mafic.

Most pyrrhotite is fine-grained but in places large euhedral crystals of pyrrhotite are up to almost 0.5 cm long. Arsenopyrite is abundant in the polished section, forming sub- to euhedral crystals up to 0.5 mm in size, mainly in veinlets or masses that appear to replace the cores of former pyrrhotite veinlets or areas, or in separate cross-cutting veins. Rarely, minor chalcopyrite as fine-grained anhedral to ragged crystals is mixed with the pyrrhotite.

The breccia appearance in hand specimen is not obvious in thin section, where the main impression is of an intensely silicified and sulfidized rock, possibly of mafic parentage.

SAMPLE: R96-60c

Deposit: Gertrude

Summary: Massive pyrrhotite±chalcopyrite-arsenopyrite, inclusions of calcic plagioclase-carbonate-tremolite-biotite-quartz-chlorite-sphene.

Hand sample description: Massive, partly oxidized pyrrhotite that is strongly magnetic with minor patchy chalcopyrite, siliceous quartz-rich matrix, possibly diopside; minor orangey-coloured inclusions react strongly to cold dilute HCl.

Petrography:

Modal mineralogy in polished thin section:

Pyrrhotite 85%

Plagioclase feldspar (?bytownite) 8-10%

Carbonate (?siderite; calcite) 1-2%

Amphibole (?tremolite-actinolite) 1-2%

Quartz 1%

Biotite (green and brown) 1%

Chlorite <1%

Sphene <1%

K-feldspar <1%

Arsenopyrite, sphalerite tr

This slide consists almost entirely of pyrrhotite with minor silicate inclusions (<15%) that are mostly <3 mm in diameter and irregular in shape; their composition is variable and difficult to determine exactly, but possibly suggestive of prograde and retrograde skarn assemblages.

Pyrrhotite forms large subhedral crystals, mostly partly altered along fractures to intermediate FeS phases with typical secondary textures. Rare euhedral crystals of arsenopyrite are included in the pyrrhotite. Minor chalcopyrite forms crystals that are mostly <0.2 mm in diameter. Rare sphalerite forms tiny red-brown crystals.

A few silicate inclusions contain quartz (forming sub- to anhedral crystals up to 0.35 mm in diameter) plus a high-relief mineral with low (first-order grey) birefringence, minor brown biotite and a green amphibole and chlorite. Subhedral amphibole crystals up to 0.1 mm long are very pale green, suggesting a member near the tremolite end of the series. There may be minor relict feldspar, suggested by cloudy areas with common fine-grained sericite. Apparently negative relief of some of the feldspar crystals (subhedral, to 25 microns diameter) suggests the presence of ?K-feldspar. However, most silicate inclusions are rich in plagioclase feldspar as indicated by the presence of polysynthetic twinning with extinction angle up to 45 degrees, suggesting a very calcic plagioclase feldspar (possibly bytownite). Minor sphene is present.

In other silicate inclusions, euhedral to subhedral flakes of a greenish brown (probably Fe-rich) biotite up to 0.15 mm in diameter intimately mixed with what is probably an iron carbonate (?siderite) and minor amounts of calcite. The ?iron carbonate is strongly limonite-stained and has a curious, distinctive habit, forming worm-like aggregates of fine sub- to anhedral crystals mostly <50 microns in diameter. This texture is reminiscent of high-Fe chlorite; there is a suggestion of radiating rosettes to the crystals. Low-Fe carbonate, probably calcite, forms coarser, subhedral crystals up to 0.25 mm in diameter that lack limonite staining.

SAMPLE: R96-62b

Deposit: Giant

Summary: ?Arsenopyrite-?Kfeldspar-epidote veins with silicified envelopes cutting ?fine tuff or metasediment (plagioclase, secondary amphibole-biotite-epidote).

Hand sample description: Grey possible bedded, silicified rock with minor pyroxene alteration; 10% silvery mineral in irregular patches to possibly vein controlled (fractures); some molybdenite, chalcopyrite. The rock is not magnetic and shows no reaction to cold dilute HCl.

Petrography:
Modal mineralogy in thin section:

?Plagioclase (groundmass) 50%

Amphibole (?actinolitic) 10%

?Secondary biotite 10%

Epidote 10%

Opaque (?arsenopyrite) 10%

?K-feldspar (veins) 5%

Quartz (vein envelopes) 3-5%

Sphene 1%

In thin section, this rock is very fine-grained, making identifications difficult, but it appears to be composed mainly of small clotty mafic minerals (amphibole, both green and brown biotite, ?epidote, sphene) in finer grained matrix of ?plagioclase, with a bedded ?ash tuff appearance. The sulfides (mostly arsenopyrite) are surrounded by zones of coarse ?feldspar as subhedral crystals up to 1 mm long (possibly Kspar) and fine-grained epidote/clinozoisite. In an irregular, poorly defined zone next to the vein, what appears to be very fine secondary quartz (relief positive compared to the feldspar host) defines a ?silicified envelope.

SAMPLE: R96-65a

Deposit: Robert E. Lee

Summary: Semi-massive arsenopyrite, quartz, rare biotite+pyrite ?matrix to clasts of ?relict feldspar-sericite-quartz-sphene/rutile-apatite.

Hand sample description: Semi-massive arsenopyrite-pyrrhotite-chalcopyrite in grey, fine-grained quartz, minor coarse pyrite. Hand specimen shows irregular pinkish (?Fe-stained) areas. The rock is not magnetic and shows no reaction to cold dilute HCl.

Petrography:
Modal mineralogy in polished thin section:

Arsenopyrite 30%

?Relict feldspar 30%

Quartz (secondary) 20%

Sericite 15%

Biotite 1-2%

Sphene 1%

Rutile 1%

Apatite <1%

?Zoisite <1%

This slide consists mainly of arsenopyrite as a breccia matrix to clasts of silicate rock up to about 1.5 cm in diameter. In these ?clasts, the rock is very fine grained and appears to be mostly quartz and sericitized ?feldspar. Quartz occurs mostly in irregular veins (up to 1 mm thick, except where with significant arsenopyrite, where they may be up to 1 cm thick). The quartz forms subhedral crystals with strong undulose extinction indicating strain; ribboned growth in pressure shadows of arsenopyrite crystals is also noted. Outside the veins, it is very difficult to identify the ?relict feldspar (relief difference against quartz is virtually impossible since there are always intervening flakes of sericite present, but in places apparently negative relief of the feldspar suggests ?K-spar, or perhaps albitic plagioclase). Sericite forms fine-grained flakes, but in places up to 0.1 mm across (these could be after former mafic minerals since they also contain

or are associated with Ti-minerals and apatite; *see* below). Apatite crystals are subhedral and mainly <0.1 mm long.

Most of the sulfide in this section is arsenopyrite, forming euhedral crystals up to about 1 mm in diameter. Only rarely is there any pyrite present, forming aggregates up to several mm across of euhedral to subhedral crystals (some of which contain minute inclusions). Associated with the pyrite and arsenopyrite aggregates are clusters of Ti-minerals (sphene and rutile) forming fine-grained crystals; these may suggest a former mafic to intermediate protolith. Chalcopyrite is not seen in the section.

One through-going fracture is marked by distinctive pale brown secondary biotite as subhedral flakes up to 0.1 mm in diameter and fine-grained, euhedral arsenopyrite. Similar pale biotite is also found around some larger arsenopyrite crystals in parts of the section; a few high-relief crystals may be ?zoisite.

The protolith to the siliceous clasts is not obvious; it could have been an intermediate rock as suggested by the abundance of feldspar and presence of rutile and sphene.

SAMPLE: R96-66a

Deposit: Bluebird

Summary: Semi-massive pyrite-sphalerite-arsenopyrite-galena-sulfosalt in quartz-calcite-sericite gangue.

Hand sample description: Massive medium-grained pyrite with streaks of massive fine-grained sphalerite plus galena, trace arsenopyrite in host of quartz and calcite. Vein margins are brecciated. Hand sample is essentially non-magnetic, but reacts to cold dilute HCl.

Petrography:
Modal mineralogy in polished thin section:

Pyrite 40%

Quartz 35%

Sphalerite 10%

Carbonate (?mainly calcite) 5%

Arsenopyrite 5%

Sericite 3%

Galena 1%

Sulfosalt (?boulangerite) <1%

Limonite <1%

Chalcopyrite tr

This slide consists of over 50% sulfides, mainly pyrite intergrown with lesser sphalerite and arsenopyrite plus minor galena. Pyrite forms mainly euhedral crystals up to about 1.5 mm in diameter. Arsenopyrite forms euhedral crystals up to 1 mm in diameter, and is commonly confined to certain zones (?vein-like areas) rather than evenly distributed. Sphalerite occurs in ragged aggregates that are mainly interstitial to pyrite, composed of subhedra with bright red-brown colour indicating moderate to high Fe content and containing trace chalcopyrite. Minor galena forms subhedral crystals or interstitial aggregates either associated with sphalerite (typically most abundant in arsenopyrite-rich zones) or rarely included in pyrite. Rare sulfosalt crystals form somewhat plumose subhedra with reflectance very similar to or slightly less than galena and distinct anisotropism under crossed polars. Possible choices include the relatively common boulangerite or bournonite, both Pb-Sb sulfosalts; probably boulangerite, as there is not much copper in the specimen.

Gangue minerals are mainly quartz and carbonate (?calcite). Quartz forms subhedral to rarely euhedral crystals up to about 1.2 mm long, although there has been some recrystallization that blurs their outlines. Strain and associated recrystallization are also indicated by undulose extinction and minor sub-grain development. Relict wall-rock fragments are marked by areas of very fine-grained quartz, carbonate and sericite (which may also contain some relict feldspar). The sericite forms subhedral flakes that in places have pale green colour, indicating some Fe may be present (phengitic composition); aggregates up to 0.2 mm across may represent the sites of former ?mafic mineral crystals. Some areas of sericite are stained by limonite. Calcite crystals are generally subhedral, and in places are found with quartz along what appear to be late veinlets cutting the sulfides.

SAMPLE: R96-67a

Deposit: Homestake

Summary: Semi-massive pyrite (±marcasite)-sphalerite-pyrrhotite±galena in matrix of quartz-epidote-chorite-biotite-amphibole-apatite.

Hand sample description: Massive sulfides - 50% arsenopyrite with streaks of massive pyrite and pyrrhotite, 20% sphalerite in arsenopyrite and as segregations; galena and chalcopyrite not noted, trace quartz gangue. The rock is magnetic but shows no reaction to cold dilute HCl.

Petrography:
Modal mineralogy in polished thin section:

Pyrite 30%

Quartz 20%

Sphalerite 15%

Pyrrhotite 10%

Marcasite 5%

Epidote (?clinozoisite) 5%

Chlorite 5%

Biotite 2-3%

Amphibole (?tremolite-actinolite) 2-3%

Galena <1%

Apatite <1%

This slide consists of coarse-grained pyrite and interstitial sphalerite and pyrrhotite in a matrix of quartz and other silicates.

Pyrite forms mainly subhedral (partly broken) to euhedral crystals up to about 1.5 mm in diameter, commonly hosted in a matrix of finer grained pyrrhotite and sphalerite. Individual crystals are difficult to see in the

sphalerite, but probably average around 0.2 mm; bright red-brown colour indicates a moderate to high Fe content. Much of the pyrrhotite forms subhedral crystals less than 0.5 mm diameter, with incipient oxidation evident at margins. In places, intergrown lamellae and flame-shaped crystals (possibly secondary) of a whitish, more highly reflective, anisotropic sulfide are likely ?marcasite,. The habit, which is typically less euhedral (more "sponge-textured") than pyrite, supports the interpretation as a secondary product after pyrrhotite. In parts of the slide, pyrrhotite is absent and its place is taken by lamellar aggregates of marcasite up to 0.5 mm in diameter. Rare galena forms subhedral crystals enclosed in the sphalerite; however, sulfosalt as seen in R96-66c is not evident.

Most of the gangue mineralogy is dominated by quartz, forming subhedral to rarely euhedral crystals up to 0.75 mm long, but also commonly as extremely fine-grained aggregates that likely represent former fragments of wallrock that have been intensely silicified. Other silicates include clear (colourless) epidote-group mineral, probably ?clinozoisite as euhedral prisms up to 0.15 mm long associated with apatite prisms, pale brownish to greenish biotite and pale greenish tremolite-actinolite. In places there is also chlorite, forming pale yellowish-green subhedral flakes (with moderate to high Fe content). The chlorite is commonly closely associated with sphalerite and pyrrhotite. It is possible that the apatite, which is significant in places, indicates an intermediate-mafic protolith for the intensely altered wallrock fragments in this vein.

SAMPLE: R96-67c

Deposit: Homestake

Summary: Massive pyrite+chalcopyrite-sphalerite-galena, veined by arsenopyrite-carbonate, gangue of sericite-biotite-tourmaline-chlorite.

Hand sample description: Massive pyrite with streaks of sphalerite and arsenopyrite. Hand sample is not magnetic and shows no reaction to cold dilute HCl.

Petrography:
Modal mineralogy in polished thin section:

Pyrite 70%

Arsenopyrite 10%

Sericite 10%

Biotite (partly chloritized) 5%

Tourmaline (schorl) 1-2%

Chalcopyrite 1-2%

Carbonate (?ankerite) 1%

Chlorite <1%

Sphalerite, galena <1% each

This slide is essentially coarse-grained pyrite with minor interstitial chalcopyrite and lesser sphalerite, cut by zones of fine-grained arsenopyrite, which is also commonly interstitial to pyrite.

Pyrite forms coarse subhedral to rarely euhedral crystals. Both chalcopyrite and sphalerite form anhedral crystals or aggregates confined to areas between the pyrite crystals, in places mixed with galena.

Arsenopyrite crystals are mainly subhedral, either interstitial to pyrite (in places mixed with sphalerite or less commonly chalcopyrite) or, where best developed, in fine crackle veinlets or zones cutting the massive pyrite.

Gangue minerals are mainly fine-grained sericite in masses up to several mm across that include lesser tourmaline and pale brown (partly chloritized) biotite. In places the chlorite is better developed, forming subhedral flakes with optical character suggesting moderately Fe-rich composition. In these areas, minor carbonate also occurs as stringers or veinlets. The carbonate may be ?dolomite or ankerite as indicated by its lack of reaction in hand specimen. The carbonate (and chlorite) is loosely associated with arsenopyrite veining.

Thus the protolith for the altered wallrock appears to have been a fairly mafic rock that has been replaced by pyrite with traces of chalcopyrite, sphalerite and galena, and later by arsenopyrite with a carbonate-chlorite alteration.

SAMPLE: R96-67d

Deposit: Homestake

Summary: Amphibole-epidote-clay/sericite±calcite-pyrrhotite-quartz-sphene-chlorite altered intermediate intrusive rock (Rossland monzonite).

Hand sample description: Rare skarn-altered Rossland monzonite with epidote, amphibole and ?pyroxene veining and brecciation associated with pyrrhotite, commonly veined by late calcite±quartz. The rock is weakly magnetic and shows trace reaction to cold dilute HCl.

Petrography:
Modal mineralogy in thin section:

Plagioclase (sericitized, ?albitic) 60%

Amphibole (secondary, ?actinolitic) 20%

Epidote 7%

Clay-sericite 5%

Carbonate (mostly calcite) 2-3%

Opaque (mostly pyrrhotite) 1-2%

Quartz (secondary) 1-2%

Sphene 1-2%

Chlorite <1%

Apatite <1%

This is a strongly altered rock in which the original igneous texture has been largely destroyed. Relict plagioclase occurs as subhedral crystals up to almost 1.5 mm long, largely altered to fine clay-sericite, amphibole and epidote; sub-grain development indicates that most plagioclase is likely of secondary, ?albitic composition. Relict mafic crystals are altered to amphibole (pale green, ?actinolitic) and epidote (pale yellow pleochroism), largely concentrated along fracture zones, plus sphene and minor apatite. Opaque (?mainly pyrrhotite) is only loosely associated with these fracture zones; some is also associated with the later, cross-cutting calcite-quartz-epidote-chlorite fractures.

SAMPLE:R96-68

Deposit: California

Summary: Clinopyroxene skarn retrograded to amphibole-alkali feldspar-epidote-sphene, fracture-controlled pyrrhotite-chalcopyrite-pyrite.

Hand sample description: Rare occurrence of diopside skarn with quartz-rich wallrock and disseminated pyrrhotite. Hand specimen is strongly magnetic but does not react to cold dilute HCl.

Petrography:

Modal mineralogy in polished thin section:

Clinopyroxene (diopside) 40%

Amphibole (secondary, ?actinolite) 30%

Alkali feldspar (?albitic) 15%

Pyrrhotite 10%

Epidote-group (?clinozoisite) 3%

Sphene 1%

Chalcopyrite <1%

Pyrite <1%

Limonite <1%

This slide consists mainly of clinopyroxene (similar to samples R96-39a, 48a and 51c), with locally significant alteration to secondary amphibole and minor epidote-group minerals (clinozoisite and ?zoisite) that are closely associated with sulfide mineralization.

Clinopyroxene forms mainly coarse to medium-grained subhedral crystals up to 4 mm long. Extinction angle is around 40 degrees, and colour is very pale green (non-pleochroic) implying a low Fe content (?diopside). The crystals are extensively fractured, with incipient to minor development of pale green secondary amphibole along some of the fractures (Photo A5-5), and traces of limonite along most fractures. In places, the amphibole completely replaces the pyroxene, leading to an assemblage of feathery to fibrous amphibole, abundant sphene (not seen with the pyroxene and therefore likely a product of the alteration), epidote-group minerals and alkali feldspar.

Amphibole forms subhedral crystals with pale green pleochroism suggesting moderate Fe content (actinolite). The alkali feldspar occurs as sub- to anhedral crystals with tightly interlocking irregular shapes up to about 0.5 mm in diameter. Vaguely developed twinning suggests plagioclase of albitic composition. Epidote forms subhedra up to about 0.5 mm diameter with no yellow pleochroism suggesting Fe-poor clinozoisite (anomalous blue birefringence in some suggests ?zoisite). Sphene forms small sub- to euhedral crystals with reddish-brown pleochroism, closely associated with sulfides.

Pyrrhotite forms irregular masses that appear to be interconnected along a vaguely developed network of fractures. Most pyrrhotite crystals are fine grained but in places larger sub- to anhedral crystals up to 1 mm occur; the larger crystals in particular are oxidized, with development of intermediate FeS phases and bird's-eye marcasite along crystal margins and cleavages (Photo A5-6). Minor chalcopyrite is associated with pyrrhotite or found along narrow veins.

Photo A5-5. Sample R96-68, California deposit: Fringing alteration of secondary amphibole (pale colours) around large crystals of clinopyroxene (?diopside) in massive skarn; transmitted light, crossed polars, field of view 2.5 mm.

Rare pyrite occurs as cubic euhedra contained within the pyrrhotite masses, in places associated with chalcopyrite.

SAMPLE: R96-74

Deposit: Josie dump

Summary: Massive pyrrhotite-pyrite (trace magnetite, chalcopyrite) with matrix of amphibole-calcite-?garnet.

Hand sample description: Skarn - well developed biotite hornfels, siliceous, cut by medium grey, probable pyroxene and pyrrhotitic sulfides. Hand sample and, in particular, the polished thin section, are mainly strongly magnetic massive sulfides (pyrrhotite, minor pyrite, rare chalcopyrite) in a greenish matrix, part of which reacts to cold dilute HCl.

Petrography:

Modal mineralogy in polished thin section:

Pyrrhotite 65%

Pyrite 10%

Carbonate (?mostly calcite) 10%

Amphibole (?tremolite/actinolite) 10%

Photo A5-6. Sample R96-68, California deposit: Typical "bird's-eye" alteration of pyrrhotite to intermediate FeS phases and marcasite (due to supergene oxidation) in clinopyroxene skarn; reflected light, uncrossed polars, field of view 1.5 mm.

?Garnet 3-5%

Magnetite <1%

Chalcopyrite <1%

Most of the pyrrhotite occurs as small subhedral to rounded crystals rarely intergrown with trace amounts of chalcopyrite. In some subparallel zones (possibly mimicking former ?bedding), magnetite is found as small sieve-like to subhedral crystals. Inclusions in magnetite are mostly very fine-grained pyrrhotite and silicates, but some euhedral pyrite also occurs.

Pyrite forms coarse subhedral to rarely euhedral crystals, commonly containing minor to abundant inclusions of silicate minerals and rare chalcopyrite and pyrrhotite.

Gangue minerals include mainly amphibole (probably secondary) and carbonate, commonly in either vague, sub-parallel ?layers (parallel to the zones with magnetite) or in anastomizing, oblique veinlets <1 mm thick. Amphibole forms subhedral crystals with very pale green pleochroism indicating low Fe content (tremolite-actinolite). Carbonate forms interlocking sub- to anhedral crystals (?calcite). In certain areas there are concentrations of what appear to be garnets (isotropic, pale pinkish to brownish where altered, rounded subhedra up to 0.25 mm in diameter). Alteration at margins appears to be to carbonate, leading to the speculation that part or all of the carbonate in the specimen may be retrograde, after former more extensive ?garnet. Brownish staining of the rimming carbonate suggests it may contain significant Fe, and that therefore the garnet may also be Ca-Fe bearing (?andradite).

APPENDIX 6A
ANALYSES OF SAMPLES FROM THE ROSSLAND CAMP (BUY ICP)

Lab No.	Field No.	Mo	Cu	Pb	Zn	Ag	Ni	Co	Mn	Fe*	As	U	Au	Th	Sr	Cd	Sb	Bi
		ppm	ppm	ppm	ppm	ppm	ppm	ppm	ppm	%	ppm	ppm	ppm	ppm	ppm	ppm	ppm	ppm
	detection limit	2	2	5	2	0.5	2	2	5	0.01	5	10	4	2	2	0.4	5	5
052136	R96-4	23437	181	35	97	< .5	42	36	1065	6.13	7	< 10	< 4	6	487	1.4	< 5	8
052137	R96-6	8815	27	38	73	< .5	20	23	636	2.67	5	30	< 4	6	690	1.1	< 5	< 5
052138	R96-7A	48644	880	19	94	11.1	15367	34551	374	12.18	7078	165	138	9	232	1.5	87	8515
052139	R96-7B	11088	8	11	24	0.5	2235	11664	301	1.31	5014	270	47	13	330	< .4	33	2065
052140	R96-8	11633	2620	< 5	115	3.8	760	120	1229	11.86	31	< 10	< 4	3	50	2.7	< 5	10
052142	R96-12A	37059	26	132	131	0.8	11	46	579	2.26	166	4380	< 4	124	2445	3.5	< 5	13
052143	R96-12D	51	2836	167	286	14	192	150	1077	20.26	29	< 10	< 4	5	197	8.7	11	10
052144	R96-15	24944	42	9	51	< .5	21	31	482	1.76	< 5	< 10	< 4	5	358	1.3	7	10
052145	R96-17	86697	325	< 5	64	< .5	125	< 2	1012	5.84	< 5	< 10	< 4	13	310	1.6	164	< 5
052146	R96-18C	29303	5788	< 5	311	17	114	54	1094	8.23	< 5	< 10	< 4	6	279	29.3	9	17
052147	R96-19A	38392	675	< 5	42	1.9	93	60	1119	7.72	< 5	25	< 4	7	132	1.2	< 5	21
052148	R96-19B	293	3951	37	119	10.6	136	46	471	13.43	99	< 10	< 4	6	219	2.6	5	59
052149	R96-19C	38075	547	62	60	2.1	29	44	505	5.68	11	< 10	< 4	28	175	1.8	< 5	32
052150	R96-20B	74	1217	208	162	8.4	142	237	2300	16.51	15	< 10	< 4	3	118	3.9	8	6
052152	R96-20C	21931	272	26	56	< .5	24	39	613	5.86	14	< 10	< 4	5	363	0.6	10	7
052153	R96-24A	30	24726	12	489	55.6	18	19	681	8.76	< 5	< 10	< 4	2	241	9	15	8
052154	R96-24D	25	4442	8	105	14.3	37	90	606	15.08	5	< 10	59	3	205	2.3	< 5	< 5
052155	R96-24C	13	99999	< 5	1919	73.5	58	190	655	25.91	< 5	< 10	26	3	108	27.7	33	14
052157	R95-28A	16	1578	< 5	99	1.4	64	60	1117	15.24	16	< 10	< 4	3	251	2.1	< 5	32
052158	R96-28D	15	5254	12	59	8.4	126	125	669	21.55	18	< 10	< 4	4	234	3.5	< 5	16
052159	R96-31A	83	13860	14	226	23.9	86	127	344	19.86	72	< 10	< 4	3	175	4.3	< 5	< 5
052160	R96-31B	20	1926	400	12612	13	110	60	947	22.49	92	< 10	< 4	2	125	160.3	< 5	17
052162	R96-35C	222	6279	< 5	40	1.8	151	301	175	42.04	< 5	14	< 4	5	73	2.7	< 5	< 5
052163	R96-39A	2	5709	< 5	90	8.4	70	458	223	27.55	< 5	< 10	< 4	8	173	3.1	< 5	18
052164	R96-40B	6	1476	26	29	3.7	85	3755	144	30.74	3346	< 10	13	4	118	2.4	64	42
052165	R96-42A	< 2	2511	6	22	3.6	20	174	1142	35.7	93	< 10	11	3	3	3.7	< 5	200
052166	R96-42B	4	67	12	13	1.1	13	2406	292	23.96	11788	< 10	8	3	91	1.3	129	105
052168	R96-44A	9	3395	< 5	50	9.5	83	2864	441	32.53	1168	< 10	108	2	144	3.6	15	35
052169	R96-45B	10	4014	< 5	19	1.4	127	2731	204	45.2	1249	10	< 4	4	84	2.3	9	56
052170	R96-46A	419	10306	17	134	7	46	982	314	37.97	104	< 10	< 4	10	65	2.2	11	< 5
052172	R96-47A	2	13537	13	141	12.3	3	132	3385	14.62	162	< 10	9	< 2	257	2.9	< 5	37
052173	R96-48A	4	22722	< 5	265	30.4	127	170	929	30.75	18	< 10	5	3	12	4.5	< 5	15
052174	R96-51B	80	48076	7	1085	141.4	205	393	264	39.55	90	12	< 4	4	47	28.2	< 5	85

APPENDIX 6A, CONTINUED

Lab No.	Field No.	Mo	Cu	Pb	Zn	Ag	Ni	Co	Mn	Fe*	As	U	Au	Th	Sr	Cd	Sb	Bi
		ppm	ppm	ppm	ppm	ppm	ppm	ppm	ppm	%	ppm	ppm	ppm	ppm	ppm	ppm	ppm	ppm
	detection limit	2	2	5	2	0.5	2	2	5	0.01	5	10	4	2	2	0.4	5	5
052175	R96-51C	26	1736	130	14099	18.6	48	75	471	11.61	66	< 10	< 4	3	42	214.4	15	74
052176	R96-51C	43	4785	214	919	29.8	77	64	119	34.4	79	< 10	< 4	2	29	16.5	24	25
052177	R96-52	6	17557	< 5	135	22.8	85	1103	102	39.85	1345	< 10	6	5	19	3.1	76	41
052178	R96-53A	69	8152	21	528	22.4	120	110	702	25.73	36	< 10	< 4	2	35	6.7	< 5	21
052179	R96-53D	71	35816	6	1295	91.6	54	131	1672	18.05	20	< 10	< 4	2	34	10.6	13	21
052180	R96-54	12	12234	109	375	28.8	263	3637	699	24.58	4512	< 10	< 4	2	165	5.1	78	19
052182	R96-55	28	13060	683	2018	46	164	27	377	18.28	86	< 10	< 4	2	73	19.2	7	94
052183	R96-60A	3	376	33	46	2.3	12	17	912	6.54	173	10	< 4	3	728	0.8	6	< 5
052184	R96-60B	45	919	49	145	4.1	359	431	353	32.47	433	12	< 4	4	94	2.4	< 5	16
052185	R96-60C	2	3181	11	54	3.6	238	131	447	49.13	< 5	< 10	< 4	4	19	2.5	< 5	5
052186	R96-61A	19	499	36	92	1	81	46	1212	7.3	20	< 10	< 4	3	637	0.6	6	< 5
052187	R96-61B	8	1077	36	33	4.3	47	105	306	21.1	20	< 10	8	3	91	0.4	< 5	43
052188	R96-62A	7614	117	32	16	2.8	811	7358	192	11.86	9111	15	7	5	191	0.4	233	4981
052189	R96-62B	467	135	39	41	3.3	14	3147	481	8.78	12703	12	17	5	390	1.1	258	3316
052190	R96-62C	327	971	54	75	2.8	611	5150	552	12.64	1347	100	15	5	251	1.7	35	823
052192	R96-62D	6468	1079	7	190	< .5	243	427	994	9.69	841	1530	27	26	226	3.1	12	775
052193	R96-63	23	739	12	131	0.8	45	3	2589	7.67	74	< 10	< 4	4	425	1	< 5	16
052194	R96-64A	9	323	28380	99999	169.6	37	124	526	27.17	1406	< 10	< 4	4	48	1645.9	591	33
052195	R96-64B	41	2243	25462	55175	230.6	55	208	398	24.77	1276	< 10	28	3	52	779.7	360	18
052196	R96-64C	8	665	5814	7851	64	7	6	883	11.87	5	< 10	< 4	2	51	89.2	37	< 5
052197	R96-65A	6	1049	69	136	6.5	24	8	238	9.35	1162	< 10	< 4	2	67	1	22	5
052198	R96-65B	2	3358	479	22845	17.7	38	12	702	23.28	379	< 10	< 4	3	32	302.6	9	21
052199	R96-66A	4	175	18672	59340	235.5	19	14	1528	26.9	840	< 10	< 4	3	43	610.6	629	< 5
052200	R96-66B	22	153	24051	20226	266.1	31	5	1316	21.58	1321	< 10	< 4	3	72	200.8	847	< 5
052202	R96-67A	< 2	366	4194	99999	110.3	29	107	1041	25.72	6395	< 10	5	4	92	1532.7	214	189
052203	R96-67B	27	13840	1004	2686	208.7	25	170	662	21.66	31	< 10	< 4	3	64	24.4	37	213
052204	R96-67C	29	2578	40367	20777	767.5	26	203	385	31.53	3107	< 10	< 4	3	17	263.6	404	1052
052205	R96-69	< 2	6736	46	92	7.5	110	290	496	24.04	13	< 10	< 4	2	72	2.2	< 5	< 5
052156	R96-70	31	2722	11	55	3	60	938	567	22.57	< 5	< 10	< 4	2	246	2.9	14	< 5
052206	R96-70A	< 2	1354	22	46	1.6	30	445	537	18.57	< 5	< 10	< 4	3	407	2.5	6	8
052207	R96-71A	153	15272	14	119	14.2	24	116	227	27.38	< 5	< 10	< 4	3	203	4.1	6	< 5
052161	R96-72	< 2	12360	29	254	18	35	79	660	20.91	48	< 10	< 4	2	248	4.4	18	< 5
052208	R96-73	7	9436	37	214	33.9	185	210	339	22.35	89	< 10	6	4	146	4.2	< 5	1211
052209	R96-74A	7	7527	13	93	9.1	276	345	715	33.58	< 5	< 10	< 4	2	122	6.3	< 5	< 5
052210	R95-74B	235	1508	9	99	1.6	41	86	1248	13.15	< 5	< 10	5	< 2	122	1.6	< 5	10

APPENDIX 6A, CONTINUED

Lab No.	Field No.	V	Ca	P	La	Cr	Mg	Ba	Ti	Al	Na	K	W	Zr	Sn	Y	Nb	Be	Sc
		ppm	%	%	ppm	ppm	%	ppm	%	%	%	%	ppm	ppm	ppm	ppm	ppm	ppm	ppm
	detection limit	2	0.01	0.002	2	2	0.01	1	0.01	0.01	0.01	0.01	4	2	2	2	2	1	1
052136	R96-4	474	7.78	0.223	33	138	2.63	432	0.29	5.26	0.8	4.04	13	25	< 2	30	< 2	2	14
052137	R96-6	589	5.99	0.102	15	165	1.75	3852	0.39	8.03	1.25	5.64	12	16	< 2	24	< 2	2	12
052138	R96-7A	156	4.31	0.053	8	135	0.34	101	0.41	5.14	1.47	1.04	17	8	< 2	21	2	1	3
052139	R96-7B	117	2.92	0.116	21	64	0.32	914	0.48	9.17	3.2	4.49	6	26	3	32	4	< 1	4
052140	R96-8	200	9.3	0.317	14	41	8.55	81	0.08	1.5	0.25	0.5	200	6	4	14	< 2	< 1	10
052142	R96-12A	53	10.15	0.18	14	109	1.1	241	0.15	3.02	0.19	2.61	24	3	3	36	4	< 1	< 1
052143	R96-12D	173	2.39	0.441	31	151	0.63	95	0.17	2.9	0.1	1.63	32	10	< 2	33	< 2	< 1	13
052144	R96-15	395	4.26	0.116	41	199	0.59	278	0.32	6.92	1.2	4.57	28	16	3	28	3	< 1	9
052145	R96-17	351	9.05	0.378	41	49	2.46	56	0.2	3.4	0.4	2.51	2506	11	< 2	36	2	< 1	< 1
052146	R96-18C	490	7.28	0.14	71	112	1.62	183	0.15	3.27	0.46	2.29	158	9	< 2	26	< 2	< 1	10
052147	R96-19A	468	7.2	0.183	31	119	3.38	130	0.25	4.2	0.53	4.38	546	17	2	22	< 2	< 1	13
052148	R96-19B	227	3.8	0.318	36	101	2.65	43	0.21	3.71	0.3	3.03	3757	11	< 2	25	< 2	6	23
052149	R96-19C	748	3.92	0.194	1699	153	1.49	113	0.25	4.74	0.33	4.53	343	30	< 2	26	3	< 1	12
052150	R96-20B	212	1.27	0.27	22	164	0.7	58	0.17	3.07	0.06	1.87	56	7	< 2	30	< 2	2	15
052152	R96-20C	224	3.49	0.298	19	171	1.29	116	0.29	5.18	0.9	3.94	51	21	< 2	36	4	< 1	12
052153	R96-24A	193	3.26	0.094	53	105	2.81	157	0.35	6.54	2.76	0.84	< 4	10	13	19	< 2	2	17
052154	R96-24D	263	4.1	0.056	17	143	3.46	68	0.47	5.04	1.18	3.39	< 4	9	15	25	< 2	3	27
052155	R96-24C	163	2.64	< .002	8	46	2.32	42	0.27	3.01	0.53	1.94	< 4	6	15	14	< 2	1	11
052157	R95-28A	214	13.88	0.037	9	48	5.02	42	0.13	2.43	0.13	0.07	4	19	3	15	2	4	12
052158	R96-28D	288	4.87	0.159	2	61	1.61	38	0.19	3.32	0.19	3.29	< 4	9	< 2	25	< 2	< 1	15
052159	R96-31A	131	2.32	0.088	5	47	1.58	68	0.29	4.96	2.08	1.76	< 4	5	3	16	< 2	< 1	13
052160	R96-31B	164	2.25	0.032	6	94	2.06	115	0.19	3.14	0.09	1.34	15	4	2	7	< 2	< 1	13
052162	R96-35C	79	1.85	0.045	42	57	0.48	32	0.11	1.67	0.7	0.1	< 4	4	< 2	8	< 2	< 1	8
052163	R96-39A	53	1.14	0.092	43	61	0.33	72	0.34	4.65	1.32	1.66	8	5	3	10	< 2	< 1	8
052164	R96-40B	36	0.94	0.041	< 2	37	0.27	48	0.12	2.91	0.38	2.65	< 4	5	< 2	11	< 2	< 1	10
052165	R96-42A	11	13.41	< .002	7	66	0.21	1	< .01	0.09	0.01	< .01	6	< 2	35	27	< 2	< 1	19
052166	R96-42B	65	0.82	0.053	< 2	49	0.75	49	0.19	2.29	0.41	1.15	< 4	5	< 2	8	< 2	4	9
052168	R96-44A	49	3.5	0.007	< 2	29	0.74	85	< .01	3.37	0.47	0.9	< 4	< 2	< 2	3	< 2	< 1	10
052169	R96-45B	13	1.52	0.017	9	26	0.39	108	0.03	1.77	0.32	0.66	< 4	2	< 2	6	< 2	< 1	7
052170	R96-46A	34	0.98	0.127	9	63	0.7	127	0.26	2.35	0.22	0.99	< 4	3	3	16	5	2	9
052172	R96-47A	27	17.61	0.025	< 2	51	0.45	8	0.08	3.11	0.01	0.04	79	7	37	112	< 2	2	39
052173	R96-48A	91	6.26	0.002	< 2	35	2.6	86	< .01	0.47	0.05	0.2	< 4	< 2	2	4	< 2	< 1	20

APPENDIX 6A, CONTINUED

Lab No.	Field No.	V	Ca	P	La	Cr	Mg	Ba	Ti	Al	Na	K	W	Zr	Sn	Y	Nb	Be	Sc
		ppm	%	%	ppm	ppm	%	ppm	%	%	%	%	ppm	ppm	ppm	ppm	ppm	ppm	ppm
	detection limit	2	0.01	0.002	2	2	0.01	1	0.01	0.01	0.01	0.01	4	2	2	2	2	1	1
052174	R96-51B	42	0.47	0.008	< 2	39	0.32	95	0.03	1.1	0.07	0.77	4439	< 2	3	4	< 2	3	6
052175	R96-51C	111	0.77	0.054	2	182	0.29	113	0.12	3.75	0.13	2.59	13	6	4	3	< 2	< 1	14
052176	R96-51C	20	0.2	0.002	< 2	231	0.06	33	0.02	0.6	0.03	0.25	43	3	2	3	< 2	< 1	5
052177	R96-52	12	0.25	0.018	< 2	21	0.1	27	0.03	0.59	0.03	0.45	4180	2	< 2	4	< 2	2	6
052178	R96-53A	221	1.48	0.079	2	121	2.94	102	0.12	2.64	0.1	1.24	11	4	4	5	< 2	< 1	10
052179	R96-53D	310	5.97	0.064	33	124	5.56	41	0.21	2.42	0.32	0.29	< 4	5	10	13	< 2	2	17
052180	R96-54	74	2.82	0.043	2	123	0.67	41	0.18	3.31	0.23	1.76	38	4	4	7	< 2	4	7
052182	R96-55	64	0.42	0.077	< 2	107	0.53	98	0.21	3.46	0.12	2.94	< 4	8	3	11	< 2	1	8
052183	R96-60A	253	4.86	0.154	12	48	2.32	199	0.77	8.56	3.08	1.65	7	10	< 2	32	< 2	1	21
052184	R96-60B	146	1.02	0.067	4	92	0.3	31	0.11	2.37	0.13	1.88	731	5	< 2	14	< 2	< 1	8
052185	R96-60C	11	0.98	0.005	< 2	15	0.18	20	< .01	0.21	0.01	0.05	< 4	< 2	6	6	< 2	< 1	3
052186	R96-61A	270	6.92	0.161	15	39	2.03	225	0.56	7.6	2.95	0.59	8	17	3	31	2	1	21
052187	R96-61B	109	0.71	0.051	5	125	0.36	120	0.17	2.35	0.44	1.18	12	3	< 2	13	< 2	< 1	8
052188	R96-62A	122	2.53	0.475	23	128	0.34	105	0.33	4.59	0.4	4.76	15	12	< 2	50	4	< 1	6
052189	R96-62B	180	4.34	0.339	23	130	1.04	289	0.33	6.66	3.42	0.75	7	13	< 2	50	2	< 1	13
052190	R96-62C	373	4.52	0.175	12	160	1.59	51	0.27	5.3	0.5	4.38	7	15	< 2	43	2	< 1	15
052192	R96-62D	910	6.08	0.271	7	73	3.06	88	0.3	4.14	2.08	0.75	143	11	< 2	52	< 2	< 1	< 1
052193	R96-63	204	11.21	0.11	51	86	5.39	219	0.25	4.81	1.21	0.76	5	15	< 2	29	< 2	1	13
052194	R96-64A	52	0.49	0.017	5	94	0.23	67	0.07	1.37	0.12	0.25	< 4	2	3	6	< 2	< 1	7
052195	R96-64B	42	0.33	0.017	4	100	0.28	25	0.07	1.42	0.13	0.4	< 4	2	< 2	7	< 2	< 1	7
052196	R96-64C	197	0.77	0.123	11	82	1.04	197	0.47	6.77	0.22	2.87	< 4	7	11	19	< 2	< 1	17
052197	R96-65A	298	1.68	0.155	11	113	0.51	147	0.38	6.94	0.48	2.41	15	2	13	26	< 2	< 1	30
052198	R96-65B	227	0.44	0.106	11	71	1.55	37	0.33	5.04	0.17	1.73	< 4	< 2	7	19	< 2	3	20
052199	R96-66A	45	2.08	0.011	4	143	0.15	29	0.01	0.44	0.01	0.17	< 4	4	5	7	< 2	< 1	4
052200	R96-66B	89	2.25	0.055	12	146	0.15	66	0.04	0.79	0.03	0.3	< 4	6	4	18	< 2	< 1	5
052202	R96-67A	74	2.28	0.024	4	143	0.25	40	0.14	2.1	0.04	0.56	< 4	6	17	7	< 2	2	10
052203	R96-67B	105	0.91	0.024	15	134	0.44	37	0.2	2.57	0.09	0.45	28	4	7	10	< 2	1	12
052204	R96-67C	47	0.66	0.017	17	108	0.19	31	0.13	3.27	0.05	1.33	10	2	10	11	< 2	< 1	4
052205	R96-69	143	6.23	0.065	< 2	38	3.37	6	0.05	1.6	0.39	0.07	< 4	< 2	< 2	6	< 2	< 1	33
052156	R96-70	104	5.11	0.076	< 2	43	1.44	70	0.15	4.12	0.83	0.91	5	3	2	10	4	< 1	12
052206	R96-70A	40	4.67	0.067	2	30	1.97	42	0.15	6.49	0.92	0.56	< 4	< 2	< 2	12	< 2	3	4
052207	R96-71A	80	1.16	0.073	29	44	0.78	31	0.21	3.85	0.42	3.84	< 4	3	2	11	3	1	9
052161	R96-72	156	3.26	0.049	2	90	1.81	62	0.41	4.22	0.35	3.22	177	3	3	26	< 2	< 1	17
052208	R96-73	136	1.28	0.058	3	232	1.49	40	0.3	4.62	0.2	4.23	824	7	3	8	< 2	< 1	11
052209	R96-74A	43	7.42	0.026	5	67	2.42	9	0.03	0.9	0.03	0.01	< 4	< 2	3	9	< 2	< 1	3
052210	R95-74B	276	9.77	0.047	210	158	4.95	90	0.13	2.63	0.89	1.04	9	4	5	11	< 2	< 1	11

Notes

Fe*, Cr = Possible Fe & Cr contamination from grinding

Method = HClO4-HNO3-HCl-HF digestion - inductively coupled plasma emission spectroscopy

Lab = ACME Analytical

APPENDIX 6B
ANALYSES OF SAMPLES FROM DEPOSITS IN THE ROSSLAND CAMP (BY INA)

Lab No.	Field No.	Au	Ag	As	Ba	Br	Ca	Co	Cr	Cs	Fe	Hf	Hg	Ir	Mo	Na	Ni	Rb	Sb	Sc	Se	Sn	Sr	Ta	Th	U	W	Zn	La	Ce	Nd	Sm	Eu	Yb	Yb	Lu	Mass
	Detection Limit	ppm 2	ppm 5	ppm 0.5	ppm 50	ppm 0.5	% 1	ppm 1	ppm 5	ppm 1	% 0.01	ppm 1	ppm 1	ppm 5	ppm 1	% 0.01	ppm 20	ppm 15	ppm 0.1	ppm 0.1	ppm 3	ppm 0.01	ppm 0.05	ppm 0.5	ppm 0.2	ppm 0.5	ppm 1	ppm 50	ppm 0.5	ppm 3	ppm 5	ppm 0.1	ppm 0.2	ppm 0.5	ppm 0.2	ppm 0.05	g 0
052136	R96-4	138	-5	30	3500	-0.5	8	13	190	5	6.67	6	-1	-5	17400	0.86	-25	230	2.7	17	-3	-0.02	-0.05	1.6	4.8	15	24	119	41	46	100	4.7	0.9	1.1	2.2	0.39	30.99
052137	R96-6	23	-5	16	4600	7.3	7	9	290	18	2.96	3	-1	-5	6790	1.39	-23	290	3	16	-3	-0.01	0.08	-0.5	5.5	29	17	-50	19	33	50	4.3	1	-0.5	2.6	0.47	31.08
052138	R96-7A	111000	-30	56900	-1000	-16	-8	34000	-35	-5	10.8	-4	-12	-44	25000	1.33	9400	-160	63	4.9	-25	-0.34	-0.28	-5	58	180	-40	-489	19	-227	-227	-227	-1.9	-4.8	-3.7	-0.73	31.82
052139	R96-7B	43300	-5	3900	1700	-4	-2	8800	-5	-1	1.32	-5	-1	-5	9400	3.24	2300	-46	29	5.1	-5	-0.08	-0.05	-0.5	14	250	-10	-83	35	31	30	-0.1	-0.2	-0.5	3.2	0.48	29.64
052140	R96-8	140	-5	47	150	-0.5	11	93	57	4	13.1	-1	-1	-5	8530	0.28	660	55	2.4	8.9	21	-0.01	-0.05	-0.5	1.4	-0.5	260	115	16	17	62	1.6	0.2	0.5	1.3	0.21	32.75
052142	R96-12A	-5	-5	58	-230	-1.8	-3	12	200	5	2.33	-1	-5	-5	40000	0.17	700	180	1.9	2.4	-5	-0.05	-0.05	-0.5	3.3	2.7	37	339	34	44	30	5	1.2	1.1	2.5	0.39	30.44
052143	R96-12D	538	16	61	310	-0.5	3	130	210	3	22	-1	-1	-5	51	0.1	130	91	7.7	8.3	32	-0.02	-0.05	-0.5	5.3	7.3	41	136	53	62	25	4.2	0.9	0.9	2.4	0.38	30.66
052144	R96-15	16	-5	14	3300	-0.5	5	7	310	5	1.91	5	-1	-5	21000	1.38	-24	230	3.1	19	40	-0.02	-0.05	-0.5	3.6	34	15000	92	55	61	84	4.9	1.3	1.4	2.9	0.43	30.01
052145	R96-17	332	-5	17	1400	-2.6	12	31	110	7	6.11	2	3	-5	92000	0.46	-20	140	8.3	14	45	-0.01	-0.05	-0.5	3.6	34	15000	92	55	61	84	4.9	1.3	1.4	2.9	0.43	30.01
052146	R96-18C	922	21	31	1200	-0.5	9	21	140	4	8.54	-1	-1	-5	21600	0.52	-25	130	4.5	12	-3	-0.02	-0.05	-0.5	3.9	3.6	130	236	84	72	130	3	1	-0.5	2.5	0.45	30.62
052147	R96-19A	72	-5	13	1800	-0.5	8	20	170	4	7.03	1	-1	-5	29000	0.52	110	200	2.3	17	-3	-0.02	-0.05	-0.5	3.7	44	580	-50	40	43	80	2.3	0.8	-0.5	1.6	0.25	31.95
052148	R96-19B	175	-5	4.5	800	-0.5	4	45	140	3	13.6	-1	3	-5	320	0.49	-20	140	3.6	20	-3	-0.01	-0.05	0.9	3.6	6.8	7000	134	51	55	30	3.6	1	-0.5	2.3	0.38	30.75
052149	R96-19C	30	-5	6.7	1800	-0.5	-1	9	150	5	5.31	-1	6	-5	29000	0.37	-34	100	1.7	15	-3	-0.02	-0.05	-0.5	26	14	370	-50	1800	1100	150	6.6	1.8	1.5	2.2	0.34	32.51
052150	R96-20B	77	9	100	400	-0.5	3	190	220	3	16.6	3	-1	-5	78	0.37	-25	88	3.8	8.8	26	-0.01	-0.05	-0.5	3.3	1.5	80	173	23	35	10	3.8	0.9	0.6	2.7	0.35	30.31
052151	R96-20C	41	-5	25	1700	-0.5	5	14	230	4	5.58	3	-1	-5	16500	0.82	-30	170	6.9	12	-3	-0.01	-0.05	-0.5	2.6	8.5	64	70	23	37	20	3.9	0.8	1	2.9	0.48	30.74
052152	R96-20D	41	-5	25	1700	-0.5	5	14	230	4	5.58	3	-1	-5	16500	0.82	-30	170	6.9	12	-3	-0.01	-0.05	-0.5	2.6	8.5	64	70	23	37	20	3.9	0.8	1	2.9	0.48	30.74
052153	R96-24A	2460	55	19	310	-0.5	5	19	110	2	7.88	2	-1	-5	32	2.66	-23	57	4.4	13	-3	-0.01	-0.05	0.5	1.8	2.6	-1	131	19	32	-5	2.6	1.2	-0.5	2.7	0.44	32.1
052154	R96-24D	1770	-5	28	1300	-0.5	5	77	150	-1	14	2	-1	-5	23	1.14	120	120	2.6	29	-3	-0.01	-0.05	-0.5	1	-0.5	-1	1410	8.6	18	-5	1.4	0.7	-0.5	1.8	0.31	30.4
052155	R96-24C	27500	75	12	850	-0.5	4	130	45	-1	23.1	1	-1	-5	15	0.48	-27	77	2.9	8.4	-3	-0.02	-0.05	-0.5	1.6	1.6	4	110	11	22	-5	1.8	0.8	-0.5	1.5	0.2	30.44
052157	R95-28A	2100	-5	44	-50	-0.5	15	55	58	4	15	1	-1	-5	32	0.16	-21	-15	2.1	4.4	17	-0.01	-0.05	-0.5	1.6	1.6	4	110	11	22	-5	1.8	0.8	-0.5	1.5	0.2	30.44
052158	R96-28D	1370	6	51	1700	-0.5	5	110	83	6	22.4	2	-1	-5	18	0.21	-25	140	5.3	14	33	-0.01	-0.05	-0.5	1.3	-0.5	-1	82	3.9	10	5	1.7	0.5	-0.5	2.3	0.36	31.91
052159	R96-31A	11000	33	810	580	-0.5	3	110	69	-1	20.5	2	-1	-5	80	2.28	-25	100	4.8	9.6	7	-0.02	-0.05	-0.5	1.2	3.1	-1	269	8.4	16	6	2.1	0.5	-0.5	1.8	0.35	31.68
052160	R96-31B	2610	10	2400	-50	-0.5	2	53	120	4	23.4	1	-1	-5	9	0.1	-28	80	12	9.8	-3	-0.02	-0.05	-0.5	1.1	-0.5	28	11600	6.1	10	-5	0.7	0.5	-0.5	0.8	0.12	32.2
052162	R96-35C	14400	-5	13	-50	-0.5	4	230	71	-1	43.3	-1	-1	-5	195	0.76	-32	-15	3.7	9.2	40	-0.02	-0.05	-0.5	1	3.1	-1	-50	43	51	14	1.4	0.4	-0.5	0.7	0.13	30.6
052163	R96-39A	160	5	12	320	-0.5	2	370	76	4	30	2	-1	-5	-1	1.5	-30	120	0.9	5	25	-0.01	-0.05	-0.5	6.2	-0.5	13	167	48	78	28	3.3	0.6	-0.5	0.9	0.15	31.18
052164	R96-40B	15800	-5	78000	-220	-8.2	-2	2700	-10	-1	29.4	-1	-1	-5	-23	0.47	-120	100	120	8	-4	-0.05	-0.05	-0.5	-0.5	-5.3	-10	-50	-1	-20	-25	-0.3	-0.5	-1.5	-0.5	-0.08	30.8
052165	R96-42A	24100	-5	280	160	-0.6	11	160	63	-1	31.9	-1	-1	-5	-4	0.01	-44	-15	1.6	23	-3	-0.03	-0.05	0.8	-0.2	-0.5	-2	-50	7.4	23	-5	3.7	1	-0.5	2.6	0.48	30.99
052166	R96-42B	8960	-5	190000	-410	-10	-5	1900	-10	-1	20.1	-1	-5	-5	-38	0.56	-170	-44	280	5.9	-10	-0.15	-0.11	-3	-1.9	-11	-24	-72	-1	-3	-5	-0.5	-0.4	-0.5	-1.6	-0.25	33.25
052167	R96-44A	1190000	27	27000	-180	-4	-4	2300	72	-1	31.8	-1	-1	-5	-22	0.52	-110	100	33	10	-4	-0.05	-0.05	-1.5	-0.5	-4.8	-10	-50	2	-3	-5	-0.1	-0.2	-0.5	-0.5	-0.08	32.14
052168	R96-44B	119000	27	27000	-180	-4	-4	2300	72	-1	31.8	-1	-1	-5	-22	0.52	-110	100	33	10	-4	-0.05	-0.05	-1.3	8.6	-3.7	-10	-50	12	-12	-5	0.3	-0.2	-0.5	2.3	0.35	31.48
052169	R96-45B	21000	-5	38000	-160	-4.1	-5	2100	-7	-1	44.8	-1	-1	-5	-11	0.34	-100	100	41	4.4	-4	-0.04	-0.05	-0.8	7.7	-0.9	-3	-50	9.8	29	-5	2.1	-0.2	-0.5	2.1	0.35	31.86
052170	R96-46A	944	-5	3000	-85	-1.1	-2	980	88	7	40.4	-1	-1	-5	500	0.27	-71	67	42	6.7	-4	-0.04	-0.05	-0.8	7.7	-0.9	-3	-50	9.8	29	-5	2.1	-0.2	-0.5	2.1	0.35	31.86
052172	R96-47A	15300	13	4100	510	-1.1	19	120	56	3	13.8	-1	-1	-5	-1	0.03	-36	-15	9.1	4.8	-3	-0.02	-0.05	-0.5	-0.2	-0.5	-2	235	-0.5	-3	-5	-0.1	-0.2	-0.5	0.4	0.08	30.41
052173	R96-48A	6190	34	250	-54	-0.9	7	170	44	-1	31.4	-1	2	-5	-1	0.07	-36	25	7.5	23	-3	-0.02	-0.05	-0.5	-0.2	-0.5	5300	1220	-0.5	-3	-5	0.2	-0.2	-0.5	-0.2	-0.05	32.46
052174	R96-51B	1610	150	55	-56	-1.6	-3	400	42	-1	44.2	-1	4	-5	120	0.1	330	50	1.8	2.6	30	-0.02	-0.05	-0.5	-0.2	-0.5	19	11800	2.3	5	-5	0.5	-0.2	-0.5	0.3	-0.05	30.33
052175	R96-51C	1200	21	620	-64	-0.7	-1	69	220	-1	10.8	2	-1	-5	32	0.13	90	140	33	9.8	-3	-0.02	-0.05	-0.5	-0.2	-0.5	30	763	-0.5	-3	-5	-0.1	-0.2	-0.5	-0.2	-0.05	33.48
052176	R96-51C	906	33	850	-63	-0.7	-2	68	290	-1	31.9	-1	2	-5	46	0.04	-28	-15	4.5	2.8	25	-0.02	-0.05	-0.5	-0.2	-0.5	7200	-50	-0.5	-3	-5	-0.1	-0.2	-0.5	1.6	0.25	32.38
052177	R96-52	413	-5	38000	-110	-4.5	-3	850	33	-1	39.2	-1	-1	-5	-5	0.06	-56	-15	86	0.6	-3	-0.02	-0.05	-0.5	-0.2	-0.5	19	534	1.7	-3	-5	0.5	0.3	-0.5	0.9	0.15	31.55
052178	R96-53A	2440	32	1000	-50	-0.8	1	120	150	7	28.9	-1	-1	-5	53	0.14	160	140	3.4	10	16	-0.01	-0.05	-0.5	-0.2	-0.5	-2	1190	33	52	18	2.8	1.2	-0.5	1.3	0.2	30.58
052179	R96-53D	5600	99	43	-50	7	6	140	140	-1	17.7	1	-1	-5	95	0.38	-32	-15	2.8	18	-3	-0.01	-0.05	-0.5	1	-0.5	-2	1190	33	52	18	2.8	1.2	-0.5	-0.5	-0.07	30.33
052180	R96-54	3020	58	120600	-160	-13	-4	3000	140	-1	28.6	2	-2	-5	-10	0.46	370	180	120	8.4	-3	-0.05	-0.05	-1	-0.5	-5.1	-31	560	-0.5	-3	-5	-0.1	-0.2	-0.5	1.3	0.22	32.5
052182	R96-55	4460	50	970	220	-0.5	-1	28	150	3	21.1	1	-1	-5	28	0.12	180	190	5.6	6.3	-3	-0.02	-0.05	-0.5	1.5	-0.5	9	1830	1.3	3	-5	0.7	0.2	-0.5	1.3	0.22	31
052183	R96-60A	83	-5	660	1100	-0.5	5	22	70	3	6.6	4	-1	-5	-2	3.45	-27	120	6.5	21	-3	-0.02	-0.05	-0.5	2.6	-0.5	-1	-50	14	33	15	4.1	1.6	-0.5	3.6	0.61	30.67
052184	R96-60B	88	-5	13000	1300	-1.4	-2	420	130	2	33.6	-1	-2	19	-1	0.13	-63	71	3.2	6.2	-5	-0.05	-0.05	-0.7	-0.4	3.9	630	277	5.7	-3	-5	1.5	0.7	-0.5	1.5	0.23	31
052185	R96-60C	19	-5	230	-50	-0.5	2	130	18	-1	46.9	-1	-1	-5	-1	-0.01	250	45	12	0.6	35	-0.02	-0.05	-0.5	-0.2	-0.5	-2	79	2.1	6	-5	0.3	-0.2	-0.5	-0.2	-0.05	32.79
052186	R96-61A	109	-5	17	380	-0.5	8	46	62	-1	7.19	3	-1	-5	24	3.25	190	-15	4.7	20	25	-0.01	-0.05	-0.5	3	4.3	-1	159	17	43	26	4.7	1.7	-0.5	3.2	0.44	30.64
052187	R96-61B	10500	-5	600	320	-0.5	2	92	150	-1	22.8	-1	-1	-5	-3	0.49	70	55	6.7	5.7	28	-0.02	-0.05	-0.5	1.2	-0.5	11	88	5.4	11	-5	1.5	0.3	-0.5	1.1	0.18	30.99
052188	R96-62A	5000	-10	180000	2500	-15	-4	6000	-10	-1	10.4	-1	-5	-5	8400	0.57	1600	-46	280	4.1	-10	-0.1	-0.05	-3.2	9.8	-0.1	-37	669	26	60	20	5.8	0.3	-0.5	-1.2	-0.3	31.6
052189	R96-62B	17300	-5	89000	-150	-7.1	-2	2500	120	-1	8.55	3	-1	-5	330	4.04	-68	-22	280	9.2	42	-0.04	-0.05	-0.5	4.4	-3.4	-18	-50	31	42	20	5.8	1	-0.5	3.2	0.49	32.62
052190	R96-62C	13800	-5	11000	2600	-2.6	-2	4100	180	-1	12.7	-1	-1	-5	380	0.66	500	250	45	15	40	-0.04	-0.05	-0.5	4.4	-3.4	-18	-50	31	42	20	5.8	1	-0.5	3.2	0.49	32.62
052192	R96-62D	38500	-5	10000	14000	-2.8	7	340	84	-1	9.11	2	-1	-5	68000	2.16	350	85	18	21	76	-0.03	-0.05	-0.5	16	1520	190	190	94	-227	140	-227	1.4	-0.5	3.6	0.54	32.11
052193	R96-63	11	-5	200	910	-0.5	14	7	100	2	7.46	4	-1	-5	30	1.23	-21	46	2.3	9.7	17	-0.01	0.08	-0.5	5	2.8	-1	141	55	77	26	3.7	0.8	-0.5	2.5	0.39	30.34
052194	R96-64A	27400	260	26000	720	-2.2	-2	160	100	-1	22.6	-1	-1	-5	-1	0.19	-100	-17	280	5.2	-9	-0.11	-0.05	-1.1	-0.9	13	-5	49700	3.6	-3	-5	0.5	-0.2	-0.5	-0.5	-0.1	30.62
052195	R96-64B	29600	240	27000	520	-2.3	-2	160	120	-1	23.2	-1	-1	-5	6	0.16	-51	50	380	5.5	-3	-0.04	-0.05	-0.5	2.4	-2.8	-6	50000	4.4	-5	-5	1.1	0.2	-0.5	-0.3	-0.05	30.1

APPENDIX 6B, CONTINUED

Lab No.	Field No.	Au	Ag	As	Ba	Br	Ca	Co	Cr	Cs	Fe	Hf	Hg	Ir	Mo	Na	Ni	Rb	Sb	Sc	Se	Sm	Ta	Th	U	W	Zn	La	Ce	Nd	Sm	Eu	Yb	Yb	Lu	Barren
	Detection	ppm	ppm	ppm	ppm	ppm	%	ppm	ppm	ppm	%	ppm	ppm	ppb	ppm	%	ppm	ppm	ppm	ppm	ppm	ppm	ppm	ppm	ppm	ppm	ppm	ppm	ppm	ppm	ppm	ppm	ppm	ppm	ppm	ppm	
	Limit	2	5	0.5	50	0.5	1	1	5	1	0.01	1	1	5	1	0.01	20	10	0.1	0.1	3	0.01	0.05	0.5	0.2	0.5	1	50	0.5	3	5	0.1	0.2	0.5	0.2	0.05	0
052196	R86-64C	226	60	53	730	-0.5	-1	10	54	5	11.8	3	-1	-5	11	0.24	-20	130	36	16	-3	-0.01	-0.05	-0.5	2.4	1.8	-1	6630	11	26	11	2.6	0.4	-0.5	2.6	0.45	30.01
052197	R86-65A	910	-5	6660	280	-0.5	2	12	140	-1	9.7	2	-1	-5	-1	0.51	-20	55	35	29	-3	-0.03	-0.05	-0.5	2	3	16	167	12	31	11	4.4	0.4	0.6	2.8	0.5	29.61
052198	R86-65B	3440	27	6320	550	-0.5	-1	15	76	-1	23	1	-1	-5	-3	0.18	-37	36	33	29	-3	-0.03	-0.05	-0.5	1	-0.5	-2	17300	10	24	15	2.9	0.4	0.7	2.1	0.39	31.55
052200	R86-66B	4660	280	24800	-100	-2.1	-3	15	130	-1	28.4	-1	5	-5	-2	0.07	-50	-15	670	1.2	13	-0.03	-0.05	-0.5	-0.3	-2.4	-5	54800	3.3	-4	-5	0.8	0.6	-0.5	-0.2	-0.05	31.41
052202	R86-67A	12660	120	129000	-120	-2.1	-3	68	550	5	34.3	-1	-1	-5	-5	0.2	-50	-15	390	8.4	-3	-0.03	-0.05	-0.5	-0.5	-4.3	-10	88800	1	-3	-5	-0.1	-0.2	-0.5	-0.2	-0.05	31.43
052203	R86-67B	13290	280	880	-50	-0.5	2	130	980	5	23.2	-1	-1	-5	27	0.09	-20	41	38	12	-3	-0.02	-0.05	-0.5	1.4	0.8	39	2410	17	31	10	2.7	0.3	-0.5	1.4	0.10	30.68
052204	R86-67C	5900	630	54900	-120	-4.6	-3	160	100	-1	27.7	-1	-1	-5	-5	0.1	-50	-94	320	3.7	-4	-0.05	-0.05	-0.5	-0.5	-3.1	-13	16200	22	20	5	1.7	-0.2	-0.5	-0.4	-0.07	30.45
052205	R86-69	340	-5	52	-50	7.3	7	200	63	-1	28.8	-1	-1	-5	-2	0.43	-30	-15	1.8	20	10	-0.01	-0.05	-0.5	-0.2	-0.5	-2	174	1.1	5	9	0.5	-0.2	-0.5	0.5	0.15	31.46
052196	R86-70	374	-5	65	360	-0.5	6	600	54	7	24.9	2	-1	-5	36	0.80	-30	65	10	9	10	-0.02	-0.05	1.1	1.5	-0.5	-1	157	2.0	9	-5	1.2	0.6	-0.5	1.2	0.10	31.03
052206	R86-70A	59	-5	150	410	-0.5	6	480	58	4	21.4	2	-1	-5	-1	1.09	-27	-15	11	4.3	5	-0.01	0.09	-0.5	1.6	2.2	-1	101	3.2	7	-5	1.3	0.5	-0.5	1.4	0.22	30.6
052207	R86-71A	2460	13	33	1600	-0.5	2	100	62	1	28.6	2	-1	-5	169	0.44	-26	130	10	8.7	6	-0.01	-0.05	-0.5	3.1	2.9	-1	132	45	59	17	2.4	0.8	-0.5	1.2	0.2	32.65
052161	R86-72	1150	20	220	1300	-0.5	3	73	120	7	21.5	1	-1	-5	-1	0.38	-25	180	4.9	16	-3	-0.01	-0.05	-0.5	0.8	-2.7	160	210	2.8	7	-5	2	0.8	-0.5	3	0.45	31.08
052208	R86-73	8660	37	560	2300	-0.5	2	180	280	7	25.4	-1	1	-5	21	0.24	160	240	11	9.9	25	-0.02	-0.05	-0.5	2.7	6.6	840	220	5.8	10	12	0.8	0.6	-0.5	1.2	0.10	31.26
052209	R86-74A	6550	-5	63	-50	-0.5	8	360	110	-1	37.7	-1	-1	-5	-2	0.03	370	-15	7.8	3.3	16	-0.01	-0.05	-0.5	-0.2	-0.5	-1	137	5.4	13	6	1.1	0.9	-0.5	-0.2	-0.05	30.9
052210	R86-74B	4650	-5	10	330	-0.5	12	70	200	-1	14	1	-1	-5	270	0.96	-24	85	2.8	9.8	7	-0.01	-0.05	-0.5	1.4	-0.5	-2	116	260	280	73	7.1	2.5	-0.5	1.4	0.3	31.39

Notes
Fe*, Cr - Possible Fe & Cr contamination from grinding
Method (INA) - Thermal neutron activation analysis
Lab - ActLabs, Ancaster, Ontario
BAL - Balance

APPENDIX 7
RE-OS DATING OF MOLYBDENITE, COXEY DEPOSIT, RED MOUNTAIN, B.C.

By Holly Stein, P.Geo., AIRIE Program
Department of Earth Resources, Colorado State University
Fort Collins, CO 80523-1482 USA

INTRODUCTION

Molybdenite mineralization in the Rossland camp, southern British Columbia, occurs in a breccia-skarn complex within metasedimentary rocks of the Early Jurassic Elise Formation. The molybdenite breccia complex lies structurally and stratigraphically above veins of the main Rossland copper-gold camp. Molybdenite from the Coxey deposit in the breccia complex was dated using the Re-Os method in order to determine its relationship, if any, with the gold-copper mineralization and to attempt to relate it to one of the many magmatic and tectonic events affecting the region.

Molybdenite presents a unique situation for the Re-Os dating method in that it usually contains ppm level Re and essentially no initial or common Os, making it a single mineral chronometer. Hence, single sample dating of molybdenite yields accurate and precise ages using this method, even for deposits that have undergone high grade metamorphism and deformation (*e.g.*, Stein *et al.*, 1998a; Raith and Stein, 2000).

SAMPLE R96-17

A molybdenite separate from a hand sample of skarn ore from the B pit on the Coxey claim was analyzed. In this sample, the molybdenite is fine-grained and massive, and occurs with minor pyrrhotite in a 2 centimeter wide vein cutting pale green, brecciated diopside skarn.

METHODOLOGY

General principles and methodology for molybdenite separation, preparation and analyses are outlined in Stein *et al.* (submitted; 1998a; 1998b). For this sample, a Carius-tube digestion was used, whereby molybdenite is dissolved and equilibrated with Re and Os spikes in a HNO_3-HCl (*aqua regia*) by sealing in a thick-walled glass ampule and heating for 12 hours at 230°C.

The Os is subsequently recovered by solvent extraction using CCl_4 and the Re is recovered by anion exchange. Purified Re and Os are loaded onto Pt filaments and isotopic compositions are determined using NTIMS on a NBS 12-inch radius, 90° sector mass spectrometer at CSU. Two in-house molybdenite standards, developed at AIRIE, are run routinely as an internal check (Markey *et al.*, 1998).

RESULTS

Listed below are the are the results with the absolute 2-sigma uncertainties (in parentheses) for the last digit indicated.

AIRIE Run # CT-371
Sample R96-17
Re = 25.08 (1) ppm
^{187}Os = 42.83 (4) ppb
Age = 162.9 ± 0.5 Ma (2-sigma)

REFERENCES

Markey, R.J., Stein, H.J. and Morgan, J.W. (1998): Highly precise Re-Os dating of molybdenite using alkaline fusion and NTIMS; *Talanta*, v. 45, p. 935-946.

Raith, J.G. and Stein, H.J. (2000): Re-Os dating and sulfur isotope composition of molybdenite from tungsten deposits in western Namaqualand, South Africa: implications for ore genesis and the timing of metamorphism; *Mineralium Deposita*, v. 35, no. 8, p. 741-753.

Stein, H.J., Sundblad, K., Markey, R.J., Morgan, J.W. and Motuza, G. (1998a): Re-Os ages for Archean molybdenite and pyrite, Kuittila-Kivisuo, Finland and Proterozoic molybdenite, Kabeliai, Lithuania: testing the chronometer in a metamorphic and metamorphic setting; *Mineralium Deposita*, v. 33, p. 392-345.

Stein, H.J., Morgan, J.W. Markey, R.J. and Hannah, J.L. (1998b): An introduction to Re-Os: What's in it for the mineral industry? *SEG Newsletter*, v. 32, p. 1,8-15.

Stein, H.J., Markey, R.J., Morgan, J.W., Hannah, J.L., and Scherstén, A. (submitted) The remarkable Re-Os chronometer in molybdenite: how and why it works: *Terra Nova*.

APPENDIX 8
ISOTOPE CHARACTERIZATION OF LEAD IN GALENA FROM MINERAL DEPOSITS IN THE TRAIL MAP SHEET (082F-SW), SOUTH-CENTRAL BRITISH COLUMBIA

By Colin I. Godwin, P.Eng and Janet Gabites, P.Geo
Department of Earth and Ocean Science, The University of British Columbia, Vancouver, British Columbia, Canada V6T 1Z4

ABSTRACT

Lead isotope analyses of galena from 39 mineral occurrences in the Trail map sheet (082F-SW) in south central British Columbia (between latitude 49.0° and 49.5° north and longitude 117.0° and 118.0° west) are reported. These isotope analyses of deposits in the Trail map sheet plot as three distinct clusters that appear to be related to three distinct mineralizing events. Each cluster is summarized below.

Cluster 1 is characterized by: (i) deposit occurrences in the Patterson area and the Keystone-Erie area, (ii) polymetallic veins in Quesnel terrane, (iii) a pronounced Mantle lead component that may have been derived from primitive basement to Quesnel terrane and/or from Tertiary lamprophyre dykes, and (iv) a linear trend to lead isotope data that may represent deposits of variable ages from Carboniferous to Tertiary.

Cluster 2 is characterized by: (i) deposit occurrences in the Rossland, Nelson, Ymir and Sheep Creek camps, and the Keystone-Erie area, (ii) polymetallic veins, many within or spatially related to Jurassic intrusions, mainly in the Quesnel terrane, but also in the Sheep Creek camp in ancestral North America, (iii) a pronounced Upper Crustal component to the lead isotopes such that they plot close to the Pericratonic lead isotope model that is relevant to terranes immediately marginal to North America, and (iv) a mixing trend from a Jurassic point on the Pericratonic model toward the lead isotope composition of the Mantle modeled in the Jurassic-Cretaceous.

Cluster 3 is characterized by: (i) deposit occurrences in the Salmo Camp, the border between the Salmo and Sheep Creek camps, and the Keystone-Erie area near the border with the Salmo Camp, (ii) numerous Salmo-type carbonate-hosted deposits, several polymetallic veins in North America terrane, and one polymetallic vein in Quesnel terrane, (iii) an Upper Crustal type of lead isotope that plots close to the Shale lead isotope model for North America, and (iv) a mixing trend from a Jurassic point on the Shale model toward the lead isotope composition of the Upper Crust in the Jurassic-Cretaceous.

Mixing trends in galena lead isotope data indicate that Cluster 2 and Cluster 3 may be related to I-type and S-type plutons, respectively. Deposits associated with I-type plutons show a variable component of Mantle lead, whereas those associated with the S-type show variable mixing with Lower Crustal lead. Thus, the Salmo carbonate-hosted zinc-lead deposits, which might be associated with S-type plutons, may be metamorphosed and deformed manto deposits.

INTRODUCTION

This paper presents a compilation of galena lead isotope compositions for 77 samples from 39 mineral occurrences in the Trail map sheet (082F-SW) in south-central British Columbia (between latitude 49.0° and 49.5° north and longitude 117.0° and 118.0° west). Important towns in the region include Trail, Rossland, Salmo, Castlegar, Nelson and Ymir.

Mineral deposits analyzed in the Trail map sheet (082F-SW) are located on Figure A8-1. Galena lead isotopic analyses from these occurrences are in Table A8-1, and the isotope data are plotted in Figures A8-2 to 5. Detailed location data of the deposits are in TableA8- 2 and general geology is in Table A8-3.

GALENA LEAD ISOTOPE ANALYSES

Galena samples of the mineral occurrences reported in Tables 1 to 3 are from a number of sources. Apart from those analyses obtained from published articles, the samples analyzed in the Geochronology Laboratory, Department of Earth and Ocean Sciences, The University of British Columbia (UBC), came from the UBC Economic Geology collection, and field collections by Trygve Höy, Kathryn Dunne, Colin Godwin, Janet Gabites, Jim Logan, George Addie and Mel de Quadros.

Galena lead isotope data in Table 1 obtained prior to 1982 were normalized (outlined in Godwin *et al.*, 1988, page 26) so that they are generally consistent with values currently generated in the Geochronology Laboratory. The errors associated with some of this older data can be obtained by reference to the source of the data. However, data published prior to 1973 is difficult to evaluate in terms of current normalization and analytical errors. Consequently, this data has not been used in determining isotopic values for the deposits; data omitted from average values for the deposits are identified in Table 3 with italicized entries.

Analytical techniques used from 1982 to the present in the Geochronology Laboratory were as follows (analytical details are in Godwin *et al.*, 1988). A small, clean cleavage cube of galena (<0.1 gram), handpicked under binocular microscope from each sample, was washed and dissolved in dilute hydrochloric acid. After evaporation to lead chloride, approximately 10 to 25 nanograms of the lead were loaded on a single rhenium filament with phosphoric acid and silica gel. Isotopic compositions were determined using a modified Vacuum Generators Ltd. Isomass 54R solid-source mass spectrometer. Measured ratios were normalized for instrument mass fractionation based on replicate analyses of

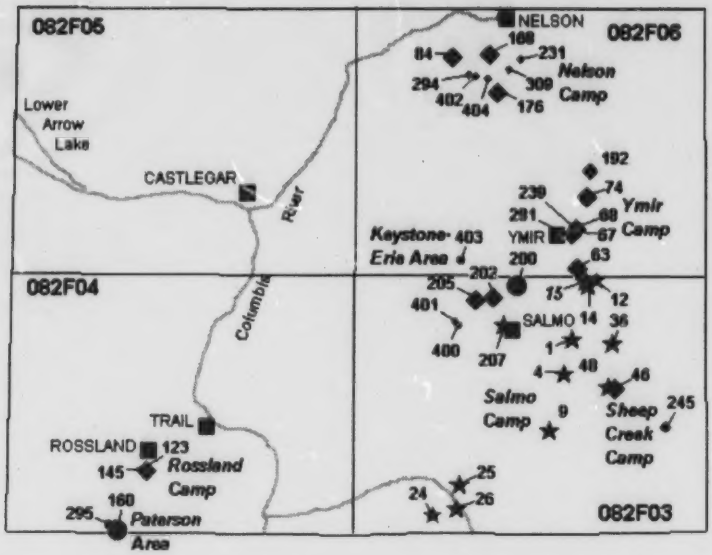

Figure A8-1. Location of mineral occurrences analyzed in the Trail map sheet (082F/SW). Galena lead isotope analyses for the occurrences are in Table A8-1. Detailed location data are in Table A8-2 and general geology is in TableA8- 3.

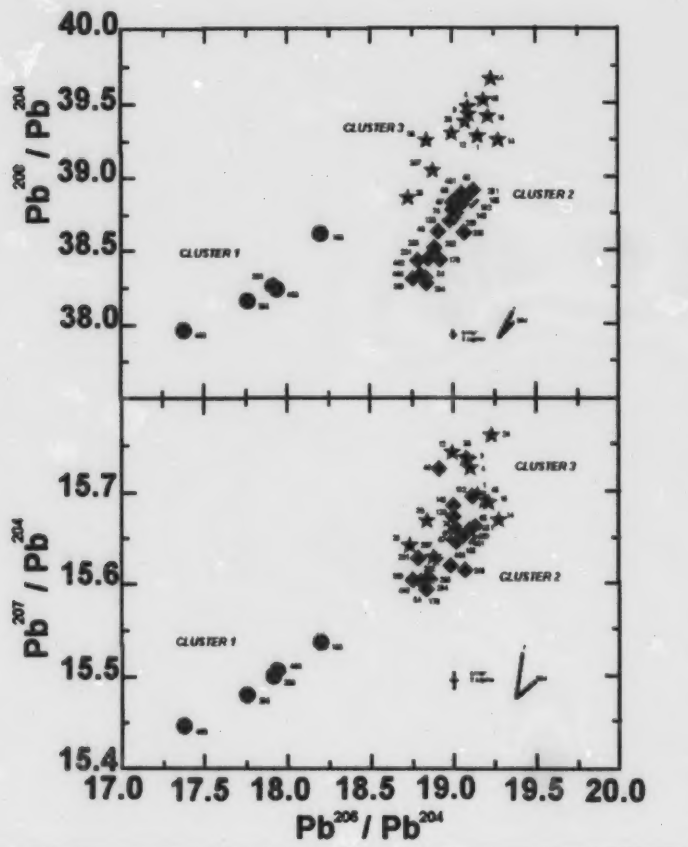

Figure A8-2. General $^{206}Pb/^{204}Pb$ versus $^{207}Pb/^{204}Pb$ and $^{206}Pb/^{204}Pb$ versus $^{208}Pb/^{204}Pb$ plots of galena lead isotopes from mineral occurrences in the Trail map sheet (082F/SW). Note that the data in the $^{206}Pb/^{204}Pb$ versus $^{208}Pb/^{204}Pb$ plot (upper part of figure) shows that the data can be divided into three clusters by inspection. Data for the deposits are from Table 1. Symbol size relates to deposit status in Table 2: large symbol = past producer, medium symbol = developed prospect, and small symbol = showing or prospect.

Numbers beside isotope symbols refer to columns labeled No. in Tables 1 to 3. Error bars at two sigma are valid only for analyses done in the Geochronology Laboratory, Department of Earth and Ocean Sciences, The University of British Columbia. Trends for fractionation error and ^{204}Pb error are shown as lines notated with an "f" and "204", respectively.

TABLE A8-1
GALENA LEAD ISOTOPE ANALYSES OF MINERAL OCCURRENCES IN THE TRAIL MAP SHEET (082F/SW)

Deposit Name	Minfile	Fig No	Camp, area	Lab no	Anal	Quality	Pb^{206}/Pb^{204}	Pb^{207}/Pb^{204}	Pb^{208}/Pb^{204}	Pb^{207}/Pb^{206}	Pb^{206}/Pb^{208}
CLUSTER 1											
Sunset	SW160	160		31067-001	91PI	fair	18.207	15.543	38.646	0.85371	2.1227
Sunset	SW160	160		31067-001	91PI	good	18.193	15.530	38.594	0.85365	2.1214
SUNSET 2	**SW160**	**160**	**PATERSON**		**AVG 2**	**GOOD**	**18.200**	**15.537**	**38.620**	**0.85400**	**2.1220**
Clubine	SW200	200		31065-001	91PI	fair	17.889	15.501	38.261	0.86652	2.1388
Clubine	SW200	200		31065-002	91PI	fair	17.934	15.501	38.268	0.86434	2.1339
Clubine	SW200	200		31065-003	91PI	fair	17.924	15.499	38.265	0.86469	2.1348
CLUBINE	**SW200**	**200**	**KEYSTONE-ERIE**		**AVG 3**	**FAIR**	**17.916**	**15.500**	**38.265**	**0.86500**	**2.1360**
Mitzie 1	SW295	295		31086-001	92PI	poor	17.753	15.472	38.141	0.87151	2.1485
Mitzie 1	SW295	295		31086-001	92PI	good	17.769	15.487	38.188	0.87158	2.1491
MITZIE 1	**SW295**	**295**	**PATERSON**		**AVG 2**	**GOOD**	**17.761**	**15.480**	**38.165**	**0.87200**	**2.1490**
Showing 31082	SW400	400		31082-001	92PI	good	17.938	15.509	38.253	0.86461	2.1325
Showing 31082	SW400	400		31082-001	92PI	fair	17.934	15.505	38.242	0.86456	2.1323
SHOWING 31082	**SW400**	**400**	**KEYSTONE-ERIE**		**AVG 2**	**GOOD**	**17.936**	**15.507**	**38.248**	**0.86500**	**2.1320**
Showing 31080	SW403	403		31080-001	92PI	fair	17.383	15.447	37.956	0.88866	2.1835
Showing 31080	SW403	403		31080-001	92PI	good	17.381	15.442	37.941	0.88845	2.1829
Showing 31080	SW403	403		31080-001	92PI	good	17.382	15.452	37.994	0.88899	2.1858
SHOWING 31080	**SW403**	**403**	**KEYSTONE-ERIE**		**AVG 3**	**GOOD**	**17.382**	**15.447**	**37.964**	**0.88900**	**2.1840**
STATISTICS: NUMBER							**5**	**5**	**5**	**5**	**5**
STATISTICS: MEAN							**17.839**	**15.494**	**38.252**	**0.86900**	**2.1446**
STATISTICS: STANDARD ERROR							**0.134**	**0.015**	**0.106**	**0.00577**	**0.0108**
CLUSTER 2											
Kootenay Belle	SW046	46		30311-001	79RY	good	18.914	15.725	38.639	0.83139	2.0429
KOOTENAY BELLE	**SW046**		**SHEEP CREEK**		**AVG 1**	**GOOD**	**18.914**	**15.725**	**38.639**	**0.83139**	**2.0429**
Porcupine (Franklin)	SE063	63		30060-001	88GA	good	19.131	15.660	38.895	0.81856	2.0331
Porcupine (Franklin)	SE063	63		30060-002	88GA	good	19.145	15.671	38.930	0.81857	2.0335
Porcupine (Franklin)	SE063	63		30060-004	88GA	good	18.901	15.629	38.626	0.82690	2.0436
Porcupine (Franklin)	SE063	63		30060-004	92PI	good	18.901	15.626	38.614	0.82674	2.0430
PORCUPINE (FRANKLIN)	**SE063**	**63**	**YMIR**		**AVG 4**	**GOOD**	**19.020**	**15.647**	**38.766**	**0.82300**	**2.0380**

TABLE A8-1, CONTINUED

Deposit Name	Minfile	Fig No	Camp, area	Lab no	Anal	Quality	Pb^{208}/Pb^{204}	Pb^{207}/Pb^{204}	Pb^{206}/Pb^{204}	Pb^{207}/Pb^{206}	Pb^{208}/Pb^{206}
Dundee	SW067	67		30061-001	88GA	good	19.055	15.653	38.826	0.82147	2.0376
DUNDEE	**SW067**	**67**	**YMIR**		**AVG 1**	**GOOD**	**19.055**	**15.653**	**38.826**	**0.82147**	**2.0376**
Yankee Girl	SW068	68		30064-001	88GA	good	19.097	15.646	38.864	0.81929	2.0351
Yankee Girl	SW068	68		30064-001	92PI	fair	19.100	15.659	38.883	0.81982	2.0357
Yankee Girl	SW068	68		30064-002	88GA	good	19.054	15.665	38.848	0.82215	2.0389
Yankee Girl	SW068	68		30064-002	92PI	good	19.050	15.646	38.798	0.82133	2.0367
Yankee Girl	SW068	68		30064-005	91PI	poor	19.191	15.675	39.002	0.81676	2.0323
Yankee Girl	SW068	68		30064-005	91PI	poor	19.191	15.675	39.002	0.81676	2.0323
Yankee Girl	SW068	68		30064-005	91PI	good	19.201	15.686	39.035	0.81694	2.0330
Yankee Girl	SW068	68		30064-005	92PI	good	19.172	15.655	38.936	0.81653	2.0309
YANKEE GIRL	**SW068**	**68**	**YMIR**		**AVG 8**	**GOOD**	**19.132**	**15.663**	**38.921**	**0.81900**	**2.0340**
Ymir	SW074	74		30451-001	82AN	good	19.055	15.660	38.841	0.82183	2.0384
Ymir	SW074	74		30451-002	82AN	good	19.076	15.696	38.934	0.82281	2.0410
Ymir	SW074	74		30451-008	91PI	fair	18.962	15.633	38.695	0.82448	2.0407
Ymir	SW074	74		30451-008	91PI	fair	18.990	15.661	38.789	0.82472	2.0426
Ymir	SW074	74		30451-008	91PI	good	18.987	15.657	38.769	0.82459	2.0419
Ymir	SW074	74		30451-501	60RUF	poor	19.224	15.892	39.239	0.82668	2.0412
Ymir	SW074	74		30451-502	73LE	good	18.989	15.675	38.776	0.82548	2.0420
YMIR	**SW074**	**74**	**YMIR**		**AVG 7**	**GOOD**	**19.019**	**15.660**	**38.807**	**0.82300**	**2.0400**
Eureka	SW084	84		31064-001	91PI	good	18.833	15.595	38.321	0.82810	2.0348
EUREKA	**SW084**	**84**	**NELSON**		**AVG 1**	**GOOD**	**18.833**	**15.595**	**38.321**	**0.82810**	**2.0348**
Homestake	SW123	123		31072-001	91PI	fair	19.004	15.674	38.728	0.82479	2.0379
HOMESTAKE	**SW123**	**123**	**ROSSLAND**		**AVG 1**	**FAIR**	**19.004**	**15.674**	**38.728**	**0.82479**	**2.0379**
Bluebird	SW145	145		31070-001	92PI	good	19.004	15.686	38.785	0.82539	2.0409
BLUEBIRD	**SW145**	**145**	**ROSSLAND**		**AVG 1**	**GOOD**	**19.004**	**15.686**	**38.785**	**0.82539**	**2.0409**
Athabaska	SW168	168		31074-001	91PI	good	19.005	15.648	38.833	0.82337	2.0433
ATHABASKA	**SW168**	**168**	**NELSON**		**AVG 1**	**GOOD**	**19.005**	**15.648**	**38.833**	**0.82337**	**2.0433**
Silver King (Nelson)	SW176	176		30911-001	87GA	poor	18.793	15.600	38.345	0.83011	2.0404
Silver King (Nelson)	SW176	176		30911-001	88GA	good	18.811	15.602	38.344	0.82944	2.0384
Silver King (Nelson)	SW176	176		30911-002	88GA	good	18.812	15.602	38.342	0.82940	2.0382
SILVER KING (NELSON)	**SW176**	**176**	**NELSON**		**AVG 3**	**GOOD**	**18.805**	**15.601**	**38.344**	**0.83000**	**2.0390**

TABLE A8-1, CONTINUED

Deposit Name	Minfile	Fig No	Camp, area	Lab no	Anal	Quality	Pb^{206}/Pb^{204}	Pb^{207}/Pb^{204}	Pb^{208}/Pb^{204}	Pb^{207}/Pb^{206}	Pb^{208}/Pb^{206}
Elise	SW192	192		30835-501	73LE	good	19.114	15.696	38.845	0.82118	2.0323
ELISE	**SW192**	**192**	**YMIR**		**AVG 1**	**GOOD**	**19.114**	**15.696**	**38.845**	**0.82118**	**2.0323**
Keystone	SW202	202		31084-001	92PI	fair	18.882	15.622	38.504	0.82733	2.0392
Keystone	SW202	202		31084-001	92PI	fair	18.896	15.636	38.542	0.82748	2.0397
KEYSTONE	**SW202**	**202**	**KEYSTONE-ERIE**		**AVG 2**	**FAIR**	**18.889**	**15.629**	**38.523**	**0.82700**	**2.0390**
Arlington	SW205	205		31073-001	91PI	fair	18.851	15.606	38.448	0.82788	2.0395
ARLINGTON	**SW205**	**205**	**KEYSTONE-ERIE**		**AVG 1**	**FAIR**	**18.851**	**15.606**	**38.448**	**0.82788**	**2.0395**
Silver 6	SW231	231		31078-001	92PI	fair	18.785	15.629	38.436	0.83201	2.0462
SILVER 6	**SW231**	**231**	**NELSON**		**AVG 1**	**FAIR**	**18.785**	**15.629**	**38.436**	**0.83201**	**2.0462**
Atlin	SW239	239		31076-001	92PI	good	19.102	15.653	38.869	0.81942	2.0348
ATLIN	**SW239**	**239**	**YMIR**		**AVG 1**	**GOOD**	**19.102**	**15.653**	**38.869**	**0.81942**	**2.0348**
Wolf Lake	SW245	245		30363-001	80RY	fair	19.075	15.616	38.628	0.81866	2.0251
WOLF LAKE	**SW245**	**245**	**SHEEP CREEK**		**AVG 1**	**FAIR**	**19.075**	**15.616**	**38.628**	**0.81866**	**2.0251**
Shiloh	SW281	281		31069-001	91PI	good	19.091	15.652	38.852	0.81986	2.0351
Shiloh	SW281	281		31069-001	91PI	poor	19.101	15.663	38.892	0.82001	2.0362
Shiloh	SW281	281		31069-001	91PI	good	19.102	15.661	38.887	0.81989	2.0358
SHILOH	**SW281**	**281**	**YMIR**		**AVG 3**	**GOOD**	**19.098**	**15.659**	**38.877**	**0.82000**	**2.0360**
Toughnut	SW294	294		30908-001	87GA	poor	18.850	15.599	38.188	0.82753	2.0259
Toughnut	SW294	294		30908-002	91PI	good	18.823	15.610	38.381	0.82933	2.0391
TOUGHNUT	**SW294**	**294**	**NELSON**		**AVG 2**	**GOOD**	**18.837**	**15.605**	**38.285**	**0.82800**	**2.0330**
Star of the West	SW309	309		30909-001	87GA	poor	18.730	15.614	38.273	0.83365	2.0435
Star of the West	SW309	309		30909-002	91PI	fair	18.752	15.595	38.312	0.83165	2.0431
Star of the West	SW309	309		30909-002	91PI	good	18.762	15.604	38.336	0.83171	2.0433
Star of the West	SW309	309		30909-002	91PI	good	18.766	15.605	38.339	0.83159	2.0430
STAR OF THE WEST	**SW309**	**309**	**NELSON**		**AVG 4**	**GOOD**	**18.753**	**15.605**	**38.315**	**0.83200**	**2.0430**
Showing 31087	SW401	401		31087-001	92PI	poor	19.058	15.648	38.878	0.82104	2.0400
Showing 31087	SW401	401		31087-001	92PI	fair	19.062	15.654	38.910	0.82124	2.0413
SHOWING 31087	**SW401**	**401**	**KEYSTONE-ERIE**		**AVG 2**	**FAIR**	**19.060**	**15.651**	**38.894**	**0.82100**	**2.0410**
Morning Toad	SW402	402		30910-001	87GA	poor	18.803	15.604	38.340	0.82985	2.0390
MORNING TOAD	**SW402**	**402**	**NELSON**		**AVG 1**	**POOR**	**18.803**	**15.604**	**38.340**	**0.82985**	**2.0390**

TABLE A8-1, CONTINUED

Deposit Name	Minfile	Fig No	Camp, area	Lab no	Anal	Quality	Pb^{206}/Pb^{204}	Pb^{207}/Pb^{204}	Pb^{208}/Pb^{204}	Pb^{207}/Pb^{206}	Pb^{208}/Pb^{206}
Blackwitch	SW404	404		31089-001	91PI	good	18.984	15.621	38.710	0.82286	2.0391
BLACKWITCH	**SW404**	**404**	**NELSON**		**AVG 1**	**GOOD**	**18.984**	**15.621**	**38.710**	**0.82286**	**2.0391**
STATISTICS: NUMBER							**22**	**22**	**22**	**22**	**22**
STATISTICS: MEAN							**18.961**	**15.642**	**38.643**	**0.82497**	**2.0380**
STATISTICS: STANDARD ERROR							**0.026**	**0.007**	**0.048**	**0.00094**	**0.0010**
CLUSTER 3											
Aspen	SW001	1		30462-003	82AN	good	18.910	15.620	38.946	0.82602	2.0595
Aspen	SW001	1		30462-003	92PI	fair	19.292	15.760	39.555	0.81689	2.0503
Aspen	SW001	1		30462-003	92PI	fair	19.258	15.726	39.447	0.81660	2.0483
Aspen	SW001	1		30462-005	82AN	good	19.002	15.628	38.946	0.82244	2.0496
Aspen	SW001	1		30462-007	92PI	good	19.289	15.760	39.546	0.81706	2.0502
ASPEN	**SW001**	**1**	**SALMO**		**AVG 5**	**GOOD**	**19.150**	**15.699**	**39.288**	**0.82000**	**2.0520**
HB (Salmo)	SW004	4		30639-501	73LE	good	19.089	15.727	39.486	0.82388	2.0685
HB (Salmo)	*SW004*	*4*		*30639-502*	*64SI*	*poor*	*19.289*	*15.947*	*40.081*	*0.82674*	*2.0779*
HB (Salmo)	*SW004*	*4*		*30639-503*	*62BR*	*poor*	*19.300*	*15.910*	*39.700*	*0.82435*	*2.0570*
HB (Salmo)	*SW004*	*4*		*30639-504*	*60RUF*	*poor*	*19.677*	*15.397*	*38.485*	*0.78249*	*1.9558*
HB (SALMO)	**SW004**	**4**	**SALMO**		**AVG 1**	**GOOD**	**19.089**	**15.727**	**39.486**	**0.82388**	**2.0685**
Jersey	SW009	9		30641-501	64SI	poor	19.310	15.937	40.106	0.82532	2.0770
Jersey	SW009	9		30641-502	64SI	poor	19.271	15.933	40.012	0.82679	2.0763
Jersey	SW009	9		30641-503	64SI	poor	19.123	15.765	39.370	0.82440	2.0588
Jersey	SW009	9		30641-504	64SI	poor	19.273	15.923	40.027	0.82618	2.0768
Jersey	SW009	9		30641-505	73LE	good	19.093	15.736	39.437	0.82418	2.0655
JERSEY	**SW009**	**9**	**SALMO**		**AVG 1**	**GOOD**	**19.093**	**15.736**	**39.437**	**0.82418**	**2.0655**
Jackpot	*SW012*	*12*		*30640-501*	*64SI*	*poor*	*19.000*	*15.731*	*39.170*	*0.82795*	*2.0616*
Jackpot	SW012	12		30640-502	73LE	good	18.992	15.744	39.304	0.82898	2.0695
JACKPOT	**SW012**	**12**	**SALMO**		**AVG 1**	**GOOD**	**18.992**	**15.744**	**39.304**	**0.82898**	**2.0695**
Hunter V	SW014	14		30356-001	80RY	fair	19.271	15.671	39.262	0.81319	2.0374
HUNTER V	**SW014**	**14**	**SALMO**		**AVG 1**	**FAIR**	**19.271**	**15.671**	**39.262**	**0.81319**	**2.0374**
Double Standard	SW015	15		30354-001	80RY	fair	19.212	15.690	39.418	0.81668	2.0517
DOUBLE STANDARD	**SW015**	**15**	**SALMO**		**AVG 1**	**FAIR**	**19.212**	**15.690**	**39.418**	**0.81668**	**2.0517**
Red Bird	SW024	24		30076-002	89PI	fair	19.219	15.753	39.645	0.81969	2.0628
Red Bird	SW024	24		30076-002	89PI	fair	19.235	15.770	39.702	0.81983	2.0640
RED BIRD	**SW024**	**24**	**SALMO**		**AVG 2**	**FAIR**	**19.227**	**15.762**	**39.674**	**0.82000**	**2.0630**

TABLE A8-1, CONTINUED

Deposit Name	Minfile	Fig No	Camp, area	Lab no	Anal	Quality	Pb^{206}/Pb^{204}	Pb^{207}/Pb^{204}	Pb^{208}/Pb^{204}	Pb^{207}/Pb^{206}	Pb^{208}/Pb^{206}
Red Rock	SW025	25		30836-501	73LE	good	18.733	15.644	38.873	0.83510	2.0751
RED ROCK	**SW025**	**25**	**SALMO**		**AVG 1**	**GOOD**	**18.733**	**15.644**	**38.873**	**0.83510**	**2.0751**
Reeves MacDonald	*SW026*	*26*		*30448-501*	*64SI*	*poor*	*19.248*	*15.911*	*39.943*	*0.82663*	*2.0752*
Reeves MacDonald	SW026	26		30448-502	73LE	good	19.076	15.738	39.386	0.82502	2.0647
Reeves MacDonald	*SW026*	*26*		*30448-503*	*64SI*	*poor*	*19.199*	*15.913*	*39.869*	*0.82885*	*2.0766*
REEVES MACDONALD	**SW026**	**26**	**SALMO**		**AVG 1**	**GOOD**	**19.076**	**15.738**	**39.386**	**0.82502**	**2.0647**
Reno Mine	SW036	36		31215-001	99GA	good	18.837	15.670	39.256	0.83190	2.0840
RENO MINE	**SW036**	**36**	**SALMO**		**AVG 1**	**GOOD**	**18.837**	**15.670**	**39.256**	**0.83190**	**2.0840**
Queen	SW048	48		30312-001	79RY	fair	19.187	15.692	39.533	0.81785	2.0604
Queen	*SW048*	*48*		*30312-501*	*62BR*	*poor*	*19.220*	*15.750*	*39.520*	*0.81946*	*2.0562*
Queen	*SW048*	*48*		*30312-503*	*60RUF*	*poor*	*19.222*	*15.748*	*39.562*	*0.81927*	*2.0582*
QUEEN	**SW048**	**48**	**SALMO**		**AVG 1**	**FAIR**	**19.187**	**15.692**	**39.533**	**0.81785**	**2.0604**
Silver Dollar	SW207	207		30014-003	88GA	good	18.878	15.631	39.057	0.82801	2.0690
SILVER DOLLAR	**SW207**	**207**	**SALMO**		**AVG 1**	**GOOD**	**18.878**	**15.631**	**39.057**	**0.82801**	**2.0690**
STATISTICS: NUMBER							**12**	**12**	**12**	**12**	**12**
STATISTICS: MEAN							**19.062**	**15.700**	**39.331**	**0.82373**	**2.0634**
STATISTICS: STANDARD ERROR							**0.049**	**0.012**	**0.062**	**0.00188**	**0.0035**

Notes:

Only boldfaced analyses are used in the interpretation presented in this paper. Where more than one analysis is available they are averaged, except those analyses deemed to be POOR by present measurement standards, which are italicized and deleted from calculation of the average.

Location and geology of the mineral occurrences are in Tables 2 and 3, respectively

The number of analyses used is indicated in the ANALYST column as AVG 1, AVG 2, etc.

Anal: Analyses by 60RUF - Russel and Farquharson, 1960; 62BR - Brown, 1962; 64SI - Sinclair, 1962; 73LE - Lecouteru, 1973; 79RY - Ryan in 1979, Dept. of Physics, UBC 82AN, 87GA, 88GA, 89PI, 92PI and 99GA: analyses in 1982, 1987, 1988, 1989 and 1999 by Anne Andrew, Janet Gabites and Anne Pickering, Geochronology Laboratory, Dept of Earth and Ocean Sciences, The University of British Columbia

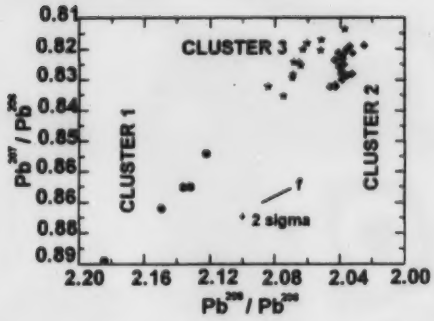

Figure A8-3. General $^{208}Pb/^{206}Pb$ versus $^{207}Pb/^{206}Pb$ plot of galena lead isotopes from mineral occurrences in the Trail map sheet (082F/SW). Note that the three clusters are distinct in this plot. Data for the deposits are from Table A8-1.Numbers beside isotope symbols and error bars are explained in Figure 2. Note that only the trend for fractionation error (line marked with an "f") is given because this plot eliminates ^{204}Pb error.

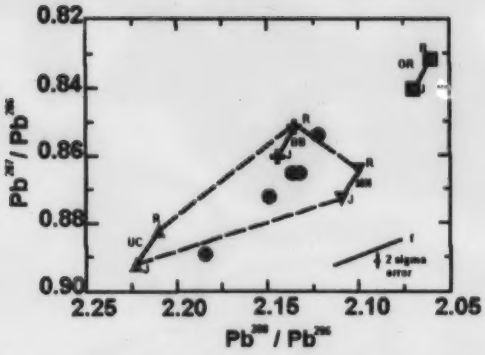

Figure A8-4. Cluster 1 data for mineral occurrences in the Trail map sheet (082F/SW) are plotted with Jurassic to Cretaceous points for lead for an idealized Mantle (MN), Lower Crust (LC) and Orogene (OR), as defined by plubotectonic models of Zartman and Doe (1981), and the Bluebell curve (BB) defined by Andrew *et al.* (1984), which is a lead model specific to the Canadian Cordillera. Data for these points are in Godwin *et al.* (1988). Lead in Cluster 1 is more primitive than orogene lead (OR) and has a marked mantle (MN) component. Isotope data are from Table 1.Symbols on the model segments represent the base of the Tertiary (R) and the base of the Jurassic (J). Therefore, the solid bars represent Jurassic and Cretaceous. Error and fraction are as described in Figure 3.

the NBS-981 common lead standard. Reported ratios in Table 1 are averages of more than two runs on a single, or sometimes multiple, dissolution. The total standard variations observed in duplicate analyses at 2 sigma are generally less than 0.2% for $^{206}Pb/^{204}Pb$, $^{207}Pb/^{204}Pb$ and $^{208}Pb/^{204}Pb$, and 0.1% for $^{207}Pb/^{206}Pb$ and $^{208}Pb/^{206}Pb$. Lead isotopic data and relevant errors are presented in Figures A8-2 to 5.

CHARACTERISTICS OF GALENA LEAD ISOTOPES FROM THE TRAIL REGION

Lead isotope data from the Trail map sheet (Table 1) can be divided into three clusters by visual examination of Figures A8-2 and 3. In these figures, Cluster 1 plots in the lower left hand corner. Cluster 2 generally plots below Cluster 3, but both plot in the upper right hand corner of the same figures. The locations of mineral occurrences, detailed in Table 2, are plotted according to cluster type in Figure A8-1. Table 3 outlines type of deposit, mineral commodities in the deposit, relevant mining camp or area, terrane, and host rock and age.

Linear trends are present within each cluster. Potential components of the mixing that might explain these trends are plotted with the data in Figures A8-4 and 5. In addition, the deposits represented by each cluster have generally different geological characteristics.

More detailed explanations for each cluster follow.

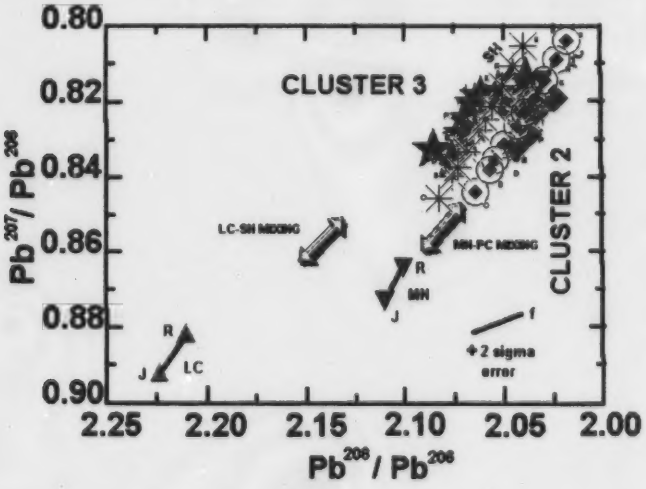

Figure A8-5. Cluster 2 and Cluster 3 data for mineral occurrences in the Trail map sheet (082F/SW) plotted with Jurassic to Cretaceous points (Zartman and Doe, 1981), for the plumbotectonic model for Mantle (MN) and Lower Crust (LC). The Shale (SH: Godwin and Sinclair, 1981) and Pericratonic (PC: Gautier, 1986) model growth curves from the Ordovician to Present are also plotted. Data for these points are in Godwin *et al.* (1988). Cluster 2 plots close to the Pericratonic curve (PC) and shows an elongated mixing trend from the Jurassic towards an idealized Jurassic-Cretaceous mantle (MN). Cluster 3 plots close to the Shale Curve (SH) and shows an elongated mixing trend from about the Cretaceous towards an idealized Jurassic-Cretaceous Lower crust (LC). Isotope data are from Table A8-1.

TABLE A8-2
LOCATION OF MINERAL OCCURRENCES ANALYZED IN THE TRAIL MAP SHEET (082F/SW)
Isotopic Analyses and Geology of the Occurrences are in Tables 1 And 3, Respectively

Minfile	Fig No	Deposit	Camp, area	Status	NTS	UTM E	UTM N	Lat N	Long W
CLUSTER 1									
082FSW160	160	SUNSET 2	PATERSON	Past Producer	082F04W	438645	5428039	49.01	117.84
082FSW200	200	CLUBINE	KEYSTONE	Past Producer	082F03W	480385	5453674	49.24	117.27
082FSW295	295	MITZIE 1	PATERSON	Showing	082F04W	437633	5428390	49.02	117.84
082FSW-400	400	SHOWING 31082	KEYSTONE	Showing	082F03W	474250	5449400	49.19	117.34
082FSW-403	403	SHOWING 31080	KEYSTONE	Showing	082F06W	474400	5456200	49.27	117.35
CLUSTER 2									
082FSW046	46	KOOTENAY BELLE	SHEEP CREEK	Past Producer	082F03E	490781	5442777	49.14	117.13
082FSW063	63	PORCUPINE	YMIR	Past Producer	082F06E	486760	5455508	49.26	117.18
082FSW067	67	DUNDEE	YMIR	Past Producer	082F06E	486122	5459122	49.29	117.20
082FSW068	68	YANKEE GIRL	YMIR	Past Producer	082F06E	486669	5459708	49.31	117.18
082FSW074	74	YMIR	YMIR	Past Producer	082F06E	487626	5463041	49.32	117.17
082FSW084	84	EUREKA 2	NELSON	Past Producer	082F06W	473546	5477883	49.46	117.37
082FSW123	123	HOMESTAKE	ROSSLAND	Past Producer	082F04W	441660	5434554	49.07	117.80
082FSW145	145	BLUEBIRD 1	ROSSLAND	Past Producer	082F04W	441595	5434215	49.06	117.80
082FSW168	168	ATHABASCA	NELSON	Past Producer	082F06W	477413	5478205	49.46	117.31
082FSW176	176	SILVER KING	NELSON	Past Producer	082F06W	478242	5474156	49.43	117.30
082FSW192	192	ELISE	YMIR	Developed Prospect	082F06E	487995	5465665	49.35	117.17
082FSW202	202	KEYSTONE	KEYSTONE	Past Producer	082F03W	477913	5452417	49.23	117.30
082FSW205	205	ARLINGTON	KEYSTONE	Past Producer	082F03W	476153	5452208	49.23	117.33
082FSW231	231	SILVER 5	NELSON	Showing	082F06W	480591	5477452	49.46	117.26
082FSW239	239	ATLIN NOME	YMIR	Showing	082F06E	486184	5459740	49.29	117.19
082FSW245	245	WOLF LAKE	SHEEP CREEK	Prospect	082F03E	498046	5438509	49.12	117.05
082FSW281	281	SHILOH	YMIR	Showing	082F06E	485273	5459063	49.28	117.21
082FSW294	294	TOUGHNUT	NELSON	Showing	082F06W	475208	5475806	49.43	117.33
082FSW309	309	STAR OF THE WEST	NELSON	Showing	082F06W	479359	5476407	49.44	117.28
082FSW-401	401	SHOWING 31087	KEYSTONE	Showing	082F03W	473900	5449600	49.20	117.35
082FSW-402	402	MORNING TOAD	NELSON	Showing	082F06W	475800	5475650	49.43	117.33
082FSW-404	404	BLACK WITCH	NELSON	Showing	082F06W	477100	5475300	49.43	117.32
CLUSTER 3									
082FSW001	1	ASPEN	SALMO	Past Producer	082F03E	486336	5447881	49.19	117.18
082FSW004	4	HB	SALMO	Past Producer	082F03E	485517	5444178	49.16	117.20
082FSW009	9	JERSEY	SALMO	Past Producer	082F03E	483940	5438222	49.10	117.22
082FSW012	12	JACKPOT MAIN	SALMO	Developed Prospect	082F03E	488636	5454052	49.24	117.15
082FSW014	14	HUNTER V	SALMO	Past Producer	082F03E	487908	5453652	49.24	117.16
082FSW015	15	DOUBLE STANDARD	SALMO	Past Producer	082F03E	487585	5453962	49.24	117.17
082FSW024	24	RED BIRD	SALMO	Developed Prospect	082F03W	471727	5429162	49.02	117.39
082FSW025	25	RED ROCK	SALMO	Past Producer	082F03W	474626	5432452	49.05	117.34
082FSW026	26	REEVES MACDONALD	SALMO	Past Producer	082F03W	474331	5430014	49.02	117.36
082FSW036	36	RENO	SALMO	Past Producer	082F03E	490485	5447502	49.16	117.11
082FSW048	48	QUEEN	SALMO	Past Producer	082F03E	490092	5442840	49.14	117.13
082FSW207	207	SILVER DOLLAR	SALMO	Past Producer	082F03W	479055	5449356	49.20	117.28

Note: Isotopic analyses and geology are in tables 1 and 3, respectively.

TABLE A8-3
GEOLOGY AND MINERAL OCCURRENCES ANALYZED IN TRAIL MAP SHEET;
FROM BC MINFILE AND APPENDIX 1

MINFILE	Fig No	Name	Status	Camp, Area	Deposit Type	C1	C2	C3	C4	C5	C6	Terrane	Host	Host Age
082FSW160	160	Sunset	Past Producer	Paterson	Vein, polymetallic	Ag	Au	Pb	Zn	Cu		Quesnel	Mt Roberts Formation	Carboniferous to Permian
082FSW200	200	Clubine	Past Producer	Keystone	Vein, polymetallic	Au	Ag	Pb	Zn	Cu		Quesnel	Hall Formation	Jurassic
082FSW295	295	Mitzie 1	Showing	Paterson	Vein, polymetallic &/or skarn	Ag	Pb	Zn	Cu	Au		Quesnel	Mt Roberts Formation	Jurassic
082FSW400	400	Showing 31082	Showing	Keystone	Vein, polymetallic	Ag	Pb	Zn				Quesnel	Archibald Formation	Jurassic
082FSW403	403	Showing 31080	Showing	Keystone	Vein, polymetallic	Ag	Pb	Zn				Quesnel	Elise Formation	Jurassic
CLUSTER 2														
082FSW046	46	Kootenay Belle	Past Producer	Sheep Creek	Vein, quartz-gold	Au	Ag	Pb	Zn	W		North America	Reno Formation	Eocambrian
082FSW063	63	Porcupine	Past Producer	Ymir	Vein, polymetallic	Au	Ag	Pb	Zn	Sn	Cu	Kootenay	Index formation	Cambrian to Ordovician
082FSW067	67	Dundee	Past Producer	Ymir	Vein, polymetallic	Au	Ag	Pb	Zn			Quesnel	Nelson intrusions & Ymir Group	Jurassic intrudes Triassic
082FSW068	68	Yankee Girl	Past Producer	Ymir	Vein, polymetallic	Au	Ag	Pb	Zn	Cd		Quesnel	Nelson intrusions & Ymir Group	Jurassic intrudes Triassic
082FSW074	74	Ymir	Past Producer	Ymir	Vein, polymetallic	Au	Ag	Pb	Zn			Quesnel	Nelson intrusions & Ymir Group	Jurassic intrudes Triassic
082FSW084	84	Eureka	Past Producer	Nelson	Vein, polymetallic	Cu	Au	Ag	Pb	Zn		Quesnel	EAgle Creek pseudodiorite	Jurassic intrusion
082FSW123	123	Homestake	Past Producer	Rossland	Vein, polymetallic	Ag	Au	Cu	Pb	Zn		Quesnel	Elise Formation	Jurassic
082FSW145	145	Bluebird 1	Past Producer	Rossland	Vein, polymetallic	Ag	Pb	Zn	Au	Cu	Sb	Quesnel	Elise Formation	Jurassic
082FSW168	168	Athabaska	Past Producer	Nelson	Vein, quartz-gold	Au	Ag	Pb	Zn	Cu	W	Quesnel	Nelson intrusions into Elise Formation	Jurassic intrudes Jurassic
082FSW176	176	Silver King	Past Producer	Nelson	Vein, polymetallic	Ag	Cu	Au	Pb	Zn		Quesnel	Silver King intrusions into Elise Formation	Jurassic intrudes Jurassic
082FSW192	192	Elise	Developed Prospect	Ymir	Vein, polymetallic	Ag	Au	Pb	Zn	Cu		Quesnel	Nelson intrusions & Ymir Group	Jurassic intrudes Triassic
082FSW202	202	Keystone	Past Producer	Keystone	Vein, polymetallic	Au	Ag	Pb	Zn	Cu		Quesnel	Hall Formation	Jurassic
082FSW205	205	Arlington	Past Producer	Keystone	Vein, polymetallic	Au	Ag	Pb	Zn			Quesnel	Hall Formation	Jurassic
082FSW231	231	Silver 5	Showing	Nelson	Volcanogenic	Ag	Pb	Zn	Cu			Quesnel	Elise Formation	Jurassic
082FSW239	239	Atlin Nome	Showing	Ymir	Vein, polymetallic	Au						Quesnel	Nelson intrusions into Ymir Group	Jurassic intrudes Triassic
082FSW245	245	Wolf Lake	Prospect	Sheep Creek	Vein, polymetallic	Au	Ag	Cu				NorthAmerica	Nelson intrusions into Windermere Group	Jurassic intrudes Proterozoic

CONTINUED TABLE A8-3

MINFILE	Fig No	Name	Status	Camp, Area	Deposit Type	C1	C2	C3	C4	C5	C6	Terrane	Host	Host Age
082FSW281	281	Shiloh	Showing	Ymir	Vein, polymetallic	Au	Zn	Pb				Quesnel	Nelson intrusions & Ymir Group	Jurassic intrudes Triassic
082FSW294	294	Toughnut	Showing	Nelson	Vein, polymetallic or porphyry	Au	Ag	Cu	Pb	Zn		Quesnel	Silver King intrusions into Elise Formation	Jurassic intrudes Jurassic
082FSW309	309	Star of the West	Showing	Nelson	Vein, polymetallic	Ag	Pb	Zn	Au			Quesnel	Elise Formation	Jurassic
082FSW401	401	Showing 31087	Showing	Keystone	Vein, polymetallic	Ag	Pb	Zn				Quesnel	Archibald Formation	Jurassic
082FSW402	402	Morning Toad	Showing	Nelson	Vein, polymetallic	Ag	Pb	Zn				Quesnel	Elise Formation	Jurassic
082FSW404	404	Black Witch	Showing	Nelson	Vein, polymetallic	Ag	Pb	Zn				Quesnel	Elise Formation	Jurassic
CLUSTER 3														
082FSW001	1	Aspen	Past Producer	Salmo	Carbonate hosted, vein	Ag	Au	Pb	Zn			North America	Reeves limestone member	Cambrian
082FSW004	4	HB	Past Producer	Salmo	Carbonate hosted, stratabound	Pb	Zn	Ag	Cd	Cu	Au	North America	Reeves limestone member	Cambrian
082FSW009	9	Jersey	Past Producer	Salmo	Carbonate hosted, stratabound	Pb	Zn	Ag	Cd	W	Mo	North America	Reeves limestone member	Cambrian
082FSW012	12	Jackpot Main	Developed Prospect	Salmo	Carbonate hosted, stratabound	Pb	Zn	Cd	W			North America	Reeves limestone member	Cambrian
082FSW014	14	Hunter V	Past Producer	Salmo	Carbonate hosted, vein	Ag	Au	Zn	Pb			North America	Reeves limestone member	Cambrian
082FSW015	15	Double Standard	Past Producer	Salmo	Carbonate hosted, vein	Ag	Au	Zn	Pb			North America	Reeves limestone member	Cambrian
082FSW024	24	Red Bird	Developed Prospect	Salmo	Carbonate hosted, stratabound	Zn	Pb	Ag	Cd			North America	Reeves limestone member	Cambrian
082FSW025	25	Red Rock	Past Producer	Salmo	Carbonate hosted, vein	Pb	Zn	Ag				North America	Reeves limestone member	Cambrian
082FSW026	26	Reeves MacDonald	Past Producer	Salmo	Carbonate hosted, stratabound	Zn	Pb	Ag	Cd	Cu	Ga	North America	Reeves limestone member	Cambrian
082FSW036	36	Reno	Past Producer	Salmo or Sheep Creek	Vein, polymetallic	Au	Pb	Zn	Ag	Cu	Hg	North America	Rano Formation	Eocambrian
082FSW048	48	Queen	Past Producer	Salmo or Sheep Creek	Vein, polymetallic	Au	Ag	Pb	Zn			North America	Quartzite Range Formation	Eocambrian
082FSW207	207	Silver Dollar	Past Producer	Salmo	Vein, polymetallic	Au	Ag	Pb	Zn	Cu		Quesnel	Hall Formation	Jurassic

Note: C1 to C6 are commodities, listed in order of importance.

CLUSTER 1

Cluster 1 occurs (Figure A8-1 and Table A8-3): (i) by itself in the Paterson area, and (ii) in the Keystone-Erie area with deposits that are part of Cluster 2. All deposits are polymetallic veins (Table 3: No. 295 may be a skarn) in Quesnel terrane.

Cluster 1 lead isotope data for mineral occurrences (Table A8-1) are plotted in Figures A8-2 to 4. Cluster 1 is compared in Figure A8-4 to the Jurassic-Cretaceous points for idealized Mantle (MN), Lower Crust (LC) and Orogene (OR), as defined by plubotectonic models of Zartman and Doe (1981; *cf.* Doe and Zartman, 1974), and the Bluebell curve defined by Andrew *et al.* (1984), which is a lead model developed for part of the southeastern Canadian Cordillera. Cluster 1 compositions are more primitive than Orogene lead (OR), and are nearly enclosed in the Jurassic-Cretaceous field made by joining the primitive model leads for the Mantle (MN), Lower Crustal (LC) and Bluebell (BB). Thus, the lead isotopes characterizing Cluster 1 are close to these primitive Jurassic - Cretaceous leads. The long linear trend of lead isotopes in Cluster 1 (Figures A8-2 to 5) may represent various lead sources and/or a range of mineralization ages from Carboniferous to Tertiary.

There are several possible explanations for a marked Mantle component to the lead isotopes in Cluster 1. Mantle lead could have been introduced from Tertiary lamprophyre dykes that are abundant near many mineral occurrences. Specifically, mineralization at one deposit (Table 3, No. 160) occurs at the contact of a lamprophyre dike. The deposits in the Paterson area are within the Mt. Roberts Formation, which contains mafic rocks that include serpentinite. As a consequence, this area has been interpreted to represent (Höy and Dunne, 1997) the early, Carboniferous-Permian, primitive basement to Quesnel terrane. The galena lead isotopes may reflect the primitive nature of Quesnel terrane before there was Upper Crustal detrital input from North America. One deposit in Cluster 1 is a possible skarn (Table 3, No. 295). If the intrusive that formed the skarn supplied the lead, the intrusive itself was more primitive than those associated with Cluster 2 deposits. However, as seems more likely, if the intrusive only remobilized lead from the primitive host rocks, two types of Jurassic intrusions would not be required.

CLUSTER 2

Cluster 2 compositions were obtained from either gold vein or polymetallic veins. This cluster represents exclusively the following camps (Figure A8-1 and Table A8-3): Nelson, Ymir, Sheep Creek and Rossland. The Keystone-Erie area hosts deposits with both Cluster 1 (relatively primitive) and Cluster 2 (relatively radiogenic) leads.

Cluster 2 is characterized by Upper Crustal and relatively radiogenic lead (Figures A8-2 to 5) that can be modeled closely with the Pericratonic (PC) model curve of Gautier (1986), which was used to model lead from Kootenay terrane deposits in the Eagle Bay Assemblage in the Adams Lake area of southeastern British Columbia.

Cluster 2 compositions (Table 1) are plotted in Figures A8-2, 3 and 5. Figure A8-5 shows Cluster 2 isotope data plotted with Jurassic to Cretaceous points for the plumbotectonic models (Zartman and Doe, 1981) for Mantle (MN) and Lower Crust (LC). The Shale (SH: Godwin and Sinclair, 1982) and Pericratonic (PC: Gautier, 1986) model growth curves from the Ordovician to Present are also plotted. Cluster 2 plots close to the Pericratonic model curve (PC), and is therefore, quite radiogenic with a substantial Upper Crustal lead isotope component. The Upper Crustal component is emphasized also by the lithophile associated tungsten, molybdenum and tin deposits represented (Table 3: Nos. 46, 63 and 168). Cluster 2 also shows an elongated mixing trend from the Jurassic on the Pericratonic model curve to Jurassic-Cretaceous Mantle model lead isotopes (MN).

Geological characteristics of Cluster 2 are presented in this bulletin and summarized in Table 3. The majority of the deposits are gold veins or polymetallic veins; one deposit (No. 294) might be a porphyry type deposit. Many are near contacts with, or within Jurassic intrusive bodies. Therefore, these intrusions appear to be deposit-causative, and this magmatism appears to have facilitated mixing of mantle and upper crustal lead. There is so much radiogenic lead that the lead isotopes plot close to the Pericratonic curve. A possible reason for the radiogenic character of lead in the area is that magmatic processes evolved from depth where a Mantle component could be inherited, but the dominant lead source involved was from assimilation of Upper Crustal material, which is relatively rich in uranium and thorium. The implication is that this part of the Quesnel terrane either received abundant Upper Crustal detritus from North America that was incorporated into subduction generated plutons, and/or was underlain by North America basement that was assimilated by intrusions. The Sheep Creek camp (Figure A8-1) within ancestral North America is characterized by quartzite-hosted gold quartz vein deposits with Cluster 2 type lead isotopes. Here, intrusive bodies in the camp presumably are linked to the deposits. If this is the case, then Cluster 2 type lead isotopes may be mainly dependent upon lead isotope mixing by magmatic contamination. Hence, the lead isotope character of Cluster 2 likely is dependent on magmatic mixing processes of several possible types, and is only indirectly terrane-specific.

CLUSTER 3

Carbonate-hosted deposits in the Salmo camp (Figure A8-1 and Table A8-3) typify Cluster 3; these are metamorphosed and highly deformed. Several polymetallic veins are represented as well. All deposits are in ancestral North America except one (Table 3: No. 207) in the Keystone-Erie area, which is in Quesnel terrane.

Cluster 3 data (Table A8-1) are plotted in Figures A8-2, 3 and 5. Figure A8-5 shows the data plotted with Jurassic to Cretaceous points (Zartman and Doe, 1981), for the plumbotectonic model for Mantle (MN) and Lower Crust (LC). The Shale (SH: Godwin and Sinclair, 1982) and Pericratonic (PC: Gautier, 1986) model growth curves from the Ordovician to Present are also plotted. Cluster 3 plots

close to the Shale curve (SH) and shows an elongated mixing trend from the Jurassic towards an idealized Jurassic-Cretaceous Lower Crust (LC). Sinclair (1966) referred to a similar elongate trend that included some of the Salmo deposits as anomalous leads with a well-defined linear trend. In summary, lead isotopes of Cluster 3 are the most radiogenic studied in the project area (Figures A8-2 to 5) and represent Upper Crustal lead that is closely modeled by the Shale curve of Godwin and Sinclair (1982). The Upper Crustal character of the mineralization is also consistent with the lithophile association of tungsten (± molybdenum) and gallium in some of the deposits (Table 3, Nos. 9, 12 and 26).

The galena lead isotope data of Cluster 3 form a linear trend in Figure A8-5. Part of the trend can be described as mixing of approximately Jurassic Upper Crustal (SH: Shale model lead) with Lower Crustal lead (LC). The Lower Crustal component might be related to S-type magmatism (see Discussion). Additionally, it is clear that the mixing trend is not toward a Mantle component, and this also distinguishes Cluster 1 from Cluster 2. The trend of Cluster 3 presumably could relate to the "markedly radiogenic" linear mixing trends common to carbonate hosted deposits in the Mississippi Valley and elsewhere (Heyl *et al.*, 1974; Godwin *et al.*, 1982; Sverjensky *et al.*, 1979; Crocetti *et al.*, 1988). In this case, the lead could be as old as the hosting Cambrian rocks. However, markedly radiogenic lead lines generally anchor on and are more radiogenic than upper crustal curves, such as the Shale curve, in which case the line would extend to the upper right beyond the shale curve in Figure A8-5. Additionally, three polymetallic vein deposits occur near the margins of the Salmo camp. Two of these vein deposits (Table 3: Nos. 36 and 48) are in the Eocambrian Reno Formation and Quartzite Range Formation, both of which are in ancestral North America. These deposits, although generally included in the Sheep Creek camp, are not related to the Cluster 2 type deposits that characterize the rest of the Sheep Creek Camp, but are superimposed on the older rocks by the mineralizing event that made the Salmo deposits. The remaining vein (207) is clearly hosted by the Early Jurassic Hall Formation in the Keystone-Erie area (Höy and Dunne, 1997), which is part of Quesnel terrane. Consequently, if all the Cluster 3 deposits formed at or about the same time, then all the Cluster 3 deposits must be Jurassic or younger. Thus, the approximate Jurassic model age for Cluster 3, defined by the intersection of the right hand end of the mixing line for Cluster 3 with the Shale curve, is compatible with available evidence.

DISCUSSION

Several metallogenic events occur together spatially. The two areas in which this occurs are: (i) the Sheep Creek camp that has mainly Cluster 2 type lead isotopes, but also has Cluster 3 lead, and (ii) the, Keystone-Erie area that has Cluster 1 type lead isotopes and Cluster 2 lead.

The trend of Cluster 3 indicates mixing of a remobilized Lower Crustal lead with an Upper Crustal lead modeled by the Shale curve. The source of this Lower Crustal component, which apparently caused the elongate mixing trend in Cluster 3, is intriguing. Could it be related to a metamorphic fluid generated in the Jurassic during metamorphism of the Lower Crust? We do not know. However, an interesting argument is made below, based on the Sheep Creek camp, on ways different types of granitic rocks could be involved in the generation of deposits associated with Clusters 2 and 3.

There are two types of granitic rock in the Sheep Creek camp that can be generalized as being similar to I-type granodiorite and S-type quartz monzonite (after Chappell and White, 1992). If we argue that Cluster 2 type lead must be I-type because of its close association with I-type granodiorite in Quesnel terrane, then the gold deposits in the Sheep Creek camp that are associated with Cluster 2 type lead are likely associated with the I-type granodiorite. Furthermore, I-type granitics can be expected to have a Mantle component, because of their typical subduction-related origin. If there is abundant Upper Crustal material in the subduction zone and/or available during ascent, then these I-type intrusives will assimilate a markedly Upper Crustal signature, as represented by the Pericratonic model curve and the Cluster 2 mineral occurrences in general. On the other hand, S-type quartz monzonites will have a Lower Crustal and lithophile (*e.g.* W, Ga and Mo) signature because they have been generated by anatexis of Lower Crustal source rocks formed of highly metamorphosed Upper Crustal rocks. The quartz monzonitic magmas generated within the bottom part of the mature North American plate will inherit the relatively high thorium signature of the Lower Crust, but will not have a Mantle component. Therefore, the mixing trend of Cluster 3 may reflect this S-type granitic event. In this regard, we also point to the close spatial association of Cluster 3 type lead-zinc carbonate-hosted mineralization with associated lithophile tungsten (±molybdenum) and gallium (*e.g.* Table A8-3, Nos. 9, 12 and 26). For an S-type magmatic event to be the source of mineralization in the Salmo camp, it has to be after deposition of the Early Jurassic Elise Formation, which hosts one of the Cluster 3 deposits. It also has to be before the Cretaceous, to be prior to the intense deformation and metamorphism that deformed the carbonate-hosted Salmo deposits. A mid-Jurassic age for an S-type plutonic event would fit this interpretation well, but has not been identified. Further constraints on the ages of: (i) metamorphic deformation of the carbonate-hosted deposits in the Salmo camp, and (ii) granitic events spatially related to the Salmo and Sheep Creek camps are critical to understanding the detailed metallogeny of this area.

CONCLUSIONS

Galena lead isotope analyses divide the deposits in the Trail map sheet into three distinct clusters. These three clusters appear to be related to three distinct mineralizing events. Each cluster is summarized below.

Cluster 1 is characterized by: (i) deposit occurrences in the Patterson area, and the Keystone-Erie area, (ii) polymetallic veins in Quesnel terrane, (iii) a pronounced

Mantle component to lead isotopes that may have been derived from primitive basement to Quesnel terrane and/or from Tertiary lamprophyre dykes, and (iv) a linear trend to lead isotope data that may represent deposits of variable age from Carboniferous to Tertiary.

Cluster 2 is characterized by: (i) most deposit occurrences within the Quesnel terrane in the Rossland, Nelson and Ymir camps, and the Keystone-Erie area, (ii) deposit occurrences within ancestral North America in the Sheep Creek camp, (iii) polymetallic veins, and possibly porphyry deposits, that are mainly within or spatially related to what are interpreted to be Jurassic intrusions, (iv) a pronounced Upper Crustal component to the lead isotopes such that they plot closely to the Pericratonic lead isotope model that is relevant to terranes immediately marginal to ancestral North America, and (v) a mixing trend from a Jurassic point on the Pericratonic model toward the lead isotope composition of the Mantle in the Jurassic-Cretaceous. It is concluded that an I-type Jurassic magmatic event generated the mineral occurrences of Cluster 2. The I-type magmatic processes facilitated mixing lead isotopes from the Mantle and Upper Crust. A substantial input of Upper Crustal component from North America into Quesnel terrane is indicated by the proximity of the cluster to the Pericratonic curve. The North American Upper Crustal component could have been incorporated into the magma as a result of subduction, or as a result of magma assimilation during ascent.

Cluster 3 is characterized by: (i) deposit occurrences in the Salmo Camp, at the border between the Salmo and Sheep Creek camps, and in the Keystone-Erie area near the border with the Salmo Camp, (ii) numerous Salmo-type carbonate-hosted deposits and several polymetallic veins in ancestral North America, and one polymetallic vein in the Quesnel terrane, (iii) an Upper Crustal type of lead isotope that plots close to the Shale lead isotope model for North America, and (iv) a mixing trend from a Cretaceous point on the Shale model toward the lead isotope composition of the Upper Crust in the Jurassic-Cretaceous. An approximate Jurassic model age for Cluster 3 is supported by the upper right hand intersection of the Cluster 3 trend with the Shale curve. A Jurassic age is also compatible with the occurrence of one deposit in the Early Jurassic Hall Formation in Quesnel terrane that has Cluster 3 type Salmo-lead. The trend of Cluster 3 indicates mixing of a remobilized Lower Crustal lead with an upper crustal lead modeled by the Shale curve. An S-type granitic event could facilitate such mixing. The Salmo carbonate-hosted deposits are interpreted to be metamorphically deformed, Jurassic manto deposits.

ACKNOWLEDGEMENTS

The writers thank Trygve Höy and Kathryn Dunne of the British Columbia Ministry of Energy, Mines and Petroleum Resources for collecting most of the galena samples for this project. Trygve Höy also enthusiastically encouraged us to complete the interpretation of all analyses available for this project area, most of which had not been published. Anne Andrew, Anne Pickering, Janet Gabites, Jim Mortensen and Colin Godwin of the Geochronology Laboratory, Department of Earth and Ocean Science, The University of British Columbia, Canada, were involved with the analysis of samples for this project. Critical editing by Alastair Sinclair and James Mortensen are gratefully acknowledged.

REFERENCES

Andrew, A., Godwin, C.I. and Sinclair, A.J. (1984): Mixing Line Isochrons: a New Interpretation of Galena Lead Isotope Data from Southeastern British Columbia, *Economic Geology*, Volume 79, pages 919-932.

Brown, J.S. (1962): Ore Leads and Isotopes, *Economic Geology*, Volume 57, pages 673-720.

Chappell, B.W. and White, A.J.R. (1992): I-Type and S-Type Granites in the Lachlan Fold Belt, *Transactions of the Royal Society of Edinburgh-Earth Sciences*, Volume 83, Part 1-2, pages 1-26.

Crocetti, C.A., Holland, H.D. and McKenna, L.W. (1988): Isotopic Composition of Lead in Galenas from the Viburnum Trend, Missouri, *Economic Geology*, Volume 83, pages 355-376.

Doe, B.R and Zartman, R.E. (1979): Chapter 2. Plumbo-tectonics I, The Phanerozoic, *in* H.L. Barnes (editor), "Geochemistry of Hydrothermal Ore Deposits, 2nd Edition", *Wiley Interscience*, New York, N.Y., pages 22-70.

Godwin, C.I., Gabites, J.E. and Andrew, A. (1988): LEADTABLE: A Galena Lead Isotope Data Base for the Canadian Cordillera, With a Guide to its Use by Explorationists, *British Columbia Ministry of Energy, Mines and Petroleum Resources*, Paper 1988-4, 188 pages.

Godwin, C.I. and Sinclair, A.J. (1981): Preliminary Interpretations of Lead Isotopes in Galena-Lead from Shale-Hosted Deposits in British Columbia and Yukon Territory, *British Columbia Ministry of Energy, Mines and Petroleum Resources*, Geological Fieldwork 1980, Paper 1981-1, pages 185-194.

Godwin, C.I. and Sinclair, A.J. (1982): Average Lead Isotope Growth Curves for Shale-Hosted Zinc-Lead Deposits, Canadian Cordillera, *Economic Geology*, Volume 7, pages 675-690.

Godwin, C.I., Sinclair, A.J. and Ryan, B.D. (1982): Lead Isotope Models for the Genesis of Carbonate-Hosted Zn-Pb, Shale-Hosted Ba-Zn-Pb, and Silver-Rich Deposits in the Northern Canadian Cordillera, *Economic Geology*, Volume 77, pages 82-94.

Goutier, F.M. (1986): Galena Lead Isotope Study of Mineral Deposits in the Eagle Bay Formation, Southeastern British Columbia, *The University of British Columbia*, Unpublished M.Sc. thesis, 153 pages.

Heyl, A.V., Landis, G.P. and Zartman, R.E. (1974): Isotopic Evidence for the Origin of Mississippi Valley - Type Mineral Deposits: A Review, *Economic Geology*, Volume 69, pages 992-1006.

Höy, T. and Dunne, K.P.E. (1997): Early Jurassic Group, southern British Columbia; Part I - stratigraphy and tectonics; *B.C. Ministry of Employment and Investment*, Bulletin 102, 124 pages.

Lecouteur, P.C. (1973): A Study of Lead Isotopes from Mineral Deposits in Southeastern British Columbia and in the Anvil Range, Yukon Territory, *The University of British Columbia*, Unpublished Ph.D. thesis, 153 pages.

Russel, R.D. and Farquhar, R.M. (1960): Lead Isotopes in Geology, *Interscience Publishers Inc.*, New York, 243 pages.

Sinclair, A.J. (1964): A Lead Isotope Study of Mineral Deposits in the Kootenay Arc, *The University of British Columbia*, Unpublished Ph.D. thesis, 257 pages.

Sinclair, A.J. (1966): Anomalous Leads from the Kootenay Arc, *In* "Tectonic History and Mineral Deposits of the Western Cordillera", (editors H. Gunning and W.H. White), *Canadian Institute of Mining and Metallurgy*, Special Volume 8, pages 249-262.

Sverjensky, Dimitri A., Rye, Danny M. and Doe, Bruce R. (1979): The Lead and Sulfur Isotopic Compositions of Galena from a Mississippi Valley-type Deposit in the New Lead Belt, Southeast Missouri, *Economic Geology*, Volume 74, pages 149-153.

Zartman, R.E. and Doe, B.R. (1981): Plumbotectonics—the Model, *Tectonophysics*, Volume 75, pages 135-162.

APPENDIX 9A
FLUID INCLUSION DATA

By Kathryn /Dunne, P.Geo.
4610 Lakekshore Road NE
Salmon Arm, B.C. V1E 3N7

INTRODUCTION

This fluid inclusion study of deposits and occurrences in the Rossland Group was undertaken in order to:

- assist in determining environments of deposition of deposits in Rossland Group,
- determine if differences exist between mineralizing fluids associated with Early Jurassic, Early-Middle Jurassic and Middle Jurassic deposits in Rossland Group,
- improve understanding of the nature of fluids responsible for mineralization in Rossland Camp,
- define fluid characteristics of alkalic porphyry Cu-Au mineralization in the Rossland Group.

The following sections address the objectives of this study by describing sampling and analytical methods, details of fluid inclusion investigations (petrography and microthermometry) and techniques and results of geobarometry. Fluid immiscibility is discussed and relationships of fluid inclusions to deposit types and origin evaluated.

Note that the word "deposit" in this appendix includes occurrences and prospects as well as proven and past-producing mines.

SAMPLING METHODS

Samples of quartz for this fluid inclusion study were selected to satisfy the following criteria:

- Adequate representation of the dominant deposit types (vein, porphyry, skarn) in the Rossland Group
- General distribution of samples in and around Early, Early-Middle and Middle Jurassic intrusions
- Generally representative distribution of vein samples from the Rossland Camp
- Representation of as many alkalic porphyry Cu-Au deposits as possible.

Deposit locations are plotted on Figure A9-1; Table A9-1 lists deposit types and tenor, associated intrusions and estimated intrusion ages. Details on composition, geochemistry and ages of associated intrusions are in Bulletin 102.

Where possible, surface samples were taken from outcrop or trenches and underground samples from drill core or adits; however, due to the flooding of mine workings on Red Mountain, samples of some of the veins in the Rossland Camp are from dumps adjacent to portals.

Samples from a number of barren veins were taken for comparison with mineralized systems and to complete spatial distribution of samples proximal to host intrusions.

ANALYTICAL METHODS

Petrographic survey and microthermometry was conducted using doubly-polished thick sections (~80-100 microns thickness). The size of fluid inclusions varies significantly from sample to sample and different deposits. Fluid inclusions range from <1 micron to approximately 50 microns in maximum dimension. Average size of fluid inclusions in the samples from this study were 6 to 10 microns.

Thermometric data were obtained using a Fluid Inc. - adapted U.S.G.S. gas-flow heating-freezing system calibrated with synthetic quartz fluid inclusion standards with the following accuracies: at -56.6±0.2°C, 374.1±0.6°C and 0.0±0.1°C.

Fluid inclusion nomenclature is given in Table A9-2.

OCCURRENCE OF FLUID INCLUSIONS

Fluid inclusions were evaluated using the concept of fluid inclusion assemblages (FIA's). This ensures that the data was not biased by samples containing large numbers of fluid inclusions and helps to eliminate inconsistent data caused by changes in mass, volume or shape of inclusions after entrapment (ie eliminate non-representative inclusions that are the result of diffusion, stretching or necking-down processes). A fluid inclusion assemblage (FIA) is a petrographically-associated group of inclusions such as those aligned along primary growth zones or secondary fracture planes. One representative data point, rather than several data points is used for each FIA.

Fluid inclusion assemblages from Rossland Group rocks occur in many different ways as can be expected from a variety of mineral deposit types. Primary inclusions which define fluid inclusion assemblages in growth zones or overgrowths in quartz were rarely observed in only six samples, the Bluebird, Lily May, War Eagle, Evening Star, Le Roi and Jumbo deposits (Tables A9-3a to A9-3f, Photos A9-1 to A9-4). Primary inclusions are believed to have formed at the same time as the crystal and therefore represent trapped portions of the fluid that formed the crystal. Most of the fluid inclusion assemblages evaluated were comprised of secondary inclusions occurring along healed fracture planes (Photo A9-5). In many cases the abundance of microfractures in a sample results in a texture referred to by Reynolds (1991) as wispy quartz (Photo A9- 6). Secondary inclusions form after growth of the crystal by sealing and healing of fluid-filled fractures in minerals (Shelton and Orville, 1980; Smith and Evans, 1984). These inclusions are

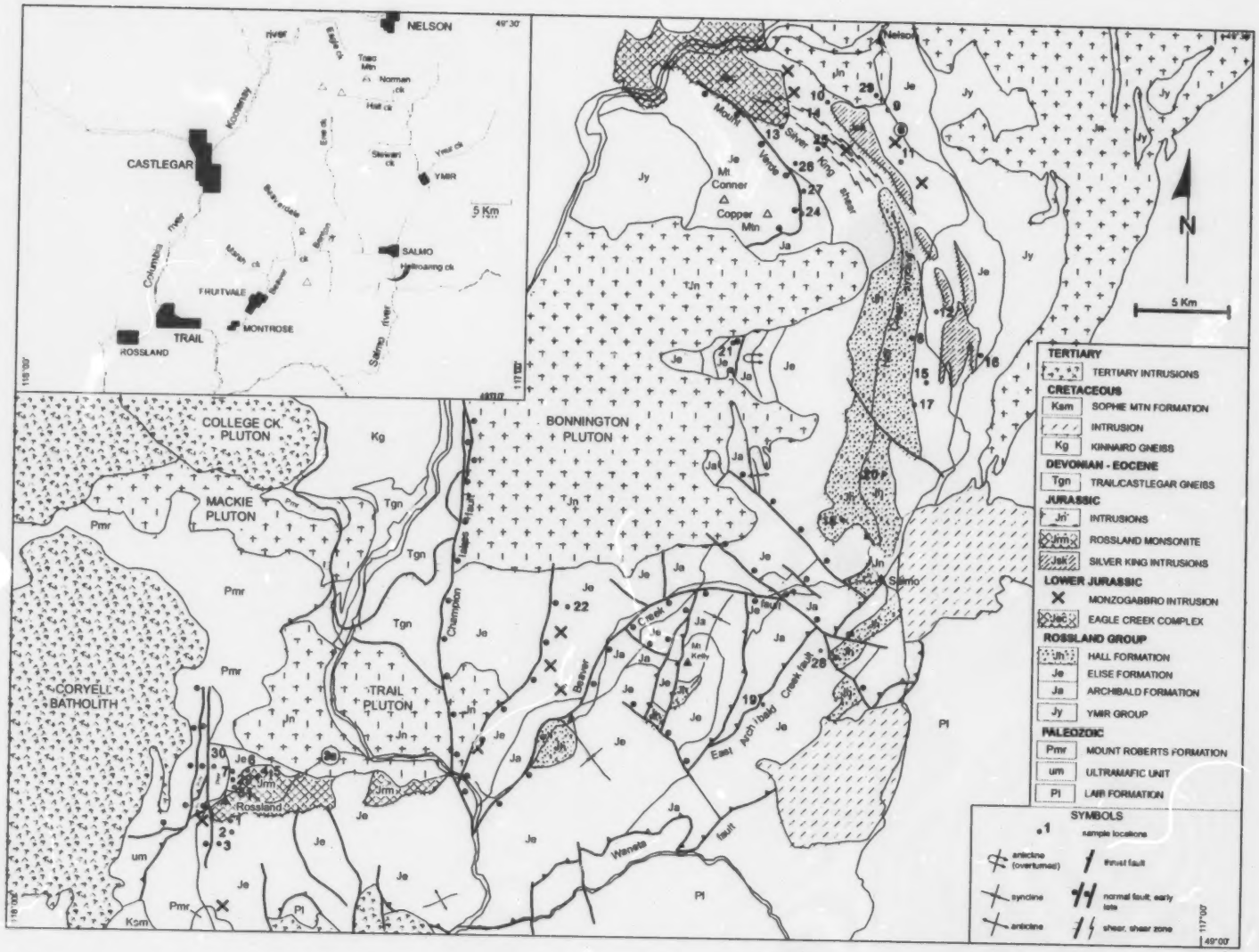

Figure A9-1. Main geologic and physiographic features in the Nelson (W1/2) southwest portion (082F/SW) showing location of intrusions and fluid inclusion sample locations by number. *See* Table A9-1 for names of occurrences and bbarren veins.

TABLE A9-1
LIST OF QUARTZ VEIN SAMPLES, OCCURRENCE NAMES, AND ESTIMATED AGE OF RELATED INTRUSIONS USED IN THIS STUDY SORTED BY DEPOSIT TYPE

Sample #	Figure #	Mining Division	MINFILE # (082FSW)	Deposit Name	Deposit Type	Area/Belt	Related Intrusion	Estimated Age of Related Intrusion	UTM North	UTM East
44-10	15	Nelson	250	Bobbi	Porphyry Mo	Stewart Ck	Nelson Batholith	Middle Jurassic	5462265	485105
Stewart	17	Nelson	229	Stewart	Porphyry Mo	Stewart Ck	Nelson Batholith	Middle Jurassic	5458519	480766
78-2B	14	Nelson	333	Great Western	Porphyry Cu-Au: Alkalic	Giveout Ck	Silver King Pluton	Early-Middle Jurassic	5476245	477274
Star	13	Nelson	83	Star	Porphyry Cu-Au: Alkalic	Morning Mtn	Eagle Creek Complex	Early Jurassic	5477250	473570
79-12	11	Nelson	331	Shaft	Porphyry Cu-Au: Alkalic	Gold Ck	Silver King Pluton	Early-Middle Jurassic	5475850	479706
DDh39-93	28	Nelson	290	Katie	Porphyry Cu-Au: Alkalic	Hellroaring Creek	Katie Stock	Early Jurassic	5443750	475500
DDH53-45	28	Nelson	290	Katie	Porphyry Cu-Au: Alkalic	Hellroaring Creek	Katie Stock	Early Jurassic	5443750	475500
DDH53-65	28	Nelson	290	Katie	Porphyry Cu-Au: Alkalic	Hellroaring Creek	Katie Stock	Early Jurassic	5443750	475500
DH53-118	28	Nelson	290	Katie	Porphyry Cu-Au: Alkalic	Hellroaring Creek	Katie Stock	Early Jurassic	5443750	475500
DH54-193	28	Nelson	290	Katie	Porphyry Cu-Au: Alkalic	Hellroaring Creek	Katie Stock	Early Jurassic	5443750	475500
DH54-197	28	Nelson	290	Katie	Porphyry Cu-Au: Alkalic	Hellroaring Creek	Katie Stock	Early Jurassic	5443750	475500
MI-123	1	Trail Creek	123	Homestake	Polymetallic Veins Ag-Pb-Zn+/-Au	Rossland/ South Belt	Rossland Pluton	Middle Jurassic	5434550	441650
M3-145	2	Trail Creek	145	Bluebird	Polymetallic Veins Ag-Pb-Zn+/-Au	Rossland/ South Belt	Rossland Pluton	Middle Jurassic	5434225	441600
MI-153	3	Trail Creek	153	Lily May	Polymetallic Veins Ag-Pb-Zn+/-Au	Rossland/ South Belt	Rossland Pluton	Middle Jurassic	5433850	440600
MI-202	18	Nelson	202	Keystone	Polymetallic Veins Ag-Pb-Zn+/-Au	Keystone Mountain	Hidden Creek Stock	Middle Cretaceous	5452417	477913
Clubine	20	Nelson	200	Clubine	Polymetallic Veins Ag-Pb-Zn+/-Au	Keystone Mountain	Hidden Creek Stock	Middle Cretaceous	5454000	479750
206-16	19	Nelson	350	Ace in the Hole	Polymetallic Veins Ag-Pb-Zn+/-Au	Hellroaring Creek	Wallack Creek Stock	Middle Cretaceous	5440519	472531
MI-068	16	Nelson	68	Yankee Girl	Polymetallic Veins Ag-Pb-Zn+/-Au	Ymir	Nelson Batholith	Middle Jurassic	5459707	486668
17-3	12	Nelson	186	Euphrates	Polymetallic Veins Ag-Pb-Zn+/-Au	Clearwater Ck	Silver King Pluton	Early-Middle Jurassic	5470405	484478
131-18B	24	Nelson	179	Golden Eagle	Polymetallic Veins Ag-Pb-Zn+/-Au	Red Mtn	Bonnington Pluton	Middle Jurassic	5471327	474964
Rozan	27	Nelson		Rozan	Polymetallic Veins Ag-Pb-Zn+/-Au	Red Mtn	Bonnington Pluton	Middle Jurassic	5471800	474800

TABLE A9-1 CONTINUED

Sample #	Figure #	Mining Division	MINFILE # 082FSW	Deposit Name	Deposit Type	Area/Belt	Related Intrusion	Estimated Age of Related	UTM North	UTM East
96-42B	5	Trail Creek	151	Columbia	Intrusion-Related Au-Pyrrhotite Veins	Rossland/Main Belt	Rossland Pluton	Middle Jurassic	5437633	442994
96-31B	29	Trail Creek	97	War Eagle	Intrusion-Related Au-Pyrrhotite Veins	Rossland/Main Belt	Rossland Pluton	Middle Jurassic	5437021	440645
96-51E	7	Trail Creek	135	Consolidated St. Elmo	Intrusion-Related Au-Pyrrhotite Veins	Rossland/ North Belt	Rossland Pluton	Middle Jurassic	5437718	440457
96-51A	7	Trail Creek	135	Consolidated St. Elmo	Intrusion-Related Au-Pyrrhotite Veins	Rossland/ North Belt	Rossland Pluton	Middle Jurassic	5437718	440457
96-58	29	Trail Creek	97	War Eagle	Intrusion-Related Au-Pyrrhotite Veins	Rossland/Main Belt	Rossland Pluton	Middle Jurassic	5436750	441150
96-28B	30	Trail Creek	111	Jumbo	Intrusion-Related Au-Pyrrhotite Veins	Rossland /North Belt	Rossland Pluton	Middle Jurassic	5437759	439138
96-24A	31	Trail Creek	93	LeRoi	Intrusion-Related Au-Pyrrhotite Veins	Rossland/Main Belt	Rossland Pluton	Middle Jurassic	5436612	440699
96-71A	29	Trail Creek	97	War Eagle	Intrusion-Related Au-Pyrrhotite Veins	Rossland/Main Belt	Rossland Pluton	Middle Jurassic	5437067	441412
96-39A	4	Trail Creek	151	Kootenay	Intrusion-Related Au-Pyrrhotite Veins	Rossland/Main Belt	Rossland Pluton	Middle Jurassic	5437695	443193
Columbia	5	Trail Creek	151	Columbia	Intrusion-Related Au-Pyrrhotite Veins	Rossland/Main Belt	Rossland Pluton	Middle Jurassic	5437450	442850
Ev-Star	6	Trail Creek	102	Evening Star	Intrusion-Related Au-Pyrrhotite Veins	Rossland/ North Belt	Rossland Pluton	Middle Jurassic	5437500	442000
51-9	9	Nelson		Giveout Creek Vein	Barren Vein	Giveout Ck	Nelson Batholith	Middle Jurassic	5477842	479419
139-4	25	Nelson		Cumberland Shaft	Barren Vein	Morning Mtn	Eagle Creek Complex	Early Jurassic	5475210	475470
165-13A	22	Trail Creek		Marsh Creek Vein	Barren Vein	Marsh Ck	Bonnington Pluton	Middle Jurassic	5442952	458251
20-1	8	Nelson		Hall Siding Vein	Barren Vein	Hall Siding	Silver King Pluton	Early-Middle Jurassic	5467705	482144
85-15C	23	Nelson	168	Athabasca	Au-Quartz Veins	Giveout Ck	Eagle Creek Complex	Early Jurassic	5478388	477352
Gold Hill	26	Nelson	92	Gold Hill	Au-Quartz Veins	Fortynine Ck	Bonnington Pluton	Middle Jurassic	5474641	473409
344-6B	21	Nelson	187	Second Relief	Au Skarns	Erie Ck	Bonnington Pluton	Middle Jurassic	5463075	471229
344-5B	21	Nelson	187	Second Relief	Au Skarns	Erie Ck	Bonnington Pluton	Middle Jurassic	5463087	471238

TABLE A9-2
FLUID INCLUSION NOMENCLATURE USED IN THIS STUDY

ABBREVIATION	DESCRIPTION
FI	fluid inclusion
FIA	fluid inclusion assemblage
P	primary origin
S	secondary origin
v	vapour phase
l	liquid phase
s	solid phase
Tm	melting temperature
Tm CO2	melting temperature of CO2 solid phase
Tm H2O	melting temperature of ice or hydrohalite
Tm hydrate	melting temperature of hydrohalite
Tm clathrate	melting of clathrate (gas hydrate) CO2 5.75H2O
Tm salt	melting of salt
Te	first observed melting event, corresponds with eutectic for stable systems; may be interpreted as metastable melting event
Te H2O	first melting of ice or hydrohalite
Th	homogenization temperature (disappearance of liquid or vapour phase)
Th CO2	homogenization temperature of CO2
Th H2O	homogenization temperature of H2O
Td	decrepitation of fluid inclusion
eq. wt.% NaCl	salinity unit expressed in terms of equivalent weight percent NaCl
XH2O	mole fraction H2O in the fluid inclusion
XCO2	mole fraction CO2 in the fluid inclusion
XNaCl	mole fraction NaCl (equivalent) in the fluid inclusion

common in rocks with low porosity or in environments in which grains are subject to tectonic or to thermal stresses during or after growth (Crawford and Hollister, 1986). Interpretation of secondary fluid inclusion data reflects the conditions of formation of post-crystal formation fluids trapped in fractures after crystal growth ceased.

The primary objective of this fluid inclusion study was to try to evaluate fluid inclusions in quartz which were related to ore minerals in the samples. Since gold or sulphide minerals could not be found within fractures clearly associated with a given generation of fluid inclusions (or fluid inclusion assemblage), where possible, fluid inclusions were sought in quartz proximal to sulphide grains. These fluid inclusions are believed to most closely approximate samples of the ore-forming fluids.

Concepts developed in this paper stem from evaluation of secondary rather than primary fluid inclusions. The occurrence of primary fluid inclusions is extremely rare, only noted in 6 samples from a total of 66 samples surveyed from deposits in the Rossland Group. It is interesting to note that the samples with primary fluid inclusions are all from the Rossland Camp though from different deposit types. We cannot confirm that secondary fluids in the Rossland Group represent the mineralizing solution for the deposit types considered in this study; however, absence of primary fluid inclusions is common in both porphyry and deep batholith-related vein deposits (Reynolds, 1991). Ideally, detailed work is required to document fluid inclusion chronology among or between fracture sets in each deposit.

COMPOSITION OF FLUID INCLUSIONS

Six compositional types of fluid inclusions have been identified in quartz from mineral occurrences in the Rossland Group through observation of phases present and volume percent phases at room temperature. For each measured fluid inclusion type within a fluid inclusion assemblage, the liquid-to-vapour ratios were relatively (+/-20 volume % vapour) consistent. The compositional types, modified from the nomenclature of Nash (1976) are: Type I aqueous liquid-rich, Type III salt-saturated, Type IV mixed aqueous and carbonic, Type V carbonic, Type VI multiphase and Type VII mixed multiphase and carbonic (Figure A9-2, Photo A9-7). Aqueous vapour-rich Type II inclusions are notably absent.

Type I fluid inclusions are characterized by 2 aqueous phases, liquid and vapour, with volume% liquid>volume% vapour. Type III inclusions comprise a liquid brine, aqueous vapour and one solid phase (salt identified by cubic shape). Type III inclusions are divided into 2 subtypes, IIIA and IIIB based on the solid crystal volume relative to the vapour phase. Type IIIA inclusions have salt volume < vapour

TABLE A9-3A
MELTING, HOMOGENIZATION AND DECREPITATION TEMPERATURE DATA FOR TYPE I FLUID INCLUSIONS

Deposit Type	Deposit Name	Sample	FIA #	Origin	Vol% Vap.	Te H2O	Tm H2O	Th H2O	Td
Au Skarns	Second Relief	344-5B	1	S	15			362.3	
Au Skarns	Second Relief	344-6B	1	S	10			352.5	
Au Skarns	Second Relief	344-6B	2	S	10		-9.3	161.7	
Au Skarns	Second Relief	344-6B	3	S	10		-9.7	281.3	403.4
Au Skarns	Second Relief	344-6B	4	S	10		-6.6		
Au Skarns	Second Relief	344-6B	5	S	30			285.1	416.2
Au-Quartz Veins	Athabasca	85-15C	1	S	2			170.9	175
Au-Quartz Veins	Athabasca	85-15C	2	S	5			174.8	
Au-Quartz Veins	Gold Hill	Gold Hill	2	S	10	-26.1	-6.4	234	
Au-Quartz Veins	Gold Hill	Gold Hill	3	S	20			300.6	
Au-Quartz Veins	Gold Hill	Gold Hill	6	S	10			271.1	
Barren Vein	Cumberland Shaft	139-4	1	S	10			260.8	
Barren Vein	Cumberland Shaft	139-4	2	S	10			326	
Barren Vein	Cumberland Shaft	139-4	3	S	10			244.6	
Barren Vein	Cumberland Shaft	139-4	4	S	5	-25	-3	186.2	
Barren Vein	Giveout Creek Vein	51-9	1	S	5		-1.7	296	
Barren Vein	Giveout Creek Vein	51-9	2	S	5		-8.6	325	327
Barren Vein	Hall Siding Vein	20-1	1	S	10			232.4	
Barren Vein	Hall Siding Vein	20-1	2	S	5	-26.1	-4.2		
Barren Vein	Hall Siding Vein	20-1	3	S	10		-1.3		
Barren Vein	Hall Siding Vein	20-1	4	S	30	-30	-4.5		
Barren Vein	Hall Siding Vein	20-1	5	S	20	-26.5	-6		
Barren Vein	Hall Siding Vein	20-1	6	S	5		-6.6	172.6	
Barren Vein	Marsh Creek Vein	165-13A	1	S	10	-27.9	-4.5	322.2	
Barren Vein	Marsh Creek Vein	165-13A	2	S	10		-2.3	246.2	
Barren Vein	Marsh Creek Vein	165-13A	3	S	30		-0.8	294.7	
Intrusion-Related	Columbia	96-42B	1-2	S	30	-22.3	-12.7	316.5	343
Intrusion-Related	Columbia	96-42B	3-2	S	40		-8.7	287.6	
Intrusion-Related	Columbia	96-42B	2-1	S	40	-22.4	-7.2	346.3	
Intrusion-Related	Columbia	Columbia	1	S	15	-18	-8.2	272	
Intrusion-Related	Columbia	Columbia	4	S	5			377	
Intrusion-Related	Columbia	Columbia	5	S	5		-3.7	302.9	
Intrusion-Related	Consolidated St Elmo	96-51A	1-2	S		-30.8	-16.7	183.4	327
Intrusion-Related	Consolidated St Elmo	96-51A	3-2	S		-26.3	-4	102.3	
Intrusion-Related	Consolidated St Elmo	96-51E	4-2	S		-27	-15.2	194.2	
Intrusion-Related	Evening Star	EV-Star	1	P	10	-25	-3.4	307.8	
Intrusion-Related	Jumbo	96-28B	1-1	S			-3.2	231.5	293
Intrusion-Related	Kootenay	96-39A	1-1	S		-23.3	-2.9	246.2	
Intrusion-Related	Kootenay	96-39A	3-1	S		-27.1	-2.7	237.5	
Intrusion-Related	War Eagle	96-31B	4-1	S		-35.7	-11.3	208.4	
Polymetallic Veins	Ace in the Hole	206-16	1	S	15		-5.3	240	
Polymetallic Veins	Ace in the Hole	206-16	2	S	15			230	
Polymetallic Veins	Ace in the Hole	206-16	3	S	5			200	
Polymetallic Veins	Ace in the Hole	206-16	4	S	5	-24		237	

TABLE A9-3A
CONTINUED

Deposit Type	Deposit Name	Sample	FIA #	Origin	Vol% Vap.	Te H2O	Tm H2O	Th H2O	Td
Polymetallic Veins	Bluebird	M3-145	1	S	5	-28.1	-14	245	
Polymetallic Veins	Bluebird	M3-145	3	P	10		-5	300	
Polymetallic Veins	Clubine	Clubine	1	S	5			200.8	
Polymetallic Veins	Clubine	Clubine	2	S	10	-23		257	
Polymetallic Veins	Clubine	Clubine	3	S	10	-16		238	270
Polymetallic Veins	Euphrates	17-3	1	S	15		-4.1	320.2	
Polymetallic Veins	Golden Eagle	131-18B	1	S	30			368.7	
Polymetallic Veins	Golden Eagle	131-18B	2	S	15		-4.2		
Polymetallic Veins	Homestake	MI-123	2	S	10	-25.1	-4.8	262	
Polymetallic Veins	Homestake	MI-123	5	S	30		-2.7		
Polymetallic Veins	Keystone	MI-202	1	S	10		-0.8	372.2	
Polymetallic Veins	Lily May	MI-153	1	P	30		-8	392.5	
Polymetallic Veins	Rozan	Rozan	1	S	15			259	
Polymetallic Veins	Rozan	Rozan	2	S	5			181.6	
Polymetallic Veins	Rozan	Rozan	3	S	5	-27.1	-5.9	160.8	
Polymetallic Veins	Rozan	Rozan	4	S	5		-5.2	228.2	
Polymetallic Veins	Yankee Girl	MI-068	1	S	5			318.5	
Polymetallic Veins	Yankee Girl	MI-068	2	S	10			314.2	
Porphyry Cu-Au	Great Western	78-2B	2	S	10			201	
Porphyry Cu-Au	Great Western	78-2B	4	S	15			313	
Porphyry Cu-Au	Katie	DDH39-93	2	S	5		-3.9	163	
Porphyry Cu-Au	Katie	DDH39-93	1	S	10		-4	239	
Porphyry Cu-Au	Katie	DDH53-65	1	S	15		-10.5	238	
Porphyry Cu-Au	Katie	DDH53-65	2	S	10		-0.9	270	
Porphyry Cu-Au	Katie	DH53-118	1	S	15		-2.6	265	
Porphyry Cu-Au	Katie	DH53-118	2	S	5		-12.7	170	
Porphyry Cu-Au	Katie	DH53-118	3	S	5	-32	-12.5	260	
Porphyry Cu-Au	Katie	DH53-118	4	S	5	-25	-8.2	236	
Porphyry Cu-Au	Katie	DH54-193	1	S	10	-28	-4.2	188	
Porphyry Cu-Au	Katie	DH54-193	2	S	5	-31	-8.2	227	339
Porphyry Cu-Au	Katie	DH54-197	1	S	15			258	293
Porphyry Cu-Au	Katie	DH54-197	2	S	30	-40		338	360
Porphyry Cu-Au	Katie	DH54-197	3	S	15		-10.3	261.8	
Porphyry Cu-Au	Shaft	79-12	2	S	5			324	
Porphyry Cu-Au	Star	Star	2	S	10			389.9	
Porphyry Cu-Au	Star	Star	3	S	10	-21.6		288.7	
Porphyry Mo	Bobbi	44-10	1	S	5			246.8	
Porphyry Mo	Bobbi	44-10	2	S	10		-8.9	217.6	
Porphyry Mo	Stewart	Stewart	2	S	40		-4.2	287.7	

TABLE A9-3B
MELTING, HOMOGENIZATION, DISSOLUTION AND DECREPITATION TEMPERATURE DATA FOR TYPE III FLUID INCLUSIONS

Deposit Type	Deposit Name	Sample	FIA #	FI Type	Origin	Vol% Vap.	Te H2O	Tm H2O	Tm Hydrate	Th H2O	Tm Salt	Td
Intrusion-Related	War Eagle	96-71A	1-1	IIIB	S	10	-32.9			156	285.5	
Intrusion-Related	War Eagle	96-71A	2-3	IIIB	S		-47.3	-23	15.9	170	331	
Polymetallic Veins	Homestake	MI-123	2	IIIA	S	10				255	184	356
Porphyry Cu-Au	Great Western	78-2B	1	IIIB	S	10	-40	-3.5		224	246.5	
Porphyry Cu-Au	Great Western	78-2B	3	IIIA	S	5				382	162	382
Porphyry Cu-Au	Great Western	78-2B	3	IIIB	S	5				206	275	328
Porphyry Cu-Au	Great Western	78-2B	4	IIIA	S	5				305	200	
Porphyry Cu-Au	Katie	DH53-118	1	IIIB	S	5	-34	-12.3		238	261	346
Porphyry Cu-Au	Katie	DH53-118	4	IIIA	S	5				262	198	
Porphyry Cu-Au	Star	Star	1	IIIB	S	15		-6.1	2.9	350.1	357.9	

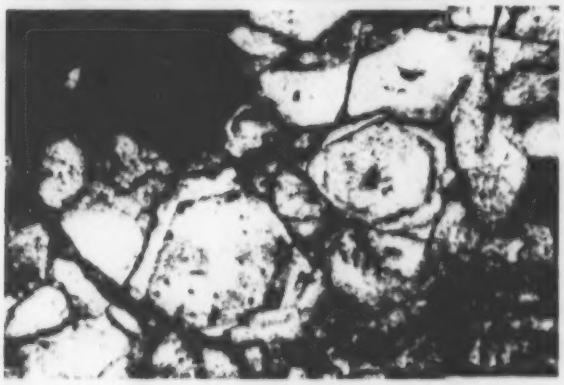

Photo A9-1. Primary inclusions trapped in quartz growth zones in quartz matrix of massive pyrite, galena sphalerite vein, Bluebird deposit. Transmitted plane light, 20X magnification, field of view = 2.5 mm.

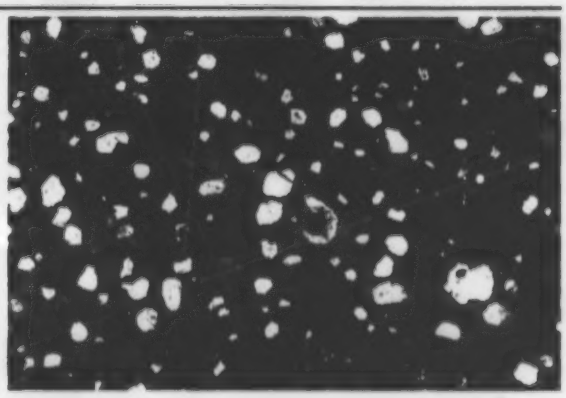

Photo A9-3. Possible primary fluid inclusions in bands or clusters in poikilitic-textured (resorbed?) quartz gangue from a massive sulphide vein, Jumbo deposit. Transmitted and reflected plane light, 6.25X magnification, field of view = 7.8 mm.

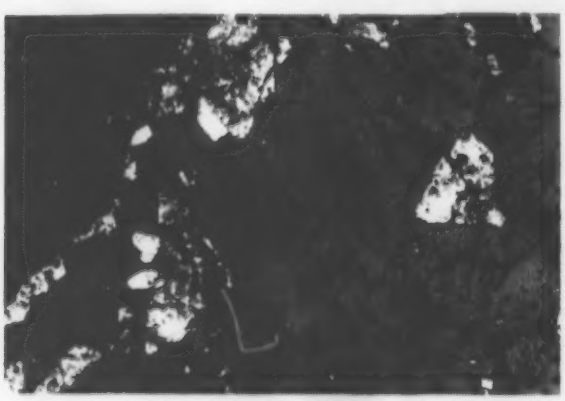

Photo A9-2. Semi-massive pyrrhotite chalcopyrite vein incorporating subhedral quartz comprising primary fluid inclusions in growth zones (right side-middle of frame quartz grain) and overgrowths (centre-top of frame quartz grain), Le Roi deposit. Transmitted and reflected plane light, 6.25X magnification, field of view = 7.8 mm.

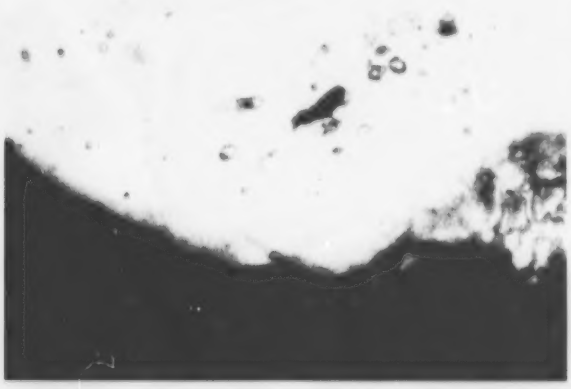

Photo A9-4. Possible primary fluid inclusions trapped in growth zones in quartz from a quartz-pyrite-calcite vein, Evening Star deposit. Transmitted plane light, 200X magnification, field of view = 0.16mm.

TABLE A9-3C
MELTING, HOMOGENIZATION AND DECREPITATION TEMPERATURE DATA FOR TYPE IV FLUID INCLUSIONS

Deposit Type	Deposit Name	Sample	FIA #	Origin	Vol% vap.	Tm CO2	Te H2O	Tm H2O	Tm Clathrat	Th CO2	Th H2O	Td
Au Skarns	Second Relief	344-5B	1	S	15	-58.1			-2.8			370
Au Skarns	Second Relief	344-6B	5	S	30	-58.5				10.2		411.9
Au-Quartz Veins	Gold Hill	Gold Hill	1	S	10		-25	-0.2	5.5			
Au-Quartz Veins	Gold Hill	Gold Hill	2	S	20	-57.3			6.7	27.9		240
Au-Quartz Veins	Gold Hill	Gold Hill	4	S	25					29.5	305.1	280
Au-Quartz Veins	Gold Hill	Gold Hill	5	S	25					29.5	300.1	
Au-Quartz Veins	Gold Hill	Gold Hill	7	S	25		-24.8	-4.1	8.3			
Barren Vein	Giveout Creek Vein	51-9	1	S	20	-57.9						
Barren Vein	Giveout Creek Vein	51-9	2	S	25						360	
Barren Vein	Marsh Creek Vein	165-13A	2	S	50	-57				13.2	324.6	
Intrusion-Related	Consolidated St Elmo	96-51A	2-2	S		-58						
Intrusion-Related	Consolidated St Elmo	96-51A	3-2	S		-55.4			5.6	25.2		
Intrusion-Related	Consolidated St Elmo	96-51A	4-1	S		-56.1				2.1		
Intrusion-Related	Consolidated St Elmo	96-51E	2-1	S	10	-58.4				23.9		371
Intrusion-Related	Evening Star	Ev-Star	2	P	40			-2.4	0.4	25.4		
Intrusion-Related	Evening Star	Ev-Star	3	P	85	-58.5			-2.8	25	351.5	
Intrusion-Related	Evening Star	Ev-Star	4	P	20	-56				10.8	312.8	
Intrusion-Related	Evening Star	Ev-Star	5	P	60	-57.1			-1.1	21.9	370	
Intrusion-Related	Jumbo	96-28B	3-1	P	35	-57.8						
Intrusion-Related	Jumbo	96-28B	6-3	P	60	-58.3						
Intrusion-Related	War Eagle	96-31B	1-1	S		-57.8				28.3	299.8	
Intrusion-Related	War Eagle	96-31B	2-2	S		-57.8			7.8		316.4	
Intrusion-Related	War Eagle	96-71A	1-1	S	60	-57.4				32.4		
Intrusion-Related	War Eagle	96-71A	2-1	S	85	-56.6			6.8	21.8		
Intrusion-Related	War Eagle	96-71A	2-4	S	80	-57			8	21.6	341.6	
Intrusion-Related	War Eagle	96-71A	3-1	S	70	-56.6			4.2	21.6	243.2	
Polymetallic Veins	Golden Eagle	131-18B	2	S	30	-57		-10		13		
Polymetallic Veins	Homestake	MI-123	1	S	50	-57.3			9.5	28.5	300.8	
Polymetallic Veins	Homestake	MI-123	3	S	60	-58.1						
Polymetallic Veins	Lily May	MI-153	1	P	80	-57		-6.3			350	
Porphyry Cu-Au	Katie	DH54-197	2	S	20	-58.2					312	366
Porphyry Cu-Au	Shaft	79-12	1	S	5					23	326	
Porphyry Cu-Au	Star	Star	1	S	15	-63.1			2.5			
Porphyry Cu-Au	Star	Star	2	S	10					10.8	385	
Porphyry Cu-Au	Star	Star	3	S	80		-22	-11.4	5.2	28.9	361.2	
Porphyry Mo	Stewart	Stewart	1	S	80	-58		-5	9.6	18.8	240	

phase and Type IIIB inclusions have salt volume > vapour phase. Type IV inclusions consist of 2 or 3 phases at room temperature. These are either an aqueous liquid and CO_2-bearing liquid or an outer aqueous liquid, inner CO_2-bearing liquid and a CO_2-bearing vapour. The CO_2 volumetric proportions of Type IV inclusions range from 10-85 % (TableA9- 3C). The whole range of CO_2 volumetric proportions may be observed within individual samples such as the Star (10 to 80 volume % CO_2). Type V inclusions consist of one or two phases at room temperature, a CO_2-bearing liquid or a CO_2-bearing vapour and a CO_2-bearing liquid. These inclusions are typically very dark. Type VI inclusions comprise aqueous liquid and vapour phases and at least one solid phase (probably not salt). Type VII inclusions are similar to type VI inclusions but in addition to an aqueous liquid and multiple solid phases they also contain a CO_2-bearing liquid and a CO_2-bearing vapour.

PHASE CHANGES ON FREEZING AND HEATING

Temperatures of measured phase changes on freezing and heating for each compositional type of fluid inclusion within a fluid inclusion assemblage (FIA) are given in Table A9-3 and Figures A9-3, A9-4 and A9-5. Only one record of each compositional type from a fluid inclusion assemblage is included in the tabular data. Variation between records of each compositional type from a fluid inclusion assemblage is consistent to moderately variable with 90% of measured temperatures falling within greater than a 10-20°C interval. The data for each fluid inclusion assemblage is denoted by

TABLE A9-3D
MELTING AND HOMOGENIZATION TEMPERATURE DATA FOR TYPE V FLUID INCLUSIONS

Deposit Type	Deposit Name	Sample	FIA #	Origin	Vol % vap.	Tm CO2	ThCO2	Td CO2
Au Skarns	Second Relief	344-5B	2	S	10	-57	24.3	
Au Skarns	Second Relief	344-6B	2	S	10	-		
Intrusion-Related	Evening Star	EV-STAR	4	P	30	-57.3	10.8	
Polymetallic Veins	Bluebird	M3-145	2	P	50	-58.2	18.3	
Polymetallic Veins	Homestake	MI-123	2	S	70	-56.8	24.1	
Polymetallic Veins	Homestake	MI-123	4	S	65	-57.3		
Polymetallic Veins	Homestake	MI-123	5	S	30	-57.3		
Polymetallic Veins	Lily May	MI-153	1	P	50	-56.8	30	
Porphyry Cu-Au	Katie	DH54-197	4	S	15	-57.2	18.7	
Intrusion-Related	Jumbo	96-28B	1-3	p	50	-58.3		
Intrusion-Related	Consolidated	96-51E	1-2	S	20	-57.8	10.2	192
Intrusion-Related	Consolidated	96-51E	3-1	S	30	-58.2	19.3	
Intrusion-Related	Kootenay	96-39A	3-1	S	75	-56.7	24	
Intrusion-Related	Kootenay	96-39A	4-1	S	85	-56.6	28.3	

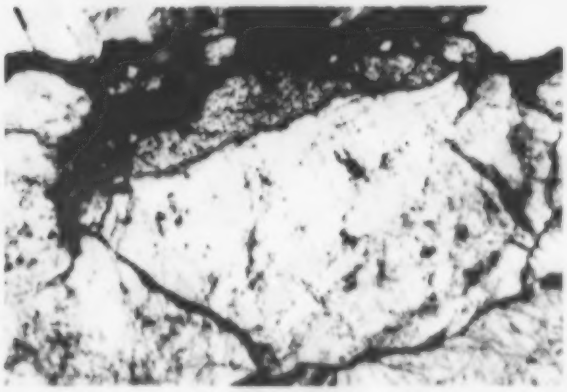

Photo A9-5. Secondary fluid inclusions occuring along healed fracture planes in quartz vein with disseminated galena, Clubine deposit. Transmitted and plane light, 20X magnification, field of view = 2.5 mm.

Photo A9-6. Wispy quartz texture: abundance of microfractures filled with tiny, secondary fluid inclusions (Reynolds, 1991) in quartz vein with disseminated galena, chalcopyrite, pyrite, and sphalerite, Ace in the Hole deposit. Transmitted plane light, 20X magnification, field of view = 2.5 mm.

sequential numerals per sample in column FIA No. For comparison of composition between deposit types and districts, deposit name and type from Table A9-1 are included. Calculation of salinity, XCO_2, XH_2O, XNaCl and pressure of entrapment were made using the computer software programs FLINCOR (Brown, 1989) and MacFlincor (Brown and Hagemann, 1994).

TYPE I: AQUEOUS LIQUID-RICH

On freezing, the fluid inclusions show metastable supercooling and form ice at temperatures below -30°C. The first melting, characterized by a sudden clearing of crystals, probably ice, from the inclusion, is typically observed on warming between -32 and -21.6°C for most deposit types (Figure A9-3A) although two fluid inclusion assemblages demonstrated low first melting temperatures of -40°C (porphyry Cu-Au) a nd -35.7°C (Intrusion-related) and two other assemblages exhibited anomalously high first melting at -18°C (Intrusion-related) and -16°C (Polymetallic vein). A second and final melting, also characterized by clearing of crystals, probably hydrohalite, and often accompanied by a jerk of the vapour bubble, occurs between -14 and 0°C for most deposit types (Figure 3A) although intrusion-related deposits exhibit melting as low as -16.7°C.

First melting temperatures below -21.2°C, the stable NaCl-H_2O eutectic, indicate the addition of small concentrations of K+, Ca2+, Mg2+ or other ions to an H_2O-NaCl fluid. The presence of low concentrations of Mg2+ ion or Ca2+ ion in some Type I fluid inclusions is suggested by pronounced first melting temperatures below -22.9°C (Figure A9-3b) and observed final ice melting behaviour (Figure A9-3c) of NaCl-MgCl-H_2O or NaCl-$CaCl_2$-H_2O fluids from Davis *et al.* (1990). Unfortunately, both extrapolations lack complementary observations of hydrate rim development, darkening of solids or nucleation of a vapour phase at lower temperatures. In conclusion, it is reasonable to model the Type I fluid overall as an NaCl brine partly because most formational fluids are NaCl dominant (Reynolds, 1991) but also because comparison of the cotectic surfaces where ice

TABLE A9-3E
MELTING, HOMOGENIZATION AND DECREPITATION TEMPERATURE DATA FOR TYPE VI FLUID INCLUSIONS

Deposit Name	Deposit Type	Sample	FIA #	Origin	Vol% vap.	Te H2O	Tm H2O	Tm Hydrate	Th H2O	#Solids	Td	Ts
Columbia	Intrusion-Related	96-42B	1-1	S		-20.6	-9.9		303.1	3	343	
Columbia	Intrusion-Related	96-42B	2-3	S		-23	-4		157.7	1		
Columbia	Intrusion-Related	96-42B	3-1	S		-22.7	-10.5		254.7	2		
Columbia	Intrusion-Related	96-42B	3-3	S		-27.8	-15.1		236.4	3		
Columbia	Intrusion-Related	96-42B	4-1	S		-23	-9.2		281.3	4	337	
Columbia	Intrusion-Related	Columbia	1	S	10	-25	-13.8		199	3	280	
Columbia	Intrusion-Related	Columbia	2	S	5	-28	-8		217	•	295	
Columbia	Intrusion-Related	Columbia	3	S	5	-22	-7		236	3	273	
Columbia	Intrusion-Related	Columbia	4	S	5				370	1		
Columbia	Intrusion-Related	Columbia	5	S	15		-3		292.8	1		
Consolidted St Elmo	Intrusion-Related	96-51E	1-1	S		-29.7	-12.5		116.2	3	300	
Consolidted St Elmo	Intrusion-Related	96-51A	1-3	S			-6.5		186.1	1	327	
Consolidted St Elmo	Intrusion-Related	96-51A	2-1	S			-16.5		183.1	1		
Consolidted St Elmo	Intrusion-Related	96-51E	4-2	S					170.3	1		
Jumbo	Intrusion-Related	96-28B	2-1	p		-23	-0.9		145	2		
Jumbo	Intrusion-Related	96-28B	4-1	p					267.1	3	268	
Jumbo	Intrusion-Related	96-28B	5-1	p		-21		10.4	210.5	4		
Jumbo	Intrusion-Related	96-28B	6-1	p		-25.4		9.7		4	337	
Jumbo	Intrusion-Related	96-28B	1-1	S		-23.6	-3.7		228	1	293	
Jumbo	Intrusion-Related	96-28B	3-1	S		-25.6	-0.1		183.1	1	184	
Kootenay	Intrusion-Related	96-39A	1-1	S			-2.3		301.1	3		
Kootenay	Intrusion-Related	96-39A	2-1	S		-22.3	-2.2		269.2	1		
Leroi	Intrusion-Related	96-24A	1-1	S	10	-36.8	-24.2			2	407	
Leroi	Intrusion-Related	96-24A	2-1	S	10	-43.2		4.3		1	210	
War Eagle	Intrusion-Related	96-31B	4-2	S		-34.4	-10.6		205.7	3	338	
War Eagle	Intrusion-Related	96-31B	1-2	S					160	1	400	
War Eagle	Intrusion-Related	96-31B	2-1	S		-36	-8		229.9	1	294.1	
War Eagle	Intrusion-Related	96-31B	2-4	S		-31.6	-14.5		298.7	5		330
War Eagle	Intrusion-Related	96-31B	3-2	S		-23			289	1	402	
War Eagle	Intrusion-Related	96-31B	4-1	S			-10.8		214.9	1		
War Eagle	Intrusion-Related	96-58	1-1	S		-24		4.3	141	1	305	
Bluebird	Polymetallic Vein	M3-145	1	S	10	-32	-19.4		248	1	248	
Bluebird	Polymetallic Vein	M3-145	2	P	5	-23.6	-8.1	5.4	286.5	1		
Bluebird	Polymetallic Vein	M3-145	3	P	10				310	1		
Homestake	Polymetallic Vein	M3-123	3	S	20	-21.8	-0.7		245.3	1	310	
Katie	Porphyry Cu-Au	DDH39-93	2	S	5	-19			166	1		
Katie	Porphyry Cu-Au	DDH39-93	3	S	10		-16.5		180.5	1		
Katie	Porphyry Cu-Au	DDH39-93	3	S	5	-28.4	-15		175	1		
Katie	Porphyry Cu-Au	DDH53-45	1	S	5				321	1	322	
Katie	Porphyry Cu-Au	DDH53-65	1	S	15	-25	-8.8		215	1		
Katie	Porphyry Cu-Au	DDH53-65	2	S	15		-8		270	1	370	
Katie	Porphyry Cu-Au	DDH53-65	3	S	5				259	1		
Katie	Porphyry Cu-Au	DH53-118	1	S	5	-28.1	-11		195.1	3	222	
Katie	Porphyry Cu-Au	DH53-118	3	S	5	-37	-12.1		269	1		
Katie	Porphyry Cu-Au	DH54-197	3	S	10				284	1		
Shaft	Porphyry Cu-Au	79-12	1	S	5				217	1		
Shaft	Porphyry Cu-Au	79-12	2	S	5				276	1		

TABLE A9-3F
MELTING, HOMOGENIZATION AND DECREPITATION TEMPERATURE DATA FOR TYPE VII FLUID INCLUSIONS

Deposit Type	Deposit Name	Sample	FIA #	Origin	Vol% Vap.	Tm CO2	Tm Clathrate	Th CO2	Th H2O	Td	# Solids
INTRUSION-RELATED	CONSOLIDATED ST ELMO	96-51E	4-1	S	25	-58	5.3	14.8			3
INTRUSION-RELATED	JUMBO	96-28B	2-2	P	20	-57		19.2		249	2
INTRUSION-RELATED	LEROI	96-24A	1-1	S	30	-56.8		24.2	206.2	352	3
INTRUSION-RELATED	WAR EAGLE	96-31B	3-1	S	40	-57.9		27.9	294.6	400	4

melts for various systems (Figure A9-6, from Crawford, 1981) shows relatively small variations (<5 wt.% change).

Using the H_2O-NaCl model composition and method of Hall *et al.* (1988), salinity of Type I fluid inclusions in Rossland Group deposits varies from 1.3 to 20 equivalent weight % (eq. wt. %) NaCl (Table A9-4). Variation in salinity range in relation to deposit type (Table A9-4) is more pronounced as expected for deposits formed under different conditions.

Homogenization temperatures of liquid-rich aqueous inclusions in Rossland Group deposits range from 160.8°C to 392.5°C (Figure A9-3d) with the bulk of data between 220°C and 320°C. Variation in homogenization temperature range in relation to deposit type is plotted in Figure A9-6. Porphyry Cu-Au, polymetallic vein, intrusion-related and Au skarn deposits have the highest homogenization temperatures.

TYPE III: SALT SATURATED

Type III fluid inclusions contain one cubic salt crystal (daughter mineral) in addition to a vapour bubble; this means that the contained fluid precipitated a salt crystal because it was saturated with respect to salt at the pressure of formation. Salt-saturated fluid inclusions must have salinities > 26.3 eq. wt. % NaCl. Salinities of Type III fluid inclusions are usually determined using the melting temperature of the salt phase and a phase diagram which represents the composition of the fluid. Sometimes the salt sylvite (KCl) can be optically distinguished from halite (NaCl) in the fluid inclusion, thus contributing to the understanding of fluid composition.

On freezing, the Rossland Group Type III fluid inclusions show metastable supercooling and form ice at temperatures below -30°C. The first documented melting, characterized by a sudden clearing of crystals from the inclusion, ranges from -47.3 to -32.9°C for most deposit types (Figure A9-4a). A second and final melting, also characterized by clearing of crystals and often accompanied by a jerk of the vapour bubble, occurs between -23 and -3.5°C for most deposit types (Figure A9-4b). The crystalline substance is interpreted to be metastable hydrohalite ($NaCl.2H_2O$).

As for Type I fluid inclusions, the presence of low concentrations of Mg^{2+} ion or Ca^{2+} ion in some Type III fluid inclusions is suggested by pronounced first melting temperatures below -22.9°C and observed final ice and hydrate melting behaviour of $NaCl-MgCl-H_2O$ or $NaCl-CaCl_2-H_2O$ fluids from Davis *et al.* (1990). But similar to Type I inclusions, both extrapolations lack complementary observations of hydrate rim development, darkening of solids or nucleation of a vapour phase at lower temperatures. As in the case of Type I fluid inclusions, the Type III fluid is modeled overall as an NaCl brine.

TABLE A9-4
SALINITY (eq. wt. % NaCl) IN RELATION TO DEPOSIT TYPE

	Type I minimum	Type I maximum	Type III minimum	Type III maximum	Type IV minimum	Type IV maximum
Porphyry Cu	1.5	16.6	31.8	43.1	8.7	-
Porphyry Mo	6.7	12.7	-	-	0.8	-
Au Skarn	13.2	13.6	-	-	-	-
Polymetallic vein	1.3	17.8	31.1	-	-	-
Au Quartz vein	-	9.7	-	-	-	-
Intrusive-Related	4.4	20	37.1	40.7	4	-
Barren vein	1.3	12.4	-	-	-	18.5

Type I
aqueous
salt undersaturated
liquid rich
H_2O-NaCl (equivalent)

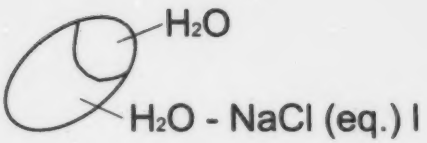

Type IIIA
salt saturated
Tmsalt < Thvapour
H_2O-NaCl (equivalent)

Type IIIB
salt saturated
Thvapour < Tmsalt
H_2O-NaCl (equivalent)

Type IV
aqueous
salt undersaturated
CO_2 bearing
H_2O-NaCl-CO_2 (equivalent)

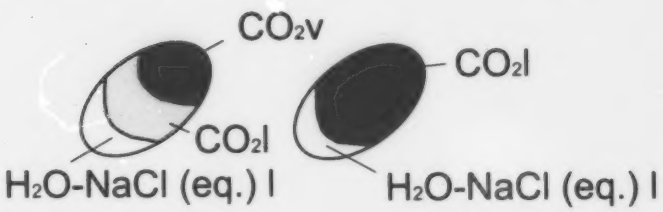

Type V
carbonic
$CO_2 \pm CH_4$ or N_2

Type VI
multiphase
solid
Thvapour < Tm solid (not observed)
H_2O-NaCl-unknown phases

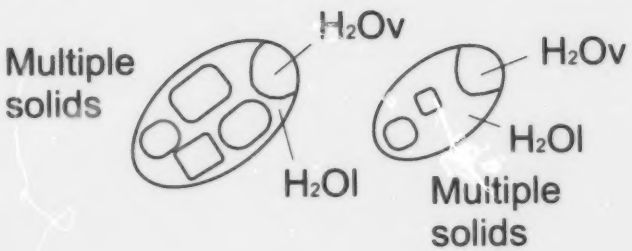

Type VII
multiphase
carbonic
H_2O-NaCl-CO_2-unknown phases

Figure A9-2. Sketches of six compositional types of fluid inclusions identified in quartz from mineral occurrences in the Rossland Group (modified from Nash, 1976).

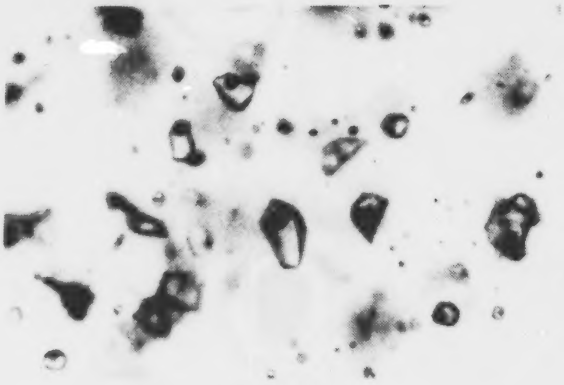

Photo A9-7a.

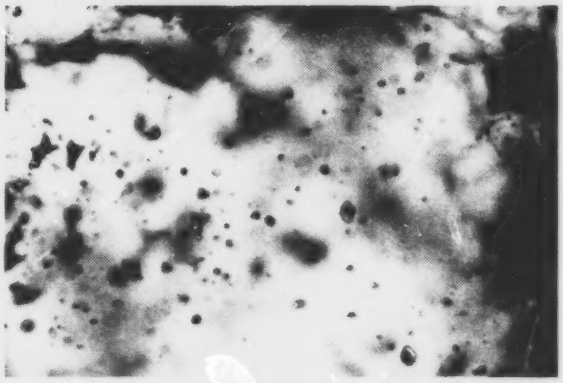

Pnoto A9-7b.

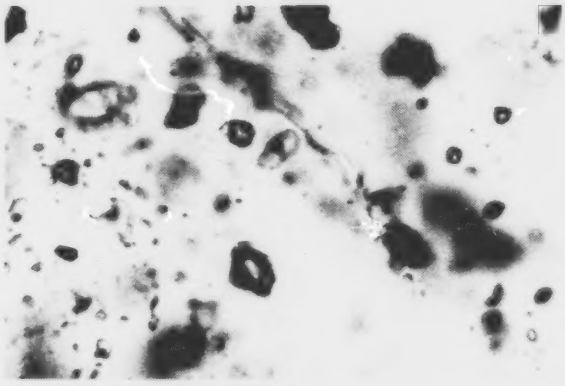

Photo A9-7c.

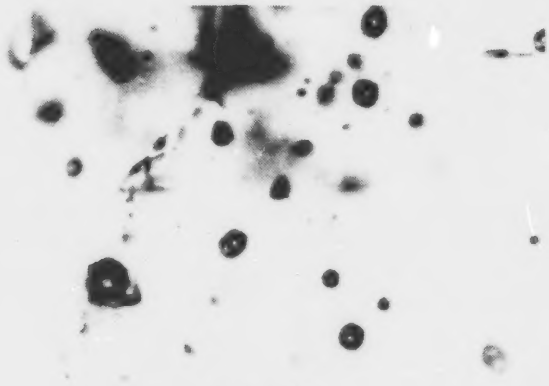

Photo A9-7d.

Photo A9-7f.

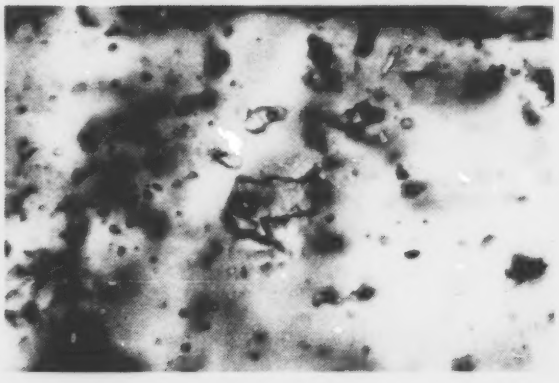

Photo A9-7e.

Photo A9-7. Composite plate with examples of type I, type IIIA, type IV, type V, type VI and type VII fluid inclusions at 20°C. A) Type I fluid inclusions, Cumberland shaft massive quartz vein. Transmitted plane light, 160X magnification, field of view = 0.3 mm. B) Type IIIA fluid inclusions, Homestake polymetallic vein (sample M1-123). Transmitted plane light, 160X magnification, field of view = 0.3 mm. C) Type IV fluid inclusions, War Eagle semi-massive pyrrhotite chalcopyrite vein (sample 96-31BA). Transmitted plane light, 160X magnification, field of view = 0.3 mm. D) type V fluid inclusions, Columbia-Kootenay deposit (Columbia portal massive arsenopyrite, quartz chalcopyrite vein). Transmitted plane light, 160X magnification, field of view = 0.3 mm. E) Type VI fluid inclusions, Columbia-Kootenay deposit (Columbia portal massive arsenopyrite, quartz chalcopyrite vein). Transmitted plane light, 160X magnification, field of view = 0.3 mm. F) Type VII fluid inclusion, War Eagle semi-massive pyrrhotite chalcopyrite vein (sample 96-31B). Transmitted plane light, 160X magnification, field of view = 0.3 mm.

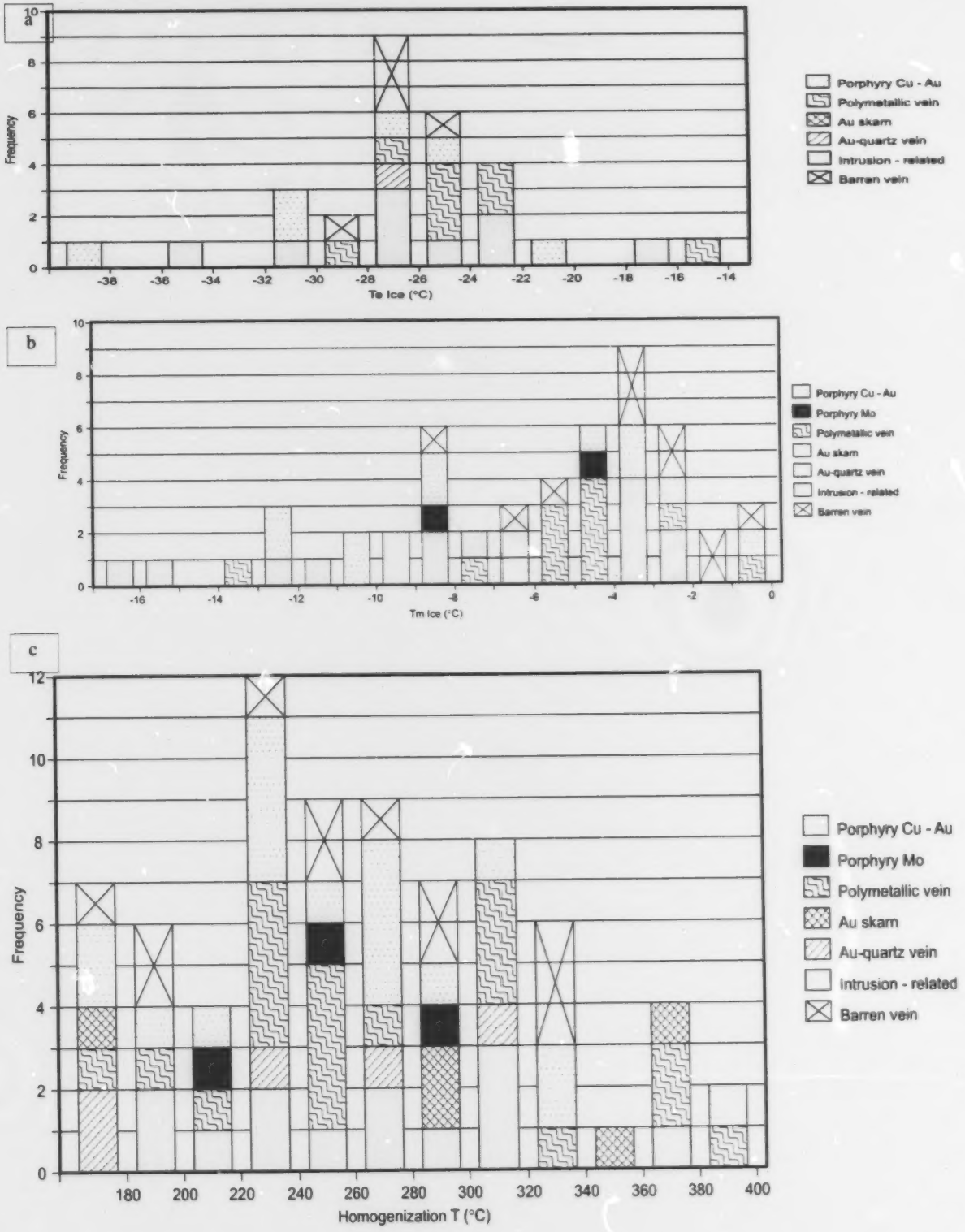

Figure A9-3a. Histograms of temperature data. Type I fluid inclusiions: a) first melting. b) last ice melting and c) homogenization.

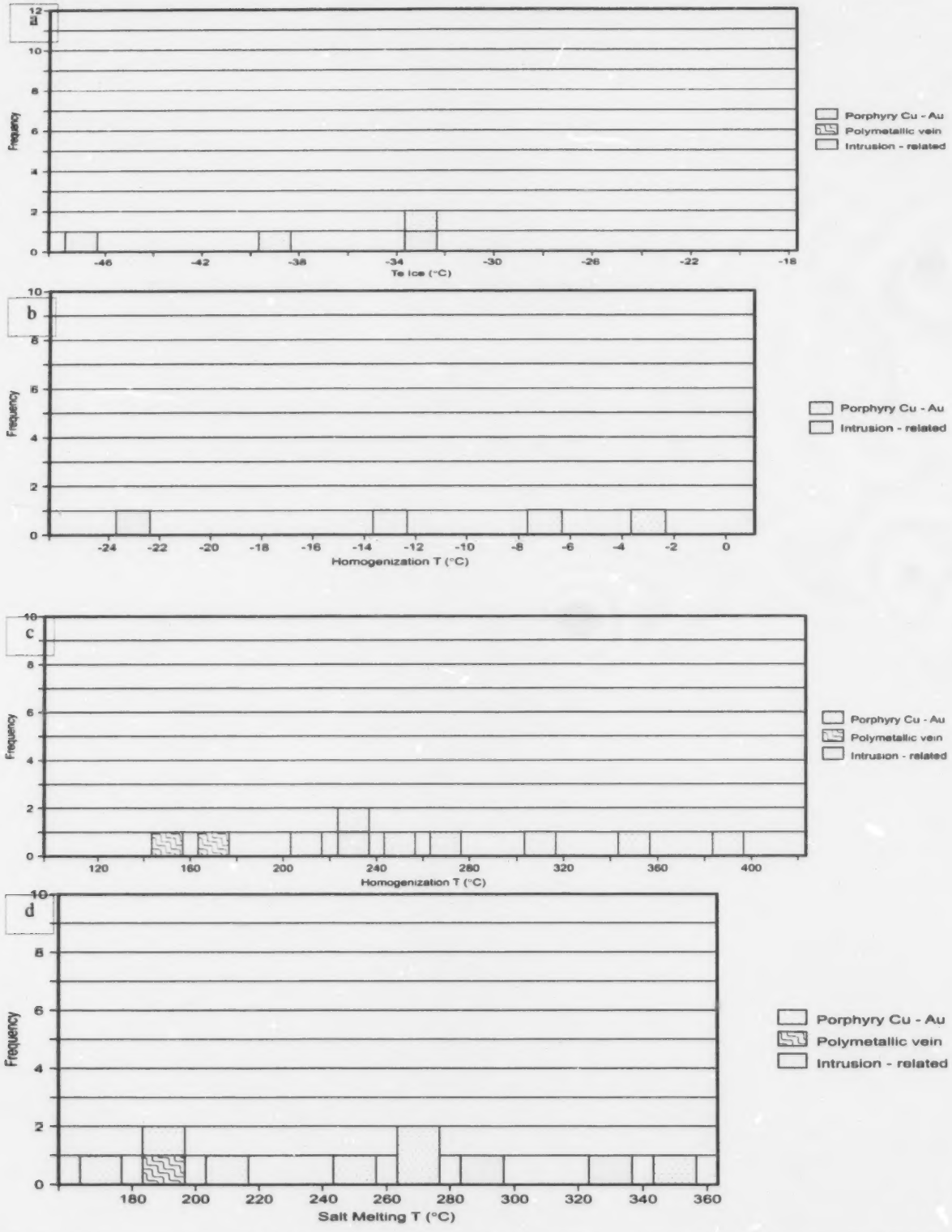

Figure A9-4. Histograms of temperature data, Type III fluid inclusions: a) first melting, b) last ice melting, c) homogenization and d) salt melting.

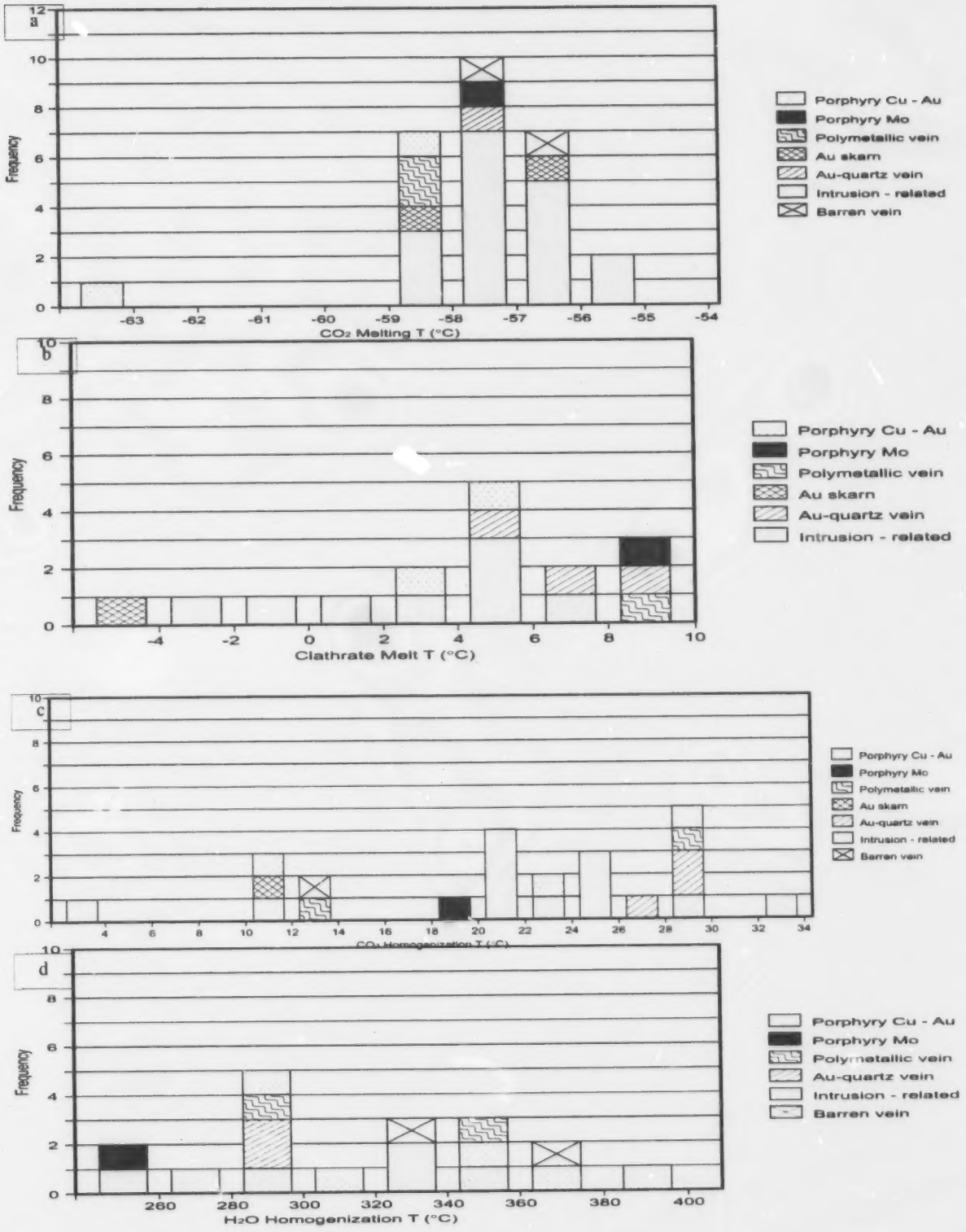

Figure A9-5. Histograms of temperature data, Type IV fluid inclusions: a) CO_2-melting, b) clathrate melting, c) homogenization of CO_2 liquid and vapour phases d) final homogenization.

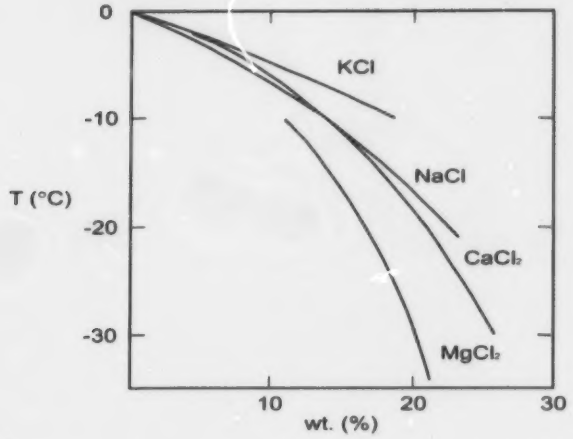

Figure A9-6. Freezing point depression of water for NaCl, KCl, CaCl2, and MgCl2 solutions (from Reynolds, 1991; modified from Crawford, 1981).

Salinities of Types III fluid inclusions (Figure A9-4c) were calculated using the H_2O-NaCl model composition and equations of Knight and Bodnar (1989) and are shown in Table A9-5. These vary from 30.0 to 31.9 equivalent weight percent (eq. wt. %) NaCl for Type IIIA inclusions, where the salt crystal melts prior to homogenization of the vapour bubble, and from 34.5 to 43.1 eq. wt.% NaCl for Type IIIB inclusions, where the salt crystal melts after homogenization of the vapour bubble. Variation in salinity range in relation to deposit type (Table A9-4) cannot be evaluated due to insufficient data.

Homogenization temperatures of salt-saturated inclusions in Rossland Group deposits range from 156°C to 382°C (Figure A9-4D). Salt-saturated (Type III) fluid inclusions occur mostly in porphyry Cu-Au and intrusion-related deposits.

TYPE IV: MIXED AQUEOUS AND CARBONIC

On cooling below 20°C, two-phase aqueous and CO_2 inclusions nucleate a vapour bubble within the CO_2 liquid phase of the inclusion. This bubble grows rapidly in size with further cooling as does the vapour bubble already present in three-phase aqueous and CO_2 inclusions on freezing. Between -90 and -100°C, Type VI inclusions exhibit metastable super cooling and crystallize CO_2 as a dark solid. With slow warming, CO_2 melting temperatures range from -58.5 to -56.6°C (Figure 5a). Only one inclusion exhibited suppressed CO_2 melting at -63.1°C and an inclusion melted above -56.6°C (probably due to a fast warming rate).

Clathration, formation of carbon dioxide hydrate ($CO_2.5.75H_2O$), was detected in most Type IV inclusions by noting a decrease in volume of the CO_2-bearing liquid phase during cooling. Clathrate melting temperatures, however, were only observed in less than half of the fluid inclusion assemblages since the clathrate crystals were difficult to detect in fluid inclusions smaller than 10 microns. Clathrate melting temperatures, dominantly from intrusion-related samples, are from -5.8 to 9.6°C (Figure A9-5b). Clathrate melting for most deposit types occurs above 2°C.

Documentation of CO_2 melting 2 degrees below the melting point of pure CO_2, indicates the presence of very small concentrations of CH_4 or possibly N_2. The occurrence of three-phase fluid inclusions and evidence for clathrate melting confirms the presence of a brine. Considering the almost negligible contribution of CH_4 or N_2 based on CO_2 melting temperatures near the melting point of pure CO_2, it is reasonable to model the Type IV fluid as a H_2O-CO_2-NaCl fluid. Salinities are therefore calculated based on clathrate melt temperatures rather than ice melt temperatures (used for H_2O-NaCl fluids) using the program FLINCOR. A compilation of salinities for Type IV inclusions is in Table A9-5. Salinities of fluid inclusions from intrusion-related deposits vary from 0.8 to 18.5 eq. wt. % NaCl.

On heating, the CO_2 liquid and vapour phases homogenize by vapour bubble disappearance over a range of 2.1 to 31.1°C (the critical point for pure CO_2) with most recorded temperatures between 18 and 30°C (Figure A9-5c). The CO_2 homogenization temperature is used to estimate the density of the homogeneous CO_2 phase and this measurement combined with optical measurements of volume percent CO_2 and aqueous phases yields an estimate of the overall CO_2 and H_2O concentration, expressed as mole percent, in the fluid (Table A9-6). Bulk inclusion mole percent CO_2 varies from 0.637 to 0.064 and mole percent H_2O from 0.918 to 0.355 (Table A9-6).

Homogenization temperatures of mixed aqueous and CO_2 inclusions in Rossland Group deposits range from 240 to 385°C (Figure A9-5d). Variation in homogenization temperature range in relation to deposit type is shown in Figure A9-5d. Porphyry Cu-Au, intrusion-related and polymetallic vein deposits have the highest homogenization temperatures.

TYPE V: CARBONIC

These inclusions consist of one or two CO_2-bearing phases at room temperature. The vapour phase of these fluid inclusions appears relatively dark in comparison to Type I or III fluid inclusions with volume % vapour ranging from 10 to 85% at CO_2 melting temperatures.

Two phase inclusions exhibit similar freezing behaviour to Type IV inclusions: crystallization of CO_2 at approximately -90 to -100°C and melting of CO_2 between -58.2 and -56.8°C (Table A9-3d). The presence of trace amounts of methane (CH_4) or nitrogen(N_2) is suggested by depression of the triple point for pure CO_2 by 1.6°C (Table A9-3e). Crushing tests of samples containing Type V fluid inclusions proved negative for dispersion of vapour bubbles in kerosene, indicating no CH_4. Considering the almost negligible contribution of CH_4 or N_2, it is reasonable to model the Type V fluid as a virtually pure CO_2 fluid.

Homogenization temperatures of CO_2 inclusions in Rossland Group deposits range from 10.8 to 30°C (Table A9-3d). Insufficient data precludes evaluation of homogenization temperature range in relation to deposit type.

TABLE A9-5
PAIRED SALINITY (eq. wt. % NaCl) AND HOMOGENIZATION TEMPERATURE (Th) DATA

Deposit Type	Deposit Name	Sample	FIA #	FI Type	Origin	Th H2O	Wt% NaCl (eq.)
Au Skarns	Second Relief	344-6B	2	I	S	161.7	13.2
Au Skarns	Second Relief	344-6B	3	I	S	281.3	13.6
Au-Quartz Veins	Gold Hill	Gold Hill	2	I	S	234	9.7
Barren Vein	Cumberland Shaft	139-4	4	I	S	186.2	4.9
Barren Vein	Giveout Creek Vein	51-9	1	I	S	296	2.8
Barren Vein	Giveout Creek Vein	51-9	2	I	S	325	12.4
Barren Vein	Highway Vein	20-1	6	I	S	172.6	10
Barren Vein	Marsh Creek Vein	165-13A	1	I	S	322.2	7.1
Barren Vein	Marsh Creek Vein	165-13A	2	I	S	246.2	3.8
Barren Vein	Marsh Creek Vein	165-13A	3	I	S	294.7	1.3
Intrusion-Related	Columbia	96-42B	1-2	I	S	316.5	16.6
Intrusion-Related	Columbia	96-42B	01-Feb	I	S	346.3	10.7
Intrusion-Related	Columbia	96-42B	02-Mar	I	S	287.6	12.5
Intrusion-Related	Columbia	Columbia	1	I	S	272	11.9
Intrusion-Related	Columbia	Columbia	5	I	S	302.9	5.9
Intrusion-Related	Consolidated St Elmo	96-51A	1-1	I	S	183.4	20
Intrusion-Related	Consolidated St Elmo	96-51A	3-2	I	S	102.3	6.4
Intrusion-Related	Consolidated St Elmo	96-51E	4-2	I	S	194.2	18.8
Intrusion-Related	Evening Star	Ev-Star	1	I	P	307.8	5.5
Intrusion-Related	Evening Star	Ev-Star	3	IV	P	351.5	18.5
Intrusion-Related	Evening Star	Ev-Star	5	IV	P	370	16.8
Intrusion-Related	Jumbo	96-28B	1-1	I	S	231.5	5.2
Intrusion-Related	Kootenay	96-39A	1-1	I	S	246.2	4.7
Intrusion-Related	Kootenay	96-39A	01-Mar	I	S	237.5	4.4
Intrusion-Related	War Eagle	96-31B	4-1	I	S	208.4	15.3
Intrusion-Related	War Eagle	96-71A	1-1	IIIB	S	156	37.1
Intrusion-Related	War Eagle	96-71A	2-3	IIIB	S	170	40.7
Intrusion-Related	War Eagle	96-71A	02-Feb	IV	S	341.6	4
Intrusion-Related	War Eagle	96-71A	01-Mar	IV	S	243.2	10.2
Polymetallic Veins	Ace in the Hole	206-16	1	I	S	240	8.2

TABLE A9-5 CONTINUED

Deposit Type	Deposit Name	Sample	FIA #	FI Type	Origin	Th H2O	Wt% NaCl (eq.)
Polymetallic Veins	Ace in the Hole	206-16	4	I	S	237	14.2
Polymetallic Veins	Bluebird	M3-145	1	I	S	245	17.8
Polymetallic Veins	Bluebird	M3-145	3	I	P	300	7.8
Polymetallic Veins	Euphrates	17-3	1	I	S	320.2	6.5
Polymetallic Veins	Homestake	MI-123	2	I	S	262	7.5
Polymetallic Veins	Homestake	MI-123	2	IIIA	S	255	31.1
Polymetallic Veins	Keystone	MI-202	1	I	S	372.2	1.3
Polymetallic Veins	Lily May	MI-153	1	I	P	392.5	11.7
Polymetallic Veins	Rozan	Rozan	3	I	S	160.8	9.1
Polymetallic Veins	Rozan	Rozan	4	I	S	228.2	8.1
Porphyry Cu-Au	Great Western	78-2B	1	IIIB	S	224	34.5
Porphyry Cu-Au	Great Western	78-2B	3	IIIB	S	206	36.3
Porphyry Cu-Au	Great Western	78-2B	3	IIIA	S	382	30
Porphyry Cu-Au	Great Western	78-2B	4	IIIA	S	305	31.9
Porphyry Cu-Au	Katie	DDH39-93	1	I	S	239	6.4
Porphyry Cu-Au	Katie	DDH39-93	2	I	S	163	6.2
Porphyry Cu-Au	Katie	DDH53-65	1	I	S	238	14.5
Porphyry Cu-Au	Katie	DDH53-65	2	I	S	270	1.5
Porphyry Cu-Au	Katie	DH53-118	1	IIIB	S	238	35.4
Porphyry Cu-Au	Katie	DH53-118	1	I	S	265	4.2
Porphyry Cu-Au	Katie	DH53-118	2	I	S	170	16.6
Porphyry Cu-Au	Katie	DH53-118	3	I	S	260	16.4
Porphyry Cu-Au	Katie	DH53-118	4	I	S	236	11.9
Porphyry Cu-Au	Katie	DH53-118	4	IIIA	S	262	31.8
Porphyry Cu-Au	Katie	DH54-193	1	I	S	188	6.7
Porphyry Cu-Au	Katie	DH54-193	2	I	S	227	11.9
Porphyry Cu-Au	Katie	DH54-197	3	I	S	261.8	14.3
Porphyry Cu-Au	Star	Star	1	IIIB	S	350.1	43.1
Porphyry Cu-Au	Star	Star	3	IV	S	361.2	8.7
Porphyry Mo	Bobbi	44-10	2	I	S	217.6	12.7
Porphyry Mo	Stewart	Stewart	1	IV	S	240	0.8
Porphyry Mo	Stewart	Stewart	2	I	S	287.7	6.7

TABLE A9-6
FLUID INCLUSION COMPOSITION DATA: TYPE IV FLUID INCLUSIONS

Deposit Type	Deposit Name	Sample	FIA #	FI Type	Origin	wt% NaCl (eq.)	XNaCl	XH2O	XCO2
AU-QUARTZ VEINS	Gold Hill	Gold Hill	2	IV	S	6.3	0.019	0.918	0.064
Intrusion-Related	Consolidated St Elmo	96-51A	3-1	IV	S	8.1	0.025	0.907	0.068
Intrusion-Related	Evening Star	Ev-Star	2	IV	P	15.2	0.044	0.794	0.163
Intrusion-Related	Evening Star	Ev-Star	3	IV	P	18.5	0.025	0.625	0.35
Intrusion-Related	Evening Star	Ev-Star	5	IV	P	16.8	0.04	0.642	0.318
Intrusion-Related	Kootenay	96-39A	3-1	IV	S	10.6	0.019	0.526	0.455
Intrusion-Related	Kootenay	96-39A	4-1	IV	S	7.9	0.01	0.387	0.603
Intrusion-Related	War Eagle	96-71A	2-1	IV	S	6.1	0.007	0.355	0.637
Intrusion-Related	War Eagle	96-71A	2-4	IV	S	4	0.006	0.44	0.555
Porphyry CU-AU	Star	Star	3	IV	S	8.7	0.014	0.475	0.511
Porphyry MO	Stewart	Stewart	1	IV	S	0.8	0.001	0.434	0.565

TYPE VI: MULTIPHASE

Type VI fluid inclusions contain at least one to five solid phases (possibly salts?, carbonate?, unknowns and rare opaque minerals) in addition to aqueous liquid and vapour phases. Behaviour on cooling of type VI inclusions is similar to Type III (salt-saturated) inclusions: eutectic? Or metastable hydrate melting is observed from -43.2 to -19°C (Table A9-3e) but is typically observed between -21 and -30°C. Last melting ranges from -24.2 to -0.1°C but is typically observed at temperatures greater than -16°C. These melting observations indicate the addition of small concentrations of ions such as Ca2+ or Mg2+ to an H_2O-NaCl fluid.

Homogenization temperatures of multiphase fluid inclusions range from 116.2 to 310°C (Table A9-3e). Salinity of Type VI fluid inclusions cannot be estimated since the solid phases do not dissolve prior to decrepitation of the fluid inclusions at temperatures between 184 and 444°C. The abundance of apparent "salts" would indicate salinities typically > 30 eq. wt. % NaCl.

Given the high probability of contained solid salt phases in Type VI inclusions, the absence of melting prior to decrepitation of the inclusion is unusual. Roedder (1984) suggested that the lack of dissolution of solid salt phases may be the result of sluggish kinetics (heating rate too fast), necking down (recrystallization), H_2 leakage (by diffusion) or the trapping of **accidental** solid inclusions (not part of the original fluid). We would argue that the large numbers of Type VII fluid inclusions examined in each fluid inclusion assemblage would negate the possibility of accidental trapping of solid daughter minerals. Also, we suggest that the relatively similar ratios of liquid to vapour and the close proportions of solid phases in most of the Type VII fluid inclusion assemblages are an indication that the fluid inclusions have not necked down. Roedder (1984) implied that sluggish kinetics are an unlikely explanation for failure of daughter minerals to dissolve since many long, slow heating experiments have been conducted without achieving dissolution to test this hypothesis. The lack of dissolution of most daughter minerals in Type VII fluid inclusions in Rossland Group deposits may be attributed to small amounts of H_2 leakage, not visible as the intersection of a fluid inclusion assemblage by a microfracture but perhaps by the intersection of a dislocation. We believe that either there are no soluble salt phases present in the Type VI inclusions, or, more likely, the pressure in Type VII fluid inclusions increases with heating to values >2 kbars which results in decrepitation of the fluid inclusions (Bodnar and Vityk, 1994) prior to the onset of solid phase dissolution. Evidence for very high pressures in Type IIIB fluid inclusions is below in the section on geobarometry estimates.

Multiphase fluid inclusions occur mostly in intrusion-related gold vein deposits and rarely in porphyry and polymetallic vein deposits. Elsewhere, this type of inclusion is commonly found in pegmatites which are characteristic of deep environments (Reynolds, 1991).

TYPE VII: MULTIPHASE AND CARBONIC

Type VII fluid inclusions contain multiple solid phases (possibly salts?, carbonate?, unknowns and rare opaque minerals) in addition to CO_2-bearing liquid and vapour phases. Behaviour on cooling of Type VII inclusions is sim-

ilar to Type IV inclusions: CO_2 melting is observed between -56.8 and -58°C, clathrate melting rarely observed and homogenization of CO_2 liquid and vapour phases occurs between 14.8 and 27.9°C. Behaviour on heating of Type VII inclusions is also similar to Type IV inclusions with final H_2O-NaCl-CO_2 homogenization temperatures above 200°C (Table A9-3e). In all cases, the solid phases do not dissolve prior to decrepitation of the fluid inclusion between 250°C and 400°C.

Type VII inclusions are rarely documented in fluid inclusion literature. As a result, virtually no experimental data has been undertaken to enable quantitative calculation of composition and pressure/temperature relations. Recent work by McCoy *et al.* (1997) includes description of similar inclusions associated with intrusion-related gold systems.

We have modelled the Type VII fluid as NaCl-H_2O-CO_2 fluid since fluid inclusions probably contain salts and definitely exhibit melting behaviour which indicates presence of CO_2. As a guess, the salinity of Type VII fluid inclusions may be > 30 eq. wt.% NaCl and probably >60 eq. wt. % NaCl given probable salt abundance.

GEOBAROMETRY ESTIMATES

Two methods are used to approximate the temperature of trapping (Tt) and pressure of trapping (Pt) or minimum Tt and Pt from the fluid inclusions studied. The first method requires Th and Ts data from Type IIIB inclusions where dissolution of halite occurs after homogenization of liquid and vapour phases. This method yields a minimum pressure of trapping at the halite dissolution temperature. The second method requires three-phase Type IV inclusions and also yields a minimum pressure of trapping at the homogenization temperature of CO_2 and H_2O-NaCl liquids. Stratigraphic depth is calculated for deposits in the Nelson area. Lithostatic pressure calculated from estimates of stratigraphic depth provides an independent comparison to the two methods used above.

The first method uses Type IIIB inclusions which exhibit salt dissolution after liquid-vapour homogenization. The minimum trapping pressure is defined using the salt melt temperature point along the liquidus calculated from the homogenization of liquid and vapour phases. Calculated minimum pressures using isochores predicted by equations of Brown and Lamb (1989) vary from 2443 to 2872 bars for intrusion-related deposits and from 292 to 1412 for porphyry Cu-Au deposits (Table A9-7).

The second method uses mixed three-phase Type IV inclusions with recorded homogenization temperatures of CO_2 liquid and vapour as well as final homogenization of CO_2 liquid and H_2O liquid phases. Calculated minimum pressures range from 1529 to 2273 bars for intrusion-related deposits, 1262 bars for polymetallic vein deposits, 1084 for porphyry Mo deposits and 1330 for porphyry Cu-Au deposits (Table A9-7) using the program FLINCOR and the equations of Bowers and Helgeson (1983). Unfortunately final homogenization temperatures are not abundant for three phase Type IV fluid inclusions (Table A9-3c). Many of these inclusions decrepitate prior to final homogenization. Roedder (1984, p. 280) suggests that the high internal pressure developed during homogenization of many CO2-H2O inclusions is the reason that decrepitation is common before homogenization is reached.

Stratigraphic depth provides an independent comparison of pressure of formation of the Star and Gold Hill deposits in the Nelson area. These deposits are both hosted by lower Elise Formation augite porphyry flows and flow breccias adjacent to the Eagle Creek pluton. The thickness of the upper Elise Formation in the area of these deposits is at least 2 kilometres (Höy and Andrew, 1989a, Fig. 1-4-2a). The Elise Formation is overlain by 1150 metres of the Hall Formation in Hall Creek to the southwest (Andrew *et al.*, 1991). Total minimum thickness of strata overlying the lower Elise Formation in the area is about 3.15 kilometres. Based on this depth, the lithostatic pressure acting on the deposits is estimated as 834 bars. This calculated lithostatic pressure falls within the range of minimum pressures estimated for the Star deposit using methods 1 (292 bars) and 2 (1330 bars).

SUMMARY

Geobarometry estimates from fluid inclusion data and stratigraphic depth provide a range of pressure data for the evaluation of the environment of deposition of intrusion-related Au-pyrrhotite veins, polymetallic veins and porphyry deposits (Table A9-7). These estimates also place limits on the depth of emplacement of the Rossland, Katie, Silver King plutons and Eagle Creek Complex.

Minimum pressures of formation of three intrusion-related Au-pyrrhotite vein deposits related to the Rossland pluton estimated using the methods above range from 1529 to 2872 bars (Table A9-7). Assuming lithostatic load, this corresponds to minimum depths of emplacement of between about 5.8 and 10.8 kilometres. The occurrence in the veins of abundant readily observable CO_2-bearing fluid inclusions, typically found in deep environments proximal to batholiths, is additional evidence that corroborates a deep setting for the intrusion-related deposits related to the Rossland monzonite. As well, the wispy quartz texture noted in early quartz from the War Eagle and Le Roi deposit samples is characteristic for deep vein environments (> 4 to 8 km) related to batholiths (Reynolds, 1991). The presence of Type III fluid inclusions with homogenization temperatures < 220°C and salinities < 35 eq. wt. % NaCl are also common in deep environments of deposition (Reynolds, 1991). The abundance of Type VII fluid inclusions is common in pegmatites at these depths. The failure of these Type VI inclusions to exhibit salt melting prior to decrepitation may be further confirming evidence of a very high pressure/depth environment of formation for these veins.

The Homestake polymetallic vein deposit, located at the southern margin of the Rossland Pluton, formed under a pressure of 1262 bars using method 2 above. The depth of emplacement of this deposit, assuming lithostatic load, is 4.8 km.

Porphyry Cu-Au deposits related to the Eagle Creek Complex, Silver King pluton and Katie pluton formed at minimum pressures of formation between 292 to 1412 bars

TABLE A9-7
ESTIMATES OF MINIMUM PRESSURE OF TRAPPING USING:
METHOD 1: SALT DISSOLUTION AFTER LIQUID-VAPOUR HOMOGENIZATION (TYPE IIIB INCLUSIONS),
AND METHOD 2: THREE-PHASE, MIXED AQUEOUS AND CO2-BEARING INCLUSIONS (TYPE IV)

Deposit Type	Deposit Name	Sample	FIA #	FI Type	Origin	Vol% vap.	Th CO2	Th H2O
Intrusion-Related	Evening Star	Ev-Star	3	IV	P	85	25	351.5
Intrusion-Related	Evening Star	Ev-Star	5	IV	P	60	21.9	370
Intrusion-Related	War Eagle	96-71A	1-1	IIIB	S	10		156
Intrusion-Related	War Eagle	96-71A	2-3	IIIB	S	10		170
Intrusion-Related	War Eagle	96-71A	2-4	IV	S	80	21.6	341.6
Polymetallic Veins	Homestake	MI-123	1	IV	S	50	28.5	300.8
Porphyry Cu-Au	Great Western	78-2B	1	IIIB	S	10		224
Porphyry Cu-Au	Great Western	78-2B	3	IIIB	S	5		206
Porphyry Cu-Au	Katie	DH53-118	1	IIIB	S	5		238
Porphyry Cu-Au	Star	Star	1	IIIB	S	15		350.1
Porphyry Cu-Au	Star	Star	3	IV	S	80	28.9	361.2
Porphyry Mo	Stewart	Stewart	1	IV	S	80	18.8	240
Intrusion-Related	Evening Star	Ev-Star			18.5		1529	
Intrusion-Related	Evening Star	Ev-Star			16.8		2273	
Intrusion-Related	War Eagle	96-71A	285.5		37.1	2443		
Intrusion-Related	War Eagle	96-71A	331		40.7	2872		
Intrusion-Related	War Eagle	96-71A			4		1629	
Deposit Type	**Deposit Name**	**Sample**	**FIA #**	**FI Type**	**Origin**	**Vol% vap.**	**Th CO2**	**Th H2O**
Polymetallic Veins	Homestake	MI-123			1		1262	
Polymetallic Veins	Lily May	MI-153		475	11.7			750
Porphyry Cu-Au	Great Western	78-2B	246.5		34.5	447		
Porphyry Cu-Au	Great Western	78-2B	275		36.3	1412		
Porphyry Cu-Au	Katie	DH53-118	261		35.4	468		
Porphyry Cu-Au	Star	Star	357.9		43.1	292		
Porphyry Cu-Au	Star	Star			8.7		1330	
Porphyry Mo	Stewart	Stewart			0.8		1084	

(Table A9-7) using methods 1 and 2 above. This corresponds to minimum depths of emplacement of between about 1.1 and 5.3 kilometres assuming lithostatic load. These calculated depths of emplacement are within the typical range for porphyry copper deposits (Bodnar, 1995; Sillitoe, 1995). Insufficient numbers of calculated pressure/depth estimates preclude specific breakdown of depth ranges for the three plutons related to alkalic porphyry Cu-Au deposits in this study.

The Stewart porphyry Mo deposit, located near a Middle Jurassic stock (Höy and Andrew, 1989b), formed at a minimum pressure of approximately 1084 bars using method 2 above. The possible depth of emplacement of this deposit, assuming lithostatic load, is 4 km which is within the range expected for porphyry Mo deposits (Sillitoe, 1995). This deposit is the only recorded porphyry Mo deposit with estimated pressures of formation.

To summarize, the Rossland monzonite is believed to have been emplaced at depths up to 11 kilometres based on calculated pressures of formation under lithostatic load of intrusion-related Au-pyrrhotite veins and polymetallic veins and corroborating petrographic evidence. Porphyry Cu-Au deposits and their associated plutons, the Eagle Creek Complex, Silver King pluton and Katie pluton, formed at minimum depths between 1 and 5 kilometres which is similar to typical emplacement depths of calc-alkaline porphyry deposits. Insufficient data precludes evaluation of the overall pressures and depths of formation of polymetallic and porphyry Mo deposits and their associated plutons.

FLUID IMMISCIBILITY

The occurrence of fluid inclusion assemblages with combinations of CO_2-bearing, mixed aqueous-CO_2, mixed salt-saturated CO_2, salt-saturated and aqueous fluid inclusions strongly suggests close genetic relationships among these fluids. The hypothesis of fluid immiscibility is evaluated for fluid inclusion assemblages containing combinations of Types I, IV, and V inclusions as well as for assemblages containing Types IV, V and III inclusions and Type VII, IV and III inclusions.

Heterogeneous trapping, entrapment of two fluids in the same inclusion, is good evidence for fluid immiscibility providing leakage or necking-down has not occurred. Mixed Types V and I inclusions might produce heterogeneous entrapment of a Type IV inclusion as documented by Robert and Kelly (1987) and mixed Types V and III inclusions might produce heterogeneous entrapment of a Type IV inclusion as documented by Bowers and Helgeson (1983a). It is unclear what phases could mix to produce a Type VII inclusion but we would speculate Types V and III inclusions or even Types IV and III inclusions. Criteria for heterogeneous trapping include: simultaneous trapping of all the inclusions of the population of interest and very scattered degree of filling and compositions (Ramboz *et al.*, 1982).

Fluid inclusion assemblages with Type IV, mixed aqueous and carbonic, and Type VII, mixed multiphase and carbonic fluid inclusions are evidence for heterogeneous trapping of a CO_2-bearing fluid and both low and high salinity aqueous fluids in Rossland Group deposits (Tables A9-3c and 3d). Type IV inclusions occur in all deposit types. Fluid inclusion assemblages with multiple Type IV inclusions satisfy criteria for heterogeneous trapping since they trap inclusions with varying degrees of fill of CO_2 and therefore composition. Type VII inclusions are rare; these inclusions are limited to deposits related to the Rossland pluton. They occur in isolation or trapped in with Type III inclusions in varying degrees of fill. Insufficient data for Type VII inclusions preclude evaluation of homogenization temperature scatter.

Evidence for fluid unmixing, the coexistence in the same rock of two different types of inclusions that correspond to two immiscible phases, is more stringent (Ramboz *et al.*, 1982). First, good evidence for contemporaneous trapping is must be confirmed (*i.e.*, both immiscible phases in the same fluid inclusion assemblage). Second, one inclusion must homogenize to the liquid and the other to the vapour phase within the same temperature range. Third, decrepitation temperatures and behaviour of both types of inclusion should be similar.

Several fluid inclusion assemblages in the Rossland Group comprise fluid inclusions that might represent two separate immiscible phases. However, further detailed work, as outlined above, is required to confirm any hypothesis of fluid unmixing. The possible immiscible phase "pairs" trapped together in fluid inclusion assemblages are as follows: 1) coexisting liquid and vapour-rich Type IV fluid inclusions at the Gold Hill deposit which homogenize within 20°C of each other and 2) coexisting type I, III, V and VI fluid inclusions at the Homestake deposit which homogenize within 15°C of each other. Immiscible entrapment of H_2O-CO_2 phases is therefore indicated at the Gold Hill deposit and possible vapour-brine partitioning at the Homestake deposit. Unfortunately, homogenization of Type IIIB inclusions at the War Eagle deposit by halite dissolution precludes immiscible entrapment although Types III and IV fluid inclusions coexist in fluid inclusion assemblages. Additional fluid inclusion analyses for the War Eagle may yield data on coexisting Type IIIA and IV fluid inclusions.

RELATIONSHIPS OF FLUID INCLUSIONS TO DEPOSIT TYPE AND ORIGIN

ENVIRONMENT OF DEPOSITION OF DEPOSITS

The range of salinity and homogenization temperature compiled from the literature from fluids in different ore deposit environments is indicated in Figure A9-7 (modified from Reynolds, 1991 and Lattanzi, 1991). Calculated salinities and homogenization temperatures for deposit types in the Rossland Group (Table A9-5) are plotted on Figure A9-7 for comparison. Results of this comparison are discussed below.

PORPHYRY MO

Two samples from the Stewart porphyry Mo deposit fall within the lower range of porphyry deposits defined on FigureA9-7. One sample from the Bobbi deposit falls above the lower "porphyry box" on Figure A9-7 but within the range of homogenization temperatures for porphyry deposits.

PORPHYRY CU-AU: ALKALIC

The fields for porphyry Cu-Au deposits are not defined on Figure A9-7. Virtually no fluid inclusion data is reported on this deposit type partially because of the paucity of usable quartz for fluid inclusion samples in most alkalic porphyry systems. Fluid inclusion data from the Katie, Great Western and Star deposits have been collected from mineralized quartz veinlets and are used in this study to define initial ranges for alkalic porphyry Cu-Au deposits on Figure A9-7. The alkalic porphyry Cu-Au data are defined by two boxes with dashed lines: a lower range from 0 to 17 eq. wt. NaCl and 150 to 400°C and an upper range of approximately 30 to 44 eq. wt. % NaCl and 175 to 400°C. Although the regions of the graph defined by the alkalic boxes are different to those for calc-alkalic systems, evidence for both low and high salinity fluids in both alkalic and calc-alkalic systems is irrefutable.

POLYMETALLIC VEINS: AG-PB-ZN-±AU

Fluid inclusion data from seven polymetallic veins encompasses a wide range in salinity and homogenization temperature (Figure A9-7). The veins are best defined as moderate salinity (7-18 eq. wt. % NaCl) and low-moderate temperature (150-400°C) veins with the exception of one high salinity data point from the Homestake deposit and one low salinity point from the Keystone deposit. It should be noted that the only Type III fluid inclusions documented for polymetallic veins are from samples peripheral to the Rossland pluton.

INTRUSION-RELATED AU-PYRRHOTITE VEINS

Intrusion-related Au-pyrrhotite veins have moderate and high salinity ranges (4-20 eq. wt. % NaCl and 37-41 eq. wt. % NaCl) and low to moderate homogenization temperatures (150-400°C) as defined on Figure A9-7. The complete range of high salinities for this deposit type is probably not reflected in Figure A9-7 due to the absence of calculated salinities for Type VI and VII inclusions as discussed above.

AU SKARNS

One sample from the Second Relief Au skarn deposit falls within the lower range of skarn deposits as defined on Figure A9-7. The sample possibly represents a "retrograde" skarn fluid.

AU-QUARTZ VEINS

One sample from the Gold hill deposit falls within the area defined as a mesothermal vein environment on Figure A9-7. Although this is the only sample with both recorded homogenization temperature and salinity, the ranges of recorded homogenization temperatures and salinities for Au-quartz deposits, 170 to 305°C and 6.2 to 9.7 eq. wt. % NaCl (Tables A9- 3a and 3c) also fall within the area defined as a mesothermal vein environment.

BARREN VEINS

Samples from "barren" veins, sampled from unmineralized roadcuts, have a broad range of salinities and homogenization temperatures that encompass the epithermal, mesothermal and low-salinity porphyry environments. Although they cannot be distinguished from mineralized samples on the basis of fluid inclusion composition and temperature alone, it is interesting to note that none of the four samples investigated contain high salinity Type III fluid inclusions.

SUMMARY

There are several important conclusions to this evaluation of environments of deposition of deposit types examined in this study:

1. This is the first study that defines the alkalic porphyry Cu-Au environment based on homogenization temperature and salinity ranges of fluid inclusions in quartz from a number of deposits. Figure A9-7 shows evidence for both low and high salinity fluids in alkalic porphyry systems which is similar to that seen in calc-alkalic systems. However, the regions of the graph defined by the alkalic boxes are different to those for calc-alkalic systems (Figure A9-7).
2. Deposits described as Au-skarn, Mo porphyry and Au-quartz vein fall within the defined fields for skarn, porphyry and mesothermal vein on Figure A9-7.
3. Intrusion-related Au-pyrrhotite veins comprise both low and high salinity fluids, similar to intrusion-related gold vein deposits elsewhere (FigureA9- 7).
4. Polymetallic veins are generally of moderate salinity and low to moderate temperature with the exception of veins associated with the Rossland pluton.
5. Unmineralized or "barren" veins generally cannot be distinguished from mineralized veins on the basis of fluid inclusion composition, temperature or composition.

ASSOCIATED INTRUSIONS

One of the objectives of this study was to evaluate variation in fluid characteristics of deposits associated with Early Jurassic, Early-Middle Jurassic, Middle Jurassic and Middle Cretaceous intrusions in the Rossland Group. The location of each deposit in this study has been evaluated with respect to a potential related intrusion (Table A9-1). In some cases where deposits are proximal to more than one intrusion, such as at the Great Western deposit, the nearest intrusion is selected. Fluid characteristics of deposits associated with each intrusion are listed in Table A9-8 and described below.

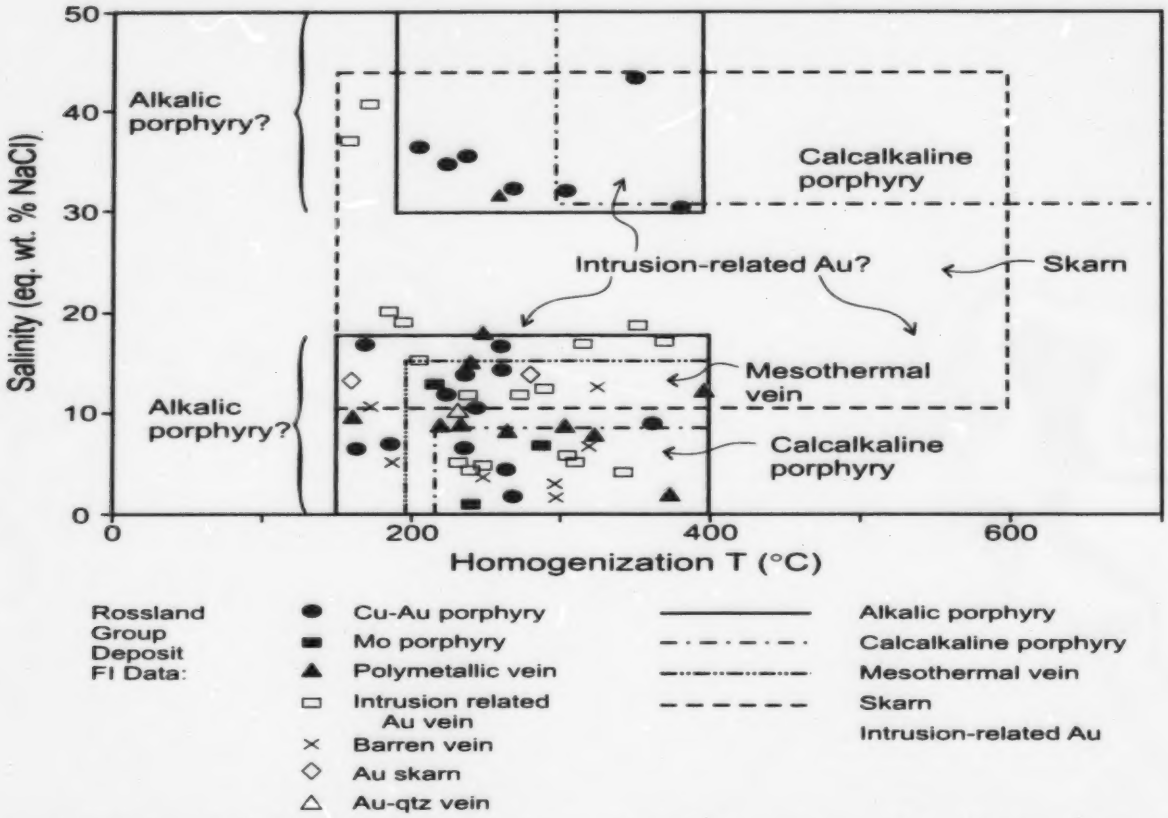

Figure A9-7. Comparison of range of salinity and homogenization temperature of Rossland Group deposits to fluids in different ore deposit environments (modified from Reynolds, 1991 and Lattanzi, 1991).

EARLY(?) JURASSIC: EAGLE CREEK COMPLEX AND KATIE STOCK

Deposit types associated with Early(?) Jurassic intrusions that have been evaluated on the basis of fluid inclusions include porphyry Cu-Au, Au-quartz veins and barren veins.

The porphyry Cu-Au deposits are characterized dominantly by Type I aqueous and Type III salt-saturated fluid inclusions. Type IV mixed aqueous and Type V carbonic fluid inclusions are rarely observed. Porphyry Cu-Au deposits associated with the Eagle Creek Complex and Katie stock are estimated to have formed at minimum depths of between 1 and 5 kilometres. The Star deposit, associated with the Eagle Creek Complex, has evidence for heterogeneous entrapment.

Types I, IV and V aqueous and carbonic fluid inclusions are documented in Au-quartz veins associated with the Eagle Creek Complex. Evidence for heterogeneous entrapment of Type IV fluid inclusions is noted at the Gold Hill deposit (*see* above).

EARLY-MIDDLE JURASSIC: SILVER KING PLUTON

Porphyry Cu-Au, polymetallic veins and barren veins are evaluated from deposits associated with the Silver King pluton. Similar to Eagle Creek complex, porphyry Cu-Au deposits are characterized dominantly by Type I aqueous and Type III salt-saturated fluid inclusions with Type IV mixed aqueous and carbonic, Type V carbonic and Type VII mixed multiphase and carbonic inclusions only rarely observed. Polymetallic and barren veins are characterized only by Type I aqueous fluids. The Great Western porphyry Cu-Au deposit is estimated to have formed at depths within 1 and 5 kilometres. No evidence of heterogeneous entrapment or fluid immiscibility is recognized with deposits associated with this pluton.

MIDDLE JURASSIC INTRUSIONS: ROSSLAND PLUTON, BONNINGTON BATHOLITH, NELSON BATHOLITH

Polymetallic, intrusion-related and barren veins as well as Au skarns and porphyry Mo deposits associated with Middle Jurassic intrusions are evaluated. Polymetallic and barren veins, Au skarns and Mo porphyries are dominated by both Type I aqueous and Type IV mixed aqueous and car-

TABLE A9-8
FLUID CHARACTERISTICS OF DEPOSITS ASSOCIATED WITH THE EARLY JURASSIC EAGLE CREEK COMPLEX AND KATIE STOCK, THE EARLY-MIDDLE JURASSIC SILVER KING PLUTON, THE MIDDLE JURASSIC ROSSLAND GROUP, BONNINGTON PLUTON AND NELSON BATHOLITH AND THE MIDDLE CRETACEOUS HIDDEN AND WALLACK CREEK STOCKS

Est. Intrusion Age	Related Intrusion	Area/Belt	Deposit Type	Deposit Name	Sample #	Type I	Type III	Type IV	Type V	Type VI	Type VII
Early Jurassic	Eagle Creek Complex	Morning Mtn	Porphyry Cu-Au: Alkalic	Star	Star	Y	Y	Y			
Early Jurassic	Eagle Creek Complex	Morning Mtn	Barren Vein	Cumberland Shaft	139-4	Y					
Early Jurassic	Eagle Creek Complex	Giveout Ck	Au-Quartz Veins	Athabasca	85-15C	Y					
Early Jurassic	Eagle Creek Complex	Fortynine Ck	Au-Quartz Veins	Gold Hill	Gold Hill	Y		Y			
Early Jurassic	Katie Stock	Hellroaring Creek	Porphyry Cu-Au: Alkalic	Katie	DDH39-93	Y				Y	
Early Jurassic	Katie Stock	Hellroaring Creek	Porphyry Cu-Au: Alkalic	Katie	DDH53-45					Y	
Early Jurassic	Katie Stock	Hellroaring Creek	Porphyry Cu-Au: Alkalic	Katie	DH53-65	Y				Y	
Early Jurassic	Katie Stock	Hellroaring Creek	Porphyry Cu-Au: Alkalic	Katie	DH53-118	Y	Y			Y	
Early Jurassic	Katie Stock	Hellroaring Creek	Porphyry Cu-Au: Alkalic	Katie	DH54-193	Y					
Early Jurassic	Katie Stock	Hellroaring Creek	Porphyry Cu-Au: Alkalic	Katie	DDH54-197	Y		Y	Y	Y	
Early-Middle Jurassic	Silver King Pluton	Giveout Ck	Porphyry Cu-Au: Alkalic	Great Western	78-2B	Y	Y			Y	
Early-Middle Jurassic	Silver King Pluton	Gold Ck	Porphyry Cu-Au: Alkalic	Shaft	79-12	Y		Y			
Early-Middle Jurassic	Silver King Pluton	Clearwater Ck	Polymetallic Veins Ag-Pb-Zn+/-Au	Euphrates	17-3	Y					
Early-Middle Jurassic	Silver King Pluton	Hall Siding	Barren Vein	Hall Siding Vein	20-1	Y					
Middle Jurassic	Bonnington Pluton	Red Mtn	Polymetallic Veins Ag-Pb-Zn+/-Au	Golden Eagle	131-18B	Y		Y			
Middle Jurassic	Bonnington Pluton	Red Mtn	Polymetallic Veins Ag-Pb-Zn+/-Au	Rozan	Rozan	Y					
Middle Jurassic	Bonnington Pluton	Marsh Ck	Barren Vein	Marsh Creek Vein	165-13A	Y		Y			
Middle Jurassic	Bonnington Pluton	Erie Ck	Au Skarns	Second Relief	344-5B	Y		Y	Y		
Middle Jurassic	Bonnington Pluton	Erie Ck	Au Skarns	Second Relief	344-6B	Y		Y	Y		
Middle Jurassic	Nelson Batholith	Stewart Ck	Porphyry Mo	Bobbi	44-10	Y					
Middle Jurassic	Nelson Batholith	Stewart Ck	Porphyry Mo	Stewart	Stewart	Y		Y			
Middle Jurassic	Nelson Batholith	Ymir	Polymetallic Veins Ag-Pb-Zn+/-Au	Yankee Girl	MI-068	Y					
Middle Jurassic	Nelson Batholith	Giveout Ck	Barren Vein	Giveout Creek Vein	51-9	Y		Y			
Middle Jurassic	Rossland Pluton	Rossland/South Belt	Polymetallic Veins Ag-Pb-Zn+/-Au	Bluebird	M3-145	Y				Y	
Middle Jurassic	Rossland Pluton	Rossland/South Belt	Polymetallic Veins Ag-Pb-Zn+/-Au	Homestake	MI-123	Y	Y	Y	Y	Y	

bonic fluid inclusions. Type V carbonic inclusions are only noted in polymetallic veins, Au-quartz veins and Au skarns. Type III salt-saturated fluid inclusions are absent in most of these deposits and extremely rare where noted. Insufficient data preclude estimated depths of formation for both polymetallic vein and porphyry Mo deposits. Evidence for heterogeneous entrapment exists at the Homestake and Lily May deposits adjacent to the Rossland pluton and at the Second Relief deposit associated close to the Bonnington pluton. Possible vapour-brine partiioning has been documented at the Homestake deposit.

It is interesting to note that, based on survey of 8 deposits, no Type III fluid inclusions are recognized from a variety of deposit types associated with either the Nelson or the Bonnington batholiths (Table A9-8). Although the absence of high salinity fluid inclusions from these two intrusions may be coincidence, this criteria serves to distinguish deposits associated with the Bonnington Pluton and "tail" of the Nelson Batholith from the those in the compositionally distinct but similar aged Rossland Pluton (Höy and Dunne, 1997)

Intrusion-related Au-pyrrhotite veins, within and along the margins of the Rossland pluton, are dominated by Type I aqueous, Type VI multiphase and Type IV mixed aqueous and carbonic fluid inclusions; Type V carbonic and Type III salt-saturated fluid inclusions are rare. Intrusion-related Au-pyrrhotite veins are the only deposit type to contain the unusual Type VII mixed multiphase and carbonic fluid inclusions. The Evening Star and War Eagle deposits are believed to have formed at minimum depths between 5 and 10.8 kilometres. Additional evidence for heterogeneous entrapment of fluids, in the form of both Type IV and V fluid inclusions, is noted at the Consolidated St. Elmo, War Eagle, Le Roi and Jumbo deposits.

MIDDLE CRETACEOUS: WALLACK CREEK AND HIDDEN CREEK STOCKS

Polymetallic veins are the only deposit type evaluated related to Middle Cretaceous intrusions. Based on two samples, only Type I aqueous fluid inclusions are noted in this deposit type.

SUMMARY

1. Porphyry Cu-Au deposits are associated with Early or Early-Middle Jurassic intrusions which are believed to have formed at relatively shallow depths of between 1 and 5 kilometres.
2. Intrusion-related Au-pyrrhotite and polymetallic vein deposits associated with the Rossland Pluton formed at depths of at least 5.7 to 10.8 kilometres.
3. Deposits related to the Rossland Pluton are the only Middle Jurassic deposits where coexisting Type III and IV fluid inclusions have been documented and the only deposits where Type VII inclusions are observed.
4. Evidence for heterogeneous entrapment is noted in deposits associated with the Eagle Creek Complex, the Rossland Pluton and possibly the Bonnington batholith.
5. Evidence for H_2O-CO_2 immiscibility is documented at the Gold Hill deposit.

NATURE OF FLUIDS RESPONSIBLE FOR AU-SULPHIDE AND POLYMETALLIC VEIN MINERALIZATION IN ROSSLAND CAMP

This study has examined seven intrusion-related Au-pyrrhotite and three polymetallic Ag-Pb-Zn+/-Au vein deposits associated with the Rossland pluton. These two deposit types account for most of the historic gold production from "lode" veins (Drysdale, 1915; Fyles, 1984) in the Rossland Mining Camp.

There are 2 types of occurrence of quartz associated with Au-pyrrhotite veins. Original, early formed quartz occurs as one to two centimetre subrounded "knots" comprising anhedral grains with abundant (>30%), tiny (<1 micron), secondary, wispy-textured fluid inclusions. The small size of fluid inclusions in the early formed quartz precludes fluid inclusion study. The early quartz "knots" are surrounded and cut by massive sulphide stringers which incorporate anhedral resorbed quartz grains (Photo A9-3), areas of "milled" quartz (Photo A9-8) or subhedral quartz grains (Photo A9- 2). These late? quartz grains are distinctly different from the early quartz as they are characterized by < 1 to perhaps 10% contained, relatively large (5 to 50 microns), dominantly secondary but rarely primary (Photo A9-1) fluid inclusions. We believe that the spatial relationship of the late quartz with gold-bearing sulphide stringers may imply a temporal association.

The following summarizes the nature of fluids in these later quartz associated with massive Au-sulphide and polymetallic vein mineralization in the Rossland Camp:

1. Dominantly Type I aqueous, Type VI multiphase and Type IV mixed aqueous and carbonic fluid inclusions with minor Type V carbonic and Type III salt-saturated inclu sions.
2. Unique occurrence in Rossland Camp deposits of Type VII mixed multiphase and carbonic fluid inclusions.
3. Abundant Type VI (multiphase) fluid inclusions in intrusion-related veins.
4. Overall, fluids are both low to moderate homogenization temperature (although actual trapping temperatures may be significantly higher (*see* Table A9-7 trapping temperatures of 335 to 475°C and arsenopyrite geothermometry by Thorpe, 1967), high and low salinity (Figure A9-8) and very similar to intrusion-related gold systems described by Lang *et al.* (2000), Lang ed. (2001), Thompson *et al.* (1999), McCoy *et al.* (1997) and Rowins (2000) which supports a model for dominantly magmatic fluid source, the Rossland pluton.
5. Calculated minimum depths of formation of deposits associated with the Rossland Pluton are relatively deep, greater than 5 km and possibly up to 10.8 km.

6. Evidence for heterogeneous entrapment, and perhaps fluid immiscibility, is present at a number of vein deposits associated with the Rossland Pluton.

Results from this study indicate that the fluids responsible for these veins are unique with respect to vein mineralization studied elsewhere in the Rossland Group. They from deposits associated with the Middle Jurassic Rossland pluton are also compositionally distinct from fluids from deposits associated with other Middle Jurassic intrusions.

Generally, fluid inclusion textures and compositions associated with Rossland Camp veins are characteristic of vein deposits formed in deep environments associated with batholiths: early wispy-textured quartz, readily observable CO_2, presence of NaCl-saturated inclusions with homogenization temperatures less than 220°C and salinities < 35 eq. wt. % NaCl (Reynolds, 1991). However, the occurrence of Type IIIB and VI fluid inclusions, typically found in porphyry and skarn systems, and evidence for Type VII fluid inclusions indicates a more complex environment of formation. Comparison of homogenization and salinity data to that of intrusion-related gold systems suggests, at least in part, a magmatic fluid origin; a metamorphic, or magmatic (Thompson *et al.*, 1999) fluid may be implied by the abundance of CO_2.

FLUID CHARACTERISTICS OF ALKALIC PORPHYRY COPPER-GOLD MINERALIZATION IN THE ROSSLAND GROUP

This study has examined four porphyry Cu-Au deposits in the Rossland Group. In summary:

1. The porphyry Cu-Au deposits are associated with Early or Early-Middle Jurassic intrusions in the Rossland Group.
2. Fluid inclusions are dominantly Type I aqueous and III salt-saturated H_2O-NaCl fluids with Type IV mixed aqueous carbonic and Type VI multiphase fluids only rarely observed. These fluid inclusion types are typical for classical porphyry environments (Reynolds, 1991).
3. Overall, fluids are both high and low salinity, very similar to calc-alkaline porphyry systems but ranges of salinity and homogenization temperature are distinctly different (Figure A9-7).
4. Calculated minimum depths of formation are within 1 to 5 kilometres, similar to depths for porphyry copper deposits (Bodnar, 1995; Sillitoe, 1995).
5. Evidence for heterogeneous entrapment is present at the Star porphyry Cu-Au deposit associated with the Eagle Creek Complex.

Results from this study indicate that the fluids responsible for alkalic porphyry Cu-Au deposits in the Rossland Group are similar to reported fluids responsible for calc-alkalic porphyry deposits: Types I and III fluid inclusions, both low and high salinity ranges on Figure A9-7, and minimum depths of formation from 1 to 5 kilometres. In common with porphyry environments in western Quesnellia and Stikinia, the alkalic porphyry deposits in the Rossland Group are commonly older than their calc-alkalic counterparts.

APPENDIX 9B
FLUID INCLUSION DATA, ROSSLAND CAMP

EVENING STAR (82F/SW102)

Primary fluid inclusions located along grown zones in quartz have been tentatively identified from a quartz-pyrite-calcite vein (Photo A9-4). These inclusions may have been trapped from fluids circulating at the same time as the host quartz crystal was growing and therefore may represent samples of the fluid that formed the quartz-pyrite-calcite vein. However, it is possible that the growth zones may be recrystallized bands that formed in a deep environment. If this is the case, fluid inclusions in these bands are not primary but secondary. Aqueous (H_2O-NaCl) Type I, carbonic (CO_2-trace CH_4/N_2) type V and mixed aqueous and carbonic (H_2O-CO_2-NaCl) type IV fluid inclusions characterize the primary fluid inclusion compositions (Tables A9-3a, 3c, 3d, 6).

Homogenization temperatures from Type I and IV fluid inclusions are moderately high from 307°C to 370°C (Tables A9-3a, 3c, 3d) and salinities low to moderate from 5.5 to 18.5 eq. wt. % NaCl (Table A9-5). Fluid inclusions fall in the intrusion-related Au or skarn fields of the ore deposit environment diagram (modified from Reynolds, 1991, Lattanzi, 1991) based on homogenization temperature (minimum trapping temperature estimate) and salinity and accounting for observable CO_2 phases present at room temperature (Figure A9-8).

Calculated minimum pressures of 1529 and 2273 are estimated for two Type IV inclusion assemblages using volume ratios of liquid-to-vapour and homogenization temperatures for CO_2 and H_2O (equations of Bowers and Helgeson, 1983). These minimum pressures correspond to depths of between about 5.7 and 8.6 km lithostatic load. Although the presence of readily observable CO_2 (*i.e.* Type IV and V fluid inclusions) is characteristic of these deep (>4 km at minimum) environments of deposition, primary fluid inclusions are not. In rare instances, euhedral quartz crystals can be protected from deformation and metamorphism that recrystallizes fluid inclusions in veins formed in deep environments by preservation within sulphide grains, i.e. encapsulation or cementation (Guha *et al.*, 1991).

CONSOLIDATED ST. ELMO (082F/SW135)

Fluid inclusions were evaluated in two quartz-sulphide veins that cut the skarn. Sample 96-51a is a 1 centimetre wide, fine-grained, granular quartz vein with blebs of pyrrhotite, pyrite and sphalerite. Vein sample 96-51e is over 5 cm wide with quartz comprising approximately 50% of the section, coarse pyrite and minor pyrrhotite. The quartz in both sections appears "milled" or brecciated into angular, anhedral fragments ranging from half a millimetre to less than a tenth of a millimetre. Fluid inclusions in the fine-grained quartz comprise about 30% of the grains and are secondary (formed along fracture planes). The abundance of fluid inclusion-filled fractures and small size of the inclusions resemble a quartz texture termed "wispy". The coarser grained quartz grains are clear with less than 2-3%, relatively large (5 to 50 micron), typically irregular-shaped, secondary fluid inclusions.

Fluid inclusions in the coarse-grained quartz are characterized by aqueous (H_2O-NaCl) Type I, mixed aqueous and carbonic (H_2O-CO_2-NaCl) Type IV, carbonic (CO_2-trace CH_4/N_2) type V, multiphase (H2O- NaCl- unknown phases) Type VI and mixed carbonic and multiphase (H_2O-CO_2-NaCl - unknown phases) Type VII (Tables A9-3a, 3c, 3d, 3e, 3f, 6). Multiphase and mixed carbonic and multiphase fluid inclusions have at least one contained solid phase. The liquid-vapour-solid ratios for measured fluid inclusion assemblages or groups were consistent indicating that the solid trapped phases are true "daughter minerals" and were trapped with daughter liquid and vapour phases from a homogeneous fluid rather than accidentally trapped solid inclusions. There is no evidence of sylvite, halite or other readily soluble phases since dissolution of daughter minerals is not observed on heating to decrepitation temperatures (300°C to 327°C).

Homogenization temperatures from Type I and VI fluid inclusions are unusually low, from 102°C to 194°C (Tables A9-3a and 3e), and salinities of Type I and IV inclusions low to moderate, from 6.4 to 20 eq. wt. % NaCl (Table A9-5). Strangely, the low homogenization temperatures are consistent with the generally irregular shapes of the fluid inclusions and their variable homogenization temperatures (> +/- 5°C within a fluid inclusion assemblage). However, in some cases, smooth shaped fluid inclusions are noted (*e.g.* sample 96-51a FIA #3-2). In the epithermal environment, smooth fluid inclusion shapes are consistent with temperatures of formation of about 250°C (Bodnar et al. 1985). The measured fluid inclusion temperature for an inclusion from FIA #3-2 is 102.3°C. This discrepancy in expected temperature (based on fluid inclusion shape) and actual measured temperatures suggests that a significant pressure correction is required for the data. Sample 96-51a probably formed at depths > 10 km lithostatic load given a 150°C 'pressure correction'.

JUMBO (082F/SW111)

Poikilitic-textured quartz gangue from a massive sulphide vein contains fluid inclusions formed in bands or clusters near the crystal cores or around poikilitically enclosed sulphide grains (Photo A9-3). These bands of fluid inclusions comprise approximately 10% of the volume of the quartz and may be of primary origin.

The primary fluid inclusions are small, from less than 3 to about 10 microns in diameter and comprise carbonic (CO_2-trace CH_4/N_2) Type V, mixed aqueous and carbonic (H2O-CO2-NaCl) Type IV, multiphase (H_2O- NaCl- unknown phases) Type VI and mixed carbonic and multiphase (H_2O-CO_2-NaCl - unknown phases) Type VII phases.

Secondary fluid inclusions formed in fractures are less common. Aqueous (Type I) and multiphase (Type VI) fluid inclusions were observed from one secondary fluid inclusion assemblage. The rims or margins of the quartz are clear with no fluid inclusions.

Primary fluid inclusion homogenization temperatures for multiphase Type VI fluid inclusions range from 145°C to 267°C. Fluid inclusion assemblage 5-1 exhibited homogenization to the vapour phase (vapour phase expansion) at 210°C; all other observed homogenization temperatures were to the liquid phase (vapour phase shrinks). The last melting temperature of ice is recorded as -0.9°C. The unknown composition of solid phases in these multiphase fluid inclusions precludes estimates of salinity and trapping temperature/pressure since the appropriate phase diagrams for the system cannot be selected.

Secondary fluid inclusion homogenization temperatures for Type I and VI fluid inclusions are moderate and range from 183°C to 231.5°C (Tables A9-3a, 3e). Salinities of aqueous fluid inclusions are low at 5.2 eq. wt. percent NaCl (Table A9-5).

The minimum depth of trapping for secondary Type I fluids under lithostatic load is 64 metres using equations of Bodnar and Vityk (1994) and is 300 metres based on boiling curves for NaCl solutions under hydrostatic conditions (after Haas, 1971). These are minimum estimates because there is no evidence for boiling. Thess estimates are probably an order of magnitude shallower than that expected considering the gangue mineralogy and character of the vein mineralization.

CENTRE STAR(082F/SW094) - LE ROI (082F/SW093)

Fluid inclusions in quartz were evaluated from a Le Roi dump sample of hornblende porphyrite containing fine-grained to disseminated sulphides cut by quartz - sulphide veins and brecciated? and intruded by coarse sulphide stringers. Sulphides are dominantly pyrrhotite with minor chalcopyrite.

Quartz from the quartz-sulphide veins typically occur as anhedral, irregular-shaped grains with abundant tiny (less than 1 micron diameter) fluid inclusions which give the grains a cloudy appearance. Rarely, cloudy grains have euhedral quartz overgrowths with virtually no contained fluid inclusions yielding a clear appearance (Photo A9- 2). Neither the cloudy quartz nor clear quartz overgrowths were suitable for fluid inclusion work. The cloudy quartz texture resembles 'wispy' quartz (Reynolds, 1991) which forms in deep environments.

The coarse sulphide stringers from sample R96-24a have trapped a broken fragment of a different generation of quartz vein containing 10 to 15 percent fluid inclusions up to 5 microns and rarely 10 microns in size (Photo A9-2). Petrographic observation of these fluid inclusions indicate a secondary origin and aqueous (H_2O-NaCl) Type I, multiphase (H_2O- NaCl- unknown phases) Type VI and mixed carbonic and multiphase (H_2O-CO_2-NaCl - unknown phases) Type VII phases. Heating and freezing of fluid inclusions from this fragment yield inconclusive results mainly due to difficulties in recognizing last ice melt temperatures due to the small size of the inclusions and early decrepitation of the fluid inclusion chips prior to vapour bubble homogenization or daughter crystal melting. The only homogenization temperature attained was 206.2°C for a fluid inclusion assemblage containing Type VII inclusions.

WAR EAGLE (082F/SW097) - No. 1

Fluid inclusions from three samples from the War Eagle deposit were evaluated to better understand the nature of fluids responsible for mineralization in this Main vein system. The samples are R96-31b, taken from the footwall of the War Eagle vein system; R96-58, from the northwest ex-

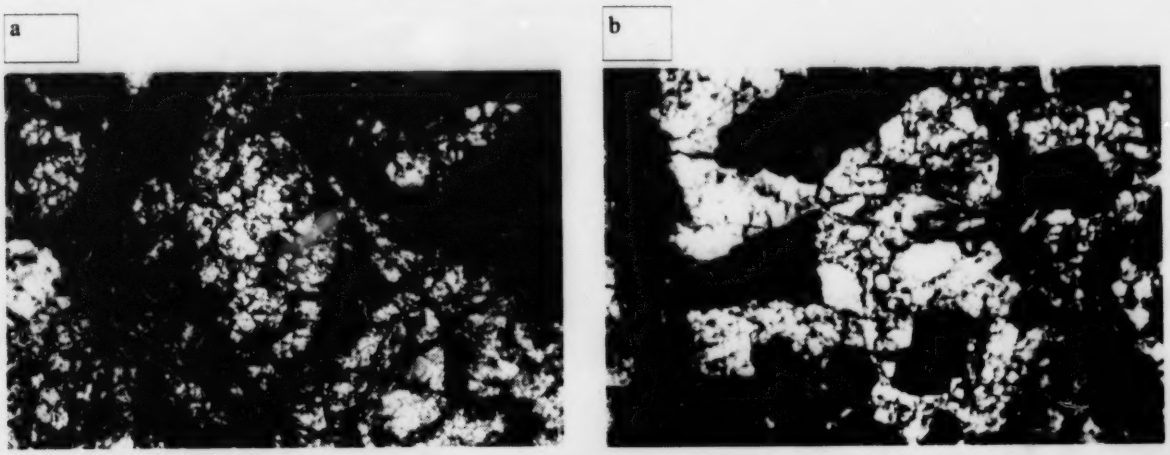

Photo A9-8. "Milled" quartz grains in a) a semi-massive to poorly banded pyrrhotite chalcopyrite vein at the Columbia-Kootenay deposit (Kootenay portal) and b) a quartz vein with minor pyrite and pyrrhotite at the Consolidated St. Elmo deposit. This quartz texture may be the result of brittle deformation. Transmitted and reflected plane light, 6.25X magnification, field of view = 7.8 mm.

tension of the War Eagle vein; and R96-71a, from the entrance to the War Eagle portal.

Sample R96-31b comprises mainly semi-massive pyrrhotite and pyrite, with minor chalcopyrite and traces of a magnetite? in a siliceous country rock. Siliceous ore from the Centre Star-War Eagle group is described by Drysdale (1915, p. 100) as "...closely associated with an intrusive tongue of diorite porphyrite and in many places represents the latter replaced, carries higher gold values than that of the upper levels which represents chiefly replaced augite porphyrite." The semi-massive ore in sample R96-31b is associated with approximately 5% euhedral to subhedral, clear quartz and cut by a one centimetre wide vein comprising anhedral quartz grains approximately 0.5 mm in diameter. Note that secondary quartz is associated with sulphides in sample R96-31c from the same location (Appendix 5).

The euhedral to subhedral quartz in sample R96-31b appears to share crystal boundaries with pyrrhotite and may have precipitated together with the semi-massive ore. This clear quartz exhibits rare primary growth zones, or possibly recrystallized bands?; unfortunately, the growth zones are defined by fluid inclusions less than one micron in diameter which are too small for fluid inclusion petrography. Since the "primary" fluid inclusions in this sample occur within semi-massive sulphides they may have been protected from deformation and metamorphism that recrystallized fluid inclusions in veins formed in deep environments (similar to Evening Star sample, described above).

Fluid inclusions in anhedral quartz from the vein in sample R96-31b are secondary occurring typically along healed fractures. They are characterized by aqueous (H_2O-NaCl) Type I, mixed aqueous and carbonic (H_2O-CO_2-NaCl) Type IV, multiphase (H_2O- NaCl- unknown phases) Type VI and mixed carbonic and multiphase (H_2O-CO_2-NaCl - unknown phases) Type VII (Tables A9-3a, 3c, 3e, 3f, 6). Multiphase and mixed carbonic and multiphase fluid inclusions have at least one contained solid phase which is commonly birefringent (possibly a carbonate phase?). Rarely, opaque phases are observed in the multiphase inclusions (Photo A9-9). The liquid-vapour-solid ratios for measured fluid inclusion assemblages or groups were consistent indicating that the solid trapped phases are true "daughter minerals" and were trapped with daughter liquid and vapour phases from a homogeneous fluid rather than accidentally trapped solid inclusions. Multiphase fluid inclusion assemblage 2-4 exhibits evidence of sylvite, halite or another readily soluble phase since dissolution of one of 5 daughter minerals occurs at 329°C, after homogenization at 298°C (Table A9-3e).

The homogenization temperature from a secondary Type I assemblage of fluid inclusions was 208°C (Table A9-3a) and corresponding salinity moderate at 15 eq. wt. % NaCl (Table A9-5).

Homogenization temperatures from secondary Type VI fluid inclusions are low to moderate from 160°C to 300°C (Tables A9-3a and 3e). Homogenization of fluid inclusions was to the liquid phase. Last melting temperatures of ice for Type VI inclusions range from -14°C to -8°C. The unknown composition of solid phases in these multiphase fluid inclusions precludes estimates of salinity and trapping temperature pressure since the appropriate phase diagrams for the system cannot be selected.

Melting of carbonic phases in Type IV and VII fluid inclusions is up to 1.3°C below the melting point of pure CO_2 which indicates the presence of trace concentrations of CH_4 or N_2. Insufficient data and unknown daughter phases preclude calculation of salinities for Type IV and VII fluids. Homogenization temperatures from secondary Type IV and VII fluid inclusions are moderate from 295°C to 316°C.

Secondary Type I fluid inclusions fall in the intrusion-related Au or skarn fields of the ore deposit environment diagram (modified from Reynolds, 1991; Lattanzi, 1991). The minimum depth of trapping for these fluids under lithostatic load is 38 metres using equations of Bodnar and Vityk (1994) and is 180 metres based on boiling curves for NaCl solutions under hydrostatic conditions (after Haas, 1971). This is a minimum estimate because there is no evidence for boiling and is probably at least an order of magnitude shallower than that expected considering the skarn alteration and character of the vein mineralization.

Sample R96-58 is a clinopyroxene, amphibole skarn with minor quartz and associated fracture-controlled? pyrrhotite and chalcopyrite. The quartz is cloudy comprising anhedral grains approximately 0.5 centimetres in diameter with abundant microfractures filled with less than one micron sized secondary fluid inclusions. The abundance of fluid inclusion filled fractures and small size of the fluid inclusions resembles a quartz texture characteristic of deep environments (> 4 km depth) termed "wispy" (*see* for example Photo A9-6).

Rare fluid inclusions large enough to observe in the quartz are characterized by multiphase (H_2O- NaCl- unknown phases) Type VI fluid inclusions. One Type VI assemblage homogenization temperature of 141°C was recorded from smooth-shaped fluid inclusions; the section decrepitated at 305°C.

Photo A9-9. Secondary multiphase (H_2O-NaCl-unknown phases) Type VI fluid inclusions in anhedral quartz vein, War Eagle deposit (sample 96-31b). Note birefringent clear solid inclusions and opaque phases. Transmitted plane light, 160X magnification. Field of view 0.3mm.

In the epithermal environment, smooth fluid inclusion shapes are consistent with temperatures of formation of about 250°C (Bodnar *et al.*, 1985). The measured fluid inclusion temperature for an inclusion from FIA #1-1 is 141°C. This discrepancy in expected temperature (based on fluid inclusion shape) and actual measured temperatures suggests that a significant pressure correction is required for the data. Unfortunately, since the salinity for the fluid inclusion assemblage is not known, the depth of lithostatic load given a 100°C 'pressure correction' cannot be calculated but, as an estimate, must be at least 5 km.

Sample R96-71a consists of highly fractured, cloudy, anhedral quartz with fractures filled with dominantly chalcopyrite and pyrrhotite, trace magnetite? and associated clear, subhedral to anhedral. Rarely, clear euhedral quartz crystals, approximately one millimetre in diameter, are cemented or encapsulated within sulphide grains (Photo A9-10). Occasionally, the clear quartz exhibits an embayed texture with the embayment filled with sulphides.

Fluid inclusions in the early, cloudy quartz are typically less than one micron in size which renders them unusable for fluid inclusion petrography. The texture of the quartz resembles wispy quartz characteristic of deep environments (> 4 km).

The late, clear quartz, which appears to be associated with sulphide precipitation in fractures, consists of approximately 1% fluid inclusions that occur as isolated inclusion assemblages or clusters of inclusions. The origin of these fluid inclusions is ambiguous. They do not occur in obvious growth zones or bands nor do they occur along defined secondary fracture planes. The fluid inclusions are characterized by salt-saturated (H_2O-NaCl) Type III and carbonic (H_2O-CO_2-NaCl) Type IV inclusions (Tables A9-3b, 3c, 6).

Salt-saturated fluid inclusions have one contained solid phase, commonly cubic, which is approximately the same size as the vapour bubble. Usually, in inclusions of this type, the vapour bubble homogenization temperature is approximately the same as the salt melting temperature. However, homogenization temperatures from fluid inclusions in assemblages FIA # 1-1 and 2-3 are low at 156°C and 170°C and the two salt phases, presumably halite, were observed to melt at 285°C and 331°C respectively (Table A9-3e). Calculated salinities for these samples based on salt melt temperatures are 37 and 41 eq. wt. % NaCl..

Homogenization temperatures from Type IV fluid inclusions are moderately from 243°C to 342°C (Tables A9-3c) and salinities low, from 4 to 10 eq. wt. % NaCl (Table A9-5). Fluid inclusions fall in the intrusion-related Au field of the ore deposit environment diagram (modified from Reynolds, 1991; Lattanzi, 1991) based on homogenization temperature (minimum trapping temperature estimate) and salinity and accounting for observable CO_2 phases present at room temperature.

Two methods are used for estimating fluid pressures from fluid inclusion data in this sample. The first method uses dissolution of halite since it dissolves after vapour-liquid homogenization in Type III inclusions (*see* Appendix 9a). Calculated minimum pressures are 2443 bars and 2872 bars (Table A9-7). These trapping pressures correspond to trapping depths of about 9.2 km and 10.8 km lithostatic load. The second method uses volume ratios of liquid-to-vapour and homogenization temperatures for CO_2 and H_2O in Type IV inclusions. The minimum estimated trapping pressure is 1692 bars for fluid inclusion assemblage 2-4. This trapping pressure corresponds to a trapping depth of about 6.4 km lithostatic load.

In summary, the War Eagle vein system, mined to depths of nearly 700 metres (Drysdale, 1915; Figure. 14), includes both skarn altered rocks (sample R96-58) and fracture controlled? mineralization (samples R96-31b, R96-71a) which formed in deep environments. The paragenetic sequence of quartz vein deposition is as follows: anhedral quartz with wispy texture, euhedral to subhedral clear quartz, sometimes embayed, associated with sulphides, late anhedral quartz veinlets cutting massive to semi-massive sulphides.

Fluid inclusions in the early anhedral quartz formed in a deep environment (> 4 km, probably > 8 km) based on the evident wispy texture of fluid inclusions in quartz (Reynolds, 1991). The clear quartz associated with sulphides contains fluid inclusions with readily observable CO_2 (Type IV) and NaCl-saturated inclusions with liquid-vapour homogenization temperatures less than 220°C and salinity of < 41 eq. wt. percent NaCl. Although coexistance of Type III and IV fluid inclusions is supported by spatial association, homogenization by halite dissolution (Type III inclusions) rather than vapour loss precludes confirmation of brine-vapour partitioning.

Minimum fluid pressure calculations for Types III and IV fluid inclusions yield corresponding minimum trapping depths that range from about 6.4 km to 10.8 km lithostatic load. Evidence in conflict with this interpretation is the fracture controlled? nature of the sulphide-quartz deposition in sample R96-71a. Fluid inclusions in the late anhedral quartz veinlets are characterized by readily observable CO_2 (Type IV inclusions) which are, again, indicative of formation in deep environments.

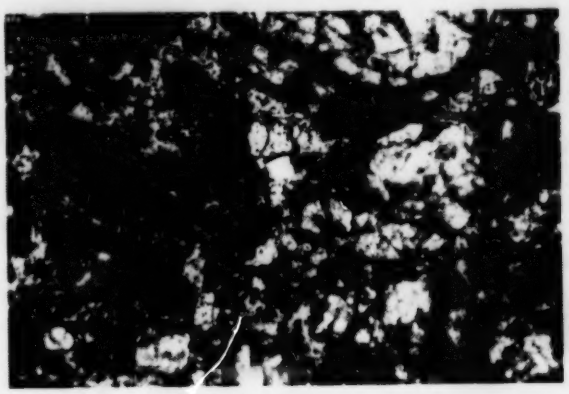

Photo A9-10. Clear, euhedral quartz crystal encapsulated within pyrrhotite grain, War Eagle deposit (sample 96-71a). Transmitted and reflected plane light, 6.25X magnification. Field of view = 7.8mm.

COLUMBIA-KOOTENAY (082F/SW151)

Fluid inclusions from three samples from the Columbia - Kootenay deposit were studied. All samples are from the Columbia waste dump.

Sample R96-39a consists of a clinopyroxene-plagioclase? skarn retrograde altered to actinolite (Appendix 8), and associated with stringers of pyrrhotite, minor chalcopyrite, quartz and trace magnetite. Poikilitic crystals (embayed) of quartz are intergrown mostly with pyrrhotite. Fluid inclusions in the quartz are secondary and include aqueous (H_2O-NaCl) Type I, carbonic (CO_2-trace CH_4/N_2) Type V and multiphase (H_2O- NaCl- unknown phases) Type VI inclusions (Tables A9-3a, 3c, 3e).

Fluid inclusion homogenization temperatures for type I inclusions are moderate at 237°C and 246°C with corresponding salinities of 4.4 and 4.7 eq. wt. percent NaCl. Homogenization temperatures for type VI inclusions are slightly higher at 269°C and 301°C. The unknown composition of solid phases in these multiphase fluid inclusions precludes estimates of salinity and trapping temperature/pressure since the appropriate phase diagrams for the system cannot be selected.

Separate Type I and Type V fluid inclusions are trapped as immiscible endmembers of an H_2O-CO_2-NaCl fluid within FIA 3-1. The Type V inclusion represents a virtually pure CO_2 system as CO_2 melting occurs at -56.7°C, only 0.1°C below the pure CO_2 triple point of -56.6°C. Homogenization of the CO_2 liquid and vapour phases occurs at 27.1°C. The Type I inclusion has a salinity of 4.4 eq. wt. percent NaCl and homogenizes at 237.5°C.

Sample R96-42b comprises massive arsenopyrite, pyrite, pyrrhotite, minor chalcopyrite and quartz in a crudely banded, folded and almost gneissic-textured altered rock. Pyrrhotite, pyrite and chalcopyrite form the matrix to rounded, fractured quartz vein fragments. The quartz vein fragments comprise multiple anhedral grains from one to 5 millimetres in diameter. Euhedral arsenopyrite overprints and is later than the other sulphides and quartz.

Fluid inclusions occur as clusters, isolated and in linear planes that probably represent healed fractures. The inclusions are assigned a secondary origin as no evidence of primary growth zones or overgrowths is observed. Aqueous (H_2O-NaCl) Type I, carbonic (CO_2-trace CH_4/N_2) Type V and multiphase (H_2O- NaCl- unknown phases) Type VI inclusions characterize the fluid inclusion compositions (Tables 3a, 3d, 3e).

Fluid inclusion homogenization temperatures for type I inclusions are moderate from 288°C to 346°C with corresponding salinities from 10.7 to 16.6 eq. wt. percent NaCl. Volume percent vapour in the Type I inclusions is high at 30 to 40% but homogenization of the fluid inclusion is to the liquid phase. Type VI fluid inclusions homogenize at significantly lower temperatures than the Type I inclusions between 157°C and 303°C. Daughter crystal phases do not dissolve prior to decrepitation of the Type VI fluid inclusions at temperatures measured from 337°C to 343°C. The unknown composition of solid phases in these multiphase fluid inclusions precludes estimates of salinity and trapping temperature/pressure since the appropriate phase diagrams for the system cannot be selected.

Type I fluid inclusions fall in the intrusion-related Au or skarn fields of the ore deposit environment diagram (modified from Reynolds, 1991;Lattanzi, 1991) based on homogenization temperature (minimum trapping temperature estimate) and salinity. This depositional environment is reasonable considering additional evidence of observable CO_2 phases present at room temperature.

The minimum depth of trapping for secondary Type I fluids under lithostatic load is 185 to 419 metres using equations of Bodnar and Vityk (1994) and is 1.0 to 1.7 km based on boiling curves for NaCl solutions under hydrostatic conditions (after Haas, 1971). These are minimum estimates because there is no evidence for boiling. These estimates are probably considerably shallower than that expected considering the skarn alteration and character of the vein mineralization.

Sample "Columbia" consists of a quartz, calcite, chlorite, biotite vein with sulphides and broken fragments. The quartz forms anhedral grains with < 2% fluid inclusions which occur as clusters, isolated or in linear planes that may be secondary. The inclusions are approximately 2 to 5 microns in diameter, smooth to negative-crystal shaped and include aqueous (H_2O-NaCl) Type I and multiphase (H_2O-NaCl- unknown phases) Type VI inclusions (Tables A9-3a, 3e, 5). Fluid inclusions in subhedral calcite are smooth-shaped, less than one micron in diameter, which precludes fluid inclusion petrography, occur in secondary fracture planes and comprise less than 1% of the mineral.

Fluid inclusion homogenization temperatures for Type I inclusions are moderate, similar to sample R96-42b, from 272oC to 377°C with corresponding salinities from 6 to 12 eq. wt. percent NaCl. Type VI fluid inclusions homogenize at lower temperatures than the Type I inclusions, between 199oC and 293°C. Daughter crystal phases do not dissolve prior to decrepitation of the Type VI fluid inclusions. The unknown composition of solid phases in these multiphase fluid inclusions precludes estimates of salinity and trapping temperature/pressure since the appropriate phase diagrams for the system cannot be selected.

Type I fluid inclusions fall in the intrusion-related Au field of the ore deposit environment diagram (modified from Reynolds, 1991;Lattanzi, 1991) based on homogenization temperature (minimum trapping temperature estimate) and salinity. However, this sample shows no fluid inclusion petrographic evidence of a deep environment such as observable CO_2 phases present at room temperature, wispy quartz texture or Type III fluid inclusions which homogenize the vapour phase below 200°C.

The minimum depth of trapping for secondary Type I fluids under lithostatic load is 139 to 238 metres using equations of Bodnar and Vityk (1994) and is 600 m to 1.1 km based on boiling curves for NaCl solutions under hydrostatic conditions (after Haas, 1971). These are minimum estimates because there is no evidence for boiling. These estimates are probably considerably shallower than that ex-

pected considering the skarn alteration and character of the vein mineralization.

In summary, the Columbia - Kootenay vein system, mined to depths of 200 m (Drysdale, 1915, Fig. 21), includes both skarn altered rocks (sample R96-39a) and metamorphosed and folded rocks (sample R96-42b) which indicate formation in deep environments. Gangue quartz occurs as poikilitic crystals intergrown with pyrrhotite (sample R96-39a) and as anhedral grains in veins or fragments from veins that formed prior to? sulphide deposition (sample R96-42b, Columbia).

The environment of deposition of the early anhedral quartz vein may have been deep (> 4 km), based on readily observable CO_2 (Type IV inclusions) in sample R96-42b . However, absolute minimum fluid pressure calculations for Type I fluid inclusions range from trapping depths of about 600 m to 1.7 km hydrostatic load or 139 to 238 metres lithostatic load.

Fluid inclusions in the later poikilitic-textured quartz associated with pyrrhotite deposition do contain readily observable CO_2 (Type IV inclusions) and may have formed at depths of >4 km.

HOMESTAKE (082F/SW123) and GOPHER (082F/SW125)

The Homestake vein (MI-123) consists of quartz intergrown with sulphides and chlorite as well as crushed and broken quartz fragments. The sample is cut by a calcite-quartz vein.

Quartz typically occurs as anhedral grains with approximately 20% smooth-shaped fluid inclusions from 5 to 15 microns in diameter. Crushed quartz appears recrystallized with less than 10% smooth-shaped fluid inclusions. The late quartz vein contains about 10% smooth-shaped fluid inclusions. The origin of fluid inclusion in all three types of quartz is ambiguous but probably secondary as no primary growth zones or overgrowths are observed.

Fluid inclusions in the early quartz, intergrown with sulphide, comprise aqueous (H_2O-NaCl) Type I, salt-saturated (H_2O-NaCl) Type III, carbonic (CO_2-trace CH_4/N_2) Type V, mixed aqueous and carbonic (H_2O-CO_2-NaCl) Type IV and multiphase (H_2O- NaCl- unknown phases) Type VI inclusions (Tables A9-3a, 3b, 3c, 3d, 3e).

Useful but limited fluid inclusion homogenization data is available from two fluid inclusion assemblages in the early quartz. Assemblage 2 contains separate Type I, Type III and Type V fluid inclusions trapped in the cluster. The Type I inclusion has a salinity of 7.5 eq. wt. % NaCl and homogenizes at 262°C. The type IIIA inclusion homogenizes by vapour disappearance at 255°C with salt melt occurring at 184°C; its salinity is 31.1 eq. wt. % NaCl. The Type V inclusion is a virtually pure CO_2 inclusion as CO_2 melting occurs at -56.8°C, only 0.2°C below the eutectic point for pure CO_2 at -56.6°C. Homogenization of the CO_2 liquid and vapour phases occurs at 24.1°C Assemblage 1 comprises Type IV fluid inclusions that exhibit clathrate melting at 9.5°C, CO_2 homogenization at 28.5°C and H_2O homogenization at 300.8°C.

Fluid pressure is estimated using volume ratios of liquid-to-vapour and homogenization temperatures for CO_2 and H_2O in Type IV inclusions. The minimum trapping pressure is approximately 1262 bars using equations of Kerrick and Jacobs (1981) for the system H_2O-CO_2-CH_4-NaCl. This minimum trapping pressure corresponds to a depth of about 4.8 km lithostatic load.

BLUEBIRD (082F/SW145) AND MAYFLOWER (082F/SW146)

Sample M3-145 consists of angular and brecciated, hornfelsed siltstone clasts in a matrix of pyrite, galena and minor chalcopyrite in a quartz gangue. Euhedral quartz in quartz overgrowths contains <1 to 2% smooth to negative crystal-shaped primary fluid inclusions and anhedral grains, up to 10% smooth-shaped secondary fluid inclusions occurring as fracture-filled planes. It is possible that the overgrowth zones may be recrystallized bands rather than primary growth features. Recrystallization and strain are also indicated by undulose extinction and minor sub-grain development in sample R96-66a from the Bluebird deposit (*see* Appendix 8). If this is the case, fluid inclusions in the euhedral quartz are secondary bands are not primary growth zones.

Fluid inclusions in quartz overgrowths are characterized by aqueous (H_2O-NaCl) Type I, carbonic (CO_2-trace CH_4/N_2) Type V and multiphase (H_2O- NaCl- unknown phases) Type VI fluid inclusions (Tables A9-3a, 3d, 3e). Multiphase fluid inclusions have one contained solid phase which is commonly birefringent. The liquid-vapour-solid ratios for measured fluid inclusion assemblages or groups were consistent indicating that the solid trapped phases are true "daughter minerals" and were trapped with daughter liquid and vapour phases from a homogeneous fluid rather than accidentally trapped solid inclusions. Homogenization temperatures for Types I and VI fluid inclusions are moderate from 286°C to 310°C. Salinity for Type I inclusions is low at 7.9 eq. wt.% NaCl.

Secondary fluid inclusions in anhedral quartz are characterized by aqueous (H_2O-NaCl) and multiphase (H_2O-NaCl- unknown phases) type fluid inclusions (Tables A9-3a, 3e). Homogenization temperatures for Types I and VI fluid inclusions are moderate from 245°C to 248°C but cooler than those from primary inclusions. Salinity for Type I inclusions is moderate at 17.8 eq. wt. % NaCl.

Type I fluid inclusions fall in the intrusion-related Au field of the ore deposit environment diagram (modified from Reynolds, 1991; Lattanzi, 1991) based on homogenization temperature (minimum trapping temperature estimate) and salinity. This depositional environment is reasonable considering additional evidence of observable CO_2 phases present at room temperature in the quartz overgrowths which is typical for deep depositional environments (>4 km).

The minimum depth of trapping for primary Type I fluids under lithostatic load is 227 metres using equations of

Bodnar and Vityk (1994) and is 1.0 km based on boiling curves for NaCl solutions under hydrostatic conditions (after Haas, 1971). The minimum depth of trapping for secondary Type I fluids under lithostatic load is 83 metres using equations of Bodnar and Vityk (1994) and is 350 metres based on boiling curves for NaCl solutions under hydrostatic conditions (after Haas, 1971). These are minimum estimate because there is no evidence for boiling. These estimates are probably considerably shallower than that expected considering evidence of observable CO_2 phases present at room temperature.

LILY MAY (082F/SW153)

Fluid inclusions in quartz from a quartz- carbonate-sulphide vein (Sample M3-153) were studied. Quartz occurs as euhedral crystals with about 10% negative crystal-shaped fluid inclusions occurring in what appears to be growth zones. However, the quartz is intergrown with recrystallized calcite and may also be recrystallized. If this is the case, the "growth zones" may be recrystallized bands of contained fluid inclusions of secondary rather than primary origin. The calcite contains rare fluid inclusions less than one micron in diameter formed along healed fractures. A thin quartz veinlet that cuts the sample is characterized by anhedral quartz grains with up to 5% irregular-shaped small secondary fluid inclusions that occur as fracture-filled planes.

Fluid inclusions in the euhedral quartz are characterized by aqueous (H_2O-NaCl) Type I, carbonic (CO_2-trace CH_4/N_2) Type V and mixed aqueous and carbonic (H_2O-CO_2-NaCl) Type IV fluid inclusions (TablesA9- 3a, 3c, 3d,).

Separate Type I and Type V fluid inclusions are trapped as immiscible endmembers of an H_2O-CO_2.NaCl fluid within FIA 1. The Type V inclusion represents a virtually pure CO_2 system as CO_2 melting occurs at -56.8°C, only 0.2°C below the pure CO_2 riple point of -56.6°C. Homogenization of the CO_2 liquid and vapour phases occurs at 30°C. The Type I inclusion has a salinity of 11.7 eq. wt. 5 NaCl and homogenizes to the liquid phase at 392.5°C.

REFERENCES

Andrew, K.P.E., Höy, T. and Simony, P. (1991): Geology of the Trail map-area, southeastern British Columbia; *B.C. Ministry of Energy, Mines and Petroleum Resources*, Open File 1991-16.

Bodnar, R.J. (1995): Fluid-inclusion evidence for a magmatic source for metals in porphyry copper deposits; in Magmas, Fluids and Ore Deposits, J.F.H. Thompson, Editor, *Mineralogical Association of Canada*, Short Course volume 23, pages 139-152.

Bodnar, R.J. and Vityk, M.O. (1994): Interpretation of Microthermometric Data for H_2O-NaCl Fluid Inclusions; in Fluid Inclusions in Minerals: Methods and Applications, De Vivo, B. and Frezzotti, M.L., Editors, Short course of the Working Group (IMA), *Virginia Tech*, Blacksburg, Virginia, U.S.A., pages 117-130.

Bowers T.S. and Helgeson H.C. (1983): Calculation of the thermodynamic and geochemical consequences of nonideal mixing in the system H_2O-CO_2-NaCl on phase relations in geologic systems: equation of state for H_2O-CO_2-NaCl fluids at high pressures and temperatures; *Geochimica et Cosmochimica Acta*, volume. 47, pages 1247-1275.

Brown P.E. (1989): FLINCOR: A microcomputer program for the reduction and investigation of fluid-inclusion data; *American Mineralogist*, volume 74, pages 1390-1393.

Brown, P.E. and Hagemann, S.G. (1994): MacFlincCor: A Computer Program for Fluid Inclusion Data Reduction and Manipulation; *in* Fluid Inclusions in Minerals: Methods and Applications, De Vivo, B. and Frezzotti, M.L., Editors, Short course of the Working Group (IMA), *Virginia Tech*, Blacksburg, Virginia, U.S.A., pages 231-250.

Brown P.E. and Lamb W.M. (1989): P-V-T properties of fluids in the system H_2O-CO_2-NaCl: new graphical presentations and implications for fluid inclusion studies; *Geochim. Cosmochim. Acta.*, volume 53, pages 1209-1221.

Crawford, M.L. (1981): Fluid Inclusions in metamorphic rocks - low and medium grade; *in* Short Course in Fluid Inclusions: Applications to Petrology, *Mineralogical Association of Canada*, L.S. Hollister and M.L. Crawford Editors, pages 39-69.

Crawford, M.L. and Hollister, L.S. (1986): Metamorphic fluids: the evidence from fluid inclusions; in Fluid-Rock Interactions during Metamorphism, Advances in Physical Geochemistry 5, Walther, J.V. and Wood, B.J., Editors.

Davis, D.W., Lowenstein, T.K. and Spences, R.J. (1990): Melting behaviour of fluid inclusions in laboratory-grown halite crystals in the systems NaCl-H_2O, NaCl-KCl-H_2O, NaCl-$MgCl_2$-H_2O, and NaCl-$CaCl_2$-H_2O*; *Geochim. Cosmochim. Acta.*, volume. 54, pages 591-601.

Drysdale, C.W. (1915): Geology and ore deposits of Rossland, British Columbia; *Geological Survey of Canada*, Memoir 77.

Fyles, J.T. (1984): Geological setting of the Rossland mining camp; *B.C. Ministry of Energy, Mines and Petroleum Resources*, Bulletin 74, 61 pages.

Goldstein, R.H. and Reynolds, T.J., (1994): Systematics of fluid inclusions in diagenetic minerals; *Society for Sedimentary Geology*, Short course 31, 199 pages.

Hall, D.L., Sterner, S.M. and Bodnar, R.J. (1988): Freezing point depression of NaCl-KCl-H_2O solutions; *Economic Geology*, volume 83, pages 197-202.

Höy, T. and Andrew, K.P.E. (1989a): The Rossland Group, Nelson map area, southeastern British Columbia; in Geological Fieldwork 1988, Newell, J.M. and Grant, B., Editors, *B.C. Ministry of Energy, Mines and Petroleum Resources*, Paper 1989-1, pages 33-43.

Höy, T. and Andrew, K.P.E. (1989b): Geology of the Rossland Group, Nelson map-area, southeastern British Columbia; *B.C. Ministry of Energy, Mines and Petroleum Resources*, Open file map 1989-1.

Höy, T. and Dunne, K.P.E. (1997): Early Jurassic Rossland Group, southern British Columbia, Part I - stratigraphy and tectonics; *B.C. Ministry of Energy, Mines and Petroleum Resources*, Bulletin 102, 124 pages.

Kerrick, D.M. and Jacobs G.K. (1981): A modified Redlich-Kwong equation for H_2O, CO_2 and H_2O-CO_2 mixtures at elevated pressures and temperatures; *American Journal of Science*, Volume 281, pages 735-767.

Knight, C.L. and Bodnar, R.J. (1989): Synthetic fluid inclusions. IX. Critical PVTX properties of NaCl-H2O solutions; *Geochim.* Cosmochim. Acta., volume 53, pages 3-8.

Lang, J.R., Baker, T., Hart, J.R. and Mortensen, J.K. (2000): An Exploration Model for Intrusion-Related Gold Systems; *Society of Economic Geologists*, Newsletter, January 2000, Number 40, p. 1-15.

Lang, J. editor (2001): Regional and System-Scale Controls on the Formation of Copper and/or Gold Magmatic-Hydrothermal Mineralization; Mineral Deposit Research Unit, *The University of British Columbia*, Special Publication Number 2.

Lattanzi, P. (1991): Applications of fluid inclusions in the study and exploration of mineral deposits; *European Journal of Mineralogy*, volume 3, pages 689-701.

McCoy, D.T., Newberry, R.J., Layer, P., DiMarchi, J.J., Bakke, A., Masterman, J.S. and Minehane, D.L. (1997): Plutonic-related gold deposits of interior Alaska, *Economic Geology*, Monograph 9, p. 191-241.

Nash, J.T. (1976): Fluid inclusion petrology - data from porphyry copper deposits and applications to exploration; *United States Geological Survey*, Professional paper 907D, 16 pages.

Ramboz, C., Pichavant, M. and Weisbrod, A. (1982): Fluid immiscibility in natural processes: use and misuse of fluid inclusion data II. Interpretation of fluid inclusion data in terms of immiscibility; *Chemical Geology*, volume 37, pages 29-48.

Reynolds, T.J., (1991): Short course on fluid inclusions, Mineral Deposit Research Unit, *The University of British Columbia*; Short course 6.

Robert, F. and Kelly, W.C. (1987): Ore-forming fluids in Archean gold-bearing quartz veins at the Sigma mine, Abitibi greenstone belt, Quebec, Canada; *Economic Geology*, volume. 82, pages 1464-1482.

Roedder E. (1984): Fluid inclusions; *Mineralogical Society of America*, Reviews in Mineralogy, volume 12, Bookcrafters Inc., Chelsea, Michigan, 644 pages.

Rowins, S. (2000): Reduced porphyry copper-gold deposits: a new variation on an old theme; *Geology*, Volume 28, pages 491-494.

Shelton, K.L. and Orville, P.M. (1980): Formation of synthetic fluid inclusions in natural quartz; *American Mineralogist*, volume 65, pages 1233-1236.

Sillitoe, R.H. (1995): The influence of magmatic-hydrothermal models on exploration strategies for volcano-plutonic arcs; *in* Magmas, Fluids and Ore Deposits, J.F.H. Thompson, Editor, *Mineralogical Association of Canada*, Short Course volume 23, pages 511-525.

Smith, D.L. and Evans, B. (1984): Diffusional crack healing in quartz; *Journal of Geophysical Research*, volume 89, pages 4125-4135.

Thompson, J.F.H., Sillitoe, R.H., Baker, T., Lang, J.R. and Mortensen, J.K. (1999): Intrusion-related gold deposits associated with tungsten-tin provinces; *Mineralium Deposita*, v. 34, p. 323-334.

Thorpe, .R.I. (1967): Mineralogy and zoning of the Rossland area; Unpublished Ph.D. thesis, *University of Wisconsin*.

MAPS NOT FILMED

CARTES NON REPRODUITES

micromedia
a division of IHS Canada

20 Victoria Street
Toronto, Ontario M5C 2N8
Tel.: (416) 362-5211
Toll Free: 1-800-387-2689
Fax: (416) 362-6161
Email: info@micromedia.on.ca